# Innovative techniques for selecting the dose of antibiotics in empiric therapy - focus on beta-lactams and cystic fibrosis patients

Dissertation zur Erlangung des
naturwissenschaftlichen Doktorgrades
der Bayerischen Julius-Maximilians-Universität Würzburg

vorgelegt von
Jürgen Bulitta
aus Scheinfeld

Würzburg 2006

**Eingereicht am:** ……

Bei der Fakultät für Chemie und Pharmazie

1. Gutachter: ……

2. Gutachter: ……

**der Dissertation**

1. Prüfer: ……

2. Prüfer: ……

3. Prüfer: ……

**des Öffentlichen Promotionskolloquiums**

Tag des Öffentlichen Promotionskolloquiums: ……

Doktorurkunde ausgehändigt am: ……

*Für meine Familie und Freunde*

**Acknowledgement**

The work for this thesis has been accomplished under the supervision of Professor Dr Fritz Sörgel, Institute for Biomedical and Pharmaceutical Research – IBMP in Nürnberg-Heroldsberg, and Professor Dr Ulrike Holzgrabe, Department of Pharmaceutical Chemistry, University of Würzburg.

First and foremost, I most cordially thank Professor Dr Fritz Sörgel for the assignment of the scientific topic for this Ph.D. thesis, for providing the raw data used in the data analyses of this thesis, for his continuous support, advice and guidance during this thesis, and for making it possible for me to work with the groups in Auckland, New Zealand, in Brisbane, Australia, and in Albany, NY, USA.

My warmest thank you goes to Professor Dr Ulrike Holzgrabe for supporting this Ph.D. work, for her time, for her help in organizational issues, and for reading and constructive commenting on the text of this thesis.

I am very thankful to Dr Martina Kinzig-Schippers and the whole laboratory team of the IBMP who did the analysis of the samples for all studies described in this thesis. I am very grateful to all clinical study teams and all people otherwise involved in those studies, without their work the data which were analyzed in this thesis would not exist.

My most sincere thank you goes to Professor Dr Nick Holford, University of Auckland, Auckland, New Zealand, for teaching me population pharmacometric data analyses and simulations, for showing me how to use NONMEM and how to greatly accelerate working with NONMEM, for valuable guidance on data analyses and simulations, and for comments on draft manuscripts that were incorporated in this thesis.

I most cordially thank Professor Dr George L. Drusano, Ordway Research Institute, Albany, New York, USA, for showing me how to do nonparametric population pharmacokinetic analysis, for valuable guidance on analyses, simulations, and interpretation of results, and for his comments on draft manuscripts that were the basis for this thesis.

My warmest thank you also goes to Professor Dr Stephen B. Duffull, University of Queensland, Brisbane, Australia, (now at the University of Otago, Dunedin, New Zealand) for the opportunity of training at the University

of Queensland, for his support in analysis and interpretation of pharmacometric data analyses, for discussions on modeling questions, and for his comments on draft manuscripts, posters and oral presentations.

I thank Cornelia Landersdorfer very much for proof reading this thesis. I am very happy to thank all my friends at the IBMP, in GoldLab and at the Ordway Research Institute and Rune Overgaard (whom I met at the University of Auckland in New Zealand) who all made the time of my Ph.D. work unforgettable.

**Legal notice**

The author of this thesis takes no responsibility and no liability for any dosing recommendation or related statement in this thesis. Drugs should be taken according to the approved manufacturer's guidelines (e. g. the German "Fachinformation" or the Summary of Product Characteristics [SPC] in the UK) and as recommended by the physician in charge.

**Rechtlicher Hinweis**

Für die in dieser Arbeit beschriebenen Dosierungs- und Verabreichungsempfehlungen übernimmt der Autor keinerlei Verantwortung und keinerlei Haftung. Arzneimittel sind nach den Vorschriften der Fachinformation und wie vom verantwortlichen Arzt empfohlen einzunehmen.

## Publications

The work described below has been published between 1998 and 2006. Some of those presentations are not part of this thesis.

## Full papers


1. Kinzig-Schippers M, Fuhr U, Zaigler M, Dammeyer J, Rüsing G, Labedzki A, Bulitta J, Sörgel F: Interaction of pefloxacin and enoxacin with the human cytochrome P450 enzyme CYP1A2. Clin Pharmacol Ther 1999; 65:262-74.
2. Sörgel F, Kinzig-Schippers M, Sauber C, Bulitta J: Pharmakokinetik und Pharmakodynamik von Levofloxacin. Chemotherapie J 1999; 8(suppl 18):19-27.
3. Sörgel F, Kinzig-Schippers M, Steinhauer S, Bulitta J: Chemie und Pharmakokinetik von Linezolid. In von Eiff C. (Eds.): Oxazolidinone: Eine neue Klasse von Antibiotika. 47-60; SM Verlagsgesellschaft mbH, Wessobrunn; 1999.
4. Sörgel F, Kinzig-Schippers M, Bulitta J: Pharmakokinetisches Profil von Quinupristin-Dalfopristin. Chemotherapie J 2000; 9(suppl 19):42-53.
5. Sörgel F, Bulitta J, Kinzig-Schippers M: How well do gyrase inhibitors work? The pharmacokinetics of quinolones. Pharm Unserer Zeit 2001; 30:418-27.
6. Jetter A, Kinzig-Schippers M, Walchner-Bonjean M, Hering U, Bulitta J, Schreiner P, Sörgel F, Fuhr U: Effects of grapefruit juice on the pharmacokinetics of sildenafil. Clin Pharmacol Ther 2002; 71:21-29.
7. Sörgel F, Bulitta J, Kinzig-Schippers M: Pharmakokinetik der Chinolone. Chemotherapie J 2002; 11(suppl 20):25-33.
8. Pletz MW, Preechachatchaval V, Bulitta J, Allewelt M, Burkhardt O, Lode H: ABT-773: Pharmacokinetics and Interactions with Ranitidine and Sucralfate. Antimicrob Agents Chemother 2003; 47:1129-31.
9. Sörgel F, Landersdorfer C, Bulitta J: Zur Pharmakokinetik von Linezolid und Telithromycin: Zwei neue Antibiotika mit besonderen Eigenschaften. Pharm Unserer Zeit 2004; 33:28-36.
10. Sörgel F, Bulitta J, Holzgrabe U: Paul Ehrlich, seine Forschungsgebiete und ihre Wirkung auf die Gegenwart - Gedanken zu seinem 150. Geburtstag. Pharm. Ztg. 2004; 149: 1038-42.
11. Sörgel F, Landersdorfer C, Bulitta J, Keppler B: Vom Farbstoff zum Rezeptor: Paul Ehrlich und die Chemie. Nachrichten aus der Chemie 2004; 52:777-782.
12. Pletz MW, Rau M, Bulitta J, De Roux A, Burkhardt O, Kruse G, Kurowski M, Nord CE, Lode H: Ertapenem pharmacokinetics and impact on intestinal microflora, in comparison to those of ceftriaxone, after multiple dosing in male and female volunteers. Antimicrob Agents Chemother 2004; 48:3765-72.
13. Krueger WA, Bulitta J, Kinzig-Schippers M, Landersdorfer C, Holzgrabe U, Naber KG, Drusano GL, Sorgel F. Evaluation by Monte Carlo Simulation of the Pharmacokinetics of Two Doses of Meropenem Administered Intermittently or as a Continuous Infusion in Healthy Volunteers. Antimicrob Agents Chemother 2005;49: 1881-9.

## Oral presentations

1. Bulitta J, Hess KJ, Sörgel F, Jaehde U, Kinzig-Schippers M: Modellierung der Resistenzentwicklung von *Staphylococcus epidermidis* gegen Gyrasehemmer. Oral Presentation at the PEG-Consensus-Conference for parenteral antibiotics; Frankfurt/Main, Germany; October 24, 1998.
2. Bulitta J, Hess KJ, Sörgel F, Jaehde U, Kinzig-Schippers M: Modellierung der Resistenzentwicklung von *Staphylococcus epidermidis* gegen Gyrasehemmer. Abstr. KP27, Pre-symposium: Clinical pharmaceutics in science and practice: Oral presentation about the rational use of antibiotics at the annual meeting of the German Pharmaceutical Society (Deutsche Pharmazeutische Gesellschaft, DPhG); Tübingen, Germany; November 5 - 6, 1998.
3. Bulitta J: Introduction into pharmacokinetics, pharmacodynamics and in-vitro/in-vivo correlations using WinNonlin® Professional for physicians, pharmacists and scientists of other natural sciences. Institute for Clinical Pharmacology – Department of Clinical Pharmacology, University of Cologne, Cologne, Germany; April 23, 1999.
4. Bulitta J: Workshop: Pharmacokinetic and pharmacodynamic calculations with WinNonlin®. Institute for Clinical Pharmacology – Department of Clinical Pharmacology, University of Cologne, Cologne, Germany; November 17, 2001.
5. Bulitta J: Ab initio-Vorhersage der Pharmakokinetik von Chinolonen in silico. Pre-symposium: Annual meeting of the German Pharmaceutical Society (Deutsche Pharmazeutische Gesellschaft, DPhG); Würzburg, Germany; October 8 - 11, 2003.
6. Bulitta J, Horn AH, Sörgel F, Holzgrabe U, Clark T: Quantitative Struktur Pharmakokinetik Beziehungen (QSPKR) bei Chinolonen – Vorhersage von Plasmakonzentrationen in silico. Oral Presentation at a Ph.D. student meeting of the German Pharmaceutical Society (DPhG); Freudenstadt-Lauterbad, Germany; March 26, 2004.
7. Bulitta J: Quantitative Structure Pharmacokinetics Relationships (QSPKR): How to estimate pharmacokinetic parameters. World Conference on Magic Bullets - Pre-Conference Workshops; Nürnberg, Germany; September 8, 2004.
8. Bulitta J, Holford NHG: Assessment of predictive performance of pharmacokinetic models based on plasma and urine data. PAGANZ 05 Population Approach Group in Australia & New Zealand, Brisbane, Australia; February 9, 2005.
9. Bulitta J, Duffull SB, Kinzig-Schippers M, Holzgrabe U, Stephan U, Sörgel F: Cystic Fibrosis Patients are Pharmacokinetically Comparable to Healthy Volunteers; 15th symposium of the International Society of Anti-Infective Pharmacology; Washington, DC, USA; December 19, 2005.

## Congress presentations

1. Sörgel F, Bulitta J, Naber KG, Kinzig-Schippers M, Jaehde U: Standardized measurement of sweat concentration (SC) of quinolones (QU) and their potential relationship to selection of resistant mutants of *staphylococcus epidermidis* (SE). Abstr. T115, 2nd European Congress of Chemotherapy (ECC) and 7th Biennial Conference on Antiinfective Agents and Chemotherapy, Hamburg, Germany; May 10 - 13, 1998.
2. Sörgel F, Bulitta J, Gatchev E, Kinzig-Schippers M, Rüsing G, Doser K, Thyroff-Friesinger U, Rauch C, Vlahov V: Results from pharmacokinetic (PK) studies analyzed by most modern LC-MS/MS – do we need to rewrite the PK of "old" antibiotics? Astr. M 336, 2nd European Congress of Chemotherapy (ECC) and 7th Biennial Conference on Antiinfective Agents and Chemotherapy, Hamburg, Germany; May 10 - 13, 1998.
3. Naber KG, Kinzig-Schippers M, Jaehde U: Standardized measurement of sweat concentration (SC) of quinolones (QU) and their potential relationship to selection of resistant mutants of *staphylococcus epidermidis* (SE). Abstr. T 115, 2nd European Congress of Chemotherapy (ECC) and 7th Biennial Conference on Antiinfective Agents and Chemotherapy, Hamburg, Germany; May 10 - 13, 1998.
4. Sauber C, Rüsing G, Bulitta J, Kinzig-Schippers M, Sörgel F: Analysis of rifampicin, isoniazid and pyrazinamide by LC-MS/MS in plasma. Abstr. 276, The 46th ASMS Conference on Mass Spectrometry and Allied Topics; Orlando, Florida/USA; May 31 - June 4, 1998.
5. Vycudilik W, Rüsing G, Sauber C, Kinzig-Schippers M, Bulitta J, Sörgel F: Application of LC-MS/MS to pharmacokinetic and forensic issues of glibenclamide. Abstr. 279, The 46th ASMS Conference on Mass Spectrometry and Allied Topics; Orlando, Florida/USA; May 31 - June 4, 1998.
6. Sauber C, Vycudilik W, Kinzig-Schippers M, Rüsing G, Bulitta J, Holzgrabe U, Sörgel F: Die LC-MS/MS als Methode zur Klärung pharmakokinetischer und forensischer Fragen zu Glibenclamid. Abstr. KP5, Pre-symposium: Clinical pharmaceutics in science and practice: Poster presentation: Rational use of antibiotics at the annual meeting of the German Pharmaceutical Society (Deutsche Pharmazeutische Gesellschaft, DPhG); Tübingen, Germany; November 5 - 6, 1998.
7. Rüsing G, Kinzig-Schippers M, Rangoonwala R, Vlahov V, Bulitta J, Bacracheva N, Hess KJ, Nickel P, Sörgel F: Bioinäquivalenz als Faktor zunehmender Resistenzentwicklung gegen Tuberkulostatika. Abstr. KP11, Pre-symposium: Clinical pharmaceutics in science and practice: Poster presentation: Rational use of antibiotics at the annual meeting of the German Pharmaceutical Society (Deutsche Pharmazeutische Gesellschaft, DPhG); Tübingen, Germany; November 5 - 6, 1998.
8. Rüsing G, Bulitta J, Müller C, Kinzig-Schippers M, Sörgel F: Sensitive analysis of naloxon-3-glucuronide by LC-MS/MS in plasma. Abstr. 2170, AAPS Annual Meeting and Exposition; San Francisco, California/USA; November 15 - 19, 1998.
9. Bulitta J, Hess KJ, Sörgel F, Kinzig-Schippers M: Modeling the emergence of resistance against quinolone (QU) antibiotics in *staphylococcus epidermidis (SE).* Abstr. 2357, AAPS Annual Meeting and Exposition; San Francisco, California/USA; November 15 - 19, 1998.
10. Kinzig-Schippers M, Rangoonwala R, Vlahov V, Rüsing G, Bulitta J, Bacracheva N, Hess KJ, Sörgel F: Bioinequivalence of tuberculostatics as a possible contributing factor to emergence of pathogen resistance. Abstr. 3437, AAPS Annual Meeting and Exposition; San Francisco, California/USA; November 15 - 19, 1998.
11. Jetter A, Bulitta J, Zaigler M, Sauber C, Fuhr U, Kinzig-Schippers M, Sörgel F: Modelling of intestinal absorption of clavulanic acid. Abstr. A19 (podium discussion), Annual congress for clinical pharmacology 1999; Berlin, Germany; June 10 – 12, 1999.
12. Steinhauer S, Kinzig-Schippers M, Kleinschnitz M, Sauber C, Bulitta J, Sörgel F: Most sensitive analysis of felodipine in human plasma by LC-MS/MS after special sample work-

up. Abstr. 2178, AAPS Annual Meeting and Exposition; New Orleans, Louisiana/USA; November 14 - 18, 1999.

13. Sauber C, Kinzig-Schippers M, Rüsing G, Heuberger S, Bulitta J, Holzgrabe U, Sörgel F: Determination of trovafloxacin by LC-MS/MS in human plasma and urine. Abstr. 2841, AAPS Annual Meeting and Exposition; New Orleans, Louisiana/USA; November 14 - 18, 1999.
14. Steinhauer S, Kinzig-Schippers M, Rüsing G, Wenner M, Heuberger S, Bulitta C, Bulitta J, Sörgel F: Sensitive analysis of roxithromycin in human plasma by LC-MS/MS. Abstr. 2844, AAPS Annual Meeting and Exposition; New Orleans, Louisiana/USA; November 14 - 18, 1999.
15. Rüsing G, Kinzig-Schippers M, Sauber C, Steinhauer S, Wahode H, Bulitta J, Holzgrabe U, Sörgel F: Sensitive analysis of diclofenac (DIC) in human plasma by LC-MS/MS after special sample work-up. Abstr. 2847, AAPS Annual Meeting and Exposition; New Orleans, Louisiana/USA; November 14 - 18, 1999.
16. Sörgel F, Allen A, Pay V, Bygate E, Kinzig-Schippers M, Bulitta J, Bird N, Naber KG: Distribution of gemifloxacin into saliva, sweat, tears, and nasal secretion in healthy volunteers. Abstr. M117, 3rd European Congress of Chemotherapy; Madrid, Spain; May 7 - 10, 2000.
17. Bulitta J, Kinzig-Schippers M, Naber CK, Naber KG, Sauber C, Kleinschnitz M, Wahode H, Rodamer M, Sörgel F: Limitations in the use of drug cocktails (DC) to compare the pharmacokinetics (PK) of drugs: ciprofloxacin (CIP) vs. levofloxacin (LEV). Abstr. 506, 40th Interscience Conference on Antimicrobial Agents and Chemotherapy; Toronto, Canada; September 17 - 20, 2000.
18. Kinzig-Schippers M, Hinder M, Loos U, Sauber C, Bulitta J, Holzgrabe U, Sörgel F: Tissue Penetration of Cefditoren (CEE) into Bronchial Mucosa (BM) and Epithelial Lining Fluid (ELF) in Patients Undergoing Fiberoptic Bronchoscopy. Poster T3282, AAPS Annual Meeting and Exposition; Denver, Colorado/USA; October 21 - 25, 2001.
19. Bulitta J, Kinzig-Schippers M, Naber CK, Naber KG, Sauber C, Kleinschnitz M, Wahode H, Rodamer M, Sörgel F: Limitations in the use of drug cocktails (DC) to compare the pharmacokinetics (PK) of drugs: ciprofloxacin (CIP) vs. levofloxacin (LEV). Poster R5168, AAPS Annual Meeting and Exposition; Denver, Colorado/USA; October 21 - 25, 2001.
20. Bulitta J, Horkovics-Kovats S, Borek M, Skott A, Illauer M, Rodamer M, Kinzig-Schippers M, Sörgel F: Self-Inhibition of Clarithromycin's (CLA) Metabolism in Humans at Steady-State. Poster A-1625, 43rd Interscience Conference on Antimicrobial Agents and Chemotherapy; Chicago, Illinois/USA; September 14 - 17, 2003.
21. Sörgel F, Bulitta J, Kinzig-Schippers M, Landersdorfer C, Tomalik-Scharte D, Jetter A, Fuhr U, Cascorbi I: Dosing of antiinfectives – "One size fits all" vs. individualized therapy. Poster P K18, Annual meeting of the German Pharmaceutical Society (Deutsche Pharmazeutische Gesellschaft, DPhG); Würzburg, Germany; October 8 - 11, 2003.
22. Bulitta J, Kinzig-Schippers M, Jetter A, Tomalik-Scharte D, Szymanski J, Fuhr U, Illauer M, Skott A, Sörgel F: Pharmacokinetics and pharmcodynamics of subcutaneous interferon alpha-2b. Poster P K2, Annual meeting of the German Pharmaceutical Society (Deutsche Pharmazeutische Gesellschaft, DPhG); Würzburg, Germany; October 8 - 11, 2003.
23. Gareis J, Hüttner S, Kinzig-Schippers M, Bulitta J, Heß K-J, Sörgel F: Evidence of opiates in human urine after consumption of poppy seed cake. Poster P K5, Annual meeting of the German Pharmaceutical Society (Deutsche Pharmazeutische Gesellschaft, DPhG); Würzburg, Germany; October 8 - 11, 2003.
24. Rodamer M, Horkovics-Kovats S, Borek M, Skott A, Illauer M, Bulitta J, Kinzig-Schippers M, Sörgel F: Self-inhibition of clarithromycin's (CLA) metabolism in humans at steady-state. Poster P K13, Annual meeting of the German Pharmaceutical Society (Deutsche Pharmazeutische Gesellschaft, DPhG); Würzburg, Germany; October 8 - 11, 2003.

25. Hüttner S, Holt DW, Bulitta J, Heß K-J, Sörgel F: Effects of freshly squeezed grapefruit juice on CYP 3A4 activity. Poster P K7, Annual meeting of the German Pharmaceutical Society (Deutsche Pharmazeutische Gesellschaft, DPhG); Würzburg, Germany; October 8 - 11, 2003.

26. Jakob V, Rodamer M, Bulitta J, Kinzig-Schippers M, Heß K-J, Sörgel F: Prediction of caffeine half-life by subject age. Poster P K8, Annual meeting of the German Pharmaceutical Society (Deutsche Pharmazeutische Gesellschaft, DPhG); Würzburg, Germany; October 8 - 11, 2003.

27. Bulitta J, Horkovics-Kovats S, Borek M, Hüttner S, Kinzig-Schippers M, Sörgel F: Self-inhibition of clarithromycin's (CLA) metabolism in humans at steady-state; Abstract no. 081, World Conference on Magic Bullets; Nürnberg, Germany; September 9 - 11, 2004.

28. Bulitta J, Fuhr U, Landersdorfer C, Tomalik-Scharte D, Szymanski J, Kinzig-Schippers M, Sörgel F: Pharmacokinetics and pharmacodynamics of subcutaneous interferon alpha-2b; Abstract no. 082, World Conference on Magic Bullets; Nürnberg, Germany; September 9 - 11, 2004.

29. Naber KG, Bulitta J, Jakob V, Kinzig-Schippers M, Sörgel F: Limitations in the use of drug cocktails (DC) to compare the pharmacokinetics (PK) of drugs: ciprofloxacin (CIP) vs. levofloxacin (LEV); Abstract no. 213, World Conference on Magic Bullets; Nürnberg, Germany; September 9 - 11, 2004.

30. Wagenlehner F, Naber KG, Kinzig-Schippers M, Bulitta J, Sörgel F: Plasma concentrations, urinary excretion and bactericidal activity of linezolid (LIN) (600mg) versus ciprofloxacin (CIP) (500mg) in healthy volunteers after a single oral dose; Abstract no. 255, World Conference on Magic Bullets; Nürnberg, Germany; September 9 - 11, 2004.

31. Rodamer M, Fuhr U, Tomalik-Scharte D, Jetter A, Bulitta J, Kinzig-Schippers M, Sörgel F: Personalized isoniazid (INH) dosing based on genotyping for arylamine *N*-Acetyltransferase Type 2 (NAT2); Abstract no. 447, World Conference on Magic Bullets; Nürnberg, Germany; September 9 - 11, 2004.

32. Sakka SG, Glauner A, Bulitta J, Kinzig-Schippers M, Sörgel F: Continuous versus intermittent bolus administration of imipenem in critically ill patients with pneumonia; Abstract no. 467, World Conference on Magic Bullets; Nürnberg, Germany; September 9 - 11, 2004.

33. Sörgel F, Bulitta J, Kinzig-Schippers M, Hüttner S: Dosing of antiinfectives - "one size fits all" vs. individualized therapy; Abstract no. 517, World Conference on Magic Bullets; Nürnberg, Germany; September 9 - 11, 2004.

34. Sorgel F, Bulitta J, Horkovics-Kovats S, Kinzig-Schippers M, Borek M, Nesme B, Jakob V: Crucial role of "appropriate" reference product and food effects in clinical trials - a plea for drug level measurements in phase III – trials; 44th Interscience Conference on Antimicrobial Agents and Chemotherapy, Chicago, Illinois/USA; October 30 - November 2, 2004.

35. Horkovics-Kovats S, Nesme B, Kinzig-Schippers M, Bulitta, J, Sörgel F: Gender Differences in the Metabolism of Clarithromycin after Oral Doses of 500 mg; Presentation number: A-8; 45th Interscience Conference on Antimicrobial Agents and Chemotherapy, Washington, DC, USA; December 16 - 19, 2005.

36. Bulitta J, Duffull SB, Kinzig-Schippers M, Holzgrabe U, Stephan U, Sörgel F: Cystic Fibrosis Patients are Pharmacokinetically Comparable to Healthy Volunteers; Presentation number: A-12; 45th Interscience Conference on Antimicrobial Agents and Chemotherapy, Washington, DC, USA; December 16 - 19, 2005.

37. Bulitta J, Kinzig-Schippers M, Holzgrabe U, Sörgel F, Holford NHG: Replicate Design to Study the Population Pharmacokinetics (PopPK) of Piperacillin (PIP). Description of Saturable Elimination (EL) and Application to the Design of Optimal Dosage Regimens; Presentation number: A-30; 45th Interscience Conference on Antimicrobial Agents and Chemotherapy, Washington, DC, USA; December 16 - 19, 2005.

38. Bulitta J, Horkovics-Kovats S, Kinzig-Schippers M, Holzgrabe U, Sörgel F, Holford NHG: Use of Replicated Design to Assess Between Occasion Variability (BOV) of Oral Amoxicillin / Clavulanic Acid (AM / C) and for Monte Carlo Simulations (MCS); Presentation number: A-32; 45th Interscience Conference on Antimicrobial Agents and Chemotherapy, Washington, DC, USA; December 16 - 19, 2005.

39. Bulitta J, Lodise TP, Drusano GL, Kinzig-Schippers M, Holzgrabe U, Sörgel F: Bias and Uncertainty of Monte Carlo Simulations with Beta-Lactams Abstract 969, 15th Annual Meeting of the Population Approach Group in Europe (PAGE); Brugge, Belgium; June 14 - 16, 2006.

40. Landersdorfer C, Kirkpatrick CMJ, Kinzig-Schippers M, Bulitta J, Holzgrabe U, Sörgel F: New Insights into the Most Commonly Studied Drug Interaction with Antibiotics: Pharmacokinetic Interaction between Ciprofloxacin, Gemifloxacin and Probenecid at Renal and Non-renal Sites. Abstract 882, 15th Annual Meeting of the Population Approach Group in Europe (PAGE); Brugge, Belgium; June 14 - 16, 2006.

41. Bulitta J, Landersdorfer C, Kinzig-Schippers M, Jakob V, Rodamer M, Drusano GL, Thyroff-Friesinger U, Holzgrabe U, Sörgel F: Population Pharmacokinetics (PK), Pharmacodynamics (PD) and Breakpoints of Cefuroxime Axetil in Healthy Volunteers via Monte Carlo Simulation (MCS). Presentation number: A-1119; 46th Interscience Conference on Antimicrobial Agents and Chemotherapy, San Francisco, CA, USA; September 27 - 30, 2006.

**Table of contents**

**List of figures**

**List of tables**

## List of chemical structures

# 1 Background on pharmacokinetic-pharmacodynamic modeling

## 1.1 Pharmacokinetics

### 1.1.1 Definition of pharmacokinetics

Pharmacokinetics (PK) relates the drug doses to the time course of drug and metabolite concentrations at various sites in the body. PK is a rather young field of science. Some of its pioneers are Paul Ehrlich (1854 - 1915), P. Hanzlik (175, 176), Harry Gold, Torsten Teorell (367, 489, 490), Friedrich Hartmut Dost (106), Ekkehard Krüger-Thiemer (262-264), and A. Augsberger (22, 23).

Holford and Sheiner (197) defined PK as follows: “Pharmacokinetics encompasses the study of movement of drugs into, through and out of the body. It describes the processes and rates of drug movement from the site of absorption into the blood, distribution into the tissues and elimination by metabolism or excretion.”

### 1.1.2 The individual pharmacokinetic approach

The individual pharmacokinetic (PK) approach attempts to describe the time course of drug concentrations in the body for one individual. Commonly applied methods for individual PK are non-compartmental analysis (NCA) or modeling by the standard-two-stage (STS) approach. Both methods require frequent concentration time points (e. g. 6 or more samples per subject).

NCA is the simplest method of analyzing concentration time profiles. The observed concentrations are connected by linear (or log-linear) interpolation and no functional model is applied to interpolate between observed concentration time points (see Figure 1.1-1).

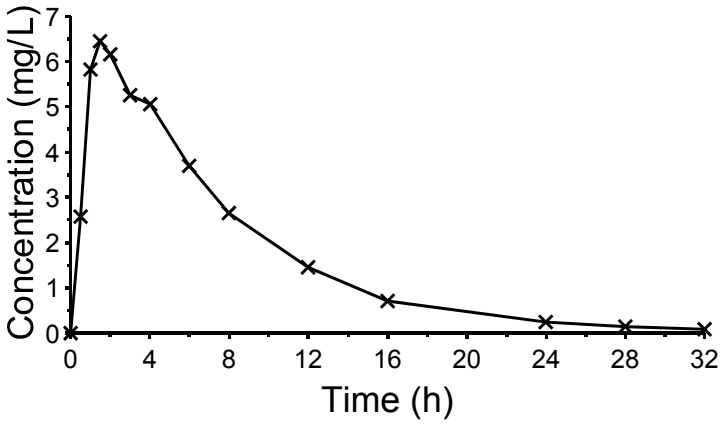


**Figure 1.1-1** Area under the curve calculation by the linear trapezoidal rule (non-compartmental analysis)

The STS approach uses a compartmental model like the one shown in Figure 1.1-2. All processes in this two-compartment model follow first order kinetics. Based on this scheme, an equation which describes the whole concentration time curve (see Figure 1.1-3) can be derived. The concentration time profile of each subject is described by a set of PK parameters for this equation.

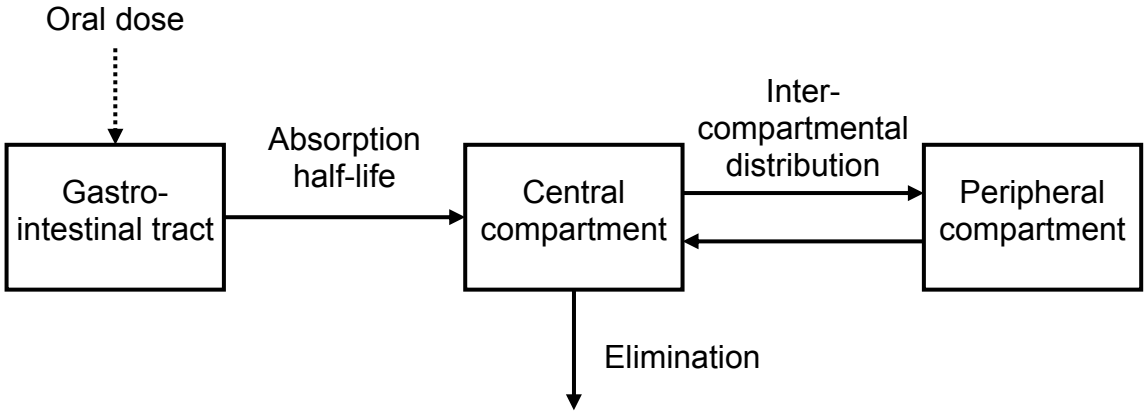


**Figure 1.1-2** Scheme of a two-compartment model with first-order oral absorption

The STS approach yields a smooth curve fit (see Figure 1.1-3) and integrates the area under the fitted curve, whereas NCA calculates the area under the curve as the sum of trapezoidals (see Figure 1.1-1).

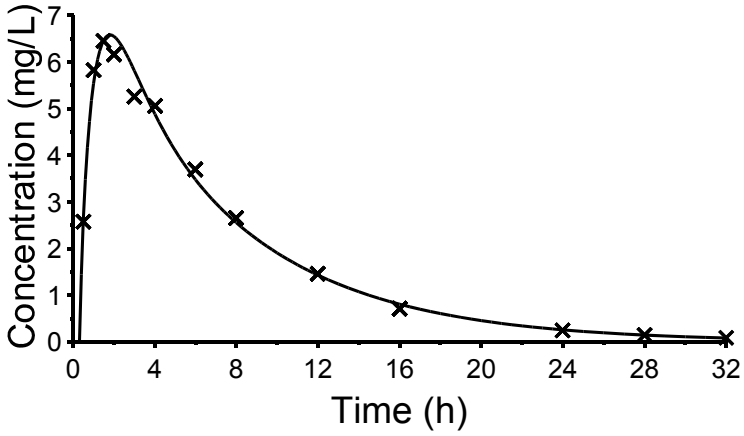


**Figure 1.1-3** Curve fit and area under the curve calculation by the standard-two-stage approach (modeling)

The STS approach is especially more powerful compared to NCA, if plasma concentration time profiles of new dosage regimens are to be simulated or if a drug obeys saturable elimination.

### 1.1.3 Population pharmacokinetics

The main conceptual difference between the individual PK approach and population PK is that the individual PK approach attempts to describe the concentration time curve for a single individual, whereas population PK attempts to describe the diversity of concentration time curves for a whole population. Descriptive statistics are usually used to characterize the distribution of PK parameters which were estimated by the STS approach. Thus, the STS approach comprises two separate data analytical steps: 1) estimation of the PK parameters separately for each subject, and then 2) use of descriptive statistics to characterize the distribution of PK parameters.

Population PK combines steps 1 and 2 in a single step. A statistical model is therefore required as one part of the population PK model to describe the variability of PK parameters. This part is called the parameter variability model. It describes the variability of PK parameters and the pairwise correlation of PK parameters for the whole study population. Figure 1.1-4 shows the raw data and the fitted plasma concentration time profiles for twelve subjects.

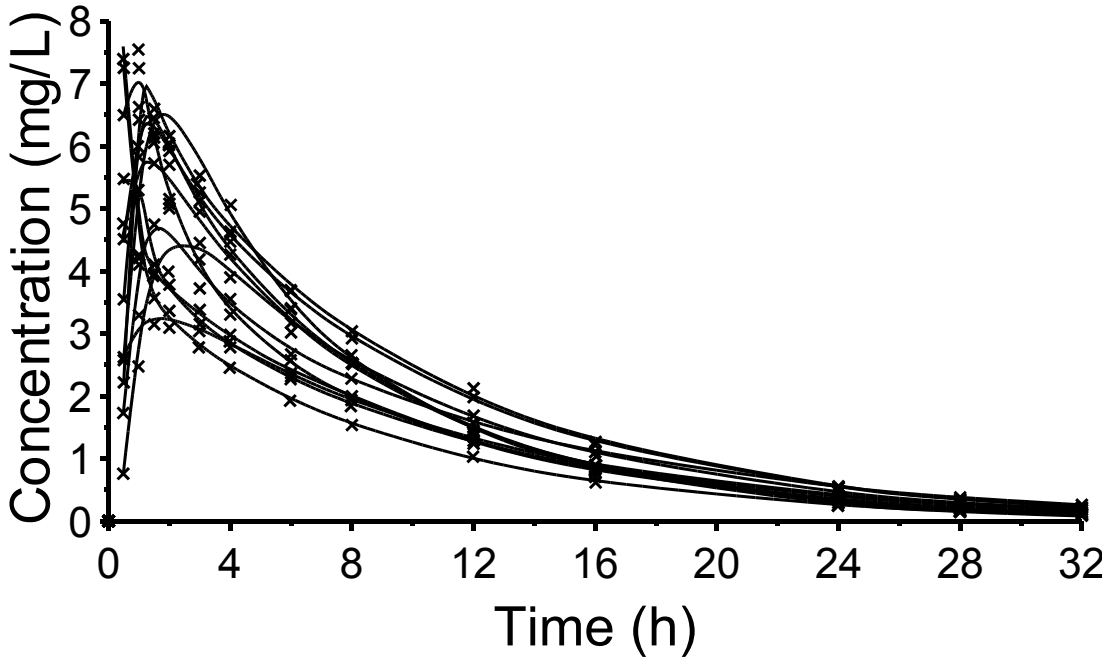


**Figure 1.1-4** Curve fits of a population PK model for twelve subjects

One set of PK parameters is used to describe the plasma concentration time profile of each subject. Based on the parameter variability model, sets of PK parameters for thousands of virtual subjects can be generated in a simulation. If the corresponding plasma concentration time profiles are simulated for each of those virtual subjects, one can study the expected range of concentration time profiles for the chosen dosage regimen.

### 1.1.4 Advantages of population pharmacokinetics

The difference between individual and population PK may seem small, however, there are significant advantages of population PK compared to individual PK. A population PK model is estimated from all concentrations observed in a whole clinical study in a single data analytical step ("one stage approach"). A population PK model can predict the variability of concentration time profiles for the whole study population for any dosage regimen. It is further possible to explain the observed variability in PK parameters by covariates like body size, body composition, and renal function. On average, patients with renal insufficiency will have a lower renal clearance than healthy volunteers. Older patients might have an altered body composition and

therefore have lower or higher volumes of distribution depending on the physicochemical properties of the drug. As a population PK model describes the variability of PK parameters of the whole study population and accounts for systematic differences of patients with altered demographic data, a population PK model can be used:

1) To simulate the expected concentration time curves for new dosage regimens in order to study:
   a. how many subject will achieve the desired drug exposure.
   b. how many subjects will achieve a certain peak concentration.
   c. how many subjects will achieve a desired concentration at the end of the dosing interval.
2) To study the influence of multiple covariates like body size, body composition, and renal function on PK parameters simultaneously.
3) To derive dosing guidelines for specific patients groups, e. g. for obese or undernourished patients and for patients with various degrees of renal impairment.
4) To repeat a clinical trial e. g. 1,000 times by simulation and to study how often the desired results can be shown with a chosen study design.

Those are only some advantages for specific applications of population PK models. Although population PK requires more computation time than modeling by the STS approach and NCA, these advantages outweigh the increased workload for many applications.

There are also methodological advantages of population PK compared to the STS approach (238, 447) which may be significant, especially if sparse datasets are evaluated. The STS approach tends to over-estimate the between subject variability (BSV) of PK parameters and yields less precise estimates for the BSV terms (447). Those methodological details will not be discussed here, as the STS approach was not used for the data analysis in this thesis. Table 1.1-1 compares key aspects of NCA, the STS approach and population PK which are relevant for the data analysis within this thesis. In essence, one should use population PK, if the objectives require a population PK approach and if one can afford the longer computation time of population

PK. Several applications for which population PK is especially powerful have been described above and additional applications are described in chapter 1.3.3.

**Table 1.1-1** Comparison of NCA, the STS approach, and population PK

| | **NCA** | **Modeling by the STS approach** | **Population PK analysis** |
|---|---|---|---|
| | | *Types of datasets* | |
| Analysis of datasets with frequent blood samples | applicable | applicable | applicable |
| Analysis of datasets with sparse blood samples | not applicable [a] | not applicable [b] | applicable |
| | | *Methodological issues* | |
| Estimates for the between subject variability | tend to be biased and imprecise | tend to be biased and imprecise | best method |
| Uncertainty of PK parameters | methodologically inferior to population PK | methodologically inferior to population PK | can be derived, best method |
| Account for multiple covariates (e. g. age, weight, creatinine clearance) | possible, by a separate data analytical step, e. g. via ANCOVA | possible, by a separate data analytical step, e. g. via ANCOVA | most powerful method, but also longest computation time |
| Computation time | very fast (<1h) | fast (<1day) | can be <1day, but maybe weeks |
| | | *Simulations* | |
| Simulation of concentration time profiles for other dosage regimens | not applicable | possible, but not as powerful as population PK | best method |
| Account for saturable elimination | not applicable | possible, but not as powerful as population PK | most powerful method |

[a]: Bootstrap methods to analyze sparse plasma concentration time data with NCA have been developed (49, 305, 306). However, these methods are applied rarely and are computationally more intensive.

[b]: Naïve pooling or naïve averaging can be used to analyze sparse data by the STS approach. However, both naïve methods have methodological flaws and are therefore not recommended (447).

ANCOVA: Analysis of covariance, NCA: Non-compartmental analysis, STS: Standard-two-stage.

## 1.2 Pharmacodynamics - definition

Knowledge about drug concentrations in the body is of limited value, unless there is information on the effect (e. g. therapeutic or toxic) which is caused by the drug concentrations. Such a concentration-effect relationship can e. g. be seen as the affinity of a drug towards its receptor(s) or as the drug exposure required to achieve a desired therapeutic effect. Drusano (107) defined pharmacodynamics (PD) as “the study of the biochemical and physiological effects of drugs and the mechanisms of their actions”.

A concentration-effect relationship has been shown for many drugs. Ideally, the drug concentrations at the site of action should be used. However, plasma concentrations are commonly used as a surrogate measure for the drug concentrations at the site of action. If there is a fast equilibrium between plasma and the site(s) of action, this approach is often helpful, since plasma concentrations can be measured more easily and often more precisely than tissue levels. A useful separation between PK and PD is: “PK is what the body does to the drug and PD is what the drug does to the body” (197).

Antimicrobial PD has been defined by Drusano (107) as “the discipline that attempts to link measures of drug exposure to the microbiological or clinical effects that are observed once an anti-infective drug has been administered”. One specific feature of antimicrobial PD is that the concentration-effect relationship of antibiotics can be determined outside the human body, e. g. by measuring the minimal inhibitory concentration (MIC) of the infecting pathogen. This is an advantage of antimicrobial PD, since the time and costs for measuring an MIC are negligible compared to performing a clinical trial in humans.

## 1.3 Pharmacokinetics-pharmacodynamics

### 1.3.1 Definition of pharmacokinetics-pharmacodynamics

Pharmacokinetics-pharmacodynamics (PKPD) is the combination of PK and PD. Linking the concentration time profiles (PK) with the concentration-effect relationship (PD) allows one to study, whether the achieved concentrations are likely to be effective, toxic, or ineffective. Figure 1.3-1 shows a scheme of a PKPD model.

The administered dose results in a concentration time profile (see Figure 1.3-1). If one assumes a direct effect PD model, the concentration at each time point causes the drug effect (e. g. the rate of bacterial killing for antibiotics). Figure 1.3-1 shows the effect time profile for a single dose. The effect time profile for the whole duration of therapy determines the drug related response.

Treatment success or failure is determined by the drug related response and various types of patient related factors. The latter comprise disease state and disease progression, co-morbidity, co-medication, and other factors. For antibiotics, the re-growth of bacteria and selection of resistant mutants due to antibiotic use also contribute to the therapeutic success / failure. As those factors are all represented as “patient related factors”, the scheme in Figure 1.3-1 is a simplified representation of the relationship between dosage regimen and therapeutic success / failure.

Although this PKPD model is simplified, it is a useful model to draw conclusions on optimal antibiotic therapy. If patient related factors are of major importance (e. g. for a patient at an intensive care unit), the expertise of experienced physicians can not be replaced by such a PKPD model. However, valuable guidance can be provided for a physician and discussed interactively to achieve an optimal probability of successful antibiotic therapy.

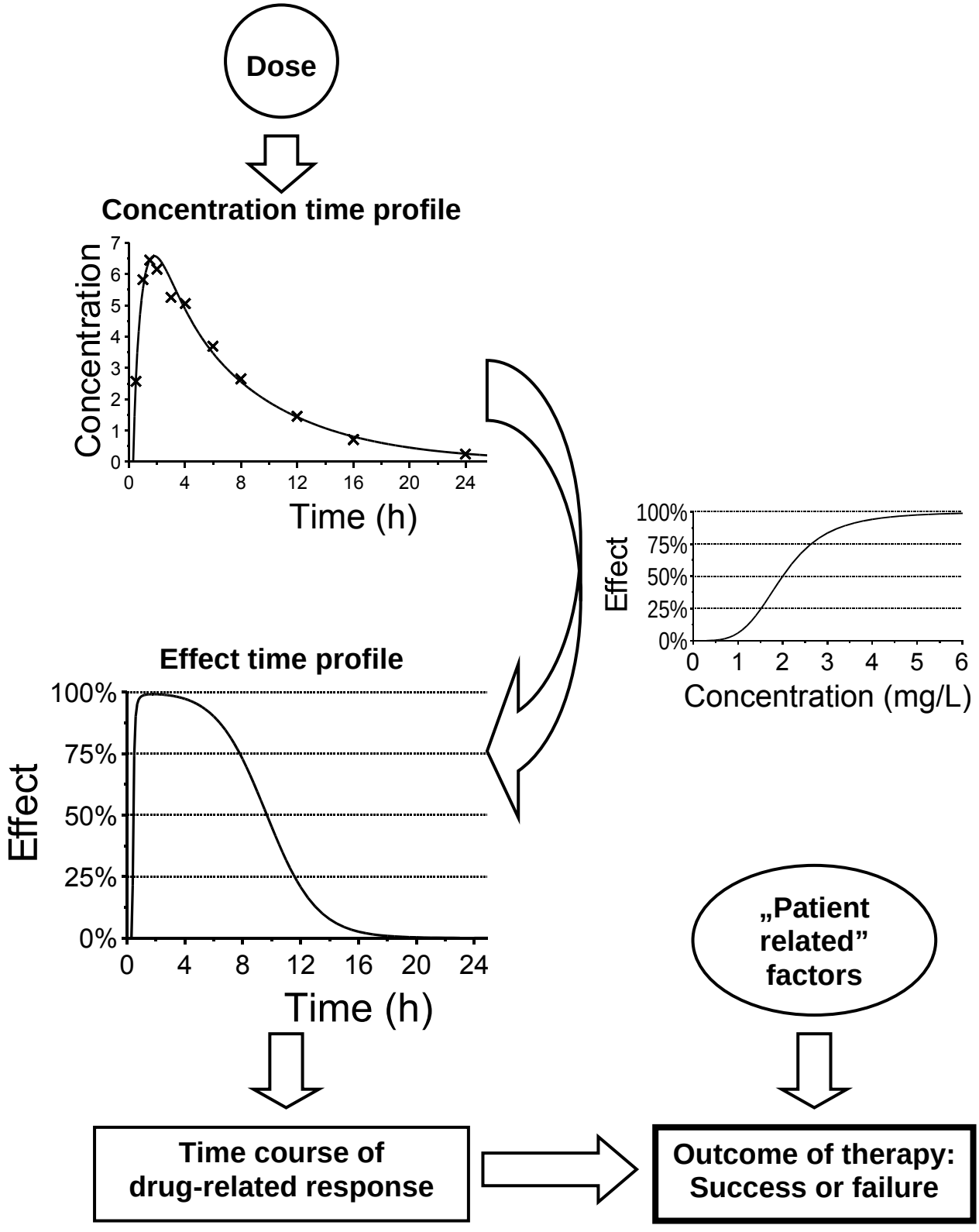


**Figure 1.3-1** Simplified scheme of a pharmacokinetic-pharmacodynamic model

### 1.3.2 Strengths of pharmacokinetic-pharmacodynamic models

The strength of PKPD models is their ability to represent all processes between a dosage regimen and the drug related response. The time course of drug related response can be compared between various dosage regimens and “the best” dosage regimen can be selected. It is important to consider the true BSV in all processes involved in Figure 1.3-1. The time course of drug related response will therefore not be the same in each patient, even if all patients receive exactly the same dosage regimen. A population PKPD model can account for the BSV and therefore allows one to predict the drug related response and its variability for a whole patient population.

It is appealing to further assume that the drug related response is the main determinant of the therapeutic response (i. e. the effect of non-drug related factors on therapeutic success/failure is small). This assumption may not be always true, e. g. in critically ill patients who might die from a co-morbidity not related to the infection. However, this assumption is often a useful simplification which applies to “standard” situations of antibiotic therapy. Although a population PKPD model accounts for the BSV in the drug related response, one still needs to be cautious in interpreting the results of such predictions, since the assumptions of such a simulation might not always be adequate. However, the ability to predict the probability of therapeutic success or failure makes population PKPD models a powerful tool for optimal antibiotic therapy and also for clinical drug development.

### 1.3.3 Important applications of pharmacokinetic-pharmacodynamic models

#### 1.3.3.1 Background and examples

The power of a population PKPD model to predict the drug related response for a whole patient population is the basis of their use for several

important applications. This chapter introduces some general applications of population PKPD models and then presents specific applications for antibiotics.

*General applications of population PKPD models:*

1. Optimization of dosage regimens
    a. Which dose level?
    b. Which mode of administration (e. g. bolus, prolonged or continuous infusion)?
    c. How long is the optimal dosing interval?
2. Derive dosage regimens which provide the optimal probability for successful therapy in specific patient populations.
3. Which is the best descriptor for body size (e. g. total body weight, body surface area, or lean body mass)?
4. Assessing the power of a clinical trial to show a desired trial result
5. Optimization of clinical trial designs
6. Visualization of already available knowledge for interpretation and discussion.

*Applications of population PKPD models for antibiotics:*

1. Determination of the highest MIC with a high probability of successful treatment.
2. Predicting the probability of successful treatment in empiric therapy.
3. Which doses / dosage regimens are required to prevent amplification of resistant mutants due to antibiotic exposure?

Many important applications of population PKPD models are based on their ability to predict the expected range of plasma concentration time profiles or the range of the time course of drug related response. As those simulations include random components, the BSV of PK (and PD) parameters, they are called Monte Carlo simulations (MCS) or stochastic simulations. Whereas deterministic simulations always provide the same answer when the same model inputs are used, two stochastic simulations (=MCS) with a large sample

size will yield similar but not identical results, if the random number generator uses a different starting point (=seed number).

The plasma concentration time profiles and effect vs. time profiles are usually simulated for many virtual patients based on the estimated population PKPD model. If the profiles of e. g. 10,000 virtual patients are simulated for each competing dosage regimen, the predicted plasma concentrations and drug effects can be compared between dosage regimens. Besides comparing the average concentrations and effects, it is important to compare the predicted variability of concentrations and effects. The patients with very low and very high concentrations are the most interesting patients, as those patients are likely to show therapeutic failure or toxicity, respectively. This allows one to assess the “optimal” dose, mode of administration (e. g. short-term, prolonged, or continuous infusion), and dosing interval.

#### 1.3.3.2 Accounting for the effect of covariates

Additionally, the effect of covariates like age, body size, body composition, and renal function on PK and PD parameters can be studied. If there is a statistically significant and clinically relevant influence of one or more covariates on the PK or PD parameters, those covariates might need to be considered for dose selection not only for dosing of special patient groups. MCS in special patient groups can provide optimal dosage regimens for patient groups with specific covariates (e. g. patients older than 65 years with a certain degree of renal failure).

One can also compare dose selection based on various descriptors for body size and body composition. Such an analysis might select total body weight, body surface area, or lean body mass to be most suitable for dose calculation. However, selection of the best body size descriptor usually requires a clinical trial with a large number of patients and with a large range in body size.

#### 1.3.3.3 Assessing the power of clinical trials and optimization of clinical trial designs

Another application of population PKPD models is based on their ability to simulate clinical trials. One can simulate a clinical trial with a specific trial design and evaluate the simulated plasma concentration time or effect time profiles. Those clinical trial simulations are usually repeated for a large number of times and the frequency of how often a desired trial result can be shown is recorded. If a sufficiently large number (e. g. >200 trials) of trials is simulated, this frequency approximates the probability of showing the desired trial result. By doing so, one can calculate the chance (power) to show bioequivalence or the chance to show a test treatment to be superior to the reference treatment in a phase II/III clinical trial. If the probability to show the desired trial result is low (e. g. <80%), then one should consider to optimize the study design or to increase the sample size. Those power calculations are inherently important for large clinical trials, since it is unethical to perform a study with a low probability of success.

For large clinical trials which may cost several million US$, it is vitally important to optimize the chance of success. The BSV needs to be considered for selecting an optimized trial design, since the BSV affects the results of the study. Optimal trial design (114, 118, 119, 160, 163, 354, 407, 488, 495, 528) has gained more interest during the last years, since this technique is computationally intensive and the computational power increased dramatically over the last decades. A population PK or PKPD model is usually the basis for the optimal trial design algorithms. As the time and costs spent especially on phase II/III clinical trials are significant, the clinical drug development process can be greatly accelerated by optimization of clinical trial designs. Additionally, more specific dosing guidelines can be derived e. g. for special patient groups, if the clinical trial design has been optimized before performing a clinical study.

#### 1.3.3.4 Visualization of clinical trial results

It may be difficult to visualize the results of a large clinical trial. This is especially true, if only sparse concentration time data are available. A group of patients may contain patients with very diverse demographic characteristics or various types of co-morbidity. In such cases, a population PKPD model is not only an elegant way to analyze the data, but may also be the “only” method to visualize the available data. It may be difficult to impossible for the reader to interpret data, if there are multiple influential covariates which affect the observed drug effect. In those cases, simulating the concentration and effect time profiles as well as the probability of successful treatment based on a population PKPD model is a valuable method of visualization.

#### 1.3.3.5 Predicting the probability of successful antibiotic treatment and of emergence of resistance

Specific applications of population PKPD models for antibiotics usually include simulation of the range of expected plasma concentrations for an antibiotic by MCS. Applications of MCS for anti-infectives were pioneered by Drusano et al. (113) who presented the first such analysis for evernimicin at an FDA meeting in 1998. Their population PKPD model suggested a low probability of successful treatment which was later found in phase II/III clinical trials. Therefore, population PKPD had the power to suggest stopping clinical drug development for evernimicin.

The MIC of the infecting pathogen and the plasma concentration time profile are the two main factors which determine the drug related response for antibiotics. The drug related response is then used to predict the probability of successful treatment. Once the MIC has been determined for a patient, the expected plasma concentration time curves can be simulated and the range of concentrations can be compared to this MIC. This allows one to predict the probability of successful treatment for this pathogen and to derive the so called PKPD breakpoint (see definition and application below).

**Definition:** The **PKPD breakpoint** is the highest MIC with a high (≥90%) probability for successful treatment (see also chapter 2.7.2).

**Application:** If the MIC of the infecting organism is at or below the PKPD breakpoint, there is a ≥90% chance for successful treatment, whereas the probability for successful treatment is below 90% for MICs above the PKPD breakpoint.

However, the MIC of the infecting pathogen is unknown in empiric antibiotic therapy. In absence of knowledge about the MIC at initiation of therapy, one may use the susceptibility data of the patients with similar infections who were treated at the respective hospital during the last year. There is often a large variability in the observed MICs which is described by the MIC distribution for the respective pathogen. Combining the MIC distribution and the variability in expected plasma concentrations allows one to predict the probability of successful treatment in empiric therapy. This probability can guide the choice of the best antibiotic and of the most appropriate dosage regimen for a clinician. Those simulations can also be applied, if there are multiple possible causative pathogens for the infection.

More recently, mathematical models were built to predict the required drug exposure to prevent emergence of resistance. The group of Drusano identified dosage regimens which were intended to suppress amplification of resistant mutants during antibiotic therapy for levofloxacin (239) or moxifloxacin (169). Those models are mathematically more complex as they require to describe the bacterial killing, growth, and re-growth at each time point. They describe the PK of the antibiotic and the killing and growth of bacteria in a much more detailed way. Although those models are computationally more intensive, they provide additional information on the expected probability of selection of resistant mutants and may become more popular in the future.

## 1.4 Study populations: Healthy volunteers or patients?

### 1.4.1 Pharmacokinetic studies in healthy volunteers and in patients

Healthy volunteers aged 18 to 45 years are a relatively homogeneous group of subjects. The BSV in PK parameters for ill patients is often 2-10 fold higher than for healthy volunteers. The low variability in healthy volunteers is caused by several factors: Healthy volunteers span a narrow range in age and total body weight, have a similar body composition (obese and undernourished subjects are typically excluded from those studies), and have a normal renal function (creatinine clearance). The lower BSV in healthy volunteers helps to estimate more complex PK models with e. g. a parallel saturable renal elimination besides the non-saturable glomerular filtration.

The clinical procedures of healthy volunteer studies are (much) more standardized than studies in patients. Drug administration, food and fluid intake, and sample preparation can be very standardized, if e. g. 12 healthy volunteers are dosed within 30 min and are studied on the same day. Studies in healthy volunteers are usually performed by professionals who work full time on clinical trials, whereas studies in patients are often performed (at least in part) by nurses who have to work on routine medical care simultaneously.

Another limitation for studying ill patients is the total amount of blood to be collected. A commonly applied limit for healthy volunteer studies is to draw no more than about 400 mL blood (e. g. 80 blood samples each of 5 mL) within four weeks. As ill patients may have a considerable amount of blood drawn for other clinical procedures and tests, only a smaller number of blood samples can be taken from patients for medical and ethical reasons.

Two-, three- or four-way crossover studies are commonly performed in healthy volunteers to remove the BSV for the comparison between treatments. As each subject serves as his/her own control, only within subject variability remains as an error term for the comparison. Medical and technical reasons may however not allow one to perform crossover studies in ill patients. Consequently, treatment comparisons have to be made with BSV as error term which is usually larger than within subject variability (198).

Studies in healthy volunteers can be performed in less than five months in total (from start of preparation of the clinical protocol to finishing the complete study report), whereas studies in patients usually require much more time. A good strategy is often 1) to start with a (small) study in healthy volunteers, 2) to use those data for optimal trial design in ill patients, and 3) to perform a clinical study in patients.

### 1.4.2 Pharmacokinetic studies in patients with cystic fibrosis

Cystic fibrosis CF is the most common inherited disease in the Caucasian population and causes a high morbidity and mortality secondary to respiratory tract infections (12, 283, 400). The PK of patients with cystic fibrosis (CF) is a major part of this thesis. Therefore, the pathophysiological alterations in CF-patients which may become relevant for PK will be described in this chapter. Cystic fibrosis affects all exocrine glands and causes alterations of various organs which might affect the PK of drugs.

***Gastrointestinal tract:*** About 85-90% of CF-patients have symptoms of dysfunctions in the gastrointestinal (GI) tract (374). Cox et al. (81) reported an hypersecretion of gastric acid in CF-patients. A small volume, high viscosity, and low concentration of hydrogencarbonate and pancreatic enzymes of duodenal aspirates has be found in CF-patients (157, 170). Most (14 of 16) CF-patients show an injury of the proximal small intestinal mucosa (81). Data on *d*-xylose (64), *d*-fructose (138), and $^{51}$Cr-ethylenediaminetetracetic acid (281) show an increased intestinal permeability of these probe molecules in CF-patients. It has been hypothesized that the presence of abnormal mucus on the intestinal mucosa may affect the intestinal absorption (138) and that abnormalities of the tight (occluding) junctions of the intestinal epithelial cells might cause this increased permeability (159). In summary, there are various factors which might result in an altered rate or extent of absorption in CF-patients compared to healthy volunteers.

Secondary to their GI alterations, CF-patients are leaner than healthy volunteers. Therefore, CF-patients have on average a higher ratio of lean

body mass (LBM) to total body weight (WT) than healthy volunteers. This altered body composition of CF-patients may need to be considered for dose selection in CF-patients.

***Blood:*** CF-patients with moderately severe pulmonary disease have an increased plasma volume and red blood cell count, when those quantities are normalized by WT. Plasma volume per kg WT was increased by 44.7% (417) and by 29.4% in another study (480) relative to healthy young adults. Average blood volume per kg WT was increased by 40.6% (417). These differences were less pronounced, if height was used instead of WT to normalize the respective volumes or if the values were compared to healthy children and healthy adolescents (66). These data suggest that it is important to account for the altered body composition of CF-patients.

***Hepatobiliary system:*** Hepatic abnormalities are found in about 20 to 50% of studied CF-patients (82, 247, 278, 374, 549). Approximately 5% of CF-patients develop cirrhosis and about 2% have severe liver disease. Fatty liver is one of the most frequent hepatic abnormalities in CF-patients (82). CF-patients have a reduced total bile acid output with a delayed peak of this output relative to control subjects, which was independent of the patients' pancreatic function level. Weizman et al. (535) suggested that this is probably due to a defect in gall-bladder responsiveness in CF-patients.

An altered bile acid metabolism and bile acid malabsorption has been shown in CF-patients by several groups (135, 157, 529-531). Children aged 2 months to 9 years have high faecal losses of bile acids (531). Even during replacement therapy with pancreatic enzymes, large amounts of bile acid are still excreted. This suggests that the enterohepatic circulation of bile acids is still interrupted even during enzyme therapy. A defect of the ileal mucosal cells causing a lack of active transport mechanism is a possible reason for the bile acid malabsorption in CF-patients (135).

These alterations in the hepatobiliary system of CF-patients might affect the hepatic elimination of drugs and affect the enterohepatic recirculation.

***Renal function:*** An about 50% increased kidney weight compared to healthy subjects has been found in CF-patients (515). Additionally

glomerulomegaly was found in 34 of 34 CF-patients aged 4 months to 35 years with glomeruli being about 1.5 to 2.0 times the normal size (2). Some authors found an unchanged average glomerular filtration rate in CF-patients and healthy volunteers, whereas others found up to about 30% increased glomerular filtration rates (unit: mL/min/1.73 $m^2$) in CF-patients (182, 183, 390, 469, 526). Berg et al. (37) found no difference in renal plasma flow (measured by para-aminohippuric acid) between CF-patients and healthy volunteers. Some authors found an increased urine flow rate in CF-patients compared to healthy volunteers (167, 389).

In part, those conflicting results may arise from differences in age, body composition, and body size between the studied CF-patients and healthy volunteers. A systematic analysis of body size and body composition to scale the observed results would be important, but was often not performed by the authors. All alterations involved in the renal function can possibly lead to an increased renal clearance in CF-patients relative to healthy volunteers, which might warrant dose adjustment.

## 1.5 Allometric scaling for pharmacokinetics

Size is an inherently important variable in nature (543). Size affects different variables in different ways. This is also important for PK, especially for datasets with a wide range in body size. It is important to adequately account for body size and body composition to compare the PK in CF-patients and in healthy volunteers, since CF-patients have on average a lower total body weight but also an altered body composition relative to healthy volunteers.

***For conventional Euclidean geometry:*** The surface area A is proportional to the square of the length L of an object ($A \propto L^2$) and the volume V is proportional to the cube of L ($V \propto L^3$) for conventional Euclidean geometry. Assuming a uniform density (i. e. volume $\propto$ mass), mass M is proportional to $L^3$. Rearrangement yields: $L \propto M^{1/3} \propto A^{1/2}$ and $A \propto M^{2/3}$. Doubling the length L of an object while keeping the proportions the same will

result in a fourfold increase in surface area and in an eightfold increase in volume. These isometric relationships hold true for the conventional Euclidean geometry.

As heat produced by metabolic processes of an organism is lost through the body surface, it seems conceivable that metabolic rate (MR) would be proportional to $M^{2/3}$. Thus, the amount of heat to be dissipated would match the surface area. This relationship between metabolic rate MR and mass ($MR \propto M^{2/3}$) has been first suggested by Sarrus and Ramaeux in 1838 (cited by Brody (57)) and has been supported by Rubner in 1883 (423) who found that the metabolic rate of resting dogs was proportional to their surface area.

***Allometric scaling – observations and theory:*** Kleiber (258, 259) found in 1932 that metabolic rate is proportional to mass raised to an exponent significantly greater than 2/3. An exponent of 3/4 was finally estimated which yields: $MR \propto M^{3/4}$. Kleiber's work was expanded by Benedict (34) and Brody (57) who published the famous mouse-to-elephant curve covering a mass range of more than five orders of magnitude between the smallest and the largest mammal. Nowadays, data on organisms from the smallest microbe ($\approx 10^{-13}$ g) to the largest mammals and plants ($\approx 10^{8}$ g) support an exponent of 3/4 for the relationship between metabolic rate and mass (184, 357, 540). Besides those impressive data on a mass range of 21 orders of magnitude, theoretical models (538, 539) have been derived to support an exponent of 3/4. An exponent of 3/4 is the upper limit for an "optimal" organism. Sub-optimal organisms will have slightly lower exponents (538). An "ideal" organism has a minimal internal path length for an optimal supply of resources and the largest possible effective surface area for metabolic processes (=maximizing fitness). As the evolution selected organisms which are ideal for these two criteria, the exponent 3/4 is found over a huge range of organisms in nature.

The term allometry has been used to describe systems which scale by exponents other than those for conventional Euclidean geometry. The word allometry comes from *allo metron* which means "a strange measure". There

are two assumptions of this allometric model which are important for the PK analysis within this thesis: 1) It is assumed that small and large animals (including humans) have the same density, and 2) similar organisms have to be compared (i. e. it is not allowed to compare an “adult” dog with a growing child who both have a total body weight of 10 kg). If those assumptions are not met, additional “correction terms” may need to be incorporated into the model.

***Effect of allometric scaling on PK:*** Allometric scaling has an important effect on the elimination of drugs. Clearance is the most important PK parameter and describes the relationship between the drug concentration (e. g. in the central compartment) and the rate of drug elimination. Clearance (CL) is proportional to mass with an exponent of 3/4 ($CL \propto M^{3/4}$). This has also been confirmed experimentally (202), although there is an ongoing debate whether the exact exponent is 3/4 or 2/3 ($CL \propto M^{2/3}$) (537, 543). Importantly, both models suggest that clearance should not be divided by total body weight, as this would erroneously assume an exponent of 1.0 ($CL \propto M$). On the contrary, volume of distribution (V) follows the exponent of conventional Euclidean geometry and a proportionality of V and M is often found experimentally ($V \propto M$). As elimination half-life ($t_{1/2}$) is $\ln(2) \cdot V / CL$, the exponent for $t_{1/2}$ is 0.25 ($t_{1/2} \propto M^{1/4}$). Consequently, elephants will have a longer average elimination half-life than mice for the same drug and adults will have a longer elimination half-life than children who have reached the normal renal and hepatic function and body composition of adults, but are just smaller than adults. Importantly, standard allometric theory does not account for developmental changes and changes in body composition of newborns and children which are most important during the first days and months of life (14, 26, 51, 62, 168, 324, 421, 534).

With a standard body weight of 70 kg and a standard clearance ($CL_{70kg}$), volume of distribution ($V_{70kg}$), and half-life ($t_{1/2,\ 70kg}$) the following three equations describe a standard allometric model.

$$CL = CL_{70kg}\left(\frac{WT}{70kg}\right)^{\frac{3}{4}} \qquad \text{Formula 1.5-1}$$

$$V = V_{70kg}\frac{WT}{70kg} \qquad \text{Formula 1.5-2}$$

$$t_{1/2} = t_{1/2,70kg}\left(\frac{WT}{70kg}\right)^{\frac{1}{4}} \qquad \text{Formula 1.5-3}$$

These three relationships are important, if one compares the PK in two subject groups of different body size. Figure 1.5-1 shows the relationship between body size and clearance, volume of distribution, and elimination half-life for an allometric model with exponent 3/4. Volume of distribution decreases linearly with body size, when one compares a standard 70 kg subject to smaller subjects. Clearance decreases slightly less than linearly with body size. Secondary to the effect of body size on clearance and volume of distribution, the average half-life is slightly shorter in smaller subjects.

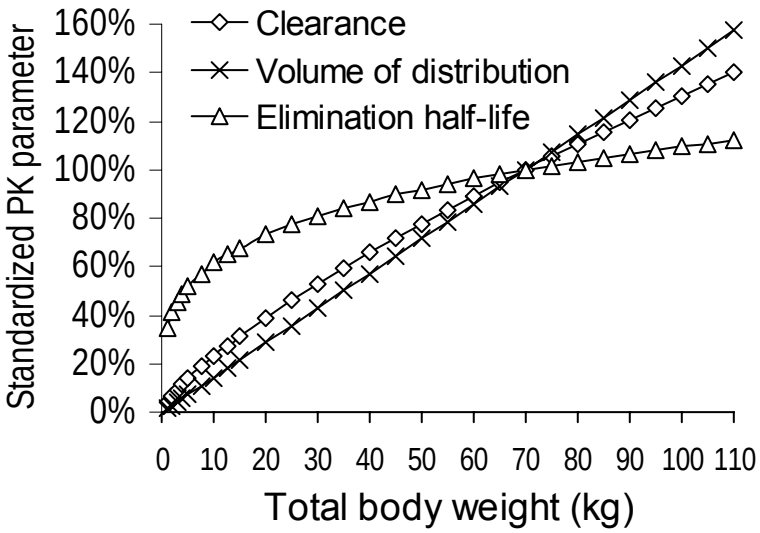


**Figure 1.5-1** Clearance, volume of distribution, and elimination half-life standardized to their value for a normal subject with WT 70 kg for an allometric model

Normalizing clearance by WT (exponent: 1.0) results in a constant ratio of clearance and volume over the whole weight range. Consequently, half-life would be predicted to be constant for all weights. As elimination half-life is

usually shorter in children than in adults, it seems more appropriate to describe clearance by the allometric model (exponent: 0.75) than by the linear model (exponent: 1.0).

## 1.6 Why are we studying antibiotics?

Patients with cystic fibrosis (CF) have a life-long need for antibiotics, because they are highly prone to respiratory tract infections secondary to structural defects in the respiratory tract. Morbidity and mortality in CF patients are primarily caused by progressive lung diseases (> 90% of deaths) (283). Therefore, CF-patients have a vital need for optimal antibiotic therapy.

*Haemophilus influenzae* and *Staphylococcus aureus* are usually the first pathogens encountered in the lungs of CF-patients. With progression of lung disease, colonization and infection by *P. aeruginosa* is often seen. About 70-80% of adults with CF are infected by *P. aeruginosa* (88). Optimal antibiotic therapy in CF-patients should address these questions:

1. Do CF-patients need much higher doses (in mg/kg WT) compared to “normal patients”, because they have a much higher size adjusted clearance than healthy volunteers?
2. Which descriptor of body size and body composition is most appropriate to select doses in CF-patients?
3. Are there reasons other than PK which might require higher doses in CF-patients?
4. Do CF-patients need altered oral doses due to a possibly altered rate or extent of absorption?
5. How can we optimize antibiotic dosage regimens against *P. aeruginosa*?
6. Can we reduce or postpone the use of antibiotics which are active against *P. aeruginosa* for treatment of *H. influenzae* and *S. aureus* to limit the emergence of resistance against *P. aeruginosa*.
7. What are the most efficacious antibiotic regimens to eradicate *P. aeruginosa* with combination therapy?

These are important questions for antibiotic treatment of CF-patients. This thesis addresses all but the last question, since we did not have appropriate data to answer the last question.

## 1.7 Why is pharmacokinetic-pharmacodynamic modeling of antibiotics important?

Some applications of PKPD models shown in chapter 1.3.3 underline that PKPD models can be used to accelerate clinical drug development and to achieve optimal antibiotic treatment for patients. Optimal clinical trial design specifically aims at an optimal allocation of resources in clinical trials. Allometric theory is important when data from various animal species are combined to predict the PK data in humans and when datasets with a wide range in body size are to be analyzed.

Besides those important applications, PKPD models for antibiotics improve our understanding of the interaction between drugs, the human body, and bacteria. It is often difficult to think about processes with multiple random components which are commonly present in population PKPD models. MCS based on those models greatly help to visualize the available data. MCS are very important to visualize modeling results and communicate them to clinicians, pharmacists, bio-analysts, sponsors, and other people involved.

## 1.8 Objectives

### 1.8.1 Overall objectives

Within this thesis, population PKPD was applied to optimize antibiotic dosage regimens based on data from CF-patients and healthy volunteers. The following general objectives were addressed:

1. Optimal dosage regimens of beta-lactams and quinolones for intravenous and oral treatment of CF-patients:
   a. Which body size descriptor should be used to select doses?

   b. Which mode of administration is most appropriate?
   c. Which antibiotic is most adequate for treatment of relevant pathogens?
2. Optimized dosage regimens of cefuroxime axetil and a meta-analysis of oral levofloxacin and ciprofloxacin all based on healthy volunteer data.
3. Studying the between occasion variability of oral amoxicillin / clavulanic acid and of piperacillin. What are the consequences for target concentration intervention and for drug development?
4. How large is the bias and uncertainty of PKPD simulations from a data analytical point of view? How much can we “trust” MCS with beta-lactams?

**Our hypotheses for those four general objectives were as follows:**

1. Optimized antibiotic dosing of CF-patients:
   a. A size descriptor which accounts for body composition and body size (like LBM) should be used to select doses in CF-patients. This might allow one to select doses and to achieve target effects more precisely in CF-patients compared to dose selection based on WT.
   b. Allometric dosing should be applied to select doses more precisely for CF-patients, since clearance does not scale linearly with body size. This can be done by use of a small reference table.
   c. Prolonged and continuous infusion of intravenous beta-lactams and more frequent dosing of oral beta-lactams (e. g. giving the same daily dose as q6h instead of q8h) may improve the probability of successful treatment significantly.
   d. Cephalosporins without activity against *P. aeruginosa* might be used to treat infections by *S. aureus* or *H. influenzae* in CF-patients.
   e. Monotherapy of oral ciprofloxacin against *P. aeruginosa* is possibly inadequate to eradicate initial infections by this pathogen in CF-patients.
2. Administering cefuroxime axetil q8h instead of q12h might improve the chance of successful treatment significantly.
3. Between occasion variability (BOV) of oral amoxicillin / clavulanic acid and intravenous piperacillin:

a. A high between occasion variability of clavulanic acid either in clearance or extent of absorption probably causes the low probability to show bioequivalence for clavulanic acid.
b. Bioequivalence might not always assure similar PKPD profiles for beta-lactams and vice versa. Consequently, similarity of PKPD profiles should be studied in parallel to bioequivalence for beta-lactams.
c. The elimination of piperacillin might be saturable. A low BOV for piperacillin might support the use of target concentration intervention.

4. Assuring the predictive performance of a population PK model is vital for MCS with beta-lactams. Uncertainty in PK and PD must be considered to compare the PKPD profiles of various beta-lactams statistically.

### 1.8.2 Pharmacokinetic and pharmacodynamic comparison of patients with cystic fibrosis and healthy volunteers

We performed a meta-analytical population PKPD analysis with data on intravenous and oral beta-lactams and quinolones with these objectives:

1. Do CF-patients have an altered drug disposition compared to healthy volunteers after accounting for body size and body composition?
2. Which body size descriptor should be used for dose selection?
3. Do CF-patients have an altered rate or extent of absorption?
4. Which dosage regimens provide optimized probabilities of successful treatment in CF-patients?
5. Does oral ciprofloxacin monotherapy achieve appropriate probabilities of target attainment against *P. aeruginosa* in CF-patients?
6. Should we account for allometric theory for dose selection in CF-patients? Do CF-patients require “higher” doses compared to healthy volunteers, because CF-patients are on average smaller?
7. Do CF-patients require higher doses for reasons other than PK?

### 1.8.3 Selection of pharmacokinetic-pharmacodynamic breakpoints for oral antibiotics – consequences for therapy

Our objectives were to predict the highest MIC with a high probability of successful treatment for cefuroxime axetil, oral ciprofloxacin, and oral levofloxacin. We studied the possibly saturable rate of absorption for cefuroxime axetil and assessed the advantages of three times daily dosing compared to twice daily dosing for this drug. We compared the probability of successful treatment of immediate and extended release ciprofloxacin and immediate release levofloxacin by a population PKPD meta-analysis for treatment of infections caused by *S. pneumoniae*, *P. aeruginosa*, and *S. aureus*. Additionally, we explored and discussed possible implications for selection of resistant mutants for ciprofloxacin and levofloxacin.

### 1.8.4 The importance of between occasion variability for drug development and for optimized dosage regimens

Therapeutic drug monitoring and target concentration intervention can only be successfully applied, if the variability e. g. in clearance between one drug administration and the next is smaller than the safe and effective variability (194, 195) of the respective drug.

We therefore studied the sources of between occasion variability (BOV) for oral amoxicillin / clavulanic acid and for piperacillin. A high BOV in the absorption or disposition of clavulanic acid may also require large sample sizes (>50 subjects) in bioequivalence trials. Improvements in the pharmaceutical formulation might reduce the high BOV in the absorption e. g. of clavulanic acid. We assessed the effect of BOV in the absorption and disposition parameters on the chance to show bioequivalence and studied, if bioequivalence guarantees similarity in the PKPD profile for amoxicillin.

### 1.8.5 Bias and uncertainty of Monte Carlo simulations with beta-lactams

Since its first application for anti-infectives in 1998 (113), MCS has become a very popular technique in this field. Several methods of MCS are being applied and the MCS results of some of those methods might yield biased results. Additionally, the uncertainty of the results of a MCS for beta-lactams has not yet been assessed. Therefore, we studied the bias and uncertainty of various methods for MCS from a data analytical point of view. Additionally, we critically discussed the uncertainty which arises from assumptions being made for a MCS which can not easily be tested by a simulation estimation study. Our results may have significant consequences for the majority of MCS which have been published on beta-lactams.

## 1.9 What was contributed by the author of this thesis

### 1.9.1 Overview

The studies described within this thesis have been planned, performed, and analyzed by many people. The contributions of various people are described in this chapter and in the acknowledgement. In brief, the pharmacometric data analyses and simulations were performed by the author of this thesis. These population PK analyses and MCS required model development for 16 antibiotics. The study objectives and the number of analyses required a substantial amount of programming by the author of this thesis. The methods of population PK analysis and MCS were developed during the last 30 years and the general methods used in this thesis were applied by other pharmacometricians for antibiotics and other drugs.

### 1.9.2 Development and application of new techniques

***Population PK analyses and MCS with antibiotics:*** The MCS technique has first been applied to anti-infectives in 1998 by Prof. Dr. George

Drusano and this technique became increasingly popular since then. However, MCS based on full population PK models are currently only performed by a few pharmacometricians in the field of anti-infectives (probably less than 20 people from academia worldwide on a full-time basis).

There is no standard software package which does a population PK analysis, MCS, and evaluation of the simulation results. There is especially no standard software package which can run MCS at an appreciable rate as was required for the objectives in this thesis. Such an interface for high-throughput MCS for antibiotics was programmed by the author of this thesis. Importantly, these programs used to run MCS allow one to run MCS for subjects with a specific set of covariates (e. g. a specific renal function and a specific body size). Covariate specific MCS have rarely been reported in literature for antibiotics, although covariates might be very important for MCS.

***Visual predictive checks (VPCs):*** There is currently no consensus on the most appropriate method to qualify a population PK model for its applications. The method of qualification depends on the applications of the model. Our primary application was simulation of concentration time profiles. A set of programs was developed by the author of this thesis under the supervision of Prof. Dr. Nick Holford which can run VPCs automatically for all models of interest. The exhaustive application of VPCs in this thesis was the basis for qualifying our population PK models for MCS. VPCs have rarely been performed by other authors for population PK models in literature and have to the best of my knowledge not yet been applied for antibiotics.

***Optimized dosage regimens for beta-lactams:*** Continuous infusion has been proposed as an optimized dosage regimen for beta-lactams by several authors and some authors proposed prolonged infusion to reduce the duration of infusion and to gain more flexibility for the patient. However, the optimal duration of infusion has not yet been systematically assessed via MCS. The author of this thesis performed such an analysis under the supervision of Prof. Dr. George Drusano. Additionally, possible advantages of a new dosage regimen, a loading dose to be followed by a prolonged infusion, were studied. Importantly, the loading dose is given at the beginning of each dosing interval to achieve effective concentrations as soon as possible.

***Effect of allometric theory on the PK of antibiotics:*** We performed a systematic analysis with linear and allometric models for body size in CF-patients. A few papers have been published on allometric scaling of anti-infectives between animals and humans. We are not aware of any systematic comparison of linear and allometric scaling for the PK of antibiotics in CF-patients or other patients. Allometric size models have rarely been applied for population PK analyses of antibiotics. This thesis contains the first statistical comparison (meta-analysis) of allometric and linear size models for antibiotics.

***Consequences of allometric theory on MCS with beta-lactams:*** We are not aware of any study which assessed the consequences of allometric theory on the results of MCS for antibiotics in patients with various body size. The author of this thesis performed a large series of MCS for our five intravenous beta-lactams to derive dosing guidelines for the following objective: How should the beta-lactam doses be calculated for which dosage regimen to achieve similar probabilities of successful treatment in patients of various body size? The author of this thesis developed a new equation for short-term infusion which should achieve this objective. This formula was evaluated in a series of MCS for our five intravenous beta-lactams and the consequences on optimal dose selection for intravenous beta-lactams were systematically studied. This simulation study was planned and performed by the author of this thesis.

***Uncertainty and bias of MCS with beta-lactams:*** The uncertainty and bias of MCS with beta-lactams has not yet been assessed. Therefore, it was not possible to answer the following question: “Is the probability of successful treatment for beta-lactam A significantly higher than for beta-lactam B ?” The uncertainty in the MCS results must be considered to answer this type of questions. We performed the first analysis of the uncertainty of MCS with beta-lactams (see chapter 6). Additionally, we systematically assessed the influence of model misspecification for MCS of beta-lactams. Depending on our results, this might warrant caution for interpretation of more than half of the papers on MCS with beta-lactams which have been published until beginning of 2006 (see chapter 6 for details). This simulation study was planned and performed by the author of this thesis.

### 1.9.3 Technical details and people involved

***Study design, clinical study, and bio-analysis:*** The clinical and bio-analytical part of the studies in this thesis was planned and performed by the group of Professor Dr. Fritz Sörgel, head of the Institute for Biomedical and Pharmaceutical Research – IBMP. The clinical and bio-analytical part of these studies was performed prior to initiation of this thesis and therefore the author of this thesis was not involved in these parts.

***Data transmission and raw data processing:*** The concentration time data and the demographic data of the clinical studies were entered manually or transferred electronically to the author of this thesis. Data entry and raw data checks were done by Cornelia Landersdorfer and the author of this thesis. Importantly, these raw data came in the format of clinical study reports or as electronic files in spreadsheet format. This format has to be modified considerably for a population PK analysis.

The design of the master raw data files used to generate the raw data file of each population PK analysis in this thesis was developed by Cornelia Landersdorfer and the author of this thesis. The generation of the raw data files for each population PK analysis was done by Perl scripts which were programmed, qualified, and validated by the author of this thesis. Prof. Dr. Nick Holford showed the author of this thesis how to set up raw data files for NONMEM® and how to do this efficiently and with a good flexibility.

The ability to automatically generate raw data files for NONMEM® is essential, as different versions of the same raw data file are often required for different structural PK models. If this process was not automated, the number of studies analyzed in this thesis would have been lower, as the additionally required raw data checks would have consumed a vast amount of time.

***NCA and statistics:*** The NCAs and statistical analyses of the original raw data for each study were performed by the author of this thesis with WinNonlin™ Pro. This program is a validated standard software which can run NCAs conveniently and efficiently. However, WinNonlin™ Pro is not suitable to do a NCA for thousands or millions of simulated concentration time profiles. This was required for the MCS in this thesis. These NCAs were run by Perl

scripts (primarily) and by an AWK script (some analyses). These Perl scripts were developed, qualified, and validated by the author of this thesis. The AWK script for NCA was programmed by Prof. Dr. Nick Holford. The author of this thesis modified this AWK script and qualified it for the NCA in this thesis.

***Population PK analyses and MCS:*** The population PK analyses were performed by the author of this thesis. Prof. Dr. Nick Holford taught the author of this thesis how to use NONMEM® and how to develop a population PK analysis plan for specific objectives. The population PK analysis and simulations of the amoxicillin/clavulanic acid study and of the piperacillin study (see chapter 5.2 and chapter 5.3) were performed by the author of this thesis under the supervision and guidance of Prof. Dr. Nick Holford. The population PK analysis plan of the CF-studies (see chapter 3.3 and chapter 3.4) and the associated meta-analysis (see chapter 3.5) were proposed by the author of this thesis and the analyses were performed under the supervision of Prof. Dr. Stephen Duffull. Prof. Dr. George Drusano reviewed and revised the MCS of the CF-studies and gave very helpful comments on the reporting and interpretation of the results (see chapter 3.3 and chapter 3.4).

NONMEM® was used as a robust and flexible population PK software. Standard structural PK models are implemented in NONMEM®. However, each NONMEM® model requires that the user programs the parameter variability model and error model in combination with the structural model in a format similar to FORTRAN. Nonlinear PK models have to be programmed by the user. NONMEM® does not provide the required graphical output for model diagnostics. The author of this thesis wrote a program which automatically generates these plots, some diagnostic statistics, and report tables.

***Reporting:*** All literature searches and preparation of the draft manuscripts, draft posters, and draft oral presentations were done by the author of this thesis. These manuscripts, posters, and oral presentations gained greatly from the revisions and guidance of Prof. Dr. George Drusano, Prof. Dr. Nick Holford, Prof. Dr. Stephen Duffull, and Prof. Dr. Fritz Sörgel. This thesis was revised by Prof. Dr. Ulrike Holzgrabe and Prof. Dr. Fritz Sörgel and improved very much from their comments and revisions.

# 2 Materials and methods

## 2.1 Study design

We had data from ten PK studies in CF-patients. Each study included a healthy volunteer control group. The studies were single dose, single-center, open, parallel group studies. The only exception was the pefloxacin study which was a single center, open, randomized, two-way crossover.

The study on cefuroxime axetil was a single dose, single-center study. Our data on ciprofloxacin and levofloxacin included data from three single dose, single-center, open, randomized, two-way crossover studies. Crossover study 1 compared 1000 mg extended release (XR) ciprofloxacin to 500 mg immediate release (IR) levofloxacin, crossover study 2 compared 500 mg IR ciprofloxacin to 500 mg IR levofloxacin, and crossover study 3 compared 500 mg IR ciprofloxacin to another comparator drug (data not shown).

The amoxicillin/clavulanic acid study and the piperacillin study were replicate dose studies in healthy volunteers with the same formulation being administered twice (amoxicillin/clavulanic acid study) or five times (piperacillin study) at subsequent study periods (occasions).

## 2.2 Study participants

Subjects participated in the study after they had given their written informed consent. The subjects' health status was assessed by physical examination, electrocardiography and laboratory tests including urine analysis and screening for drugs of abuse. Consumption of alcohol, methylxanthines, and tobacco in any form or of other medication (including antibiotics) was forbidden from at least 24 h before study drug administration until the last sample of the respective study period. Consumption of grapefruit products was forbidden from 7 days before the first dose until end of follow-up. For the studies with oral treatment, CF-patients abstained from taking pancreatic enzymes as supplement therapy from at least 10 h prior to until 4 h post study drug administration, except for the fleroxacin study in which the CF-patients

continued intake of pancreatic enzymes, multivitamins, and any other medications required for treatment of their disease.

The subjects fasted overnight and received standardized food on the day of study drug administration, if not otherwise indicated. In the studies with CF-patients, the food served included a standard breakfast (at 1h post dose), a standard lunch (at 4h to 6h post dose), and a standardized dinner or snack (for studies with blood samples over more than 12 h). Sufficient fluid intake of mineral water was assured during the study. All volunteers were closely observed by physicians for the occurrence of adverse events during the period of drug administration. The study protocols had been approved by the local ethics committee. All studies were performed following the Declaration of Helsinki and relevant guidelines from regulatory authorities.

## 2.3 Drug administration

All study drug administrations were in the fasting state. Oral study drug administrations were given together with a standardized volume (range: 150 mL to 240 mL, depending on the study) of calcium poor low-carbonated mineral water at room temperature. All infusions were given intravenously. The instruments (perfusors or motor syringes, depending on the study) were checked on a daily basis by weighing defined volumes delivered by the perfusor or motor syringe.

## 2.4 Sample collection

***Blood:*** All blood samples were drawn from a forearm vein into heparinized plastic tubes. Samples were taken from the arm contralateral to the one used for drug administration for the studies with intravenous administration. Blood samples were centrifuged for about 10 min. In studies with beta-lactams, blood samples were cooled in an ice-water bath at 4°C for approximately 10 minutes, and then centrifuged immediately at about 3600 rotations/min at 4°C for 10 min.

***Urine:*** Urine samples were stored at 4°C during the collection period of the beta-lactam studies. The pH and amount of urine were measured for each urine sample. After shaking the samples, aliquots were taken, immediately frozen and stored at -70°C (beta-lactams) or -20°C (quinolones) until analysis.

***Storage:*** Samples from quinolone studies were frozen and stored at -20°C until analysis and samples from beta-lactam studies were frozen and stored at -70°C until analysis. The amoxicillin/clavulanic acid samples were frozen on dry ice and stored at -70°C until analysis due to the instability of clavulanic acid (and amoxicillin). Quinolone samples were protected from sunlight throughout sample preparation and bio-analysis to prevent degradation of the study drugs due to daylight exposure.

## 2.5 Quantification of drug concentrations

Drug concentrations in plasma and urine were determined by reversed phase high performance liquid chromatography (HPLC) with UV (HPLC-UV) or fluorescence (HPLC-Fluo) detection for most studies described in this thesis. Amoxicillin, clavulanic acid and cefuroxime were quantified by HPLC coupled with a tandem mass spectrometer (LC-MS/MS).

As the bio-analysis was not performed by the author of this thesis, bio-analytical assays and sample analysis are described in brief in the individual chapters of each publication. All assays included an internal standard and the bio-analysis was in accordance to the bio-analytical guidelines

## 2.6 Pharmacokinetic calculations

### 2.6.1 Non-compartmental analysis

Non-compartmental analysis (NCA) is the most commonly applied standard technique for PK analysis of datasets with frequent plasma concentrations (observations) for each profile. NCA relies on fewer assumptions than compartmental modeling, but is not as powerful as the latter

(see Table 1.1-1, page 6). NCA requires very little computation time and the terminal half-life is the only PK parameter which is estimated. Therefore, the methods used for NCA are usually well comparable between authors.

The maximal observed plasma concentration (Cmax) and its timing (tmax) are read directly from the plasma concentration time raw data. The terminal half-life ($t_{1/2}$) is determined by the slope ($-\lambda_z$) of the terminal phase of the plasma concentration time profile on semi-logarithmic scale (see Figure 2.6-1). The last three to six plasma concentrations are usually used to determine the terminal phase. The following formula is used to calculate $t_{1/2}$:

$$t_{1/2} = \frac{\ln(2)}{\lambda_z}$$ Formula 2.6-1

The area under the plasma concentration time curve is determined by the trapezoidal method. The plasma concentration time profile is usually linearly (or log-linearly) interpolated between two observations ("i" denotes the $i^{th}$ observation, see also Figure 2.6-2).

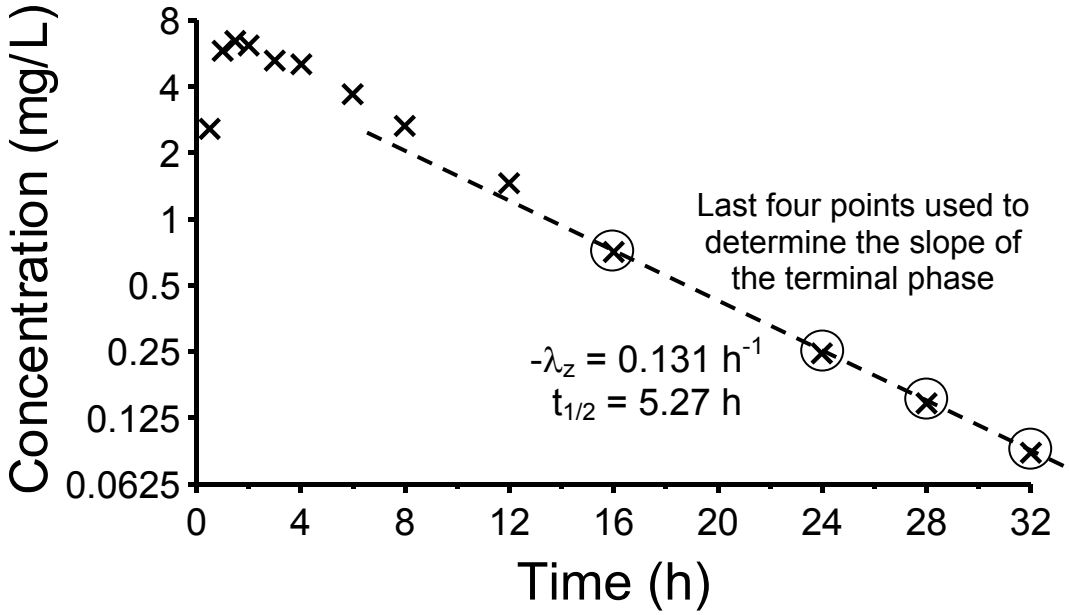


**Figure 2.6-1** Determination of terminal half-life

*Formula for linear interpolation:*

$$AUC_i^{i+1} = \Delta t \cdot \frac{C_i + C_{i+1}}{2} = (t_{i+1} - t_i) \cdot \frac{C_i + C_{i+1}}{2}$$ Formula 2.6-2

*Formula for logarithmic interpolation:*

$$AUC_i^{i+1} = \Delta t \cdot \frac{C_{i+1} - C_i}{\ln\left(\frac{C_{i+1}}{C_i}\right)}$$ Formula 2.6-3

We used the “linear-up log-down” method in WinNonlin™. This means that linear interpolation is used for $C_i \leq C_{i+1}$ and log-linear interpolation is used for $C_i > C_{i+1}$. The area under the curve from time zero to the last quantifiable concentration is calculated as the sum of these trapezoidals:

$$AUC_{0\text{-last}} = \sum_i AUC_i^{i+1}$$ Formula 2.6-4

The area under the curve from the last quantifiable concentration ($C_{last}$) to time infinity ($AUC_{last\text{-}\infty}$) is extrapolated by the following formula:

$$AUC_{last-\infty} = \frac{C_{last}}{\lambda_z}$$ Formula 2.6-5

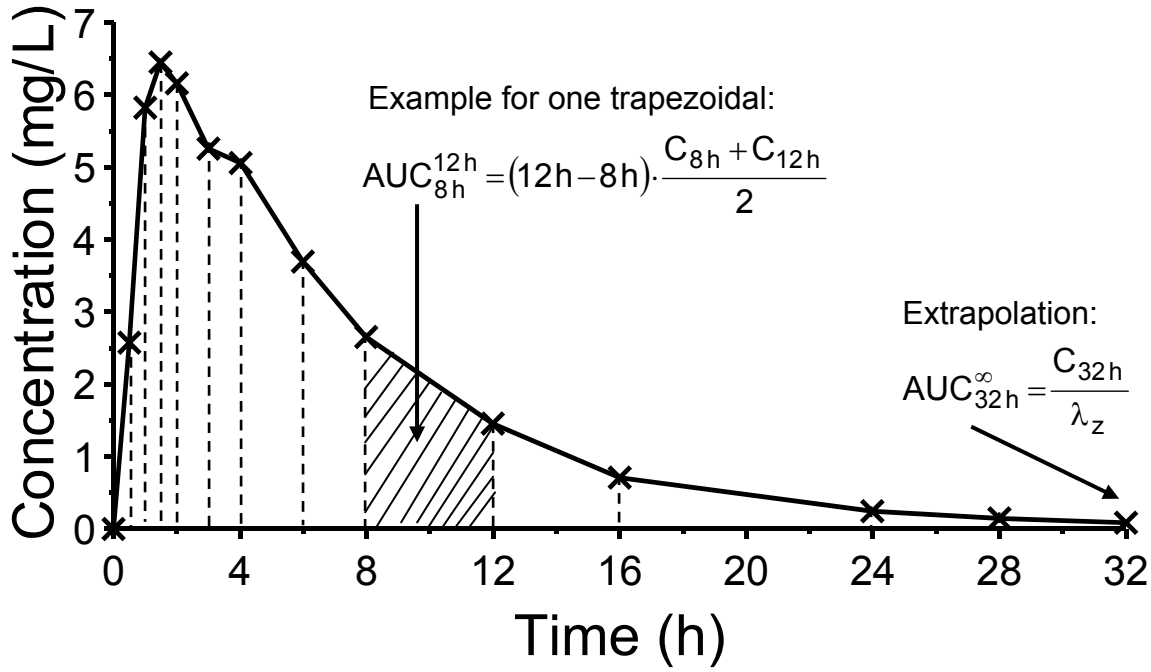


**Figure 2.6-2** Determination of the area under the curve (AUC) by linear interpolation between observations

The area under the curve from time zero to infinity ($AUC_{0-\infty}$) is calculated as follows:

$$AUC_{0-\infty} = AUC_{0-last} + AUC_{last-\infty}$$ Formula 2.6-6

Total clearance ($CL_T$), renal clearance ($CL_R$), and nonrenal clearance ($CL_{NR}$) after a single intravenous dose are calculated as follows:

$$CL_T = \frac{Dose}{AUC_{0-\infty}}$$ Formula 2.6-7

$$CL_R = \frac{\text{Amount excreted unchanged in urine until time } T_{urine}}{AUC_{0-Turine} \text{ in plasma}}$$ Formula 2.6-8

$$CL_{NR} = CL_T - CL_R$$ Formula 2.6-9

For oral administration, the formulas for the apparent total clearance ($CL_T/F$) and the apparent nonrenal clearance ($CL_{NR}/F$) are (F denotes the extent of absorption, the formula for $CL_R$ is the same as for iv administration):

$$\frac{CL_T}{F} = \frac{Dose}{AUC_{0-\infty}}$$ Formula 2.6-10

$$\frac{CL_{NR}}{F} = \frac{CL_T}{F} - CL_R$$ Formula 2.6-11

The volume of distribution during the terminal phase for intravenous administration (Vz) and the apparent volume of distribution during the terminal phase for oral administration (Vz/F) are calculated as follows:

$$Vz = \frac{CL_T}{\lambda_z}$$ Formula 2.6-12

$$\frac{Vz}{F} = \frac{CL_T}{F \cdot \lambda_z}$$ Formula 2.6-13

The mean residence time (MRT) is the average time which a drug molecule stays within the body (excluding urine and GI tract) after an intravenous administration. The MRT is the ratio of the Area Under the first Moment plasma Concentration time curve ($AUMC_{0-\infty}$, see formula below) and the $AUC_{0-\infty}$ ($T_{inf}$: duration of infusion, $T_{inf}/2$ is the mean input time, MIT):

$$MRT(iv) = \frac{AUMC_{0-\infty}}{AUC_{0-\infty}} - \frac{T_{inf}}{2}$$ Formula 2.6-14

The same formula for oral administration yields the mean body residence time (MBRT) which is the sum of the MIT and the MRT:

$$MBRT(oral) = MIT + MRT = \frac{AUMC_{0-\infty}}{AUC_{0-\infty}}$$ Formula 2.6-15

The AUMC is calculated by linear (or log-linear) interpolation between plasma concentration time points:

*Formula for linear interpolation:*

$$AUMC_i^{i+1} = \Delta t \cdot \frac{t_i \cdot C_i + t_{i+1} \cdot C_{i+1}}{2}$$ Formula 2.6-16

*Formula for logarithmic interpolation:*

$$AUMC_i^{i+1} = \Delta t \cdot \frac{t_{i+1} \cdot C_{i+1} - t_i \cdot C_i}{\ln\left(\frac{C_{i+1}}{C_i}\right)} - \Delta t^2 \cdot \frac{C_{i+1} - C_i}{\ln\left(\frac{C_{i+1}}{C_i}\right)}$$ Formula 2.6-17

Summing up the interpolated AUMCs yields $AUMC_{0\text{-last}}$ and extrapolation to time infinity yields $AUMC_{0\text{-}\infty}$:

$$AUMC_{0\text{-last}} = \sum_i AUMC_i^{i+1}$$ Formula 2.6-18

$$AUMC_{0\text{-}\infty} = AUMC_{0-\text{last}} + \frac{C_{\text{last}} \cdot t_{\text{last}} \cdot t_{1/2}}{\ln(2)} + \frac{C_{\text{last}} \cdot (t_{1/2})^2}{[\ln(2)]^2}$$ Formula 2.6-19

The volume of distribution at steady-state (Vss) is a more reliable measure for the volume of distribution compared to Vz as discussed by Gobburu and Holford (153). Vss is calculated based on the whole plasma concentration time profile. Vss is often less variable than Vz, because the uncertainty in the estimation of terminal half-life directly translates into uncertainty in Vz. Vss is calculated as follows:

$$Vss = MRT_{iv} \cdot CL_T$$ Formula 2.6-20

To calculate Vss after oral administration, a correction procedure is required to subtract the MIT from the MBRT, since the MRT after intravenous administration is required to calculate Vss.

### 2.6.2 Population pharmacokinetics

Population PK tries to describe and explain the variability in the observations (e. g. plasma concentration time data). Patient specific factors are used to reduce the random (unexplained) between patients variability to improve predictions for future patients. A population PK model is a nonlinear mixed-effects model, as it contains fixed and random effects. Figure 2.6-3 shows the four components of a population PK model.

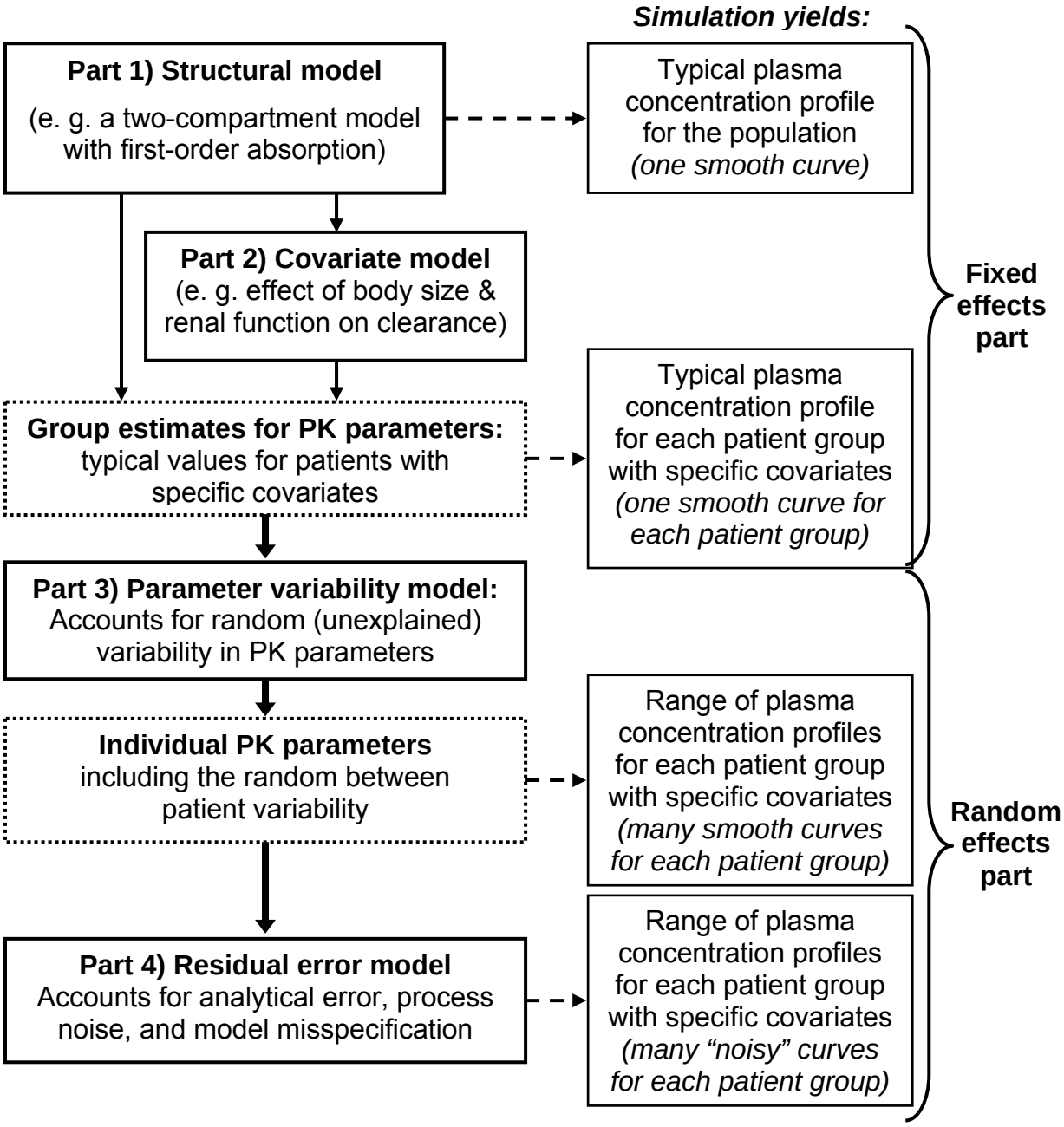


**Figure 2.6-3** Schematic diagram of a population PK model

#### 2.6.2.1 Structural model

The structural model is the first part of a population PK model (see Figure 2.6-3). It defines the structure of the PK processes which define the movement of drug in the body. The structural model belongs to the fixed-effects part of the population PK model. One-, two-, or three-compartment models are commonly used. The number of compartments required to describe the PK of a drug appropriately depends on the physicochemical properties of the drug, the rate of drug input, and the sampling schedule. In general, two- or three-compartment models tend to be more often required, if the drug input is fast (e. g. short-term infusion or rapid oral absorption) and if frequent samples, especially within the first two hours after dosing, are drawn. One-compartment models are often adequate, if the drug input is slow or if there are less frequent samples within the first hours after dosing.

We used two-compartment models (excluding the compartment for the GI tract) for most of our drugs. We used a three- or a one-compartment model for some drugs. The drug input for intravenous infusions was described as time delimited zero-order input process (see Figure 2.6-4). The oral absorption was modeled as first-order absorption from the GI tract into the central compartment including a lag-time for oral drug absorption (see Figure 2.6-5). The GI tract and the urine compartment describe the amount of drug, whereas the central and the peripheral compartment describe the drug concentrations.

The drug in the central compartment is in a dynamic equilibrium with the peripheral compartment. The three parameters which describe this equilibrium are the volume of the central (V1) and of the peripheral compartment (V2) and the intercompartmental clearance (CLic). It is assumed that there is no elimination from the peripheral compartment. The drug elimination from the central compartment is described by the renal clearance ($CL_R$) and nonrenal clearance ($CL_{NR}$). The sum of $CL_R$ and $CL_{NR}$ equals the total clearance. As the transport processes in this model follow first-order kinetics, it is assumed that there is no (or only negligible) saturation of those processes at therapeutic doses.

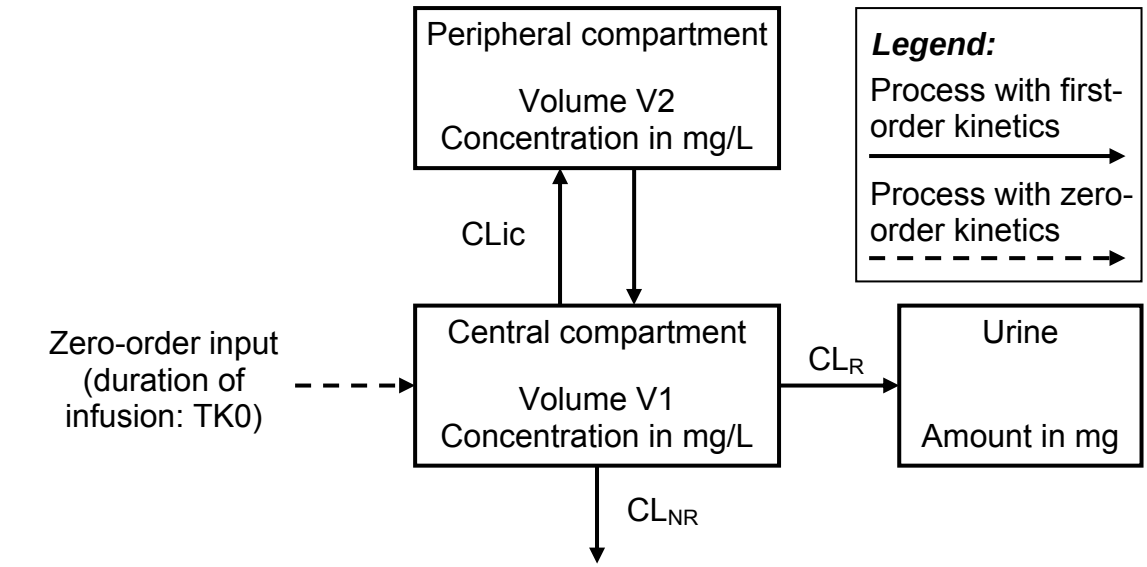


**Figure 2.6-4** Two-compartment model with time delimited zero-order input to describe an intravenous infusion

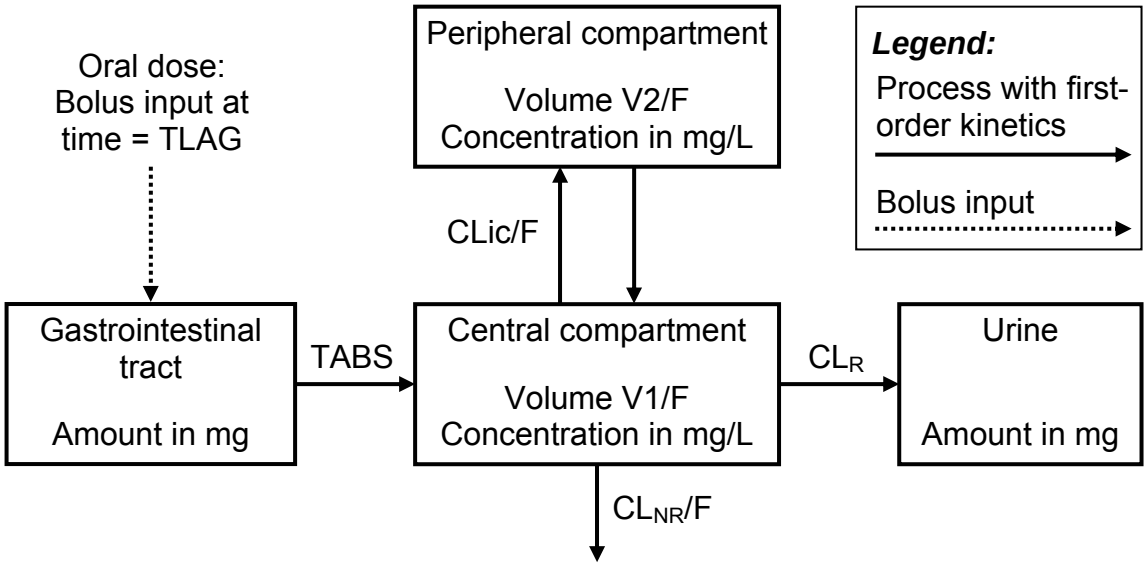


**Figure 2.6-5** Two-compartment model with first-order oral absorption

TK0: Duration of infusion (unit: min), TLAG: lag time of absorption (unit: min), TABS: half-life of absorption (unit: min), F: extent of absorption (unit: none), V1: volume of distribution for the central compartment (unit: L), V2: volume of distribution for the peripheral compartment (unit: L), CLic: intercompartmental clearance between the central and the peripheral compartment (unit: L/h), $CL_R$: renal clearance (unit: L/h), and $CL_{NR}$: nonrenal clearance (unit: L/h). V1/F, V2/F, CLic/F, and $CL_{NR}$/F denote the apparent volumes or apparent clearances after oral administration, as F is mathematically not identifiable based only on data after oral dosing.

A one-compartment model can be derived from the models shown in Figure 2.6-4 and Figure 2.6-5 by removing the peripheral compartment. A three-compartment model contains two peripheral compartments and has three volume of distributions (V1, V2, and V3) and two intercompartmental clearances ($CLic_{shallow}$ and $CLic_{deep}$). The shallow peripheral compartment is in a fast equilibrium with the central compartment and the deep peripheral compartment is in a slower equilibrium with the central compartment. The PK parameters of a three-compartment model are therefore as follows: V1: volume of distribution for the central compartment, V2: volume of distribution for the shallow peripheral compartment, V3: volume of distribution for the deep peripheral compartment, $CLic_{shallow}$: intercompartmental clearance between the central and the shallow peripheral compartment, and $CLic_{deep}$: intercompartmental clearance between the central and the deep peripheral compartment. The total, renal, and nonrenal clearances are defined in the same way for a one-, two-, and three-compartment model.

#### 2.6.2.2 Covariate model

The covariate model belongs to the fixed-effects part of a population PK model, as it contains no random components. The covariate model describes the effect of covariates on the PK parameters of the structural model. Some examples for those effects are:

1) Effect of renal function (e. g. measured by creatinine clearance) on renal clearance.
2) Effect of body size (and body composition) on volume of distribution and clearance.
3) Effect of smoking, alcohol intake, sex, or race on hepatic function.
4) Effect of disease state on clearance or volume of distribution.
5) Effect of nutritional state (or body composition) on rate or extent of absorption.

***Purpose of the covariate model:*** The PK parameters have a total between subject variability (BSV) in the studied population. The total BSV can be split into a predictable component ($BSV_{Predictable}$) and a random component ($BSV_{Random}$) by use of the covariate model:

$$BSV_{Total} = BSV_{Predictable} + BSV_{Random} \qquad \text{Formula 2.6-21}$$

$BSV_{Random}$ represents the unexplained fraction of $BSV_{Total}$. The covariate model seeks to reduce $BSV_{Random}$ as much as possible, because a low $BSV_{Random}$ allows one to predict the individual PK parameters more precisely. If the individual PK parameters can be predicted more precisely based on the patient's covariates, target concentrations, target effects, and therapeutic response can be optimized more precisely for this patient. The ability to simultaneously account for multiple covariates and to account for time dependent covariates is a powerful feature of population PK. Such a covariate model might be a prerequisite for successful application of therapeutic drug monitoring and target concentration intervention.

***Typical values:*** If a PK parameter is affected by one (or more) covariate(s), there is a specific group estimate for this PK parameter for a specific value of this (these) covariate(s). This group estimate is called the typical value. Examples are a) the typical volume of distribution for a subject with 70 kg total body weight (WT), b) the typical renal clearance for a subject with normal renal function (creatinine clearance 7.2 L/h) and 70 kg WT, and c) the typical total clearance of a CF-patient and a healthy volunteer both with an lean body mass (LBM) of 53 kg. There are two types of covariates, continuous and categorical covariates. Example a) and b) here show the effect of continuous covariates, whereas example c) shows the influence of a categorical covariate.

***Covariate model building:*** It needs to be decided by the pharmacometrician, which covariate influences which PK parameter. The functional form for the influence of a covariate on the structural parameter also needs to be chosen. The effect of covariates on renal clearance or volume of distribution is commonly included in a population PK model, whereas other PK

parameters like the parameters for oral absorption often lack a clear relationship with covariates. As shown in Figure 2.6-3, some PK parameters of the structural model may be affected by covariates, whereas others are not.

If a PK dataset comprises less than 50 subjects, it is important to rely on prior knowledge for covariate model building. For small datasets, the effect of a covariate on a PK parameter might occur just by chance and one might erroneously conclude such a relationship to be true (411).

***Effect of body size on clearance and volume of distribution:*** We used WT to describe body size of normal healthy volunteers. We considered other body size descriptors for our studies in CF-patients and healthy volunteers to account for the altered body composition of CF-patients. The details on those models are described in chapter 3.2.

We considered linear and allometric scaling (193, 538, 539) of clearance and volume of distribution by body size. We will use WT to describe body size in the following equations. $F_{Size,V,i}$ and $F_{Size,CL,i}$ are the fractional changes in volume of distribution and clearance for the $i^{th}$ subject (with $WT_i$) standardized to a weight $WT_{STD}$ of 70 kg.

*Linear scaling of volume of distribution and clearance:*

$$F_{Size,V,i} = \frac{WT_i}{WT_{STD}} \qquad \text{Formula 2.6-22}$$

$$F_{Size,CL,i} = \frac{WT_i}{WT_{STD}} \qquad \text{Formula 2.6-23}$$

Our allometric model assumes that volume of distribution scales linearly (allometric exponent 1.0) with body size, whereas clearance scales slightly less than linearly with body size (allometric exponent 0.75). The allometric exponent was fixed to 1.0 for all volume terms and fixed to 0.75 for all clearance terms.

*Allometric scaling of volume of distribution and clearance:*

$$F_{Size,V,i} = \frac{WT_i}{WT_{STD}} \qquad \text{Formula 2.6-24}$$

$$F_{Size,CL,i} = \left( \frac{WT_i}{WT_{STD}} \right)^{0.75} \qquad \text{Formula 2.6-25}$$

***Effect of renal function on renal clearance:*** We used renal function as a covariate on renal clearance for our amoxicillin/clavulanic acid study and for our carumonam (a monobactam which is currently only marketed in Japan) study. This allowed us to estimate renal clearance of amoxicillin and clavulanic acid without urine data by our population PK model. As we applied this covariate relationship only in this study, the details are described in chapter 3.3.3.3 (see pages 131ff, for details).

***Effect of disease on clearance and volume of distribution:*** We determined group specific estimates for renal and nonrenal clearance and for volume of distribution in CF-patients and healthy volunteers. This was done by using cystic fibrosis as a categorical covariate for our studies in CF-patients and healthy volunteers. The details are described in chapter 3.2.

### 2.6.2.3 Parameter variability model

The parameter variability model describes the variability of PK parameters in the study population. We used parametric population PK models which means that we assumed a functional form for the distribution of PK parameters. Assuming a normal distribution of the log-transformed PK parameters is often a reasonable assumption in PK. Distributions of PK parameters tend to be skewed to the right (see Figure 2.6-6). The log-normal distribution used to simulate this distribution of half-lives had a (geometric) mean of 5.0 h and a coefficient of variation of 30%.

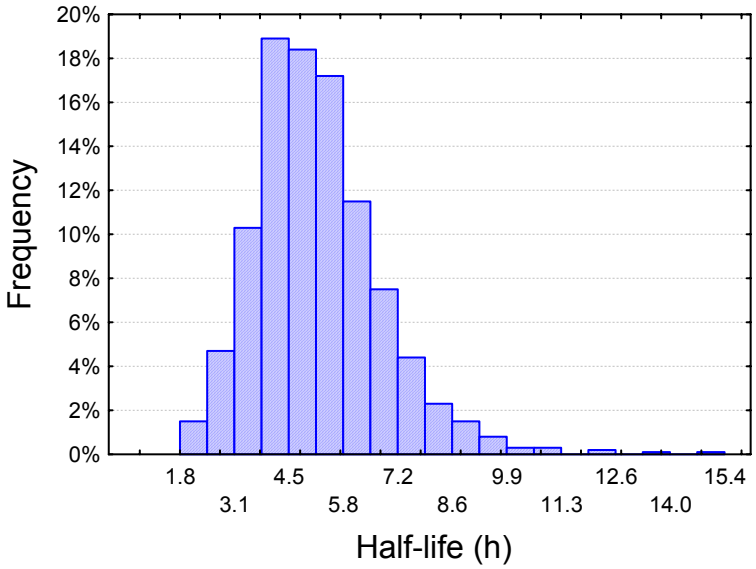


**Figure 2.6-6** Log-normal distribution of half-life (simulation example)

We estimated the BSV by assuming a log-normal distribution for the PK parameters. $\eta_{BSVi}$ is the log scale difference of the individual PK parameter estimate from its population mean for the ith subject. $\eta_{BSV}$ is assumed to be a normally distributed random variable with mean zero and standard deviation BSV. BSV was estimated as variance, but we report the square root of the estimate. We have expressed these values in the text as a percentage, because this quantity is an approximation to the apparent coefficient of variation of a normal distribution. In absence of a covariate model, renal clearance can then be described as:

$$CL_{R,i} = CL_{POP,R} \cdot \exp(\eta_{BSVCLRi}) \qquad \text{Formula 2.6-26}$$

$CL_{POP,R}$ is the population estimate for renal clearance and $CL_{Ri}$ is the individual estimate for renal clearance for the $i^{th}$ subject. We used such an exponential parameter variability model for all PK parameters except for intercompartmental clearance, unless otherwise indicated.

***Parametric parameter variability models:*** The variability of PK parameters is often correlated between pairs of PK parameters. Parametric parameter variability models describe the variability and pairwise correlation of PK parameters by a variance-covariance matrix. An example for a variance-covariance matrix is shown in Table 2.6-1 which shows the between subject

variance on log-scale. The variance-covariance matrices are symmetrical. Therefore, only the lower triangle matrix is shown.

**Table 2.6-1** Variance-covariance matrix for clearance and volume of distribution (an example)

| | BSVCL | BSVV |
|---|---|---|
| BSVCL | 0.09 | |
| BSVV | 0.081 | 0.09 |

BSVCL: Between subject variability in total clearance.

BSVV: Between subject variability in volume of distribution.

The apparent coefficient of variation is the square root of the diagonal elements (i. e. 30% for both clearance and volume of distribution in this example). The off-diagonal element is the covariance of clearance and volume of distribution. The coefficient of correlation between clearance and volume of distribution [r(CL,V)] can be calculated by the following formula:

$$r(CL,V)=\frac{Cov(CL,V)}{\sqrt{Var(CL)\cdot Var(V)}}$$ Formula 2.6-27

“Cov” denotes the covariance and “Var” the variance of the respective parameters. In this example, the coefficient of correlation is 0.9. If one simulates from this multivariate normal-distribution on log-scale, one gets the scatterplots of clearance and volume of distribution shown in Figure 2.6-7.

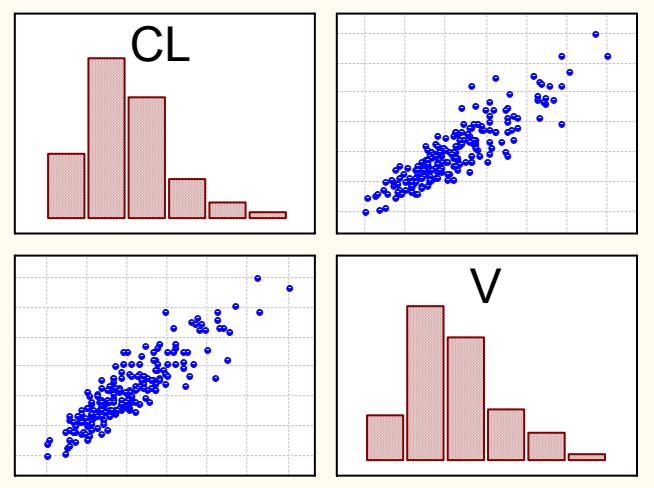


**Figure 2.6-7** Clearance and volume of distribution on linear scale for 200 subjects sampled from a multivariate log-normal distribution (a simulation example)

See Table 2.6-1 for explanation of parameters.

If one assumes a one-compartment model, the elimination half-life ($t_{1/2}$) can be derived by the following formula:

$$t_{1/2} = \frac{V \cdot \ln(2)}{CL}$$ Formula 2.6-28

The apparent coefficient of variation is 30% for clearance and volume of distribution in this simulation example. However, the coefficient of variation was only 13% for the derived elimination half-life due to the correlation between clearance and volume of distribution. Accounting for covariance terms is therefore important, especially for MCS with beta-lactams.

A real data example for a variance-covariance matrix for levofloxacin in healthy volunteers is shown in Table 2.6-2. We used a three-compartment model with first-order absorption (half-life: TABS) and a lag-time (TLAG). CL denotes the total clearance. V1 is the volume of the central compartment, V2 the volume of the shallow peripheral compartment, and V3 the volume of the deep peripheral compartment.

**Table 2.6-2** Variance-covariance matrix for levofloxacin in healthy volunteers

| | BSVCL | BSVV1 | BSVV2 | BSVV3 | BSVTABS | BSVTLAG |
|---|---|---|---|---|---|---|
| BSVCL | 0.0175 | | | | | |
| BSVV1 | -0.00604 | 0.112 | | | | |
| BSVV2 | 0.0197 | -0.172 | 0.290 | | | |
| BSVV3 | 0.0217 | 0.0237 | -0.0177 | 0.126 | | |
| BSVTABS | -0.00452 | 0.0182 | -0.0802 | 0.0547 | 0.535 | |
| BSVTLAG | -0.00686 | 0.0970 | -0.193 | -0.00637 | -0.0895 | 0.322 |
| Coefficient of variation | 13% | 33% | 54% | 35% | 73% | 57% |

BSVCL: Between subject variability in total clearance.

BSVV1: Between subject variability in volume of distribution for the central compartment.

BSVV2: Between subject variability in volume of distribution for the shallow peripheral compartment (fast equilibrium with the central compartment).

BSVV3: Between subject variability in volume of distribution for the deep peripheral compartment (slow equilibrium with the central compartment).

BSVTABS: Between subject variability in half-life of absorption.

BSVTLAG: Between subject variability in lag-time of absorption.

The correlation matrix is shown in Table 2.6-3. The coefficients of correlation for pairs of random BSV were derived as shown above for clearance and volume of distribution.

**Table 2.6-3** Correlation matrix for levofloxacin in healthy volunteers

| | BSVCL | BSVV1 | BSVV2 | BSVV3 | BSVTABS | BSVTLAG |
|---|---|---|---|---|---|---|
| BSVCL | 1 | | | | | |
| BSVV1 | -0.136 | 1 | | | | |
| BSVV2 | 0.277 | -0.954 | 1 | | | |
| BSVV3 | 0.462 | 0.200 | -0.093 | 1 | | |
| BSVTABS | -0.047 | 0.074 | -0.204 | 0.211 | 1 | |
| BSVTLAG | -0.091 | 0.511 | -0.632 | -0.032 | -0.216 | 1 |

See Table 2.6-2 for explanation of parameters.

The following scatterplots show the samples of 200 subjects whose PK parameters were simulated from this multivariate log-normal distribution (see Figure 2.6-8).

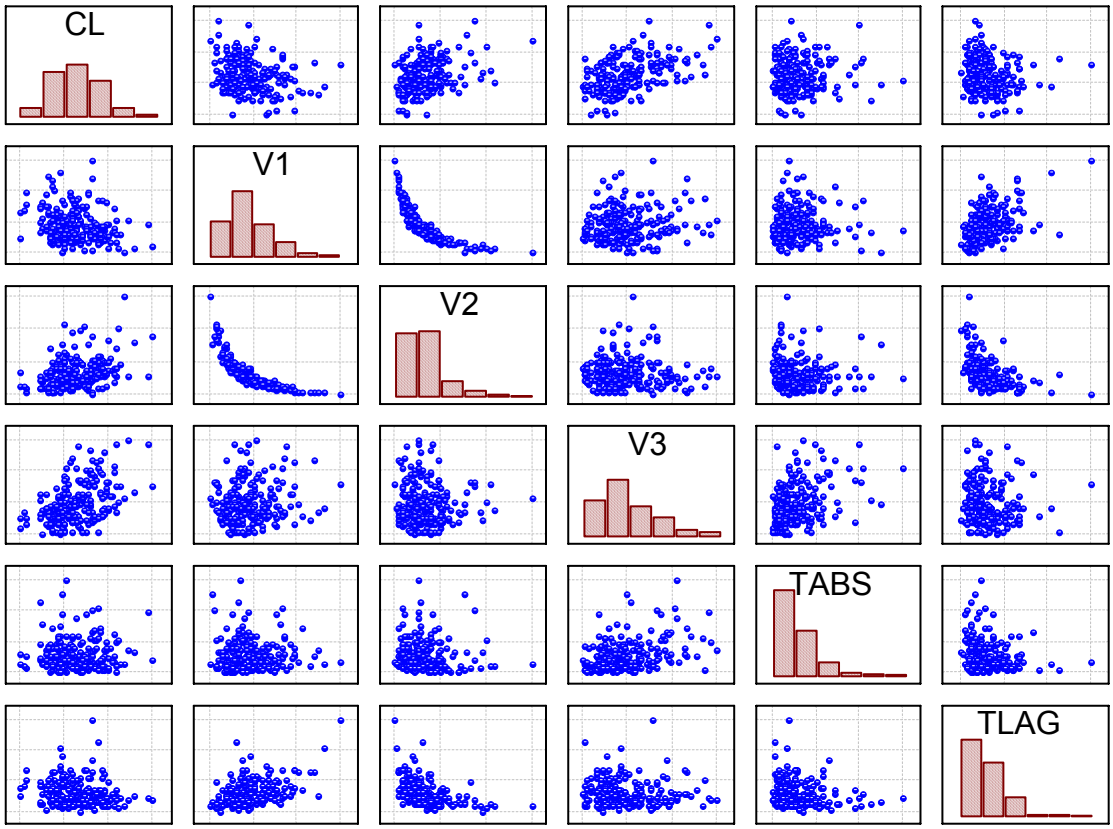


**Figure 2.6-8** PK parameters of 200 healthy volunteers on linear scale sampled from a multivariate log-normal distribution for levofloxacin

See Table 2.6-2 for explanation of parameters.

This real data example for levofloxacin shows a strong negative correlation between V1 and V2 (r = -0.954). The next highest coefficient of correlation was -0.632 between V2 and TLAG. The full variance-covariance matrix in this example contains 21 variance and covariance parameters to be estimated.

It may be difficult to estimate all those parameters for datasets with less than about 30 subjects. One option in this situation is to estimate only a subset of the full matrix. One could e. g. estimate the 4 x 4 variance-

covariance matrix with CL, V1, V2, and V3 (=10 parameters) and estimate another 2 x 2 matrix (=3 parameters) with TABS and TLAG. This yields 13 parameters in total. For even smaller datasets, one option is to estimate only the diagonal elements of the variance-covariance matrix and to assume that the off-diagonal elements are zero. This would result in 6 variance parameters to be estimated for this example.

Irrespective of the chosen parameter variability model, it is important to assure that the chosen parameter variability model is adequate to resemble the variability of the available raw data. This is especially important, if the population PK models are used for MCS, as in this thesis. The visual predictive check (VPC) described in chapter 2.6.3 is a powerful method to assure that the parameter variability model is adequate.

#### 2.6.2.4 Residual error model (residual unidentified variability)

We described the residual unidentified variability by a combined additive and proportional error model. C denotes the predicted concentration without residual error, whereas $Y_C$ is the individual prediction including a proportional ($CV_C$) and additive ($SD_C$) residual error component. The random variables $\varepsilon_{CVC}$ and $\varepsilon_{SDC}$ are normally distributed with mean zero and standard deviations $CV_C$ and $SD_C$, respectively.

$$Y_C = C*(1+\varepsilon_{CVC})+\varepsilon_{SDC} \qquad \text{Formula 2.6-29}$$

The same model for residual unidentified variability was used for the amounts excreted unchanged in urine. AU denotes the predicted amount excreted in urine without residual error, whereas $Y_{AU}$ is the individual prediction including a proportional ($CV_{AU}$) and additive ($SD_{AU}$) residual error component. The random variables $\varepsilon_{CVAU}$ and $\varepsilon_{SDAU}$ are normally distributed with mean zero and standard deviations $CV_{AU}$ and $SD_{AU}$, respectively.

$$Y_{AU} = AU*(1+\varepsilon_{CVAU})+\varepsilon_{SDAU} \qquad \text{Formula 2.6-30}$$

### 2.6.3 Model discrimination

There are various commonly applied methods for model discrimination. Most often, a criterion addresses one of the following two questions:

1) How well does the model fit to the raw data?
2) How well do the model predictions mirror the central tendency and the variability of the observed concentrations?

Most model selection criteria address the first question. The second criterion considers the predictive performance of a model which is especially important for the use of a population PK model for MCS.

***Assessing the model fit:*** NONMEM's objective function is a sensitive measure to compare the model fit of two competing population PK models. NONMEM's objective function is -2 times the log of the likelihood (plus a constant). The likelihood is the probability that the observed data come from the chosen model and its parameters. NONMEM searches the lowest possible objective function which is equivalent to searching the highest probability for the data. The model with the smallest objective function is regarded to give the best fit to the data. If two nested models had an insignificant difference in NONMEM's objective function, we chose the simpler model. The term nested means that the more complex model includes the simpler model, if the estimate for a model parameter has a specific value (most often zero). A one-compartment model is e. g. nested within a two-compartment model. If the intercompartmental clearance was estimated to be zero, there is no drug transport between the central and the peripheral compartment which results in a one-compartment model.

We used NONMEM's objective function and standard diagnostic plots (including residual analysis) to assess the model fit of our population PK models. We could show that these criteria were not as powerful as the visual predictive checks (VPCs) for model selection, as will be shown in chapter 6.2.

***Assessing the predictive performance:*** We evaluated the predictive performance of our population PK models by VPCs. We simulated the plasma (and urine) profiles for 4,000 to 10,000 virtual subjects for each competing model. We derived the median, the nonparametric 50% prediction interval

(25% to 75% percentile), and the nonparametric 80% prediction interval (10% to 90% percentile) from the predicted profiles. The prediction interval lines were then over-layed on the original raw data.

If the model described the data correctly, the median should adequately mirror the central tendency of the raw data, 50% of the observed data points should fall outside the 50% prediction interval, and 20% of the observed data points should fall outside the 80% prediction interval at each time point. We compared the median predicted concentrations and the prediction intervals with the raw data and assessed visually, whether the predicted profiles mirrored the central tendency and the variability of the raw data adequately for the respective model. An example for a VPC is shown in Figure 2.6-9.

The VPC tests whether the chosen structural and parameter variability model is adequate. A VPC is easy to interpret and visualizes the importance of model misspecification. It directly shows if the problems arise e. g. during the absorption phase or during the terminal phase. We applied the VPC to all tested models and used it as our primary model selection criterion, since we used our models extensively for simulations.

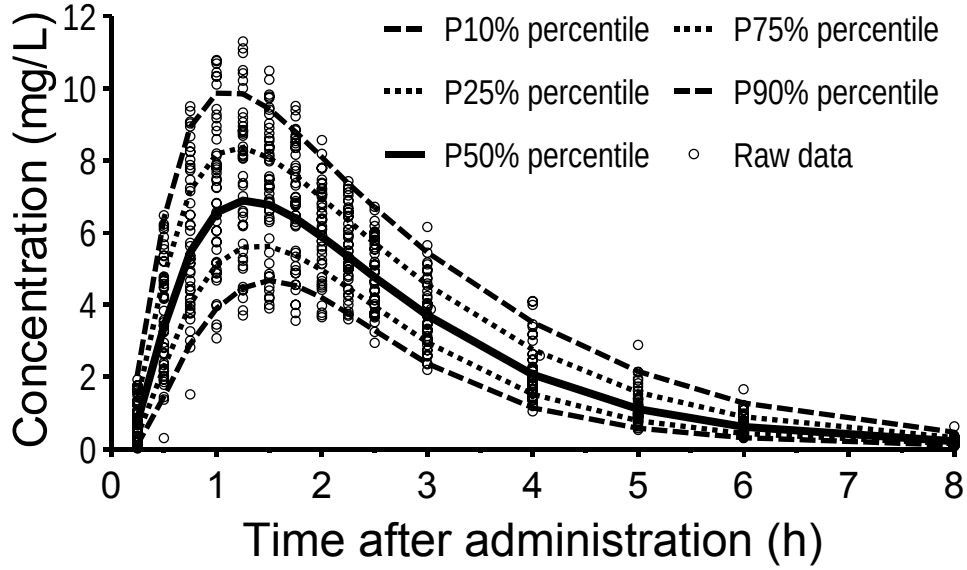


**Figure 2.6-9** VPC showing the median, 50% and 80% prediction interval of the simulated plasma concentrations

### 2.6.4 Assessing the uncertainty of pharmacokinetic parameters by non-parametric bootstrap techniques

The parameters of a population PK model are determined based on a limited amount of data. Consequently, there is always uncertainty in the estimated parameters. In general, the fewer data are available, the wider is the 90% confidence interval for a given parameter.

If one was e. g. interested in the average clearance in healthy volunteers and if there are data on two studies: Study 1 included 10 subjects and showed a clearance of 10 L/h [6-16 L/h] (average [90% confidence interval]); study 2 included 40 subjects and showed a clearance of 12 L/h [10-15 L/h]. Intuitively, one would tend to trust the results of study 2 more than study 1, because study 2 included 4 times as many subjects. It is especially important to account for the uncertainty (e. g. in average clearance), if one pools data from different studies. This was important for our meta-analysis in CF-patients and healthy volunteers.

There are various methods to determine the 90% confidence interval of a PK parameter. Some methods only yield confidence intervals for the parameters of the structural model, whereas other methods also yield confidence intervals for the BSV parameters (i. e. all elements of the variance-covariance matrix). It is important to note that these confidence intervals are often asymmetric (both on linear and on log-scale), although some parametric methods by definition yield symmetric confidence intervals.

To the best of my knowledge, non-parametric bootstrap techniques are among the most powerful methods to determine the uncertainty (e. g. in form of 90% confidence intervals) for all parameters of a population PK model. Non-parametric bootstrapping requires very few assumptions compared to other methods which assess the uncertainty of population PK parameters. Importantly, non-parametric bootstrapping makes no assumption on the form of the uncertainty distribution from which the confidence intervals are derived. This technique is easy to apply and very robust.

The only drawback of non-parametric bootstrapping is that the computation time required is about 1000 times longer (or more) than for the

estimation of the final population PK model. Modern computation power usually allows one to apply this technique for one-, two-, and three-compartment models with first-order drug disposition. If the elimination of a drug is saturable, those population PK models need to be solved by differential equations which often precludes the use of non-parametric bootstrapping due to exhaustive computation times.

***The technique of non-parametric bootstrapping:*** The technique as it was applied in this thesis is easy to implement. The general idea is to generate pseudo datasets from which the population PK model is re-estimated. If one has a raw dataset of e. g. 10 subjects, one can randomly draw new raw datasets each of 10 subjects. It is allowed to draw one subject multiple times (see Table 2.6-4).

Each of the new randomly drawn datasets is called a pseudo sample of the original dataset. We used at least 1000 pseudo-samples to assess the uncertainty of our PK parameters. The population PK model is re-estimated for each of the 1000 pseudo samples. This causes the 1000 fold increase in computation time and yields 1000 estimates for all parameters of the population PK model. The distribution of those 1000 estimates approximates the uncertainty distribution of the respective model parameter. The 5% and 95% percentile of this uncertainty distribution are the limits of the 90% confidence interval for the respective model parameter.

**Table 2.6-4** Illustration of the generation of bootstrap raw datasets to assess the uncertainty of population PK parameters

| | **Subject** | | | | | | | | | |
|---|---|---|---|---|---|---|---|---|---|---|
| **Original dataset** | 1 | 2 | 3 | 4 | 5 | 6 | 7 | 8 | 9 | 10 |
| *Bootstrap datasets* | *Random datasets each containing data from 10 subjects* | | | | | | | | | |
| Pseudo sample 1 | 1 | 2 | 4 | 4 | 7 | 7 | 7 | 8 | 10 | 10 |
| Pseudo sample 2 | 1 | 1 | 3 | 3 | 4 | 5 | 5 | 6 | 9 | 9 |
| Pseudo sample 3 | 2 | 2 | 3 | 5 | 5 | 6 | 7 | 8 | 9 | 10 |
| Pseudo sample 4 | 3 | 5 | 5 | 7 | 8 | 8 | 8 | 9 | 10 | 10 |
| ... | ... | | | | | | | | | ... |
| Pseudo sample 1000 | 1 | 1 | 5 | 5 | 6 | 6 | 6 | 8 | 8 | 8 |

There is one possibly critical assumption of non-parametric bootstrapping, especially for small raw datasets. It is assumed that the subjects in the raw dataset are representative of the whole population. If there are data on 10-20 subjects, this assumption might become critical and the results should be interpreted with some caution. However, non-parametric bootstrapping is one of the most powerful and robust techniques to directly determine the uncertainty of all parameters of a population PK model.

## 2.7 Pharmacodynamic simulations

### 2.7.1 Background

MCS with antibiotics aim at predicting the probability of successful clinical or microbiological treatment for empiric therapy. This probability depends on the antibiotic, the dosage regimen, the patient population, and the susceptibility of the organisms which cause the infection. MCS should identify dosage regimens with an optimal probability for successful treatment. Covariates like renal function and body size might be included to individualize antibiotic dosage regimens. As described in chapter 1.3 it is often assumed that the drug related response is the main determinant of successful antibiotic treatment.

As early as in the 1940s and 1950s, Eagle et al. (120) found in a mouse infection model that the shape of the concentration time profiles also affects the chance of successful treatment besides the total drug exposure. Their work was continued and expanded by the group of Craig (524) and others since the 1980s who found that the rate of bacterial killing reaches its maximum at concentrations of about 4 to 6 times the MIC of the infecting pathogen for beta-lactams. Therefore, beta-lactams show a relatively concentration independent rate of bacterial killing. The results from the groups of Eagle, Craig, and others have led to the separation between concentration-dependent and concentration independent antibiotics.

#### 2.7.1.1 Concentration-dependent and concentration-independent antibiotics

Antibiotics are often categorized into concentration-dependent and concentration-independent drugs. Quinolones and aminoglycosides belong to the group of concentration-dependent antibiotics, whereas beta-lactams belong to the group of concentration-independent antibiotics. The rate of bacterial growth and killing due to antibiotic concentrations is often described by the following equation (341) (see parameter explanation below):

$$\frac{dN}{dt} = \left( \text{growth term} - \varepsilon \frac{Conc^{Hill}}{Conc^{Hill} + EC_{50}{}^{Hill}} \right) N \qquad \text{Formula 2.7-1}$$

N denotes the number of bacteria present at time t, $\varepsilon$ is the maximum kill rate, Conc the antibiotic concentration, $EC_{50}$ the concentration at which 50% of the maximum kill rate is reached, and Hill is the Hill coefficient. The Hill coefficient defines the steepness of the concentration effect relationship and effect is the bacterial kill rate in this example. Concentration-dependent antibiotics have a lower Hill coefficient than concentration-independent antibiotics. An example with data from Mouton et al. (341) is shown in Figure 2.7-1.

The concentration axis is shown in multiples of $EC_{50}$. Tobramycin has a maximum kill rate of 13.4 $h^{-1}$ which is much larger than the maximum kill rate of 2.57 $h^{-1}$ for ceftazidime in this *in vitro* experiment. Ceftazidime reaches 92% of its maximum kill rate at a concentration of two times the $EC_{50}$, whereas tobramycin reaches only 62% of its maximum kill rate at two times the $EC_{50}$. Due to their steep concentration effect relationship, beta-lactams are called concentration-independent antibiotics. Tobramycin still shows an increase in the rate of bacterial killing between concentrations of two to ten times the $EC_{50}$. Mouton et al. (341) did not report data for quinolones for this experiment. Quinolones would be expected to have a Hill coefficient similar to tobramycin.

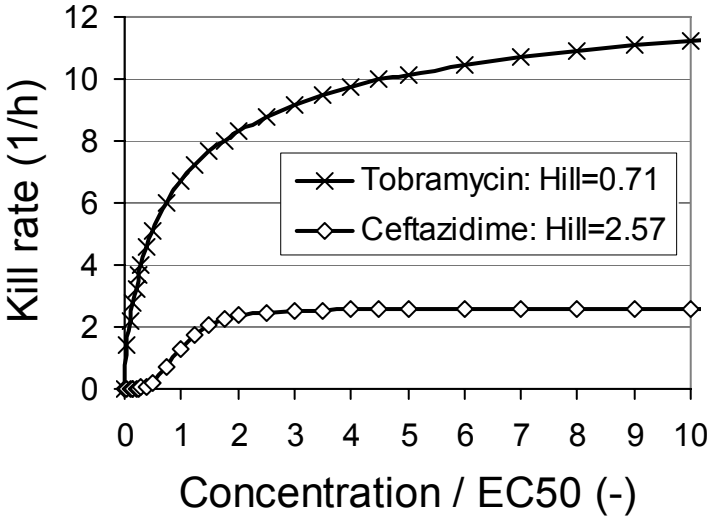


**Figure 2.7-1** Comparison of concentration-dependent killing (tobramycin) and concentration-independent killing (ceftazidime) against *P. aeruginosa*

Parameters to generate this plot from Mouton et al. (341)

#### 2.7.1.2 Pharmacokinetic-pharmacodynamic indices and targets

It is complex to predict the bacterial growth and killing over the whole time course of antibiotic therapy. Consequently, simplified PKPD statistics have been evaluated and validated to predict the chance of a successful microbiological or clinical treatment. These statistics are also called PKPD indices (334). They are based on the plasma concentration time course and the MIC of the infecting pathogen.

Different PKPD statistics were developed for concentration-dependent and concentration-independent antibiotics. As protein binding reduces the microbiological activity of antibiotics (45, 319), only free (non-protein bound) antibiotic concentration is considered to be microbiologically active (107).

The time during that the non-protein bound plasma (or serum) concentration remains above the MIC ($fT_{>MIC}$) is the PKPD statistic (84, 107) that best predicts microbiological success for beta-lactams. The $fT_{>MIC}$ should be reported as cumulative percentage of a 24h interval that the drug concentration exceeds the MIC at steady-state (334).

The rate of bacterial killing for quinolones is concentration-dependent over a wide range of concentrations. The PKPD statistic that best predicts microbiological success for quinolones (84, 107, 137) is the ratio of the free area under the concentration-time curve over 24h to the MIC (*f*AUC/MIC). An example for calculation of $fT_{>MIC}$ and *f*AUC/MIC is shown in Figure 2.7-2.

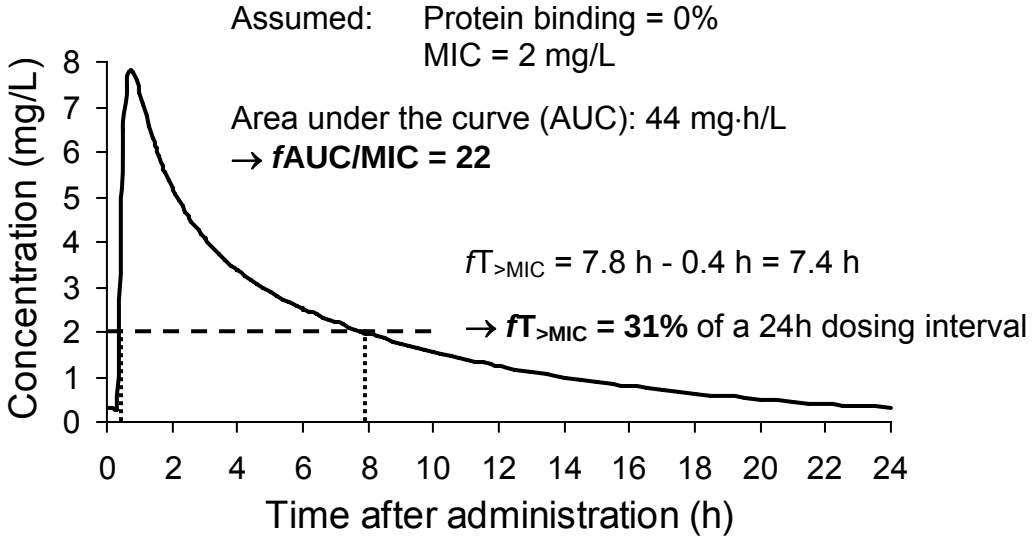


**Figure 2.7-2** Derivation of the PKPD statistics *f*AUC/MIC and $fT_{>MIC}$

The PKPD statistic $fT_{>MIC}$ assumes that the concentration effect relationship (e. g. of beta-lactams) is steep and that there is only a narrow range between zero and full drug effect (see ceftazidime in Figure 2.7-1). The PKPD statistic *f*AUC/MIC assumes that a continuous and a short term infusion yield the same effect, if both result in the same AUC over 24h. This assumption is useful, because there is a wide range of concentrations between zero and full effect in the concentration effect relationship (see tobramycin in Figure 2.7-1). The attained PKPD statistics are usually compared to a validated PKPD target which indicates a high or low probability for successful microbiological or clinical outcome (see below).

It is important that those two PKPD statistics are simplifications. Both statistics over-simplify the concentration effect relationship. The presence of resistant sub-populations and selection of resistant mutants are not addressed. These PKPD statistics also do not provide information on the

optimal duration of therapy. However, these statistics can provide valuable information to guide antibiotic therapy and to optimize antibiotic dosage regimens. Therefore, they have been widely applied in MCS with antibiotics.

### 2.7.2 Monte Carlo simulations with antibiotics

#### 2.7.2.1 Background

Originally, MCS was called “statistical sampling”. A series of pseudo-random numbers is used to account for random effects in such a simulation. This series of pseudo-random numbers approximates a series of truly random numbers, as pseudo-random numbers follow a complex algorithm which is implemented in the respective program. If one simulates a large number of events, then this approximation is usually good enough. Due to the use of random numbers, a MCS is also called a stochastic simulation.

MCS has been used in the 1930s for studying the properties of the neutron and has been applied to develop the hydrogen bomb in the 1950s. Drusano et al. (113) first used this technique to optimize antibiotic dosage regimens and to specify susceptibility breakpoints in 1998. They showed that MCS is a valuable tool in rational dose selection for phase II/III clinical trials.

#### 2.7.2.2 Calculation of the probability of target attainment vs. MIC profiles

A MCS for antibiotics combines the predicted variability in plasma concentration time profiles with the variability in bacterial susceptibility (described by an MIC distribution). The plasma concentration time profiles for a large number of subjects, typically 5,000 to 10,000, are simulated.

The steps involved in a MCS with antibiotics are illustrated in Figure 2.7-3. These steps apply to all MCS in this thesis:

1) Simulation of the plasma concentration time profiles for many subjects (e. g. 10,000) at steady-state. These profiles are to be simulated for the chosen dosage regimen. It is often helpful to derive the median and the prediction intervals to visualize the range of simulated profiles.
2) Calculate the unbound plasma concentration by multiplying each concentration with the fraction unbound which was assumed to be 100% for the example shown in Figure 2.7-3.
3) Calculate the $fT_{>MIC}$ (e. g. for beta-lactams) or the *f*AUC/MIC (e. g. for quinolones) for each of the 10,000 simulated profiles at one MIC of interest.
4) Choose a validated PKPD target. The PKPD targets $fT_{>MIC} \geq 40\%$ or *f*AUC/MIC $\geq 33.7$ were chosen in this example (see Figure 2.7-3).
5) Count the number of subjects who attained this PKPD target at the selected MIC. The fraction of subjects who attained the PKPD target approximates the probability to attain this target.
6) Repeat steps 3) to 5) for all relevant MICs. Ideally, the lowest studied MIC should have a probability of target attainment of 100% and the highest studied MIC should have a probability of target attainment of 0%.
7) Plot these probabilities (fractions) of target attainment as a function of the MIC for the selected PKPD target (see Figure 2.7-3).
8) Repeat steps 3) to 7) for all PKPD targets of interest.

The results of the probability of target attainment (PTA) vs. MIC plot depend on the chosen population PK model, on the dosage regimen, and on the covariates (e. g. demographic data) of the subjects studied in the MCS. Additionally, the selected PKPD target influences the PTA vs. MIC profiles. The meaning of several PKPD targets for beta-lactams and quinolones from literature is shown in chapter 2.7.3. It is very important to assure that the population PK model has adequate predictive performance to obtain unbiased PTAs.

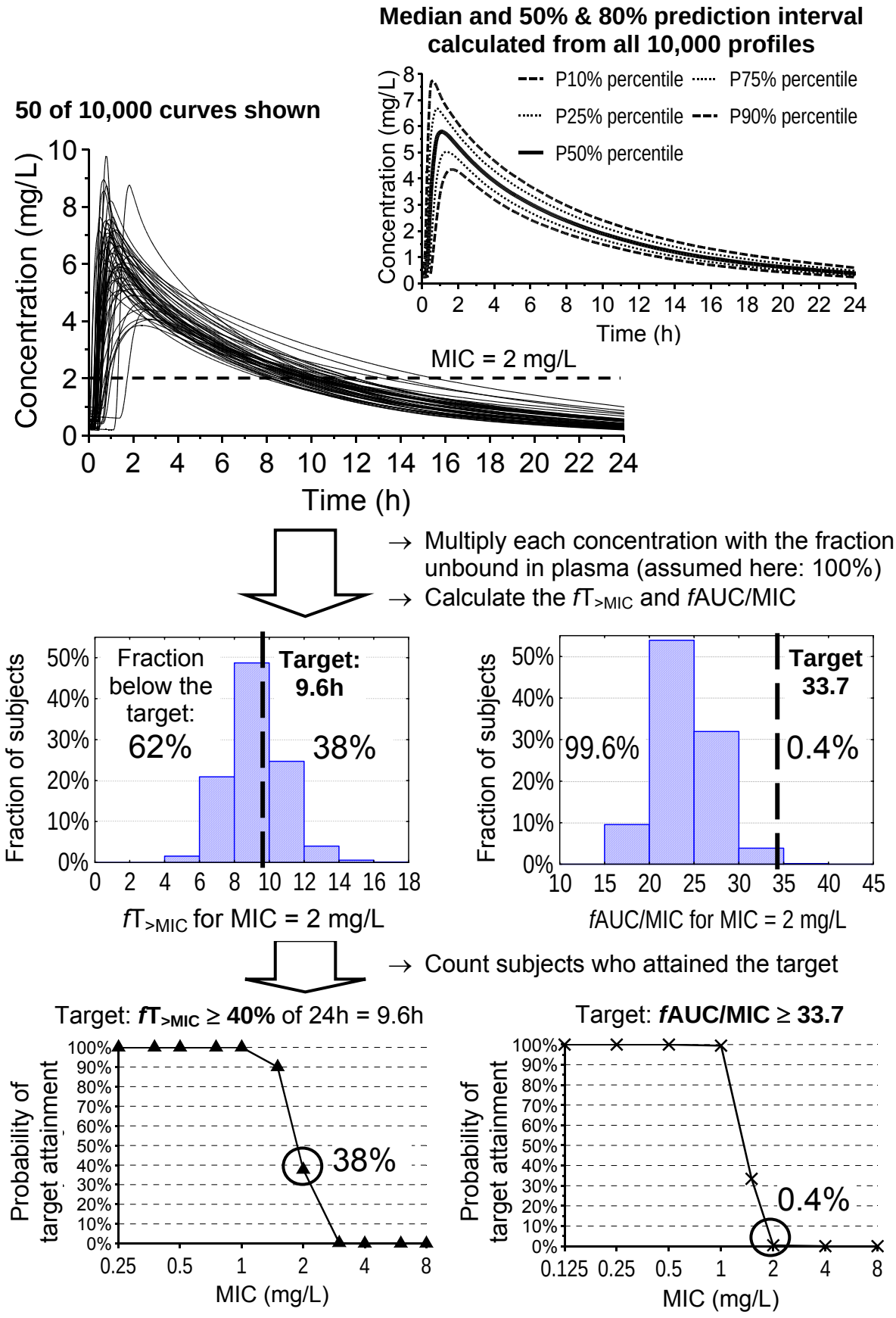


**Figure 2.7-3** Monte Carlo simulation for antibiotics

#### 2.7.2.3 Derivation of PKPD breakpoints and probabilities of target attainment for specific MIC distributions

***PKPD breakpoint:*** It is important to know the highest MIC with a high probability of successful treatment for the chosen dosage regimen. Attainment of the selected PKPD target is used as a surrogate measure for microbiological or clinical success. The PKPD breakpoint is usually defined as the highest MIC for which at least 90% of the subjects attain the PKPD target. The PKPD breakpoint can be derived from the PTA vs. MIC profiles. In the example shown in Figure 2.7-4, the PKPD breakpoint is 1.5 mg/L.

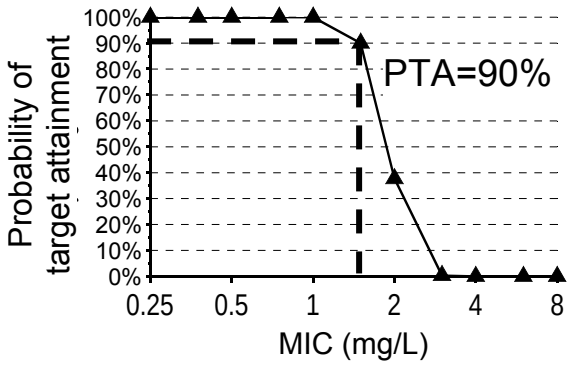


**Figure 2.7-4** Probability of target attainment vs. MIC profile for the PKPD target $fT_{>MIC} \geq 40\%$

If the MIC of an infecting organism is higher than the PKPD breakpoint, alternative dosage regimens or an alternative drug should be selected. It is important that the method of specifying the PKPD breakpoint is different from the methods of national organizations like the DIN (Deutsches Institut für Normung), the BSAC (British Society for Antimicrobial Chemotherapy), and the CLSI (Clinical and Laboratory Standards Institute) used to specify their susceptibility breakpoints. This methodological difference may cause differences between the PKPD breakpoint and the susceptibility breakpoint by more than a factor of four.

***PTA expectation value:*** In order to put the PTA vs. MIC profiles into clinical perspective, one should calculate the expected PTA for treatment of infections caused by bacteria from a specific MIC distribution. This expected PTA is called the PTA expectation value and is also called cumulative fraction

of response (334). The PTA expectation value provides valuable information for empiric treatment. It depends on:

1) the chosen antibiotic and dosage regimen,
2) the specific PK profile of the patient population of interest,
3) the covariates (e. g. demographic data) of the patient(s), and on
4) the expected bacterial susceptibility (MIC distribution).

The PTA expectation value is calculated by multiplying the PTA at each MIC by the fraction of the population of microorganisms at each MIC.

$$\text{PTA expectation value} = \sum_i f(MIC_i) \cdot PTA(MIC_i) \qquad \text{Formula 2.7-2}$$

$PTA(MIC_i)$ is the probability of target attainment at the $i^{th}$ MIC and $f(MIC_i)$ is the fraction of bacterial isolates with $MIC_i$ (see Figure 2.7-5 for an example).

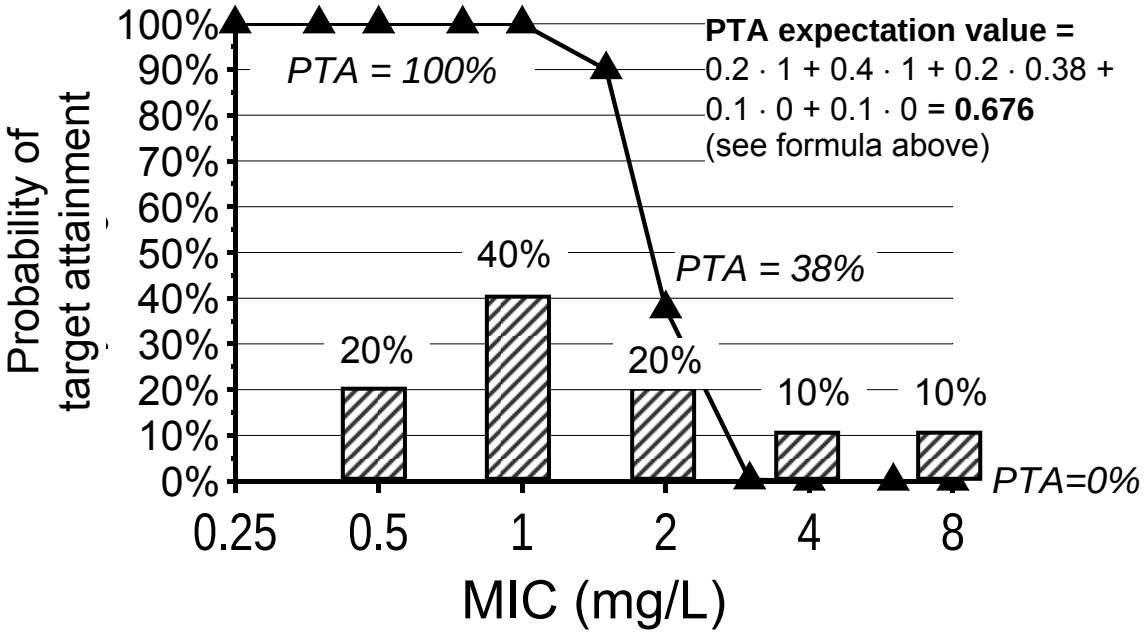


**Figure 2.7-5** Calculation of the PTA expectation value from the PTA vs. MIC profile and the MIC distribution of the expected pathogen

Ideally, a population PK model which has been derived in the patient population of interest should be combined with the expected MIC distribution

in this patient population at a local hospital. The PTA expectation value can then be used to predict the probability of successful microbiological or clinical outcome for the desired patient population at the local hospital.

The selected dosage regimens can be individualized based e. g. on body size and renal function. If no MIC data from the local hospital are available, MIC distributions from published databases on bacterial susceptibility in one or several countries can be used for calculation of the PTA expectation value.

### 2.7.3 PKPD targets for beta-lactams and quinolones

***Beta-lactams:*** The PKPD targets are an important component of a MCS simulation. Some targets have been evaluated in a mouse infection model, whereas other targets were determined in specific patient groups. Importantly, there are no established PKPD targets in CF-patients. The group of Craig (84) determined the PKPD targets for beta-lactams shown in Table 2.7-1 in a mouse infection model (107).

**Table 2.7-1** PKPD targets for beta-lactams against *Enterobacteriaceae* determined in a mouse infection model

| **Drug group** | Bacteriostasis[a] | Near-maximal bactericidal activity[a] |
|---|---|---|
| | $fT_{>MIC}$ as fraction of the dosing interval | |
| Cephalosporins | 40% | 65%[b] |
| Penicillins | 30% | 50% |
| Carbapenems | 20% | 40% |

[a]: Determined 24h after initiation of drug treatment.

[b]: Range: About 60-70%.

The PKPD targets shown in the right column of Table 2.7-1 are also called the targets for near-maximal bactericidal activity and the targets in the second column are called bacteriostasis targets.

***Quinolones:*** Various *f*AUC/MIC targets have been established for different endpoints of treatment with quinolones. For our MCS with levofloxacin and ciprofloxacin based on PK data from healthy volunteers, we used the PKPD target *f*AUC/MIC ≥ 33.7 for fluoroquinolones against *S. pneumoniae* from Ambrose et al. (9) which is predictive of successful microbiological response in patients with community-acquired respiratory tract infections. Additionally, we used the target AUC/MIC ≥ 125 (corresponding to a *f*AUC/MIC ≥ 87.5 assuming a 30% protein binding for ciprofloxacin) which correlates with clinical and microbiological success in seriously ill patients infected with gram-negative bacteria including *P. aeruginosa* (137). In absence of a PKPD target for fluoroquinolones in CF-patients, we back-engineered the required PKPD target for ciprofloxacin in CF-patients.

Attainment of a PKPD target is commonly used as a surrogate marker for successful microbiological or clinical outcome. Selection of the most appropriate PKPD target depends on the seriousness of the infection and on the status of the patient's immune system, besides other factors (84). While achieving a bacteriostatic target might be sufficient for treatment of minor infections, near-maximal bacterial killing should be achieved in immuno-compromised patients with severe infections (107). It seems conceivable that infections at infection sites which are difficult to treat like the stagnant mucus of CF-patients might require higher PKPD targets than for infections which are possibly less difficult to treat.

## 2.8 Objective driven PK analysis and simulations

Maybe the most important step of a pharmacometric data analysis is a clear statement of the objectives. All pharmacometric data analyses should start with a discussion of the purpose of the analysis between all people involved. The most appropriate pharmacometric analysis will be driven by the type of questions raised in the objectives and by the available raw data. This chapter assumes that the data from one (or more) clinical studies are already available. This is usually a more difficult situation compared to the analysis of

clinical studies whose design has already been optimized by optimal trial design techniques. Therefore, the first two questions before starting a population PK analysis are:

1) Do we really need this work intensive technique?
2) Why?

Unfortunately, there is no generally applicable answer to these two questions. Chapter 1, chapter 2.6, and chapter 2.7 present an overview of several methods of pharmacometric data analysis. Table 1.1-1 compares specific features of NCA, modeling by the STS approach, and population PK modeling. This chapter will present some guidance to choose the most appropriate method of pharmacometric data analysis and simulation. Some of the issues discussed below would require large simulation studies. Therefore, this chapter contains the opinion of the author of this thesis and is not based on large simulation studies. The issues described in this chapter should be discussed for each PKPD analysis on a case by case basis.

### 2.8.1 Helpful things to do before starting a PK data analysis

It is almost always helpful to plot the available raw data. For concentration time data, these plots should be prepared both on linear and on semi-logarithmic scale and might comprise some or all of the following plots:

1) Individual concentration time raw data for all subjects.
2) Individual concentration time raw data for each subject; if data for more than one treatment from a subject have been collected, it is often helpful to combine those data in one plot per subject.
3) Summary statistic plot of the concentration time raw data for each treatment separately. Most authors prefer to plot the average ± SD concentration time profiles. However, sometimes plotting the median [range] or median and [10-90% percentile] is more appropriate. If only data on a few subjects are available, plotting the median and [25-75% percentile] may be helpful.

4) Summary statistic plot of the concentration time raw data for each group of patients separately (e. g. young vs. old patients, males vs. females, undernourished vs. normal weight vs. obese patients, etc.).
5) Comparing the average ± SD or the median [10-90% percentile] of each treatment or of each patient group in one plot.
6) Splitting the plots described above in single dose and steady-state data, if applicable.

These plots can be easily prepared for a crossover study in healthy volunteers or patients. They are almost always helpful before starting the PK analysis and may guide some of the decisions during model building. Modifications may be required for large clinical trials with sparse sampling. Important issues to keep in mind for interpretation of raw data plots (especially of clinical trials in sick patients) are:

1) If there are dropouts, e.g. due to adverse events or for other reasons, raw data plots maybe misleading. If one treatment resulted in higher concentrations than the other treatments and if subjects with the highest concentrations were most likely to drop out, the average concentration of this treatment may be biased towards lower values.
2) The average or median plasma concentration time course should be interpreted cautiously, as it may:
   a. erroneously lead to the conclusion that there are two or three slopes on semi-logarithmic scale, because more and more concentrations were below the quantification limit for the last time points,
   b. hide a saturable clearance component due to averaging the data.

### 2.8.2 Choice of method for derivation of PK parameters

#### 2.8.2.1 Datasets often occurring in PK studies

The types of available datasets can be roughly split into the four categories shown in Table 2.8-1. The categories shown in this table are no

strict categories, as both axes (columns and rows) would be better described by a continuous scale. It is important to note that optimal sampling time theory may greatly improve the amount of information contained in the same number of data points.

**Table 2.8-1** Types of datasets which typically arise from PK studies

| | **1)** Many (>10) samples per subject (per profile) | **2)** Few (1-5) samples per subject (per profile) |
|---|---|---|
| **A:** Data on many (more than ca. 50) subjects available | **A1**<br>NCA: applicable & robust<br>STS: applicable & robust<br>PopPK: applicable & robust<br>PopPK (and STS) modeling may be superior to NCA<br>Average parameters and BSV term well estimable, covariate effect estimable. | **A2**<br>NCA: not applicable<br>STS: not applicable<br>PopPK: applicable & robust<br>PopPK is the most appropriate technique.<br>Often only simple structural models can be estimated, covariate effect estimable. |
| **B:** Data on few (less than ca. 16) subjects available | **B1**<br>NCA: applicable<br>STS: applicable<br>PopPK: applicable<br>*all methods require caution*<br>PopPK (and STS) modeling may be superior to NCA.<br>Average parameters estimable, BSV terms can not be soundly estimated. Empiric covariate effects not well estimable. | **B2**<br>NCA: not applicable<br>STS: not applicable<br>PopPK: applicable, but caution is required<br>Even PopPK results to be interpreted cautiously.<br>Often only very simple structural models can be estimated. Empiric covariate effects not well estimable. |

NCA: Non-compartmental analysis, STS: individual PK modeling by the standard-two-state approach, PopPK: population PK modeling.

**Case A1** in Table 2.8-1 contains the largest amount of data. As there are more than 50 subjects, estimation of average PK parameters is usually

very robust and estimation of BSV terms is robust. Additionally, the effect of covariates on PK parameters can be empirically estimated. Small covariate effects may require more than 100 subjects for a sound estimation of covariate effects (411). The BSV e. g. in terminal half-life might be biased towards higher values by NCA due to analytical error. Therefore, population PK and the STS approach might be superior to NCA for some PK parameters. The BSV of the absorption parameters (lag time and absorption half-life) may be biased towards higher values for the STS approach. Therefore, population PK is still the most powerful technique, but has only limited advantages compared to the STS approach and NCA (depending on the objective).

**Case B1** in Table 2.8-1 has plenty of information for each subject, but contains data on fewer subjects. The average PK parameters can still be estimated reasonably, however, the estimates for the BSV terms are often less precise than for case A1. Additionally, covariate model building should probably be limited to known covariate relationships (like the effect of body size on clearance and volume of distribution or the effect of renal function on renal clearance) for case B1. Empiric covariate model building should not be performed in this case. As population PK can provide more accurate and more precise estimates for the BSV compared to the STS approach and NCA, population PK is superior for incorporation of (multiple) covariate relationships which should be based on prior knowledge. Therefore, there may be some advantages of population PK for case B1 compared to the STS approach and NCA (depending on the objectives of the study).

**Case A2** in Table 2.8-1 is the situation when population PK has its greatest merits. Both NCA and the STS approach are usually not applicable, whereas population PK can obtain reasonable estimates for the average PK parameters and their BSV. Covariate effects can usually be identified, especially if data on more than 100 subjects are available. Optimal sampling time strategies can greatly increase the amount of information in the data for case A2. Prior information on the model parameters may be incorporated into the analysis by a Bayesian approach. This additional information, e. g. from studies of case A1 or B1 may support the analysis of studies of case A2. This might allow to estimate more complex structural models.

**Case B2** requires the most caution for interpretation of the results as the least amount of information is contained in the data. Especially the BSV terms can often not be well estimated. Therefore, incorporation of a Bayesian analysis strategy has its greatest merits in this case. Prior information on the average PK parameters and their BSV terms is often very helpful to obtain reasonable estimates for data of case B2. Such an analysis can be performed as individual PK analysis (e. g. with the program ADAPT II) or as population PK analysis (e. g. with the program WinBugs or PKBugs).

#### 2.8.2.2 Typical objectives for NCA

For studies of case A1 or B1 (see Table 2.8-1), there are several objectives for which NCA is sufficient:

1) Determination of the average AUC and its 90% confidence interval (to characterize its uncertainty).
2) Determination of the average (median) volume of distribution (volume of distribution at steady-state can usually be estimated more reliably than volume of distribution during the terminal phase, especially if low concentrations can not be determined reliably).
3) Determination of the BSV in clearance and volume of distribution (with some limitations)
4) Determination of the average terminal half-life. The BSV in terminal half-life is often biased towards higher values.
5) Characterizing the average extent of a PK drug-drug interaction at the studied dose level (but not the time course of interaction).
6) Comparing the average rate of absorption (time to peak concentration) between various oral formulations.
7) and others.

For studies of cases A1 and B1, NCA should probably always be performed, as most studies in literature report NCA results and as NCA results may be helpful during modeling.

#### 2.8.2.3 Typical objectives which greatly gain from modeling

PKPD modeling either by the STS approach or by the population approach is especially superior to NCA for the following objectives:

1) Modeling the time course of drug concentrations and prediction of concentration time profiles for other than the studied dosage regimens.
2) Modeling the time course for PKPD models where the drug effect at each time is required as an input variable of the PD model or disease progression model.
3) Modeling the time course of a PK drug-drug interaction and suggesting a possible mechanism.
4) Modeling dynamic systems like the emergence of resistance of bacteria.
5) Modeling the oral absorption profile and prediction of the absorption profile for other dose levels (with some limitations).
6) and others.

#### 2.8.2.4 Choice of STS approach or population approach

There are some modeling objectives for which the population approach is particularly advantageous compared to the STS approach:

1) Estimation of the variability for PK and PD parameters.
2) Estimation of different sources of variability (see e. g. chapter 5.1).
3) Simulation of the expected range of predicted concentration or effect profiles (=MCS or stochastic simulations).
4) Accounting for the effect of (multiple) covariates on model parameters (for both structural and variance parameters).
5) Incorporation of allometric theory or similar concepts.
6) Estimation of saturable and non-saturable elimination pathways.
7) Accounting for the residual unidentified variability (including analytical error) in the residual error model.
8) Estimation of the uncertainty of all model parameters.

9) Simulation of clinical trials.
10) Simulation of the predicted response for a whole study population.
11) Simulation of the predicted response for patient groups with a specific set of covariates.
12) Selecting dosage regimens for one patient or a group of patients.
13) Meta-analysis of clinical studies (see chapter 3.5 and chapter 4.3)
14) and others.

In essence, population PK is the most powerful technique and is always superior or comparable to NCA or the STS approach. However, there are situations for which the STS approach might be a more reasonable choice:

1) Estimation of mechanistic interaction models for which model development would consume a vast amount of time via population PK (computation times of weeks to months for one estimated model).
2) (Initial) search for the most appropriate structural PK model, if complex models are required. Final model should be estimated with population PK, if possible.
3) Finding initial estimates for complex population PK models.
4) and others.

#### 2.8.2.5 Choice of parametric or non-parametric population approach

There is an ongoing debate which has started more than 20 years ago whether parametric or nonparametric population PK analysis is the better approach. There are strengths of both approaches. Importantly, some parametric population PK programs (including NONMEM®) approximate the true log-likelihood and use this approximated log-likelihood as their objective function to be optimized (see chapter 2.6.3). Although this increases the speed of computation, the validity of the results depends on the appropriateness of this approximation. There are both parametric population approach programs (like PEM and MCPEM) and non-parametric population

approach programs (like NPEM or NPAG) that calculate the true log-likelihood without an approximation. This is a considerable advantage.

The main difference between parametric and non-parametric population PK analysis lies in the parameter variability model. Parametric population PK models describe the BSV e. g. as a multivariate log-normal distribution. (Sometimes other parametric distributions are also applied.) Non-parametric population PK does not assume any shape of the distribution and just describes the data from each subject as one specific set of PK parameters which is called a support point. Each support point has an associated weight w which is 1 / sample size of the study in the simplest case. A support point may combine the PK data from two, three, or more subjects which would result in weights of 2 / sample size, 3 / sample size etc. Therefore, each support point is its own sub-population of subjects.

Sub-populations of subjects with a different set of PK parameters can also be estimated in a parametric population PK analysis (e. g. in NONMEM®). These models are called MIXTURE models in NONMEM®. The number of sub-populations has to be pre-specified by the user in NONMEM®, whereas non-parametric population PK programs choose the most appropriate number of sub-populations automatically. This is an advantage of non-parametric population PK programs. Several parametric and non-parametric population PK estimation methods were compared by Bustad et al. (63) and by Girard and Mentré (152). The discussions about the most appropriate population PK analysis programs will probably be ongoing for many more years.

Although NONMEM® approximates the true log-likelihood, NONMEM® has been proven to be a robust, extremely flexible, and reasonably fast program for population PKPD analysis during the last 30 years. NONMEM® is the most widely used population PKPD program and has been used for the vast majority of population PK analyses for submission to regulatory authorities in the past (and presence).

It is unlikely that a multi-model distribution of renal clearance would appear for the drugs described in this thesis. Glomerular filtration is a passive process which is not subject to genetic polymorphism and most of our studied

drugs were eliminated primarily via the renal pathway. As none of our drugs had a protein binding above 60%, glomerular filtration comprises a significant part of the total clearance. It is also unlikely for studies with less than 30 subjects (as for most studies in this thesis, see case B1 in Table 2.8-1) that two or more distinct subpopulations can be identified. Therefore, parametric or non-parametric population PK models would have probably led to the same conclusions in this thesis and parametric PK software seems to be a reasonable choice for this thesis.

It is the opinion of the author of this thesis that it was more important for the results and conclusions in this thesis to choose the population PK models with the best predictive performance. The reason for this is that almost all applications of population PK models described in this thesis were based on MCS.

### 2.8.3 Choice of method for stochastic simulations (MCS)

As described in chapter 2.8.2.4, many of the applications of population PK models are based on stochastic simulations (also called MCS). For MCS applications, the population approach is most likely always the most powerful method and should be preferred, unless other limitations exist.

The differences in the parameter variability model between the parametric and non-parametric population approach affect the type of output from a MCS. A parametric population PK model tries to estimate the form of a multivariate distribution of PK parameters. This multivariate distribution should describe the parameter variability of the whole population, although it is only based on data from e. g. 24 subjects. Importantly, the number of subjects simulated in a MCS (e. g. 10,000) does not imply that the MCS is representative for the whole subject population. The number of subjects on which the MCS is based is far more important than the number of simulated subjects. A sound MCS should just simulate more than 2,000 (better 10,000) subjects to adequately represent the statistical distribution which is a methodological issue. Simulating 100,000 subjects usually does not improve the results of a MCS (depending on the problem and its objectives).

If the PK parameters of several thousand subjects are randomly sampled from this multivariate distribution, the expected range of concentration time profiles can be predicted.

Non-parametric population PK models use support points to describe the parameter variability. If a non-parametric population PK model comprises e. g. 80 support points, a non-parametric MCS would predict the concentration time profiles for exactly 80 subjects (with equal or different weights). The set of support points can, however, also be used to generate a variance-covariance matrix of e. g. a multivariate log-normal distribution as for a parametric population PK model. And then the same approach as for parametric MCS can be applied. This leads to three possible methods for estimation of population PK models and subsequent MCS. These are summarized in Table 2.8-2.

The hypotheses in Table 2.8-2 have not been generated and tested by large simulation-estimation studies. These would consume a vast amount of time and probably none of the options shown in Table 2.8-2 will be the most appropriate in all circumstances. If one has true concerns about the appropriateness of parametric or non-parametric population PK estimation and simulation, the most reasonable way to go would be to use both approaches. However, this is very rarely performed as it requires many efforts and time and only few people have sufficient experience with more than one population approach software to perform such a systematic comparison. Project deadlines often do not allow one to use more than one population PK software in parallel. Although this hypothesis is unproven, the use of option 1, 2, or 3 shown in Table 2.8-2 would possibly not affect the final conclusions drawn in this thesis. Choosing one or the other option might cause a shift in the results for some of the comparisons in this thesis. However, the general conclusions will probably not change, as our studies came from small and homogeneous datasets with a high proportion of healthy volunteers.

**Table 2.8-2** Three methods of population PK model estimation and Monte Carlo simulation

<table>
<tr><th></th><th>Option 1</th><th>Option 2</th><th>Option 3</th></tr>
<tr><td>Estimation<br>Simulation</td><td>Parametric<br>Parametric</td><td>Non-parametric<br>Parametric</td><td>Non-parametric<br>Non-parametric</td></tr>
<tr><td>A: Data on very many subjects available (e. g. > 1,000)</td><td colspan="2">Simulation will be robust as mixture models can adequately identify subpopulations and as the parameter variability model (variance-covariance matrix) is well supported by the data.</td><td>Simulations might be more powerful, as no parametric distribution is assumed.</td></tr>
<tr><td>B: Data on many subjects available (e. g. 50 - 300)</td><td colspan="2">Simulation will be reasonably robust. Subpopulations may or may not be well identifiable, but a reasonable amount of data is available to describe the parameter variability model.</td><td>Simulations might be more powerful, as no parametric distribution is assumed.</td></tr>
<tr><td>C: Data on few subjects available (e. g. < 20)</td><td colspan="3">The results of all three options should be interpreted with caution, as the number of subjects to describe the population is small.</td></tr>
<tr><td></td><td colspan="2">Parametric MCS will generate a smooth distribution of simulated subjects (smooth curve in the PTA vs. MIC plot).</td><td>Non-parametric MCS will generate a step function like in a survival plot.</td></tr>
</table>

### 2.8.4 Why did we choose which methods for PK analysis and simulation?

As described above, there are various reasons why to choose which method of PK analysis. Our choice was driven by the following arguments. This choice appears as a practical approach for analyses of datasets of case B1 shown in Table 2.8-1.

Step 1: We applied NCA for all studies investigated to use the method which has been used by the vast majority of investigators in the past (and presence).

Those NCAs provided reasonable initial estimates for our population PK models. Therefore, we did not need the STS approach to find initial estimates for our population PK analyses.

Step 2: Our objectives required MCS for other than the studied dosage regimens. Additionally, we had to account for the uncertainty in PK parameters for our meta-analyses. These two objectives are strong arguments to use population PK.

Therefore, we used parametric population PK analysis in NONMEM® for model estimation. Non-parametric bootstrapping to estimate the uncertainty of model parameters is supported by the computation time of NONMEM® for models with non-saturable drug transfer. Additionally, NONMEM® is a flexible platform which can be easily automated via additional programming.

Step 3: We used parametric MCS (option 1 in Table 2.8-2) as we estimated our population PK models by the parametric approach. Importantly, we selected the most appropriate population PK model by VPCs (and other model diagnostics) before use of these models in our MCS.

## 2.9 Computation

***Population PK:*** We built all population PK models with NONMEM® version V release 1.1 (NONMEM Project Group, University of California, San Francisco, CA, USA) (33). The first order conditional estimation (FOCE) method with the INTERACTION estimation option was applied for all model building and bootstrap runs. We used the G77 FORTRAN compiler or the Compaq Visual Fortran version 6.6 Upgrade C compiler (with options /fltconsistency /optimize:4 /fast) both with double precision.

We used Wings for NONMEM (WFN) Version 408b to greatly increase the productivity of our NONMEM® runs. WFN is a set of DOS batch command files and AWK scripts written by Professor Dr Nick Holford.

The non-parametric bootstrapping was supported by a series of Perl scripts used to generate the raw datasets for bootstrapping and to evaluate the bootstrap results. These Perl scripts were written by the author of this thesis.

***NCA and statistics:*** We used WinNonlin™ Professional (version 4.0.1, Pharsight Corp., Mountain View, CA, USA) for NCA and ANOVA statistics (including bioequivalence statistics).

***PKPD simulations:*** The NCA for our PKPD simulations with 10,000 subjects per run were performed with validated Perl scripts.

# 3 Pharmacokinetic and pharmacodynamic comparison of patients with cystic fibrosis and healthy volunteers

## 3.1 Background and literature data on the pharmacokinetic in CF-patients

The PK in CF-patients has been extensively reviewed (389, 390, 408, 499, 502). The majority of studies investigates less than 30 subjects in total (CF-patients and healthy volunteers). Many studies lack a control group of healthy volunteers. CF-patients are on average smaller and leaner compared to healthy volunteers. However, most PK studies in CF-patients use WT or BSA which both ignore body composition for their comparison of CF-patients and healthy volunteers.

Some of the PK studies in CF-patients and healthy volunteers compared study populations with considerable differences in age. This makes such a PK comparison more difficult. To the best of my knowledge, none of the studies in CF-patients and healthy volunteers compared the PK in both subject groups by allometric size models based WT or LBM. Overall, it seems not surprising that there is a large between study variability for the comparison of CF-patients and healthy volunteers.

### 3.1.1 Disposition of antibiotics after intravenous administration

Most studies comparing clearance in CF-patients and healthy volunteers find higher size adjusted clearances in CF-patients (389, 390, 408, 499, 502). Some studies report similar size adjusted clearances in both subject groups. Higher clearances in CF-patients were reported for dicloxacillin (+197% after oral dose, renal clearance: 282 $\pm$ 135 mL/min/1.73 $m^2$ in CF-patients vs. 95 $\pm$ 28 mL/min/1.73 $m^2$ in healthy volunteers) (241), cloxacillin (+114%, unit: L/h/kg WT, iv dose) (470), ceftazidime (+65%, unit: L/h/kg WT, iv dose) (282), ticarcillin (+50%, unit: L/h/1.73 $m^2$ BSA, iv dose) (100), and ciprofloxacin (+46%, unit: L/h/1.73 $m^2$ BSA, iv dose) (75).

Similarly, increased volumes of distribution were reported for methicillin (+36%) (550), cloxacillin (+38%) (470), cefepime (+44%) (203), and ciprofloxacin (+62%) (75). The majority of those differences in volume of distribution tend to disappear (408, 502), if LBM was used to scale volume instead of WT.

These pronounced differences, especially in clearance, have led to the common impression that CF-patients require higher doses than would be predicted based on PK data from healthy volunteers. However, some of those data are more than 30 years old. During the last decades, the therapy and life expectancy of CF-patients has increased tremendously. Almost none of the studies in CF-patients have been evaluated by population PK, although the possible influence of multiple covariates like body size, body composition, and disease specific renal function seems likely.

This calls for a series of well-controlled studies in CF-patients with an age-matched collective of healthy volunteers and PK analysis by population PK as has been pointed out by Touw et al. (502). Ten studies in CF-patients with a healthy volunteer control group and PK evaluation by population PK will be described in chapter 3. A meta-analysis of those ten studies by population PK will conclude this chapter.

### 3.1.2 Oral absorption of antibiotics

Pathophysiological changes in the GI tract of CF-patients may potentially interfere with the oral absorption. These changes occur frequently in CF-patients and comprise gastric acid hypersecretion, injury of the proximal small intestinal mucosa (31, 81), and bile acid malabsorption (135). Other pathophysiological alterations in CF-patients are described in chapter 1.4.2.

There are some data (71) on a possibly accelerated rate of gastric emptying relative to control subjects in n=4 infants (age: 5 weeks to 4 months) with CF after intake of a milk-meal. The influence of these changes on the rate and extent of oral absorption has rarely been studied. The extent of absorption is slightly higher (not significant) in CF-patients (50 $\pm$ 26%, n=16)

than in healthy volunteers (38 ± 17%, n=12) for cloxacillin (470) and more variable in CF-patients. A 36% longer absorption half-life has been reported for cloxacillin in CF-patients. Although there are reports on an increased extent of absorption for ciprofloxacin (75) with 80 ± 18% in CF-patients and 57 ± 12% in healthy volunteers, Davis et al. (98) found an extent of absorption of 72 ± 18% in CF-patients and of 70 ± 21% in healthy volunteers. Other authors report a slower rate of absorption for ciprofloxacin (98) and fleroxacin (325) in CF-patients. However, there are also conflicting data from other studies on the extent of absorption for quinolones which showed no differences between CF-patients and healthy volunteers (408).

Several authors (98, 280, 325, 403) used the STS approach and report a longer absorption half-life of ciprofloxacin and fleroxacin in CF-patients. However they find a large BSV with coefficients of variation of 46 to 100% for the absorption half-life. Rajagopalan et al. (398) combined data from five studies in pediatric patients and analyzed them with population PK. Nineteen percent of their patients had CF. They report a 61% slower rate and a similar extent of absorption for ciprofloxacin in children with CF relative to other pediatric patients. However, their CF-patients come from two of their five studies which did not include a control group of healthy volunteers or other patients. Therefore, they compared the rate of absorption between CF-patients and other pediatric patients from different studies.

Similar clinical study performance and standardized clinical procedures for CF-patients and healthy volunteers are essential to compare the rate of oral absorption. It may also be important to compare the oral absorption between CF-patients and healthy volunteers in absence of pancreatic enzymes, although the effect of pancreatic enzymes on the absorption of ciprofloxacin has been reported to be small (302, 403).

## 3.2 Common methods for analysis of our studies in CF-patients

We applied the methods described in chapter 2, to perform and evaluate our ten studies in CF-patients.

### 3.2.1 Literature background on descriptors for body size and body composition

CF-patients are often undernourished and have a paucity of adipose tissue. There are reports that lean body mass (LBM) better describes volume of distribution (323, 408, 499-501) and clearance in CF-patients than does WT (323). Consequently, Touw et al. (500, 501) proposed to calculate the initial daily dose of tobramycin in CF-patients based on LBM rather than on WT. LBM was also proposed to be used as size descriptor in CF-patients (390) and has been proposed to be a superior predictor of drug dosage compared to other measures of body size (e. g. WT or body surface area, BSA) (171, 328). Although there are some studies (323, 408, 499-501) in CF-patients which show that LBM might be superior to WT for dose selection in CF-patients, this superiority needs to be shown on a statistical basis and its possible clinical relevance needs to be assessed.

As beta-lactams are hydrophilic molecules, we expect them to distribute primarily into lean body compartments. We believed *a priori* for beta-lactams that body size is better described by LBM or fat-free mass (FFM) than by WT, since WT does not account for differences in body composition for a given mass. It is important to note that LBM and FFM are essentially the same metric. From a measurement perspective there are no defined methods for estimating LBM, whereas methods do exist for FFM. FFM differs from LBM in that FFM does not include the fat component of cellular membranes and cell walls, whereas LBM does. This difference is however relatively small, of the order of 2-3%. In contrast to the beta-lactams, most quinolones have a higher n-octanol water partition coefficient at pH 7.4 than our studied beta-lactams

(see Table 3.2-1). The combination of these antibiotics therefore poses a potentially challenging quest for a single size descriptor.

**Table 3.2-1** Study overview and log P of the ten studied antibiotics in CF-patients and healthy volunteers

| Drug | Dose (mg) | Route of administration | Log P[§] at pH 7.4 | Reference for physico-chemical data |
|---|---|---|---|---|
| Carumonam | 2166 | 15 min iv infusion | | |
| Cefaclor | 1000 | oral | -1.76 | (28) |
| Cefadroxil | 1000 | oral | -3.40 | (28) |
| Cefotiam | 1027.5 | 3 min iv infusion | | |
| Cefpirome | 2000 | 10 min iv infusion | -1.70[&] | (342) |
| Ceftazidime | 2000° | 5 min iv infusion | -1.60 or -3.69 | (28, 320) |
| Piperacillin | 4000[#] | 5 min iv infusion | -3.30 | (320) |
| Ciprofloxacin | 750 | oral | -1.1 | (174, 562) |
| Fleroxacin* | 800 | oral | -0.75 | (562) |
| Pefloxacin | 400 / 400 (crossover study) | 30 min iv infusion and oral dose | 0.2 | (562) |

°: Instead of 2000 mg, one CF-patient each received 1000 mg, 1500 mg, or 3000 mg ceftazidime.

[#]: One CF-patient received 3000 mg instead of 4000 mg.

*: We used data from Mimeault et al. (325) after a single dose of fleroxacin.

[§]: Logarithm (base 10) of the n-octanol water partition coefficient.

[&]: In distilled water.

Several equations have been developed to estimate FFM. The Cheymol & James equation (72, 222) was developed for epidemiological purposes to describe the rising prevalence of obesity in the UK (164). The Cheymol & James equation is empirical and was not intended to be used for selecting drug doses. Subsequently, a new equation for estimating FFM has been developed by Janmahasatian et al. (224) which has a semi-mechanistic basis and was developed for use as a size descriptor in PK. The predicted FFM from both of these equations approximates LBM. FFM is possibly a

valuable descriptor of body size/composition in PK, because most metabolic processes are in the aqueous body space and distribution of hydrophilic drugs like beta-lactams is likely to be primarily restricted to blood and interstitial fluid. The group of Duffull (117, 223) developed formulas for the predicted normal weight (PNWT) in obese and normal weighted patients. PNWT is a size descriptor which was specifically designed to be used for dose selection. We studied PNWT and BSA estimated by the Mosteller formula (332) in addition to WT and FFM.

The following formulas were applied for calculation of size descriptors. WT is total body weight in kg, HT is height in m, and BMI is body mass index in kg $m^{-2}$ (BMI is calculated as $WT/HT^2$).

*Cheymol & James equation* (72, 222) *for estimation of FFM ($FFM_C$):*

$$FFM_C(\text{female}) \text{ in kg} = 1.07 \cdot WT - 0.0148 \cdot BMI \cdot WT \qquad \text{Formula 3.2-1}$$

$$FFM_C(\text{male}) \text{ in kg} = 1.1013 \cdot WT - 0.01281 \cdot BMI \cdot WT \qquad \text{Formula 3.2-2}$$

*New equation from Janmahasatian et al. (224) for estimation of FFM ($FFM_J$):*

$$FFM_J(\text{female}) \text{ in kg} = \frac{9270 \cdot WT}{8780 + 244 \cdot BMI} \qquad \text{Formula 3.2-3}$$

$$FFM_J(\text{male}) \text{ in kg} = \frac{9270 \cdot WT}{6680 + 216 \cdot BMI} \qquad \text{Formula 3.2-4}$$

*Equation from Duffull et al.* (117) *for estimation of PNWT based on the Cheymol & James equation ($PNWT_C$):*

$$PNWT_C(\text{female}) \text{ in kg} = 1.75 \cdot WT - 0.0242 \cdot BMI \cdot WT - 12.6 \qquad \text{Formula 3.2-5}$$

$$PNWT_C(\text{male}) \text{ in kg} = 1.57 \cdot WT - 0.0183 \cdot BMI \cdot WT - 10.5 \qquad \text{Formula 3.2-6}$$

*Equation from Janmahasatian et al. (223) for estimation of PNWT based on the Janmahasatian equation ($PNWT_J$):*

$$\mathrm{PNWT_J(female)\ in\ kg} = \frac{\mathrm{WT} - 0.169 \cdot \mathrm{BMI} - 6.076}{0.014 \cdot \mathrm{BMI} + 0.515} \qquad \text{Formula 3.2-7}$$

$$\mathrm{PNWT_J(male)\ in\ kg} = \frac{\mathrm{WT} - 0.201 \cdot \mathrm{BMI} - 6.216}{0.016 \cdot \mathrm{BMI} + 0.487} \qquad \text{Formula 3.2-8}$$

*Mosteller equation (332) for estimation of body surface area (BSA):*

$$\mathrm{BSA\ in\ m^2} = \sqrt{\frac{\mathrm{WT} \cdot \mathrm{HT}}{36}} \qquad \text{Formula 3.2-9}$$

All of the formulas shown above (except the Mosteller equation) account for the different body composition of males and females.

### 3.2.2 Essential properties of a descriptor for body size and body composition

The two essential properties of a size descriptor are: 1) The composition/size descriptor should be able to describe body structure and functional capacity in relation to drug distribution and clearance, respectively, for a wide range of body sizes including normal, undernourished and the obese. In terms of CF, the critical area of importance lies in the ability of the size descriptor to accommodate the undernourished CF-patient as well as the normal weighted healthy volunteer. 2) A size descriptor should explain as much of the random BSV as possible. Reducing the unexplained BSV allows one to more accurately predict the effects of any given dose and therefore select doses that are most likely to achieve the desired therapeutic response. A population PK analysis can be used to directly rank different descriptors of body size and body composition based on their performance for these two criteria.

### 3.2.3 Models for scaling clearance and volume of distribution by body size and body composition

We considered the ten size models shown in Table 3.2-2 for analysis of our studies in CF-patients. The meta-analysis of all ten studies shows the results for all ten size descriptors, whereas the chapters on the individual drugs focus on the following five size models: 1) No_size, 2) WT1, 3) WT, 5) FFMc, and 7) FFMj (see Table 3.2-2).

**Table 3.2-2** Overview of size models used in our studies comparing CF-patients and healthy volunteers

| Abbreviation for size model | Size descriptor | Standard value | Allometric exponent | Type of scaling | Accounts for body composition | Reference for size descriptor |
|---|---|---|---|---|---|---|
| 1) No_size | none | none | none | unscaled | No | none |
| 2) WT1 | WT | 70 kg | 1 | linear | No | (193, 538, 539) |
| 3) WT | WT | 70 kg | 0.75 | allometric | No | (193, 538, 539) |
| 4) FFMc1 | $FFM_C$ | 53 kg | 1 | linear | Yes | (72, 222) |
| 5) FFMc | $FFM_C$ | 53 kg | 0.75 | allometric | Yes | (72, 222) |
| 6) FFMj1 | $FFM_J$ | 53 kg | 1 | linear | Yes | (224) |
| 7) FFMj | $FFM_J$ | 53 kg | 0.75 | allometric | Yes | (224) |
| 8) PNWTc | $PNWT_C$ | 70 kg | 0.75 | allometric | Yes | (117) |
| 9) PNWTj | $PNWT_J$ | 70 kg | 0.75 | allometric | Yes | (223) |
| 10) BSA | BSA | 1.73 $m^2$ | 0.67[a] | "linear" by BSA | No | (332) |

[a]: Exponent for conventional Euclidian geometry.

WT: Total body weight.

$FFM_C$: Fat-free mass calculated by the formula of Cheymol and James (72, 222).

$FFM_J$: Fat-free mass calculated by the formula of Janmahasatian et al. (224).

$PNWT_C$: Predicted normal weight based on the Cheymol & James equation for $FFM_C$ developed by Duffull et al. (117).

$PNWT_J$: Predicted normal weight based on the equation from Janmahasatian et al. (223).

BSA: Body surface area calculated by the Mosteller formula (332).

The number "1" in the abbreviation WT1, FFMc1, and FFMj1 indicates that the respective size model used linear scaling of clearance by the respective descriptor of body size/composition.

The background on allometric scaling is described in chapter 1.5. The models based on linear scaling by WT, $FFM_C$, $FFM_J$, or BSA assume that clearance and volume of distribution scale linearly with body size (i. e. WT, $FFM_C$, $FFM_J$, or BSA). The equations for linear scaling describing the fractional changes in volume of distribution ($F_{Size,V,i}$) and clearance ($F_{Size,CL,i}$) for the $i^{th}$ subject (with $WT_i$) standardized to a weight $WT_{STD}$ of 70 kg are shown in chapter 2.6.2.2. We exchanged WT by the respective other size descriptor shown in Table 3.2-2 and used the respective standard value for each size descriptor also shown in Table 3.2-2.

Our allometric model assumes that volume of distribution scales linearly (allometric exponent 1.0) with body size, whereas clearance scales slightly less than linearly (allometric exponent 0.75) with body size. The allometric exponent was fixed to 1.0 for all volume terms and fixed to 0.75 for all clearance terms. The equations for $F_{Size,V,i}$ and $F_{Size,CL,i}$ for our allometric model based on WT is shown in chapter 2.6.2.2. We applied the same allometric size model for $FFM_C$, $FFM_J$, $PNWT_C$, and $PNWT_J$ (model for $FFM_J$ shown below as an example, $FFM_{J,STD}$ is the standard value of $FFM_J$ which we chose as 53 kg).

*Allometric scaling of volume of distribution and clearance by $FFM_J$:*

$$F_{Size,V,i} = \frac{FFM_{J,i}}{FFM_{J,STD}} \qquad \text{Formula 3.2-10}$$

$$F_{Size,CL,i} = \left( \frac{FFM_{J,i}}{FFM_{J,STD}} \right)^{0.75} \qquad \text{Formula 3.2-11}$$

### 3.2.4 Between-subject variability model for our studies in CF-patients

We estimated the BSV of PK parameters by assuming a log-normal distribution as described in chapter 2.6.2.3. We used disease (CF) specific scale factors for renal clearance ($FCYF_{CLR}$), nonrenal clearance ($FCYF_{CLNR}$), and volume of distribution at steady-state ($FCYF_V$). For some studies with

sparse urine data, we additionally estimated the total clearance instead of renal and nonrenal clearance. We used a disease specific scale factor for total clearance ($FCYF_{CLT}$) in those analyses. The disease specific scale factors (FCYF) were set to 1.0 for healthy volunteers and were estimated for the population of CF-patients.

The individual PK parameters were calculated as follows (parameters explained below):

$$CL_{R,i} = CL_{POP,R} \cdot F_{Size,CL,i} \cdot FCYF_{CLR} \cdot \exp(\eta_{BSVCLRi}) \quad \text{Formula 3.2-12}$$

$$CL_{NR,i} = CL_{POP,NR} \cdot F_{Size,CL,i} \cdot FCYF_{CLNR} \cdot \exp(\eta_{BSVCLNRi}) \quad \text{Formula 3.2-13}$$

$$CL_i = CL_{R,i} + CL_{NR,i} \quad \text{Formula 3.2-14}$$

$CL_{POP,R}$ and $CL_{POP,NR}$ are the population estimates for the renal and nonrenal clearance of a healthy volunteer with standard size. $CL_i$, $CL_{Ri}$, and $CL_{NRi}$ are the individual estimates for total, renal, and nonrenal clearance for the $i^{th}$ subject, respectively. $\eta_{BSVCLRi}$ and $\eta_{BSVCLNRi}$ are log scale differences of the individual estimates from their population means ($CL_{POP,R}$ and $CL_{POP,NR}$) for the $i^{th}$ subject, respectively. The variance of these log scale differences is the random unexplained BSV between patients.

The disease specific scale factor for renal clearance ($FCYF_{CLR}$) characterizes the ratio of renal clearance in CF-patients divided by renal clearance in healthy volunteers of the same body size. If the scale factor $FCYF_{CLR}$ is 1.0, CF-patients and healthy volunteers of the same body size will have identical group estimates for renal clearance. We also estimated a disease specific scale factor for nonrenal clearance ($FCYF_{CLNR}$). The disease specific scale factor for total clearance ($FCYF_{CLT}$) was calculated as weighted average of $FCYF_{CLR}$ and $FCYF_{CLNR}$ by the following formula:

$$FCYF_{CLT} = \frac{CL_{POP,R} \cdot FCYF_{CLR} + CL_{POP,NR} \cdot FCYF_{CLNR}}{CL_{POP,R} + CL_{POP,NR}} \quad \text{Formula 3.2-15}$$

For our studies with sparse urine data, we used the following formula which directly estimates $FCYF_{CLT}$ instead of $FCYF_{CLR}$ and $FCYF_{CLNR}$ (parameters explained below):

$$CL_i = CL_{POP} \cdot F_{Size,CL,i} \cdot FCYF_{CLT} \cdot \exp(\eta_{BSVCLi}) \quad \text{Formula 3.2-16}$$

$CL_{POP}$ is the population estimate for total clearance of a healthy volunteer with standard size. $CL_i$ is the individual estimate for total clearance for the $i^{th}$ subject. $\eta_{BSVCLi}$ is the log scale difference of the individual estimates from their population mean ($CL_{POP}$) for the $i^{th}$ subject.

The individual volumes of distribution of a two-compartment model were estimated as follows (parameters explained below):

$$V1_i = V1_{POP} \cdot F_{Size,V,i} \cdot FCYF_V \cdot \exp(\eta_{BSVV1i}) \quad \text{Formula 3.2-17}$$

$$V2_i = V2_{POP} \cdot F_{Size,V,i} \cdot FCYF_V \cdot \exp(\eta_{BSVV2i}) \quad \text{Formula 3.2-18}$$

$$Vss_i = V1_i + V2_i \quad \text{Formula 3.2-19}$$

For a three-compartment model, the corresponding formulas are:

$$V1_i = V1_{POP} \cdot F_{Size,V,i} \cdot FCYF_V \cdot \exp(\eta_{BSVV1i}) \quad \text{Formula 3.2-20}$$

$$V2_i = V2_{POP} \cdot F_{Size,V,i} \cdot FCYF_V \cdot \exp(\eta_{BSVV2i}) \quad \text{Formula 3.2-21}$$

$$V3_i = V3_{POP} \cdot F_{Size,V,i} \cdot FCYF_V \cdot \exp(\eta_{BSVV3i}) \quad \text{Formula 3.2-22}$$

$$Vss_i = V1_i + V2_i + V3_i \quad \text{Formula 3.2-23}$$

$V1_{POP}$, $V2_{POP}$, and $V3_{POP}$ are the population estimates for the volume of distribution of the central compartment (V1), (shallow) peripheral compartment (V2), and deep peripheral (V3) compartment of a healthy volunteer with standard size. $Vss_i$, $V1_i$, $V2_i$, and $V3_i$ are the individual estimates for volume of distribution at steady-state, volume of central compartment, volume of the (shallow) peripheral compartment, and volume of the deep peripheral compartment for the $i^{th}$ subject, respectively. $\eta_{BSVV1i}$, $\eta_{BSVV2i}$, and $\eta_{BSVV3i}$ are log scale differences of the individual estimates from their population means ($V1_{POP}$, $V2_{POP}$, and $V3_{POP}$) for the $i^{th}$ subject, respectively.

### 3.2.5 Group estimates for CF-patients and healthy volunteers

As described above, we used body size/composition as a continuous covariate and presence or absence of CF as a categorical covariate in our BSV model. We tested for the effect of other covariates by plotting the individual estimates for clearance and volume of distribution vs. other covariates. However, there was often no obvious trend in those scatterplots.

We report the group estimates of clearance and volume of distribution for CF-patients and healthy volunteers of standard body size. The standard values for body size are shown in Table 3.2-2. The group estimates for renal ($CL_R$) and nonrenal clearance ($CL_{NR}$) as well as for volume of central (V1), (shallow) peripheral (V2), and deep peripheral compartment (V3) and for volume of distribution at steady-state (Vss) in CF-patients (CF) and healthy volunteers (H) are calculated as follows:

$$CL_R(CF) = CL_{POP,R} \cdot FCYF_{CLR} \quad \text{Formula 3.2-24}$$

$$CL_R(H) = CL_{POP,R} \cdot 1.0 \quad \text{Formula 3.2-25}$$

$$CL_{NR}(CF) = CL_{POP,NR} \cdot FCYF_{CLNR} \quad \text{Formula 3.2-26}$$

$$CL_{NR}(H) = CL_{POP,NR} \cdot 1.0 \quad \text{Formula 3.2-27}$$

$$V1(CF) = V1_{POP} \cdot FCYF_V \quad \text{Formula 3.2-28}$$

$$V1(H) = V1_{POP} \cdot 1.0 \quad \text{Formula 3.2-29}$$

$$V2(CF) = V2_{POP} \cdot FCYF_V \quad \text{Formula 3.2-30}$$

$$V2(H) = V2_{POP} \cdot 1.0 \quad \text{Formula 3.2-31}$$

$$Vss(CF) = (V1_{POP} + V2_{POP}) \cdot FCYF_V \quad \text{Formula 3.2-32}$$

$$Vss(H) = (V1_{POP} + V2_{POP}) \cdot 1.0 \quad \text{Formula 3.2-33}$$

*For a three-compartment model, group estimates for V3 and Vss were calculated as follows:*

$$V3(CF) = V3_{POP} \cdot FCYF_V \quad \text{Formula 3.2-34}$$

$$V3(H) = V3_{POP} \cdot 1.0$$ Formula 3.2-35

$$Vss(CF) = (V1_{POP} + V2_{POP} + V3_{POP}) \cdot FCYF_V$$ Formula 3.2-36

$$Vss(H) = (V1_{POP} + V2_{POP} + V3_{POP}) \cdot 1.0$$ Formula 3.2-37

*Group estimates for total clearance (CL) in studies with sparse urine data:*

$$CL(CF) = CL_{POP} \cdot FCYF_{CL}$$ Formula 3.2-38

$$CL(H) = CL_{POP} \cdot 1.0$$ Formula 3.2-39

$F_{Size,CL,i}$ and $F_{Size,V,i}$ are 1.0 for standard body size and therefore do not appear in these equations.

### 3.2.6 Selecting the number of compartments for the analysis of an individual antibiotic and for the meta-analysis

Our meta-analysis of all ten studies in CF-patients was based on estimates for two-compartment models for all drugs except fleroxacin, for which a one compartment model was more appropriate. The use of the same number of compartments is an essential advantage for a meta-analysis.

For analysis of the individual antibiotics, we selected the best structural model. Three compartment models were slightly superior to two-compartment models for some drugs. Therefore, the results of these three compartment models are described in the individual chapters for each antibiotic, although the meta-analysis was based on two-compartment models for those drugs.

### 3.2.7 Assessing the uncertainty of population PK parameters by non-parametric bootstrap techniques

To quantify the uncertainty in the estimated PK parameters and their BSV, we used non-parametric bootstrap techniques and ran (at least) 1,000 replicates for each size model (see also chapter 2.6.4). Each replicate contained the raw data of the same number of CF-patients and healthy

volunteers as the original raw dataset (balanced bootstrap datasets). The non-parametric 90% confidence intervals (5% to 95% percentile) were derived for each PK parameter from the 1,000 estimated PK parameter sets of each size model.

As the distribution of the population PK parameters from those 1,000 bootstrap replicates represents the uncertainty in the PK parameter estimates, it is possible to derive a p-value by comparing the percentiles of this distribution against a reference value (for example, how many of the 1,000 runs had an estimated $FCYF_{CLR} > 1.0$). The corresponding percentile of this distribution represents a one-sided p-value.

### 3.2.8 Monte Carlo simulations for CF-patients and healthy volunteers

We used the methods described in chapter 2.7.2 for the MCS of our studies in CF-patients and healthy volunteers. We used the PKPD targets shown in Table 2.7-1 (page 67). We simulated all dosage regimens at steady-state in absence of residual error. At least 9,000 virtual CF-patients and 9,000 virtual healthy volunteers with the same demographic data as the subjects in the respective study were simulated for each dosage regimen.

As described in chapter 2.7.2, we derived the PTA by calculating the fraction of subjects who attained the PKPD target at each MIC. The PKPD breakpoint was defined as the highest MIC for which the PTA was at least 90%. In order to determine the clinical relevance of the differences in PTAs between CF-patients and healthy volunteers, we calculated the PTA expectation value (also called cumulative fraction of response (334)). The PTA expectation value is the probability of target attainment in a specific target population (e. g. CF-patients) with infections caused by bacteria from a specific MIC distribution (ideally the MIC distribution of each local hospital). Thus, the PTA expectation value can be interpreted as the probability of successful treatment of CF-patients at the local hospital in empiric therapy.

## 3.3 Systematic comparison of the PKPD of intravenous antibiotics between CF-patients and healthy volunteers

### 3.3.1 Population pharmacokinetics and pharmacodynamics of piperacillin

#### 3.3.1.1 Chemical structure of piperacillin

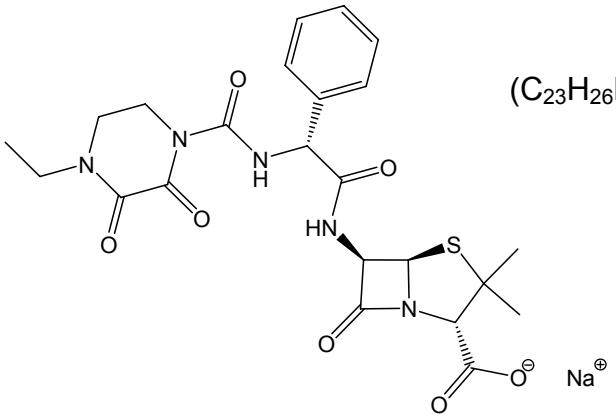

($C_{23}H_{26}N_5NaO_7S$, Mol. Wt.: 539.54)

**Chemical structure 3.3-1** Piperacillin

#### 3.3.1.2 Use of piperacillin in patients with cystic fibrosis

About 30% of the children aged 2-5 years and 81% of adults (aged 26-30 years) with CF are infected by *P. aeruginosa* (105) and respiratory diseases are the primary reason for frequent hospitalization of CF-patients and a primary cause of mortality (12, 283, 400). Piperacillin in combination with the beta-lactamase inhibitor tazobactam has good bactericidal activity against gram-positive microorganisms and *P. aeruginosa* also in CF-patients (308, 317, 383, 437). The combination is frequently used in the empirical treatment of hospital acquired infections and for treatment of pulmonary exacerbations in CF-patients (217). There are reports that *P. aeruginosa*

isolates from non-CF-patients show a better susceptibility to antipseudomonal agents (185) than isolates from CF-patients (386, 486). As *P. aeruginosa* can only be eradicated in the early stage in therapy of CF-patients (65), early aggressive treatment against this pathogen is vital (191) as is optimization of the probability of successful treatment against *P. aeruginosa*.

It is now generally agreed upon that population PK in combination with MCS is the method of choice to predict the probability of successful antibiotic treatment. However, a MCS has not yet been used to determine the PKPD profile of piperacillin in CF-patients. Even though knowledge of the PK in the desired patient population (e. g. in CF-patients) is a prerequisite for a well-founded MCS, there is no PK study with piperacillin in CF-patients which included a healthy volunteer control group. Such a comparison would help to explain a possibly altered PK in CF-patients which could affect the PKPD profile in CF-patients (105, 502).

Population PK can directly study the influence of body size, body composition, and disease state on PK and is also a powerful concept to compare the PKPD characteristics between CF-patients and healthy volunteers. Therefore, our first objective was to compare the PK of piperacillin between CF-patients and healthy volunteers via population PK. As our second objective, we studied whether the average differences and the BSV in clearance and volume of distribution are better described by $FFM_C$ or $FFM_J$ than by WT. Our third objective was to study the influence of patient related differences in PK parameters on PD characteristics of piperacillin given as various dosage regimens.

#### 3.3.1.3 Methods

The general clinical and sample handling procedures, the methods for PK analysis (including NCA and population PK), and the general methods for MCS are described in chapter 2. Chapter 3.2 shows the specific methods applied for analysis of our CF-studies.

***Subjects:*** A total of 34 Caucasian volunteers (eight adult CF-patients and 26 adult healthy volunteers) of both sexes participated in the study. Table 3.3-1 shows the demographic data.

**Table 3.3-1** Demographic data of the piperacillin study (average ± SD)

| | **CF-patients** | **Healthy volunteers** |
|---|---|---|
| Number of subjects (males / females) | 8 (5 / 3) | 26 (13 / 13) |
| Height (cm) | 160 ± 11.9 | 174 ± 8.4 |
| Total body weight (kg) | 43.1 ± 7.8 | 71.1 ± 11.8 |
| Fat-free mass° (kg) | 37.2 ± 6.9 | 56.4 ± 7.2 |
| Fat-free mass# (kg) | 36.0 ± 8.1 | 55.8 ± 6.8 |
| Body mass index (kg $m^{-2}$) | 16.7 ± 1.1 | 23.6 ± 3.7 |

°: Calculated by the formula of Cheymol and James (72, 222).

#: Calculated by the formula of Janmahasatian et al. (224).

***Drug administration:*** Each subject received a dose of 4g piperacillin as 5 min intravenous infusion except for one CF-patient who received a dose of 3g piperacillin. All infusions were administered with a BRAUN-Perfusor® (Braun, Melsungen, Germany).

***Blood sampling:*** Blood samples were drawn immediately before start of infusion (0 min), at the end of infusion (5 min), as well as at 5, 10, 15, 20, 30, 45, 60, 90 min and 2, 2.5, 3, 3.5, 4, 5, 6, 8, 10, 12, and 24 h post end of infusion.

***Drug analysis:*** Piperacillin concentrations in plasma were determined by HPLC. For determination of piperacillin in plasma 100 µL of the sample were deproteinized with 200 µL acetonitrile containing the internal standard. After mixing and centrifugation at 15,000 rpm, 40 µL were injected onto the HPLC-system. Piperacillin was determined using a reversed phase column, potassium dihydrogen phosphate/acetonitrile mobile phase (pH 6.2) with a flow of 2 mL/min. Piperacillin and the internal standard were detected at 220 nm.

The plasma samples were measured against a plasma calibration row. The calibration row was prepared by a 10:1 dilution of a tested drug-free plasma with a stock solution to obtain the highest calibration level. The other calibration levels were obtained by 1:1 dilution of the highest calibration level or a level of higher concentration with drug-free plasma.

For control of inter-assay variation spiked quality controls in plasma were prepared by adding defined volumes of the stock solution or the spiked control of higher concentration to defined volumes of tested drug-free plasma. No interferences were observed in plasma for piperacillin and the internal standard. Calibration was performed by linear regression. The linearity of piperacillin calibration curves in plasma was shown between 0.200 and 150 mg/L. The quantification limits were identical with the lowest calibration levels. The inter-day precision and the analytical recovery of the spiked quality control standards of piperacillin in human plasma ranged from 3.5 to 9.2% and from 95.0 to 106.9%, respectively.

***MCS:*** We studied the following dosage regimens: 1) continuous infusion of 9g / 70kg WT per day, 2) prolonged (4 h) infusion of 3g / 70kg WT q8h (daily dose: 9g), and 3) short-term (30 min) infusion of 3g / 70kg WT q4h (daily dose: 18g). We studied a range of MICs from 0.5 to 128 mg/L and assumed a protein binding of 30% for piperacillin (13, 459).

The PTA expectation value was calculated based on published MIC distributions. These comprised susceptibility data on *P. aeruginosa*, *E. coli*, and *K. pneumoniae* from the 2002 MYSTIC program in North America (273) and in South America (254), *P. aeruginosa* data from the Hartford Hospital, CT, USA (274), as well as data on non-mucoid and mucoid *P. aeruginosa* isolates from CF-patients in Freiburg, Germany (437), and in Leipzig, Germany (467).

#### 3.3.1.4 Results

***NCA:*** Figure 3.3-1 shows the average plasma concentrations of CF-patients and healthy volunteers after a 5 min infusion of 4g piperacillin. Table 3.3-2 lists the results of NCA for CF-patients and healthy volunteers. These parameters are not scaled by any size descriptor. Total clearance was 25% lower in CF-patients and volume of distribution at steady-state was 31% smaller in CF-patients than in healthy volunteers. CF-patients had higher peak concentrations, a shorter half-life, and a shorter mean residence time compared to healthy volunteers.

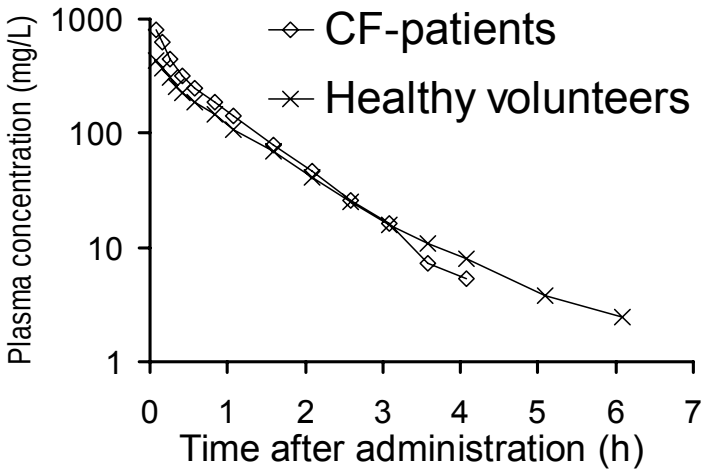


**Figure 3.3-1** Average plasma concentrations of piperacillin for CF-patients and healthy volunteers after a single 5 min intravenous infusion of 4g piperacillin

***Population PK analysis:*** The VPC indicated a very good predictive performance for the two and three compartment model. The one compartment model had insufficient predictive performance. The objective function was 253 points better for the two than for the one compartment model. As the two compartment model had highly sufficient predictive performance, we selected it as our final model.

**Table 3.3-2** Unscaled PK parameters derived by NCA (median [range])

| | CF-patients | Healthy volunteers |
|---|---|---|
| Total clearance (L/h) | 8.78 [6.39 - 12.1] | 11.7 [6.25 - 14.5] |
| Volume of distribution at steady-state (L) | 8.13 [5.16 - 10.8] | 11.8 [9.06 - 30.6] |
| Peak concentration (mg/L) | 767 [408 - 1044]*,# | 446 [272 - 721] |
| Terminal half-life (L) | 0.69 [0.34 - 1.19] | 1.05 [0.49 - 7.52] |
| Mean residence time (h) | 0.85 [0.66 - 1.03] | 1.02 [0.79 - 3.49] |

*: Normalized to a dose of 4g piperacillin, since one CF-patient received a dose of 3g instead of 4g.

#: Only four CF-patients had a blood sample drawn directly at the end of the infusion. The other four CF-patients had blood draws 5-12 min post end of infusion. The peak concentration provided here was the highest observed concentration in all eight CF-patients. The true peaks in CF-patients were probably higher than the observed peaks.

Figure 3.3-2 reveals the very good predictive performance for the final model which was based on allometric scaling by $FFM_C$. The final estimates for this model are shown in Table 3.3-3. The disease specific scale factors $FCYF_{CLT}$ and $FCYF_V$ shown in Table 3.3-4 are the ratios of group estimates between CF-patients and healthy volunteers after accounting for body size (functional capacity) by the respective size model.

We distinguished the different size models 1) by their estimates for the disease specific scale factors FCYF and 2) by their ability to describe the BSV in clearance and volume of distribution. CF-patients had a 27% lower total clearance and a 40% lower volume of distribution compared to healthy volunteers, when no size descriptor was included (see size model A, Table 3.3-4). For all other size models $FCYF_V$ was close to the ideal value of 1.0 (range: 0.926 to 0.999). However, total clearance was estimated to be 20% larger in CF-patients than in healthy volunteers for linear scaling by WT. For the three allometric size models, total clearance was estimated to be very similar (range: 1.00 to 1.06) between both subject groups.

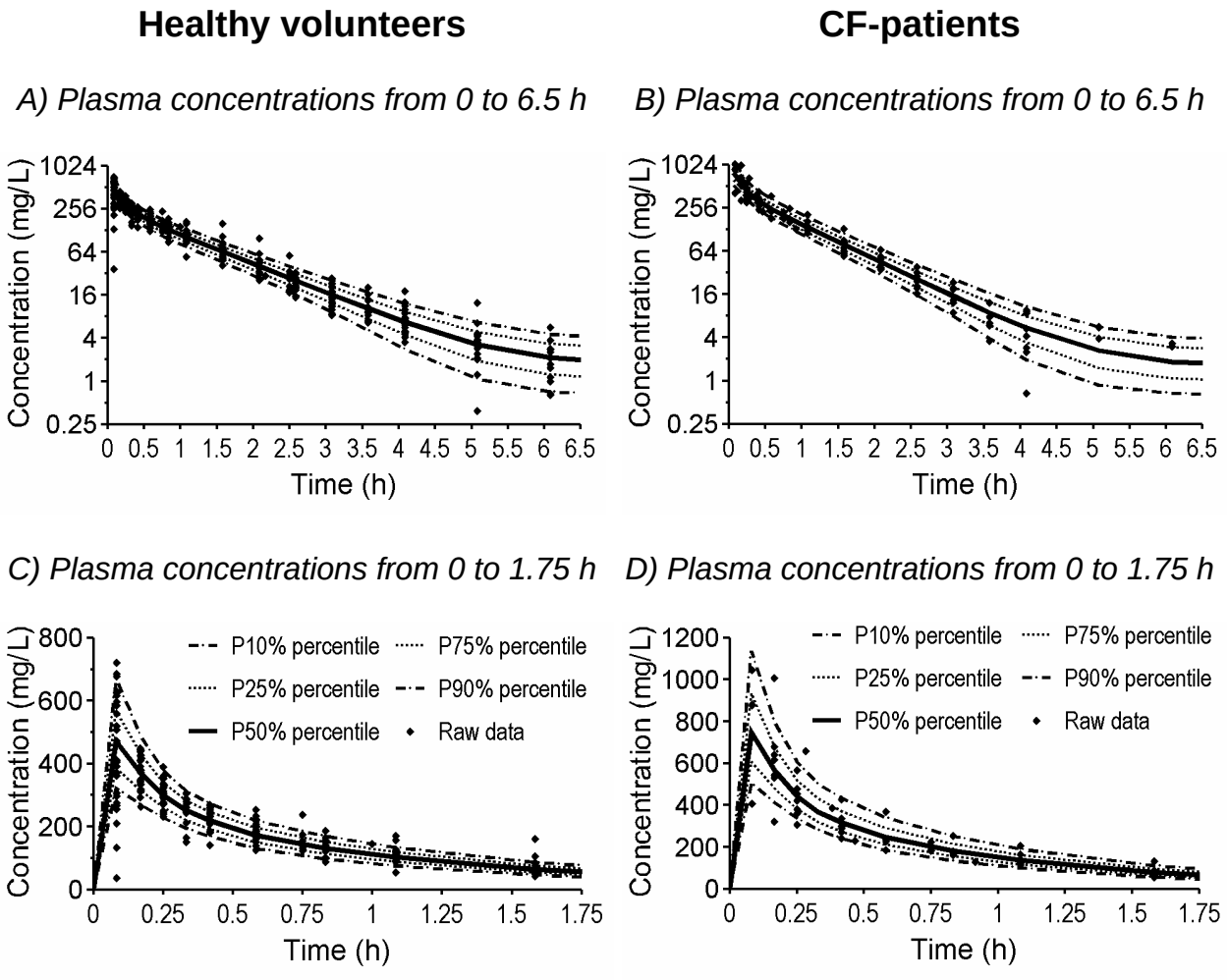


**Figure 3.3-2** VPC based on 8,000 CF-patients and 26,000 healthy volunteers for the two compartment model based on $FFM_C$ (see Table 3.3-3).

See chapter 2.6.3 for interpretation of VPCs.

We also compared the ability of the different size models to explain the BSV. Table 3.3-5 shows that allometric scaling by $FFM_C$ or $FFM_J$ explained more of the variability than linear scaling by WT. Allometric scaling by $FFM_C$ or $FFM_J$ reduced the BSV in clearance by about 25% and the BSV in volume of central compartment by about 12% relative to linear scaling by WT.

**Table 3.3-3** PK parameter estimates for the allometric size model based on $FFM_C$

| Parameter | Unit | Estimate for | | Coefficient of variation (%)° |
|---|---|---|---|---|
| | | CF-patients | healthy volunteers | |
| CL | L $h^{-1}$ | 11.3* | 11.3* | 10.4 |
| Vss^ | L | 9.61* | 10.4* | |
| V1 | L | 6.49* | 7.01* | 26.0# |
| V2 | L | 3.12* | 3.37* | 34.2# |
| CLic | L $h^{-1}$ | 12.8* | | |
| TK0 (fixed) | min | 5 | | |
| $CV_C$ | % | 13.2 | | |
| $SD_C$ | mg/L | 1.88 | | |

*: Group estimate for subject of standard size ($FFM_C$ = 53 kg).

^: Derived from model estimates, not an estimated parameter.

°: Apparent coefficients of variation for the BSV.

#: Coefficient of correlation for the random variability between V1 and V2, r = -0.80.

See chapter 2.6.2 for explanation of model parameters.

**Table 3.3-4** Ratios of group estimates (CF-patients / healthy volunteers) for clearance and volume of distribution for different size models

| Size model | $FCYF_{CLT}$ | $FCYF_V$ |
|---|---|---|
| A) No size model | 0.729 | 0.598 |
| B) WT linear scaling | 1.20 | 0.997 |
| C) WT allometric | 1.06 | 0.999 |
| D) $FFM_C$ allometric | 1.00 | 0.926 |
| E) $FFM_J$ allometric | 1.03 | 0.957 |

$FCYF_{CLT}$: Ratio of group estimates for total clearance in CF-patients divided by total clearance in healthy volunteers.

$FCYF_V$: Ratio of group estimates for volume of distribution at steady-state in CF-patients divided by volume of distribution at steady-state in healthy volunteers.

**Table 3.3-5** Comparison of BSV (variances) between various size models: The table shows the relative between subject variances for the respective PK parameter and size models.

| Size model | Relative between subject variance | | |
|---|---|---|---|
| | CL | V1 | V2 |
| B) WT linear scaling | 100%* | 100%* | 100%* |
| C) WT allometric | 88%° | 101% | 105% |
| D) $FFM_C$ allometric | 74%° | 87% | 95% |
| E) $FFM_J$ allometric | 75%° | 88% | 91% |

*: The BSV for linear scaling by WT was used as reference.

°: The lower this number, the more variability was explained by the respective size model. These values mean that the BSV (variance) for total clearance was reduced by 12% for allometric scaling by WT, by 26% for allometric scaling by $FFM_C$, and by 25% for allometric scaling by $FFM_J$, all compared to linear scaling by WT.

***MCS:*** CF-patients had slightly lower PTAs which resulted in similar PKPD breakpoints for the studied dosage regimens (see Figure 3.3-3). Continuous infusion of 9g / 70kg WT per day had a PKPD breakpoint of 16 mg/L for both targets in CF-patients and healthy volunteers. For a dose of 3g / 70kg WT q8h (daily dose: 9g), prolonged (4 h) infusion had a PKPD breakpoint of 16 mg/L in CF-patients and healthy volunteers for near-maximal bactericidal activity. For this dosage regimen, CF-patients had a breakpoint of 24 mg/L and healthy volunteers of 32 mg/L for bacteriostasis. At a daily dose of 18g, the short-term infusions of 3g / 70kg WT q4h had a near-maximal kill breakpoint of 12 mg/L in CF-patients and 16 mg/L in healthy volunteers and a bacteriostasis breakpoint of 32 mg/L in both subject groups.

The PTA expectation values for CF-patients and healthy volunteers with the same demographic data as the subjects in our study are shown in Table 3.3-6. PTA expectation values differed only by 3.2% or less between the three dosage regimens in each subject group, although daily doses of 9g and 18g were studied in these dosage regimens.

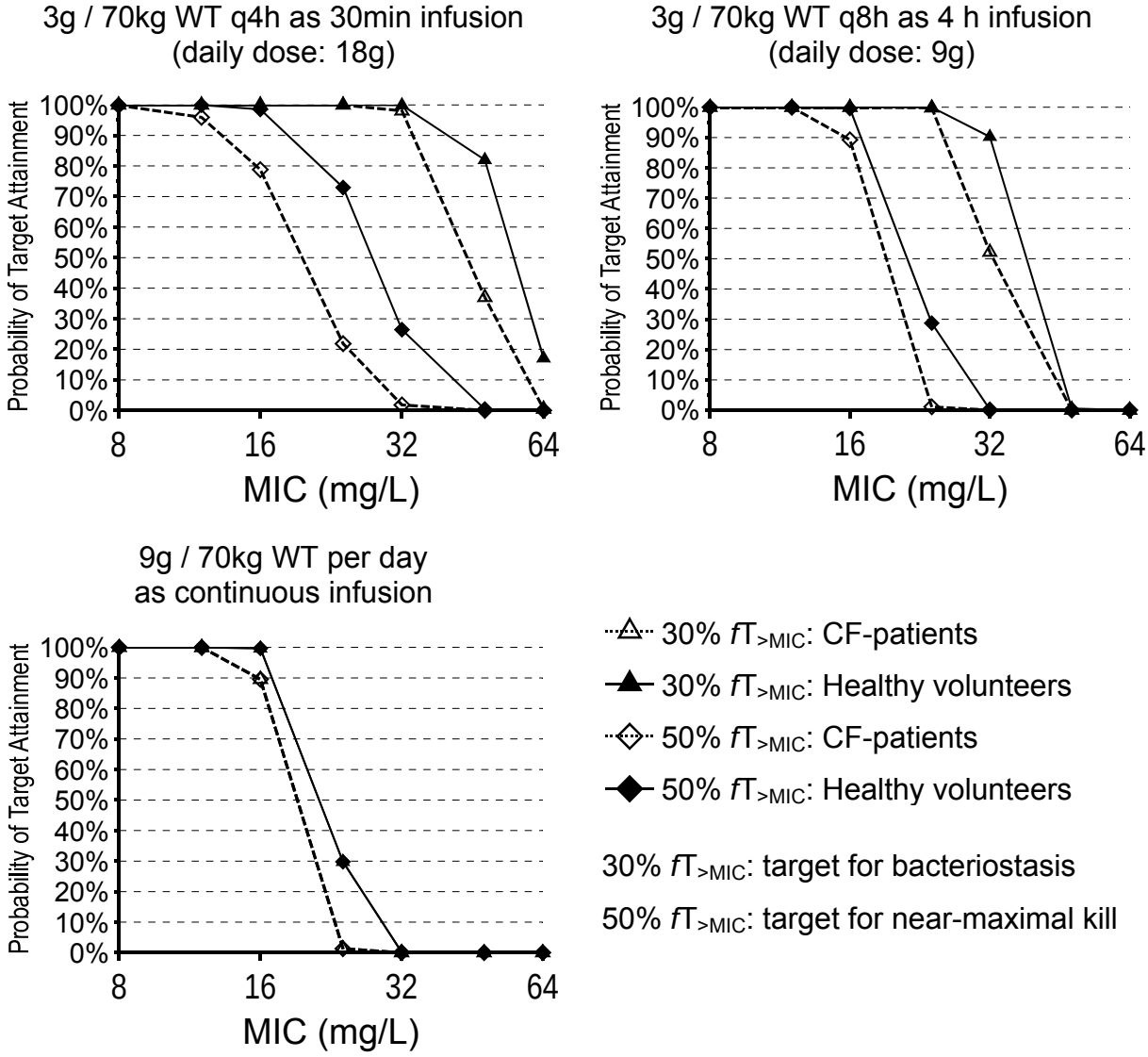


**Figure 3.3-3** Probability of target attainment for various dosage regimens of piperacillin at steady-state

The maximum difference in PTA expectation values between CF-patients and healthy volunteers was 5.5%. When we calculated the individual PTA expectation values shown in Table 3.3-6 for the bacteriostasis target ($fT_{>MIC} \geq 30\%$) instead of the near-maximal kill target, we obtained the same PTA expectation values for the bacteriostasis target for continuous infusion. When we calculated the PTA expectation values based on the bacteriostasis target for prolonged and short term infusion, we obtained slightly higher individual PTA expectation values (median [range]: 4.5% [0.2 to 14.8%]) for the bacteriostasis target than for the near-maximal kill target ($fT_{>MIC} \geq 50\%$).

**Table 3.3-6** Expectation values for target attainment for the CF-patients and healthy volunteers in our study based on the PKPD target for near-maximal bactericidal effect ($fT_{>MIC} \geq 50\%$) in combination with published MIC distributions

| Source | Pathogen | **Continuous infusion** | | **Prolonged (4h) infusion** | | **Short-term (30min) infusion** | |
|---|---|---|---|---|---|---|---|
| | | 9g/70kg WT / day | | 3g / 70kg WT q8h | | 3g / 70kg WT q4h | |
| | | CF-patients | Healthy volunteers | CF-patients | Healthy volunteers | CF-patients | Healthy volunteers |
| MYSTIC 2002, North America (273) | *P. aeruginosa* (n=427) | 82.2% | 83.4% | 82.2% | 83.4% | 81.0% | 84.9% |
| | *E. coli* (n=433) | 97.3% | 97.4% | 97.3% | 97.4% | 97.1% | 97.4% |
| | *K. pneumoniae* (n=288) | 94.3% | 94.8% | 94.3% | 94.8% | 93.8% | 95.0% |
| MYSTIC 2002, South America (254) | *P. aeruginosa* (n=233) | 43.2% | 44.2% | 43.1% | 44.1% | 42.4% | 47.1% |
| | *E. coli* (n=98) | 85.6% | 86.8% | 85.6% | 86.8% | 84.5% | 88.0% |
| | *K. pneumoniae* (n=92) | 71.3% | 71.8% | 71.3% | 71.7% | 70.9% | 72.9% |
| Hartford, CT, USA (274) | *P. aeruginosa* (n=557) | 92.7% | 93.6% | 92.7% | 93.6% | 92.6% | 95.0% |
| ***Isolates from CF-patients*** | | | | | | | |
| Freiburg, Germany (437) | *P. aeruginosa*, non-mucoid strains (n=229) | 64.5% | 65.9% | 64.4% | 65.9% | 63.1% | 68.0% |
| | *P. aeruginosa*, mucoid strains (n=156) | 65.5% | 66.7% | 65.4% | 66.6% | 64.4% | 69.9% |
| Leipzig, Germany (467) | *P. aeruginosa* (n=38) | 88.6% | 89.5% | 88.6% | 89.4% | 87.8% | 90.1% |

WT: Total body weight.

PTA expectations values were lower for susceptibility data from South America (86% for *E. coli* and 71% for *K. pneumoniae*) than from North America (97% for *E. coli* and 94% for *K. pneumoniae*), as shown in Table 3.3-6. The differences between PTA expectation values from different regions were even more pronounced for *P. aeruginosa*. PTA expectation values were about 93% for the MIC distribution of the Hartford Hospital, 82% for the 2002 MYSTIC data from North America, and only 43% for the 2002 MYSTIC data from South America. For the *P. aeruginosa* isolates from German CF-patients, PTA expectation values were about 89% for Leipzig and about 65% for Freiburg. PTA expectation values for the non-mucoid and mucoid strains were similar.

#### 3.3.1.5 Discussion

Medical advances have led to tremendous improvements in the life-expectancy and quality of life for CF-patients during the last 70 years. In the 1930s, the average life-expectancy of CF-patients was only a few months. The median survival age of CF-patients increased to 14 years in 1969 and to 31.3 years in 1996 in the US (12). The probability of surviving 40 years was even 83.3% in 1995 in Denmark for a diagnosed CF-patient (141). This improved life-expectancy seems to correlate with early treatment of *P. aeruginosa* (141) as it is almost impossible to eradicate this pathogen once a chronic infection is established. Early aggressive treatment was shown to prevent or delay chronic *P. aeruginosa* infection significantly (139, 192) and resulted in a probability of >80% for still not having developed a chronic *P. aeruginosa* infection 7 years after the first isolation of this pathogen in the respective patient (140).

European experts strongly recommended the use of local susceptibility patterns for treatment of *P. aeruginosa* (105). As the time required to identify *P. aeruginosa* and to assess its antibiotic susceptibility from a sputum culture is about 3-4 days, efficacious empiric therapy is very important. Data on the effectiveness of intravenous antibiotic treatment in CF-patients are rather sparse and large randomized controlled trials are required (80, 125, 310).

There is also no ideal biomarker for the long-term progression of respiratory insufficiency or survival of CF-patients (310).

MCS offers a tool to overcome this shortage of data. A PKPD target, e. g. for near-maximal bactericidal activity, is used as surrogate marker for successful clinical outcome in a MCS. However, knowledge of the PK in the relevant patient population (e. g. in CF-patients) is a prerequisite to apply a MCS, since MCS combines the patient specific PK parameters and their variability with the specific susceptibility data from a local hospital.

Population PK is a powerful method to study the influence of body size, body composition, and disease state on the PK in CF-patients quantitatively. Our population PK analysis aimed at estimating both the differences in average PK parameters between CF-patients and healthy volunteers as well as the PK parameter variability. Our final model had a highly sufficient predictive performance for both the average plasma concentration time profiles of piperacillin and their variability (see Figure 3.3-2). Therefore, we used it to compare the PD profiles between both subject groups via MCS.

Our results for the PK parameters of piperacillin in healthy volunteers were well within the range of those from other authors (32, 39, 297, 493). The literature data on the PK of piperacillin in CF-patients are sparse. The data reported show a rather wide variability in PK parameters. None of the studies included a healthy volunteer control group which makes it difficult to interpret the differences in the observed results between studies. The average terminal half-life of piperacillin is between 0.54 and 0.89 h in children and adolescents (101, 200, 217, 315, 393) with CF and 1.2 $\pm$ 0.9 h in adult (age: 25.8 $\pm$ 3.6 yrs) CF-patients (520). We determined a terminal half-life of 0.69 [0.34 - 1.19] h (median [range]) in our adult CF-patients (age: 21.1 $\pm$ 3.8 yrs) which is well within the range of half-lives reported by other authors.

For CF-patients volume of distribution was reported to be 0.4 L/kg (217) in children, 0.64 L/kg (101, 200) and 0.17 L/kg in juveniles and young adults (101, 393), and 0.296 $\pm$ 0.11 L/kg (520) in adult CF-patients. Differences by a factor of 3.8 (maximum / minimum) are unlikely to be caused by differences in body composition (e. g. between young and adult CF-

patients). Total clearance was reported to be about 0.43 L/h/kg in children (age: 5 yrs, (217)), 0.497 L/h/kg (age: 8-16 yrs, (101, 200)) and 0.188 L/h/kg (age: 12-21 yrs, (101, 393)) in juveniles and young adults, 0.23 ± 0.04 L/h/kg for intermittent treatment and 0.43 ± 0.21 L/h/kg for continuous infusion in adult CF-patients (520). Although higher clearances in L/h/kg are often observed in younger (and smaller) patients compared to adults, a difference by a factor of 2.6 between the two juvenile-adult subject groups seems very large. This underlines the need to include a healthy volunteer control group to compare the PK of CF-patients to the PK in healthy volunteers within the same study. Some of those large differences might also be due to inadequate scaling of CF-patients for body size and body composition.

Our CF-patients had a 39% lower WT than the healthy volunteers (see Table 3.3-1) and $FFM_C$ as well as $FFM_J$ were about 35% lower in CF-patients. Our NCA showed a 31% lower unscaled volume of distribution at steady-state and a 25% lower unscaled total clearance in CF-patients (see Table 3.3-2). The terminal-half-life was 34% shorter and the mean residence time was 17% shorter in CF-patients.

Our population PK analysis aimed at ranking the different size models according to 1) their ability to describe the average differences between CF-patients and healthy volunteers and 2) their ability to reduce the unexplained BSV. In the absence of a size descriptor (size model A, Table 3.3-4), CF-patients had a 27% lower clearance and a 40% lower volume of distribution, because they were smaller. Size models B to E estimated $FCYF_V$ very close to 1.0 (range: 0.926-0.999). Scaling clearance linearly by WT over-accounted for the fact that our CF-patients were smaller. CF-patients had a 20% higher clearance expressed as L/h/kg (linear scaling by WT), because WT ignores that CF-patients were leaner than healthy volunteers. Allometric scaling by WT, $FFM_C$, or $FFM_J$ yielded estimates very close to 1.0 (range: 1.00-1.06). Therefore, all three allometric size models explained the average differences in volume of distribution and clearance between CF-patients and healthy volunteers adequately.

Besides the ability of the various size models to describe the average differences in clearance and volume, we studied the ability of these models to explain the BSV. This is important in empiric therapy, as target concentrations can be attained more precisely the more BSV is explained by a size descriptor. Allometric scaling by $FFM_C$ or $FFM_J$ (see Table 3.3-5) reduced the unexplained BSV in CL by about 25% and the unexplained BSV in V1 by about 12% compared to linear scaling by WT. Thus, allometric scaling by $FFM_C$ or $FFM_J$ described the average differences in clearance and volume and reduced the unexplained BSV compared to linear or allometric scaling by WT. This result seems reasonable, because $FFM_C$ and $FFM_J$ account for body composition, whereas WT does not.

We used the population PK model based on $FFM_C$ to calculate the PTA in CF-patients. In our PK model we used a non-saturable elimination, although the elimination of piperacillin may be saturable (39, 493, 520). However, we could show by exhaustive MCS for our three studied dosage regimens and for the MIC distributions used herein, that this model choice did not affect the PKPD breakpoints and that the differences between saturable and non-saturable PK models is less than ±3% for the PTA expectation values for the selected dose range of 9 to 18g daily. Therefore, the PKPD breakpoints and PTA expectation values from our non-saturable PK model are valid for the studied dosage regimens, since the PK of piperacillin appears as “pseudo-linear” for the studied dosage regimens, although it is truly nonlinear.

CF-patients had only slightly lower PTAs (see Figure 3.3-3) which resulted in similar PKPD breakpoints compared to healthy volunteers. We studied continuous infusion and prolonged (4 h) infusion q8h at a daily dose of 9g / 70kg WT as well as short-term (30 min) infusion q4h at a daily dose of 18g / 70kg WT. Remarkably, continuous and prolonged infusions achieved the same PKPD breakpoint for near-maximal killing of about 16 mg/L at a 50% lower daily dose compared to short-term infusions. Our PKPD breakpoint is in good agreement with the PKPD breakpoint determined by Lodise et al. (297) via MCS and with the breakpoint of 16 mg/L for susceptibility specified by the BSAC (56) and the CLSI (353), as well as the DIN breakpoints (104) of ≤4 mg/L for susceptibility and >32 mg/L for resistance. The dose reduction

from 18g to 9g daily underlines the benefit of prolonged and continuous infusion compared to short-term infusion with regard to drug acquisition costs and a possibly lower risk for adverse events.

Early aggressive treatment of *P. aeruginosa* may require very high piperacillin doses which carry an increased risk for adverse events. Doses up to 900 mg/kg daily divided into six doses (equivalent to 63g for a 70kg patient, assuming a linear increase of dose with WT) have been administered to CF-patients aged 12 years or less (402). A distinct serum-sicknesslike adverse reaction was observed in 32% of these patients and its incidence appeared to be correlated with the piperacillin dose. Adverse events after piperacillin treatment in CF-patients were also reported by other authors (370, 427, 473, 475).

As the options for efficacious antipseudomonal treatment become increasingly fewer due to emergence of resistance, prolonged infusion of piperacillin seems to be an appealing option which can combine a high probability for clinical success and a possibly lower risk for adverse events secondary to considerably lower daily doses.

To determine the clinical relevance of the observed PTAs, we calculated the PTA expectation values for various MIC distributions. The PTA expectation values differed only slightly (<5.5%) between CF-patients and healthy volunteers for the studied MIC distributions. PTA expectation values for *E. coli* and *K. pneumoniae* from the 2002 MYSTIC data in North America as well as for the *P. aeruginosa* data at the Hartford Hospital were robust (>92%) for all three studied dosage regimens (see Table 3.3-6). Secondary to a decreased susceptibility of the *P. aeruginosa* isolates in the 2002 MYSTIC data, PTA expectation values were only 82% in North America and 43% in South America. When we studied MIC distributions in German CF-patients, PTA expectation values against *P. aeruginosa* were between 64 and 89%. These differences underline the importance to use the MIC distribution of each local hospital to calculate the PTA expectation value for successful empiric treatment against each pathogen (105).

In conclusion we found a 25% lower unscaled total clearance and a 31% lower volume of distribution at steady-state in CF-patients compared to

healthy volunteers, because our CF-patients were smaller. Allometric scaling by WT, $FFM_C$, or $FFM_J$ explained the average differences in PK parameters better than linear scaling by WT. Linear scaling by WT predicted clearance in CF-patients to be 20% higher than in healthy volunteers, probably because WT does not account for body composition. Allometric scaling by $FFM_C$ or $FFM_J$ reduced the unexplained BSV by 25% for clearance and by 12% for volume of the central compartment relative to linear scaling by WT. This is important to achieve target concentrations more precisely in empiric therapy. Large clinical studies are warranted to show a higher probability of successful clinical outcome for dose selection in CF-patients based on $FFM_C$. The PKPD breakpoint for near-maximal bactericidal activity was 16 mg/L in CF-patients and healthy volunteers for 3g / 70kg WT q8h given as prolonged (4 h) infusion. PTA expectation values were between 64% and 89% for *P. aeruginosa* isolates from CF-patients in Germany. Clinical trials are warranted to compare the clinical cure rates and adverse events for prolonged infusion at an about 50% lower daily dose vs. short-term infusions at the full daily dose.

### 3.3.2 Population pharmacokinetics and pharmacodynamics of ceftazidime

#### 3.3.2.1 Chemical structure of ceftazidime

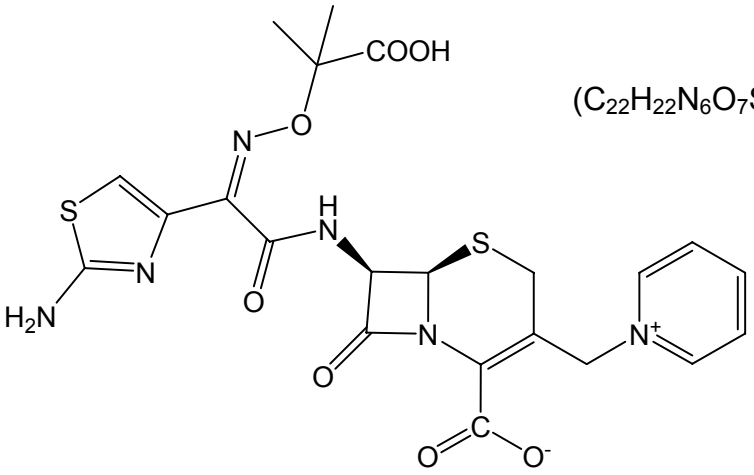


($C_{22}H_{22}N_6O_7S_2$, Mol. Wt.: 546.58)

**Chemical structure 3.3-2** Ceftazidime

#### 3.3.2.2 Use of ceftazidime in patients with cystic fibrosis

As described for piperacillin above, treatment of *P. aeruginosa* in CF-patients poses a significant challenge (105). Ceftazidime has a broad spectrum of activity against Gram-positive and Gram-negative aerobic bacteria (413), is one of the most active agents against *P. aeruginosa* isolates from CF-patients, and has some activity against *B. cepacia* (44, 68, 101, 308, 415, 418). Ceftazidime is an effective agent for the treatment of respiratory infections in CF- and other patients (17, 47, 397, 505). As *P. aeruginosa* can only be eradicated in the early stage in therapy of CF-patients (65), efficacious anti-infective treatment against *P. aeruginosa* is vital to prevent chronic infection by this pathogen (191). Therefore, the probability to achieve a successful microbiological and clinical outcome is very important.

Two groups compared the PK in CF-patients and healthy volunteers within the same study (182, 282). The authors find higher clearances (in L/h/kg) and shorter terminal half-lives in CF-patients, but did not systematically study the influence of these PK alterations on the PD profile of ceftazidime. As both a higher clearance and a shorter terminal half-life will decrease the probability to attain a PKPD target, this calls for identification of optimal dosage regimens in CF-patients.

We used population PK to study the influence of body size, body composition, and disease state on the PK of ceftazidime in CF-patients and healthy volunteers and to compare their PKPD profile. Our first objective was to compare the PK of ceftazidime between CF-patients and healthy volunteers. As our second objective, we studied whether the average differences and the BSV in clearance and volume of distribution are better described by LBM or FFM than by WT. Our third objective was to compare the PTA between various dosage regimens of ceftazidime.

#### 3.3.2.3 Methods

The general clinical and sample handling procedures, the methods for PK analysis (including NCA and population PK), and the general methods for MCS are described in chapter 2. Chapter 3.2 shows the specific methods applied for analysis of our CF-studies.

***Subjects:*** A total of 15 Caucasian volunteers (eight CF-patients and seven healthy volunteers) participated in the study. Table 3.3-7 shows the demographic data.

***Drug administration:*** The subjects received 2g ceftazidime as 5 min intravenous infusion. One CF-patient received 1.5g, one CF-patient received 1g, and one CF-patient received 3g instead of 2g ceftazidime. All infusions were administered with a BRAUN-Perfusor® (Braun, Melsungen, Germany).

***Blood sampling:*** Blood samples were drawn immediately before start of infusion (0 min), at end of infusion (5 min), as well as at 5, 10, 15, 20, 30, 45, 60, 90 min and 2, 2.5, 3, 3.5, 4, 5, 6, 8, 10, and 12 h post end of infusion.

**Table 3.3-7** Demographic data of the ceftazidime study (median [range])

| | **CF-patients** (n=8) | **Healthy volunteers** (n=7) |
|---|---|---|
| Height (cm) | 164 [105 - 176] | 175 [164 - 191] |
| Total body weight (kg) | 37.9 [14.2 - 73.5] | 67 [56 - 71] |
| Fat-free mass° (kg) | 34.7 [13.3 - 58.6] | 54.5 [46.7 - 60.5] |
| Fat-free mass# (kg) | 35.9 [13.9 - 57.7] | 54 [46.4 - 60.5] |
| Body mass index (kg $m^{-2}$) | 15.0 [12.5 - 23.7] | 21.7 [19.5 - 23.7] |

°: Calculated by the formula of Cheymol and James (72, 222).

#: Calculated by the formula of Janmahasatian et al. (224).

***Drug analysis:*** We determined the concentration of ceftazidime in plasma by reversed phase HPLC. An amount of 100 µL of $NaH_2PO_4$ buffer was added to 100 µL of each sample. Acetonitrile (400 µL) was used to deproteinize each sample. After centrifugation 1,000 µL of dichloromethane were added for extraction of the organic phase. From the remaining aqueous phase, 20 µL were injected into the HPLC system. After sample preparation, the prepared samples were stored in an ice-water bath until injection. We assured stability of ceftazidime under these conditions and used a LiChrosphere RP 18-5 µ (50 x 4mm) column with a water / acetonitrile mixture at pH 5.0. Ceftazidime was detected at a wavelength of 275 nm. Calibration was performed by linear regression. The ceftazidime assay was linear between 1.56 and 200 mg/L We took 30-40 mL blood from one additional subject at three time points with a high, intermediate, and low concentration. This subject did not participate in the PK study. Those blood samples were prepared like all other samples as described above and used as biological quality controls. We included these biological quality controls and spiked quality controls in each analytical run.

***MCS:*** We compared five dosage regimens all at a daily dose of 6g / 70kg WT ceftazidime: 1) 2g / 70kg WT q8h as short-term (30min) infusion, 2) 1.5g / 70kg WT q6h as short-term (30min) infusion, 3) 2g / 70kg WT q8h as prolonged (5h) infusion, 4) 1.5g / 70kg WT q6h as prolonged (4h) infusion,

and 5) continuous infusion of 6g / 70kg WT. We studied a range of MICs from 0.125 to 128 mg/L. As the protein binding for ceftazidime has been reported to range between 2 and 19% (178, 282, 335, 359), we assumed an average protein binding of 11% for ceftazidime.

We calculated the PTA expectation value based on published MIC distributions. These comprised susceptibility data on *P. aeruginosa*, *E. coli*, and *K. pneumoniae* from the 2002 MYSTIC program in North America (273) and in South America (254), *P. aeruginosa* isolates from three European CF-centers (158), as well as non-mucoid and mucoid *P. aeruginosa* isolates from CF-patients in Freiburg, Germany (437), and in Leipzig, Germany (467).

#### 3.3.2.4 Results

***NCA:*** Figure 3.3-4 shows the average plasma concentrations of CF-patients and healthy volunteers. The results from NCA are listed in Table 3.3-8. These parameters are not scaled by any size descriptor. Total clearance was 19% lower in CF-patients and volume of distribution at steady-state was 36% smaller in CF-patients compared to healthy volunteers. CF-patients had a 112% higher average peak concentration, a 24% shorter terminal half-life, and a 27% shorter mean residence time relative to healthy volunteers.

***Population PK analysis:*** The VPC indicated a highly sufficient predictive performance for the three compartment model which was slightly better than for the two compartment model. The one compartment model had insufficient predictive performance. The objective function was 46 points better for the three than for the two compartment model. Therefore, we selected the three compartment model as our final model.

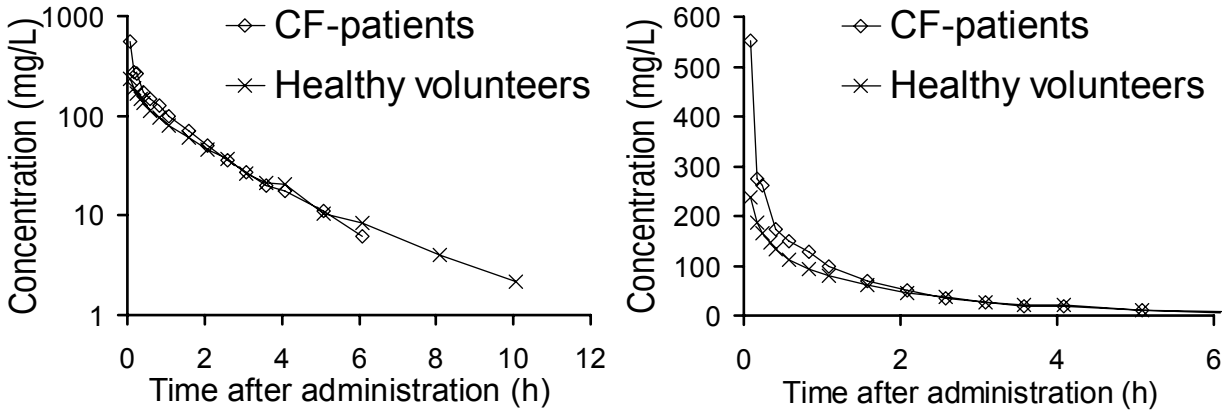


**Figure 3.3-4** Average plasma concentrations of ceftazidime for CF-patients and healthy volunteers after a single 5 min intravenous infusion of 2g ceftazidime

Concentrations were dose-normalized to 2g ceftazidime since three CF-patients received slightly lower or slightly higher doses.

**Table 3.3-8** Unscaled PK parameters derived by NCA (median [range])

| | **CF-patients** | **Healthy volunteers** |
|---|---|---|
| Total clearance (L/h) | 5.37 [3.35 - 12.8] | 6.59 [4.87 - 9.50] |
| Volume of distribution at steady-state (L) | 9.14 [2.77 - 19.9] | 14.3 [10.8 - 17.1] |
| Peak concentration (mg/L) | 445 [151 - 1200]* | 210 [148 - 397] |
| Terminal half-life (L) | 1.48 [0.49 - 1.78] | 1.94 [1.28 - 2.78] |
| Mean residence time (h) | 1.54 [0.62 - 2.35] | 2.10 [1.71 - 2.87] |

*: Normalized to a dose of 2g ceftazidime, since three CF-patient received slightly higher or slightly lower doses.

Figure 3.3-5 reveals the very good predictive performance for the final model which was based on allometric scaling by $FFM_J$. The final PK parameter estimates for this model are shown in Table 3.3-9. The disease specific scale factors $FCYF_{CLT}$ and $FCYF_V$ shown in Table 3.3-10 represent the ratios of group estimates between CF-patients and healthy volunteers after adjusting for body size by the respective size descriptor (WT, $FFM_C$ or $FFM_J$).

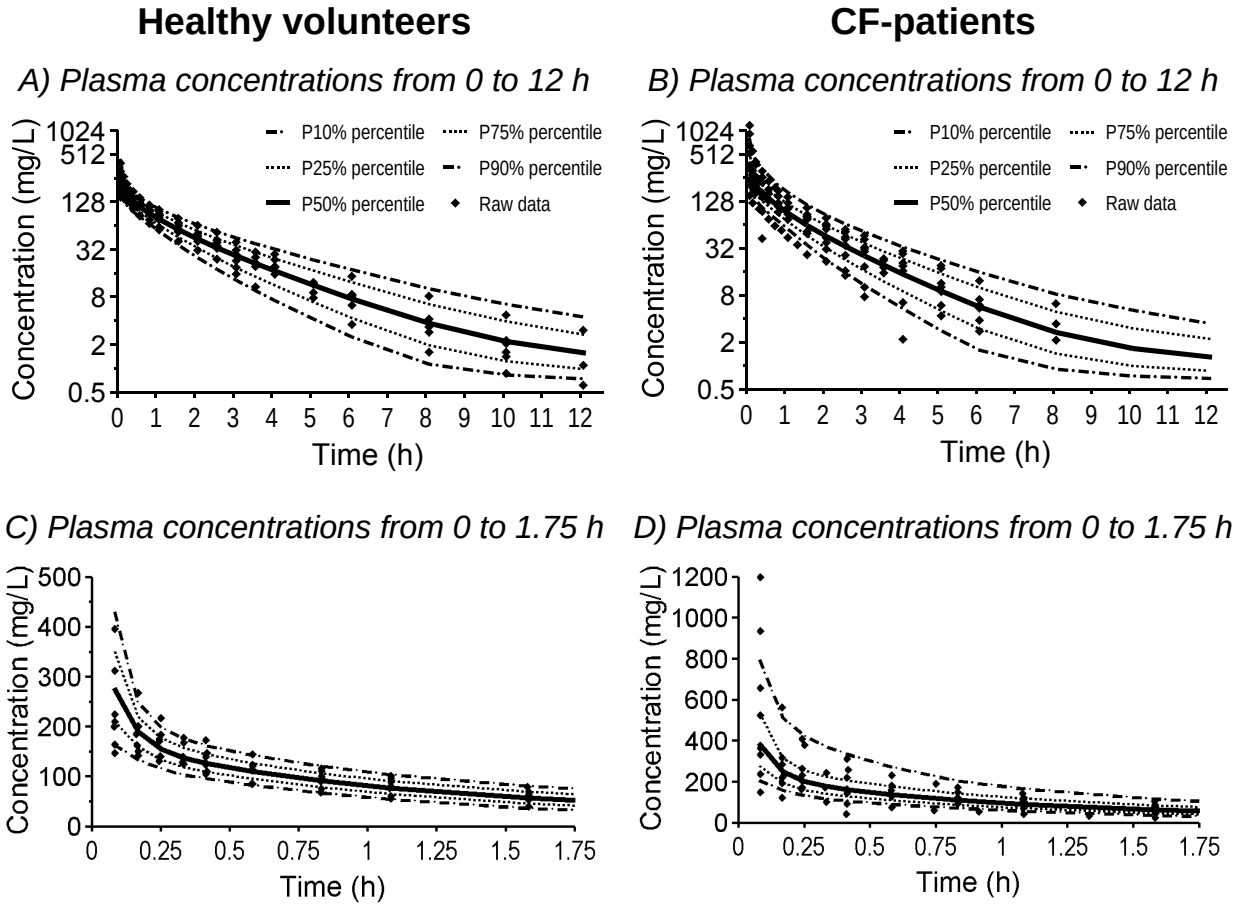


**Figure 3.3-5** VPC based on 8,000 CF-patients and 7,000 healthy volunteers for the three compartment model based on $FFM_J$ (see Table 3.3-9).

See chapter 2.6.3 for interpretation of VPCs.

**Table 3.3-9** PK parameters for the allometric size model based on $FFM_J$

| Parameter | Unit | Estimate for CF-patients | Estimate for healthy volunteers | Coefficient of variation (%)° |
|---|---|---|---|---|
| CL | L $h^{-1}$ | 7.82* | 6.68* | 28.3 |
| Vss^ | L | 12.8* | 12.7* | |
| V1 | L | 5.73* | 5.67* | 45.2# |
| V2 | L | 3.92* | 3.88* | 25.0# |
| V3 | L | 3.16* | 3.13* | 29.1# |
| $CLic_{shallow}$ | L $h^{-1}$ | 27.9* | | |
| $CLic_{deep}$ | L $h^{-1}$ | 2.57* | | |
| TK0 (fixed) | min | 5 | | |
| $CV_C$ | % | 12.2 | | |
| $SD_C$ | mg/L | 0.059 | | |

*: Group estimate for subject of standard size ($FFM_J$ = 53 kg).

°: Apparent coefficients of variation for the BSV.

^: Derived from model estimates, not an estimated parameter.

#: Coefficient of correlation for the random variability between pairs of random effects, r(V1,V2) = -0.67, r(V1,V3) = 0.56, r(V2,V3) = -0.59.

See chapter 2.6.2 for explanation of model parameters.

**Table 3.3-10** Ratios of group estimates (CF-patients / healthy volunteers) for clearance and volume of distribution for different size models

| Size model | $FCYF_{CLT}$ | $FCYF_V$ |
|---|---|---|
| A) No size model | 0.861 | 0.853 |
| B) WT linear scaling | 1.45 | 1.13 |
| C) WT allometric | 1.27 | 1.13 |
| D) $FFM_C$ allometric | 1.20 | 1.04 |
| E) $FFM_J$ allometric | 1.17 | 1.01 |

$FCYF_{CLT}$: Ratio of group estimates for total clearance in CF-patients divided by total clearance in healthy volunteers.

$FCYF_V$: Ratio of group estimates for volume of distribution at steady-state in CF-patients divided by volume of distribution at steady-state in healthy volunteers.

**Table 3.3-11** BSV (variances) for different size models: The table shows the relative between subject variances for the respective PK parameter and size models.

| Size model | Relative between subject variance | | | |
|---|---|---|---|---|
| | CL | V1 | V2 | V3 |
| B) WT linear scaling | 100%* | 100%* | 100%* | 100%* |
| C) WT allometric | 75%° | 97% | 96% | 89% |
| D) $FFM_C$ allometric | 69%° | 101% | 78% | 84% |
| E) $FFM_J$ allometric | 68%° | 104% | 74% | 82% |

*: The BSV for linear scaling by WT was used as reference.

°: The lower this number, the more variability was explained by the respective size model. These values indicate that the BSV (variance) for total clearance was reduced by 25% for allometric scaling by WT, by 31% for allometric scaling by $FFM_C$, and by 32% for allometric scaling by $FFM_J$, all compared to linear scaling by WT.

We distinguished the size models by their estimates for the disease specific scale factors FCYF. CF-patients had a 14% lower total clearance and a 15% lower volume of distribution compared to healthy volunteers, if no size descriptor was included (see size model A, Table 3.3-10). Linear scaling by WT resulted in a 45% higher total clearance and in a 13% higher volume of distribution. The average differences in volume of distribution between CF-patients and healthy volunteers were well described by allometric scaling with $FFM_C$ or $FFM_J$ which yielded point estimates very close to 1.0. Size adjusted total clearance was estimated to be 17-20% higher for allometric scaling by $FFM_C$ or $FFM_J$ (see Table 3.3-10) which was evidence for a slightly higher clearance of ceftazidime in CF-patients after adjusting for body size and body composition.

Additionally we compared the ability of each size model to reduce the unexplained BSV in clearance and volume of distribution. Table 3.3-11 shows that allometric scaling by $FFM_C$ or $FFM_J$ reduced the unexplained BSV relative to linear scaling by WT. Allometric scaling by $FFM_C$ or $FFM_J$ reduced the unexplained BSV by about 32% for total clearance, by about 24% for volume

of distribution for the shallow peripheral compartment, and by about 17% for volume of distribution for the deep peripheral compartment relative to linear scaling by WT.

***MCS:*** CF-patients had lower PTAs than healthy volunteers which resulted in 1.5 to 3 times lower PKPD breakpoints for the studied dosage regimens (see Figure 3.3-6). Continuous infusion of 6g / 70kg WT per day achieved a PKPD breakpoint of 12 mg/L in CF-patients and 16 mg/L in healthy volunteers for both targets. For the near-maximal kill target ($fT_{>MIC} \geq$ 65%), the PKPD breakpoints were 8-12 mg/L in CF-patients and 16 mg/L in healthy volunteers for both prolonged (4-5h) infusion regimens. For this target, CF-patients had a breakpoint of 2 mg/L for short-term infusion q6h and of 1 mg/L for short-term infusion q8h at a daily dose of 6g / 70kg WT. Healthy volunteers had a breakpoint of 4 mg/L for short-term infusion q6h and of 3 mg/L for short-term infusion q8h at a daily dose of 6g / 70kg WT.

For the bacteriostasis target ($fT_{>MIC} \geq$ 40%), the PKPD breakpoints were 16 mg/L in CF-patients and 24 mg/L in healthy volunteers for both prolonged (4-5h) infusion regimens. For this target, CF-patients had a breakpoint of 6 mg/L for short-term infusion q6h and of 4 mg/L for short-term infusion q8h at a daily dose of 6g / 70kg WT. Healthy volunteers had a breakpoint of 12 mg/L for short-term infusion q6h and of 8 mg/L for short-term infusion q8h at a daily dose of 6g / 70kg WT.

Table 3.3-12 shows the PTA expectation values in CF-patients with the same demographic data as the subjects in our study for the near-maximal kill target. Healthy volunteers achieved higher PTA expectation values than CF-patients (median [range]: 3.7% [0.8-17.9%] for the near-maximal kill target; PTA expectation values for healthy volunteers not shown elsewhere). The PTA expectation values for the bacteriostasis target and the near-maximal kill target were identical for continuous infusion. For short-term and prolonged infusion, the PTA expectations values of the bacteriostasis target were higher (4.4% [0.6-26.9%]) than for the near-maximal kill target.

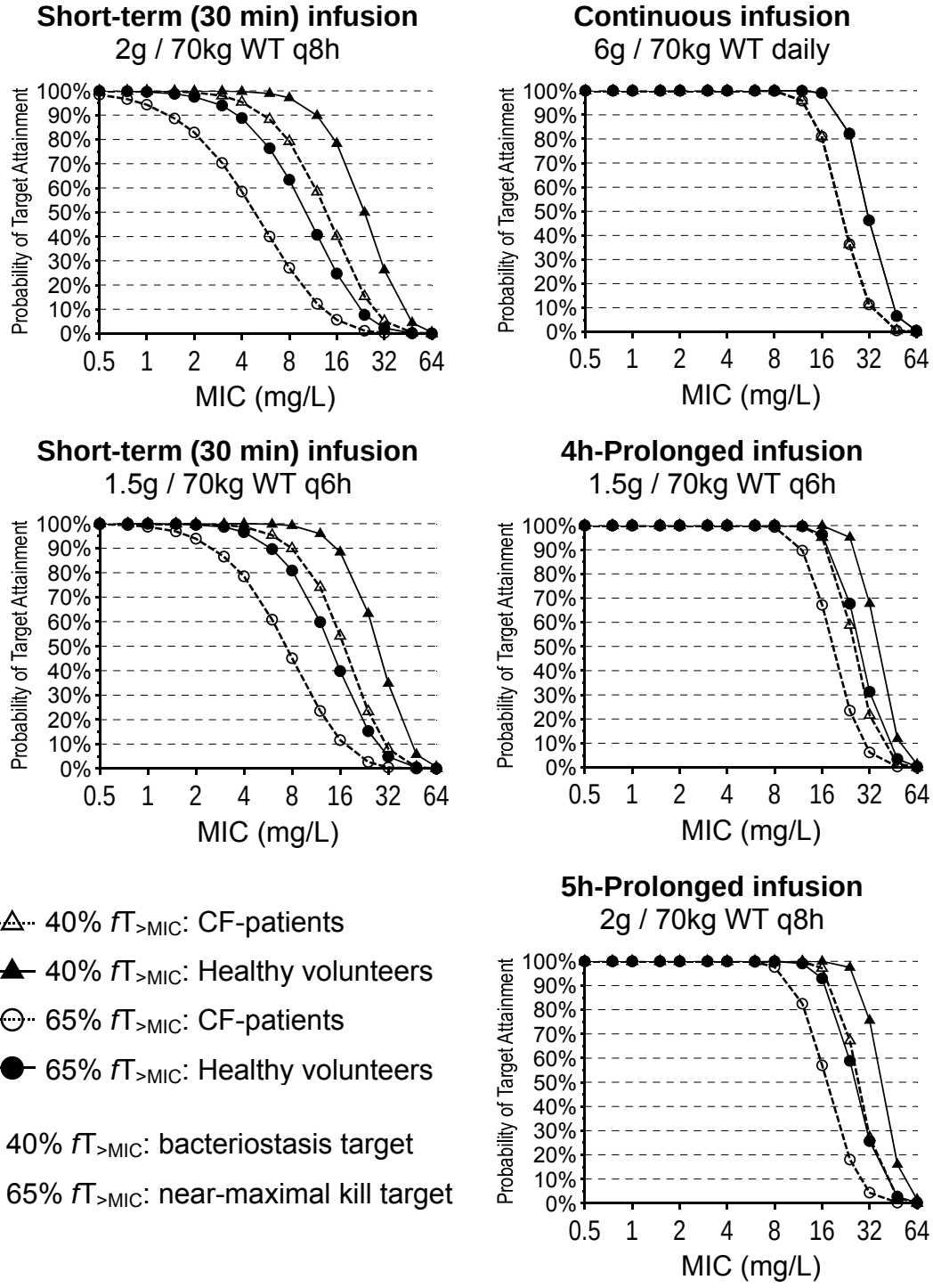


**Figure 3.3-6** Probability of target attainment for different dosage regimens of 6g ceftazidime daily at steady-state

**Table 3.3-12** PTA expectation values for the CF-patients in our study at a daily dose of 6g / 70 kg WT based on the PKPD target for near-maximal bactericidal effect (*f*T>MIC ≥ 65%) and published MIC distributions

| **Source** | **Dosage regimen** | **Continuous infusion** | **Prolonged infusion** | | **Short-term infusion** | |
|---|---|---|---|---|---|---|
| | Duration of infusion | 24h | 4h | 5h | 30min | 30min |
| | Dose for a CF-patient with 70 kg WT | 6g / day | 1.5g | 2g | 1.5g | 2g |
| | Dosing interval | | q6h | q8h | q6h | q8h |
| MYSTIC 2002, North America (273) | *E. coli* (n=433) | 96.4% | 96.1% | 96.0% | 94.9% | 94.0% |
| | *K. pneumoniae* (n=288) | 91.4% | 90.9% | 90.7% | 89.8% | 89.0% |
| | *P. aeruginosa* (n=427) | 89.2% | 88.0% | 87.2% | 73.5% | 62.9% |
| MYSTIC 2002, South America (254) | *E. coli* (n=98) | 96.1% | 95.4% | 94.8% | 89.3% | 86.1% |
| | *K. pneumoniae* (n=92) | 85.5% | 84.1% | 83.1% | 73.4% | 68.8% |
| | *P. aeruginosa* (n=233) | 61.6% | 60.3% | 59.4% | 51.0% | 45.5% |
| ***Isolates from CF-patients*** | | | | | | |
| 3 CF-centers: Italy, UK, and Germany (158) | *P. aeruginosa* (n=101) | 78.1% | 75.6% | 73.9% | 55.7% | 46.2% |
| Freiburg, Germany (437) | *P. aeruginosa*, non-mucoid strains (n=229) | 83.4% | 82.5% | 81.8% | 66.2% | 55.7% |
| | *P. aeruginosa*, mucoid strains (n=156) | 93.2% | 92.8% | 92.3% | 79.9% | 70.3% |
| Leipzig, Germany (467) | *P. aeruginosa* (n=38) | 96.2% | 94.9% | 94.1% | 86.6% | 79.5% |

WT: Total body weight.

Continuous infusion achieved slightly higher (1.4% [0.3-7.0%]) PTA expectation values than both prolonged infusion regimens for the near-maximal kill target (see Table 3.3-12). Administering the same dose as prolonged infusion instead of as short-term infusion increased the PTA expectation values considerably (14.0% [1.1-33.6%]). For the *E. coli* and *K. pneumoniae* isolates from the MYSTIC 2002 North America data, all five dosage regimens had PTA expectation values ≥89%. For those two pathogens, the superiority of the prolonged infusion was more pronounced for the less susceptible isolates from South America. Prolonged infusion reached high (>87%) PTA expectation values for the *P. aeruginosa* isolates from North America, whereas the PTA expectation values for the less susceptible *P. aeruginosa* isolates from South America were only about 60%.

The prolonged ceftazidime infusions achieved PTA expectation values of ≥82% for the *P. aeruginosa* isolates from CF-patients in Freiburg, Germany, and in Leipzig, Germany, whereas the PTA expectation values were only about 74% for the *P. aeruginosa* isolates from three CF-centers in Italy, UK and Germany. Prolonged infusion achieved notably higher PTA expectation values for isolates from CF-patients (median [range]: 21.0% [8.3-33.6%]) than short-term infusions.

#### 3.3.2.5 Discussion

The life-expectancy and quality of life for CF-patients improved impressively during the last 70 years. Optimal treatment of *P. aeruginosa* (141) is an important factor for improving the quality of life and life-expectancy of CF-patients. Ceftazidime has been shown to be a valuable treatment option in anti-pseudomonal therapy in CF-patients (17, 47, 404, 486). We compared the differences in average PK parameters of ceftazidime between CF-patients and healthy volunteers in our population PK analysis. Additionally, we studied the unexplained BSV after accounting for body size by each size model. Our final model had a highly sufficient predictive performance for both the average plasma concentration time profiles of ceftazidime as well as their BSV (see

Figure 3.3-5). The variability in the raw data was well captured by the predicted plasma concentration time curves in CF-patients. The predictions were slightly too wide for healthy volunteers. This results in slightly more conservative (lower) predicted PTAs in healthy volunteers. The highly sufficient predictive performance qualified our final model to compare the PD profiles between both subject groups and to identify optimal dosage regimens via MCS.

Our results for the PK parameters of ceftazidime in healthy volunteers were in good agreement with those from other authors (15, 115, 252, 335, 377, 494, 525). There are only two studies on ceftazidime in CF-patients which included a healthy volunteer control group. Leeder et al. (282) find a total clearance of 8.5 ± 1.0 L/h/1.73 $m^2$ and Hedman et al. (182) find 7.6 ± 0.7 L/h/1.73 $m^2$ in CF-patients. Although some authors report (312, 369, 509) higher clearances of 0.23-0.36 L/h/kg WT (equivalent to 16-25 L/h/70 kg WT, if one assumes linear scaling by WT) for ceftazidime in CF-patients, most studies (253, 333, 338, 380, 519, 521) in juvenile to adult CF-patients find an average total clearance of 8-11 L/h for CF-patients of standard body size (i. e. 70 kg WT or 1.73 $m^2$ body surface area) and a coefficient of variation of 9-26% for the BSV of total clearance. Our geometric mean of 7.82 L/h (28.3% CV) for total clearance in CF-patients with 53 kg $FFM_J$ (see Table 3.3-9) was in good agreement with the reported clearances in CF-patients.

The reported average volume of distribution ranges between 0.237 and 0.46 L/kg WT (equivalent to 16.6 and 32 L/70 kg) with coefficients of variation between 14 and 53% in CF-patients (253, 282, 312, 333, 338, 369, 380, 521). Our geometric mean of 12.8 L for a CF-patient with 53 kg $FFM_J$ and coefficients of variation between 25 and 45% for the individual volumes (see Table 3.3-9) was in agreement with the literature values, given that arithmetic means are larger than (or equal to) geometric means and volume of distribution is often log-normally rather than normally distributed. Our results on terminal half-life (see Table 3.3-8) were in good agreement with the shorter terminal half-life of 1.5 ± 0.2 h in CF-patients compared to 1.76 ± 0.2 h in healthy volunteers reported by Leeder et al. (282). The report average half-

lives range between 1 and 2 h in juvenile to adult CF-patients (253, 312, 333, 369, 380, 477, 509, 521).

Some of the reported differences in clearance and volume of distribution between various studies might arise from inadequate scaling of CF-patients for body size. Our CF-patients had a 43% lower WT than our healthy volunteers (see Table 3.3-7) and $FFM_C$ as well as $FFM_J$ were about 35% lower in CF-patients. Our NCA showed a 36% lower unscaled volume of distribution at steady-state and a 19% lower unscaled total clearance in CF-patients (see Table 3.3-8). The terminal-half-life was 24% shorter and the mean residence time was 27% shorter in CF-patients.

Our population PK analysis aimed at comparing various size models by their ability 1) to explain the average differences between CF-patients and healthy volunteers and 2) to reduce the unexplained BSV. In absence of a size descriptor (size model A, Table 3.3-10), CF-patients had a 14% lower clearance and a 15% lower volume of distribution, because they were smaller. Linear and allometric scaling by WT predicted clearance (by 45 and 27%) and volume of distribution (by 13%) to be higher in CF-patients (see Table 3.3-10). Allometric scaling by $FFM_C$ or $FFM_J$ yielded very similar volumes of distribution for both subject groups and a 17-20% higher size adjusted total clearance in CF-patients compared to healthy volunteers. Therefore, we observed a 17-20% increased total clearance in CF-patients after adjusting for body size and body composition.

These results are similar to those from Leeder et al. (282) who find a 42% increased total clearance (142 $\pm$ 17 mL/min/1.73 $m^2$ in CF-patients vs. 101 $\pm$ 10 mL/min/1.73 $m^2$ in healthy volunteers) and Hedman et al. (182) who find a 25% increased renal clearance (125 $\pm$ 20 mL/min/1.73 $m^2$ in CF-patients and 100 $\pm$ 9 mL/min/1.73 $m^2$ in healthy volunteers) for ceftazidime. The latter authors could explain this increased renal clearance primarily by an increased glomerular filtration rate in CF-patients determined via inulin clearance. The reason for the increased glomerular filtration rate in CF-patients is not well known. CF-patients have a 16% higher resting energy expenditure possibly due to a higher energy need secondary to chronic lung

infection would be another explanation (514). This might be one reason for their higher clearance. An altered glomerulotubular balance due to a primary tubular transport defect has also been hypothesized as explanation (19, 37).

Besides the ability of the different size models to describe the average differences between both subject groups, we studied by how much each size model reduced the unexplained BSV in clearance and volume of distribution. Reducing the unexplained BSV allows one to achieve target concentrations more precisely in empiric therapy. Allometric scaling by $FFM_J$ or $FFM_C$ (see Table 3.3-11) reduced the BSV in CL by about 32%, the BSV in V2 by about 24%, and the BSV in V3 by about 17% relative to linear scaling by WT. This result seems reasonable, because $FFM_J$ and $FFM_C$ account for body composition, but WT does not.

We used the population PK model based on $FFM_J$ to predict the PTA in CF-patients and healthy volunteers. CF-patients had lower PTAs (see Figure 3.3-6) than healthy volunteers. For the near-maximal kill target ($fT_{>MIC} \geq 65\%$), CF-patients had a breakpoint of 1 mg/L for the short-term infusion of 2g / 70 kg WT q8h, whereas healthy volunteers had a breakpoint of 3 mg/L for this dosage regimen. Administering the same daily dose q6h instead of q8h increased the breakpoint to 2 mg/L in CF-patients. Mouton et al. (338) found a PTA ≥90% for MICs ≤4 mg/L in CF-patients and for MICs ≤8 mg/L in healthy volunteers for a fixed dose of 2g q8h and the target $fT_{>MIC} \geq 60\%$. When we used this target and a fixed dose of 2g q8h as 30 min infusion, we got a comparable breakpoint of 3 mg/L in CF-patients.

To improve the PTA in CF-patients, Mouton et al. (338) proposed therapeutic drug monitoring based on a population PK model with a Bayesian approach to increase the dose or dosing frequency in individual CF-patients if required. Doses of 150-250 mg/kg/day ceftazidime split into 3 or 4 intermittent doses have been recommended for CF-patients (105) up to a maximum daily dose of 12g. However, it has been argued that even high intermittent doses (289) might not be sufficient for treatment of CF-patients. Subsequently, continuous infusion of ceftazidime has been proposed and studied in CF-patients (25, 96, 275, 399, 517, 521).

We studied continuous and prolonged infusion to identify optimal dosage regimens in CF-patients at a daily dose of 6g / 70kg WT. Prolonged (5h) infusions of 2g / 70 kg WT q8h and prolonged (4h) infusion of 1.5g / 70 kg WT q6h achieved PKPD breakpoints of 8-12 mg/L in CF-patients which was about 10 times higher than the breakpoint for standard short-term infusions q8h at the same daily dose. For comparison, giving the same daily dose q6h instead of q8h as a 30 min infusion only increased the breakpoint by a factor of 2 (from 1 mg/L for q8h to 2 mg/L for q6h) in CF-patients. The prolonged infusion regimens achieved notably higher PTA expectation values, especially against the less susceptible pathogens. For the isolates from CF-patients (see Table 3.3-12), prolonged infusion achieved 21.0% [8.3-33.6%] (median [range]) higher PTA expectation values compared to short-term infusions at the same daily dose. Prolonged infusion reached only slightly lower PTA expectation values (1.4% [0.3-7.0%]) than continuous infusion (see Table 3.3-12). However, ceftazidime at a concentration of 120 g/L is only 90% stable for 8h at 37°C (517). Continuous infusion bears a risk for line infections and is less convenient than prolonged infusions which seem the most reasonable choice to improve the PTA expectation values for ceftazidime.

Prolonged infusions achieved PTA expectation values in CF-patients of about 94% for *P. aeruginosa* isolates from Leipzig (467), Germany, of 92% for the mucoid *P. aeruginosa* isolates and of 82% for the non-mucoid *P. aeruginosa* isolates from Freiburg (437), Germany, and of 74% for *P. aeruginosa* isolates from three CF-centers (158) in Italy, UK and Germany. These differences between the PTA expectation values from different CF-centers underline the importance to use the MIC distributions of the local hospital to predict the probability of successful treatment with ceftazidime for each CF-clinic.

In conclusion we found a 19% lower unscaled total clearance and a 36% lower volume of distribution at steady-state in CF-patients compared to healthy volunteers, because our CF-patients were smaller. Allometric scaling by $FFM_J$ or $FFM_C$ explained the average differences in PK parameters better than linear scaling by WT. The latter model predicted clearance in CF-patients to be 45% higher, probably because WT does not account for body

composition. Allometric scaling by $FFM_J$ indicated a 17% higher total clearance and a similar (1% higher) volume of distribution after adjusting for body size. More importantly, allometric scaling by $FFM_J$ reduced the unexplained BSV by 32% for clearance and by 18-26% for volume of the peripheral compartments relative to linear scaling by WT. This is important to achieve target concentrations more precisely in empiric therapy. The PKPD breakpoint for near-maximal bactericidal activity was 1 mg/L in CF-patients and 3 mg/L in healthy volunteers after short-term infusions of 2g / 70kg WT q8h. As an alternative mode of administration prolonged (5 h) infusion of 2g / 70kg WT q8h achieved a breakpoint of 8-12 mg/L in CF-patients and 16 mg/L in healthy volunteers. For this dosage regimen, the PTA expectation values were between 74% and 94% for *P. aeruginosa* isolates of CF-patients from various European CF-centers. Large clinical trials in CF-patients are warranted to compare the clinical cure rates for prolonged and short-term infusion of ceftazidime and to study the probability of successful clinical outcome for dose selection based on $FFM_J$.

### 3.3.3 Population pharmacokinetics and pharmacodynamics of carumonam

#### 3.3.3.1 Chemical structure of carumonam

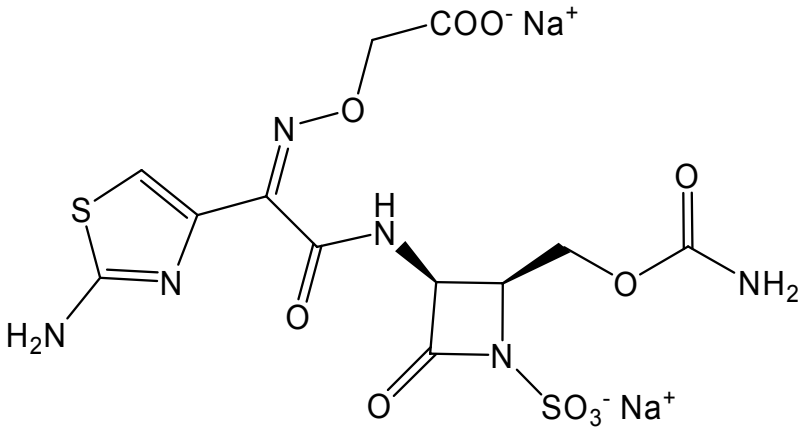


($C_{12}H_{12}N_6Na_2O_{10}S_2$, Mol. Wt.: 510.37)

**Chemical structure 3.3-3** Carumonam (disodium salt)

Although carumonam is only marketed in Japan, our study with carumonam contributed valuable information to our PK comparison between CF-patients and healthy volunteers and especially to our meta-analysis.

#### 3.3.3.2 Possible use of carumonam in patients with cystic fibrosis

The high morbidity and mortality involved in this pulmonary disease underlines the need for optimal anti-infective treatment of CF-patients. After initial infection by *H. influenzae* or *S. aureus*, many CF-patients suffer from infections by *P. aeruginosa*, *methicillin resistant S. aureus*, or *Burkholderia cepacia*. The latter three pathogens are often resistant to many antibiotics. In order to postpone or limit the emergence of resistance, it seems advisable to limit the use of quinolones, cephalosporins, carbapenems, aminoglycosides, and glycopeptides against the latter pathogens, whenever an alternative

treatment option with a high probability for successful treatment e. g. against *H. influenzae* or *S. aureus* is available.

Carumonam is active against *H. influenzae* (213), *K. pneumoniae* (211, 213, 266), *P. aeruginosa* (210, 212, 451), *E. coli* (265, 450), and *Serratia marcescens* (209, 266, 269) and may be a promising treatment option for infections caused by those pathogens. Carumonam shows synergy with gentamicin in experimental urinary tract infections in mice (362). However, there is no study on the PK of carumonam in CF-patients. Many PK studies on other beta-lactams in CF-patients did not include a control group of healthy volunteers. This lack of data may hamper dose selection in CF-patients.

Therefore, we compared the population PK of carumonam between CF-patients and healthy volunteers and studied whether $FFM_C$ or $FFM_J$ is a more appropriate descriptor of body size and functional capacity compared to WT. Additionally, we studied the PTA for CF-patients and healthy volunteers based on various PKPD targets via MCS.

#### 3.3.3.3 Methods

The general clinical and sample handling procedures, the methods for PK analysis (including NCA and population PK), and the general methods for MCS are described in chapter 2. Chapter 3.2 shows the specific methods applied for analysis of our CF-studies.

***Subjects:*** A total of 28 Caucasian volunteers (ten CF-patients and 18 healthy volunteers) of both sexes participated in the study. Table 3.3-13 shows the demographic data.

***Study design and drug administration:*** Each subject received a dose of 2166 mg of carumonam as a 15 min intravenous infusion. All infusions were administered with a BRAUN-Perfusor® (Braun, Melsungen, Germany).

***Blood and urine sampling:*** All blood samples were drawn in vials containing citric acid. Blood samples were drawn immediately before start of the infusion (0 min) and at 5, 10, and 15 min post start of infusion as well as at 5, 15, 20, 30, 45, 60, 75, 90 min and 2, 3, 4, 5, 6, 8, 10, 12, and 24 h post end of infusion. Urine was collected from the start of the infusion until 1 h post end

of infusion as well as at 1 to 2, 2 to 3, 3 to 4, 4 to 6, 6 to 8, 8 to 10, 10 to 12, and 12 to 24 h after end of infusion.

**Table 3.3-13** Demographic data of the carumonam study (median [range])

| | **CF-patients** | **Healthy volunteers** |
|---|---|---|
| Number of subjects (males / females) | 10 (9 / 1) | 18 (12 / 6) |
| Age (yr) | 21 [19 - 25] | 25 [21 - 37] |
| Height (cm) | 178 [167 - 183] | 174 [160 - 203] |
| Total body weight (kg) | 54 [47 - 61] | 61 [50 - 107] |
| Fat-free mass° (kg) | 47.9 [41.9 - 52.9] | 49.7 [40.0 - 82.2] |
| Fat-free mass# (kg) | 48.6 [37.3 - 53.3] | 49.3 [35.1 - 80.7] |
| Body mass index (kg $m^{-2}$) | 18.0 [14.5 - 19.2] | 20.6 [18.1 - 26.0] |
| Serum creatinine concentration (µmol $L^{-1}$) | 64 [49 - 80] | 80 [71 - 95] |
| Renal function* (mL $min^{-1}$) | 162 [132 - 193] | 115 [97 - 133] |

*: Estimated renal function for a subject with nominal total body weight of 70 kg (see paragraph “Population PK analysis” in chapter 3.3.3.3 for details).

°: Calculated by the formula of Cheymol and James (72, 222).

#: Calculated by the formula of Janmahasatian et al. (224).

***Drug analysis in plasma and urine:*** We determined the concentration of carumonam in plasma and urine by HPLC. Plasma samples (200 µL) were deproteinized by addition of 400 µL acetonitrile. This mixture was centrifuged at 10,000 rpm for 5 min and 1,000 µL of dichloromethane were added to the supernatant. Ten (10) µL of the aqueous phase were injected onto the system. We used a Hypersil ODS 5, 125 x 4 mm column and a 1% acetic acid (glacial) / 2% methanol, 0.3% $(NH_4)_2SO_4$ eluent at pH 2.9. Carumonam was detected at a wavelength of 293 nm. The limit of quantification was 0.2 mg/L for plasma and 7 mg/L for urine. The coefficients of variation for inter-day precision were between 4.1 and 5.5% for plasma and between 2.6 and 6.0% for urine.

***Population PK analysis:*** In addition to the covariate model described in chapter 3.2, we used renal function as a covariate for renal clearance. The glomerular filtration rate of the $i^{th}$ subject ($GFR_i$) was estimated by the Cockcroft & Gault formula (78) for a nominal 70 kg subject:

$$GFR_i = \left[\left(140 - \frac{age_i}{yrs}\right) \cdot \frac{mg/dL}{\text{Serum Creatinine Concentration}_i}\right] \frac{mL}{min} \qquad \text{Formula 3.3-1}$$

We scaled the estimated glomerular filtration rate by a standard glomerular filtration rate ($GFR_{STD}$) of 120 mL/min/70kg. Renal function of the $i^{th}$ subject ($RF_i$) can then be predicated as:

$$RF_i = \frac{GFR_i}{GFR_{STD}} \qquad \text{Formula 3.3-2}$$

We assumed a nonrenal ($CL_{NR}$) and a renal ($CL_R$) component of clearance. We estimated the renal clearance of carumonam based on the amount of carumonam excreted unchanged into urine and used RF as a covariate on renal clearance. We assumed that renal clearance is linearly related to RF (see chapter 3.2.4 for explanation of the parameters in this equation):

$$CL_{R,i} = CL_{POP,R} \cdot F_{Size,CL,i} \cdot FCYF_{CLR} \cdot RF_i \cdot \exp(\eta_{BSVCLRi}) \qquad \text{Formula 3.3-3}$$

***ANOVA statistics:*** As we had data on 28 subjects in this study, ANOVA and equivalence statistics were used to test for significant differences and their possible clinical relevance via ANOVA statistics. We estimated the population PK model both with or without the disease specific scale factors $FCYF_{CLR}$, $FCYF_{CLNR}$ and $FCYF_V$. We used the individual estimates for the random deviates ($\eta_{BSVi}$) on renal clearance, nonrenal clearance and volume of distribution of the population PK model without the scale factors to calculate point estimates and 90% confidence intervals for the ratio of group estimates between CF-patients and healthy volunteers by ANOVA statistics. The $\eta_{BSVi}$ were used as dependent variables in the ANOVA statistics. Using the $\eta_{BSVi}$ is superior to using the individual estimates for clearance and volume of

distribution, because the $\eta_{BSVi}$ are the individual random components for the respective PK parameter after adjusting for body size and renal function, whereas the individual PK parameters are neither adjusted for body size nor for renal function.

***MCS:*** There are much fewer studies which evaluated appropriate PKPD targets for monobactams than for penicillins, cephalosporins, or carbapenems. As carumonam is a beta-lactam we assumed that $fT_{>MIC}$ is the most suitable PKPD statistic to describe the antibacterial effect of carumonam. We calculated the PTA for the PKPD targets $fT_{>MIC}$ to be at least 20%, 40%, 60%, 80%, or 100% within the MIC range from 0.25 to 64 mg/L. As monobactams, like carumonam, reach near-maximal bactericidal activity at a target of about 50-60% $fT_{>MIC}$, we reported the PKPD breakpoints for near-maximal bactericidal activity based on the target $fT_{>MIC} \geq 60\%$. We used a protein binding of 23% for carumonam which was shown (316) to be independent of plasma concentration between 25 and 400 mg/L. We compared a daily carumonam dose of 6 g per 70 kg WT at steady-state given either 1) as continuous infusion, or 2) split into three 15 min infusions (q8h), or 3) split into three 4 h infusions (q8h).

#### 3.3.3.4 Results

***NCA:*** Figure 3.3-7 shows the average plasma concentrations of CF-patients and healthy volunteers. Table 3.3-14 lists the results of the NCA. These parameters are not scaled by any size descriptor. CF-patients had a 16% higher unscaled total clearance compared to healthy volunteers which was caused by a 24% higher unscaled renal clearance. The unscaled volume of distribution at steady-state was similar between both subject groups.

Several PK parameters determined by NCA are plotted vs. $FFM_C$ in Figure 3.3-8. The volume of distribution at steady-state, total clearance, renal clearance, and mean residence time showed a tendency to increase with $FFM_C$. This trend was more pronounced for our healthy volunteers, as their

range in $FFM_C$ was much wider and as their variability tended to be lower than for our CF-patients.

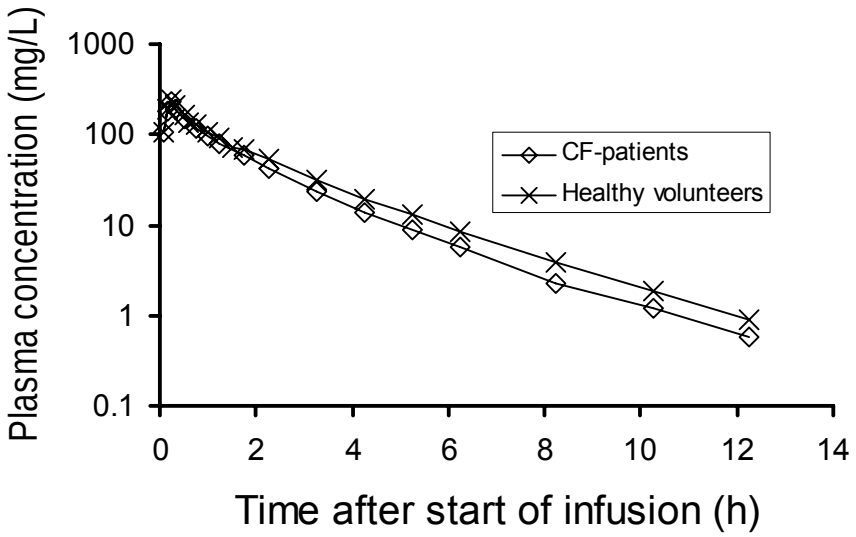


**Figure 3.3-7** Average plasma concentrations of carumonam for CF-patients and healthy volunteers after a single 15 min intravenous infusion of 2166 mg carumonam

**Table 3.3-14** Unscaled PK parameters derived by NCA (median [range])

| | **CF-patients** | **Healthy volunteers** |
|---|---|---|
| Total clearance (L/h) | 7.00 [6.14 - 8.67] | 6.05 [4.94 - 7.46] |
| Renal clearance (L/h) | 5.72 [3.08 - 7.19] | 4.62 [2.40 - 5.93] |
| Nonrenal clearance (L/h) | 1.55 [0.04 - 3.64] | 1.39 [0.63 - 2.91] |
| Volume of distribution at steady-state (L) | 12.8 [8.01 - 15.5] | 12.1 [9.65 - 18.4] |
| Fraction excreted unchanged in urine (%) | 80 [46 - 99] | 76 [45 - 89] |
| Peak concentration (mg/L) | 207 [174 - 472] | 248 [153 - 352] |
| Terminal half-life (L) | 2.00 [1.43 - 3.10] | 2.02 [1.50 - 2.61] |
| Mean residence time (h) | 1.88 [1.13 - 2.19] | 2.02 [1.65 - 2.47] |

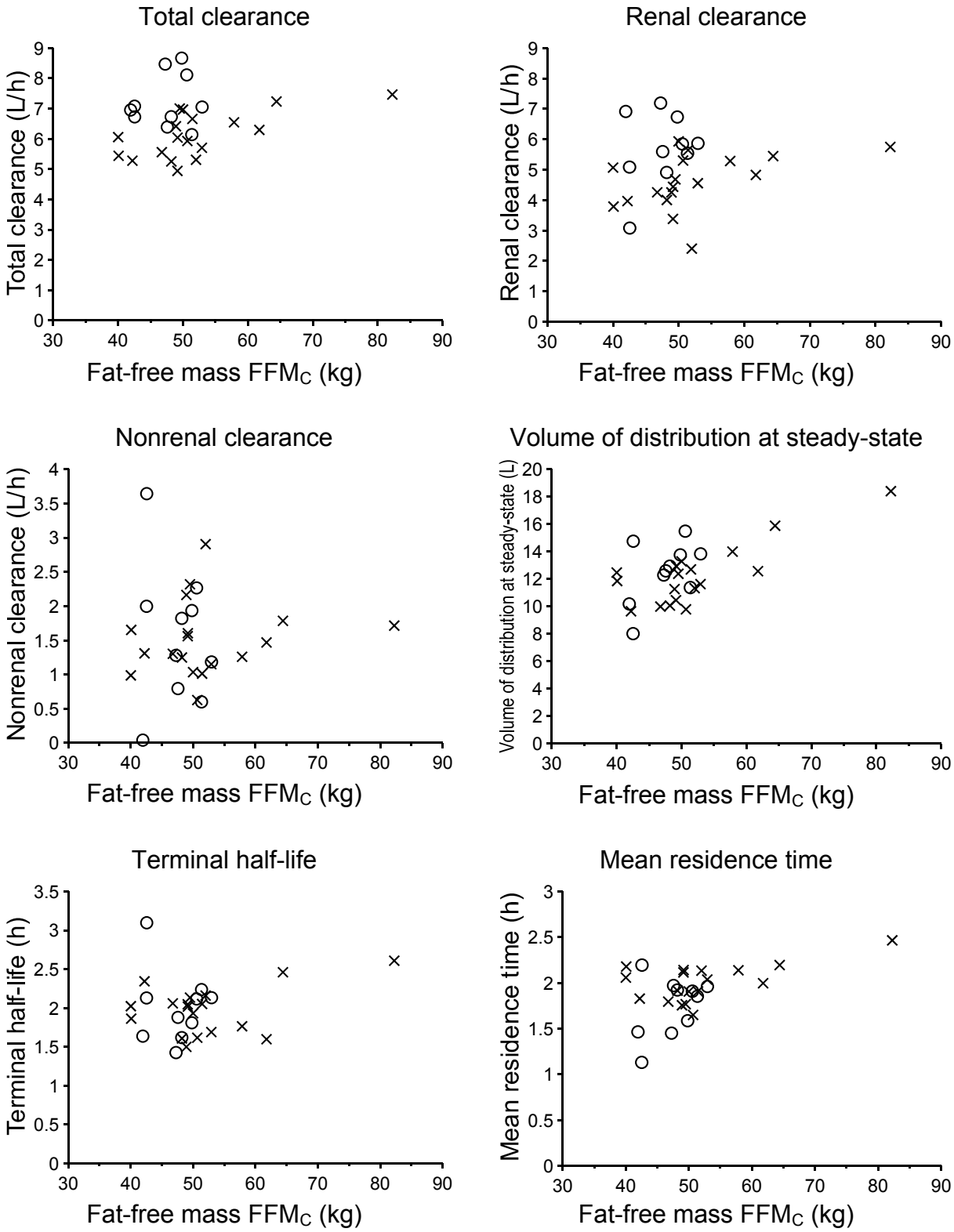


**Figure 3.3-8** PK parameters determined by NCA plotted vs. FFM$_C$

Circles: CF-patients, X: healthy volunteers

***Population PK analysis:*** The VPC indicated a better predictive performance for the three compartment model than for the two compartment model. The one compartment model had insufficient predictive performance. Figure 3.3-9 reveals the highly sufficient predictive performance of the three compartment model with $FFM_C$ as size descriptor for plasma concentrations and amounts excreted in urine at all sampling times. This VPC showed that the model was able to capture the plasma and urine profiles for CF-patients and healthy volunteers well. NONMEM's objective function favored the three compartment model by 164 points relative to the two compartment model. Therefore, we chose the three compartment model. The final estimates for the population PK model based on $FFM_C$ are shown in Table 3.3-15.

We studied 1) which size model best described the average differences in clearance and volume of distribution between CF-patients and healthy volunteers and 2) which size model reduced the unexplained BSV most. The ability of the size models to describe the average differences between both patient groups is shown in Table 3.3-16. The scale factors $FCYF_{CLR}$, $FCYF_{CLNR}$ and $FCYF_V$ are the ratios of group estimates between CF-patients and healthy volunteers after accounting for body size and renal function. A value of 1.0 for FCYF indicates that CF-patients and healthy volunteers have the same group estimate for the respective PK parameter. A value above (below) 1.0 means that CF-patients have a higher (lower) estimate for the respective PK parameter than healthy volunteers with the same body size and renal function. It is important to note that the estimate for $FCYF_{CLR}$ was derived for a model that included renal function as a covariate on renal clearance. As shown in Table 3.3-13, CF-patients had a 20% lower serum creatinine concentration and a 41% higher estimated renal function for a nominal 70 kg subject. The estimates for $FCYF_{CLR}$ (see Table 3.3-16) were very close to 1.0 (range: 0.92 to 1.06 for the different size models). Thus, CF-patients had both an increased creatinine clearance (renal function) and a higher renal clearance of carumonam compared to healthy volunteers.

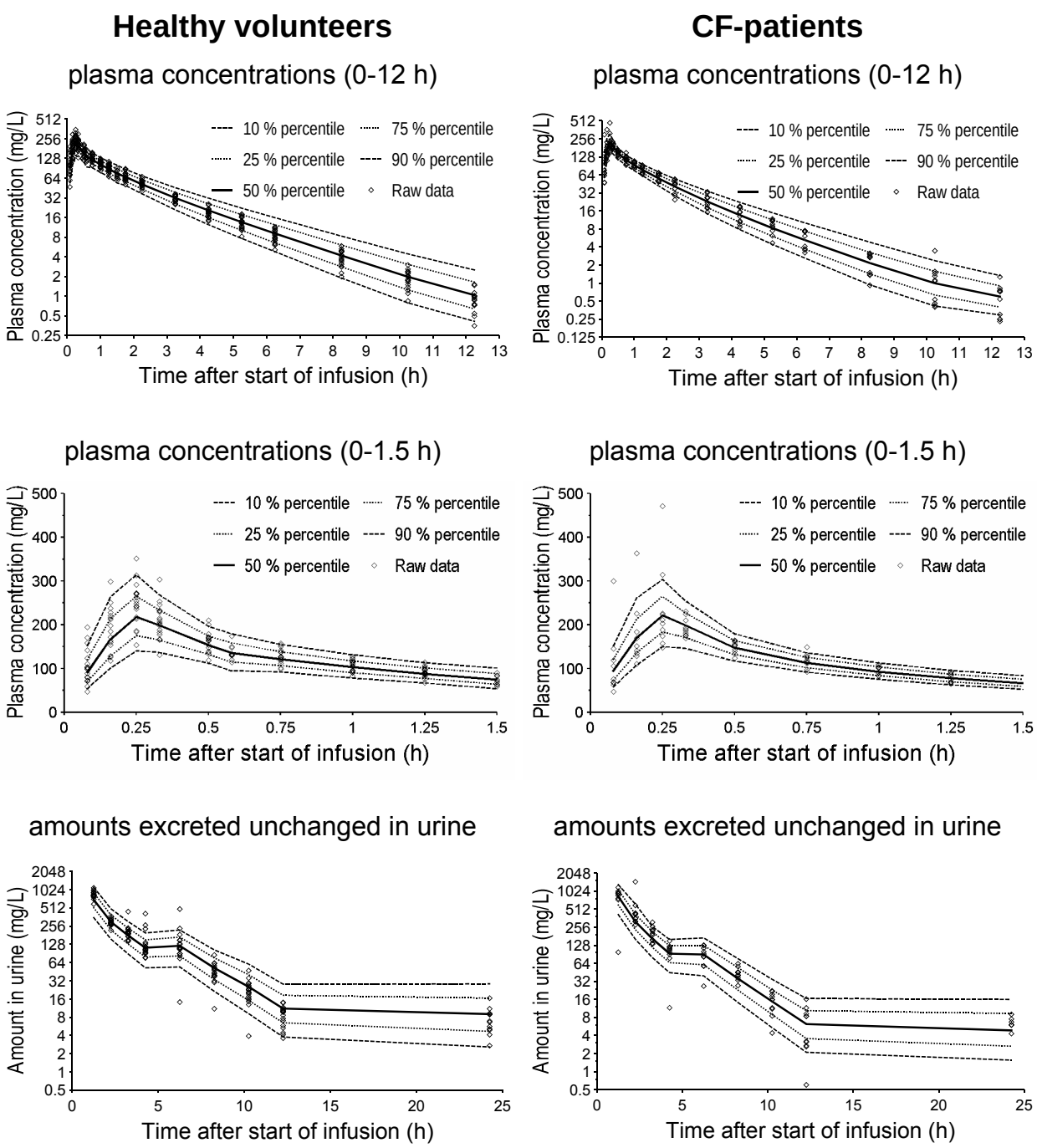


**Figure 3.3-9** VPC based on 5,000 CF-patients and 9,000 healthy volunteers for the three compartment model based on $FFM_C$ (see Table 3.3-15).

See chapter 2.6.3 for interpretation of VPCs.

**Table 3.3-15** PK parameter estimates for the allometric size model based on $FFM_C$

| Parameter | Unit | Estimate for | | Coefficient of variation (%)° |
|---|---|---|---|---|
| | | CF-patients | healthy volunteers | |
| $CL_{TOT}$ | L $h^{-1}$ | 6.33* | 6.25* | |
| $CL_R$ | L $h^{-1}$ | 4.36* | 4.54* | 12 |
| $CL_{NR}$ | L $h^{-1}$ | 1.97* | 1.71* | 39 |
| Vss^ | L | 13.2* | 12.7* | |
| V1# | L | 7.14* | 6.87* | 36 |
| V2# | L | 3.70* | 3.56* | 18 |
| V3# | L | 2.38* | 2.29* | 16 |
| $CLic_{shallow}$ | L $h^{-1}$ | 14.9* | | |
| $CLic_{deep}$ | L $h^{-1}$ | 1.55* | | |
| TK0 (fixed) | min | 15 | | 16 |
| $CV_C$ | % | 8.7 | | |
| $SD_C$ | mg/L | 0.26 | | |
| $CV_{AU}$ | % | 38 | | |
| $SD_{AU}$ | mg | 0.26 | | |

*: Group estimate for subject of standard size ($FFM_C$ = 53 kg).

^: Derived from model estimates, not an estimated parameter.

°: Apparent coefficient of variation for the BSV.

#: The coefficient of correlation for the random effects for pairs of volumes of distribution were: $r_{BSV}$(V1,V2) : -0.61, $r_{BSV}$(V1,V3) = -0.22, and $r_{BSV}$(V2,V3) = 0.06.

See chapter 2.6.2 for explanation of model parameters.

Linear and allometric scaling by WT (size models B and C) estimated clearance and volume of distribution to be 7-11% higher in CF-patients relative to healthy volunteers (see Table 3.3-16). Allometric scaling by $FFM_C$ or $FFM_J$ explained the average differences in total clearance and volume of distribution between CF-patients and healthy volunteers (range: 0.98 to 1.06 for $FCYF_{CLT}$ and $FCYF_V$, see Table 3.3-16).

**Table 3.3-16** Ratios of group estimates (CF-patients / healthy volunteers) for clearance and volume of distribution for different size models

| Size model | $FCYF_{CLR}$ | $FCYF_{CLNR}$ | $FCYF_{CLT}$[#] | $FCYF_{V}$ |
|---|---|---|---|---|
| A) No size model | 0.921 | 1.02 | 0.95 | 0.99 |
| B) WT linear scaling | 1.06 | 1.25 | 1.11 | 1.10 |
| C) WT allometric | 1.02 | 1.19 | 1.07 | 1.11 |
| D) $FFM_C$ allometric | 0.960 | 1.15 | 1.01 | 1.04 |
| E) $FFM_J$ allometric | 0.935 | 1.08 | 0.98 | 1.06 |

$FCYF_{NNN}$: Ratio of group estimates for parameter NNN (group estimate for CF-patients divided by group estimate for healthy volunteers).

[#]: Calculated as weighted average of $FCYF_{CLR}$ and $FCYF_{CLNR}$.

**Table 3.3-17** Comparison of BSV (variances) between the various size models: The table shows the relative between subject variances for the respective PK parameter and size models

| Size model | Relative between subject variance | | | | |
|---|---|---|---|---|---|
| | $CL_R$ | $CL_{NR}$ | V1 | V2 | V3 |
| B) WT linear scaling | 100%* | 100% | 100% | 100% | 100% |
| C) WT allometric | **62%°** | 94% | 98% | 99% | 101% |
| D) $FFM_C$ allometric | **70%°** | 103% | 115% | **73%** | **70%** |
| E) $FFM_J$ allometric | 116% | 106% | 99% | 83% | 130% |

*: The BSV for linear scaling by WT was used as reference.

°: The lower this number, the more variability was explained by the respective size model. These values mean that the BSV (variance) for renal clearance is reduced by 38% for allometric scaling by WT, and by 30% for allometric scaling by $FFM_C$, both compared to linear scaling by WT.

Table 3.3-17 shows the ability of the various size models to reduce the unexplained BSV. There was a trend that the allometric size models reduced the BSV better than linear scaling by WT (size model B). Allometric scaling by WT reduced the unexplained BSV in renal clearance by 38% and allometric scaling by $FFM_C$ reduced the unexplained BSV by 30% compared linear scaling by WT. There was no clear trend, which of the allometric size models reduced the unexplained BSV most.

***ANOVA statistics:*** The equivalence statistics for the comparison of CF-patients and healthy volunteers are shown in Table 3.3-18. CF-patients had a significantly (p=0.01) higher volume of distribution for both size models based on WT. We observed the same trend for total clearance scaled linearly by WT. The allometric scaling by $FFM_C$ or $FFM_J$ had point estimates very close to 100% (range: 94 to 107%) and their 90% confidence intervals all included 100%.

**Table 3.3-18** Equivalence statistics for the comparison of CF-patients and healthy volunteers after adjusting for body size by the respective size model

| Size model | Total clearance | | Volume of distribution at steady-state[#] | |
|---|---|---|---|---|
| | PE (90% CI)* | p-value | PE (90% CI)* | p-value |
| A) No size model | 92 (83 - 101) | 0.15 | 100 (90 - 111) | 0.98 |
| B) WT linear scaling | 107 (96 - 118) | 0.29 | 115 (106 - 124) | 0.01 |
| C) WT allometric | 103 (94 - 112) | 0.61 | 115 (106 - 124) | 0.01 |
| D) $FFM_C$ allometric | 97 (89 - 106) | 0.58 | 107 (99 - 115) | 0.13 |
| E) $FFM_J$ allometric | 94 (85 - 105) | 0.34 | 103 (94 - 113) | 0.53 |

*: Point estimate (PE) and 90% confidence interval (CI) for the ratio of least square means.

#: These point estimates and 90% confidence intervals were derived for a three compartment model without the scale factors FCYF (see chapter 3.3.3.3 for details). In this model the variability of volume of distribution at steady-state was calculated instead of the variability of the individual volumes of distribution V1, V2, and V3.

***MCS:*** PTAs were lower for CF-patients than for healthy volunteers (see Figure 3.3-10). Both subject groups had a PKPD breakpoint for near maximal bactericidal activity ($fT_{>MIC} \geq 60\%$) of 16 mg/L for continuous infusion at a daily carumonam dose of 6 g / 70 kg WT at steady-state (see Figure 3.3-10, panels E and F). For prolonged (4 h) infusions of 2 g / 70 kg WT q8h, the PKPD breakpoint was 16 mg/L in healthy volunteers and 8-12 mg/L (PTA=87% for an MIC of 12 mg/L) in CF-patients (Figure 3.3-10, panels C and D). For short-term (15 min) infusions of 2 g / 70 kg WT q8h, the PKPD breakpoint was 6 mg/L in healthy volunteers and 3 mg/L in CF-patients (see Figure 3.3-10, panels A and B). This 2 fold difference in PKPD breakpoints between both subject groups for short-term intermittent infusion may seem small. However, the dose in mg/kg WT would have to be doubled in CF-patients, if CF-patients should achieve the same PTAs as healthy volunteers in empiric therapy.

#### 3.3.3.5 Discussion

Secondary to medical advances, there has been major progress in increasing the life-expectancy and quality of life of CF-patients during the last 70 years (485). This longer life-expectancy has led to a significantly increased use of antibiotics in adult patients with CF. Although there is an increased usage of antibiotics in this patient group, only a few studies systematically compared the PK of antibiotics in CF-patients and healthy volunteers. Consequently, there is often not enough data for optimal selection of doses in CF-patients.

The two key questions for the comparison of CF-patients and healthy volunteers and for dose selection of CF-patients from a PK point of view are: Do CF-patients have altered PK compared to healthy volunteers? If yes, how should doses be adjusted? To answer these questions we used population PK and MCS. We compared a variety of descriptors for body size (functional capacity) with or without the allometric model.

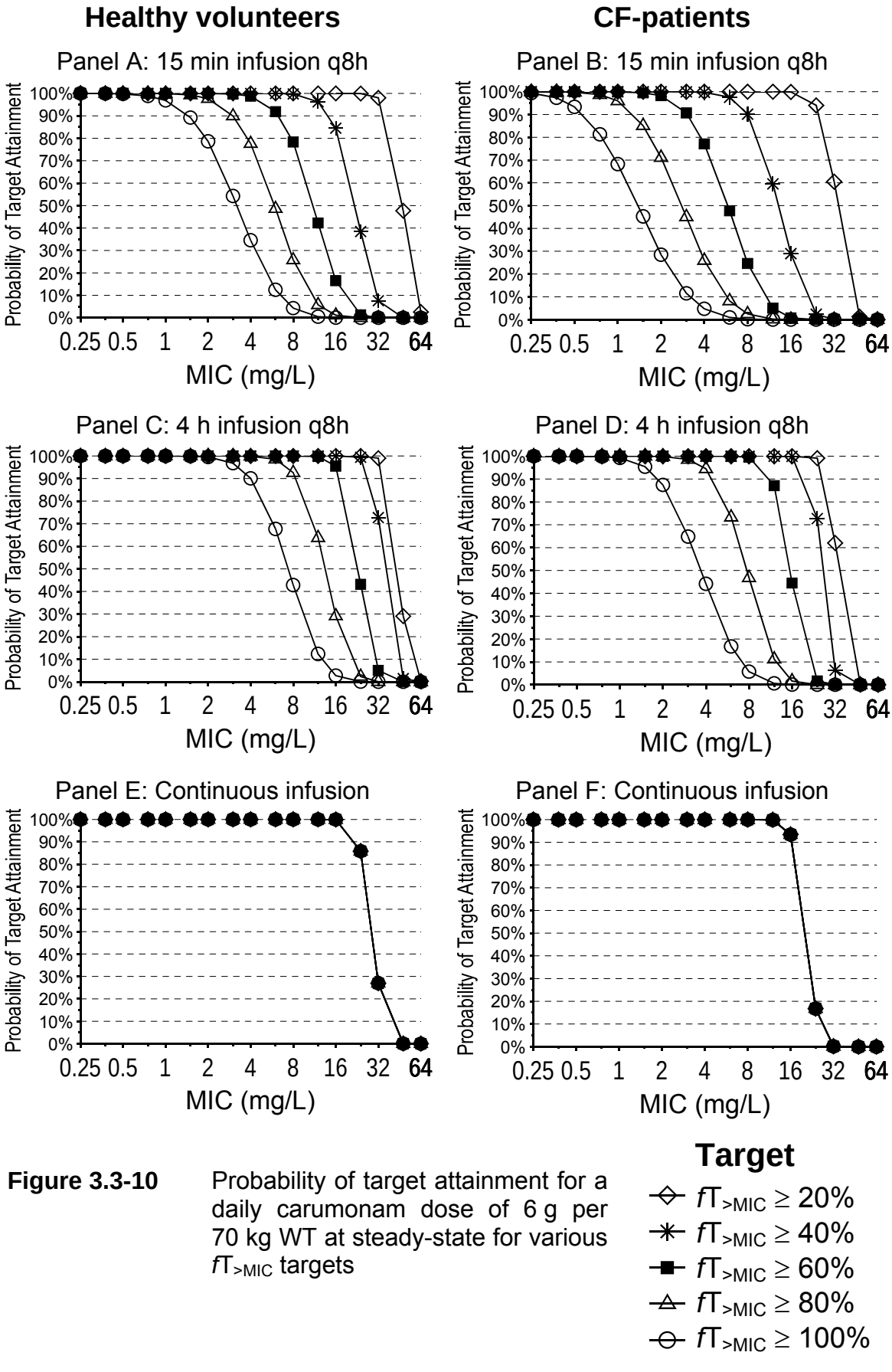


**Figure 3.3-10** Probability of target attainment for a daily carumonam dose of 6 g per 70 kg WT at steady-state for various $fT_{>MIC}$ targets

Our CF-patients had an 11% lower WT than the healthy volunteers, whereas $FFM_C$ and $FFM_J$ were similar (see Table 3.3-13). Thus both groups were likely to have a comparable amount of aqueous body space. This is probably the reason why we found similar volumes of distribution for CF-patients and healthy volunteers in the NCA (see Table 3.3-14). Our results for the PK parameters of carumonam were in good agreement with those of other authors (43, 260) for healthy volunteers. We are not aware of any reports on carumonam in CF-patients. NCA (see Table 3.3-14) showed a 24% higher unscaled renal clearance in CF-patients which corresponded to the higher renal function in our CF-patients compared to our healthy volunteers. This might be explained e. g. by an increase in glomerular filtration rate or in net tubular secretion. Hedman et al. (182, 183) found an increased renal clearance of ceftazidime and cefsulodin which was caused by an increased glomerular filtration rate. Wang et al. (526) found an enhanced renal clearance of ticarcillin in CF-patients due to a higher affinity of ticarcillin to the renal transporter in CF-patients relative to healthy volunteers.

We used renal function as a covariate on renal clearance in our population PK models which explained the average differences in renal clearance of carumonam between CF-patients and healthy volunteers. The model without any size descriptor (size model A) had scale factors for clearance and volume of distribution close to 1.0 (see FCYF in Table 3.3-16) – most likely because both subject groups were matched in $FFM_C$ and $FFM_J$. When we scaled clearance and volume of distribution by WT (size models B and C), CF-patients had higher clearances and a higher volume of distribution, probably because WT neglects differences in body composition. Both size models based on WT predicted volume of distribution to be significantly ($p=0.01$) higher in CF-patients (see Table 3.3-18). Allometric scaling by $FFM_C$ or $FFM_J$ (size models D and E) resulted in scale factors close to 1.0 (see Table 3.3-16). For the latter two size models, the 90% confidence intervals for the ratio of group estimates (CF-patients vs. healthy volunteers) all included 100% (see Table 3.3-18). We found that $FFM_C$ reduced the unexplained BSV by 30% for renal clearance and for volume of distribution of the shallow and deep peripheral compartment (see Table 3.3-17). This allows

one to predict the individual clearance and volume of distribution more precisely by allometric scaling with $FFM_C$. Therefore, target concentrations can be achieved more precisely in empiric therapy by use of $FFM_C$.

Although renal function and $FFM_C$ or $FFM_J$ explained the average difference in PK parameters between both subject groups, CF-patients still had a higher renal clearance than healthy volunteers. We observed a two times lower PKPD breakpoint for near-maximal bactericidal effect ($fT_{>MIC} \geq 60\%$) for intermittent short term infusions with carumonam and dose selection on a mg per kg WT basis (see Figure 3.3-10, panels A and B). The lower PKPD breakpoint in CF-patients is a consequence 1) of the slightly higher renal clearance (and renal function) and 2) of the altered body composition of CF-patients. The lower PKPD breakpoints were not caused by a larger variability in CF-patients (data not shown).

A two times lower PKPD breakpoint (6 mg/L in healthy volunteers vs. 3 mg/L in CF-patients for $fT_{>MIC} \geq 60\%$) may not seem much. However, carumonam doses in CF-patients would have to be doubled on a mg per kg WT basis, if CF-patients should achieve the same PKPD breakpoints as healthy volunteers. Such larger doses would possibly carry more severe side effects and a higher frequency of adverse events. Instead of increasing the dose, we studied prolonged and continuous infusion as alternative dosage regimens to increase the PKPD breakpoints. For the near-maximal kill target ($fT_{>MIC} \geq 60\%$), we found a PKPD breakpoint of 8-12 mg/L (PTA=87% at an MIC of 12 mg/L) in CF-patients and of 16 mg/L in healthy volunteers for prolonged (4 h) infusions of 2 g / 70 kg WT q8h (see Figure 3.3-10, panels C and D). Continuous infusion at the same daily dose of 6 g / 70 kg WT achieved a PKPD breakpoint of 16 mg/L in both subject groups.

To put these PTAs into clinical perspective, the PTA expectation value for treatment of infections caused by bacteria from a specific MIC distribution needs to be calculated (e. g. for the MIC distribution of a local hospital). It is important to note, for which MIC range prolonged and continuous infusions will be superior to short-term infusions or when CF-patients should receive prolonged infusions instead of short-term infusions. Carumonam showed good

activity against *Proteus mirabilis* ($MIC_{90} \leq 0.125$ mg/L) (267, 268), *K. pneumoniae* ($MIC_{90} \leq 0.125$ mg/L) (211, 266, 268), *S. marcescens* ($MIC_{90}$ = 0.5 mg/L (209); $MIC_{50}$ = 0.25 mg/L (266)), *S. liquefaciens* ($MIC_{90}$ = 0.25 mg/L) (209), and *E. coli* ($MIC_{90} \leq 0.125$ mg/L) (265). If the $MIC_{90}$s are below 1 mg/L, there is almost no improvement with prolonged or continuous infusion in the PTA expectation value, since the PTA expectation value will be >95% for short-term, prolonged, and continuous infusion.

However, other authors report considerably lower susceptibility to carumonam. *S. marcescens* has been reported to have an $MIC_{90}$ of 16 mg/L (269) and the mucoid strains of *P. aeruginosa* had an $MIC_{80}$ of 2 mg/L for carumonam (210, 212). Although infections with an $MIC_{80}$ of 2 mg/L can still be treated successfully by short-term infusions of carumonam for some patients, it is these infections for which prolonged and continuous infusion will have considerably higher PTA expectation values compared to short-term infusion. This applies especially to CF-patients, since they had a breakpoint of 3 mg/L for short-term infusions of 2 g / 70 kg WT q8h and a breakpoint of 8-12 mg/L for prolonged infusions of the same dose. Continuous infusion requires an additional line and this increases the risk for line infections. As prolonged infusion does not require an additional line, we would propose prolonged (4 h) infusions q8h for carumonam as the most reasonable option to increase PTAs and PKPD breakpoints.

Recent reports (86, 92, 199, 360) identified a significant role of *Burkholderia pseudomallei* (previously known as *Pseudomonas pseudomallei*) for CF-patients living or making holidays in the tropical regions of Northern Australia or Southeast Asia. This pathogen is the causative bacterium for melioidosis, an infectious disease endemic in Southeast Asia and Northern Australia (166, 201). $MIC_{50}$'s of 2 to 3 mg/L and $MIC_{90}$'s of 2 to 4 mg/L (21, 457, 552) have been reported for carumonam against *B. pseudomallei*. As the mortality associated with the acute stage of this infection is as high as 75% (166, 416), it is infections caused by bacteria in this MIC range for which the observed difference in PKPD breakpoints is most important. As for treatment of infections caused by *P. aeruginosa*, patients will have considerably higher

PTA expectation values, if they receive prolonged instead of short-term infusions against *B. pseudomallei*. However, it is important to calculate the PTA expectation value for the MIC distribution of a local hospital for each relevant pathogen to determine, whether carumonam will be a valuable treatment option.

In conclusion we found a 24% higher unscaled renal clearance in CF-patients compared to healthy volunteers, which could be explained by an enhanced glomerular filtration rate in CF-patients. The average differences in PK parameters between CF-patients and healthy volunteers could be explained by body size, body composition, and renal function. $FFM_C$ and $FFM_J$ explained the average differences in PK parameters between CF-patients and healthy volunteers better than WT. Linear scaling by WT resulted in significantly higher clearances and volumes of distribution in CF-patients. Allometric scaling by $FFM_C$ reduced the unexplained BSV in renal clearance and volume of distribution of both peripheral compartments by about 30% relative to linear scaling by WT. Therefore, dosing of CF-patients based on an allometric model with $FFM_C$ or $FFM_J$ should be superior to dosing by WT. Future clinical studies are warranted to show a higher probability of successful clinical outcome for dose selection in CF-patients based on $FFM_C$ or $FFM_J$. Prolonged and continuous infusion achieved higher PKPD breakpoints than short-term infusions q8h at the same daily dose. At a daily dose of 6 g / 70 kg WT, CF-patients had a PKPD breakpoint for near-maximal bactericidal activity of 3 mg/L for 15 min infusions q8h, of 8-12 mg/L (87% PTA for MIC=12 mg/L) for 4 h infusions q8h, and of 16 mg/L for continuous infusion. Therefore, prolonged infusion will be superior to short-term infusions, if the $MIC_{50}$'s and $MIC_{90}$'s fall between 2 and 8 mg/L. For infections caused by those pathogens, treatment of CF-patients by prolonged or continuous infusion of carumonam seems the most reasonable option to optimize dosage regimens.

### 3.3.4 Population pharmacokinetics and pharmacodynamics of cefpirome

#### 3.3.4.1 Chemical structure of cefpirome

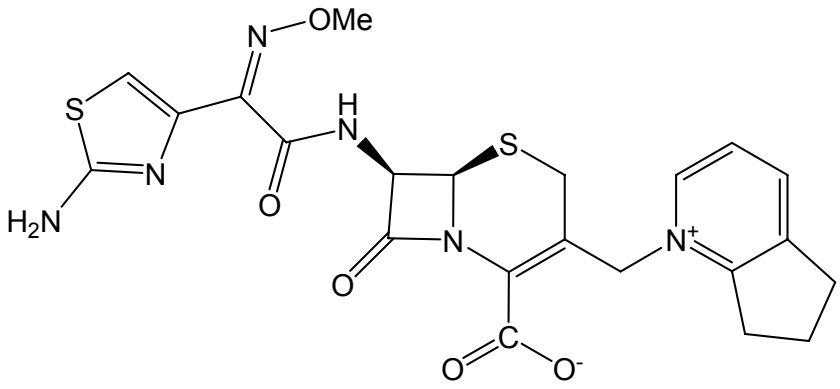


($C_{22}H_{22}N_6O_5S_2$, Mol. Wt.: 514.58)

**Chemical structure 3.3-4** Cefpirome

#### 3.3.4.2 Possible use of cefpirome in patients with cystic fibrosis

Cystic fibrosis (CF) is the most common life-shortening genetic disorder in the Caucasian population and affects about 60,000 individuals worldwide (88). The pulmonary disease causes most of the morbidity and mortality in CF-patients. *P. aeruginosa* is the most significant pathogen in this patient group (151) with a prevalence of up to 80% in adult CF-patients (88). Aminoglycosides, some beta-lactams, and ciprofloxacin are recommended for treatment of infections by *P. aeruginosa* (105, 151). Chronic infection by *P. aeruginosa* can be delayed or prevented by early efficacious treatment against this pathogen (139, 140, 192). Therefore, the use of antibiotics with activity against *P. aeruginosa* should be limited to preserve their effectiveness, when it is vitally needed. Alternative treatment options should

be considered for treatment of infections caused by *S. aureus* or *H. influenzae* that frequently occur in the first years of life in CF-patients.

Cefpirome is one such alternative treatment option with good activity against *H. influenzae* and methicillin susceptible *S. aureus* (MSSA) (20, 173, 474, 546), but it has insufficient activity against *P. aeruginosa*, methicillin resistant *S. aureus* (MRSA), *Burkholderia cepacia*, and *Stenotrophomonas maltophilia* as monotherapy (20, 69, 70, 173, 288, 503, 546). Although several authors have shown synergy of cefpirome and other antibiotics against MRSA (40, 41, 206), *Stenotrophomonas maltophilia* (246, 522), and *P. aeruginosa* (523) *in vitro*, the impact of those observations on the treatment of infections by those organisms *in vivo* needs to be substantiated. Zeitlinger et al. (557) proposed the combination of fosfomycin and cefpirome against *S. aureus* and *P. aeruginosa* for patients with severe soft tissue infections. Clinical and bacteriological data show good activity of cefpirome against Gram-positive and Gram-negative bacteria (42, 150, 235, 237, 287, 428, 466). Comparable or better cure rates have been found for cefpirome in comparison to ceftazidime, cefotaxime and ceftriaxone (150).

As the PK of cefpirome in CF-patients has not yet been evaluated, our first objective was to compare the average clearance and volume of distribution between CF-patients and healthy volunteers for various body size descriptors via population PK. As our second objective, we studied the ability of these body size models to reduce the unexplained BSV. Our third objective was to propose optimal dosage regimens of cefpirome in CF-patients.

#### 3.3.4.3 Methods

The general clinical and sample handling procedures, the methods for PK analysis (including NCA and population PK), and the general methods for MCS are described in chapter 2. Chapter 3.2 shows the specific methods applied for analysis of our CF-studies.

**Table 3.3-19** Demographic data of the cefpirome study (median [range])

| | **CF-patients** | **Healthy volunteers** |
|---|---|---|
| Number of subjects (males / females) | 12 (8 / 4) | 12 (6 / 6) |
| Age (yr) | 22.5 [18 - 34] | 29 [20 - 35] |
| Height (cm) | 170 [140 - 183] | 175 [161 - 182] |
| Total body weight (kg) | 53.3 [31.5 - 66.5] | 63.6 [53.0 - 85.0] |
| Fat-free mass° (kg) | 45.7 [26.2 - 55.9] | 50.0 [41.8 - 62.7] |
| Fat-free mass# (kg) | 45.8 [23.0 - 55.7] | 47.0 [36.6 - 61.5] |
| Body mass index (kg $m^{-2}$) | 19.0 [13.2 - 20.3] | 20.6 [17.7 - 28.4] |

°: Calculated by the formula of Cheymol and James (72, 222).

#: Calculated by the formula of Janmahasatian et al. (224).

***Subjects:*** We studied a total of 24 Caucasian volunteers (twelve CF-patients and twelve healthy volunteers) of both sexes. Table 3.3-19 shows the demographic data.

***Study design and drug administration:*** Each subject received a dose of 2,000 mg cefpirome dissolved in 20 mL water for injection as 10 min intravenous infusion. All infusions were administered with a BRAUN-Perfusor® (Braun, Melsungen, Germany).

***Blood and urine sampling:*** Blood samples were drawn immediately before start of the infusion (0 min) and at 5, and 10 min post start of infusion as well as at 5, 10, 15, 20, 30, 45, 60, 75, 90 min and 2, 2.5, 3, 4, 5, 6, 7, 8, 10, 12, 16, and 24 h post end of infusion. Urine was collected from the start of the infusion until 1 h post end of infusion as well as at 1-2, 2-3, 3-4, 4-6, 6-8, 8-10, 10-12, 12-24, 12-36, and 36-48 h after end of infusion.

***Drug analysis:*** We determined the concentration of cefpirome in plasma and urine by reversed phase HPLC with an internal standard. An equivalent amount of 0.1 M sodium hydrogen sulfate buffer (pH 5.0) with the internal standard desacetyl-cefotaxime (10 mg/L) was added to the plasma samples. Urine samples were diluted by a factor of 100 with distilled water which contained the internal standard. Acetonitrile (400 µL) was used to deproteinize each sample. After centrifugation for 5 min at 11,000 rpm,

1,000 µL of dichloromethane were added to the supernatant for extraction of the acetonitrile. After centrifugation for 5 min, 10-20 µL of the aqueous phase were injected into the HPLC system.

We assured stability of cefpirome under these conditions and used a Spherisorb ODS II column (5 µm, 250 x 8 x 4.6 mm, Waters, Germany) with a water / acetonitrile mixture at pH 5.5 and tetrabutylammonium hydrogen sulfate as ion-pair reagent. Cefpirome was detected at a wavelength of 254 nm in plasma and 273 nm in urine. Calibration was performed by linear regression. The cefpirome assay was linear between 0.614 and 322 mg/L in plasma and between 17.1 and 8,000 mg/L in urine. We took 30-40 mL blood from one additional subject at three time points with low, intermediate, and high expected concentrations. This subject did not participate in the PK study. Those blood samples were prepared as the other samples (see above) and used as biological quality controls. We included these biological quality controls and spiked quality controls in each analytical run.

***MCS:*** We compared various dosage regimens at a daily cefpirome dose of 4 g / 70 kg WT: 1) 30 min infusion of 2 g / 70 kg WT q12h, 2) 5 h infusion of 2 g / 70 kg WT q12h, 3) 30 min infusion of 1.33 g / 70 kg WT q8h, 4) 5 h infusion of 1.33 g / 70 kg WT q8h, and 5) continuous infusion of 4 g / 70 kg WT per day. We studied a range of MICs from 0.125 to 64 mg/L and assumed a protein binding of 10% for cefpirome (343, 479).

#### 3.3.4.4 Results

***NCA:*** The average plasma concentrations of CF-patients and healthy volunteers are shown in Figure 3.3-11. Table 3.3-20 lists the PK parameters from NCA. Those PK parameters are not scaled by any size descriptor. CF-patients and healthy volunteers had a similar total, renal, and nonrenal clearance without size adjustment. The unscaled volume of distribution at steady-state was 6% lower in CF-patients. Several PK parameters determined by NCA are plotted vs. $FFM_C$ in Figure 3.3-12. The volume of distribution at steady-state, total clearance, renal clearance, and mean residence time

showed a (slight) trend to increase with $FFM_C$. These trends are driven by two CF-patients with a low $FFM_C$.

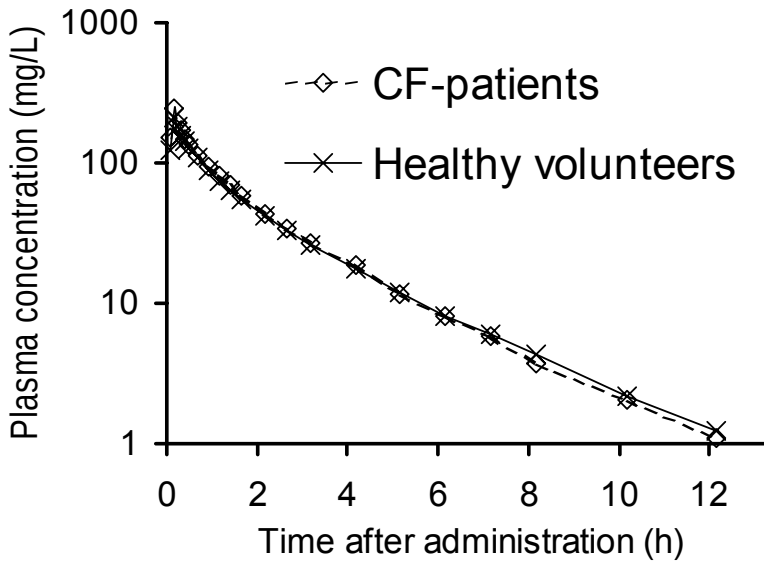


**Figure 3.3-11** Average plasma concentrations of cefpirome for CF-patients and healthy volunteers after a single 10 min intravenous infusion of 2 g cefpirome

***Population PK analysis:*** The VPC indicated a highly sufficient predictive performance for the two and the three compartment model, whereas the one compartment model had insufficient predictive performance. Figure 3.3-13 reveals the very good predictive performance of the two compartment model for plasma concentrations and amounts excreted in urine. We selected the two compartment model as our final model, because it was simpler than the three compartment model. The PK parameters for the two compartment model are shown in Table 3.3-21.

We distinguished the different size models 1) by their estimates for the disease specific scale factors FCYF and 2) by their estimates for the unexplained BSV in clearance and volume of distribution. CF-patients had lower estimates for clearance and volume of distribution than healthy volunteers, if body size was ignored (see size model A, Table 3.3-22).

**Table 3.3-20** Unscaled PK parameters derived by NCA (median [range])

| | CF-patients | Healthy volunteers |
|---|---|---|
| Total clearance (L/h) | 6.52 [4.05 - 8.51] | 6.64 [5.63 - 7.64] |
| Renal clearance (L/h) | 5.59 [3.18 - 9.98] | 5.51 [2.70 - 7.13] |
| Nonrenal clearance (L/h) | 0.842 [0.0* - 1.77] | 0.881 [0.512 - 4.28] |
| Volume of distribution at steady-state (L) | 14.4 [7.32 - 25.3] | 15.3 [12.6 - 19.4] |
| Fraction excreted unchanged in urine (%) | 84.4 [78.6 - 100*] | 87.0 [38.7 - 93.3] |
| Peak concentration (mg/L) | 221 [135 - 560] | 206 [159 - 299] |
| Terminal half-life (L) | 2.07 [1.95 - 3.29] | 2.17 [1.68 - 3.75] |
| Mean residence time (h) | 2.16 [1.58 - 3.03] | 2.33 [1.85 - 2.98] |

*: The amount excreted unchanged in urine was larger than the nominal dose for one CF-patient. This would cause the nonrenal clearance to be negative which is physiologically impossible. We therefore report 0.0 L/h for the lowest nonrenal clearance and 100% for the highest fraction excreted unchanged in urine.

The estimates for $FCYF_V$ was close to the ideal value of 1.0 (range: 0.97 to 1.05, see Table 3.3-22, panel B) for size models B to E. Linear scaling by WT (size model B) resulted in a significantly (p=0.002) higher total clearance in CF-patients compared to healthy volunteers with a 19% higher total clearance in CF-patients (see Table 3.3-22, panel B). This difference was much smaller (on average: 5-7%) and not significantly different from 0% for allometric scaling by $FFM_C$ or $FFM_J$. Allometric scaling by WT or $FFM_C$ resulted in a 21% and 16% reduction of the unexplained BSV for renal clearance (see Table 3.3-23), respectively. However, this reduction was not statistically significant at the sample size of this study.

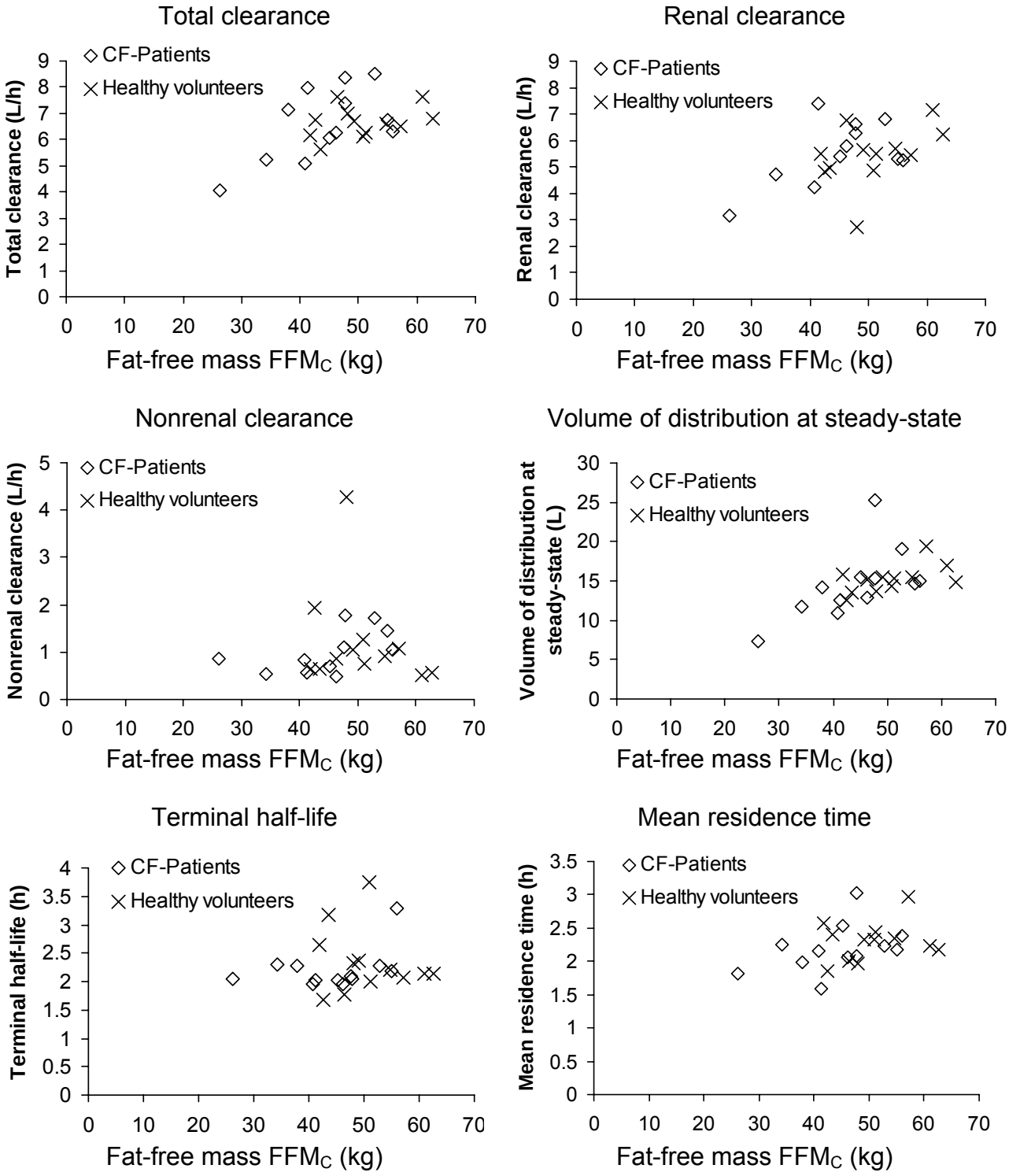


**Figure 3.3-12** PK parameters determined by NCS plotted vs. $FFM_C$

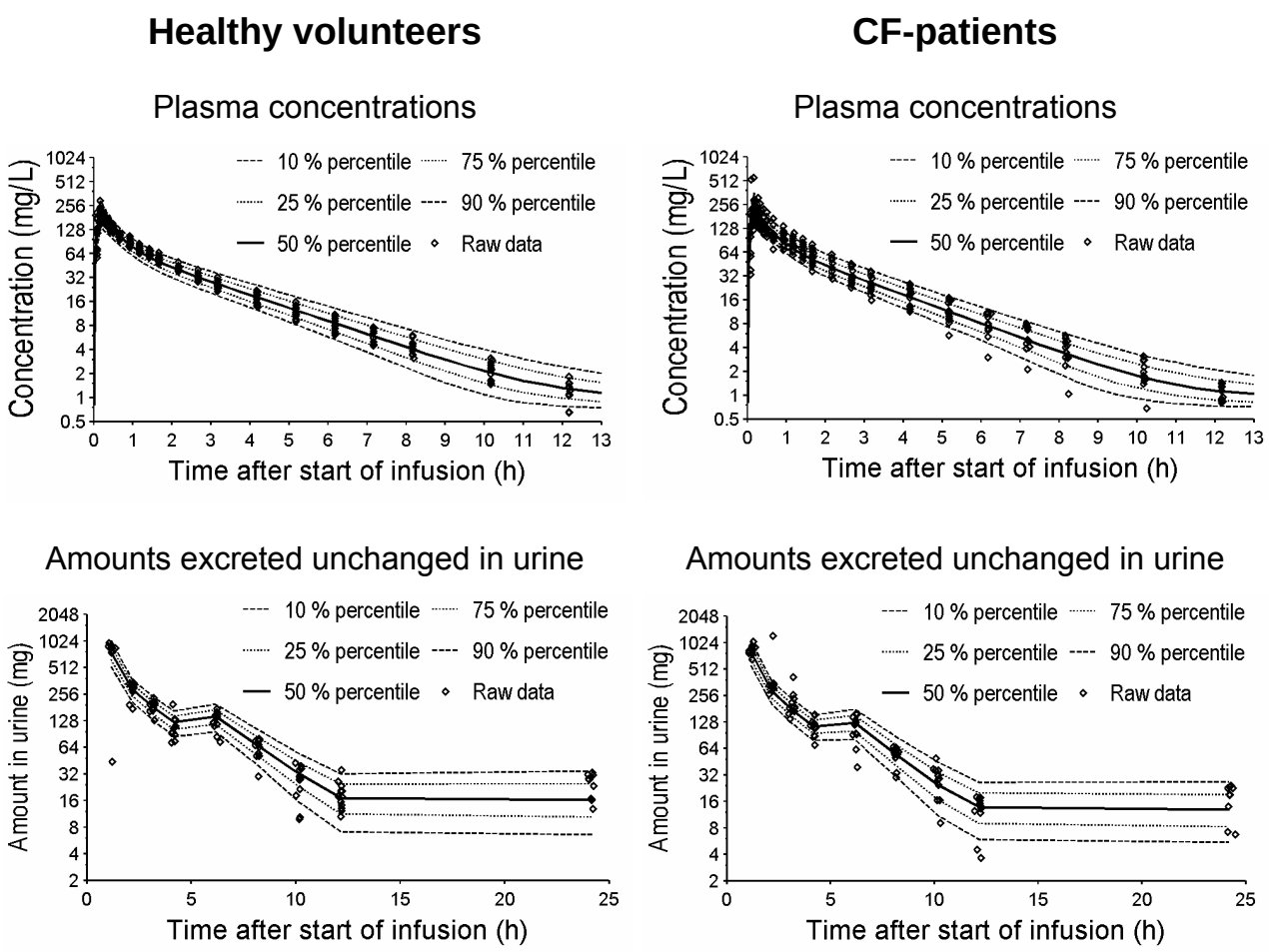


**Figure 3.3-13** VPC based on 6,000 CF-patients and 6,000 healthy volunteers for the two compartment model based on $FFM_C$ (see Table 3.3-21).

See chapter 2.6.3 for interpretation of VPCs.

***MCS:*** Figure 3.3-14 reveals that CF-patients had slightly lower PTAs than healthy volunteers, primarily because doses were selected as mg/kg WT and CF-patients had a higher total clearance per kg WT. The PKPD breakpoints in CF-patients were about 1.5 times lower compared to healthy volunteers (see Table 3.3-24). Standard short-term infusions of 2 g / 70 kg WT cefpirome q12h achieved a PKPD breakpoint of 6 mg/L for bacteriostasis and of 1.5 mg/L for near-maximal kill in CF-patients.

**Table 3.3-21** PK parameters for the allometric size model based on $FFM_C$

| Parameter | Unit | Estimate for | | Coefficient of variation (%)° |
|---|---|---|---|---|
| | | CF-patients | healthy volunteers | |
| $CL_{tot}$^ | L $h^{-1}$ | 7.55* | 7.03* | |
| $CL_R$ | L $h^{-1}$ | 6.13* | 5.78* | 13.5 |
| $CL_{NR}$ | L $h^{-1}$ | 1.43* | 1.25* | 25.8 |
| Vss^ | L | 15.3* | 15.4* | |
| V1 | L | 8.88* | 8.93* | 25.7 |
| V2 | L | 6.39* | 6.43* | 10.8 |
| CLic | L $h^{-1}$ | 6.92* | | |
| TK0 (fixed) | min | 10 | | |
| CVC | % | 12.4 | | |
| SDC | mg/L | 0.506 | | |
| CVAU | % | 20.6 | | |
| SDAU | mg | 7.54 | | |

*: Group estimate for subject of standard size ($FFM_C$ = 53 kg).

^: Derived from model estimates, not an estimated parameter.

°: Apparent coefficients of variation for the BSV.

#: The coefficient of correlation for the random effects of V1 and V2 was: $r_{BSV}(V1,V2) = -0.51$.

See chapter 2.6.2 for explanation of model parameters.

These PKPD breakpoints increased by a factor of 1.5 to 2, if the same daily dose was given as short-term infusions q8h instead of q12h (see Table 3.3-24). As alternative mode of administration, prolonged (5h) infusion of 2 g / 70 kg WT q12h achieved a bacteriostasis breakpoint of 16 mg/L and a near-maximal kill breakpoint of 4 mg/L in CF-patients. Prolonged (5h) infusion of 1.33 g / 70 kg WT q8h yielded a breakpoint of 8-12 mg/L (PTA = 85% at an MIC of 12 mg/L) and continuous infusion of 4 g / 70 kg WT per day achieved a breakpoint of 12 mg/L for near-maximal killing in CF-patients.

**Table 3.3-22** Ratios of group estimates (CF-patients / healthy volunteers) for clearance and volume of distribution for different size models

Panel A: Estimates from the original dataset

| Size model | $FCYF_{CLR}$ | $FCYF_{CLNR}$ | $FCYF_{CLT}$[#] | $FCYF_{V}$ |
|---|---|---|---|---|
| A) No size model | 0.952 | 1.04 | 0.967 | 0.861 |
| B) WT linear scaling | 1.19 | 1.23 | 1.20 | 1.04 |
| C) WT allometric | 1.12 | 1.19 | 1.13 | 1.06 |
| D) $FFM_C$ allometric | 1.06 | 1.14 | 1.07 | 0.994 |
| E) $FFM_J$ allometric | 1.05 | 1.11 | 1.06 | 0.971 |

Panel B: Median (90% confidence interval) from non-parametric bootstrap[$]

| Size model | $FCYF_{CLR}$ | $FCYF_{CLNR}$ | $FCYF_{CLT}$[#] | $FCYF_{V}$ |
|---|---|---|---|---|
| A) No size model | 0.95 (0.84-1.07) | 1.03 (0.75-1.41) | 0.97 (0.86-1.07) | 0.87 (0.80-0.95) |
| B) WT linear scaling | 1.19 (1.07-1.31) | 1.23 (0.90-1.70) | 1.19 (1.09-1.32) | 1.04 (0.96-1.12) |
| C) WT allometric | 1.12 (1.01-1.24) | 1.19 (0.87-1.64) | 1.13 (1.04-1.24) | 1.05 (0.97-1.14) |
| D) $FFM_C$ allometric | 1.06 (0.96-1.18) | 1.14 (0.85-1.61) | 1.07 (0.99-1.18) | 0.99 (0.92-1.07) |
| E) $FFM_J$ allometric | 1.04 (0.94-1.17) | 1.12 (0.84-1.58) | 1.05 (0.96-1.17) | 0.97 (0.87-1.07) |

$FCYF_{NNN}$: ratio of group estimates for parameter NNN (group estimate for CF-patients divided by group estimate for healthy volunteers).

[#]: Calculated as weighted average of $FCYF_{CLR}$ and $FCYF_{CLNR}$.

[$]: Medians and non-parametric 90% confidence intervals (5% - 95% percentile) derived from 1,000 non-parametric bootstrap runs. Each bootstrap run contained 24 subjects (12 CF-patients and 12 healthy volunteers) who were randomly drawn from the original dataset with replacement.

**Table 3.3-23** BSV (variances) for various size models relative to linear scaling by WT

Panel A: Estimates from the original dataset

| Size model | $CL_R$ | $CL_{NR}$ | V1 | V2 |
|---|---|---|---|---|
| B) WT linear scaling | 0%* | 0%* | 0%* | 0%* |
| C) WT allometric | **-19%°** | -8% | -2% | 31% |
| D) $FFM_C$ allometric | **-13%°** | -10% | -6% | 33% |
| E) $FFM_J$ allometric | 10%° | 4% | 7% | 138% |

Panel B: Median (90% confidence interval) from non-parametric bootstrap[$]

| Size model | $CL_R$ | $CL_{NR}$ | V1 | V2 |
|---|---|---|---|---|
| B) WT linear scaling | 0%* | 0%* | 0%* | 0%* |
| C) WT allometric | **-21%** (-46 to 5%) | -7% (-35 to 36%) | -2% (-9 to 5%) | 33% (-3 to 75%) |
| D) $FFM_C$ allometric | **-16%** (-51 to 25%) | -6% (-44 to 70%) | -5% (-26 to 11%) | 37% (-16 to 99%) |
| E) $FFM_J$ allometric | 6% (-35 to 70%) | 1% (-49 to 111%) | 7% (-18 to 33%) | 139% (34 to 276%) |

*: The values are (variance of test size model - variance of linear scaling by WT) / variance of linear scaling by WT. For the bootstrap estimates, the denominator was the median variance of linear scaling by WT from all 1,000 bootstrap runs.

°: The lower this number, the more variability was explained by the respective size model. A negative value indicates that the size model reduced the between subject variance compared to linear scaling by WT. These values indicate that the BSV (variance) for renal clearance was reduced by 19% for allometric scaling by WT, reduced by 13% for allometric scaling by $FFM_C$, and increased by 10% for allometric scaling by $FFM_J$, all relative to linear scaling by WT.

[$]: Medians and non-parametric 90% confidence intervals (5% - 95% percentile) derived from 1,000 non-parametric bootstrap runs. Each bootstrap run contained 24 subjects (12 CF-patients and 12 healthy volunteers) who were randomly drawn from the original dataset with replacement.

**Table 3.3-24** PKPD breakpoints for various dosage regimens of cefpirome at a daily dose of 4 g / 70 kg WT

| **Dosage regimens** | **Bacteriostasis target ($fT_{>MIC} \geq 40\%$)** | | **Near-maximal kill target ($fT_{>MIC} \geq 65\%$)** | |
|---|---|---|---|---|
| | CF-patients | Healthy volunteers | CF-patients | Healthy volunteers |
| **Dose: 2 g / 70kg WT q12h** | *PKPD breakpoints (mg/L)* | | | |
| as 30 min infusion | 6 | 8 | 1.5 | 2 |
| as 5 h infusion | 16 | 16 | 4 | 6 |
| **Dose: 1.33 g / 70kg WT q8h** | | | | |
| as 30 min infusion | 8 | 12 | 3 | 4 |
| as 5 h infusion | 16 | 16 | 8-12 | 12 |
| Continuous infusion of 4g/70kg/day | 12 | 16 | 12 | 16 |

### 3.3.4.5 Discussion

Chronic infection by *P. aeruginosa* remains a serious problem for CF-patients. It seems unlikely that many new drugs will be added to the armamentarium for treatment of this pathogen in the near future. Therefore, optimal antibiotic treatment with the currently available antibiotics which are active against *P. aeruginosa* is vital and preserving their activity by a prudent use in CF-patients is an important task (151).

MSSA or *H. influenzae* are often found as the first pathogens in the lungs of young CF patients. In order to limit the emergence of resistance of antibiotics against *P. aeruginosa*, it seems reasonable to rely on antibiotics which are not primarily used against *P. aeruginosa* for treatment of infections caused by MSSA or *H. influenzae*. Cefpirome is one such alternative with good activity against *H. influenzae* and MSSA (20, 173, 474, 546) and some activity against *P. aeruginosa*. However, we are not aware of any data on the PK of cefpirome in CF-patients or on its effectiveness in CF-patients.

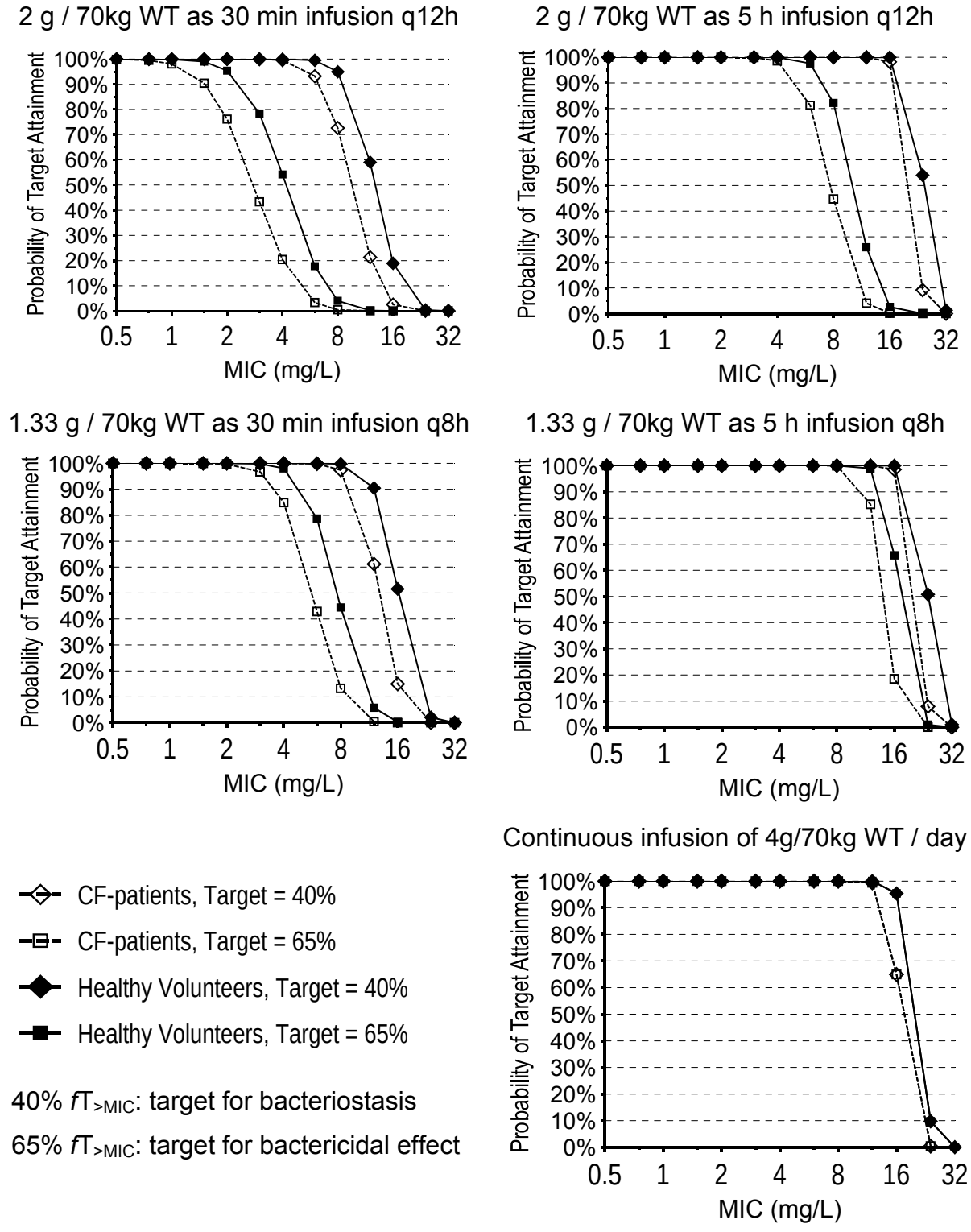


**Figure 3.3-14** Probability of target attainment for different dosage regimens of cefpirome at steady-state for a daily dose of 4 g / 70 kg total body weight

Therefore, we compared the PK of cefpirome in CF-patients and healthy volunteers by population PK and evaluated the PD profile by MCS. Our population PK model had a highly sufficient predictive performance for cefpirome in plasma and urine (see Figure 3.3-13). The prediction intervals for the plasma concentrations were very representative of the raw data for CF-patients and were slightly too wide during the terminal phase for healthy volunteers. However, the variability of the healthy volunteers' plasma concentrations was low and this results only in slightly more conservative (lower) predicted PTAs in healthy volunteers. After assuring the predictive performance of our final model, we used it to compare the PD characteristics between both subject groups via MCS.

Our results for the PK parameters of cefpirome in healthy volunteers were in good agreement with those from other authors (24, 248, 298, 299, 307, 349, 373). Our CF-patients had a 16% lower WT than our healthy volunteers, $FFM_C$ was 9% lower and $FFM_J$ was 3% lower in CF-patients (see Table 3.3-19). Our NCA analysis showed a 6% lower unscaled volume of distribution at steady-state and a 2% lower unscaled total clearance in CF-patients (see Table 3.3-20). The terminal half-life was 5% shorter and the mean residence time was 7% shorter in CF-patients. These differences were in good agreement with the slightly smaller aqueous body space in our CF-patients compared to our healthy volunteers as indicated by $FFM_C$ and $FFM_J$.

We studied the influence of body size on clearance and volume of distribution by population PK. In absence of a size descriptor (size model A, Table 3.3-22), CF-patients had slightly lower volumes of distribution and clearances, probably because they were slightly smaller. Size models B to E estimated $FCYF_V$ very close to 1.0. We observed a significantly higher (+19%, p=0.002) total clearance in CF-patients, if clearance was scaled linearly by WT (see Table 3.3-22, panel B). Allometric scaling by $FFM_C$ or $FFM_J$ resulted in similar total clearances for both subject groups (5-7% higher in CF-patients) with no statistically significant difference between CF-patients and healthy volunteers. Therefore, the average clearance and volume of distribution were well comparable between CF-patients and healthy volunteers for allometric scaling by $FFM_C$ or $FFM_J$.

Besides the ability to describe the difference in average clearance and average volume of distribution, we compared the ability to reduce the unexplained BSV between our size models. If a size descriptor reduces the unexplained BSV in clearance or volume of distribution, it allows one to predict the individual clearance or volume of distribution for a patient more precisely and subsequently permits to achieve target concentrations with a greater precision. As shown in Table 3.3-23, allometric scaling by WT or $FFM_C$ reduced the unexplained BSV in renal clearance by 16-21% relative to linear scaling by WT. However, all 90% confidence intervals included 0% and therefore none of the allometric size models (size models C to E) reduced the unexplained BSV significantly better than linear scaling by WT. Larger studies or a meta-analysis of several smaller studies are required to show that.

We used the population PK model based on allometric scaling by $FFM_C$ to predict the PTA in CF-patients and healthy volunteers. We compared the PKPD breakpoints for various dosage regimens to propose “optimal” dosage regimens for the bacteriostasis and the near-maximal kill target. Figure 3.3-14 shows that CF-patients achieved slightly lower PTAs compared to healthy volunteers, primarily because CF-patients had a 19% higher clearance per kg WT (size model B, linear scaling by WT) and doses were selected as mg/kg WT. The PKPD breakpoints were about 1.5 times lower in CF-patients relative to healthy volunteers (see Table 3.3-24). However, if CF-patients should achieve the same PTAs as healthy volunteers, CF-patients would require an about 50% higher dose in mg/kg WT. As this would possibly carry more side effects, we studied alternative modes of administration to optimize the PTA in both subject groups. Continuous infusion (124) or shorter dosage intervals (435) have also been proposed for cefpirome by other authors.

The BSAC (56) deems isolates with an MIC ≤1 mg/L as susceptible to cefpirome. Other authors use ≤4 mg/L (69) or ≤8 mg/L (149, 214, 314) to define susceptibility. For a standard regimen of 2 g / 70 kg WT q12h given as 30 min infusion, we found a PKPD breakpoint of 2 mg/L in healthy volunteers and of 1.5 mg/L in CF-patients for the near-maximal kill target $fT_{>MIC} \geq 65\%$. The PKPD breakpoints for the bacteriostasis target were 8 mg/L in healthy

volunteers and 6 mg/L in CF-patients. Therefore, our PKPD breakpoint for near-maximal killing was slightly higher than the BSAC breakpoint of 1 mg/L for cefpirome and our PKPD breakpoint for bacteriostasis was in good agreement with the higher breakpoints of 4-8 mg/L used by other authors (69, 149, 214, 314). If the bacteriostasis breakpoint was to be optimized, administering the same dose as 5 h infusion q12h instead of as 30 min infusion yielded a breakpoint of 16 mg/L in both subject groups for bacteriostasis.

To optimize the PKPD breakpoint for near-maximal killing at the same daily dose, more frequent dosing of prolonged infusions or continuous infusion would be required. Prolonged (5 h) infusion of 1.33 g / 70 kg WT q8h achieved a PKPD breakpoint of 8-12 mg/L (PTA = 85% at an MIC of 12 mg/L) and continuous infusion of 4 g / 70 kg WT per day reached a PKPD breakpoint of 12 mg/L for near-maximal killing in CF-patients. This was a 6-8 fold increase in the PKPD breakpoint compared to 30 min infusions q12h (see Table 3.3-24). It depends on the MIC distribution, if those increased PTAs will result in a higher probability of successful treatment. Prolonged infusion q8h and continuous infusion of cefpirome will especially be superior to 30 min infusion q12h, if the $MIC_{50}$ and $MIC_{90}$ fall between 2 and 16 mg/L. For $MIC_{90}$'s of 1 mg/L or less, there will be only a small advantage for prolonged or continuous infusion compared to short-term infusion, since short-term infusions q12h will achieve probabilities of successful treatment of >90% (assuming that the PTA is 100% for all MICs below the PKPD breakpoint).

The $MIC_{90}$ for cefpirome has been reported (20, 173, 288, 384, 503, 546) to be below 1 mg/L against *H. Influenzae* and about 0.5-1 mg/L against MSSA. More recently, Ishii et al. (214) find MICs between 0.38 and 4 mg/L for MSSA with an $MIC_{90}$ of 1.5 mg/L in Japan and Lewis et al. (287) report an $MIC_{90}$ of 2 mg/L in Japan. Mathai et al. (314) report an $MIC_{90}$ of 1.5 mg/L for MSSA in India and Giamarellos-Bourboulis et al. (149) find higher MICs for MSSA with an $MIC_{50}$ of 1 mg/L and an $MIC_{90}$ above 256 mg/L in Greece. It is those more resistant populations of MSSA for which prolonged infusion will be superior to short-term infusion of cefpirome in empiric therapy.

The $MIC_{90}$ of *P. aeruginosa* is often above 32 mg/L for cefpirome, which precludes the use of cefpirome in empiric monotherapy. However, the $MIC_{50}$ has been reported to range between 3 and 12 mg/L for this pathogen (69, 214, 233, 287, 314, 384). Those $MIC_{50}$'s are below the PKPD breakpoint for prolonged infusion q8h and for continuous infusion (see Table 3.3-24). Prolonged (5 h) infusion of 1.33 g / 70kg WT might be a valuable treatment option for infections caused by *P. aeruginosa* with an MIC of 12 mg/L and below, although the effectiveness of prolonged and continuous infusion of cefpirome has to be substantiated clinically.

In conclusion we found similar to slightly lower unscaled clearances and volumes of distribution of cefotiam for CF-patients compared to healthy volunteers. Allometric scaling by $FFM_C$ or $FFM_J$ explained the average differences in PK parameters better than linear scaling by WT which predicted total clearance to be 19% higher (p=0.002) in CF-patients compared to healthy volunteers. Allometric scaling by WT or $FFM_C$ reduced the unexplained BSV in renal clearance by 16-21%, but this reduction was not statistically significant. However, dose selection based on $FFM_C$ may be important to achieve target concentrations more precisely in empiric therapy. A standard dosage regimen of 2 g / 70 kg WT q12h given as 30 min infusion achieved a PKPD breakpoint of 1.5 mg/L for near-maximal killing and of 6 mg/L for bacteriostasis in CF-patients. Administering 2 g / 70 kg WT q12h as 5 h infusion was an optimized dosage regimen for bacteriostasis and achieved a PKPD breakpoint of 16 mg/L for this target. Optimal breakpoints for near-maximal killing of 8-12 mg/L were achieved by 5 h infusions of 1.33 g / 70 kg WT q8h and by continuous infusion. The superiority of prolonged and continuous infusion to standard short-term infusions will be most pronounced, if the MICs fall between 2 and 12 mg/L. Future clinical trials are warranted to show a higher probability of successful clinical outcome for dose selection in CF-patients based on $FFM_C$ and to show the superiority of prolonged or continuous infusion to standard short-term infusion.

### 3.3.5 Population pharmacokinetics and pharmacodynamics of cefotiam

#### 3.3.5.1 Chemical structure of cefotiam

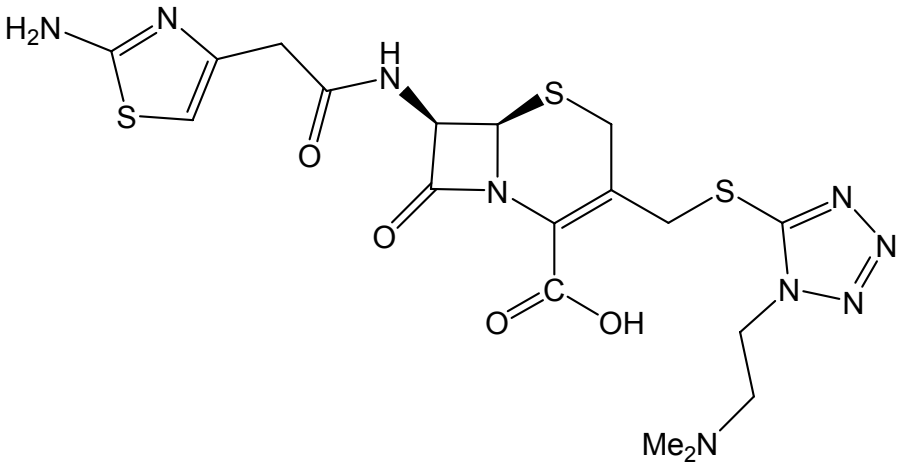

($C_{18}H_{23}N_9O_4S_3$, Mol. Wt.: 525.63)

**Chemical structure 3.3-5** Cefotiam

#### 3.3.5.2 Possible use of cefotiam in patients with cystic fibrosis

As described in chapter 3.3.4.2, it may be important to limit and postpone the use of antibiotics with high activity against *P. aeruginosa* for treatment of infections by *H. influenzae* or *S. aureus*. Cefotiam is one such alternative to antibiotics with a high activity against *P. aeruginosa* and is active against *H. influenzae* and MSSA (173, 366). Therefore, cefotiam is an appealing candidate for early use in CF-patients.

We are not aware of any reports on the PK of cefotiam in CF-patients. Therefore, our first objective was to compare the PK of cefotiam between CF-patients and healthy volunteers via population PK. As our second objective, we studied whether the average differences and the BSV in clearance and volume of distribution are better described by $FFM_C$ or $FFM_J$ than by WT. Our

third objective was to explore the PKPD profiles of various dosage regimens in CF-patients and healthy volunteers.

### 3.3.5.3 Methods

The general clinical and sample handling procedures, the methods for PK analysis (including NCA and population PK), and the general methods for MCS are described in chapter 2. Chapter 3.2 shows the specific methods applied for analysis of our CF-studies.

***Subjects:*** A total of 14 Caucasian volunteers (eight CF-patients and six healthy volunteers) participated in the study. Table 3.3-25 shows the demographic data.

**Table 3.3-25** Demographic data of the cefotiam study (median [range])

| | **CF-patients** | **Healthy volunteers** |
|---|---|---|
| Number of subjects (males / females) | 8 (4 / 4) | 6 (3 / 3) |
| Age (yrs) | 19 [17 - 24] | 23.5 [21 - 26] |
| Height (cm) | 167 [157 - 173] | 169 [164 - 190] |
| Total body weight (kg) | 45.5 [33 - 59] | 68.5 [58 - 80] |
| Fat-free mass° (kg) | 40.3 [28.8 - 46.2] | 50.6 [44.6 - 65.4] |
| Fat-free mass# (kg) | 40.2 [25.4 - 46.4] | 47.4 [39.1 - 64.7] |
| Body mass index (kg $m^{-2}$) | 17.0 [13.4 - 19.9] | 22.5 [20.3 - 27.9] |

°: Calculated by the formula of Cheymol and James (72, 222).

#: Calculated by the formula of Janmahasatian et al. (224).

***Study design and drug administration:*** All subjects received 1,027.5 mg cefotiam as 3 min intravenous infusion. All infusions were administered with a BRAUN-Perfusor® (Braun, Melsungen, Germany).

***Blood sampling:*** Blood samples were drawn immediately before start of infusion (0 min), at the end of infusion (3 min), as well as at 5, 10, 15, 20, 30, 45, 60, 90 min and 2, 3, 4, 5, 6, 8, 12, and 24 h post end of infusion.

***Drug analysis:*** We determined the concentration of cefotiam in plasma by reversed phase HPLC. An amount of 200 µL of $NaH_2PO_4$ buffer at pH 6.2 was added to 200 µL of each plasma sample. Acetonitrile (400 µL) was used to deproteinize each sample. After centrifugation 2,000 µL of dichloromethane were added for extraction of acetonitrile. From the remaining aqueous phase, 20-40 µL were injected into the HPLC system. The recovery from plasma was 99.7 ± 1.6% at a concentration of 100 mg/L, 99.6 ± 3.3% at a concentration of 25 mg/L, and 94.9 ± 5.9% at a concentration of 1 mg/L. For comparison, the corresponding recoveries from water were 97.2 ± 3.0%, 94.1 ± 2.6%, and 95.3 ± 1.9%, respectively.

We used a Novapack C18 (5 µm) column with a water / acetonitrile mixture at pH 4.7. Cefotiam was detected at a wavelength of 254 nm. Calibration was performed by linear regression. We took 30-40 mL blood from one additional subject at three time points with a high, intermediate, and low concentration. This subject did not participate in the PK study. Those blood samples were prepared like all other samples as described above and used as biological quality controls. We included these biological quality controls and spiked quality controls in each analytical run.

***MCS:*** We compared five dosage regimens in total. These comprised three dosage regimens at a daily dose of 4g / 70kg WT cefotiam: a) Short-term (30min) infusion of 1g / 70kg WT q6h, b) prolonged (4h) infusion of 1g / 70kg WT q6h, and c) continuous infusion of 4g / 70kg WT daily. The other two dosage regimens had a higher daily dose of 6g / 70kg WT cefotiam: d) Short-term (30min) infusion of 2g / 70kg WT q8h and e) prolonged (5h) infusion of 2g / 70kg WT q8h. We studied a range of MICs from 0.001 to 32 mg/L. The protein binding of cefotiam has been reported (58, 345, 394, 545) to range between 40 and 62%. Therefore, we assumed an average protein binding of 51% for cefotiam.

#### 3.3.5.4 Results

***NCA:*** Figure 3.3-15 shows the average plasma concentrations of CF-patients and healthy volunteers and Table 3.3-26 the results from NCA. These PK parameters are not scaled by any size descriptor. Total clearance was 3% lower and volume of distribution at steady-state was 3% smaller in CF-patients than in healthy volunteers. CF-patients had a 12% higher peak concentration, a 14% shorter terminal half-life and a very similar mean residence time relative to healthy volunteers.

**Table 3.3-26** Unscaled PK parameters derived by NCA (median [range])

| | CF-patients | Healthy volunteers |
|---|---|---|
| Total clearance (L/h) | 17.1 [8.97 - 27.8] | 17.7 [16.2 - 24.0] |
| Volume of distribution at steady-state (L) | 12.4 [8.80 - 18.1] | 12.8 [10.5 - 16.7] |
| Peak concentration (mg/L) | 124 [74.1 - 293] | 111 [81.7 - 130] |
| Terminal half-life (L) | 0.931 [0.881 - 1.91] | 1.08 [0.753 - 1.66] |
| Mean residence time (h) | 0.699 [0.527 - 1.22] | 0.707 [0.646 - 0.874] |

***Population PK analysis:*** The VPC indicated a similar predictive performance for the two and three compartment model, whereas the one compartment model had insufficient predictive performance. As the two-compartment model had highly sufficient predictive performance for the desired PKPD statistic $fT_{>MIC}$, we selected it as our final model.

Figure 3.3-16 shows the good predictive performance for the final model which was based on $FFM_C$ as size descriptor. The prediction intervals were slightly too wide for the healthy volunteers. However, the observed variability for the (n=6) healthy volunteers was small possibly due to highly standardized study conditions. This resulted in slightly more conservative (lower) predicted PTAs in healthy volunteers. The final parameter estimates for this model are shown in Table 3.3-27.

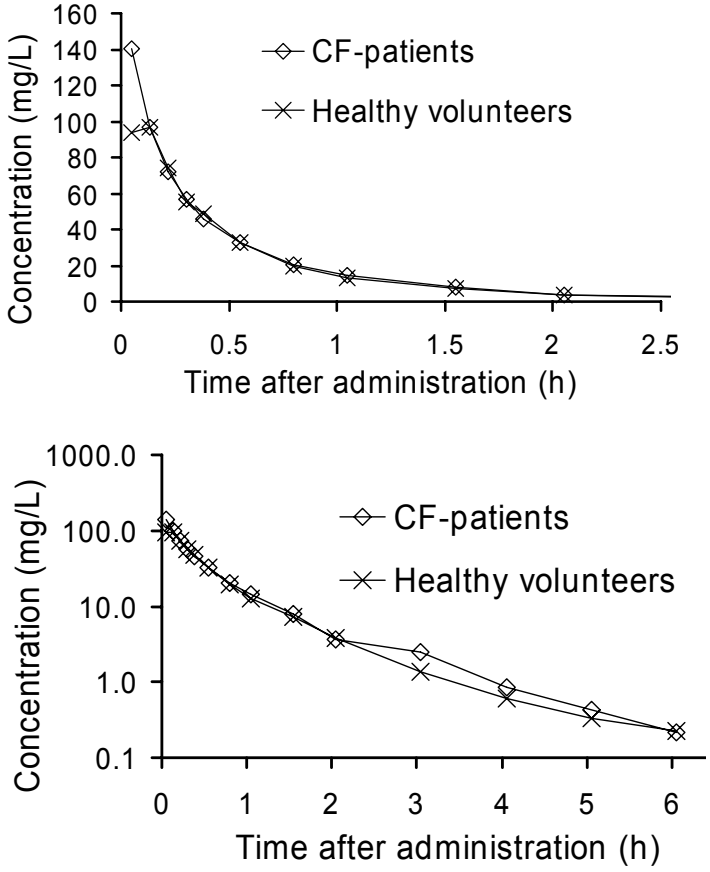


**Figure 3.3-15** Average plasma concentrations of cefotiam for CF-patients and healthy volunteers after a single 3 min intravenous infusion of 1,027.5 mg cefotiam

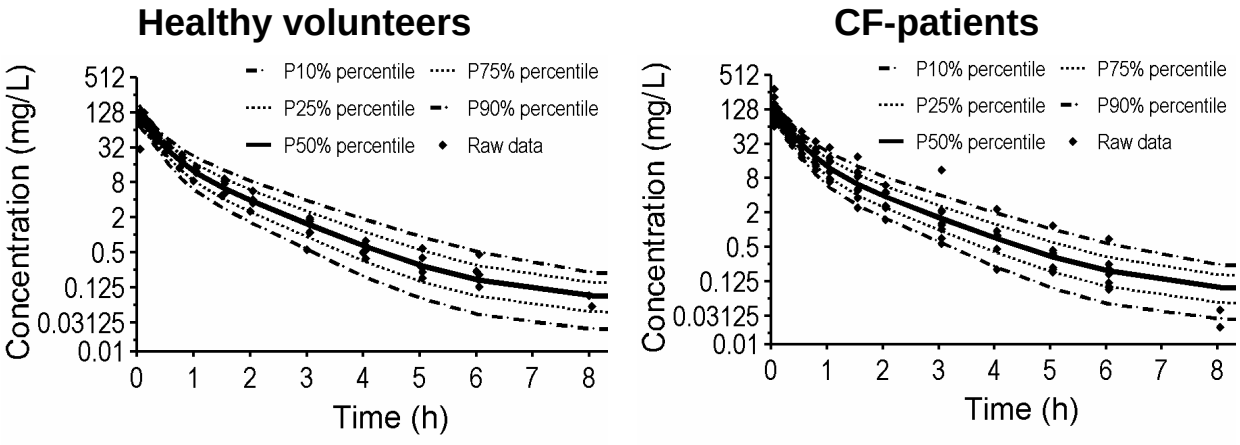


**Figure 3.3-16** VPC based on 12,000 CF-patients and 9,000 healthy volunteers for the two compartment model based on $FFM_C$ (see Table 3.3-27).

See chapter 2.6.3 for interpretation of VPCs.

**Table 3.3-27** PK parameter estimates for the allometric size model based on $FFM_C$

| Parameter | Unit | Estimate for | | Coefficient of variation (%)° |
|---|---|---|---|---|
| | | CF-patients | healthy volunteers | |
| CL | L $h^{-1}$ | 22.6* | 19.3* | 26.0 |
| Vss^ | L | 16.5* | 13.3* | |
| V1 | L | 10.8* | 8.74* | 21.5# |
| V2 | L | 5.65* | 4.56* | 14.3# |
| CLic | L $h^{-1}$ | 6.39* | | |
| TK0 (fixed) | min | 3 | | |
| $CV_C$ | % | 17.5 | | |
| $SD_C$ | mg/L | 0.0955 | | |

*: Group estimate for subject of standard size ($FFM_C$ = 53 kg).

^: Derived from model estimates, not an estimated parameter.

°: Apparent coefficient of variation for the BSV.

#: Coefficient of correlation for the random variability between V1 and V2, r(V1,V2) = -0.17.

See chapter 2.6.2 for explanation of model parameters.

We compared the size models 1) by their estimates for the disease specific scale factors FCYF and 2) by their ability to reduce the unexplained BSV in clearance and volume of distribution. In absence of a size descriptor (size model A, Table 3.3-28), CF-patients had a 4% lower total clearance and a very similar volume of distribution relative to healthy volunteers. Linear scaling by WT predicted total clearance to be 39% higher and volume of distribution to be 35% higher in CF-patients. Allometric scaling by $FFM_C$ or $FFM_J$ resulted in a 16-18% higher total clearance and in an about 25% higher volume of distribution in CF-patients (see Table 3.3-28). Therefore, CF-patients had a slightly higher clearance and volume of distribution of cefotiam after adjusting for body size and body composition.

**Table 3.3-28** Ratios of group estimates (CF-patients / healthy volunteers) for clearance and volume of distribution for different size models

| Size model | Estimates from original dataset | | Median (90% confidence interval) from non-parametric bootstrap[#] | |
|---|---|---|---|---|
| | $FCYF_{CLT}$ | $FCYF_V$ | $FCYF_{CLT}$ | $FCYF_V$ |
| A) No size model | 0.955 | 0.980 | 0.96 (0.76 - 1.19) | 1.00 (0.82 - 1.23) |
| B) WT linear scaling | 1.37 | 1.32 | 1.39 (1.14 - 1.66) | 1.35 (1.18 - 1.55) |
| C) WT allometric | 1.25 | 1.35 | 1.26 (1.03 - 1.51) | 1.38 (1.20 - 1.57) |
| D) $FFM_C$ allometric | 1.17 | 1.24 | 1.18 (0.95 - 1.42) | 1.26 (1.10 - 1.45) |
| E) $FFM_J$ allometric | 1.15 | 1.22 | 1.16 (0.92 - 1.45) | 1.25 (1.06 - 1.46) |

$FCYF_{CLT}$: Ratio of group estimates for total clearance in CF-patients divided by total clearance in healthy volunteers.

$FCYF_V$: Ratio of group estimates for volume of distribution at steady-state in CF-patients divided by volume of distribution at steady-state in healthy volunteers.

[#]: Medians and non-parametric 90% confidence intervals (5% - 95% percentile) derived from 2000 non-parametric bootstrap runs. Each bootstrap run consisted of 14 subjects (eight CF-patients and six healthy volunteers) who were randomly drawn from the original dataset.

We also compared the ability of the different size models to reduce the unexplained BSV. Table 3.3-29 shows that there were only small differences between size models B to D in their ability to reduce the unexplained BSV. Allometric scaling by $FFM_J$ had slightly higher estimates for BSVCL and BSVV1, but described the average differences between CF-patients and healthy volunteers best compared to the other size models (see Table 3.3-28). Almost all of the 90% confidence intervals for the pairwise comparisons of BSV with linear scaling by WT as reference included 0% and these comparisons were therefore not statistically significant.

**Table 3.3-29** BSV for the different size models

| Size model | Estimates from original dataset | | | Median (90% confidence interval) from non-parametric bootstrap[#] | | |
|---|---|---|---|---|---|---|
| | CL | V1 | V2 | CL | V1 | V2 |
| B) WT linear scaling | 0%* | 0%* | 0%* | 0%* | 0%* | 0%* |
| C) WT allometric | 1%° | 0% | -4% | 1 (-13 to 12%) | 1 (-8 to 13%) | -4 (-47 to 15%) |
| D) $FFM_C$ allometric | 14%° | 13% | 9% | 11 (-9 to 39%) | 13 (-20 to 66%) | 0 (-45 to 42%) |
| E) $FFM_J$ allometric | 44%° | 71% | 17% | 38 (3 to 87%) | 75 (-3 to 185%) | 12 (-77 to 87%) |

*: The values are (variance of test size model - variance of linear scaling by WT) / variance of linear scaling by WT. For the bootstrap estimates, the denominator was the median variance of linear scaling by WT from all 2000 bootstrap runs.

°: The lower this number, the more variability was explained by the respective size model. A negative value indicates that the size model reduced the between subject variance compared to linear scaling by WT. These values mean that the BSV (variance) for total clearance was increased by 1% for allometric scaling by WT, by 14% for allometric scaling by $FFM_C$, and by 44% for allometric scaling by $FFM_J$, all compared to linear scaling by WT.

#: Medians and non-parametric 90% confidence intervals (5% - 95% percentile) estimated from 2000 non-parametric bootstrap runs. Each bootstrap run consisted of 14 subjects (eight CF-patients and six healthy volunteers) who were randomly drawn from the original dataset.

***MCS:*** CF-patients had lower PTAs than healthy volunteers which resulted in similar or slightly lower PKPD breakpoints for the studied dosage regimens (see Table 3.3-30 and Figure 3.3-17). Administering the same dose as prolonged (4-5 h) infusion instead of as short-term (30 min) infusion improved the PKPD breakpoint by a factor of 16 to 43 for the near-maximal kill target ($fT_{>MIC} \geq 65\%$) and by a factor of 5 to 12 for the bacteriostasis target ($fT_{>MIC} \geq 40\%$).

**Table 3.3-30** PKPD breakpoints for various dosage regimens of cefotiam

| **Dosage regimen** | **Bacteriostasis target ($fT_{>MIC} \geq 40\%$)** | | **Near-maximal kill target ($fT_{>MIC} \geq 65\%$)** | |
|---|---|---|---|---|
| | CF-patients | Healthy volunteers | CF-patients | Healthy volunteers |
| **Daily dose 4g / 70 kg WT** | *PKPD breakpoints (mg/L)* | | | |
| Continuous infusion | 2 | 2 | 2 | 2 |
| 4h infusion q6h | 2 | 4 | 1.5 | 2 |
| 30min infusion q6h | 0.375 | 0.5 | 0.094 | 0.094 |
| **Daily dose 6g / 70 kg WT** | | | | |
| 5h infusion q8h | 4 | 6 | 1.5 | 2 |
| 30min infusion q8h | 0.375 | 0.5 | 0.047 | 0.047 |

### 3.3.5.5 Discussion

Although there is a growing understanding of the pathophysiology and the molecular basis for CF, morbidity and mortality caused by progressive lung diseases in CF-patients is still high (283). It seems prudent to use antibiotics against infections by MSSA or *H. influenzae* which are not used to treat infections by *P. aeruginosa*. This potentially reduces the emergence of resistance of the latter pathogen.

Cefotiam is active against MSSA and *H. influenzae* and is an appealing option for treatment of those infections. However, we are not aware of any reports on the PK of cefotiam in CF-patients or on its effectiveness in CF-patients. Our population PK analysis aimed at estimating both the differences in average PK parameters of cefotiam between CF-patients and healthy volunteers as well as the PK parameter variability. Our final model had good predictive performance for both the average plasma concentration time profiles of cefotiam and their BSV (see Figure 3.3-16). The prediction intervals were slightly too wide for the healthy volunteers. However, this only resulted in slightly more conservative (lower) predicted PTAs in healthy volunteers. Therefore, we used our final model to compare the PD profile between both subject groups and to identify optimal dosage regimens.

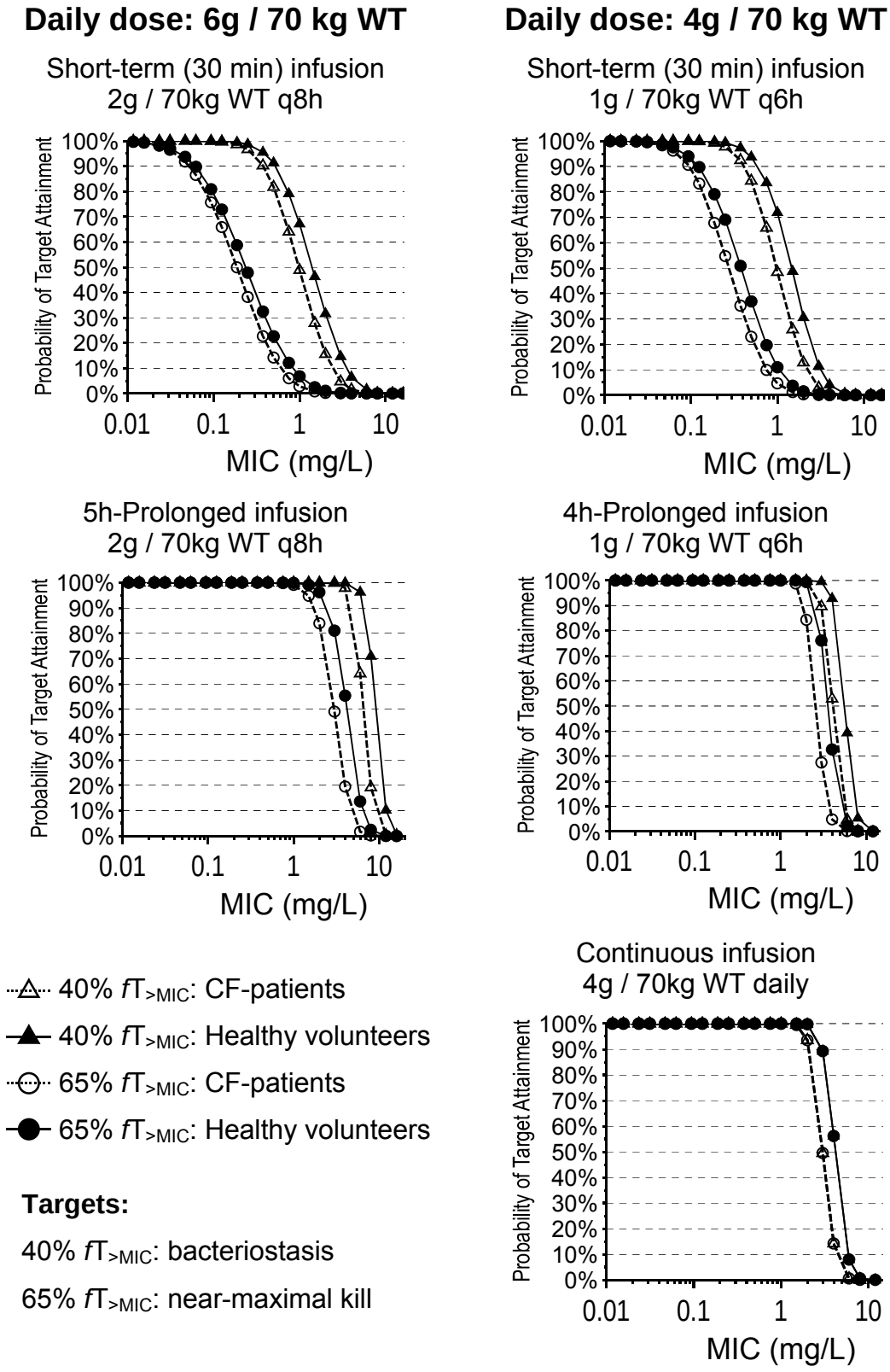


**Figure 3.3-17** Probability of target attainment for various cefotiam dosage regimens at steady-state

Our results for the PK parameters of cefotiam in healthy volunteers were in good agreement with the results from other authors (55, 73, 95, 420) and we are not aware of reports on the PK of cefotiam in CF-patients in literature. Our CF-patients had a 34% lower WT, a 20% lower $FFM_C$, and a 15% lower $FFM_J$ than our healthy volunteers (see Table 3.3-25). Although our CF-patients were smaller, NCA showed only a 3% lower unscaled total clearance and a 3% smaller unscaled volume of distribution at steady-state in CF-patients (see Table 3.3-26). The terminal-half-life was 14% shorter in CF-patients and the mean residence time was similar in both subject groups.

We studied the differences in average clearance and average volume of distribution between both subject groups via population PK. In absence of a size descriptor (size model A, Table 3.3-28), CF-patients had a 4% lower clearance and a very similar volume of distribution. Linear and allometric scaling by WT predicted clearance to be 39% and 26% higher in CF-patients (see Table 3.3-28), respectively, relative to healthy volunteers. A two-sided test based on the posterior distribution from bootstrap indicated a p-value of 0.01 for linear scaling by WT and a p-value of 0.06 for allometric scaling by WT. Allometric scaling by $FFM_C$ or $FFM_J$ showed a 16-18% higher clearance in CF-patients after accounting for body size. However, these differences were not statistically significant. These results are similar to those from other authors who find a 42% increased total clearance (L/h/1.73 $m^2$) (282) and a 25% increased renal clearance (L/h/1.73 $m^2$) (182) for ceftazidime in CF-patients. Hedman et al. (182) could explain this increased renal clearance primarily by an increased glomerular filtration rate in CF-patients determined via inulin clearance. The reason for the increased glomerular filtration rate in CF-patients is unknown. A possible explanation would be an altered glomerulotubular balance secondary to a primary tubular transport defect (19, 37). Another possibility might be that CF-patients have a 16% increased resting energy expenditure (514) due to a higher energy need secondary to chronic lung infection and might therefore also have an increased clearance.

After accounting for body size, size models B to E predicted volume of distribution to be significantly higher in CF-patients relative to healthy volunteers. Volume of distribution was predicted to be 35-38% higher for the

size models based on WT and about 25% higher for the size models based on by $FFM_C$ or $FFM_J$ in CF-patients (see Table 3.3-28). This difference was significant for all four size-models ($p<0.02$). It is difficult to explain this observation, as we already accounted for body composition by $FFM_C$ or $FFM_J$. However, the influence on the PD profile for cefotiam was small (see Table 3.3-30).

Besides the ability of $FFM_C$ or $FFM_J$ to describe the average differences in clearance and volume of distribution between both subject groups, we studied the reduction of unexplained BSV in clearance and volume relative to linear scaling by WT. This may become important in empiric therapy, as target concentrations can be attained more precisely the lower the unexplained BSV. Table 3.3-29 shows that the three allometric size models had similar or slightly higher estimates for the BSV in CL, V1, and V2 relative to linear scaling by WT. The 90% confidence interval for almost all pairwise comparisons between the allometric size models and linear scaling by WT included 0%. Therefore, none of the size descriptors reduced the unexplained BSV significantly.

We used the population PK model based on $FFM_C$ to calculate the PTA in CF-patients and healthy volunteers. CF-patients had lower PTAs (see Figure 3.3-17) compared to healthy volunteers which resulted in slightly (up to a factor of 2) lower PKPD breakpoints. We found much more pronounced differences between short-term and prolonged infusions. For the near-maximal kill target ($fT_{>MIC} \geq 65\%$), 4h-prolonged infusion of 1g / 70 kg WT cefotiam q6h achieved a breakpoint of 1.5 mg/L in CF-patients, whereas short-term (30min) infusion of the same dose reached only a breakpoint of 0.094 mg/L. Giving a higher daily dose of 2g / 70 kg WT q8h instead of 1g / 70 kg WT q6h did not improve the PKPD breakpoints (see Table 3.3-30). The short average half-life of cefotiam of about 1 h in combination with the 6 or 8 h dosing interval was the primary reason why prolonged infusions reached much higher breakpoints than short-term infusions. Although continuous infusion reached similar PKPD breakpoints as prolonged infusion, continuous infusion bears the risk for line infections and is less convenient for the patient. Therefore, prolonged infusion might be preferred to continuous infusion.

To put the superiority of the PKPD breakpoint for prolonged infusion to the breakpoint for short-term infusion into clinical perspective, these breakpoints should be compared with the MIC distributions encountered in clinical practice. The probability of successful clinical outcome will be especially favorable for prolonged infusion, if the $MIC_{50}$ and $MIC_{90}$ fall between the breakpoints for prolonged infusion (1.5 mg/L) and short-term infusion (0.094 mg/L). For MSSA and *H. influenzae*, the $MIC_{50}$ ranged between 0.39 and 0.78 mg/L and the $MIC_{90}$ ranged between 0.78 and 4 mg/L (173, 366, 527). For *S. pneumoniae*, the $MIC_{50}$ ranged between 0.06 and 0.5 mg/L and the $MIC_{90}$ ranged between 0.25 and 6.25 mg/L (173, 366, 527). Although the MIC distributions of a local hospital should be used to decide, if cefotiam is an appealing treatment option, these reported $MIC_{50}$ and $MIC_{90}$ are between the PKPD breakpoints for short-term and prolonged infusion. Prolonged infusion will have promising (>90%) probabilities of successful treatment for an $MIC_{50}$ of 0.5 mg/L and an $MIC_{90}$ of 1 mg/L, because the PTA is almost 100% for all MICs $\leq$1mg/L. However, short-term infusion will have much lower (<50%) probabilities for successful treatment for such an MIC distribution.

In conclusion we found a 3% lower unscaled total clearance and a 3% lower unscaled volume of distribution at steady-state in CF-patients compared to healthy volunteers, although our CF-patients had a 34% lower WT, a 20% lower $FFM_C$, and a 15% lower $FFM_J$. Linear scaling by WT predicted total clearance to be 39% higher and volume of distribution to be 35% higher in CF-patients. Allometric scaling by $FFM_J$ resulted in a 16% higher clearance in CF-patients (p=0.32). The average differences in volume of distribution at steady-state were best explained by $FFM_J$ which indicated a 25% higher volume of distribution in CF-patients (p=0.024). The higher clearance and volume of distribution in CF-patients after accounting for body size and body composition is probably of less clinical relevance, as the PKPD breakpoints were similar or only slightly lower in CF-patients than in healthy volunteers. Prolonged (4h) infusion of 1g / 70 kg WT q6h achieved a breakpoint of 1.5 mg/L for the near-maximal kill target in CF-patients, whereas the breakpoint for short-term infusion of the same dose was only 0.094 mg/L. As

the $MIC_{50}$ and $MIC_{90}$ for MSSA and *H. influenzae* fall between 0.06 and 4 mg/L, prolonged infusion of cefotiam will achieve considerably higher probabilities of successful treatment in CF-patients compared to short-term infusion. Large clinical trials in CF-patients are warranted to study the clinical cure rates for prolonged infusion with cefotiam.

## 3.4 Systematic comparison of the PKPD of oral antibiotics between CF-patients and healthy volunteers

### 3.4.1 Population pharmacokinetics and pharmacodynamics of cefaclor

#### 3.4.1.1 Chemical structure of cefaclor

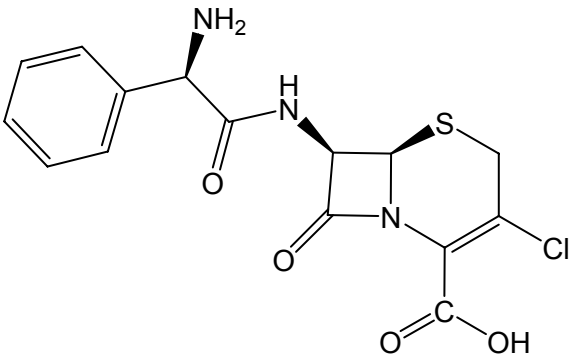


($C_{15}H_{14}ClN_3O_4S$, Mol. Wt.: 367.81)

**Chemical structure 3.4-1** Cefaclor

#### 3.4.1.2 Possible use of cefaclor in patients with cystic fibrosis

CF-Patients often have a life-long need for antibiotics because they are highly prone to respiratory tract infections secondary to structural defects in the respiratory tract. The oral route of administration is an appealing treatment option for CF-patients. Emergence of bacterial resistance may diminish the clinical effectiveness e. g. of fluoroquinolones or beta-lactams. Oral cefaclor may be a valuable alternative e. g. in chronic suppression therapy against *H. influenzae* and MSSA to save fluoroquinolones for treatment of more serious infections or to postpone their use in CF-patients. The amount of cefaclor excreted in urine at steady-state (day 10) was reported to be 77 ± 6.5% (30). Thus, cefaclor is well and reliably absorbed orally. On the contrary,

the variability of oral cloxacillin (470) which is also active against staphylococci shows a lower extent of oral absorption with a larger variability (50 ± 26%, in CF-patients and 38 ± 17% in healthy volunteers). Consequently, cefaclor is an appealing candidate for early use in CF-patients.

The use of oral antibiotics in CF-patients, however, may be prohibited by pathophysiological changes frequently occuring in the GI tract of CF-patients. The influence of these pathophysiological changes on the oral absorption of antibiotics has not been well studied. More importantly, an altered bioavailability may have a pronounced effect on the PD of antibiotics, particularly the beta-lactams. Due to the short half-life of oral cephalosporins (between 0.5 and 3 hours on average for most cephalosporins), the rate of absorption is an important determinant for the $fT_{>MIC}$.

We are not aware of any reports in literature on the PK of cefaclor in CF-patients or on a comparison of CF-patients and healthy volunteers by MCS based on data from a single study. Therefore, our first objective was to compare the PK of cefaclor between CF-patients and healthy volunteers. As our second objective we compared clearance and volume of distribution between CF-patients and healthy volunteers and studied, whether $FFM_C$ or $FFM_J$ are more appropriate descriptors of body size than WT. Our third objective was to study the influence of patient related differences in PK parameters on PD characteristics of cefaclor after oral administration.

#### 3.4.1.3 Methods

The general clinical and sample handling procedures, the methods for PK analysis (including NCA and population PK), and the general methods for MCS are described in chapter 2. Chapter 3.2 shows the specific methods applied for analysis of our CF-studies.

***Subjects:*** A total of 14 Caucasian volunteers (eight CF-patients and six healthy volunteers) of both sexes participated in the study. Table 3.4-1 shows the demographic data.

**Table 3.4-1** Demographic data of the cefaclor study (median [range])

| | **CF-patients** | **Healthy volunteers** |
|---|---|---|
| Number of subjects (males / females) | 8 (4 / 4) | 6 (3 / 3) |
| Age (yr) | 20 [15 - 24] | 24 [21 - 26] |
| Height (cm) | 168 [157 - 178] | 169 [164 - 190] |
| Total body weight (kg) | 48.5 [33 - 72] | 68.5 [58 - 80] |
| Fat-free mass° (kg) | 41.3 [28.8 - 58.3] | 50.6 [44.6 - 65.4] |
| Fat-free mass# (kg) | 39.3 [25.4 - 57.6] | 47.4 [39.1 - 64.7] |
| Body mass index (kg $m^{-2}$) | 17.2 [13.4 - 22.7] | 22.5 [20.3 - 27.9] |

°: Calculated by the formula of Cheymol and James (72, 222).

#: Calculated by the formula of Janmahasatian et al. (224).

***Study design and drug administration:*** Each subject received a total oral dose of 1,000 mg cefaclor as two capsules each containing 500 mg cefaclor (Panoral®) in the fasting state together with 150 mL of calcium poor low-carbonated mineral water at room temperature. CF-patients abstained from taking pancreatic enzymes as supplement therapy from at least 10 h prior to until 4 h post study drug administration.

***Blood and urine sampling:*** Blood samples were drawn immediately before administration (0 h) and at 0.25, 0.5, 1, 1.5, 2, 3, 4, 5, 6, 8, 12, and 24 h post dose. Urine was collected from 0 to 1, 1 to 2, 2 to 3, 3 to 4, 4 to 5, 5 to 6, 6 to 8, 8 to 12, and 12 to 24 h after dosing.

***Drug analysis in plasma and urine:*** We determined the concentration of cefaclor in plasma and urine by reversed phase HPLC with UV detection. An amount of 100 µL of $NaH_2PO_4$ buffer was added to 100 µL of each sample. Acetonitrile (400 µL) was used to deproteinize each sample. After centrifugation 1,000 µL of dichloromethane were added for extraction of the organic phase. From the remaining aqueous phase, 20 µL were injected into the HPLC system. Urine samples were diluted (ratios 1:5 to 1:50) with bi-distilled water if necessary. Ten (10) µL of the resulting mixture were injected into the HPLC system. After sample preparation, the prepared samples were stored in an ice-water bath until injection. We assured stability of cefaclor

under these conditions and used a µ-Bondapak ® C18 (10 µ) column (Waters, Germany) with a water / acetonitrile mixture at pH 7.5. The eluent included tetrabutylammonium phosphate as ion-pair reagent. Cefaclor was detected at a wavelength of 263 nm. Calibration was performed by linear regression. The linearity of cefaclor calibration curves in plasma and urine was shown between 0.5-40 mg/L and 30-400 mg/L, respectively. We took 30-40 mL blood from one additional subject at three time points with a high, intermediate, and low concentration. This subject did not participate in the PK study. Those blood samples were prepared like all other samples as described above and used as biological quality controls. We included these biological quality controls and spiked quality controls in each analytical run.

***Population PK***

***Structural model:*** We tested one, two, and three compartment disposition models. We modeled the drug input 1) as first order process from the gut into the central compartment (half-life of absorption: TABS), 2) as time delimited zero order input (duration: TK0) directly into the central compartment, and 3) as time delimited zero order input into the gut compartment (duration: TK0) with subsequent first order absorption from the gut into the central compartment (half-life of absorption: TABS). We tested all three absorption models with or without lag-time (TLAG).

***Covariate model for absorption parameters:*** In addition to the covariate model described in chapter 3.2 we used the following covariate model for the parameters of oral absorption. CF-patients often suffer from GI problems. In absence of a direct descriptor of the GI malfunctions we used body mass index (BMI) centered around 22 kg $m^{-2}$ as a surrogate measure to study the influence of BMI on the absorption parameters. This choice was based on the empirical observation that a scatterplot of the absorption parameters showed a correlation with BMI. We used an exponential covariate model (parameters explained below):

$$TLAG_i = TLAG_{POP} \cdot \exp\left(slope_{TLAG} \cdot \left(BMI_i - 22\,kg\,m^{-2}\right)\right) \cdot \exp(\eta_{BSVTLAGi})$$

Formula 3.4-1

$$TK0_i = TK0_{POP} \cdot \exp\left(slope_{TK0} \cdot \left(BMI_i - 22\,kg\,m^{-2}\right)\right) \cdot \exp(\eta_{BSVTK0i})$$

Formula 3.4-2

$$TABS_i = TABS_{POP} \cdot \exp\left(slope_{TABS} \cdot \left(BMI_i - 22\,kg\,m^{-2}\right)\right) \cdot \exp(\eta_{BSVTABSi})$$

Formula 3.4-3

$TLAG_{POP}$ is the population estimate for lag time of absorption, $TK0_{POP}$ is the population estimate for the duration of zero order input into the central (absorption model 1) or gut compartment (absorption model 3), and $TABS_{POP}$ is the population estimate for the half-life of the first order input from the gut into the central compartment for a subject with BMI 22 kg $m^{-2}$. The slopes characterize the influence of BMI on the respective PK parameter. The $\eta_{BSVi}$ are the individual differences of the respective PK parameter from its population mean on log-scale. The $\eta_{BSVi}$ represent the random variability of the absorption parameters. $TLAG_i$, $TK0_i$, and $TABS_i$ are the respective individual parameter estimates for the $i^{th}$ subject. To screen for differences between CF-patients and healthy volunteers in the absorption parameters we used a model without BMI as covariate which instead included disease specific scale factors for lag time ($FCYF_{TLAG}$), duration of zero order input ($FCYF_{TK0}$), and half-life of first order input ($FCYF_{TABS}$).

***MCS:*** We compared CF-patients and healthy volunteers at steady-state after a fixed oral dose of 1,000 mg cefaclor q8h. We studied a range of MICs from 0.0625 to 4 mg/L and used a protein binding of 25% for cefaclor (59). We calculated the PTA expectation value based on published MIC distributions of *S. pneumoniae* (313), *H. Influenzae* (409, 478), and *S. aureus* (205).

#### 3.4.1.4 Results

***NCA:*** Figure 3.4-1 shows the average plasma concentrations of CF-patients and healthy volunteers. Table 3.4-2 lists the results of the NCA for CF-patients and healthy volunteers. These parameters are not scaled by any size descriptor. Median apparent total clearance (-21%), renal clearance

(-23%), apparent non-renal clearance (-18%), and volume of distribution at steady-state (-8%) were lower in CF-patients than in healthy volunteers. The median terminal half-life was shorter in CF-patients, but the variability in terminal half-life was large.

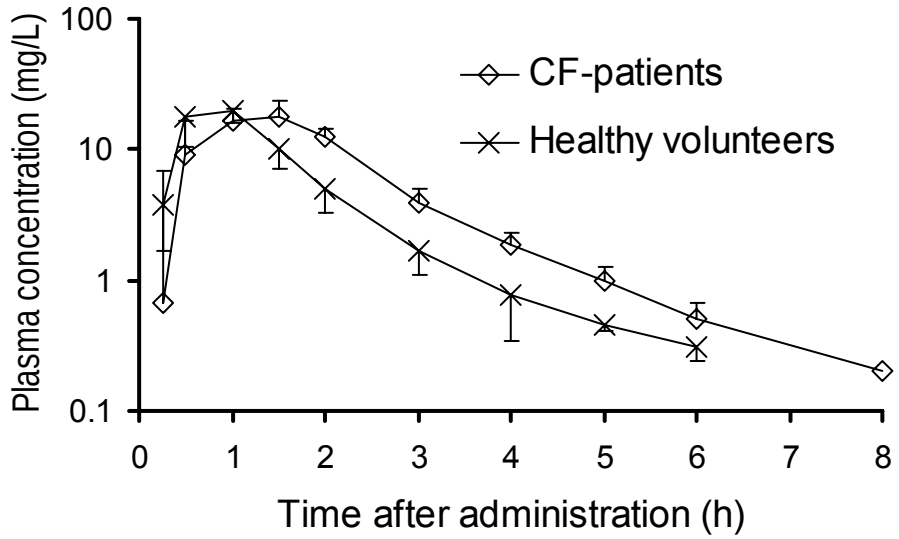


**Figure 3.4-1** Average ± SD plasma concentrations of cefaclor for CF-patients and healthy volunteers after a single oral dose of 1,000 mg cefaclor in the fasting state

**Table 3.4-2** Unscaled PK parameters derived via NCA (median [range])

| | CF-patients | Healthy volunteers |
|---|---|---|
| Apparent total clearance (L/h) | 26.0 [21.9 - 30.4] | 32.8 [22.7 - 54.1] |
| Renal clearance (L/h) | 18.7 [14.7 - 21.4] | 24.3 [18.9 - 42.7] |
| Apparent nonrenal clearance (L/h) | 6.92 [1.62 - 12.4] | 8.48 [0.553 - 11.3] |
| Apparent volume of distribution at steady-state (L) | 47.0 [38.2 - 113] | 51.0 [32.2 - 81.3] |
| Fraction excreted unchanged in urine (%) | 72.4 [54.3 - 92.6] | 77.8 [63.3 - 98.7] |
| Time to peak concentration (h) | 1.25 [1.00 - 2.00] | 1.00 [0.50 - 1.00] |
| Peak concentration (mg/L) | 21.1 [18.6 - 25.6] | 20.2 [14.4 - 31] |
| Terminal half-life (L) | 0.928 [0.891 - 7.81] | 1.30 [0.525 - 7.23] |
| Mean body residence time* (h) | 1.97 [1.44 - 4.16] | 1.42 [1.18 - 2.68] |

* Sum of mean input time and mean disposition residence time.

The terminal half-life was slightly shorter in CF-patients. However, the absorption of cefaclor and time to peak concentration were longer in CF-patients (see Figure 3.4-1). More importantly, the mean body residence time was 39% longer in CF-patients. The mean body residence time is the sum of the mean input time and the mean disposition residence time. As the half-life was slightly shorter in CF-patients, the mean disposition residence time was probably slightly shorter in CF-patients. Thus, a considerably longer mean input time caused the mean body residence time to be 39% longer in CF-patients. The extent of absorption was comparable between both subject groups, since the median fraction excreted unchanged in urine was 72.4% for CF-patients and 77.8% for healthy volunteers (see Table 3.4-2).

**Population PK analysis**

***Structural model:*** NONMEM's objective function improved by about 60 points, if lag-time was included. The objective function was 129 points better for the two compartment disposition model with absorption model 3 than for the corresponding one compartment disposition model. The data did not support a three compartment disposition model. For the two compartment disposition model, absorption model 3 had the best objective function. The objective function was 78 points worse for absorption model 1 and 61 points worse for absorption model 2.

The VPC (see Figure 3.4-2) showed a highly sufficient predictive performance of the two compartment disposition model (absorption model 3) with $FFM_C$ as size descriptor for plasma concentrations and amounts excreted in urine at all sampling times. This model was able to capture the plasma and urine profiles for CF-patients and healthy volunteers very well. We chose the two compartment disposition model with absorption model 3 as our final model due to its very good predictive performance and its considerably better objective function relative to absorption models 1 and 2.

***Covariate model:*** When we estimated $FCYF_{TLAG}$, $FCYF_{TK0}$, and $FCYF_{TABS}$, CF-patients showed a 7 min longer TLAG, a 50% longer TK0 (15 min), and a 26% (6.5 min) longer TABS. BMI as a covariate explained the average differences in all three absorption parameters between CF-patients

and healthy volunteers and improved the objective function significantly. Additionally, inclusion of BMI reduced the BSV (variance) by about 40% for volume of central compartment and by about 99% for TABS.

The final estimates for the population PK model based on $FFM_C$ as size descriptor are shown in Table 3.4-3. As we estimated a $slope_{TLAG}$ of about -0.052 $m^2\ kg^{-1}$, a $slope_{TK0}$ of about -0.085 $m^2\ kg^{-1}$, and a $slope_{TABS}$ of about -0.077 $m^2\ kg^{-1}$, the influence of BMI on TLAG, TK0, and TABS can be interpreted as follows: A decrease of BMI by 1 kg $m^{-2}$ results in an increase of about 5.2% for TLAG, of about 8.5% for TK0, and of about 7.7% for TABS. The median BMI was 5.3 kg $m^{-2}$ lower in CF-patients than in healthy volunteers. Therefore, a typical CF-patient was estimated to have an about 26% (2.6 min) longer TLAG, a 45% (13 min) longer TK0, and a 41% (9 min) longer TABS compared to a typical healthy volunteer.

We distinguished the studied size models 1) by their estimates for the disease specific factors FCYF and 2) by their ability to reduce the unexplained BSV in clearance and volume of distribution. As expected, CF-patients had a lower (17%) renal clearance and a lower (14%) volume of distribution at steady-state in absence of any size model (see FCYF in Table 3.4-4, size model A), because they were smaller than healthy volunteers. Linear scaling by WT (size model B) predicted renal clearance to be 15% higher and volume of distribution to be 7% higher in CF-patients relative to healthy volunteers. The allometric size models (size models C, D, and E) estimated the disease specific factors $FCYF_{CLR}$ and $FCYF_V$ to be very close to the ideal value of 1.0 (range: 0.969 to 1.06). Nonrenal clearance was estimated to be between 13.5 to 22.9% smaller for size models B to E.

We also compared the ability of the different size models to explain the BSV. Table 3.4-5 shows that allometric scaling by $FFM_C$ reduced the unexplained BSV in renal clearance by 35% compared to linear scaling by WT. As the BSV in renal clearance (20.9% CV, see Table 3.4-3) was larger than for nonrenal clearance (12.0% CV) and as renal clearance is about twice as large as nonrenal clearance, reducing the unexplained BSV in renal clearance is more important than for nonrenal clearance. Allometric scaling by

WT or $FFM_C$ reduced the unexplained BSV in volume of central compartment by about 30% relative to linear scaling by WT.

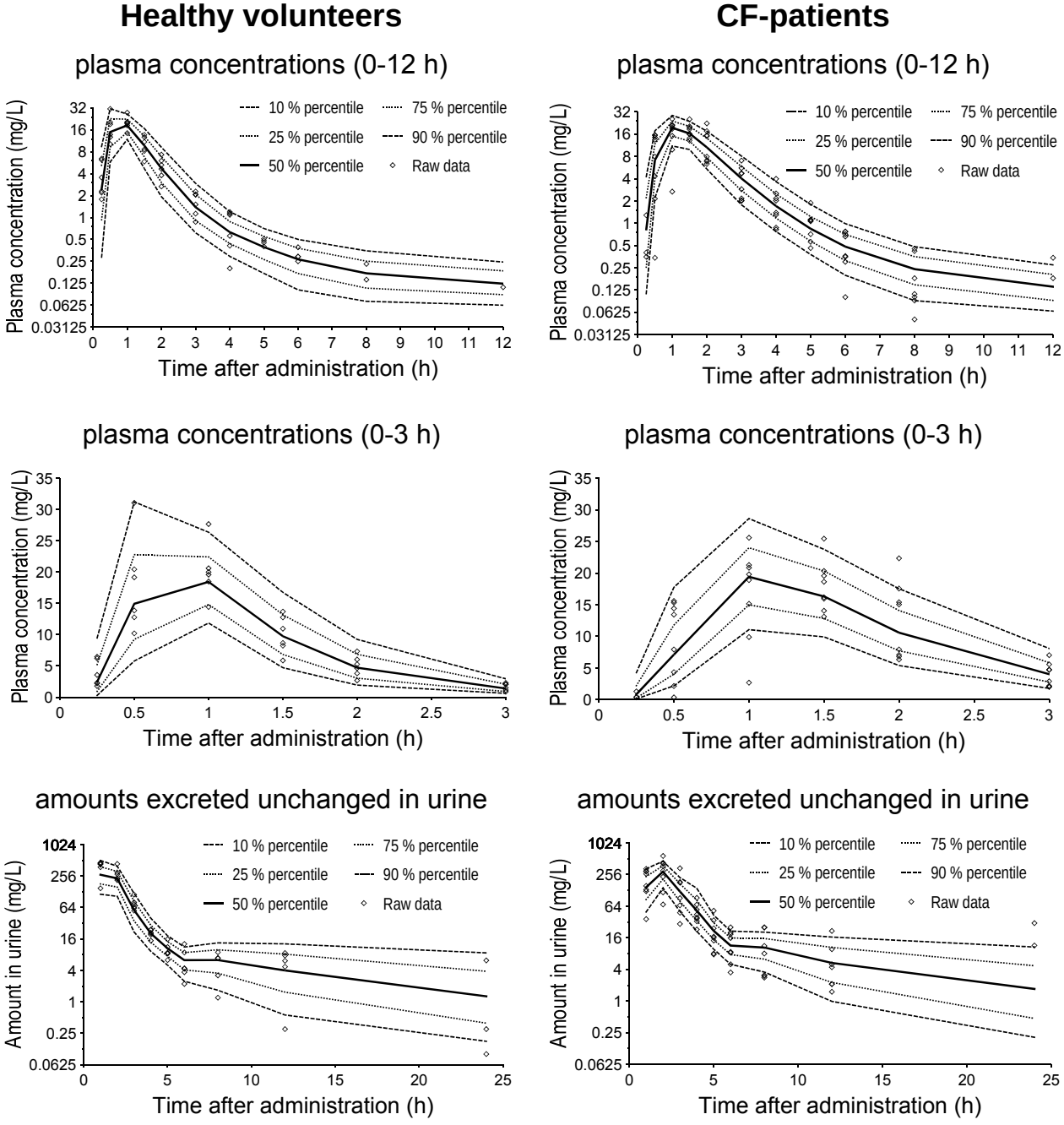


**Figure 3.4-2** VPC based on 8,000 CF-patients and 6,000 healthy volunteers for the two compartment disposition model based on $FFM_C$ with absorption model 3 (see Table 3.4-3).

See chapter 2.6.3 for interpretation of VPCs.

**Table 3.4-3** PK parameter estimates for the allometric size model based on $FFM_C$

| Parameter | Unit | Estimate for | | Coefficient of variation (%)° |
|---|---|---|---|---|
| | | CF-patients | healthy volunteers | |
| $CL_{tot}^{§,\wedge}$ | L $h^{-1}$ | 31.5* | 34.5* | |
| $CL_R$ | L $h^{-1}$ | 22.4* | 22.7* | 20.9# |
| $CL_{NR}^{§}$ | L $h^{-1}$ | 9.10* | 11.8* | 12.0# |
| $Vss^{§,\wedge}$ | L | 17.3* | 17.6* | |
| $V1^{§}$ | L | 6.60* | 6.71* | 63.8** |
| $V2^{§}$ | L | 10.7* | 10.9* | 54.7** |
| $CLic^{§}$ | L $h^{-1}$ | 5.70* | | |
| TLAG | min | 9.48* | | 36.6 |
| TK0 | min | 29.2* | | 39.7 |
| TABS | min | 22.8* | | 0.083 |
| $Slope_{TLAG}$ | $m^2$ $kg^{-1}$ | -0.0518 | | |
| $Slope_{TK0}$ | $m^2$ $kg^{-1}$ | -0.0848 | | |
| $Slope_{TABS}$ | $m^2$ $kg^{-1}$ | -0.0771 | | |
| $CV_C$ | % | 17.9 | | |
| $SD_C$ | mg/L | 0.119 | | |
| $CV_{AU}$ | % | 37.9 | | |
| $SD_{AU}$ | mg | 0.0934 | | |

*: Group estimate for a subject with standard $FFM_C$ = 53 kg and standard BMI = 22 kg $m^{-2}$.

§: Values are apparent clearances and apparent volumes of distribution (e. g. $CL_{TOT}$/F and Vss/F).

^: Derived from model estimates, not an estimated parameter.

°: Apparent coefficients of variation for the between subject variability.

#: Coefficient of correlation for random effects of $CL_R$ and $CL_{NR}$: r = 0.08.

**: Coefficient of correlation for random effects of V1 and V2: r = -0.71.

TLAG: lag-time of absorption, TK0: duration of zero order input into the gut compartment, TABS: half-life of first order absorption from the gut into the central compartment. See also chapter 2.6.2 for explanation of model parameters.

**Table 3.4-4** Ratios of group estimates (CF-patients / healthy volunteers) for clearance and volume of distribution for different size models

| Size model | $FCYF_{CLR}$ | $FCYF_{CLNR}$ | $FCYF_{CLT}^{\#}$ | $FCYF_{V}$ |
|---|---|---|---|---|
| A) No size model | 0.834 | 0.628 | 0.763 | 0.86 |
| B) WT linear scaling | 1.15 | 0.865 | 1.05 | 1.07 |
| C) WT allometric | 1.06 | 0.809 | 0.974 | 1.04 |
| D) $FFM_C$ allometric | 0.985 | 0.771 | 0.912 | 0.983 |
| E) $FFM_J$ allometric | 0.969 | 0.783 | 0.906 | 1.05 |

$FCYF_{NNN}$: Ratio of group estimates for parameter NNN (group estimate for CF-patients divided by group estimate for healthy volunteers).

#: Calculated as weighted average of $FCYF_{CLR}$ and $FCYF_{CLNR}$.

**Table 3.4-5** Comparison of BSV (variances) between various size models: The table shows the relative between subject variances for the respective PK parameter and size models

| Size model | Relative between subject variance | | | |
|---|---|---|---|---|
| | $CL_R$ | $CL_{NR}$ | V1 | V2 |
| B) WT linear scaling | 100%* | 100% | 100% | 100% |
| C) WT allometric | **71%°** | 95% | **69%** | 105% |
| D) $FFM_C$ allometric | **65%°** | 125% | **72%** | 101% |
| E) $FFM_J$ allometric | 83%° | 134% | 112% | 99% |

*: The BSV for linear scaling by WT was used as reference.

°: The lower this number, the more variability was explained by the respective size model. These values mean that the BSV (variance) for renal clearance is reduced by 29% for allometric scaling by WT, by 35% for allometric scaling by $FFM_C$, and by 17% for allometric scaling by $FFM_J$, all compared to linear scaling by WT.

***MCS:*** We found a PKPD breakpoint of 0.094 mg/L for healthy volunteers and of 0.25 mg/L for CF-patients based on the target $fT_{>MIC} \geq 65\%$ for near-maximal bactericidal effect (see Figure 3.4-3). The breakpoints for bacteriostasis (target $fT_{>MIC} \geq 40\%$) were 0.375 mg/L in healthy volunteers and 0.75 mg/L in CF-patients.

The PTA expectation values for successful empiric treatment against three different pathogens from the US, Brazil, Russia, and Germany are shown in Table 3.4-6. The expectation values for the bacteriostasis target ($fT_{>MIC} \geq 40\%$) ranged between 12 and 86%. PTA expectation values for the near-maximal bactericidal activity target ($fT_{>MIC} \geq 65\%$) were between 0 and 30%. For these MIC distributions, we found differences in the PTA expectation value of up to 50% between CF-patients and healthy volunteers. Although this is a pronounced difference, these differences depend on the individual MIC distribution used to calculate the PTA expectation value.

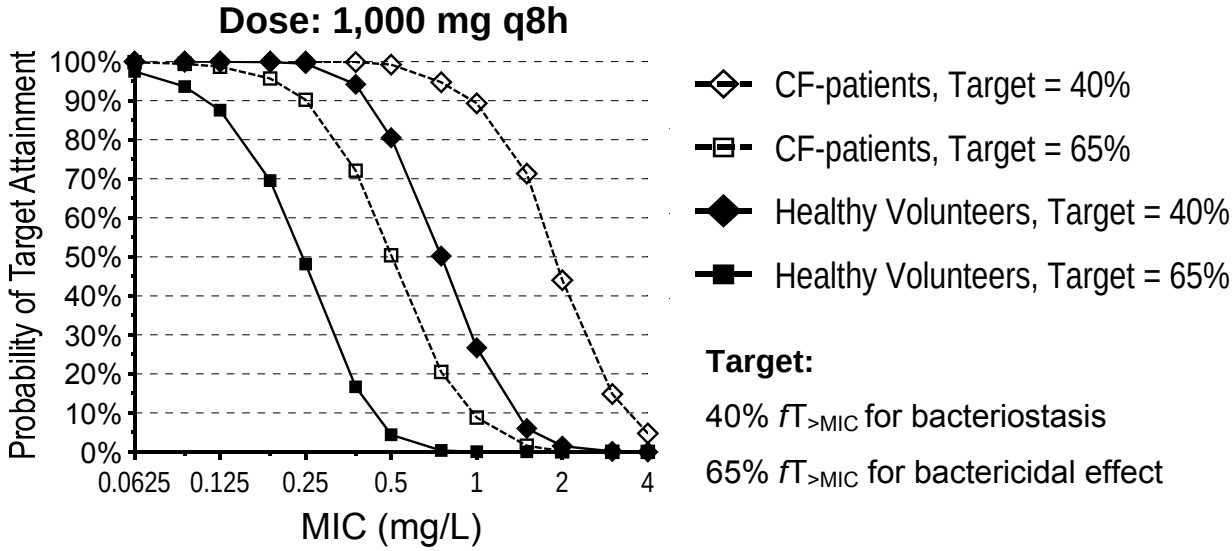


**Figure 3.4-3** Probability of target attainment for oral doses of cefaclor at steady-state based on the population PK model with $FFM_C$

**Table 3.4-6** PTA expectation values for CF-patients and healthy volunteers for various PKPD targets

| Target | Group | *S. pneumoniae* | *H. influenzae* | | *Staph. aureus* |
|---|---|---|---|---|---|
| $fT_{>MIC}$ | Region (number of isolates) | USA (n=2849) | Brazil (n=123) | Russia (n=100) | Germany (n=307) |
| 40% | Healthy volunteers | 30.3% | 48.3% | 20.2% | 12.2% |
| | CF-patients | 78.7% | 85.7% | 64.5% | 52.2% |
| 65% | Healthy volunteers | 3.4% | 8.5% | 0.9% | 0.0% |
| | CF-patients | 15.4% | 29.4% | 9.0% | 3.9% |

#### 3.4.1.5 Discussion

Respiratory diseases are the primary factor for frequent hospitalization of CF-patients and a primary cause of mortality (283, 400). The first pathogens affecting the lungs of young CF-patients are often MSSA and *H. influenzae*. Since young children with CF may require multiple courses of antibiotic treatment per year, the availability of effective oral agents with activity against these pathogens is vital. One agent that might be used for the treatment of “early” respiratory tract infections is cefaclor. Cefaclor is a second generation cephalosporin that is available orally and is active against MSSA and *H. influenzae*.

While cefaclor is active against the organisms frequently encountered in “early” stage respiratory tract infection in CF-patients, its use may potentially be prohibited by oral absorption-related issues secondary to the GI changes that frequency are observed in this population. These pathophysiological alterations in CF-patients are described in chapter 1.4.2. The influence of these alterations on the absorption of beta-lactams and quinolones is described in chapter 3.1.2.

The oral absorption in CF-patients was only studied by a few investigators via population PK (378, 398, 436) who studied oral ciprofloxacin, but did not include a control group of healthy volunteers in the same study. The oral bioavailability of beta-lactams in CF-patients has not yet been studied via population PK, although rate and extent of absorption are both important determinants for $fT_{>MIC}$. We used population PK modeling and MCS to calculate the PTA for the PKPD statistic $fT_{>MIC}$.

A flip-flop situation seems unlikely for the oral absorption of cefaclor, since its terminal half-life correlates significantly with creatinine clearance (471, 472), but is neither affected by the considerably slower rate of absorption under fed conditions (29) nor by switching from an immediate to an extended release formulation (79). These factors were not present in our study. However, the absorption of cefaclor was likely not to follow a simple first order process. Several authors found evidence for an active dipeptide

transport of cephalosporins that contributes to the intestinal absorption of cephalosporins including cefaclor (54, 94, 346, 347, 396, 430, 554).

The presence of an alpha-amino group on cephalosporins (as for cefaclor) increases their transepithelial transport which is mediated by the intestinal peptide transporter PEPT1 in a colon cell monolayer absorption model (Caco-2 monolayers) (396). Such a transport process is likely to be saturable. Additionally, we would expect the solubility and lipophilicity of cefaclor to change along the GI tract depending on the local pH. The pKa values of cefaclor are 2.43 and 7.16 (Eli Lilly and Company, Material Safety Data Sheet for cefaclor) and its solubility is rather low. One (1) g cefaclor dissolves in 93 mL water (364). Secondary to the active intestinal absorption and the solubility and lipophilicity issues for cefaclor, it was not surprising that more complex models were required to describe its oral absorption.

Some of the absorption models used here were developed by Oguma et al. (364) for cefaclor using the standard-two-stage method. They studied the oral absorption of cefaclor with or without various types and quantities of food. They used a first order or a zero order drug transport into the gut compartment with a first order link between the gut and the central compartment and included a lag-time. They pointed out that more complex absorption models might be required for cefaclor, especially if patients with GI disease are studied. Such a more complex absorption model described the absorption profile of cefaclor in our study considerably better than a standard first order or zero order absorption model.

Our final model used a zero order input into the gut compartment. We could exclude a possible bias due to intake of pancreatic enzymes in CF-patients, since our CF-patients abstained from taking pancreatic enzymes from at least 10 h prior to until 4 h post cefaclor dose. Our final population PK model had a highly sufficient predictive performance for both the average profiles of cefaclor in plasma and urine as well as their variability (see Figure 3.4-2). This allowed us to compare the PD characteristics after oral dosing between CF-patients and healthy volunteers via MCS.

Our PK parameter estimates were in agreement with those reported by other authors (59, 465) for healthy volunteers. We are not aware of any PK

studies on cefaclor in CF-patients. Our CF-patients had a 29% lower WT and an 18% lower $FFM_C$. We therefore accounted for differences in body size by population PK modeling including linear and allometric scaling based on WT, $FFM_C$, and $FFM_J$. The use of $FFM_C$ and $FFM_J$ specifically aims at accounting for body composition.

As expected, we observed lower unscaled clearances and a lower unscaled volume of distribution in CF-patients, because they were smaller (see Table 3.4-2 and Table 3.4-4). Linear scaling by WT predicted renal clearance to be 15% higher and volume of distribution at steady-state to be 7% higher in CF-patients relative to healthy volunteers. We believe that this occurred, because WT does not account for body composition. We observed the same trend to a lesser extent for allometric scaling by WT. Renal clearance and volume of distribution at steady-state were well comparable for allometric scaling by $FFM_C$ or $FFM_J$. Thus, the latter two size models were able to describe the average differences between CF-patients and healthy volunteers for clearance and volume of distribution. Our results were in good agreement with those of Spyker et al. (472) who found a significant correlation between $FFM_C$ and volume of distribution ($r = 0.572$) for cefaclor.

Besides comparing the average differences between subject groups, population PK directly estimates the variability of the PK parameters. The allometric size models showed a trend to reduce the unexplained BSV more than linear scaling by WT (size model B, see Table 3.4-5). Allometric scaling by $FFM_C$ reduced the BSV in renal clearance by 35% compared to linear scaling by WT. Reducing the unexplained BSV is important in empiric therapy. The more the unexplained BSV is reduced by a size model, the more precisely can a target concentration be achieved.

After including body size and body composition in the model we still found a significantly longer absorption phase in CF-patients. All three absorption parameters (TLAG, TK0, and TABS) were consistently longer in CF-patients than in healthy volunteers. We had no descriptor for GI malfunction in CF-patients. Hence, we used BMI as a surrogate measure to describe possible GI malfunctions, because we believed that BMI might be correlated with the degree of malfunction. In a population PK model without

BMI, the average absorption parameters TLAG, TK0, and TABS were systematically longer in CF-patients than in healthy volunteers. Inclusion of BMI explained these average differences in all three absorption parameters and reduced the BSV in the absorption parameters. Although the rate of absorption was considerably slower in CF-patients, the extent of absorption was similar to healthy volunteers, since the fraction excreted unchanged in urine was only slightly higher in healthy volunteers and its variability was large in both subject groups (see Table 3.4-2).

The prolonged absorption in our CF-patients increased the PKPD breakpoints by a factor of 2. It is important to note that those higher breakpoints in CF-patients were due to a prolonged absorption phase in CF-patients. We could show in additional simulations (data not shown) that the breakpoints in CF-patients were also twice as large as in healthy volunteers, if doses were calculated on a mg/kg WT basis. Overall, those breakpoints are rather low compared to the breakpoints specified by the CLSI (1 mg/L for *S. pneumoniae* and 8 mg/L for *H. influenzae*, (351)), BSAC (susceptible: MIC ≤ 1 mg/L, resistant: MIC > 1 mg/L, (350)) and DIN (susceptible: MIC ≤ 1 mg/L, resistant: MIC > 4 mg/L, (104)).

There is a debate about the applicability of PKPD breakpoints for cefaclor (391). Mason et al. (313) determined a PKPD breakpoint of 1 mg/L (at a dose of 13.3 mg/kg q8h) based on the target $T_{>MIC} \geq 40\%$. As we used MCS and included BSV, it is not surprising that we found a lower PKPD breakpoint of 0.375 mg/L for bacteriostasis ($fT_{>MIC} \geq 40\%$) in healthy volunteers. Based on bacteriological eradiation data Dagan et al. (90, 91) proposed a breakpoint for acute otitis media of 0.25-0.5 mg/L for pneumococcal infections and of about 0.25 mg/L for *H. influenzae*. They observed a 50% bacteriological failure rate (91) with *H. influenzae* MICs ≤1.0 mg/L. These breakpoints are in good agreement with the breakpoints identified in our MCS.

Our results for the PTA expectation values were rather low (see Table 3.4-6). The PTA expectation values differed between groups by an absolute value of up to 50%. However, these results depend on the MIC distribution

which is used for calculation. The susceptibility differs considerably between countries. $MIC_{90}$'s against *S. pneumoniae* were reported to be ≤0.5 mg/L in Brazil (419), <2 mg/L in Pakistan (4), 1 mg/L in Great Britain (410), and 1 mg/L in other European countries (232), whereas susceptibility was much lower in America ($MIC_{90}$ >32 mg/L, (231)). The $MIC_{90}$'s against *H. Influenzae* were higher with 2 mg/L in Great Britain (410), <2 mg/L in Pakistan (4), 3 mg/L in Russia (478), 4 to >32 mg/L (27, 232) in European countries, 4-64 mg/L in Japan (180), 8-32 mg/L in North and South America (231), and 16-32 mg/L in the US (234). This pronounced variability in the susceptibility between countries underlines the importance to use the MIC distribution of each hospital to calculate the expectation value for successful treatment with cefaclor based on the local resistance pattern.

In conclusion, we found a significantly prolonged absorption phase in CF-patients which could be described by BMI as covariate. The disposition parameters were similar between CF-patients and healthy volunteers after we scaled them allometrically by $FFM_C$ or $FFM_J$. The prolonged oral absorption in CF-patients resulted in two times higher PKPD breakpoints for CF-patients. A dose of 1,000 mg q8h showed robust (≥90%) PTAs for near-maximal bactericidal effect for MICs ≤0.25 mg/L in adult CF-patients and for MICs ≤0.094 mg/L in healthy volunteers. Future clinical studies are warranted to show whether the profound effect of the prolonged oral absorption phase in CF-patients on the PTA also results in a higher probability of successful clinical outcome.

### 3.4.2 Population pharmacokinetics and pharmacodynamics of cefadroxil

#### 3.4.2.1 Chemical structure of cefadroxil

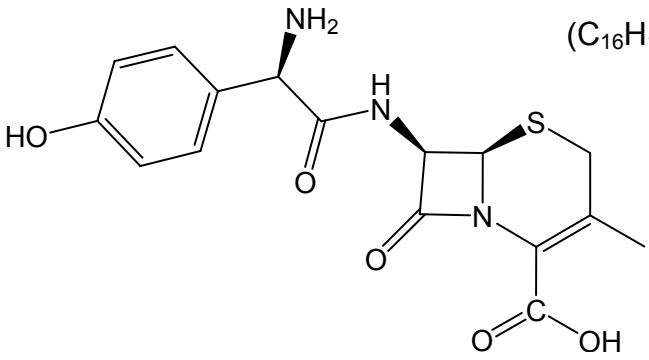


($C_{16}H_{17}N_3O_5S$, Mol. Wt.: 363.39)

**Chemical structure 3.4-2** Cefadroxil

#### 3.4.2.2 Possible use of cefadroxil in patients with cystic fibrosis

As described for cefaclor in chapter 3.4.1.2, the oral route of administration is very important for CF-patients. Oral cefadroxil is a promising and cost-effective treatment option for group A beta-hemolytic streptococcal tonsillopharyngitis (67, 102), uncomplicated urinary tract infections (242) caused by *E. coli*, *P. mirabilis*, Klebsiella, or *S. saprophyticus*, as well as skin and skin structure infections by *S. aureus*, *S. epidermidis*, and *Streptococcus pyogenes* (156, 189, 290, 544), and prevention of flare-ups in dental infections (331). As its spectrum of activity is basically restricted to Gram-positive bacteria, cefadroxil causes a lower risk for emergence of bacterial resistance than broad spectrum antibiotics. After oral administration, cefadroxil is reliably and virtually completely absorbed in presence or absence of food (296, 434), reaches about 12-15 times higher serum concentrations 6 h post dose than cefaclor (172), and is well tolerated in adults and children (148, 156, 181, 318, 433, 434, 559). Consequently, cefadroxil is an appealing candidate for oral

treatment of infections caused by the above mentioned pathogens in CF-patients, but has not yet been studied in CF-patients.

The oral route of administration is very important for CF-patients, but pathophysiological changes in their GI tract might prohibit a reliable use of oral antibiotics in CF-patients. Therefore, our first objective was to compare the PK including the rate and extent of oral absorption of cefadroxil between CF-patients and healthy volunteers via population PK. As our second objective, we compared clearance and volume of distribution between CF-patients and healthy volunteers to study which body size descriptor is most appropriate for cefadroxil in CF-patients. Our third objective was to compare the PD profile of oral cefadroxil between CF-patients and healthy volunteers.

#### 3.4.2.3 Methods

The general clinical and sample handling procedures, the methods for PK analysis (including NCA and population PK), and the general methods for MCS are described in chapter 2. Chapter 3.2 shows the specific methods applied for analysis of our CF-studies.

***Subjects:*** A total of 14 Caucasian volunteers (eight CF-patients and six healthy volunteers) of both sexes participated in the study. Table 3.4-7 shows the demographic data.

***Study design and drug administration:*** The study was a single dose, single-center, open, parallel group study. Each subject received a total oral dose of 1g cefadroxil as 2 capsules each containing 500 mg cefadroxil (Bidocef®) in the fasting state together with 150 mL of calcium poor low-carbonated mineral water at room temperature. CF-patients did not take pancreatic enzymes as supplement therapy from at least 10 h before until 4 h after cefadroxil dose.

***Blood and urine sampling:*** Blood samples were drawn immediately before administration (0 h) and at 0.25, 0.5, 1, 1.5, 2, 3, 4, 5, 6, 8, 12, and 24 h post dose. Urine was collected from 0 to 1, 1 to 2, 2 to 3, 3 to 4, 4 to 5, 5 to 6, 6 to 8, 8 to 12, and 12 to 24 h after dosing.

**Table 3.4-7** Demographic data of the cefadroxil study (average ± SD)

| | **CF-patients** | **Healthy volunteers** |
|---|---|---|
| Number of subjects (males / females) | 8 (4 / 4) | 6 (3 / 3) |
| Age (yr) | 19.8 ± 3.2 | 23.3 ± 2.1 |
| Height (cm) | 168 ± 7.5 | 173 ± 10 |
| Total body weight (kg) | 49.6 ± 10.9 | 68.8 ± 10.7 |
| Fat-free mass° (kg) | 41.8 ± 8.7 | 53.1 ± 9.5 |
| Fat-free mass# (kg) | 39.8 ± 10.4 | 49.9 ± 11.9 |
| Body mass index (kg $m^{-2}$) | 17.4 ± 2.7 | 23.0 ± 2.9 |

°: Calculated by the formula of Cheymol and James (72, 222).

#: Calculated by the formula of Janmahasatian et al. (224).

***Drug analysis in plasma and urine:*** We determined the concentration of cefadroxil in plasma and urine by reversed phase HPLC with UV detection. An amount of 100 µL of $NaH_2PO_4$ buffer was added to 100 µL of each sample. Acetonitrile (400 µL) was used to deproteinize each sample. After centrifugation 1,000 µL of dichloromethane were added for extraction of the organic phase. From the remaining aqueous phase, 20 µL were injected into the HPLC system. Urine samples were diluted (ratios 1:5 to 1:50) with bi-distilled water if necessary. Ten (10) µL of the resulting mixture were injected into the HPLC system. We assured stability of cefadroxil during sample preparation and analysis and used a µ-Bondapak® C18 (10 µ) column (Waters, Germany) with a water / acetonitrile mixture at pH 6.7. The eluent included tetrahexylammonium chloride as ion-pair reagent. Cefadroxil was detected at a wavelength of 263 nm. Calibration was performed by linear regression. The linearity of cefadroxil calibration curves in plasma and urine was shown between 0.5-40 mg/L and 30-400 mg/L, respectively. We took 30-40 mL blood from one additional subject at three time points with a high, intermediate, and low concentration. This subject did not participate in the PK study. Those blood samples were prepared like all other samples as

described above and used as biological quality controls. We included these biological quality controls and spiked quality controls in each analytical run.

***Population PK analysis:*** We used the same population PK model for cefadroxil as for cefaclor (see chapter 3.4.1.3 for details).

***MCS:*** We compared the PTAs of CF-patients and healthy volunteers at steady-state for two oral dosage regimens: 1) 1g cefadroxil q12h and 2) 1g cefadroxil q8h. We studied a range of MICs from 0.5 to 16 mg/L and assumed a protein binding of 20% for cefadroxil (60). We calculated the PTA expectation value against penicillin susceptible *Streptococcus pneumoniae* (n=283) (516) based on a published MIC distribution.

### 3.4.2.4 Results

***NCA:*** Figure 3.4-4 shows the average plasma concentrations of CF-patients and healthy volunteers and Table 3.4-8 lists the results of the NCA. These parameters are not scaled by any size descriptor. The median renal clearance was 1% lower, the terminal half-life was 16% shorter, and the volume of distribution at steady-state was 5% larger in CF-patients than in healthy volunteers.

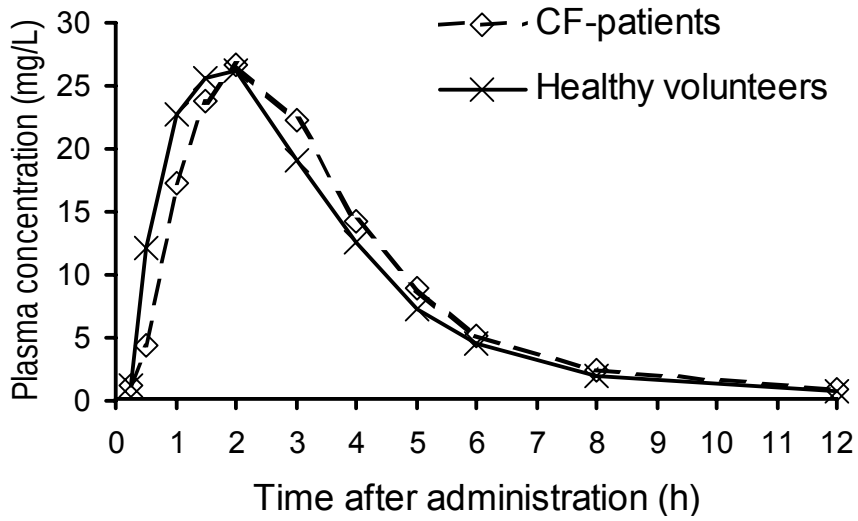


**Figure 3.4-4** Average plasma concentrations of cefadroxil for CF-patients and healthy volunteers after a single oral dose of 1g cefadroxil in the fasting state

**Table 3.4-8** Unscaled PK parameters derived via NCA (median [range])

| | CF-patients | Healthy volunteers |
|---|---|---|
| Fraction of nominal dose excreted unchanged in urine (%) | 106 [85 - 117] | 110 [98 - 118] |
| Apparent total clearance (L/h) | 9.38 [8.22 - 11.1] | 9.45 [8.86 - 10.8] |
| Renal clearance (L/h) | 10.1 [7.37 - 12.0] | 10.2 [9.16 - 11.8] |
| Apparent volume of distribution at steady-state (L) | 33.7° [28.2 - 39.1] | 32.1° [29.2 - 45.5] |
| Apparent volume of distribution during the terminal phase (L) | 26.4 [17.3 - 39.5] | 30.5 [22.4 - 55.5] |
| Time to peak concentration (h) | 2.0 [1.0 - 3.0] | 1.75 [1.0 - 2.0] |
| Peak concentration (mg/L) | 31.0 [19.9 - 35.6] | 27.9 [23.2 - 30.3] |
| Terminal half-life (L) | 1.97 [1.08 - 2.89] | 2.34 [1.66 - 3.57] |
| Mean body residence time* (h) | 3.54 [2.79 - 4.49] | 3.45 [3.11 - 4.22] |

*: Sum of mean input time and mean disposition residence time

°: The higher apparent volume of distribution at steady-state in CF-patients was probably caused by a longer mean input time for the oral absorption process.

Even though the terminal half-life was shorter in CF-patients, the mean body residence time was 3% longer in CF-patients. A longer mean input time in CF-patients probably caused the mean body residence time to be 3% longer in CF-patients. The extent of absorption was comparable between both subject groups, since the median fraction excreted unchanged in urine was 106% of the nominal dose for CF-patients and 110% for healthy volunteers (see Table 3.4-8). The pharmaceutical content of the cefadroxil formulation used in this study was 108-110% of the nominal content. Therefore, essentially all drug was recovered in urine and nonrenal clearance of cefadroxil was negligible.

**Population PK analysis**

***Structural model:*** The predictive performance during the absorption phase improved considerably through the inclusion of lag-time. NONMEM's objective function improved by 55 to 122 points (depending on the structural model), if lag-time was included. Absorption model 3 had a considerably

better predictive performance, especially during the absorption phase, compared to absorption model 2 (zero-order input) which was slightly better than absorption model 1 (first-order input). The predictive performance for the 24-h urine sample was much better for the two-compartment model than for the one-compartment model. For absorption model 3, the objective function was 52 points better for the two-compartment than for the one-compartment model. The data did not support a three-compartment model.

Figure 3.4-5 reveals the highly sufficient predictive performance of the model with two disposition compartments, absorption model 3, and $FFM_C$ as size descriptor. This applies to the plasma and urine profiles in CF-patients and healthy volunteers. The variability of the predicted plasma concentrations was slightly too large for the healthy volunteers who had a very low variability possibly due to the highly standardized study performance and drug analysis. As this PK model was able to capture the plasma and urine profiles for CF-patients and healthy volunteers well, we chose this model as our final model.

***Covariate model:*** When we estimated $FCYF_{TLAG}$, $FCYF_{TK0}$, and $FCYF_{TABS}$ CF-patients showed a 5 min longer TLAG, an 81% (17 min) longer TK0, and a 45% (11 min) longer TABS. BMI as a covariate explained the average differences in all three absorption parameters between CF-patients and healthy volunteers. Additionally, inclusion of BMI reduced the BSV by 46% for TLAG, 20% for TK0, and 36% for TABS.

The final estimates for the population PK model based on $FFM_C$ as size descriptor are shown in Table 3.4-9. As $slope_{TLAG}$, $slope_{TK0}$, and $slope_{TABS}$ had estimates between -0.05 and -0.08 $m^2\ kg^{-1}$, the influence of BMI on TLAG, TK0, and TABS can be interpreted as follows: A decrease of BMI by 1 kg $m^{-2}$ results in an increase of about 7.6% for TLAG, of about 5.2% for TK0, and of about 7.0% for TABS. The average BMI was 5.3 kg $m^{-2}$ lower in CF-patients than in healthy volunteers. Therefore, a typical CF-patient was estimated to have an about 43% (3.9 min) longer TLAG, a 29% (7.3 min) longer TK0, and a 39% (10 min) longer TABS compared to a typical healthy volunteer.

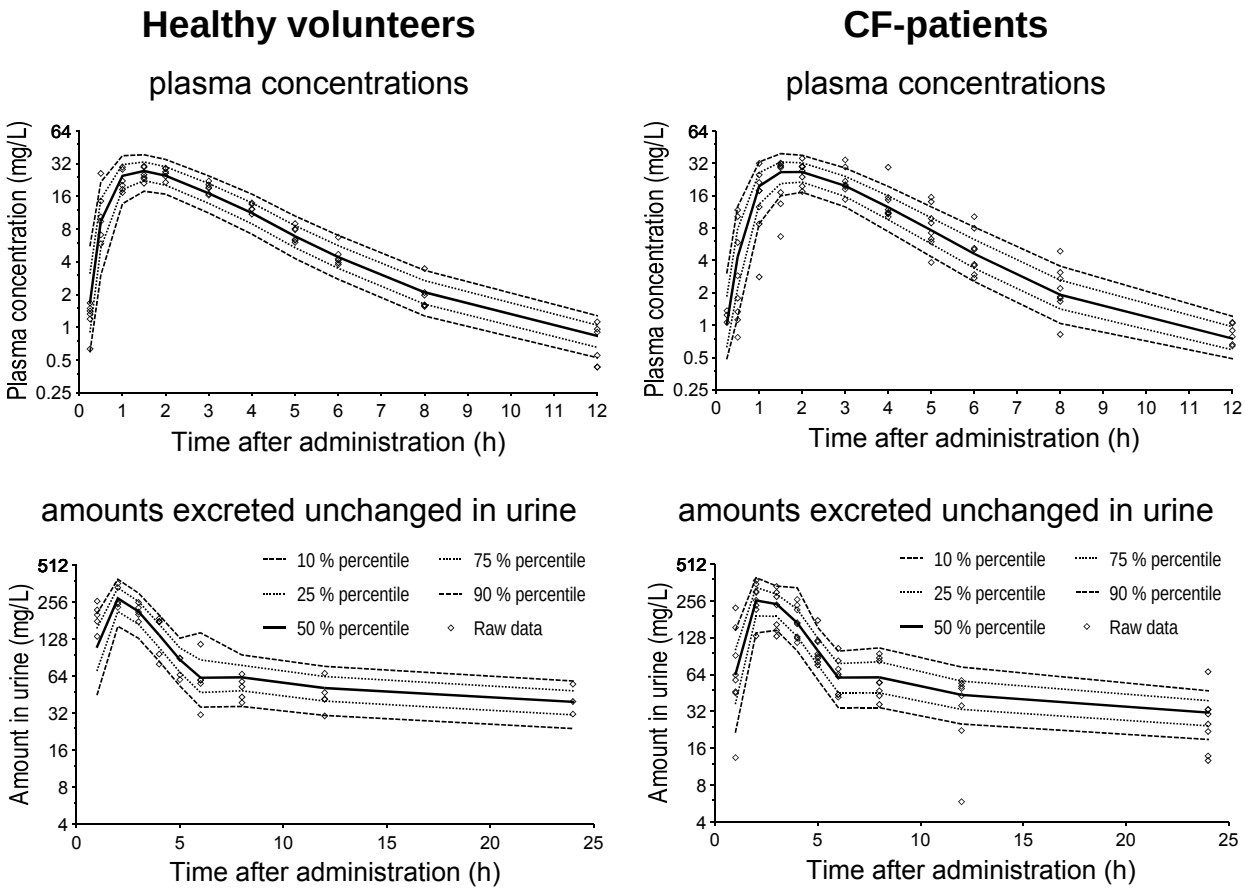


**Figure 3.4-5** VPC based on 12,000 CF-patients and 9,000 healthy volunteers for the two compartment disposition model based on $FFM_C$ with absorption model 3 (see Table 3.4-9).

See chapter 2.6.3 for interpretation of VPCs.

We distinguished the size models 1) by their estimates for the disease specific scale factors FCYF and 2) by their ability to reduce the unexplained BSV in clearance and volume of distribution. CF-patients had an identical ($FCYF_{CLR}$ = 1.00) renal clearance and a 21% lower volume of distribution at steady-state in absence of any size model (see FCYF in Table 3.4-10, size model A). Linear scaling by WT (size model B) predicted renal clearance to be 39% higher and volume of distribution to be 18% higher in CF-patients relative to healthy volunteers. Allometric scaling by WT (size model C) predicted renal clearance to be 28% higher and volume of distribution to be 15% in CF-patients. For allometric scaling by $FFM_C$ or $FFM_J$ (size models D and E), renal

clearance was estimated to be about 20% higher in CF-patients and volume of distribution at steady-state was estimated to be very similar in both subject groups.

**Table 3.4-9** PK parameter estimates for the allometric size model based on $FFM_C$

| Parameter | Unit | Estimate for | | Coefficient of variation (%)° |
|---|---|---|---|---|
| | | CF-patients | healthy volunteers | |
| $F^{§}$ | | 1.07* | | |
| $CL_R$ | L $h^{-1}$ | 12.4* | 10.3* | 6.94 |
| Vss^ | L | 30.3* | 29.4* | 5.00 |
| V1 | L | 21.9* | 21.3* | |
| V2 | L | 8.36* | 8.12* | |
| CLic | L $h^{-1}$ | 1.37* | | |
| TLAG | min | 9.24* | | 36.9 |
| TK0 | min | 25.0* | | 61.9 |
| TABS | min | 26.0* | | 37.5 |
| $Slope_{TLAG}$ | $m^2$ $kg^{-1}$ | -0.0764 | | |
| $Slope_{TK0}$ | $m^2$ $kg^{-1}$ | -0.0515 | | |
| $Slope_{TABS}$ | $m^2$ $kg^{-1}$ | -0.0701 | | |
| CVC | % | 22.5 | | |
| SDC | mg/L | 0.243 | | |
| CVAU | % | 29.5 | | |
| SDAU | mg | 0.324 | | |

*: Group estimate for a subject with standard $FFM_C$=53 kg and standard BMI = 22 kg $m^{-2}$.

§: We estimated F by the amount excreted unchanged in urine and assumed that nonrenal elimination is absent.

^: Derived from model estimates, not an estimated parameter.

°: Apparent coefficient of variation for the BSV.

F: Extent of absorption. We assumed that all drug is eliminated renally. Therefore, “F” in part accounts for the deviation between actual and nominal dose in the formulation.

TLAG: lag-time of absorption, TK0: duration of zero order input into the gut compartment, TABS: half-life of first order absorption from the gut into the central compartment. See also chapter 2.6.2 for explanation of model parameters.

**Table 3.4-10** Ratios of group estimates (CF-patients / healthy volunteers) for clearance and volume of distribution for different size models

| Size model | $FCYF_{CLR}$ | $FCYF_V$ |
|---|---|---|
| A) No size model | 1.00 | 0.79 |
| B) WT linear scaling | 1.39 | 1.18 |
| C) WT allometric | 1.28 | 1.15 |
| D) LBM allometric | 1.20 | 1.03 |
| E) $FFM_J$ allometric | 1.19 | 1.00 |

FCYF: Ratio of group estimates (group estimate for CF-patients divided by group estimate for healthy volunteers).

Additionally, we compared the ability of the different size models to reduce the unexplained BSV. Table 3.4-11 shows that allometric scaling by $FFM_C$ or WT reduced the unexplained BSV in renal clearance by 58% relative to linear scaling by WT. Allometric scaling by $FFM_C$ or $FFM_J$ reduced the unexplained BSV in volume of distribution by about 60% compared to linear scaling by WT.

**Table 3.4-11** Comparison of BSV (variances) between various size models: The table shows the relative between subject variances for the respective PK parameter and size models

| Size model | Relative between subject variance | |
|---|---|---|
| | $CL_R$ | Vss |
| B) WT linear scaling | 100%* | 100%* |
| C) WT allometric | 42%° | 91% |
| D) $FFM_C$ allometric | 42%° | 38% |
| E) $FFM_J$ allometric | 74%° | 44% |

*: The BSV for linear scaling by WT was used as reference.

°: The lower this number, the more variability was explained by the respective size model. These values mean that the BSV for renal clearance was reduced by 58% for allometric scaling by WT and allometric scaling by $FFM_C$, and by 26% for allometric scaling by $FFM_J$, all compared to linear scaling by WT.

***MCS:*** After an oral dose of 1g cefadroxil q12h at steady-state we found a PKPD breakpoint of 1 mg/L for healthy volunteers and CF-patients based on the target $fT_{>MIC} \geq 65\%$ for near-maximal bactericidal effect (see Figure 3.4-6). The breakpoint for bacteriostasis (target $fT_{>MIC} \geq 40\%$) was 3-4 mg/L for both subject groups. For 1g cefadroxil q8h the PKPD breakpoint for near-maximal killing was 3 mg/L and the bacteriostasis breakpoint was 8 mg/L in both subject groups.

The PTA expectation value for bacteriostasis ($fT_{>MIC} \geq 40\%$) against penicillin susceptible *S. pneumoniae* was 100% for CF-patients and healthy volunteers. For near-maximal bactericidal activity ($fT_{>MIC} \geq 65\%$), PTA expectation values were 94% for CF-patients and 98% for healthy volunteers after 1g q12h. A dose to 1g q8h achieved PTA expectation values of 100% for CF-patients and healthy volunteers for both PKPD targets.

#### 3.4.2.5 Discussion

Progressive lung disease causes more than 90% of deaths in CF-patients (283) and respiratory diseases are also the primary reason for frequent hospitalization of CF-patients (283, 400). Methicillin susceptible *S. aureus* (MSSA) is often one of the first pathogens infecting the lungs of young CF-patients. Cefadroxil is orally available and has been successfully used in the treatment of respiratory tract infections caused by beta-hemolytic streptococci, MSSA, and *S. pneumoniae* (395). It is a cost-effective treatment option for group A beta-hemolytic streptococcal tonsillopharyngitis (67, 102), uncomplicated urinary tract infections (1, 242), skin and skin structure infections (156, 189, 226, 290, 544), and prevention of flare-ups in dental infections (331). Cefadroxil showed a high (85.7%) clinical and microbiological cure rate in an outpatient trial in children with uncomplicated skin and skin structure infections caused by MRSA (243), which was comparable to linezolid. Cefadroxil also showed a high clinical and microbiological cure rate (~92%) (102) for treatment of pharyngitis and tonsillitis caused by group A beta-hemolytic streptococci which was superior to oral penicillin V. Casey and

Pinchichero (67) reported a significantly lower likelihood of bacteriologic and clinical failure for treatment of group A beta-hemolytic streptococcal tonsillopharyngitis in children for oral cephalosporins (including cefadroxil) than for oral penicillin.

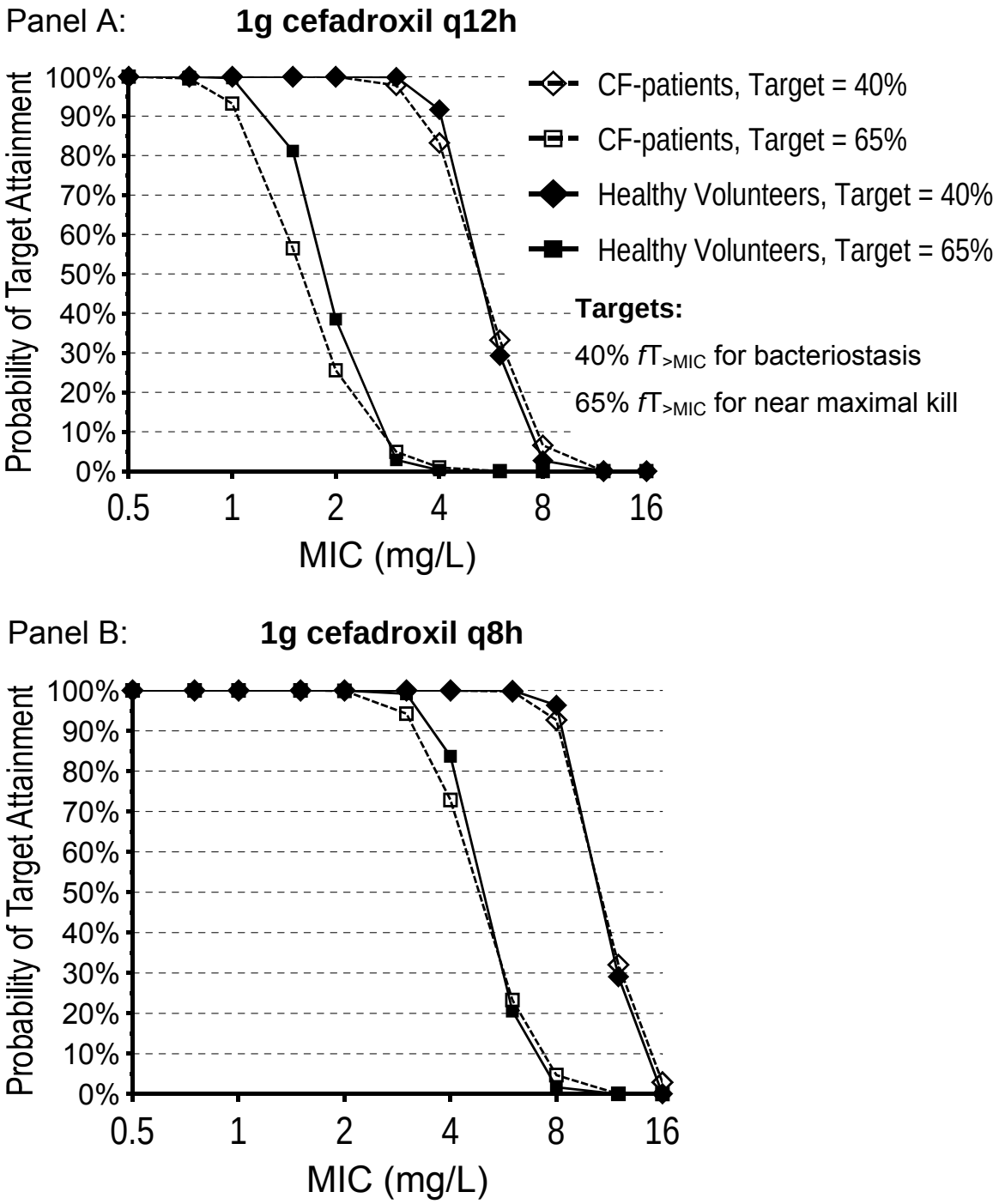


**Figure 3.4-6** Probability of target attainment for oral doses of cefadroxil at steady-state based on the population PK model with $FFM_C$

Pathophysiological changes in the GI tract of CF-patients may affect the rate and extent of oral absorption in CF-patients (see chapter 3.1.2 for details). There are only a few studies on the rate and extent of absorption of beta-lactams in CF-patients. None of those studies used population PK. As we studied cefadroxil after oral administration, it was important to build a population PK model with sufficient predictive performance during the absorption phase. A flip-flop situation seems unlikely for cefadroxil, since the terminal half-life is significantly prolonged in patients with renal failure (204), while the “absorption” half-life remains unaltered (87). Our subjects had a normal renal function.

The absorption of cefadroxil has been described not to follow a simple first order process (including a lag-time). Several authors (256, 348, 432, 508) described an active absorption of cefadroxil from the rat small intestine which was also found in humans for aminopenicillins (454). Cefadroxil resembles a dipeptide structure and is recognized by the intestinal peptide transporter PEPT1 (54, 396). Therefore, more complex absorption models were required to described the oral absorption of cefadroxil. Garrigues et al. (146) used a zero-order input process which was switched to a first order absorption after an estimated duration of the zero-order input process for cefadroxil. They also included a lag-time of absorption.

Our CF-patients abstained from taking pancreatic enzymes as supplement therapy from at least 10 h prior to cefadroxil dose. This allowed us to compare the absorption in both subject groups without a possible bias due to the intake of pancreatic enzymes. Our final model had a zero order input into the gut compartment. It had a highly sufficient predictive performance in plasma and urine (see Figure 3.4-5). The variability of the predicted concentrations for healthy volunteers was slightly wider than the variability of the raw data. However, the variability of the raw data for healthy volunteers was very small and the PKPD breakpoint will only be slightly more conservative for healthy volunteers due to this fact. The highly sufficient predictive performance qualified our population PK model to compare the PD characteristics between CF-patients and healthy volunteers via MCS.

Our PK parameter estimates were in good agreement with those reported by other authors (3, 29, 146, 204, 276, 295, 311, 452) for healthy volunteers. We are not aware of any PK studies on cefadroxil in CF-patients. Our CF-patients had a 28% lower WT and a 21% lower $FFM_C$. We therefore accounted for differences in body size by population PK including linear and allometric size models based on WT, $FFM_C$, or $FFM_J$.

As expected, we observed a lower unscaled volume of distribution in CF-patients, because they were smaller than our healthy volunteers (see Table 3.4-8 and Table 3.4-10). A longer mean input time probably caused the volume of distribution at steady-state determined via NCA to be slightly larger for CF-patients than for healthy volunteers. Our estimate for unscaled renal clearance was very similar for both subject groups.

Linear scaling by WT resulted in a 39% higher renal clearance and in an 18% higher volume of distribution for CF-patients (see Table 3.4-10). We found a similar trend for allometric scaling by WT, probably because WT does not account for body composition. Allometric scaling by $FFM_C$ or $FFM_J$ resulted in very similar volumes of distribution for CF-patients and healthy volunteers and in an about 20% higher renal clearance for CF-patients. This is evidence for a possibly slightly increased renal clearance in CF-patients for cefadroxil. This observation is in agreement with the data from Hedman et al. (182, 183) who found an increased renal clearance of ceftazidime and cefsulodin caused by an increased glomerular filtration rate.

Allometric scaling by $FFM_C$ or $FFM_J$ explained the average difference in renal clearance and volume of distribution better than both size models based on WT. Furthermore, population PK also directly estimates, whether $FFM_C$, $FFM_J$, or WT is more appropriate to reduce the unexplained BSV in clearance and volume of distribution, after accounting for the average differences between CF-patients and healthy volunteers. Table 3.4-11 shows that allometric scaling by $FFM_C$ reduced the unexplained BSV by 58% for renal clearance and by 62% for volume of distribution at steady-state relative to linear scaling by WT. Therefore, $FFM_C$ allows one to achieve target concentrations more precisely in empiric therapy compared to dose selection by WT.

After including body size and body composition we still found a longer absorption phase in CF-patients. All three absorption parameters (TLAG, TK0, and TABS) were systematically longer in CF-patients than in healthy volunteers. In absence of a descriptor for GI malfunction in CF-patients, we used BMI as a surrogate measure to describe a possible GI malfunction, because we empirically found a correlation between the absorption parameters and BMI. The population PK analysis revealed that BMI could explain the average differences in all three absorption parameters between CF-patients and healthy volunteers and reduced the BSV in all three absorption parameters by 20-46%. Although the rate of absorption was slower in CF-patients, the extent of absorption was similar to healthy volunteers. Cefadroxil was virtually completely recovered in urine within 24 h in both subject groups (see Table 3.4-8). Therefore, cefadroxil was reliably and virtually completely absorbed in both subject groups.

The prolonged absorption in our CF-patients improved the PD profile of cefadroxil for CF-patients. The 16% shorter elimination half-life of cefadroxil was counterbalanced by a prolonged absorption phase in CF-patients with regard to the $fT_{>MIC}$. A shorter elimination half-life decreases the PTA, whereas a prolonged absorption phase increases the PTA. We studied a dose of 1g either q12h or q8h and found only slightly lower or similar PTAs for CF-patients compared to healthy volunteers. For 1g q12h, the PKPD breakpoint was 3-4 mg/L for bacteriostasis and 1 mg/L for near-maximal bactericidal activity in both subject groups. This is in good agreement with the BSAC breakpoint (56) for beta-hemolytic streptococci of 1 mg/L for susceptibility. For 1g q8h, the breakpoint was 8 mg/L for bacteriostasis and 3 mg/L for near-maximal bactericidal activity in both subject groups.

To put this into clinical perspective, we calculated the PTA expectation value for successful treatment of infections caused by penicillin susceptible *S. pneumoniae* (516) isolated in Belgium. For 1g q12h, the PTA expectation values were 100% for bacteriostasis in both subject groups. The PTA expectation values were 94% for CF-patients and 98% for healthy volunteers for near-maximal killing. Giving 1g cefadroxil q8h instead of q12h, increased the PTA expectation values to 100% for near-maximal killing in both subject

groups. The superiority of 1g cefadroxil q8h to 1g q12h will be most pronounced, if the $MIC_{50}$ and $MIC_{90}$ fall between 1 and 4 mg/L. $MIC_{90}$'s of 2 mg/L (or below) have been reported (143, 147, 449) for penicillin susceptible (or intermediate) *S. pneumoniae*. Doses of 1g cefadroxil q12h will be sufficient for treatment of *S. pyogenes* with an $MIC_{90}$ of 0.13 mg/L (all MICs $\leq$ 0.25 mg/L) (143). However, the MIC distribution of the local hospitals should be used to calculate the PTA expectation value to decide, whether cefadroxil will be a promising treatment option for the respective pathogens in each local hospital.

In conclusion, cefadroxil was reliably and virtually completely absorbed and completely recovered in urine within 24 h in CF-patients and healthy volunteers. We found a prolonged absorption phase in CF-patients which could be described by BMI as a covariate. Linear or allometric scaling by WT predicted clearance and volume of distribution to be 15 to 39% higher in CF-patients. Allometric scaling by $FFM_C$ or $FFM_J$ resulted in similar volumes of distribution for both subject groups. Renal clearance was about 20% higher in CF-patients after accounting for body size and body composition via $FFM_C$ or $FFM_J$. Allometric scaling by $FFM_C$ best reduced the unexplained BSV for clearance and volume of distribution. The prolonged oral absorption in CF-patients caused the PKPD breakpoints to be the same in both subject groups, although CF-patients had a 16% shorter elimination half-life. The PTAs for the near-maximal kill target 65% $fT_{>MIC}$ were robust ($\geq$90%) for MICs $\leq$1mg/L after 1g q12h and for MICs $\leq$3 mg/L after 1g cefadroxil q8h. Future clinical trials are warranted to show whether oral cefadroxil shows promising clinical and microbiological cure rates in CF-patients.

### 3.4.3 Population pharmacokinetics and pharmacodynamics of ciprofloxacin

#### 3.4.3.1 Chemical structure of ciprofloxacin

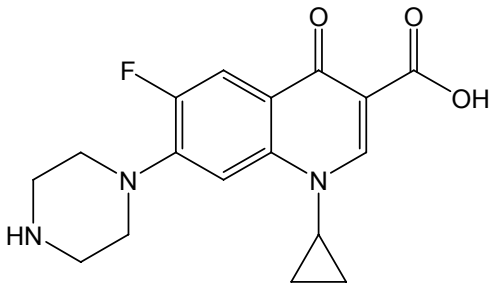


($C_{17}H_{18}FN_3O_3$, Mol. Wt.: 331.34)

**Chemical structure 3.4-3** Ciprofloxacin

#### 3.4.3.2 Use of ciprofloxacin in patients with cystic fibrosis

Chronic lung infection by *P. aeruginosa* is a major factor involved in the disease progression and mortality of CF-patients (12, 283, 400). Antibiotic therapy against this pathogen serves two objectives. As it is virtually impossible to eradicate *P. aeruginosa* once a chronic infection is established (105, 151), early aggressive treatment against this pathogen aims at preventing or delaying chronic infection (139, 192). After *P. aeruginosa* infection has become chronic, antibiotics are given to reduce the high bacterial load and improve the clinical condition of CF-patients e. g. during exacerbation of pulmonary disease (502).

Fluoroquinolones are the only available oral treatment option against *P. aeruginosa* and most of the experience has been gained with ciprofloxacin. Ciprofloxacin is active against *P. aeruginosa*, *S. aureus*, and *H. influenzae* and is therefore an appealing oral treatment option for CF-patients. Clinical experience in adult CF-patients with chronic infection by *P. aeruginosa* most often shows significant clinical improvement due to oral ciprofloxacin therapy,

although eradication of *P. aeruginosa* is almost never observed in adult CF-patients (50, 155, 188, 227, 270, 279, 422, 443, 445, 448, 455).

Two clinical studies on the effectiveness of ciprofloxacin monotherapy in children with CF (age: 5-17 yrs) show eradication rates of 30% and less at the end of treatment (77, 412), although both studies show significant clinical improvement after oral ciprofloxacin therapy. Those studies did not combine the PK of ciprofloxacin in CF-patients with the susceptibility data and the authors also did not derive a PKPD target for ciprofloxacin in CF-patients. Population PK with MCS is the method of choice to predict the probability of bacterial eradication. For fluoroquinolones, the ratio of the area under the plasma concentration time curve divided by the MIC (AUC/MIC) best predicts the clinical and microbiological success (84, 107, 111, 137). Importantly, the AUC/MIC target for ciprofloxacin which is required for treatment success has been determined based on data in patients without CF. The AUC/MIC target for ciprofloxacin in CF-patients has not yet been determined.

Besides the AUC/MIC target in CF-patients, a PK model which adequately accounts for body size in adults and children with CF is required to combine the PK data with the MIC distribution for CF-patients. It may also be necessary to account for body composition, since CF-patients often have a paucity of adipose tissue. Three groups (378, 398, 436) determined the population PK of oral ciprofloxacin in children and juveniles with CF, but did not study the PD profile of ciprofloxacin via MCS. Montgomery et al. (327) used population PK and MCS to assess the PD profile of intravenous ciprofloxacin in adult CF-patients. However, none of those four studies included a healthy volunteer control group. It is therefore difficult to decide, if CF, age, body size, or body composition may have altered the PK in these CF-patients compared to healthy volunteers. Some authors (408, 502) compared the PK of ciprofloxacin in CF-patients and healthy volunteers with data from the same study, but did not use population PK to assess the PD profile of oral ciprofloxacin via MCS.

Therefore, we applied population PK as a powerful method to compare the PK of oral ciprofloxacin between CF-patients and healthy volunteers. As our first objective, we studied the difference in average clearance and volume

of distribution after adjusting for body size by various size descriptors. As our second objective, we compared the unexplained BSV in clearance and volume of distribution between various size models. Our third objective was to back-engineer the AUC/MIC target of ciprofloxacin for eradication of *P. aeruginosa* based on clinical data from children with CF. We used this back-engineered AUC/MIC target to determine the PKPD profile of high dose oral ciprofloxacin therapy in adult CF-patients via MCS.

#### 3.4.3.3 Methods

The general clinical and sample handling procedures, the methods for PK analysis (including NCA and population PK), and the general methods for MCS are described in chapter 2. Chapter 3.2 shows the specific methods applied for analysis of our CF-studies.

***Subjects:*** Sixteen (16) Caucasian volunteers (eight CF-patients and eight healthy volunteers) participated in the study. Table 3.4-12 shows the demographic data.

***Study design and drug administration:*** All subjects received an oral dose of 750 mg ciprofloxacin together with 150 mL low-carbonated, calcium-poor mineral water at room temperature. CF-patients abstained from taking pancreatic enzymes as supplement therapy from at least 10 h before until 4 h post ciprofloxacin dose.

***Blood sampling:*** Blood samples were drawn immediately before administration (0 min) as well as at 15, 30, 60, and 90 min and at 2, 3, 4, 5, 6, 8, 10, 12, 16, and 24 h post end of infusion. Urine was collected from 0 to 1, 1 to 2, 2 to 3, 3 to 4, 4 to 5, 5 to 6, 6 to 8, 8 to 10, 10 to 12, 12 to 16, 16 to 24, and 24 to 30 h after dosing.

***Drug analysis:*** We determined the concentration of ciprofloxacin in plasma and urine by reversed phase HPLC with fluorescence detection. An amount of 200 µL acetonitrile was added to 100 µL plasma. The mixture was centrifuged and 4-8 µL of the supernatant were injected into the HPLC system. Urine samples were diluted 1:50 with bidistilled water and 4-8 µL were injected into the HPLC system. We used a Nucleosil C18 (5 µm) column

with a water / acetonitrile mixture at pH 2.4 and tetrahexylammonium chloride as ion-pair reagent.

The excitation wavelength was 275 nm and emission was detected at 445 nm. Calibration was performed by linear regression. The assay was linear between 0.079 and 5.0 mg/L ciprofloxacin in plasma and between 0.313 and 500 mg/L ciprofloxacin in urine. We took 30-40 mL blood from one additional subject at three time points with a high, intermediate, and low concentration. This subject did not participate in the PK study. Those blood samples were prepared like all other samples as described above and used as biological quality controls. We included these biological quality controls and spiked quality controls in each analytical run.

**Table 3.4-12** Demographic data of the ciprofloxacin study (median [range])

| | **CF-patients** | **Healthy volunteers** |
|---|---|---|
| Number of subjects (males / females) | 8 (4 / 4) | 8 (4 / 4) |
| Age (yrs) | 20 [17 - 26] | 24 [23 - 27] |
| Height (cm) | 168 [157 - 191] | 169 [165 - 184] |
| Total body weight (kg) | 46.8 [33.0 - 81.2] | 61.5 [53.0 - 77.0] |
| Fat-free mass° (kg) | 41.8 [28.8 - 66.3] | 48.5 [41.8 - 62.4] |
| Fat-free mass# (kg) | 40.2 [25.4 - 65.5] | 45.4 [36.6 - 61.6] |
| Body mass index (kg $m^{-2}$) | 16.5 [13.4 - 22.3] | 21.7 [19.0 - 22.7] |

°: Calculated by the formula of Cheymol and James (72, 222).

#: Calculated by the formula of Janmahasatian et al. (224).

***Population PK analysis:*** We used a standard two-compartment model with first-order absorption (half-life TABS) including a lag-time (TLAG) for oral absorption of ciprofloxacin. This model is described in chapter 2.6.2.1.

***Back-engineering of PKPD target:*** The AUC/MIC has been shown to be predictive for the microbiological and clinical outcome for fluoroquinolones in patients without CF (11, 46, 84, 110, 111, 137). We are not aware of any study in CF-patients which identified a PKPD target for the AUC/MIC ratio

which predicts clinical or microbiological outcome. Therefore, we back-engineered the AUC/MIC target for microbiological outcome based on PK data and clinical studies in CF-patients from literature.

We used the PK data in pediatric CF-patients from Rajagopalan et al. (398) and effectiveness data on oral ciprofloxacin from Richard et al. (412) who studied pediatric CF-patients (age: 5-17 yrs) with acute bronchopulmonary exacerbations. These pulmonary infections were attributable to *P. aeruginosa* susceptible to ciprofloxacin at pre-treatment (=inclusion criterion). The *P. aeruginosa* had an $MIC_{50}$ of 0.5 mg/L before therapy. Additionally we used effectiveness data for sequential iv/po ciprofloxacin therapy from Church et al. (77) in pediatric CF-patients (age: 5-17 yrs) with an acute pulmonary exacerbation associated with *P. aeruginosa* infection. We back-engineered the AUC/MIC target which would predict the observed bacteriological outcome for eradication at the end of ciprofloxacin treatment and for persistent eradication at follow-up based on MIC distributions for ciprofloxacin and *P. aeruginosa* in CF-patients (437, 467). The MIC distributions used for back-engineering (437, 467) had $MIC_{50}$s between 0.25 and 2 mg/L and $MIC_{90}$s between 1 and 8 mg/L.

***MCS:*** We studied a range of MICs from 0.001 to 128 mg/L and compared oral ciprofloxacin dosage regimens of 750 mg q12h (daily dose: 1,500 mg) and 750 mg q8h (daily dose: 2,250 mg) at steady-state. We simulated 10,400 CF-patients and 10,400 healthy volunteers with the same demographic data as the subjects in our study in absence of residual error. We used a range of AUC/MIC targets covering the targets identified by back-engineering.

We calculated the PTA expectation value based on various MIC distributions to predict the probability of successful treatment of CF-patients with oral ciprofloxacin in empiric monotherapy. We calculated the PTA expectation value based on published MIC distributions for *P. aeruginosa* from three European CF-centers (158), as well as for non-mucoid and mucoid *P. aeruginosa* isolates from CF-patients in Freiburg, Germany (437), and in Leipzig, Germany (467).

#### 3.4.3.4 Results

***NCA:*** Figure 3.4-7 shows the average plasma concentrations for CF-patients and healthy volunteers and Table 3.4-13 lists the PK parameters from NCA. These PK parameters are not scaled by any size descriptor. Apparent total clearance was 32% lower, renal clearance was 12% lower, and apparent volume of distribution at steady-state was 18% smaller in CF-patients compared to healthy volunteers. CF-patients had a 54% higher average peak concentration, but a comparable time to peak concentrations. The terminal half-life was 15% longer in CF-patients and mean body residence time was similar in both subject groups.

***Population PK analysis:*** The two and three compartment model had a similar predictive performance as assessed by VPCs, whereas the one compartment model had insufficient predictive performance. As the two-compartment model had highly sufficient predictive performance for plasma and urine profiles (see Figure 3.4-8), we selected it as our final model. The PK parameters of this model are shown in Table 3.4-14.

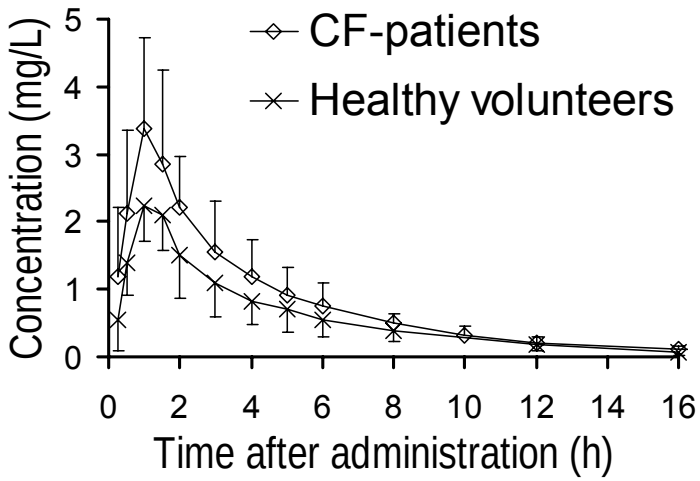


**Figure 3.4-7** Average (± standard deviation) plasma concentrations of ciprofloxacin in CF-patients and healthy volunteers after a single oral dose of 750 mg ciprofloxacin

**Table 3.4-13** Unscaled PK parameters derived by NCA (median [range])

| | CF-patients | Healthy volunteers |
|---|---|---|
| Area under the curve from time zero to infinity (L/h) | 13.8 [8.02 - 27.0] | 9.45 [5.52 - 16.5] |
| Apparent total clearance (L/h) | 54.5 [27.8 - 93.6] | 79.6 [45.3 - 136] |
| Renal clearance (L/h) | 12.7 [7.04 - 22.0] | 14.5 [12.0 - 19.0] |
| Apparent nonrenal clearance (L/h) | 41.6 [20.7 - 80.8] | 66.9 [33.3 - 117] |
| Fraction excreted unchanged in urine (%) | 23.2 [13.6 - 27.5] | 19.1 [14.0 - 26.5] |
| Apparent volume of distribution at steady-state (L) | 335 [149 - 450] | 407 [271 - 659] |
| Time to peak (mg/L) | 1.0 [0.5 - 2.0] | 1.25 [0.5 - 1.5] |
| Peak concentration (mg/L) | 3.54 [1.91 - 5.73] | 2.30 [1.68 - 3.03] |
| Terminal half-life (h) | 4.32 [1.89 - 6.31] | 3.76 [2.83 - 8.83] |
| Mean body residence time (h) | 5.09 [3.10 - 7.12] | 5.05 [3.82 - 8.96] |

We distinguished the studied size models 1) by their estimates for the disease specific scale factors FCYF and 2) by their estimates for the unexplained BSV in clearance and volume of distribution. CF-patients had lower clearances and a lower apparent volume of distribution compared to healthy volunteers, if no size descriptor was included (see size model A, Table 3.4-15). Size models B to E predicted similar ratios of average clearance and volume of distribution between both subject groups within a range of 0.77 to 1.04. None of the FCYF estimates for size models B to E (see Table 3.4-15) was significantly different from 1.0 at an $\alpha$ of 0.05 (assessed via non-parametric bootstrap techniques, data not shown). Allometric scaling by $FFM_C$ or WT reduced the unexplained BSV better than linear scaling by WT. The BSV in renal clearance was reduced by about 33% for allometric scaling by WT or $FFM_C$ relative to linear scaling by WT (see Table 3.4-16). However, non-parametric bootstrapping showed that none of the allometric size models reduced the BSV significantly better than linear scaling by WT (data not shown).

## Healthy volunteers

*A) Plasma concentrations from 0 to 30 h*

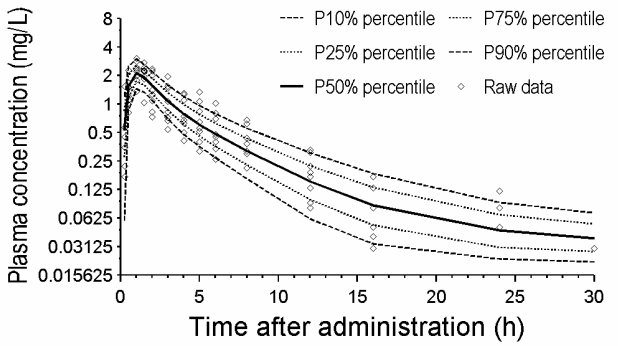


*C) Plasma concentrations from 0 to 5 h*

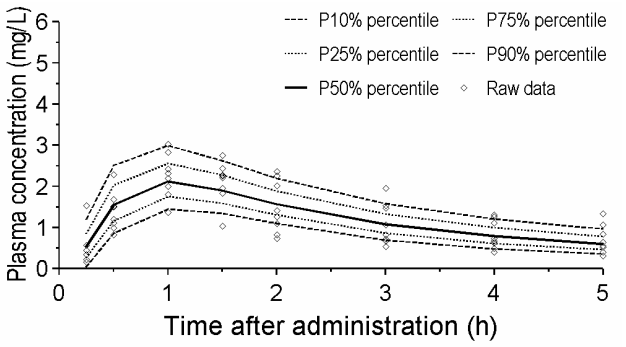


*E) Amounts excreted unchanged in urine*

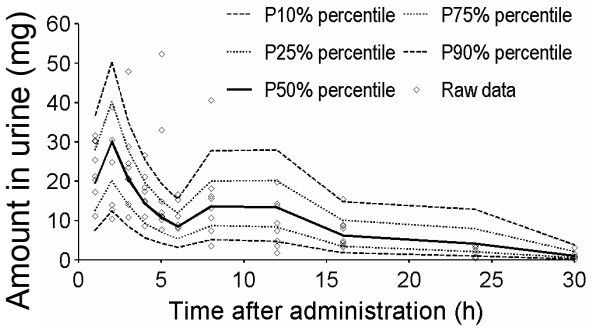


## CF-patients

*B) Plasma concentrations from 0 to 30 h*

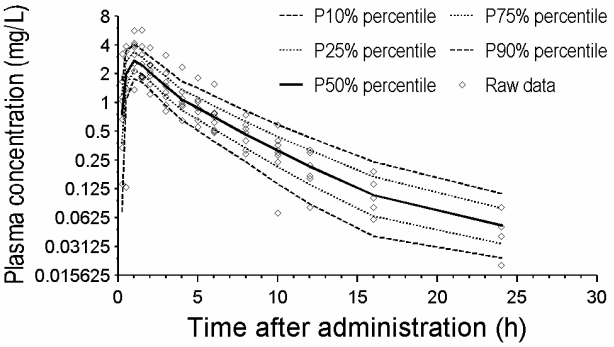


*D) Plasma concentrations from 5 h*

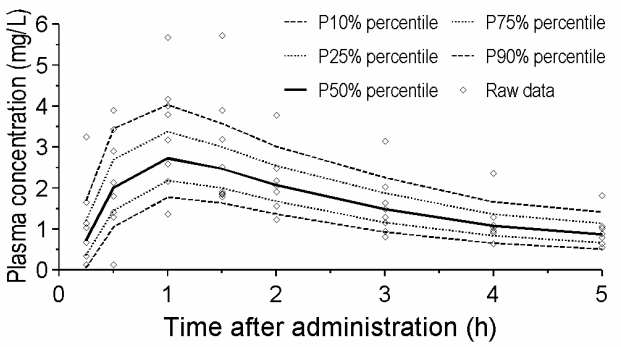


*F) Amounts excreted unchanged in urine*

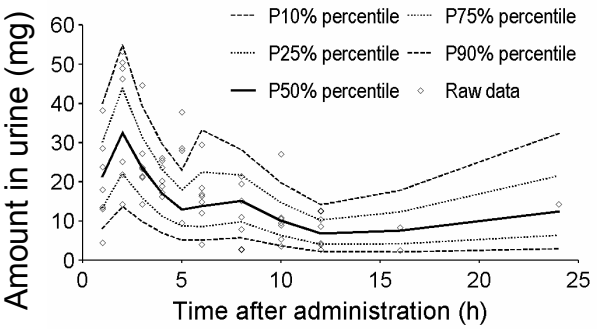


**Figure 3.4-8** VPC based on 10,400 CF-patients and 10,400 healthy volunteers for the two compartment model based on $FFM_C$ (see Table 3.4-14).

See chapter 2.6.3 for interpretation of VPCs.

**Table 3.4-14** PK parameters for the allometric size model based on $FFM_C$

| Parameter | Unit | Estimate for | | Coefficient of variation (%)° |
|---|---|---|---|---|
| | | CF-patients | Healthy volunteers | |
| $CL_R$ | L $h^{-1}$ | 15.9* | 16.7* | 13.9^ |
| $CL_{NR}$§ | L $h^{-1}$ | 53.6* | 68.1* | 30.2^ |
| V1§ | L | 83.2* | 93.4* | 32.9# |
| V2§ | L | 186* | 209* | 27.4# |
| CLic§ | L $h^{-1}$ | 99.7* | | |
| TLAG | min | 11.2 | | 42.5 |
| TABS | min | 42.5 | | 21.5 |
| $CV_C$ | % | 15.9 | | |
| $SD_C$ | mg/L | 0.0324 | | |
| $CV_{AU}$ | % | 48.6 | | |
| $SD_{AU}$ | mg/L | 0.594 | | |

*: Group estimate for a subject of standard size ($FFM_C$ = 53 kg).

§: Values are apparent clearances and apparent volumes of distribution.

°: Apparent coefficients of variation for the BSV.

^: Coefficient of correlation for the random variability between renal and nonrenal clearance, $r(CL_R,CL_{NR}) = 0.66$

#: Coefficient of correlation for the random variability between volume of central and peripheral compartment, r(V1,V2) = -0.20.

See also chapter 2.6.2 for explanation of model parameters.

***Back-engineering of PKPD target:*** Based on the clinical data from Richard et al. (412), we identified an AUC/MIC ratio of about 77-215 for *P. aeruginosa* suppression at the end of ciprofloxacin treatment and a range of about 125-340 for persistent *P. aeruginosa* suppression at follow-up. For the clinical data from Church et al. (77), we identified an AUC/MIC ratio of about 56-295 for eradication or presumed eradication of *P. aeruginosa* at the end of ciprofloxacin treatment and a range of about 108-465 for continued *P. aeruginosa* eradication at the 14- to 28-day follow-up. Those wide ranges were caused by the different MIC distributions (437, 467) used to back-

engineer the AUC/MIC target which was required to achieve the respective PTA expectation values (microbiological eradication rates). Richard et al. (412) reported the median MIC of their *P. aeruginosa* isolates to be 0.5 mg/L at pre-treatment and Church et al. (77) did not report the MICs.

**Table 3.4-15** Ratios of group estimates (CF-patients / healthy volunteers) for clearance and volume of distribution for different size models

| Size model | $FCYF_{CLR}$ | $FCYF_{CLNR}$ | $FCYF_{CLT}^{\#}$ | $FCYF_{V}$ |
|---|---|---|---|---|
| A) No size model | 0.883 | 0.691 | 0.728 | 0.794 |
| B) WT linear scaling | 1.04 | 0.859 | 0.895 | 0.934 |
| C) WT allometric | 0.991 | 0.820 | 0.854 | 0.915 |
| D) LBM allometric | 0.955 | 0.787 | 0.820 | 0.891 |
| E) FFM allometric | 0.944 | 0.770 | 0.804 | 0.884 |

$FCYF_{NNN}$: Ratio of group estimates for parameter NNN (group estimate for CF-patients divided by group estimate for healthy volunteers).

#: Calculated as weighted average of $FCYF_{CLR}$ and $FCYF_{CLNR}$.

**Table 3.4-16** Comparison of BSV between different size models

| Size model | $CL_R$ | $CL_{NR}$ | V1 | V2 |
|---|---|---|---|---|
| B) WT linear scaling | 0%* | 0%* | 0%* | 0%* |
| C) WT allometric | -32%° | -6% | -32% | 33% |
| D) LBM allometric | -34%° | -4% | -4% | 13% |
| E) FFM allometric | 49%° | 5% | 44% | 2% |

*: The values are (variance of test size model - variance of linear scaling by WT) / variance of linear scaling by WT. For the bootstrap estimates, the denominator was the median variance of linear scaling by WT from all 1000 bootstrap runs.

°: The lower this number, the more variability was explained by the respective size model. A negative value means that the size model reduced the between subject variance, and a positive value means that the respective size model increased the between subject variance compared to linear scaling by WT. These values mean that the BSV (variance) for renal clearance was reduced by 32% for allometric scaling by WT and by 34% for allometric scaling by $FFM_C$, as well as increased by 49% for allometric scaling by $FFM_J$, all compared to linear scaling by WT.

***MCS:*** Figure 3.4-9 shows the PTA vs. MIC profiles for an average AUC/MIC target of 160 representing eradication at the end of ciprofloxacin therapy and of 260 representing persistent eradication of *P. aeruginosa* at follow-up. CF-patients had higher PTAs than healthy volunteers for a fixed dose of 750 mg oral ciprofloxacin q12h or q8h (see Figure 3.4-9), because our CF-patients were smaller and therefore had a lower unscaled total clearance compared to our healthy volunteers. The PKPD breakpoint for oral ciprofloxacin and those targets was between 0.0625 and 0.125 mg/L in CF-patients.

We used MIC distributions for *P. aeruginosa* from four publications which had $MIC_{50}$s between 0.25 and 8 mg/L and $MIC_{90}$s between 1 and 64 mg/L. The PTA expectation values (see Figure 3.4-10) were below 40% for the AUC/MIC ≥ 160 target at a daily dose of 1500 mg oral ciprofloxacin. Even for 750 mg q8h the PTA expectation values were only 50% or below. All PTA expectation values were between 0 and 31% for the AUC/MIC ≥ 260 target.

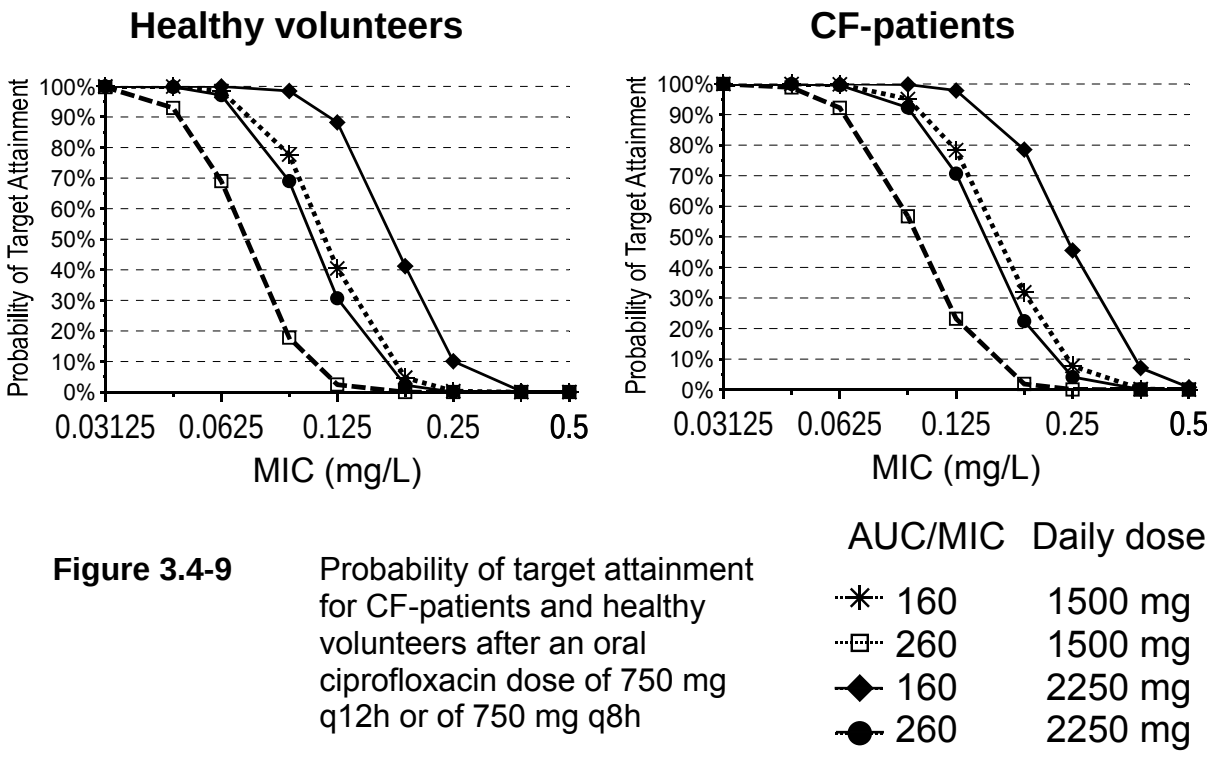


**Figure 3.4-9** Probability of target attainment for CF-patients and healthy volunteers after an oral ciprofloxacin dose of 750 mg q12h or of 750 mg q8h

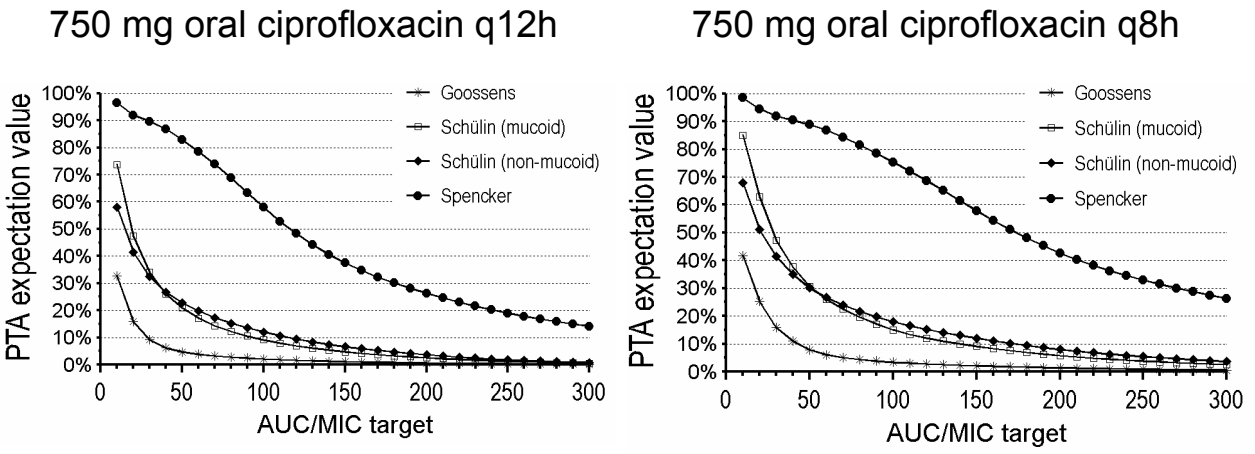


**Figure 3.4-10** PTA expectation values in CF-patients for four MIC distributions of *P. aeruginosa* isolates from CF-patients of different studies

### 3.4.3.5 Discussion

Most CF-patients develop chronic lung infection by *P. aeruginosa* which is usually preceded by a period of intermittent colonization (228). Eradication of *P. aeruginosa* is virtually impossible, once a chronic lung infection is established. Although impressive medical advances improved the median life-expectancy of CF-patients to 33.4 years in the US in 2001 (88), the survival after onset of chronic *P. aeruginosa* infection is stagnating (229). However, chronic *P. aeruginosa* infection can be significantly delayed or prevented by early aggressive therapy (139-141, 192). As chronic *P. aeruginosa* infection is a major determinant of mortality in CF-patients, identification of efficacious dosage regimens to eradicate *P. aeruginosa* during initial infection is vital.

Fluoroquinolones are the only oral treatment option against *P. aeruginosa*. Most of the experience is available for ciprofloxacin which is an appealing treatment option due to its activity against three major pathogens in CF-patients *P. aeruginosa*, *S. aureus*, and *H. influenzae*. There are only limited data on the effectiveness of ciprofloxacin monotherapy against *P. aeruginosa*. A significant clinical improvement is observed in almost all

adult CF-patients with chronic lung infection (50, 155, 188, 227, 270, 279, 422, 443, 445, 448, 455) as well as in children with CF and acute pulmonary exacerbation associated with *P. aeruginosa* infection (77, 412). However, several authors find no correlation between clinical improvement and bacteriological eradication (279, 443). Almost all children with infection by *P. aeruginosa* showed clinical improvement in those studies (77, 412), but the bacterial eradication rate at follow-up was only 13% and 15%. The authors concluded no direct correlation between bacterial eradication and clinical outcome, whereas a predictive relationship between bacterial susceptibility and microbiological outcome was found for beta-lactams in CF-patients (144).

We intended to investigate this 'lack' of correlation between drug exposure (PK) combined with bacterial susceptibility (PD) and the bacteriological outcome. We are not aware of any established PKPD target for eradication of *P. aeruginosa* in children or adults with CF. As these infections are difficult to eradicate, it is likely that PKPD targets from other patients do not apply to this situation. We used the effectiveness data from Richard et al. (412) and Church et al. (77) in children with CF (age: 5-17 yrs) to back-engineer the AUC/MIC target for ciprofloxacin which might predict persistent *P. aeruginosa* eradication at follow-up of young CF-patients with acute pulmonary exacerbation associated with *P. aeruginosa* infection. We used this back-engineered PKPD target in our MCS. We estimated the population PK in adult CF-patients and healthy volunteers and combined our patient specific PK parameters with MIC distributions for *P. aeruginosa* in CF-patients. This allowed us to estimate, if high-dose oral ciprofloxacin has a sufficient probability of successful treatment for empiric therapy.

Several authors studied the PK of ciprofloxacin in adult CF-patients and included a healthy volunteer control group. The reported average renal clearances range between 14.3 and 28.4 L/h in CF-patients (coefficients of variation between 29 and 49%) and between 13.9 and 23.7 L/h in the healthy volunteer control groups (coefficients of variation between 18 and 52%) (75, 98, 280). We observed renal clearances of 12.7 [7.04 - 22.0] L/h in CF-patients (median [range]) and 14.5 [12.0 - 19.0] L/h in healthy volunteers which was at the lower end of the range reported by other authors. The

amount of ciprofloxacin recovered unchanged in urine after an oral dose of ciprofloxacin is 34 ± 13% in CF-patients and 41 ± 14% in healthy volunteers (98). Christensson et al. (75) find lower values of 31 ± 8% in CF-patients and 23 ± 4% in healthy volunteers. We recovered 23.2% [13.6 - 27.5%] (median [range]) unchanged ciprofloxacin in urine of CF-patients and 19.1% [14.0 - 26.5%] in healthy volunteers. These values are at the lower end of those reported by Christensson et al. (75).

Apparent total clearances (CL/F) between 27 and 51 L/h with coefficients of variation between 9 and 37% were reported in CF-patients after oral administration (75, 98, 280, 403). We found an apparent total clearance of 54.5 [27.8 - 93.6] L/h in our CF-patients which was at the upper end of the range reported by other authors. The average extent of oral absorption (F) of ciprofloxacin has been reported to vary between 62 and 80% in CF-patients (75, 98, 436) with between subject coefficients of variation of up to 30% (98). Both our low urinary recovery and our high CL/F indicated that the extent of absorption in our study was probably at the lower end of this range.

The average terminal half-life of ciprofloxacin in adult CF-patients ranges from 2.6 to 4.8 h in CF-patients and from 3.1 to 5.2 h in the healthy volunteer control groups (75, 98, 280, 403, 482). Our median terminal half-life of 4.32 h in CF-patients and of 3.76 h in healthy volunteers was within the ranges reported in literature. Some authors (98, 280) reported a slower rate of absorption in CF-patients who were taking pancreatic enzymes as co-medication compared to healthy volunteers. As our CF-patients abstained from pancreatic enzymes, this could have caused the rate of absorption to be similar in our CF-patients and healthy volunteers, although the effect of pancreatic enzymes on the absorption of ciprofloxacin is small (302, 403).

When the PK of CF-patients and healthy volunteers is to be compared, it may be important to adequately account for body size and body composition. Our CF-patients had a 24% lower WT, a 14% lower $FFM_C$, and an 11% lower $FFM_J$ compared to our healthy volunteers (see Table 3.4-12). We used population PK to account for the difference in body size and body

composition. Our final population PK model had a highly sufficient predictive performance for the plasma and urine profiles (see Figure 3.4-8).

In the absence of a size descriptor (size model A, Table 3.4-15), CF-patients had a lower renal (12%), nonrenal (31%), and total clearance (27%) as well as a 21% lower apparent volume of distribution. Size model B to E indicated a ratio of 0.77 to 1.04 for the size adjusted clearance and volume of distribution between CF-patients and healthy volunteers (see Table 3.4-15). None of those ratios was significantly different from 1.0. This was in agreement with the results from other authors (98, 280, 403) who report comparable renal and total clearances in CF-patients and healthy volunteers after size adjustment. Allometric scaling by WT or $FFM_C$ reduced the unexplained BSV in renal clearance by about 33% compared to linear scaling by WT (see Table 3.4-16), but this reduction was not statistically significant.

Rajagopalan et al. (398) used an allometric size model to scale the PK parameters of ciprofloxacin in children. The children in their study weighed only about half as much as normal healthy volunteers. With those datasets allometric scaling often is superior to linear scaling by body size (193). We used a population PK model similar to the model from Rajagopalan et al. (398) to link the PK in children with CF to the expected MIC distribution. We simulated the expected AUCs in the patient population of Richard et al. (412) and Church et al. (77) according to the demographic data of their patients via MCS. Those simulated AUCs were combined with the expected susceptibility of *P. aeruginosa* in CF-patients at the time of these studies.

It is important to point out that this approach has limitations, because we neither had the individual MICs nor the individual PK data in the patients from Richard et al. (412) and Church et al. (77). For eradication of *P. aeruginosa* at the end of therapy in children with CF, we found a wide range of AUC/MIC targets of 77-215 for the study by Richard et al. (412) and of 56-295 for the study by Church et al. (77). The respective ranges of AUC/MIC targets for persistent *P. aeruginosa* eradication at follow-up were 125-340 (Richard study) and 108-465 (Church study). We subsequently used average AUC/MIC targets of about 160 for *P. aeruginosa* eradication at end of therapy and of about 260 for persistent eradication at follow-up in our MCS.

Even though those average targets had large confidence intervals, we could still draw meaningful conclusions in our MCS. For three of the four MIC distributions used in our MCS, we found PTA expectation values of 30% and below for all targets above AUC/MIC ≥ 50 (see Figure 3.4-10). As shown above, our back-engineered AUC/MIC targets were far above 50, especially for persistent eradication at follow-up. Therefore, high-dose oral ciprofloxacin monotherapy is most likely inappropriate for bacterial eradication of *P. aeruginosa* in empiric therapy of CF-patients.

Even 750 mg oral ciprofloxacin q8h only achieved robust PTAs for MICs of 0.06 mg/L and below (see Figure 3.4-9). Therefore, oral high dose monotherapy with ciprofloxacin to eradicate *P. aeruginosa* might be considered, if MICs at or below the PKPD breakpoint of 0.06 mg/L are assured in a CF-patient prior to initiation of therapy. Montgomery et al. (327) identified a PKPD breakpoint of <0.5 mg/L for susceptibility of *P. aeruginosa* for intravenous ciprofloxacin therapy in CF-patients. Our PKPD breakpoint was in agreement to the breakpoint of Montgomery et al. (327), since Montgomery et al. studied intravenous ciprofloxacin with a lower BSV in AUC and since they used a lower AUC/MIC target of 125 determined in patients without CF (137). It should be noted that the breakpoint of ≤1 mg/L for susceptibility of *P. aeruginosa* and ciprofloxacin specified by national organizations such as the CLSI (352), BSAC (350), and DIN (104) is much higher than the PKPD breakpoint in our CF-patients.

As the PK was similar in our CF-patients compared to healthy volunteers, the primary reason why our PKPD breakpoint was much lower than the standard susceptibility breakpoint is the higher PKPD target required. CF-patients with initial infection by *P. aeruginosa* require a high AUC/MIC to eradicate ciprofloxacin persistently. In contrast, the PKPD target for clinical improvement of CF-patients is probably much lower than the target for persistent eradication. The clinical studies on ciprofloxacin monotherapy in CF-patients report a clinical improvement in almost all CF-patients with lung infection by *P. aeruginosa* (50, 77, 155, 188, 227, 270, 279, 412, 422, 443, 445, 448, 455). The PKPD target for bacterial eradication is likely to increase

between initial and chronic lung infection by *P. aeruginosa* and future studies are required to identify this PKPD target in CF-patients more precisely.

As ciprofloxacin monotherapy had low PTA expectation values, combination chemotherapy against *P. aeruginosa* should be highly preferred to eradicate *P. aeruginosa* from the lungs of CF-patients. Although there are some reports (48, 130, 429, 431) on *in vitro* synergy of ciprofloxacin with other antibiotics against *P. aeruginosa* and other problematic pathogens in CF-patients, more randomized clinical trials on the optimal combination therapy to eradicate *P. aeruginosa* are urgently needed (80, 165).

In conclusion we found a similar size adjusted average clearance and volume of distribution in CF-patients relative to healthy volunteers (range of ratios: 77-104%). Those ratios between CF-patients and healthy volunteers were not significantly different from 100%. Allometric scaling by WT or $FFM_C$ reduced the unexplained BSV in renal clearance by about 33% compared to linear scaling by WT ($p>0.05$). Although CF-patients had similar size adjusted PK parameters compared to healthy volunteers, CF-patients require higher doses than “normal” patients, because the PKPD target for persistent eradication of *P. aeruginosa* in lung infection of children with CF was high. By back-engineering, we found that an AUC/MIC of about 260 was required for persistent eradication in these patients. High dose (2,250 mg/day) monotherapy of oral ciprofloxacin achieved robust PTAs only for MICs of 0.06 mg/L and below for this target. The PTA expectation values were $\leq$31% for an AUC/MIC target of 260 for MIC distributions of *P. aeruginosa* from different CF-centers. Therefore, high dose oral ciprofloxacin monotherapy is not warranted for empiric treatment to eradicate *P. aeruginosa* from CF-patients and should only be initiated after an MIC of 0.06 mg/L or less has been assured. Otherwise, combination therapy should be preferred. Future studies to assess the effectiveness of ciprofloxacin combination therapy and to identify the associated PKPD target in CF-patients to eradicate *P. aeruginosa* are warranted.

### 3.4.4 Population pharmacokinetics and pharmacodynamics of fleroxacin

#### 3.4.4.1 Chemical structure of fleroxacin

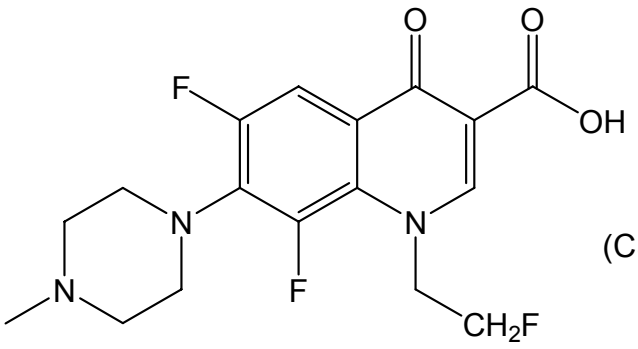


($C_{17}H_{18}F_3N_3O_3$, Mol. Wt.: 369.34)

**Chemical structure 3.4-4** Fleroxacin

Fleroxacin is currently only marketed in Japan and has been discontinued or is no longer actively marketed in several countries including Germany. However, fleroxacin is an appealing probe drug for the oral absorption and elimination in CF-patients.

#### 3.4.4.2 Fleroxacin as a probe drug

Reliable oral antibiotic therapy is very important for CF-patients to avoid excessive use of intravenous antibiotics. However, CF-patients often have pathophysiological changes of the GI tract which may interfere with the oral absorption. Oral treatment against *P. aeruginosa* is especially appealing for CF-patients, because about 30% of children aged 0-5 years and up to 80% of adults with CF have respiratory tract infections by *P. aeruginosa* (88).

Fluoroquinolones are the only oral treatment option against this pathogen. Some authors compared the bioavailability of ciprofloxacin in CF-patients and healthy volunteers by NCA or the STS method. Christensson et al. (75) find an increased extent of ciprofloxacin absorption in CF-patients compared to healthy volunteers, whereas Davis et al. (98) report a similar

extent of absorption. A slower rate of absorption has been reported for ciprofloxacin and fleroxacin by several groups (98, 280, 325, 403). We are not aware of any comparison of the rate and extent of absorption of antibiotics between CF-patients and healthy volunteers by population PK based on data from the same study. It is probably important to account for body size, body composition, and disease state for this comparison.

As fleroxacin has a log n-octanol/water partition coefficient of -0.75 at pH 7.4 (562), it is more lipophilic than beta-lactams and aminoglycosides. The volume of distribution of fleroxacin exceeds total body water and thus fleroxacin distributes both into lean and adipose tissue. However, the vast majority of metabolic processes occur in lean body tissue. Therefore, it is a difficult task for a single size descriptor to adequately account for body size with regard to clearance and volume of distribution.

Population PK is the method of choice to compare the oral absorption, drug disposition, and the BSV of the former processes between CF-patients and healthy volunteers. Fleroxacin was an appealing “probe drug” for our study, because it is rapidly and virtually completely absorbed in healthy volunteers (532, 533) and distributes both into lean and adipose tissue. We used population PK to re-analyze the data from Mimeault et al. (325), since Mimeault et al. used NCA and the STS method and did not compare various body size descriptors. Our first objective was to compare the rate of fleroxacin absorption between CF-patients and healthy volunteers via population PK. As our second objective, we systematically compared several size descriptors in their ability 1) to describe the average differences between CF-patients and healthy volunteers and 2) to reduce the unexplained BSV.

#### 3.4.4.3 Methods

The general clinical and sample handling procedures, the methods for PK analysis (including NCA and population PK), and the general methods for MCS are described in chapter 2. Chapter 3.2 shows the specific methods applied for analysis of our CF-studies.

***Subjects and Drug administration:*** The details of the clinical part of this study have been described by Mimeault et al. (325). In brief, the study was a parallel group study with 13 CF-patients and 12 healthy volunteers. CF-patients were studied during an infection-free period and stopped all prophylactic antimicrobial therapy (oral and inhaled) at least 2 weeks before the study. However, CF-patients continued to receive pancreatic enzymes, multivitamins, and any other medications required because of their disease (albuterol, acetazolamide, inhaled beclomethasone, and oral as well as intramuscular contraceptives).

The median [range] age was 22 yrs [18-28] for CF-patients and 23 yrs [20-27] for healthy volunteers. Total body weight was 55 kg [31-77] for CF-patients and 74 kg [59-86] for healthy volunteers. $FFM_C$ (72, 222) was 47 kg [27-54] for CF-patients and 58 kg [49-62] for healthy volunteers. $FFM_J$ (224) was 45 kg [24-54] for CF-patients and 57 kg [49-61] for healthy volunteers. Body mass index was 20.6 $kg/m^2$ [13.7-26.7] for CF-patients and 23.5 $kg/m^2$ [19.7 - 29.9] for healthy volunteers.

Each subject received a single oral dose of 800 mg fleroxacin on day 1. Three days later, subjects received 800 mg oral fleroxacin q24h for five days. Subjects fasted overnight and received each dose with 200 mL drinking water.

***Sample collection:*** Blood samples were collected immediately before each dose and 10, 20, 30, and 45 min and 1, 2, 3, 4, 6, 8, 12, 16, 24, 36, 48, and 72 h after the first and the last dose. Samples were protected from light to prevent degradation of fleroxacin.

***Drug analysis:*** The details of the assay have been described by Mimeault et al. (325). In brief, fleroxacin was determined by a reverse-phase ion-pair HPLC with fluorescence detection. Pipemidic acid was used as internal standard. The sensitivity limit of the assay was 0.01 mg/L. The coefficient of variation from day to day was less than 4.4% and the plasma recovery was 82%. The assay was linear between 0.05 and 10 mg/L with coefficients of correlation of at least 0.999. The method was selective and no interference was observed from endogenous compounds.

**Population PK**

***Motivation for additional PK analysis:*** Mimeault et al. (325) used NCA to derive the PK parameters in CF-patients and healthy volunteers. Additionally, they used the STS approach to model the plasma concentration time profiles and reported the absorption rate constant for fleroxacin. They scaled clearance and volume of distribution linearly (exponent: 1.0) by $FFM_C$ (72, 222) (called LBM in their paper). However, their analysis did not aim at comparing various size descriptors in their ability to describe the average differences and the BSV in clearance and volume of distribution. Population PK is superior to NCA and the STS approach, as population PK directly estimates the average PK parameters as well as their BSV.

Mimeault et al. (325) found a higher extent of fleroxacin absorption at steady-state compared to single dose based on the amounts excreted into urine. They also found a decreased renal clearance at steady-state relative to single dose for healthy volunteers. Panneton et al. (372) showed that the nonrenal clearance of fleroxacin is saturable at higher concentrations and that possibly also the renal clearance is saturable to a lesser extent. We did not intend to explore these elimination mechanisms in our population PK analysis as this would have made our analysis significantly more complex. Therefore, we used only the data after the first dose to study differences in the absorption profile and to compare the clearance and volume of distribution of fleroxacin between CF-patients and healthy volunteers.

### 3.4.4.4 Results

***Structural model:*** Inclusion of a lag-time of absorption improved the predictive performance of the population PK model and improved NONMEM's objective function by about 198 points. A one compartment model with first order absorption had highly sufficient predictive performance (see Figure 3.4-11). Therefore, we chose the one compartment model as our final structural model. The estimates of our final model are shown in Table 3.4-17.

The group estimate for the absorption lag-time in CF-patients was 1.5 (1.1 - 2.2) times as long as in healthy volunteers (see Table 3.4-17). The

individual estimates for the absorption lag-time were 18 min [8.0 - 109 min] in CF-patients and 14 min [8.4 - 27 min] in healthy volunteers (median [range]). We found no trend or correlation between lag-time and any demographic variable.

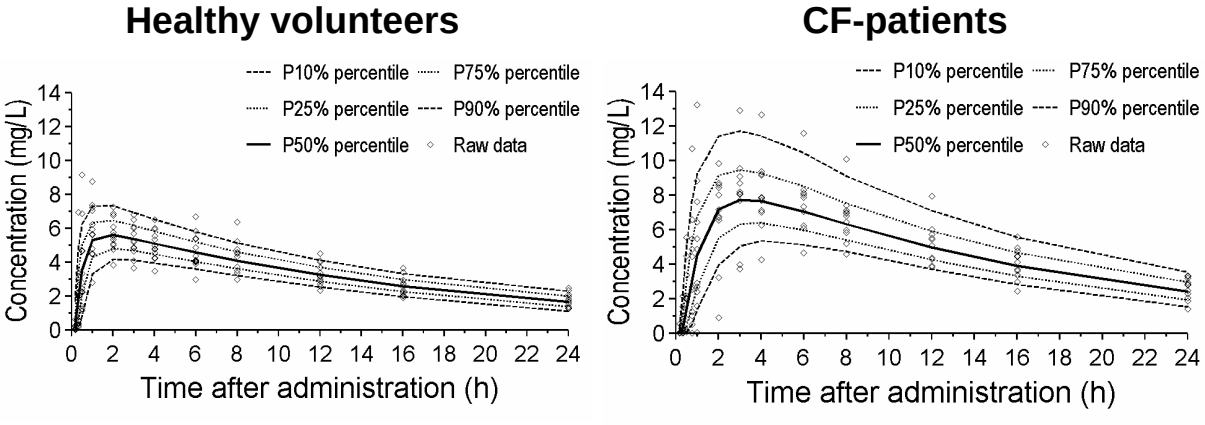


**Figure 3.4-11** VPC for the final population PK model (see Table 3.4-17).

See chapter 2.6.3 for interpretation of VPCs.

***Rate of absorption:*** CF-patients had a slower rate of absorption than healthy volunteers. The group estimate for the absorption half-life in CF-patients was 3.2 (1.9 - 5.1) times [median (90% confidence interval)] as long as in healthy volunteers (see also Table 3.4-17). The individual absorption half-lives were 39 min [9.4 - 117 min] in CF-patients and of 8.8 min [2.5 - 44 min] in healthy volunteers (median [range]). The CF-patient with the longest absorption half-life of 117 min had a BMI of 13.7 kg/m$^2$. However, there was no correlation between absorption half-life and BMI. Body surface area explained 62% of the variability in the absorption half-time ($p<0.01$ from ANOVA).

***Disposition:*** We distinguished the size models 1) by their estimates for the disease specific scale factors FCYF and 2) by their reduction of unexplained BSV in clearance and volume of distribution relative to linear scaling by WT. In absence of any size descriptor, CF-patients had a 30% lower total clearance and a 37% lower volume of distribution at steady-state (see Table 3.4-18, bootstrap results for size model A).

**Table 3.4-17** PK parameters for the allometric size model based on $FFM_J$

| Parameter | Unit | Estimate | | Median (90% confidence interval) from non-parametric bootstrap[&] | |
|---|---|---|---|---|---|
| | | CF-patients | healthy volunteers | CF-patients | healthy volunteers |
| $CL_{tot}/F$ | L $h^{-1}$ | 6.13* | 6.79* | 6.14 (5.69 - 6.58)* | 6.77 (6.10 - 7.52)* |
| BSV($CL_{tot}/F$)° | | 17.5% | | 17% (12 - 21%) | |
| V/F | L | 106* | 120* | 106 (96.4 - 116)* | 120 (109 - 131)* |
| BSV(V/F)° | | 17.5% | | 17% (12 - 20%) | |
| TLAG | min | 22.8 | 14.7 | 22.3 (16.3 - 30.0) | 14.5 (11.7 - 16.8) |
| BSV(TLAG)° | | 56.1% | | 53% (34 - 66%) | |
| TABS | min | 34.9 | 10.5 | 34.7 (24.2 - 49.4) | 10.6 (8.14 - 16.6) |
| BSV(TABS)° | | 82.0% | | 77% (56 - 94%) | |
| $CV_C$ | | 10.1% | | 10% (8.6 - 12%) | |
| $SD_C$ | mg/L | 0.164 | | 0.15 (0.088 - 0.20) | |

°: Apparent coefficient of variation for the BSV.

&: Medians and non-parametric 90% confidence intervals (5% - 95% percentile) derived from 1,000 non-parametric bootstrap runs.

*: Group estimate for a subject with standard $FFM_J$ = 53 kg.

See also chapter 2.6.2 for explanation of model parameters.

Our CF-patients had an approximately 25% lower median WT, $FFM_C$, and $FFM_J$ compared to our healthy volunteers. The size adjusted total clearance was estimated to be 5-13% lower and size adjusted volume of distribution was estimated to be 11-17% lower in CF-patients (see Table 3.4-18) by size models B to E. Allometric scaling by $FFM_C$ or $FFM_J$ reduced the unexplained BSV in clearance and volume of distribution by 23-30% relative to linear scaling by WT (see Table 3.4-19). The reduction of BSV was significant for total clearance (size model D) as well as for volume of distribution (size model E), since those 90% non-parametric confidence intervals (see Table 3.4-19) did not include 0%.

**Table 3.4-18** Ratios of group estimates (CF-patients / healthy volunteers) for clearance and volume of distribution for different size models

| Size model | Estimates from original dataset | | Median (90% confidence intervals) from 1,000 bootstrap runs[#] | |
|---|---|---|---|---|
| | $FCYF_{CLT}$ | $FCYF_V$ | $FCYF_{CLT}$ | $FCYF_V$ |
| A) No size model | 0.715 | 0.603 | 0.700 (0.614 - 0.805) | 0.627 (0.532 - 0.742) |
| B) WT linear scaling | 0.945 | 0.843 | 0.945 (0.833 - 1.070) | 0.838 (0.743 - 0.959) |
| C) WT allometric | 0.882 | 0.840 | 0.874 (0.754 - 1.010) | 0.842 (0.718 - 1.000) |
| D) $FFM_C$ allometric | 0.867 | 0.833 | 0.868 (0.762 - 0.989) | 0.832 (0.722 - 0.971) |
| E) $FFM_J$ allometric | 0.903 | 0.880 | 0.904 (0.798 - 1.030) | 0.885 (0.771 - 1.019) |

$FCYF_{CLT}$: Ratio of group estimates for total clearance in CF-patients divided by total clearance in healthy volunteers.

$FCYF_V$: Ratio of group estimates for volume of distribution at steady-state in CF-patients divided by volume of distribution at steady-state in healthy volunteers.

[#]: Medians and non-parametric 90% confidence intervals (5% - 95% percentile) derived from 1,000 non-parametric bootstrap runs.

**Table 3.4-19** Relative BSV (variances) relative to linear scaling by WT

| Size model | Estimates from original dataset | | Median (90% confidence intervals) from 1,000 bootstrap runs[#] | |
|---|---|---|---|---|
| | CL | V | CL | V |
| B) WT linear scaling | 0%* | 0%* | 0% (0 to 0%) | 0% (0 to 0%) |
| C) WT allometric | -16%° | 1% | -17% (-46 to 6%) | 0% (-24 to 27%) |
| D) $FFM_C$ allometric | -29%° | -26% | **-30% (-63 to -2%)** | -26% (-54 to 1%) |
| E) $FFM_J$ allometric | -21%° | -30% | -23% (-58 to 7%) | **-30% (-58 to -4%)** |

*: The values are (variance of test size model - variance of linear scaling by WT) / variance of linear scaling by WT. For the bootstrap estimates, the denominator was the median variance of linear scaling by WT from all 1,000 bootstrap runs.

°: The lower this number, the more variability was explained by the respective size model. These values mean that the BSV (variance) for total clearance was reduced by 16% for allometric scaling by WT, by 29% for allometric scaling by $FFM_C$, and by 21% for allometric scaling by $FFM_J$, all compared to linear scaling by WT.

[#]: Medians and non-parametric 90% confidence intervals (5% - 95% percentile) derived from 1,000 non-parametric bootstrap runs.

#### 3.4.4.5 Discussion

The oral route of treatment is very important for antibiotic therapy of CF-patients. There are pathophysiological changes in the GI tract of CF-patients which may potentially interfere with the oral absorption. Gastric acid hypersecretion, injury of the proximal small intestinal mucosa (31, 81), and bile acid malabsorption (135) commonly occur in CF-patients. However, there is debate about the influence of these changes on the rate and extent of oral absorption. Most authors (98, 280, 325, 403) find a comparable extent of absorption in CF-patients and healthy volunteers and a longer absorption half-life in CF-patients. Importantly, the influence of these alterations in rate or extent of absorption (including their BSV) in CF-patients on the PKPD profile of antibiotics has not yet been systematically studied by MCS.

Rajagopalan et al. (398) used population PK and estimated a 61% slower rate and a similar extent of absorption for ciprofloxacin in children with CF compared to other pediatric patients. However, they combined data from different pediatric studies and their comparison is a between study comparison. Standardization of the clinical procedures and similar clinical study conditions for CF-patients and healthy volunteers might be crucial, if the oral absorption is to be compared. Although intake of pancreatic enzymes affected the rate of ciprofloxacin absorption only to a small extent (302, 403), this factor might affect the rate and extent of oral absorption in CF-patients.

We used fleroxacin as a “probe drug” to study the absorption and disposition of an oral quinolone. The original analysis was prepared by Mimeault et al. (325) using NCA as well as the STS method. Modern computational power allows one to analyze these data by population PK and to derive confidence intervals of the PK parameters including their BSV terms via non-parametric bootstrapping. Such an analysis was not possible at the time of the original analysis. Fleroxacin is rapidly and virtually completely absorbed in healthy volunteers. In our re-analysis, we intended to compare the rate of fleroxacin absorption between CF-patients and healthy volunteers. Additionally, we wished to find the most appropriate size descriptor for clearance and volume of distribution.

Our estimates of the PK parameters for healthy volunteers were in agreement with the results from other authors (255, 463, 481, 532, 533). We are not aware of any studies on the PK of fleroxacin in CF-patients with exception of the original study by Mimeault et al. (325). Our population PK analysis showed a significantly slower rate of absorption in CF-patients relative to healthy volunteers. The group estimate for the absorption half-life in CF-patients was 3.2 (1.9 - 5.1) times [median (90% confidence interval)] as long as in healthy volunteers (see also Table 3.4-17). This estimate was in good agreement to the 2.6 times as long absorption half-life in CF-patients relative to other patients reported by Rajagopalan et al. (398) for ciprofloxacin.

Our median [range] for the individual absorption half-lives was 39 min [9.4 - 117 min] in CF-patients and 8.8 min [2.5 - 44 min] in healthy volunteers. Although the CF-patient with the longest absorption half-life of 117 min had a BMI of 13.7 $kg/m^2$, there was no correlation between absorption half-time and BMI. Intake of pancreatic enzymes could have been a possible factor contributing to the longer absorption half-life in CF-patients, since all except one of our CF-patients took pancreatic enzymes as co-medication. The group estimate for the absorption lag-time in CF-patients was 1.5 (1.1 - 2.2) times as long as in healthy volunteers (see also Table 3.4-17). The median [range] of the individual lag-times was 18 min [8.0 - 109 min] in CF-patients and 14 min [8.4 - 27 min] in healthy volunteers. Lag-time did not correlate with any of the demographic variables. The amounts of fleroxacin excreted unchanged in urine reported by Mimeault et al. (325) show that the extent of absorption was similar between both subject groups, although we found a significantly longer absorption half-life and lag-time in CF-patients relative to healthy volunteers. However, our sample size was very low for an empirical covariate analysis.

Our second objective was to compare the ability of various size models to describe the differences in average clearance and volume of distribution as well as to reduce the unexplained BSV in those PK parameters. Our CF-patients had a 30% lower unscaled total clearance and a 37% lower unscaled volume of distribution at steady-state (see Table 3.4-18, size model A), probably because they were smaller than our healthy volunteers. The median WT, $FFM_C$, and $FFM_J$ was approximately 25% lower in our CF-patients

relative to our healthy volunteers. As our healthy volunteers were relatively lean, healthy volunteers and CF-patients had a similar body composition in our study. After accounting for body size, total clearance was estimated to be 5-13% lower and volume of distribution was estimated to be 11-17% lower in CF-patients (see Table 3.4-18, size models B to E). There were no pronounced differences between these four studied size models in their ability to describe the difference in average clearance and volume of distribution between CF-patients and healthy volunteers. All four size models had estimates close to 1.0 and most of the 90% non-parametric confidence intervals included 1.0. Allometric scaling by $FFM_C$ or $FFM_J$ reduced the unexplained BSV in clearance and volume of distribution by 23-30% relative to linear scaling by WT (see Table 3.4-19). This reduction in unexplained BSV was significant for $FFM_C$ and total clearance as well as for $FFM_J$ and volume of distribution at steady-state, since the 90% non-parametric confidence intervals for those comparisons did not include 0%. Therefore, target concentrations can be achieved more precisely by use of an allometric size model based on $FFM_C$ or $FFM_J$ in empiric therapy.

In conclusion, the half-life of absorption in CF-patients was 3.2 (1.9 - 5.1) times as long as in healthy volunteers and lag-time of absorption in CF-patients was 1.5 (1.1 - 2.2) times as long as in healthy volunteers [point estimate (90% confidence interval)]. However, the extent of absorption was comparable in both subject groups. After accounting for body size by WT, $FFM_C$, or $FFM_J$, the size adjusted average total clearance was 5-13% lower and the size adjusted average volume of distribution was 11-17% smaller in CF-patients relative to healthy volunteers. Allometric scaling by $FFM_C$ or $FFM_J$ reduced the unexplained BSV in clearance and volume of distribution by 23-30% relative to linear scaling by WT, probably because $FFM_C$ and $FFM_J$ account for body composition whereas WT does not. Further well controlled studies on the absorption of other oral antibiotics are required to compare the rate and extent of absorption between CF-patients and healthy volunteers. Large clinical studies are required to investigate, whether $FFM_C$ or $FFM_J$ are superior size descriptors compared to WT for dose selection in CF-patients.

### 3.4.5 Population pharmacokinetics and pharmacodynamics of pefloxacin

#### 3.4.5.1 Chemical structure of pefloxacin

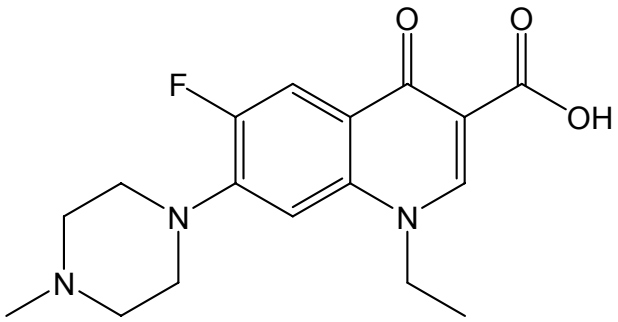


($C_{17}H_{20}FN_3O_3$, Mol. Wt.: 333.36)

**Chemical structure 3.4-5** Pefloxacin

Pefloxacin is currently marketed only in some countries like Brazil, the Czech Republic, France, Greece, Hungary, India, Italy, Malaysia, Mexico, Portugal, and Russia. It has been discontinued or is no longer actively marketed in several countries including Germany. However, pefloxacin is an appealing probe drug for the oral absorption and metabolism in CF-patients.

#### 3.4.5.2 Pefloxacin as a probe drug

Pathophysiological changes in the GI tract of CF-patients may complicate the use of oral antibiotics in this patient group. There are only limited data about the influence of these pathophysiological changes on the rate and extent of absorption for quinolones. Quinolones are especially important for CF-patients, as they are the only orally available antibiotics against *P. aeruginosa*.

As pefloxacin has a log octanol/water partition coefficient of 0.21 at pH 7.4 (562), pefloxacin is more lipophilic than beta-lactams and aminoglycosides. Pefloxacin is completely and rapidly absorbed in healthy volunteers, is extensively metabolized, and has a volume of distribution

exceeding total body water. These PK characteristics make pefloxacin an appealing “probe drug” to compare the rate and extent of oral absorption as well as renal and nonrenal clearance between CF-patients and healthy volunteers. Therefore, our first objective was to compare the rate and extent of absorption of pefloxacin between CF-patients and healthy volunteers. Our second objective was to compare clearance and volume of distribution between both subject groups to assess, whether $FFM_C$ or $FFM_J$ are better descriptors of body size than WT. As our third objective, we compared the amounts of two metabolites, norfloxacin and pefloxacin N-oxide, recovered in urine between both subject groups.

#### 3.4.5.3 Methods

The general clinical and sample handling procedures, the methods for PK analysis (including NCA and population PK), and the general methods for MCS are described in chapter 2. Chapter 3.2 shows the specific methods applied for analysis of our CF-studies.

***Subjects:*** A total of 18 Caucasian volunteers (eight CF-patients and ten healthy volunteers) participated in the study. Table 3.4-20 shows the demographic data.

***Study design and drug administration:*** The study was a randomized, single dose, single-center, open, two-way crossover. Subjects received 400 mg pefloxacin as 30 min intravenous infusion in study period I and 400 mg oral pefloxacin in study period II, or vice versa. The study periods were separated by a washout period of 10 days. For the oral administration, the subjects took pefloxacin with 150 mL low-carbonated, calcium-poor mineral water at room temperature. CF-patients abstained from taking pancreatic enzymes as supplement therapy from at least 10 h before until 4 h after pefloxacin dose. For the intravenous infusion, 400 mg pefloxacin were dissolved in 300 mL glucose solution (5%) and this mixture was shaken thoroughly for 2-3 minutes. All infusions were administered with exactly adjustable motor syringes.

**Table 3.4-20** Demographic data of the pefloxacin study (median [range])

| | **CF-patients** | **Healthy volunteers** |
|---|---|---|
| Number of subjects (males / females) | 8 (2 / 6) | 10 (5 / 5) |
| Age (yr) | 19 [17 - 24] | 24 [18 - 27] |
| Height (cm) | 166 [158 - 175] | 174 [168 - 191] |
| Total body weight (kg) | 46.3 [35.5 - 63.5] | 77.5 [55.0 - 82.0] |
| Fat-free mass° (kg) | 38.0 [31.0 - 47.1] | 55.6 [43.0 - 64.5] |
| Fat-free mass# (kg) | 33.3 [27.3 - 46.4] | 52.1 [37.7 - 64.0] |
| Body mass index (kg $m^{-2}$) | 17.6 [13.4 - 22.2] | 21.6 [19.5 - 27.3] |

°: Calculated by the formula of Cheymol and James (72, 222).

#: Calculated by the formula of Janmahasatian et al. (224).

***Blood and urine sampling:*** For intravenous treatment, blood samples were drawn immediately before start of the infusion (0 min) and at 10, 20, and 30 min post start of infusion as well as at 5, 10, 20, 30, 45, 60, 90 min and 2, 2.5, 3, 4, 5, 6, 8, 10, 12, 16, 24, 30, 36, and 48 h post end of infusion. For oral treatment, blood samples were drawn immediately before administration (0 min) and at 15, 30, 45, 60, 90 min and 2, 3, 4, 6, 8, 10, 12, 16, 24, 30, 36, and 48 h post administration. Urine was collected from 0 to 1, 1 to 2, 2 to 3, 3 to 4, 4 to 6, 6 to 8, 8 to 12, 12 to 16, 16 to 24, 24 to 36, and 36 to 48 h post dose.

***Drug analysis:*** Plasma samples were analyzed for unchanged pefloxacin and urine samples were analyzed for pefloxacin and its main metabolites, pefloxacin N-oxide and norfloxacin, by reversed-phase HPLC assays which have been described previously (309).

We used a mobile phase consisting of 50% methanol and 50% 0.1 M phosphate buffer adjusted to pH 4.9 for determination of pefloxacin in plasma. A Nucleosil C18 5-µm reversed-phase column heated to 40°C (Bischoff GmbH, Leonberg, Germany) was used as the stationary phase. Plasma samples were deproteinized by the addition of acetonitrile (1:2), and the supernatant was injected into the mobile phase (flow rate 1.2 mL/min). The mobile phase consisted of 24.1% methanol, 2.6% acetonitrile, and 73.3% 0.1

M phosphate buffer adjusted to pH 5.75 for determination of the levels of pefloxacin and its metabolites in urine. A C18 µ-Bondapak reversed-phase column (Waters Association, Eschborn, Germany) was used for this assay.

Urine samples were diluted with bidistilled water and were injected into the mobile phase at a flow rate of 1.0 ml/min. The fluorescence of the mobile phase was monitored by a Perkin Elmer 650-10 LC Fluorescence Spectrometer (Perkin-Elmer, Überlingen, Germany) to detect pefloxacin, pefloxacin N-oxide, and norfloxacin. The excitation wavelength was 275 nm, and the emission wavelength was 415 nm. The assay was linear between 0.078 and 20 mg/L for pefloxacin in plasma, 0.78 and 100 mg/L for pefloxacin in urine and between 3.13 and 200 mg/L for the metabolites in urine. The coefficients of correlation were greater than 0.999.

The within-day precision (coefficient of variation) was 3.2% for 2.5 mg/L pefloxacin in plasma, 6.9% for 0.63 mg/L pefloxacin in plasma, 3.1% for 100 mg/L pefloxacin in urine, and 5.1% for 12.5 mg/L pefloxacin in urine. The between-day precision was 2.7% for 3.8 mg/L pefloxacin in plasma, 3.4% for 1.5 mg/L pefloxacin in plasma, 3.8% for 40.2 mg/L pefloxacin in urine, and 7.3% for 8.3 mg/L pefloxacin in urine.

***Population PK:*** We considered one, two, and three compartment disposition models. The drug input for the oral absorption was described as a first order process from the gut into the central compartment (with or without lag-time) and as a zero order input into the central compartment for the intravenous infusion. As we had data after an oral and after an intravenous administration for each subject, we could estimate the extent of oral absorption (F) and its BSV using the intravenous dose as reference.

### 3.4.5.4 Results

***NCA:*** Figure 3.4-12 shows the average plasma concentrations of CF-patients and healthy volunteers after an oral and intravenous dose. Table 3.4-21 lists the results of the NCA. These parameters are not scaled by any size descriptor. CF-patients had a 19% higher unscaled renal clearance and a 28% lower nonrenal clearance than healthy volunteers. As renal elimination of

unchanged pefloxacin only accounted for about 6.5 to 13% of the total elimination (see Table 3.4-21), unscaled total clearance was 25% lower in CF-patients. CF-patients had a similar volume of distribution at steady-state, and a similar to slightly longer terminal half-life and mean residence time compared to healthy volunteers.

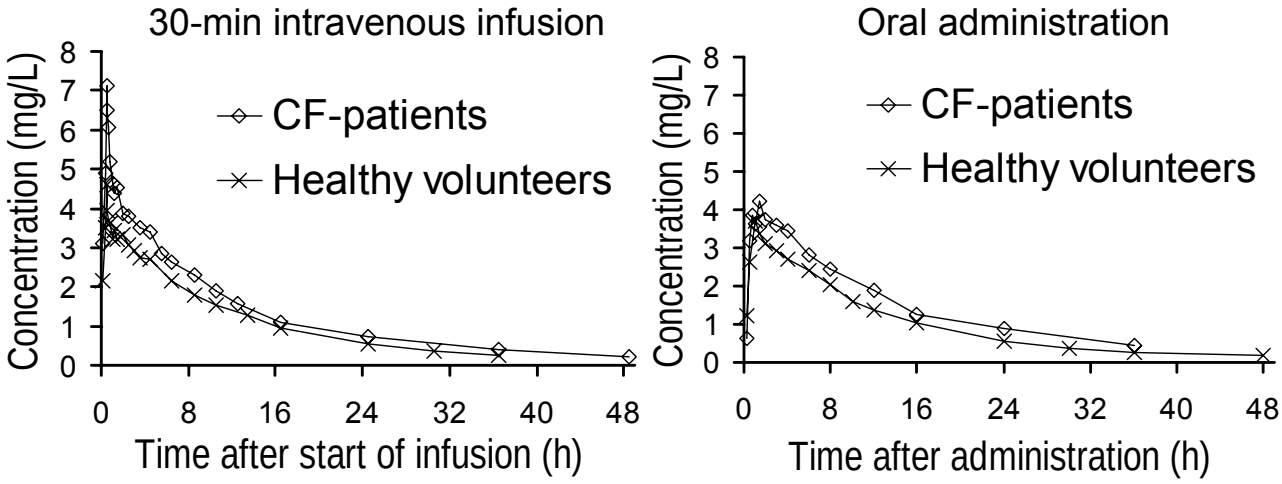


**Figure 3.4-12** Average plasma concentrations of pefloxacin for CF-patients and healthy volunteers after a single dose of 400 mg pefloxacin

CF-patients had higher peak concentrations than healthy volunteers. The times to peak concentrations as well as their BSV were comparable between both subject groups. The area under the plasma concentration time curve was similar for oral and intravenous treatment within each subject group indicating a virtually complete extent of absorption. The average amount of unchanged pefloxacin recovered in urine after oral treatment was about 14% lower relative to intravenous treatment (see Table 3.4-21) which could be explained by first-pass metabolism of pefloxacin. CF-patients excreted about 74% more pefloxacin unchanged in urine relative to healthy volunteers (see Table 3.4-21). The amount of norfloxacin and pefloxacin N-oxide recovered in urine was similar to slightly higher in CF-patients compared to healthy volunteers.

**Table 3.4-21** Unscaled PK parameters derived via NCA (median [range])

| | CF-patients | | Healthy volunteers | |
|---|---|---|---|---|
| | oral | intravenous | oral | intravenous |
| Total clearance (L/h) | 6.47 [3.50 - 10.4] | 6.47 [3.81 - 12.6] | 8.81 [4.76 - 12.6] | 8.35 [5.56 - 16.0] |
| Renal clearance (L/h) | 0.650 [0.442-0.890] | 0.796 [0.457-1.08] | 0.564 [0.426-0.870] | 0.654 [0.395-1.01] |
| Nonrenal clearance (L/h) | 5.65 [3.06 - 9.97] | 5.74 [3.23 - 11.8] | 8.32 [4.24 - 12.0] | 7.60 [5.17 - 15.0] |
| Volume of distribution at steady-state (L) | | 98.1 [82.2 - 166] | | 98.2 [80.5 - 202] |
| Time to peak concentration (h) | 1.13 [0.50 - 3.00] | 0.50 [0.50 - 0.67] | 1.50 [0.50 - 4.00] | 0.54 [0.50 - 1.50] |
| Peak concentration (mg/L) | 4.49 [3.45 - 8.94] | 7.40 [3.68 - 11.0] | 4.19 [2.68 - 5.32] | 4.76 [2.35 - 7.56] |
| Terminal half-life (L) | 11.7 [9.58 - 19.2] | 12.3 [10.6 - 20.1] | 11.7 [7.95 - 15.9] | 9.40 [6.18 - 12.4] |
| Mean residence time° (h) | 15.4 [13.3 - 25.5] | 15.4 [13.0 - 25.1] | 14.1 [10.4 - 20.1] | 13.2 [9.85 - 16.2] |
| Area under the plasma concentration time curve (mg h/L) | 61.8 [38.4 - 114] | 61.8 [31.7 - 105] | 45.4 [31.6 - 84.0] | 48.0 [25.0 - 71.9] |
| Fraction excreted as pefloxacin in urine (%) | 11.1 [4.24 - 15.6] | 13.2 [6.83 - 17.5] | 6.54 [4.73 - 10.9] | 7.44 [6.30 - 10.2] |
| Fraction excreted as norfloxacin in urine (%) | 15.9 [9.10 - 20.0] | 14.8 [8.77 - 27.1] | 15.3 [10.7 - 17.7] | 14.0 [11.6 - 22.4] |
| Fraction excreted as pefloxacin N-oxide in urine (%) | 18.3 [16.3 - 20.5] | 18.6 [15.4 - 21.7] | 17.2 [11.8 - 18.3] | 14.8 [10.3 - 17.2] |

°: Mean body residence time for oral treatment, mean residence time for intravenous treatment.

**Population PK analysis**

***Structural model:*** Inclusion of a lag-time for oral absorption improved the predictive performance of the population PK model and improved NONMEM's objective function by about 153 points. The predictive performance of the models with two and three disposition compartments was similar and highly sufficient for both models. The one-compartment model had

insufficient predictive performance. Therefore, we chose the simpler two compartment model as our final model. The VPC (see Figure 3.4-13) showed a highly sufficient predictive performance of the two-compartment model with $FFM_J$ as size descriptor for the full range of sampling times.

***Extent of absorption:*** The parameters of our final population PK model are shown in Table 3.4-22 along with the estimates of 1,000 non-parametric bootstrap replicates. The extent of absorption was 97.7% in CF-patients and 99.2% in healthy volunteers. As indicated by the bootstrap estimates and confidence intervals, the extent of absorption was not significantly different from 100% for both subject groups. The coefficient of variation for the BSV in extent of absorption was 25.8% in CF-patients and 13.5% in healthy volunteers (see Table 3.4-22). CF-patients had a 3.8 (0.91 - 11) times larger [median (90% nonparametric confidence interval)] BSV (variance) for extent of absorption than healthy volunteers, but this comparison was not statistically significant (p=0.06, one-sided test, obtained from the percentile of the bootstrap runs).

***Rate of absorption:*** The individual estimates of the population PK model (see Table 3.4-22) indicated a median [range] half-life of absorption of 12.3 min [4.1 - 109 min] in CF-patients and of 13.6 min [2.4 - 56.5 min] in healthy volunteers. One of the eight CF-patients, who had the lowest BMI of 13.4 $kg/m^2$ in our study, had an absorption half-life of 109 min. The other seven CF-patients had absorption half-lives within the range of the values seen for healthy volunteers. There was no trend in a scatterplot of the absorption half-life vs. BMI. The lag-time of absorption and its BSV were virtually identical in both subject groups with 12.1 min [11.4 - 14.6 min] in CF-patients and 12.1 min [11.0 - 14.7 min] in healthy volunteers.

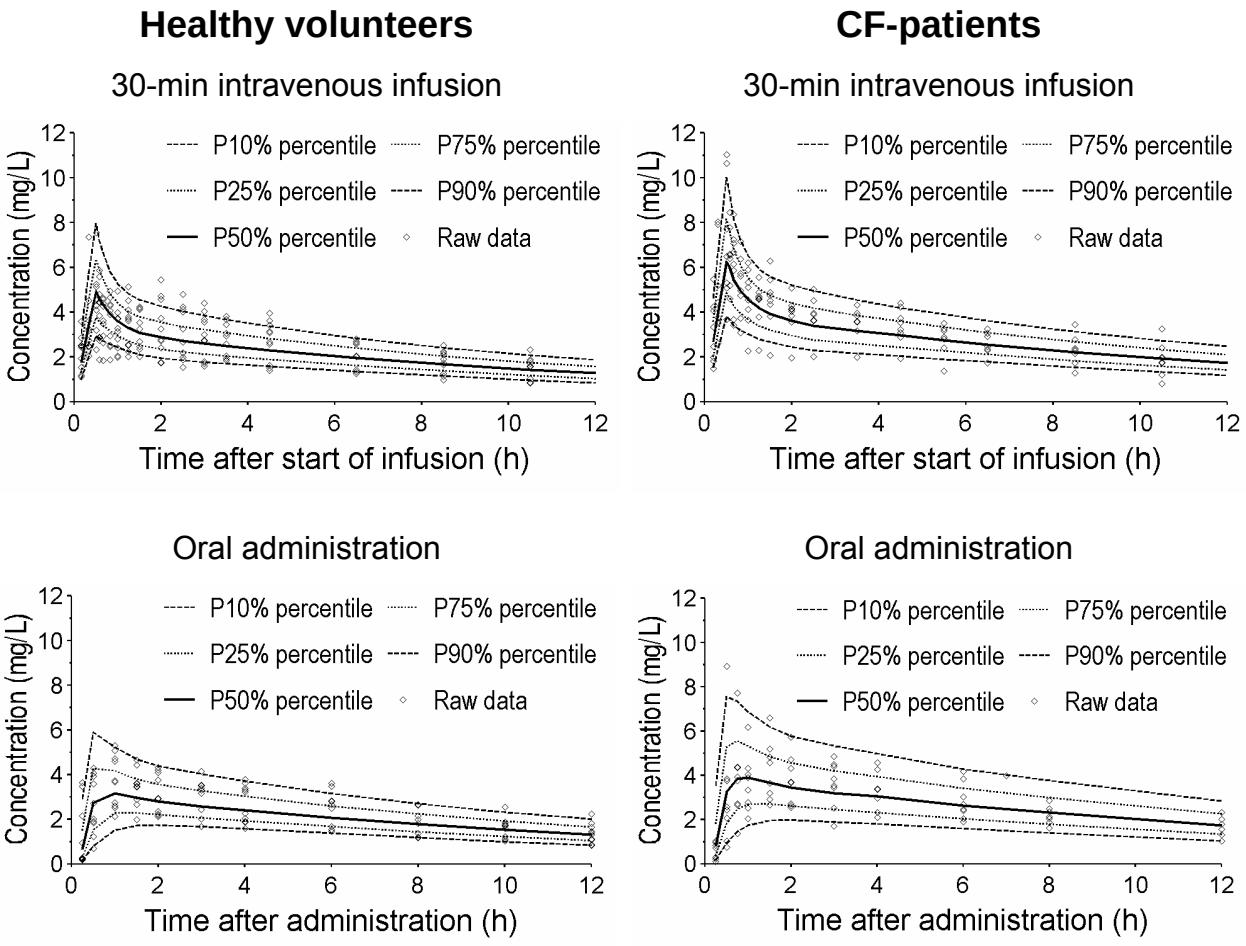


**Figure 3.4-13** VPC based on 8,000 CF-patients and 10,000 healthy volunteers for the final population PK model (see Table 3.4-22).

See chapter 2.6.3 for interpretation of VPCs.

***Disposition:*** We distinguished the size models 1) by their estimates for the disease specific scale factors FCYF and 2) by their estimates for the BSV in clearance and volume of distribution. In absence of any size descriptor, CF-patients had a 12% higher renal clearance, a 31% lower nonrenal clearance, and a 21% lower volume of distribution at steady-state (see Table 3.4-23, size model A). As our CF-patients were smaller than our healthy volunteers (see Table 3.4-20), a 12% higher unscaled renal clearance in our CF-patients was unexpected.

**Table 3.4-22** PK parameter estimates for allometric scaling by $FFM_J$

| Parameter | Unit | Estimate %CV[$] | | Median (90% confidence interval) from non-parametric bootstrap[&] | |
|---|---|---|---|---|---|
| | | CF-patients | healthy volunteers | CF-patients | healthy volunteers |
| F(oral) | % | 97.7 | 99.2 | 97.6 (83.4 - 113) | 99.1 (91.7 - 107) |
| BSV($F_{oral}$) | | 25.8% | 13.5% | 24% (13 - 33%) | 12% (7.7 - 16%) |
| $CL_{tot}$^ | L $h^{-1}$ | 8.82* | 9.30* | 8.85* (7.77 - 10.1) | 9.29* (8.3 - 10) |
| $CL_R$ | L $h^{-1}$ | 1.06* | 0.724* | 1.07* (0.877 - 1.23) | 0.726* (0.685 - 0.764) |
| BSV($CL_R$) | | 19%[#] | 19%[#] | 19% (5.1 - 25%) | 19% (5.1 - 25%) |
| $CL_{NR}$ | L $h^{-1}$ | 7.76* | 8.58* | 7.76* (6.68 - 9.16) | 8.56* (7.61 - 9.67) |
| BSV($CL_{NR}$) | | 24%[#] | 24%[#] | 22% (15 - 29%) | 22% (15 - 29%) |
| Vss^ | L | 131* | 113* | 130* (116 - 146) | 114* (101 - 129) |
| V1 | L | 78.3* | 67.5* | 77.3* (65.4 - 90.5) | 67.3* (55.6 - 80.5) |
| BSV(V1) | | 38%** | 38%** | 37% (22 - 49%) | 37% (22 - 49%) |
| V2 | L | 52.7* | 45.4* | 52.9* (41.6 - 65.8) | 46.1* (37.0 - 56.9) |
| BSV(V2) | | 43%** | 43%** | 41% (28 - 57%) | 41% (28 - 57%) |
| CLic | L $h^{-1}$ | 61.6* | | 62.2* (44.4 - 94.8) | |
| TK0 (fixed) | min | 30 | | 30 | |
| TLAG | min | 12.4 | | 12.4 (11.8 - 13.2) | |
| BSV(TLAG) | | 12% | | 11% (7.9 - 14%) | |
| TABS | min | 14.5 | | 14.7 (9.41 - 22.3) | |
| BSV(TABS) | | 112% | | 108% (78 - 139%) | |
| $CV_C$ | % | 15.5 | | 15.4 (14.1 - 16.7) | |
| $SD_C$ | mg/L | 0.0436 | | 0.0434 (0.0318 - 0.0605) | |

[$]: Coefficient of variation for BSV.

[&]: Medians and non-parametric 90% confidence intervals (5% - 95% percentile) from 1,000 non-parametric bootstrap replicates. Each bootstrap replicate consisted of 18 subjects (eight CF-patients and ten healthy volunteers) who were randomly drawn from the original dataset (with replacement).

*: Group estimate for a subject with standard $FFM_J$ = 53 kg.

^: Derived from model estimates, not an estimated parameter.

°: Apparent coefficients of variation for the BSV.

[#]: Coefficient of correlation for random effects of $CL_R$ and $CL_{NR}$: r = 0.064.

**: Coefficient of correlation for random effects of V1 and V2: r = -0.53.

See also chapter 2.6.2 for explanation of model parameters.

Size adjusted renal clearance was estimated to be 52-68% higher ($p<0.01$, one-sided test) for linear and allometric scaling by WT (size models B and C) and 44-47% higher ($p<0.01$, one-sided test) for allometric scaling by $FFM_C$ or $FFM_J$ (size models D and E). Although this is a large relative difference, renal clearance of pefloxacin accounted only for about 10% of total clearance (see Table 3.4-21) and therefore the higher renal clearance in CF-patients had a little effect on total clearance.

As the size adjusted nonrenal clearance was estimated to be slightly lower or similar in CF-patients compared to healthy volunteers, the size adjusted total clearance was estimated to be similar (range: 93-108%) in CF-Patients and healthy volunteers by size models B to E (see Table 3.4-23). The size adjusted volume of distribution at steady-state was estimated to be 12-20% higher ($p=0.07$ to $p=0.18$, one-sided test) in CF-patients by size models B to E. When we compared the ability of the different size models to reduce the unexplained BSV (see Table 3.4-24), allometric scaling by $FFM_J$ reduced the BSV of nonrenal clearance by 19% ($p=0.03$, one-sided test) and the BSV of volume of the peripheral compartment by 14% ($p=0.10$, one-sided test) relative to linear scaling by WT.

**Table 3.4-23** Ratios of group estimates (CF-patients / healthy volunteers) for clearance and volume of distribution for different size models

| **Part A** | Estimates from original dataset | | | |
|---|---|---|---|---|
| Size model | $FCYF_{CLR}$ | $FCYF_{CLNR}$ | $FCYF_{CLT}^{\#}$ | $FCYF_{V}$ |
| A) No size model | 1.12 | 0.693 | 0.726 | 0.785 |
| B) WT linear scaling | 1.68 | 1.03 | 1.08 | 1.20 |
| C) WT allometric | 1.52 | 0.934 | 0.980 | 1.19 |
| D) $FFM_C$ allometric | 1.44 | 0.885 | 0.928 | 1.12 |
| E) $FFM_J$ allometric | 1.47 | 0.904 | 0.948 | 1.16 |

| **Part B** | Median (90% confidence intervals) from bootstrap runs | | | |
|---|---|---|---|---|
| Size model | $FCYF_{CLR}$ | $FCYF_{CLNR}$ | $FCYF_{CLT}^{\#}$ | $FCYF_{V}$ |
| A) No size model | 1.12 (0.93-1.31) | 0.69 (0.54-0.91) | 0.73 (0.57-0.93) | 0.78 (0.62-1.03) |
| B) WT linear scaling | 1.68 (1.42-1.91) | 1.03 (0.83-1.31) | 1.08 (0.89-1.34) | 1.19 (0.97-1.48) |
| C) WT allometric | 1.52 (1.29-1.72) | 0.94 (0.75-1.19) | 0.98 (0.80-1.22) | 1.19 (0.97-1.47) |
| D) $FFM_C$ allometric | 1.44 (1.20-1.66) | 0.89 (0.72-1.11) | 0.93 (0.77-1.14) | 1.11 (0.92-1.35) |
| E) $FFM_J$ allometric | 1.47 (1.20-1.73) | 0.90 (0.74-1.11) | 0.95 (0.79-1.15) | 1.14 (0.96-1.37) |

$FCYF_{NNN}$: Ratio of group estimates for parameter NNN (group estimate for CF-patients divided by group estimate for healthy volunteers).

#: Calculated as weighted average of $FCYF_{CLR}$ and $FCYF_{CLNR}$.

**Table 3.4-24** Comparison of BSV (variances) between various size models: The table shows the relative between subject variances for the respective PK parameter and size models

| **Part A** | Estimates from original dataset<br>Relative between subject variance | | | |
|---|---|---|---|---|
| Size model | $CL_R$ | $CL_{NR}$ | V1 | V2 |
| B) WT linear scaling | 0%* | 0%* | 0%* | 0%* |
| C) WT allometric | -7%° | 5% | -1% | 0% |
| D) $FFM_C$ allometric | 9%° | -5% | -8% | -9% |
| E) $FFM_J$ allometric | 41%° | -19% | -6% | -14% |

| **Part B** | Median (90% confidence intervals) from bootstrap runs[#]<br>Relative between subject variance | | | |
|---|---|---|---|---|
| Size model | $CL_R$ | $CL_{NR}$ | V1 | V2 |
| B) WT linear scaling | 0% (0 to 0)* | 0% (0 to 0)* | 0% (0 to 0)* | 0% (0 to 0)* |
| C) WT allometric | -6% (-21 to 8) | 5% (-4 to 16) | -1% (-3 to 1) | 0% (-5 to 9) |
| D) $FFM_C$ allometric | 7% (-19 to 45) | -5% (-18 to 9) | -7% (-22 to 8) | -8% (-17 to 6) |
| E) $FFM_J$ allometric | 41% (-16 to 107) | **-19% (-36 to -3)** | -5% (-31 to 20) | **-14% (-27 to 7)** |

*: The value provided here is (variance of test size model - variance for linear scaling by WT) / variance for linear scaling by WT. For the bootstrap estimates, the denominator was the median variance for linear scaling by WT from all 1,000 bootstrap runs.

°: The lower this number, the more variability was explained by the respective size model. These values mean that the BSV (variance) for renal clearance was reduced by 7% for allometric scaling by WT, increased by 9% for allometric scaling by $FFM_C$, and increased by 41% for allometric scaling by $FFM_J$, all compared to linear scaling by WT.

#: Medians and non-parametric 90% confidence intervals (5% - 95% percentile) from 1,000 non-parametric bootstrap replicates. Each bootstrap replicate consisted of 18 subjects (eight CF-patients and ten healthy volunteers) who were randomly drawn from the original dataset (with replacement).

#### 3.4.5.5 Discussion

Pathophysiological changes in the GI tract of CF-patients may potentially interfere with the oral absorption. These changes occur frequently in CF-patients (for details, see chapter 1.4.2). Some examples for the influence of these changes on the absorption of beta-lactams and quinolones are shown in chapter 3.1.2. In essence, there are only a few studies which compared the rate and extent of absorption for antibiotics between CF-patients and healthy volunteers. Most authors (98, 280, 325, 403) used the STS approach. A slower rate of absorption for ciprofloxacin and fleroxacin has been observed in CF-patients. However, the reported coefficients of variation for the BSV of the absorption half-life range between 46 and 100%. Rajagopalan et al. (398) used population PK and found a 61% slower rate and a similar extent of absorption for ciprofloxacin in children with CF relative to other pediatric patients.

Pefloxacin is a fluoroquinolone which can be administered orally and intravenously. It has anti-staphylococcal activity in patients with CF (387). Pefloxacin is completely, reliably, and rapidly absorbed in healthy volunteers. We used pefloxacin as a “probe drug” to study differences in the rate and extent of absorption between CF-patients and healthy volunteers. About 90% of pefloxacin are eliminated via nonrenal pathways what makes pefloxacin an appealing candidate to compare the nonrenal elimination and metabolism between both subject groups. Additionally, we wished to compare the disposition of pefloxacin to identify the most appropriate size descriptor for clearance and volume of distribution.

We used population PK to estimate and compare both the average PK parameters and their BSV. Population PK is a powerful technique which considers all available raw data simultaneously. We used non-parametric bootstrap techniques to derive non-parametric confidence intervals of our PK parameters and the BSV terms for a statistical comparison of the PK in CF-patients and healthy volunteers. This method is superior to standard equivalence statistics (ANOVA) which describes the oral absorption on a less

mechanistic level by the peak concentrations and the area under the plasma concentration time curve and assumes that the BSV is the same in both subject groups.

We performed a two-way crossover study with eight CF-patients and ten healthy volunteers who received 400 mg pefloxacin as oral and intravenous dose. We applied a high degree of standardization of the clinical procedures to yield study conditions as similar as possible for both subject groups. Our CF-patients abstained from taking pancreatic enzymes as supplement therapy to exclude the influence of pancreatic enzymes on the absorption of pefloxacin. However, the effect of pancreatic enzymes on the absorption has been reported to be small for another fluoroquinolone [ciprofloxacin] (302, 403). The estimates of our PK parameters for healthy volunteers were in agreement with the results of other authors (142, 220, 382, 547). We are not aware of any studies on the PK of pefloxacin in CF-patients.

The average (90% confidence interval) extent of absorption was 97.6% (83.4 - 113%) in CF-patients and 99.1% (91.7 - 107%) in healthy volunteers which showed that the extent of oral absorption was virtually complete in both subject groups. Although the coefficients of variation for the BSV in extent of absorption was larger in CF-patients than in healthy volunteers (25.8% vs. 13.5%, see also Table 3.4-22), this comparison lacked statistical significance (p=0.06 from bootstrap).

The median absorption half-life was very similar between both subject groups. Seven of the eight CF-patients had individual estimates for the absorption half-life which mirrored the central tendency and the range of individual absorption half-lives seen in our healthy volunteers. The CF-patient with the lowest BMI of 13.4 $kg/m^2$ in our study had an absorption half-life of 109 min which was about twice as long as the absorption half-lives for all other subjects. However, this patient had a complete (100%) extent of absorption and an average Shwachman score of 74%. A scatterplot of the absorption half-life vs. BMI showed no correlation or trend. Although we observed a prolonged absorption half-life in one CF-patient, this was unlikely to affect the PD of pefloxacin, because the extent of absorption in CF-patients and healthy volunteers was very similar.

When we studied the differences in clearance and volume of distribution between CF-patients and healthy volunteers, we found a 31% lower nonrenal clearance and a 21% lower volume of distribution in CF-patients when no size descriptor was used (see size model A, Table 3.4-23). However, we found a 12% higher unscaled renal clearance, although our CF-patients had a 40% lower WT, a 32% lower $FFM_C$, and a 36% lower $FFM_J$ (see Table 3.4-20). Consequently, the size adjusted renal clearance was predicted to be 52-68% higher ($p<0.01$) in CF-patients than in healthy volunteers for linear or allometric scaling by WT and 44-47% ($p<0.01$) higher for allometric scaling by $FFM_C$ or $FFM_J$ (see Table 3.4-23). Although this difference was larger than expected, renal clearance contributed only about 10% to the total pefloxacin clearance and therefore the influence of the increased renal clearance on total clearance is small. Christensson et al. (75) found a 100% higher renal clearance (in L/h/1.73 $m^2$ BSA) after intravenous treatment and a 23% higher renal clearance after oral treatment of ciprofloxacin in CF-patients relative to healthy volunteers. A 50% increased kidney weight (515) and glomerulomegaly (2) in CF-patients may contribute to these observations. However, the majority of authors (390, 408, 502) found similar to about 40% higher size adjusted renal clearances for beta-lactams and aminoglycosides in CF-patients compared to healthy volunteers.

As the average size adjusted nonrenal clearance in CF-patients was similar (range: 89-103%) in CF-patients and in healthy volunteers, the size adjusted total clearance was similar in both subject groups (range: 93-108%, see size models B to E, Table 3.4-23). The size adjusted volume of distribution was slightly higher in CF-patients (range: 112-120%). Overall, there were no pronounced differences between the four size models in their ability to describe the average difference in total clearance and volume of distribution between both subject groups. Allometric scaling by $FFM_J$ (size model E) reduced the unexplained BSV in nonrenal clearance significantly by 19% ($p=0.03$, one-sided test) and the unexplained BSV in volume of the peripheral compartment by 14% compared to linear scaling by WT.

We had data on the amount of two metabolites, norfloxacin and pefloxacin N-oxide, recovered in the urine. Similar to slightly higher amounts

of those metabolites were recovered in the urine of CF-patients compared to healthy volunteers (see Table 3.4-21). Therefore, the metabolism of pefloxacin to those two metabolites was probably comparable between both subject groups. However, we do not know how much metabolite was formed, unless we assume that the metabolites were only eliminated renally. As we found a 44 to 68% higher ($p<0.01$) size adjusted renal clearance in CF-patients for pefloxacin, also the renal clearance of the metabolites might have been higher in CF-patients than in healthy volunteers. We are not aware of literature data on the disposition of norfloxacin or pefloxacin N-oxide in CF-patients. Therefore, it is difficult to interpret, whether an altered metabolite formation, an altered renal or nonrenal clearance of the metabolite(s), or both contributed to the similar to slightly higher amount of metabolite recovered in urine of CF-patients in our study.

In conclusion, pefloxacin was reliably and virtually completely absorbed in CF-patients and in healthy volunteers. The extent of absorption had a larger BSV in CF-patients (25.8% CV) than in healthy volunteers (13.5% CV), but the BSV was not significantly larger ($p=0.06$) in CF-patients. After accounting for body size by WT, $FFM_C$, or $FFM_J$, the size adjusted average total clearance and volume of distribution at steady-state of CF-patients were within $\pm$20% of the values for healthy volunteers. Therefore, the absorption and disposition of pefloxacin in CF-patients was comparable to the PK in healthy volunteers, if body size was considered. Allometric scaling by $FFM_J$ reduced the BSV in nonrenal clearance by 19% ($p=0.03$) compared to linear scaling by WT. Therefore, target concentrations can be achieved more precisely by use of $FFM_J$ for dose selection. Population PK with non-parametric bootstrap techniques was a powerful method to compare the absorption and disposition as well as their BSV in subject groups with different body size and body composition. More well controlled studies on the absorption of other oral antibiotics are required to study differences in the rate and extent of absorption between CF-patients and healthy volunteers and their variability.

## 3.5 Cystic fibrosis patients are pharmacokinetically comparable to healthy volunteers when scaled by body size / composition

### 3.5.1 Background and purpose of this meta-analysis

CF is the most common inherited disease in the Caucasian population. Respiratory diseases are the primary reason for frequent hospitalization of CF-patients and a primary cause of morbidity and shortened survival (12, 283, 400). Doses in adult CF-patients are usually calculated per kg WT (65, 105). However, there is considerable evidence that body composition influences PK (72, 164, 328, 368, 499) which requires dose adjustment for some patient groups. As most PK studies in CF-patients with a healthy volunteer control group studied less than 30 subjects (in total), a meta-analysis of several smaller studies is the method of choice to compare various descriptors for body size and body composition. A meta-analysis allows one to increase the power of a comparison and to identify studies with “outlying” results on a statistical basis. If a meta-analysis shows a statistically significant and clinically relevant superiority of dose selection by a size descriptor that accounts for body composition, large randomized clinical trials are warranted to show the clinical superiority of this descriptor. However, such a meta-analysis is indeed rare in any circumstance and has not yet been performed for the PK in CF-patients.

We performed a meta-analysis based on in-house data from ten well-controlled studies (on seven beta-lactams and three quinolones) each containing PK data from CF-patients and healthy volunteers. We compared the ability of various descriptors of body size and composition to accurately select doses with the following three objectives: 1) To study the ability of each descriptor to describe the average differences in clearance and volume of distribution between CF-patients and healthy volunteers, 2) to study the between drug variability (BDV) of these average differences, and 3) to study the reduction of unexplained BSV in clearance and volume of distribution by

incorporation of various descriptors of body size and composition compared to linear scaling by WT. We accounted for the average differences in clearance and volume of distribution between CF-patients and healthy volunteers for this comparison of unexplained BSV.

### 3.5.2 Methods

The general clinical and sample handling procedures, the methods for PK analysis (including NCA and population PK), and the general methods for MCS are described in chapter 2. Chapter 3.2 shows the specific methods applied for analysis of our CF-studies. Chapter 3.3 and chapter 3.4 show the details of the individual studies. The methods specific to the meta-analysis are described in this chapter.

***Selection of studies:*** We used in-house data from ten studies each comparing the PK in CF-patients and healthy volunteers. The physicochemical properties of the ten drugs are shown in Table 3.2-1 on page 86. A total of 201 Caucasian volunteers (90 CF-patients and 111 healthy volunteers) of both sexes participated in these studies. A summary of their demographic data is shown in Table 3.5-1.

***Dependent variables for meta-analysis:*** We used the disease specific scale factors $FCYF_{CLR}$, $FCYF_{CLNR}$, $FCYF_{CLT}$, and $FCYF_{V}$ as dependent variables in our meta-analysis to study the average differences between CF-patients and healthy volunteers after adjusting for body size by the respective size model. Chapter 3.2.4 and chapter 3.2.5 describe details about the FCYFs.

**Table 3.5-1** Demographic data of all ten studies in CF-patients and healthy volunteers (average ± SD)

| | CF-patients | Healthy volunteers |
|---|---|---|
| Number of subjects | 90 | 111 |
| Age (yr) | 21 ± 3.6 | 25 ± 3.5 |
| Height (cm) | 167 ± 11 | 174 ± 8.3 |
| Total body weight (kg) | 50 ± 11 | 68 ± 11 |
| Fat-free mass (Cheymol & James) (kg)[a] | 42 ± 8.6 | 54 ± 7.9 |
| Fat-free mass (Janmahasatian et al.) (kg)[b] | 40 ± 9.6 | 52 ± 9.2 |
| Predicted normal weight (Cheymol & James) (kg)[c] | 52 ± 12 | 68 ± 9.5 |
| Predicted normal weight (Janmahasatian et al.) (kg)[d] | 52 ± 12 | 68 ± 9.3 |
| Body surface area ($m^2$)[e] | 1.51 ± 0.21 | 1.81 ± 0.17 |
| Body mass index (kg $m^{-2}$) | 17.7 ± 2.7 | 22.5 ± 2.9 |

[a]: Fat-free mass ($FFM_C$) calculated by the formula of Cheymol and James (72, 222).

[b]: Fat-free mass ($FFM_J$) calculated by the formula of Janmahasatian et al. (224).

[c]: Predicted normal weight ($PNWT_C$) based on the Cheymol & James equation for $FFM_C$ developed by Duffull et al. (117).

[d]: Predicted normal weight ($PNWT_J$) based on the equation from Janmahasatian et al. (223).

[e]: Calculated by the Mosteller formula (332).

***Meta-analysis:*** Our meta-analysis was performed in a 2 stage process. In stage 1, we estimated the population PK parameters and their uncertainty for each drug separately. Thus, the dependent individual effect, e. g. $FCYF_{CLR}$, was derived for each drug separately. In stage 2, we estimated the overall mean effect and the between drug variability (BDV) by pooling a weighted average of the effect size (e. g. $FCYF_{CLR}$) of all drugs. This was done by using the estimated values of, e. g., $FCYF_{CLR}$, as dependent variables in a linear mixed-effects model (ANOVA). We used “size model” as fixed effect and “drug” as random effect. In this setting the BDV can be quantified. We estimated the pooled BDV across all size descriptors. The

value of the fractional scale parameters (e. g. $FCYF_{CLR}$) used as the dependent variable in this analysis was the geometric mean of the 1,000 bootstrap estimates for each drug. The analysis was performed on log-scale. We used the inverse of the variance on log-scale of the 1,000 bootstrap estimates as weight in stage 2 of our meta-analysis. We tested for all four FCYFs, whether the mean value for each size model was significantly different from 1.0 by two-sided testing at an $\alpha$ of 0.05.

***Reduction of unexplained BSV:*** We compared the estimated BSV for renal and nonrenal clearance as well as for volume of the central and peripheral compartment between the size models. As most dosing guidelines in CF-patients are based on linear scaling by WT (105, 151), we used linear scaling by WT as reference model for the comparison of BSV. We calculated the differences between BSV(test size model) and BSV(linear scaling by WT) for each bootstrap run and divided this difference by the median BSV for linear scaling by WT from all 1000 bootstrap runs for the respective drug. This scaled difference in BSV characterizes the reduction of unexplained BSV by the respective test size model compared to linear scaling by WT. We compared those scaled differences in BSV between size models by descriptive statistics.

### 3.5.3 Results

***Total clearance:*** Figure 3.5-1 (panel A) shows the disease specific scale factors for total clearance ($FCYF_{CLT}$). The ten drugs had a median unscaled total clearance that was about 19% [range: 0-30%] lower for our CF-patients relative to our healthy volunteers, most likely because our CF-patients were smaller. In the meta-analysis of all ten drugs, linear scaling by WT resulted in a 15% [4-27%] higher average total clearance in CF-patients (p=0.013, point estimate [95% confidence interval], see Table 3.5-2). Allometric scaling by WT and linear scaling by $FFM_C$ or $FFM_J$ estimated the average total clearance to be about 6-7% higher in CF-patients than in healthy volunteers.

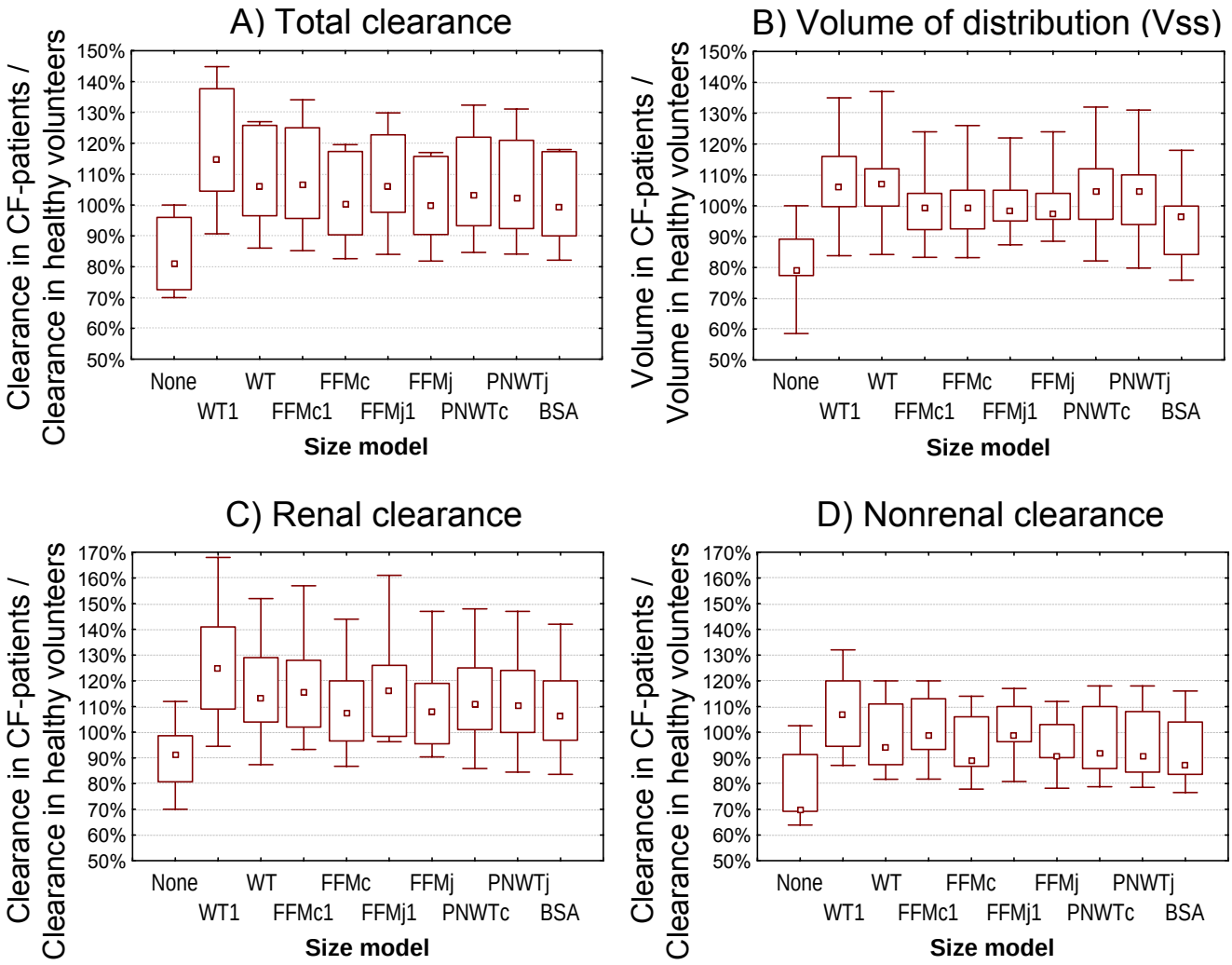


**Figure 3.5-1** Distribution of disease specific scale factors (FCYFs)

Each box-whisker shows the median (marker), interquartile range (box), and minimum/maximum (whiskers) of all ten studied drugs. Note a value of 100% indicates that CF-patients were not different to healthy volunteers.

The labels of the size models are: “None”: no size model; “WT1”: linear scaling by WT, “WT”: allometric scaling by WT, “FFMc1”: linear scaling by $FFM_C$, “FFMc”: allometric scaling by $FFM_C$, “FFMj1”: linear scaling by $FFM_J$, “FFMj”: allometric scaling by $FFM_J$, “PNWTc”: allometric scaling by $PNWT_C$, “PNWTj”: allometric scaling by $PNWT_J$, and “BSA”: linear scaling by BSA.

**Table 3.5-2** Meta-analysis of disease specific scale factors (FCYF) for all ten drugs.

The data are least square means (95% confidence intervals) and p-values for a two-sided test, if the least square mean is different from 1.0.

| **Size model** | **$FCYF_{CLT}$** | **$FCYF_{CLR}$** | **$FCYF_{CLNR}$** | **$FCYF_{V}$** |
|---|---|---|---|---|
| No size model | 0.85 (0.77-0.94) p = 0.005 | 0.94 (0.84-1.05) p = 0.211 | 0.76 (0.68-0.86) p < 0.001 | 0.83 (0.76-0.91) p = 0.001 |
| WT (linear scaling) | 1.15 (1.04-1.27) p = 0.013 | 1.23 (1.11-1.38) p = 0.002 | 1.07 (0.96-1.20) p = 0.208 | 1.06 (0.97-1.16) p = 0.191 |
| WT (allometric) | 1.06 (0.96-1.17) p = 0.215 | 1.15 (1.03-1.28) p = 0.020 | 0.99 (0.88-1.11) p = 0.789 | 1.07 (0.97-1.17) p = 0.144 |
| $FFM_C$ (linear scaling) | 1.07 (0.97-1.18) p = 0.175 | 1.14 (1.02-1.28) p = 0.021 | 1.00 (0.89-1.12) p = 0.997 | 0.99 (0.91-1.09) p = 0.879 |
| $FFM_C$ (allometric) | 1.01 (0.91-1.11) p = 0.905 | 1.08 (0.97-1.21) p = 0.136 | 0.94 (0.84-1.05) p = 0.223 | 1.00 (0.91-1.09) p = 0.976 |
| $FFM_J$ (linear scaling) | 1.07 (0.97-1.18) p = 0.172 | 1.13 (1.02-1.27) p = 0.029 | 1.01 (0.90-1.13) p = 0.863 | 0.99 (0.90-1.08) p = 0.721 |
| $FFM_J$ (allometric) | 1.00 (0.91-1.11) p = 0.922 | 1.08 (0.96-1.20) p = 0.171 | 0.94 (0.84-1.05) p = 0.260 | 0.99 (0.91-1.08) p = 0.823 |
| $PNWT_C$ (allometric) | 1.04 (0.94-1.15) p = 0.445 | 1.12 (1.00-1.25) p = 0.047 | 0.96 (0.86-1.08) p = 0.458 | 1.04 (0.95-1.14) p = 0.357 |
| $PNWT_J$ (allometric) | 1.03 (0.93-1.14) p = 0.557 | 1.11 (0.99-1.24) p = 0.060 | 0.95 (0.85-1.07) p = 0.368 | 1.03 (0.94-1.13) p = 0.480 |
| BSA (linear by BSA) | 1.00 (0.91-1.11) p = 0.982 | 1.08 (0.97-1.21) p = 0.139 | 0.93 (0.83-1.04) p = 0.164 | 0.95 (0.86-1.03) p = 0.198 |
| Between drug variability [a] | 14% | 15% | 15% | 12% |

$FCYF_{NNN}$: Ratio of group estimates for parameter NNN after accounting for body size (e. g. $FCYF_{CLT}$: group estimate of total clearance in CF-patients divided by group estimate of total clearance in healthy volunteers of the same body size).

[a]: Coefficient of variability for the between drug variability (BDV) of the disease specific scale factors (FCYF). As the BDV was similar between all size models, we estimated the pooled BDV across all size models.

The average differences between CF-patients and healthy volunteers vanished (±4%), if total clearance was scaled allometrically by $FFM_C$, $FFM_J$, $PNWT_C$, or $PNWT_J$. Linear scaling by BSA yielded an average $FCYF_{CLT}$ of 1.00. The ratio of average total clearance in CF-patients and healthy volunteers ranged between 0.82 and 1.20 for all ten drugs for allometric scaling by $FFM_C$ or $FFM_J$ and for linear scaling by BSA (see Figure 3.5-1, panel A). The BDV of the estimates for $FCYF_{CLT}$ of all ten drugs was 14% (see Table 3.5-2).

***Volume of distribution at steady-state:*** Figure 3.5-1 (panel B) shows the disease specific scale factors for volume of distribution at steady-state ($FCYF_V$). The ten drugs had a median unscaled volume of distribution that was about 21% [range: 0-41%] lower in our CF-patients relative to our healthy volunteers. Linear scaling by WT estimated the average volume of distribution to be 6% [-3 to +16%] higher (p=0.191, point estimate [95% confidence interval]) in CF-patients (see Table 3.5-2). The meta-analysis showed that the ratio of average volume of distribution in CF-patients and healthy volunteers was very close to 1.0 for the linear and allometric model based on $FFM_C$ or $FFM_J$. Virtually identical results for the linear and allometric model were expected, since those models use the same exponent of 1.0 for volume of distribution. The ratio of average volume of distribution in CF-patients and healthy volunteers ranged between 0.83 and 1.26 for all ten drugs for the size models based on $FFM_C$ or $FFM_J$ (see Figure 3.5-1, panel B). The BDV of the estimates for $FCYF_V$ of all 10 drugs was 12% (see Table 3.5-2).

***Renal and nonrenal clearance:*** The disease specific scale factors of the studied drugs are shown in Figure 3.5-1 panel C for renal clearance ($FCYF_{CLR}$) and in Figure 3.5-1 panel D for nonrenal clearance ($FCYF_{CLNR}$). For allometric scaling by $FFM_C$ or $FFM_J$, the median renal clearance of all drugs was about 8% higher in CF-patients relative to healthy volunteers and the median nonrenal clearance was about 10% lower in CF-patients. In the meta-analysis, linear scaling by WT estimated the average renal clearance to be 23% [11-38%] higher (p=0.002, point estimate [95% confidence interval]) in CF-patients and the average nonrenal clearance to be 7% [-4 to +20%] higher (p=0.208) in CF-patients (see Table 3.5-2).

Allometric scaling by $FFM_C$ or $FFM_J$ estimated renal clearance to be 8% higher in CF-patients ($p \geq 0.136$) and nonrenal clearance to be 6% lower in CF-patients ($p \geq 0.223$). The ratio of average renal clearance in CF-patients and healthy volunteers ranged between 0.87 and 1.47 for all ten drugs for allometric scaling by $FFM_C$ or $FFM_J$ (see Figure 3.5-1, panel C). The ratio of average nonrenal clearance in CF-patients and healthy volunteers ranged between 0.78 and 1.14 for all drugs for allometric scaling by $FFM_C$ or $FFM_J$ (see Figure 3.5-1, panel D) and the BDV was 15% for renal and nonrenal clearance (see Table 3.5-2). The power to detect a 20% average difference between CF-patients and healthy volunteers in the meta-analysis was >99% for all FCYFs.

***Subgroup analysis of beta-lactams and quinolones separately:*** The subgroup analysis for the disease specific scale factors (FCYFs) is shown in Table 3.5-3 for the seven beta-lactams and in Table 3.5-4 for the three quinolones. The results of the subgroup analysis for the beta-lactams was similar to the results for all ten drugs. For our three quinolones, the allometric size models predicted total clearance in CF-patients to be about 10-13% lower than in healthy volunteers. Nonrenal clearance was predicted to be about 14-16% lower and renal clearance was predicted to be 6-7% higher in CF-patients for allometric scaling by $FFM_C$ or $FFM_J$. Volume of distribution was predicted to be similar in both subject groups (2-7% lower in CF-patients) by all size models except linear scaling by BSA (see Table 3.5-4).

***Reduction of BSV:*** Figure 3.5-2 shows the distribution of the scaled unexplained BSVs relative to linear scaling by WT. Allometric scaling by WT, $FFM_C$, $PNWT_C$, or $PNWT_J$ and linear scaling by BSA reduced the unexplained BSV in renal clearance by 20 to 27% (median of 10 drugs). The size models based on $FFM_C$ or $FFM_J$ reduced the unexplained BSV in volume of the peripheral compartment by 6-10% relative to linear scaling by WT.

**Table 3.5-3** Meta-analysis of disease specific scale factors (FCYF) for the subgroup of seven beta-lactams.

The data are least square means (95% confidence intervals) and p-values for a two-sided test, if the least square mean is different from 1.0.

| Size model | $FCYF_{CLT}$ | $FCYF_{CLR}$ | $FCYF_{CLNR}$ | $FCYF_{V}$ |
|---|---|---|---|---|
| No size model | 0.91 (0.82-1.00) p = 0.059 | 0.95 (0.87-1.04) p = 0.244 | 0.80 (0.69-0.93) p = 0.013 | 0.87 (0.79-0.96) p = 0.009 |
| WT (linear scaling) | 1.23 (1.11-1.36) p = 0.002 | 1.25 (1.14-1.37) p < 0.001 | 1.14 (0.98-1.33) p = 0.080 | 1.10 (1.00-1.21) p = 0.058 |
| WT (allometric) | 1.13 (1.03-1.25) p = 0.020 | 1.16 (1.06-1.27) p = 0.005 | 1.05 (0.90-1.22) p = 0.481 | 1.11 (1.00-1.22) p = 0.044 |
| $FFM_C$ (linear scaling) | 1.13 (1.03-1.25) p = 0.020 | 1.16 (1.06-1.26) p = 0.006 | 1.06 (0.90-1.23) p = 0.425 | 1.02 (0.93-1.13) p = 0.594 |
| $FFM_C$ (allometric) | 1.07 (0.97-1.18) p = 0.157 | 1.10 (1.00-1.20) p = 0.047 | 0.99 (0.85-1.15) p = 0.840 | 1.03 (0.93-1.13) p = 0.522 |
| $FFM_J$ (linear scaling) | 1.12 (1.01-1.24) p = 0.030 | 1.14 (1.04-1.25) p = 0.011 | 1.05 (0.90-1.23) p = 0.458 | 1.00 (0.91-1.11) p = 0.925 |
| $FFM_J$ (allometric) | 1.06 (0.96-1.17) p = 0.211 | 1.08 (0.99-1.18) p = 0.077 | 0.98 (0.84-1.15) p = 0.792 | 1.01 (0.92-1.11) p = 0.851 |
| $PNWT_C$ (allometric) | 1.11 (1.00-1.22) p = 0.045 | 1.14 (1.04-1.24) p = 0.012 | 1.02 (0.88-1.19) p = 0.741 | 1.08 (0.98-1.19) p = 0.109 |
| $PNWT_J$ (allometric) | 1.10 (0.99-1.21) p = 0.060 | 1.13 (1.03-1.23) p = 0.016 | 1.01 (0.87-1.18) p = 0.854 | 1.07 (0.97-1.18) p = 0.146 |
| BSA (linear by BSA) | 1.07 (0.97-1.18) p = 0.159 | 1.10 (1.00-1.20) p = 0.043 | 0.98 (0.84-1.15) p = 0.771 | 0.98 (0.89-1.08) p = 0.630 |
| Between drug variability [a] | 11% | 9% | 15% | 10% |

$FCYF_{NNN}$: Ratio of group estimates for parameter NNN after accounting for body size (e. g. $FCYF_{CLT}$: group estimate of total clearance in CF-patients divided by group estimate of total clearance in healthy volunteers of the same body size).

[a]: Coefficient of variability for the between drug variability (BDV) of the disease specific scale factors (FCYF). As the BDV was similar between all size models, we estimated the pooled BDV across all size models.

**Table 3.5-4** Meta-analysis of disease specific scale factors (FCYF) for the subgroup of three quinolones.

The data are least square means (95% confidence intervals) and p-values for a two-sided test, if the least square mean is different from 1.0.

| **Size model** | **$FCYF_{CLT}$** | **$FCYF_{CLR}$** | **$FCYF_{CLNR}$** | **$FCYF_{V}$** |
|---|---|---|---|---|
| No size model | 0.71 (0.62-0.83) p = 0.006 | 0.88 (0.46-1.69) p = 0.499 | 0.69 (0.60-0.80) p = 0.004 | 0.72 (0.50-1.02) p = 0.056 |
| WT (linear scaling) | 0.97 (0.83-1.12) p = 0.510 | 1.19 (0.62-2.30) p = 0.387 | 0.95 (0.82-1.09) p = 0.300 | 0.97 (0.67-1.40) p = 0.774 |
| WT (allometric) | 0.90 (0.78-1.04) p = 0.097 | 1.10 (0.57-2.13) p = 0.604 | 0.88 (0.76-1.01) p = 0.059 | 0.97 (0.68-1.40) p = 0.795 |
| $FFM_C$ (linear scaling) | 0.93 (0.80-1.08) p = 0.222 | 1.12 (0.58-2.16) p = 0.548 | 0.90 (0.78-1.04) p = 0.099 | 0.94 (0.65-1.35) p = 0.538 |
| $FFM_C$ (allometric) | 0.87 (0.75-1.01) p = 0.062 | 1.06 (0.55-2.04) p = 0.765 | 0.84 (0.73-0.97) p = 0.034 | 0.94 (0.65-1.36) p = 0.571 |
| $FFM_J$ (linear scaling) | 0.97 (0.84-1.12) p = 0.525 | 1.15 (0.60-2.20) p = 0.481 | 0.92 (0.80-1.07) p = 0.173 | 0.97 (0.68-1.40) p = 0.787 |
| $FFM_J$ (allometric) | 0.90 (0.77-1.04) p = 0.100 | 1.07 (0.56-2.06) p = 0.703 | 0.86 (0.74-0.99) p = 0.045 | 0.98 (0.68-1.41) p = 0.814 |
| $PNWT_C$ (allometric) | 0.88 (0.76-1.02) p = 0.065 | 1.08 (0.56-2.08) p = 0.693 | 0.85 (0.74-0.99) p = 0.040 | 0.95 (0.66-1.36) p = 0.597 |
| $PNWT_J$ (allometric) | 0.87 (0.75-1.01) p = 0.057 | 1.07 (0.55-2.07) p = 0.716 | 0.85 (0.74-0.98) p = 0.038 | 0.93 (0.65-1.34) p = 0.504 |
| BSA (linear by BSA) | 0.85 (0.73-0.99) p = 0.043 | 1.04 (0.54-2.02) p = 0.814 | 0.83 (0.72-0.96) p = 0.027 | 0.86 (0.60-1.23) p = 0.225 |
| Between drug variability [a] | 7% | 28% | 7% | 16% |

$FCYF_{NNN}$: Ratio of group estimates for parameter NNN after accounting for body size (e. g. $FCYF_{CLT}$: group estimate of total clearance in CF-patients divided by group estimate of total clearance in healthy volunteers of the same body size).

[a]: Coefficient of variability for the between drug variability (BDV) of the disease specific scale factors (FCYF). As the BDV was similar between all size models, we estimated the pooled BDV across all size models.

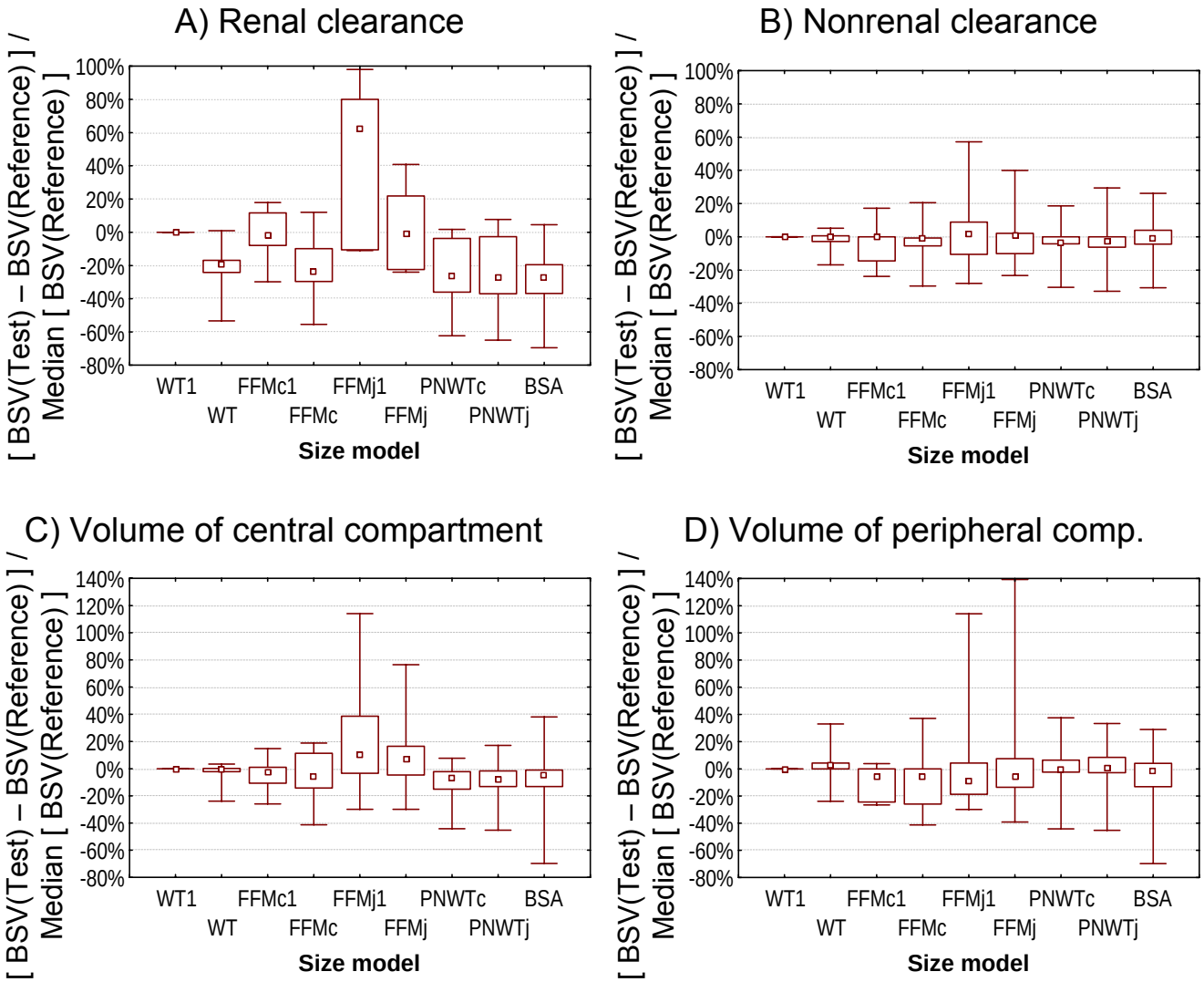


**Figure 3.5-2** Distribution of the reduction of unexplained BSV relative to linear scaling by WT (=reference) after accounting for the average difference between CF-patients and healthy volunteers.

Each box-whisker shows the median (marker), interquartile range (box), and minimum/maximum (whiskers) of all ten drugs. The BSV was expressed on variance scale for calculation. Note a negative value means that the respective size model is superior to linear scaling by WT (=reference).

The labels of the size models are: “None”: no size model; “WT1”: linear scaling by WT, “WT”: allometric scaling by WT, “FFMc1”: linear scaling by $FFM_C$, “FFMc”: allometric scaling by $FFM_C$, “FFMj1”: linear scaling by $FFM_J$, “FFMj”: allometric scaling by $FFM_J$, “PNWTc”: allometric scaling by $PNWT_C$, “PNWTj”: allometric scaling by $PNWT_J$, and “BSA”: linear scaling by BSA.

Table 3.5-5 shows the number of drugs for which the BSV in renal clearance was reduced or increased. The scaled unexplained BSVs relative to linear scaling by WT were split into five categories. Allometric scaling by $FFM_C$, $PNWT_C$, or $PNWT_J$ and linear scaling by BSA showed a reduction in the unexplained BSV in renal clearance by more than 25% for 5 of the 10 drugs and a reduction by 15-25% for 2 or 3 of the 10 drugs. The remaining 2 or 3 drugs had a comparable BSV for those four size models compared to linear scaling by WT. Interestingly, there was a trend that allometric scaling by WT, $FFM_C$ or $FFM_J$ was better than linear scaling by the respective size descriptors with regard to reducing the unexplained BSV in renal clearance.

**Table 3.5-5** Reduction of unexplained BSV in renal clearance relative to linear scaling by WT

The table shows the number of drugs in each of the five categories.

| **Category** | **Reduction by more than 25%** | **Reduction by 15 to 25%** | **Reduction by 15% to increase by 15%** | **Increase by 15 to 25%** | **Increase by more than 25%** |
|---|---|---|---|---|---|
| | *"best"* | *…* | *"unchanged"* | *…* | *"worst"* |
| WT (linear scaling) | | | 10 (reference) | | |
| WT (allometric) | 2 | 6 | 2 | | |
| $FFM_C$ (linear scaling) | 1 | 1 | 6 | 2 | |
| $FFM_C$ (allometric) | 5 | 2 | 3 | | |
| $FFM_J$ (linear scaling) | | | 3 | | 7 |
| $FFM_J$ (allometric) | | 3 | 4 | 1 | 2 |
| $PNWT_C$ (allometric) | 5 | 2 | 3 | | |
| $PNWT_J$ (allometric) | 5 | 2 | 3 | | |
| BSA (linear by BSA) | 5 | 3 | 2 | | |

Target concentrations and target effects can be achieved more precisely, if the unexplained BSV is reduced by a size model. The left data column ("best") of this table indicates the number of drugs with a reduction of unexplained BSV by more than 25%, the column in the middle ("unchanged") shows the number of drugs with a comparable BSV, and the right column ("worst") shows the number of drugs with an increase in unexplained BSV by more than 25%, all relative to linear scaling by WT.

### 3.5.4 Discussion

The life-expectancy and quality of life for CF-patients improved tremendously since the 1930s. The average life-expectancy of CF-patients was only a few months in the 1930s, whereas a diagnosed CF-patient in Denmark (141) had a chance of 83.3% to survive 40 years in 1995. There is an increased need for antibiotics to treat respiratory tract infections in CF-patients secondary to this improved life-expectancy and efficacious antibiotic treatment of CF-patients is vital. However, only a few new antibiotics have been introduced to the market during the last five years. This underlines the need for optimal antibiotic treatment with established agents. After choosing the most appropriate antibiotic, the dose and mode of administration can be optimized based on PKPD principles to yield the highest probability for successful treatment outcome (61, 107, 109, 113, 518). This meta-analysis focuses on the rationale for optimal selection of the administered dose in CF-patients from a PK point of view.

The current practice in dosing of CF-patients is dose selection based on WT (65, 105). CF-patients are often undernourished and have a paucity of adipose tissue. Some authors (323, 328, 390, 500, 501) have proposed dose selection based on $FFM_C$ which approximates LBM, because clearance and volume of distribution can be better predicted by $FFM_C$ compared to other measures of body size (e. g. WT or BSA). As most PK studies in CF-patients have a low sample size, a meta-analysis of several smaller studies is the method of choice to systematically compare various body size descriptors. A meta-analysis can greatly increase the accuracy, precision, and power of the comparison and can incorporate the uncertainty in the observed effect sizes, when multiple studies are combined. More importantly, the BDV can be estimated in a meta-analysis, i. e. clearance might be increased for one antibiotic and unchanged for another agent. Outlying results (e. g. for a specific drug) can be identified on a statistical basis. Meta-analyses in fields other than therapeutic benefits (including adverse events) have been claimed recently (18, 344).

Although the PK in CF-patients has been extensively reviewed (101, 249, 250, 389, 390, 408, 468, 499, 502), we are not aware of any meta-analyses which compared the PK between CF-patients and healthy volunteers. We combined in-house data from ten highly standardized studies in CF-patients, all including a healthy volunteer control group. The clinical study performance, drug analyses (all from a single laboratory), and the PK data analysis were very similar. Heterogeneity among the studies combined in this meta-analysis was therefore of no concern. As we used all available raw data, there was no publication bias in our meta-analysis.

One possible limitation of our analysis is that the individual studies were small. Therefore, it was not possible to identify the effect of disease state or other disease specific covariates on clearance and volume of distribution. However, the power to detect a clinically relevant difference of (e. g.) 20% in the disease specific scale factors (FCYFs) was >99% in our meta-analysis. Less than half of the PK studies in CF-patients reviewed by Touw et al. (502) included a control group of healthy volunteers and some authors compared study populations that were very heterogeneous with regard to age and body size. The demographic data of our CF-patients and healthy volunteers were comparable (see Table 3.5-1).

CF-patients were usually smaller than their healthy volunteer control groups. Consequently, most studies (389, 408, 499) find a lower unscaled total clearance and a lower unscaled volume of distribution in CF-patients. However, CF-patients often have higher clearances and volumes of distribution per kg WT (= linear scaling by WT in our analysis). Secondary to malnutrition, CF-patients are usually leaner than healthy volunteers and have a paucity of adipose tissue. Although it stands to reason to account for the altered body composition in dose selection, the possible benefits of dose selection by a size descriptor which accounts for body composition (e. g. $FFM_C$, $FFM_J$, $PNWT_C$, or $PNWT_J$) have not yet been systematically investigated on a statistical basis for CF-patients.

The differences in the average volume of distribution between CF-patients and healthy volunteers for hydrophilic drugs either vanish or become smaller (100, 132, 215, 251, 282, 286, 325, 361, 550) after adjusting for the

difference in body composition by FFM. Our results were in agreement with those reports. We could show for ten antibiotics that the ratio of size adjusted volume of distribution in CF-patients relative to healthy volunteers was between 0.99 and 1.04 for size models based on $FFM_C$, $FFM_J$, $PNWT_C$, or $PNWT_J$. Linear scaling by WT yielded a ratio of 1.06 (see Table 3.5-2). The BDV of this ratio was 12%. Consequently, an average volume of distribution expressed as L/kg WT which is reported to be more than about 30% (= 6% + 2 x 12%) higher in CF-patients relative to healthy volunteers might be specific to an antibiotic. Such increased volumes of distribution were reported for methicillin (+36%) (550), cloxacillin (+38%) (470), cefepime (+44%) (203), and ciprofloxacin (+62%) (75).

The differences in the average total clearance between CF-patients and healthy volunteers for several antibiotics (19, 98, 100, 132, 182, 183, 282, 286, 322) usually become smaller after accounting for body composition by FFM. We found a very similar total clearance (ratio of averages: 1.00 to 1.04) in CF-patients and healthy volunteers for allometric scaling by $FFM_C$, $FFM_J$, $PNWT_C$, or $PNWT_J$ (see Table 3.5-2). Linear scaling by WT predicted total clearance to be 15% higher (p=0.013) in CF-patients. The BDV of this ratio was 14%. Therefore, if total clearance expressed as L/h/kg is found to be more than about 43% (15% + 2 x 14%) higher in CF-patients, this points to possible drug specific mechanisms. Higher clearances in CF-patients were reported for dicloxacillin (+197% after oral dose, renal clearance: 282 $\pm$ 135 mL/min/1.73 $m^2$ in CF-patients vs. 95 $\pm$ 28 mL/min/1.73 $m^2$ in healthy volunteers) (241), cloxacillin (+114%, unit: L/h/kg WT after iv dose) (470), ceftazidime (+65%, unit: L/h/kg WT after iv dose) (282), ticarcillin (+50%, unit: L/h/1.73 $m^2$ BSA after iv dose) (100), and ciprofloxacin (+46%, unit: L/h/1.73 $m^2$ BSA after iv dose) (75).

*In vitro* data (484) suggest that P-glycoprotein might play a role in the increased renal tubular secretion in CF-patients secondary to increased P-glycoprotein expression, e. g. for dicloxacillin (241), trimethoprim (207), and ticarcillin (100). Wang et al. (526) find a Michaelis-Menten constant of 33.7$\pm$12.2 mg/L in CF-patients and of 77.6 $\pm$38.4 mg/L in healthy volunteers

and a similar maximal rate of renal tubular secretion of ticarcillin for both groups. Furthermore the disease state of CF-patients might complicate a comparison of PK data. CF-patients had a median survival age of 14 years in 1969 and of 31.3 years in 1996 in the US (12). Those data suggest that an average 15 year old CF-patient in the 1960s might not be well comparable to a 15 year old CF-patient in 2000. Although this is a possible reason for differences between the results of studies in CF-patients from the 1960s and e. g. in 2000, more studies about the effect of disease state on PK are required for CF-patients.

Heterogeneity between subject groups in age might play an important role. Our CF-patients were of similar age (21 ± 3.6 yrs vs. 25 ± 3.5 yrs, see Table 3.5-1) and had a 27% lower WT as well as a 22% lower $FFM_C$ and $FFM_J$ compared to our healthy volunteers. Although those differences in age and WT were rather small, we found consistently for WT, $FFM_C$ and $FFM_J$ that allometric scaling yielded disease specific scale factors closer to 1.0 than linear scaling by the respective size descriptor (see Table 3.5-2). More importantly, the unexplained BSV in renal clearance was more reduced by allometric scaling than by linear scaling for those three size descriptors.

After adjusting for body size and body composition, we found similar total clearances ($FCYF_{CLT}$ between 1.00 and 1.04) and volumes of distribution at steady-state ($FCYF_V$ between 0.99 and 1.04) in CF-patients and healthy volunteers for allometric scaling by $FFM_C$, $FFM_J$, $PNWT_C$, or $PNWT_J$ (see Table 3.5-2). The BDV of the disease specific scale factors $FCYF_{CLT}$ and $FCYF_V$ was only 12-14%. For those four size models, the vast majority of the $FCYF_{CLT}$ and $FCYF_V$ for the ten drugs were within 80-125% (see Figure 3.5-1, panels A and B).

We observed an 8-12% higher renal clearance in CF-patients compared to healthy volunteers for allometric scaling by $FFM_C$, $FFM_J$, $PNWT_C$, or $PNWT_J$ (see Table 3.5-2). We observed similar results for renal clearance in our subgroup analyses for beta-lactams (see Table 3.5-3) and quinolones (see Table 3.5-4). Possible reasons for the slightly higher renal clearances in CF-patients are disease specific changes like glomerulomegaly (2) and a 50% increased kidney weight (515), an increased urine flow rate

(389), an up to 30% increased glomerular filtration rate (mL/min/1.73 $m^2$) (182, 183, 390, 469, 526), and a 16% increased resting energy expenditure. The latter might be due to a higher energy need secondary to chronic lung infection (514). However, our data only showed a slightly higher renal clearance in CF-patients after adjusting for body size and body composition.

Allometric scaling by $FFM_C$, $FFM_J$, $PNWT_C$, or $PNWT_J$ resulted in very similar (±2%) average nonrenal clearances for beta-lactams in both subject groups (see Table 3.5-3). Those four allometric size models showed an about 15% lower average nonrenal clearance in CF-patients for quinolones (see Table 3.5-4). Pathophysiological changes like fatty liver (82), focal biliary cirrhosis, and disturbed bile acid metabolism leading to increased biliary excretion (135) are very common in CF-patients. Indocyanine green clearance as a marker for hepatic blood flow is increased by 56% (unit: L/h/kg WT) (250) in CF-patients and specific phase I and phase II metabolic pathways are enhanced (408). Although those alterations have been reported for CF-patients, we found similar to slightly lower nonrenal clearances in both subject groups in our analysis.

With regard to dose selection, we could show that CF-patients had a 15% higher average total clearance per kg WT for our ten drugs. The BDV of $FCYF_{CLT}$ was 14% (see Table 3.5-2). Therefore, CF-patients would achieve the same average drug concentration at steady-state, if they received a 15% (±14% BDV) higher dose on a mg/kg WT basis compared to doses which would be required based on healthy volunteer data. If the average drug concentration at steady-state was most relevant for therapeutic success, this procedure would account for the average difference between CF-patients and healthy volunteers from a PK perspective.

However, CF-patients often receive much higher doses than other patients for reasons other than PK e. g. in early aggressive treatment of *P. aeruginosa* (105, 389). In empiric therapy, doses are usually selected on a mg/kg WT basis to achieve the required target concentration. If a new size descriptor allowed one to achieve target concentrations more precisely, this size descriptor would be ultimately superior to the current standard. Achieving

target concentrations and effects more precisely requires a size descriptor to reduce the unexplained fraction of the BSV in clearance (and volume of distribution) after adjusting for the average differences in PK parameters.

We found several size models which reduced the unexplained BSV in renal clearance compared to linear scaling by WT for about eight of our ten antibiotics. Those models comprise allometric scaling by WT, $FFM_C$, $PNWT_C$, or $PNWT_J$ and linear scaling by BSA (see also Table 3.5-5). The median reduction of unexplained BSV in renal clearance was between 20 and 27% for those five size models and none of the 10 drugs had an increase in unexplained BSV by more than 15%. Although $FFM_C$ and $FFM_J$ are similar size descriptors and yielded virtually identical results for the FCYFs, we did not find a reduction of unexplained BSV in renal clearance for $FFM_J$. It is difficult to explain this observation, as we found very similar results for $PNWT_C$ and $PNWT_J$ which are based on $FFM_C$ and $FFM_J$, respectively. Further data are required to compare $FFM_C$ and $FFM_J$.

Allometric scaling by WT reduced the unexplained BSV in renal clearance to a similar extent as $FFM_C$, $PNWT_C$, and $PNWT_J$. However, we believe that using $FFM_C$, $PNWT_C$, or $PNWT_J$ is physiologically more plausible than using WT, because $FFM_C$, $PNWT_C$, or $PNWT_J$ account for differences in body composition, whereas WT and BSA (332) do not account for body composition. We expect allometric scaling by $FFM_C$, $PNWT_C$, or $PNWT_J$ to be especially superior to WT and BSA for the very undernourished CF-patients. More studies are required to compare those size descriptors in larger trials. The little extra effort to calculate $FFM_C$, $PNWT_C$, or $PNWT_J$ based on sex, weight, and height seems justified by the benefit of achieving target concentrations more precisely. Incorporating an allometric factor in dose calculations can be easily done by use of a reference table or chart.

In conclusion, we could show for seven beta-lactams and three quinolones that the average total clearance and volume of distribution were well comparable between CF-patients and healthy volunteers after accounting for body size and body composition by allometric scaling with $FFM_C$, $FFM_J$, $PNWT_C$, or $PNWT_J$. The BDV of the ratio of average total clearance and volume of distribution between both subject groups was small (12-14%).

Allometric scaling by $FFM_C$, $PNWT_C$, or $PNWT_J$ reduced the unexplained BSV in renal clearance by 24 to 27% relative to linear scaling by WT. This reduction of unexplained BSV allows one to achieve target concentrations and target effects more precisely. The superiority of dose selection based on $FFM_C$, $PNWT_C$, or $PNWT_J$ needs to be shown clinically. More studies are required to investigate the effect of disease severity on the PK in CF-patients.

## 3.6 Comparison of PKPD profiles in CF-patients and healthy volunteers – implications for optimization of dosage regimens

### 3.6.1 Background on the effect of covariates on the PKPD profiles

The effect of body size, body composition, and presence or absence of CF has been shown to be important for the PK in CF-patients (see chapter 3.5). Although the average differences in PK between CF-patients and healthy volunteers were small in the meta-analysis of our ten antibiotics (see Figure 3.5-1 and Table 3.5-2), it is still important to account for drug specific differences for optimization of dosage regimens for an individual antibiotic. CF-patients span a wide range in body size. Dosage regimens achieving a high probability of successful treatment in adult CF-patients with an FFM of 50kg and above might not be optimal for smaller CF-patients. It is therefore important to assess the PKPD profiles of CF-patients with a specific body size.

Therefore, our first objective was to systematically compare the difference in PKPD profiles between CF-patients and healthy volunteers for short-term, prolonged, and continuous infusion for our five intravenous beta-lactams. Importantly, these MCS used the covariates of the CF-patients and healthy volunteers in our studies. A slower rate of oral absorption in CF-patients caused higher PKPD breakpoints in CF-patients relative to healthy volunteers for oral cefaclor and cefadroxil and our PKPD breakpoints for oral ciprofloxacin in CF-patients were low. Therefore, the PKPD profiles of these oral antibiotics will not be discussed in this chapter. As our second objective, we systematically studied the reason for the differences in PKPD breakpoints between CF-patients and healthy volunteers by MCS for CF-patients of specific body size. Our third objective was to develop and evaluate formulas for dose selection of beta-lactams to achieve the same $fT_{>MIC}$ for patients with various body size. Additionally, we explored dosage regimens which possibly achieve higher PKPD breakpoints than continuous infusion.

### 3.6.2 Methods

We used the final population PK models for our five intravenous beta-lactams described in chapter 3.3 (see Table 3.3-3, Table 3.3-9, Table 3.3-15, Table 3.3-21, and Table 3.3-27). Our MCS in this chapter were based on at least 2,500 simulated subjects for each PTA vs. MIC profile.

#### 3.6.2.1 MCS for the CF-patients and healthy volunteers with the same demographic data as the subject in our studies

We derived the PTA vs. MIC profiles and the PKPD breakpoints for CF-patients and healthy volunteers with the same demographic data as the CF-patients and healthy volunteers in our respective study. Doses were selected either as mg/kg WT or by an allometric model based on FFM. We derived the following formula for dose selection from the allometric equation of scaling clearance with body size shown in chapter 1.5. This formula for allometric dose selection by FFM aims at achieving a constant average AUC in subjects with various FFM [$Dose_{STD}$: standard dose, $FFM_{STD}$: standard FFM, $FFM_i$ is FFM of the $i^{th}$ subject, and $Dose(FFM_i)$ is the dose for a subject with $FFM_i$]:

*Formula for "constant AUC dosing" based on an allometric model with FFM:*

$$Dose(FFM_i) = Dose_{STD} \cdot \left( \frac{FFM_i}{FFM_{STD}} \right)^{0.75} \qquad \text{Formula 3.6-1}$$

Figure 3.6-1 shows a flow chart of the simulation plan for our systematic comparison of PKPD breakpoints between CF-patients and healthy volunteers. We studied two methods of dose selection and three dosage regimens (six combinations in total).

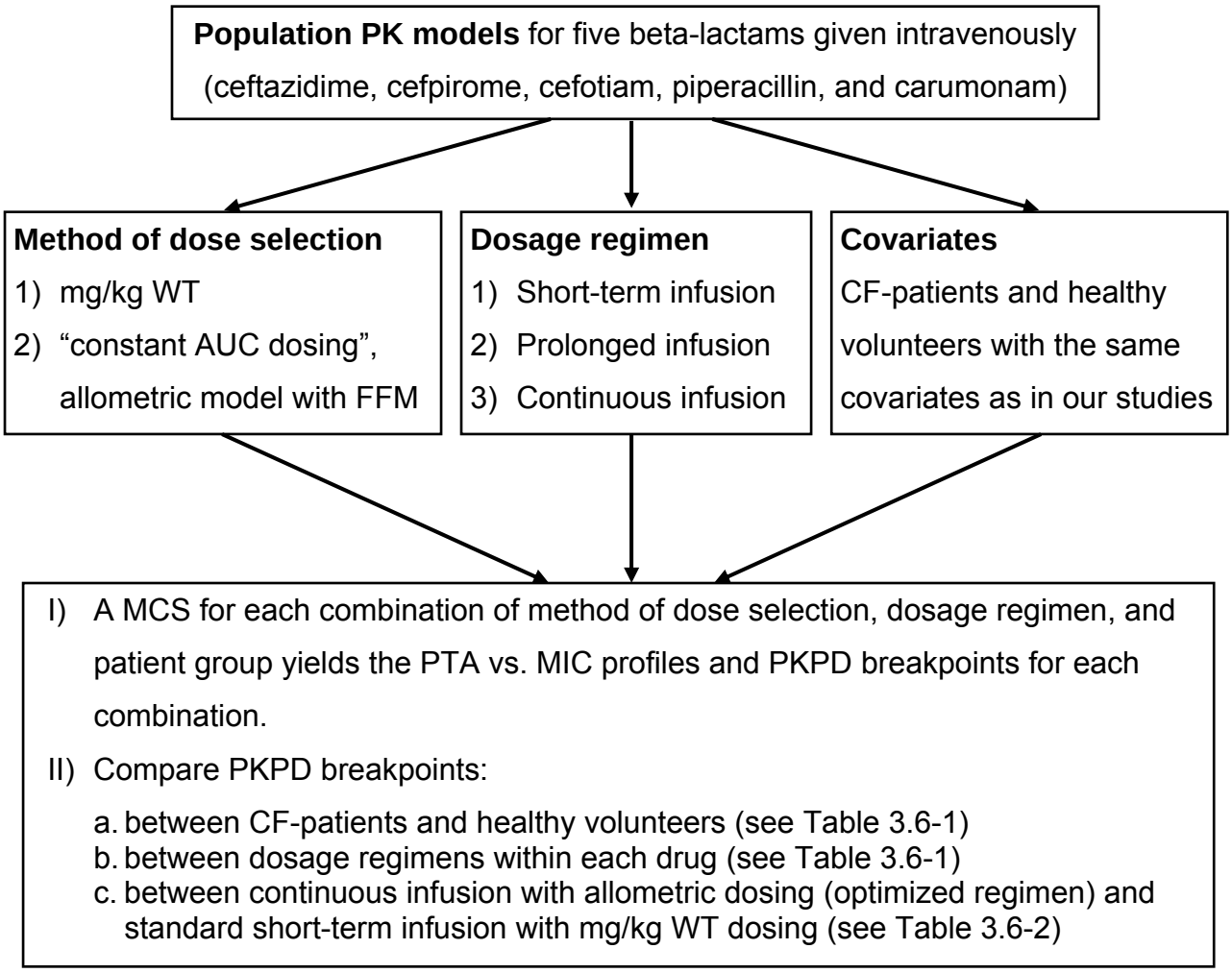


**Figure 3.6-1** Schematic for the MCS of our five intravenous beta-lactams based on the covariates of the CF-patients and healthy volunteers in the respective study

### 3.6.2.2 Effect of body size on the PTA vs. MIC profiles in CF-patients – influence of allometric theory on optimal dose selection

We found considerable evidence that allometric scaling of clearance and volume of distribution by body size is more appropriate than linear scaling for our ten studies in CF-patients and healthy volunteers (see chapter 3.5). Allometric scaling by $FFM_C$, $PNWT_C$, or $PNWT_J$ resulted in more similar average clearances between CF-patients and healthy volunteers compared to linear scaling by WT (see Table 3.5-2). Additionally, the unexplained BSV in renal clearance was about 20-27% lower for allometric scaling by WT, $FFM_C$,

$PNWT_C$, or $PNWT_J$ relative to linear scaling by WT (Figure 3.5-2 and Table 3.5-5). Overall, this is evidence that applying an allometric size model is more reasonable than a linear size model for our MCS.

Figure 3.6-2 shows clearance, volume of distribution, and elimination half-life as a function of WT for linear and allometric scaling. For simplicity, it was assumed that all subjects have the same body composition (i. e. WT and FFM were assumed to be directly proportional, FFM = 0.757 · WT). Allometric scaling predicts that a subject with WT 30kg has a 19% shorter elimination half-life relative to a subject with WT 70kg. A subject with WT 15kg has a 32% shorter average elimination half-life relative to a subject with WT 70kg.

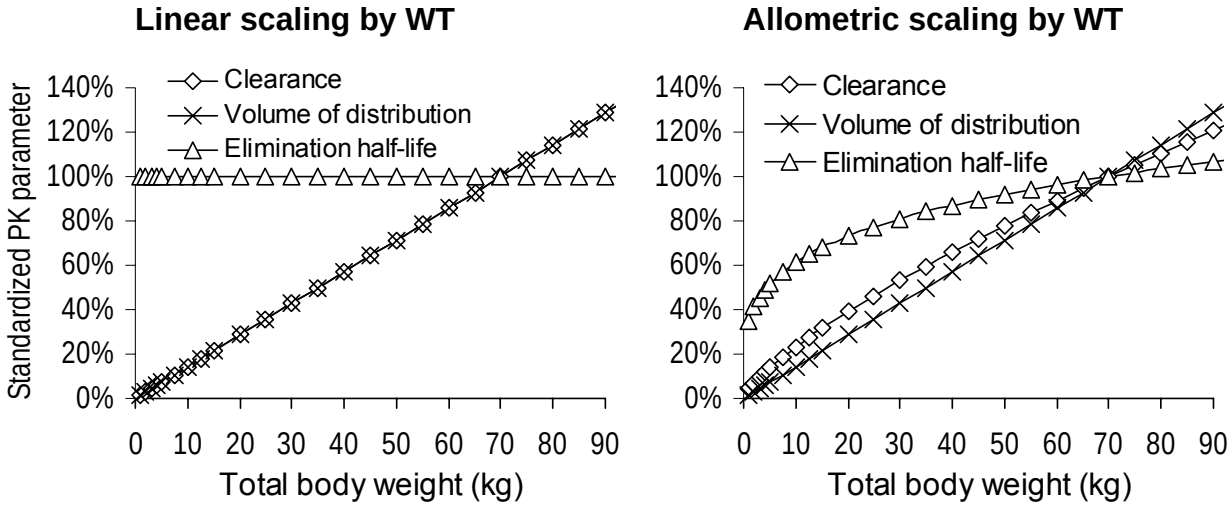


**Figure 3.6-2** Comparison of linear and allometric scaling. The plot shows clearance, volume of distribution, and elimination half-life standardized to their value for a normal subject with WT 70 kg.

The elimination half-life is the most important determinant for the $fT_{>MIC}$ of a short-term infusion, since the average elimination half-life of many beta-lactams is between 1 and 3h. For a drug with a 2h half-life, plasma concentrations are falling for about four half-lives during an 8h dosing interval which corresponds to a decline by a factor of 16. Therefore, differences in elimination half-lives as a function of body size need to be considered for dose selection of short-term infusions, if one likes to achieve the same $fT_{>MIC}$ in subjects of various body size.

For continuous infusion, unbound clearance is the only PK parameter which determines the average non-protein bound plasma concentration at steady-state and also the $fT_{>MIC}$. Therefore, differences in unbound clearance need to be considered for dose selection of continuous infusions. As shown above, a formula which yields constant average plasma concentrations at steady-state as a function of body size can be derived from the allometric equation for clearance.

The situation is more difficult for prolonged infusion. To the best of my knowledge, there are no reports on the optimal method of dose selection for beta-lactams (most important PKPD statistics: $fT_{>MIC}$) for prolonged infusion. As a simplification, we applied the formula for “constant AUC dosing” for prolonged infusion. Importantly, dose selection as mg/kg WT or mg/kg FFM neither account for the difference in elimination half-life nor for the difference in clearance between subjects of various body size for an allometric model.

We developed a new equation for dose selection to achieve similar $fT_{>MIC}$ values for a range of FFMs. This formula was qualified by MCS based on the final population PK models for our five intravenous beta-lactams. This new equation is a simplified formula based on a one-compartment model with intravenous bolus administration.

*Required dose to achieve a constant average $fT_{>MIC}$ for an iv bolus dose:*

$$\mathrm{Dose}(\mathrm{FFM_i}) = \mathrm{Dose_{STD}} \frac{\mathrm{FFM_i}}{\mathrm{FFM_{STD}}} \exp\left\{ \frac{\%\mathrm{target} \cdot \mathrm{Tau} \cdot \ln(2)}{\mathrm{half\text{-}life_{STD}}} \cdot \left[ \left( \frac{\mathrm{FFM_{STD}}}{\mathrm{FFM_i}} \right)^{0.25} - 1 \right] \right\}$$

Formula 3.6-2

$\mathrm{Dose_{STD}}$ is the standard dose for a subject with a standard FFM ($\mathrm{FFM_{STD}}$). $\mathrm{FFM_i}$ is FFM of the $i^{th}$ subject and $\mathrm{Dose(FFM_i)}$ is the dose for a subject with $\mathrm{FFM_i}$. %target is the PKPD target, Tau is the dosing interval, and $\mathrm{half\text{-}life_{STD}}$ is the typical half-life of a subject with $\mathrm{FFM_{STD}}$. We used an $\mathrm{FFM_{STD}}$ of 53kg in our MCS and assumed a constant body composition for CF-patients with various FFM. We assumed that FFM equals 75.7% of WT (i. e. an FFM of 53kg corresponds to a WT of 70kg). The median terminal half-life from NCA was used as $\mathrm{half\text{-}life_{STD}}$ in the equation above.

Our simulation plan for a systematic assessment of the optimal mode of dose selection in CF-patients of various body size is shown in Figure 3.6-3.

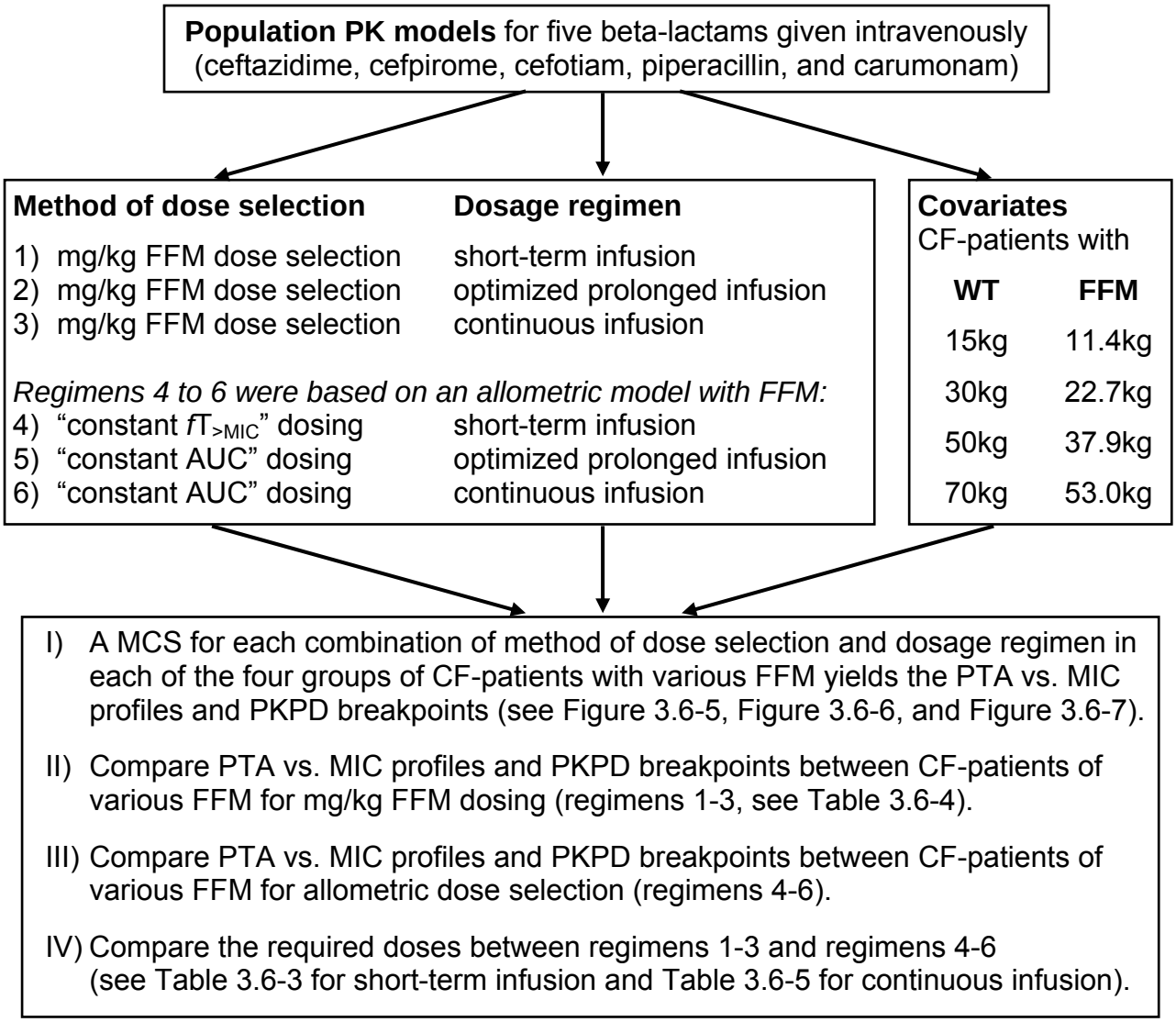


**Figure 3.6-3** Schematic for the MCS of our five intravenous beta-lactams for CF-patients of various FFM

### 3.6.2.3 Evaluation of a loading dose plus prolonged infusion dosage regimens

Figure 3.6-4 compares the plasma concentration time profiles of 2g ceftazidime in healthy volunteers at steady-state. The continuous infusion achieved a steady-state concentration of 37.4 mg/L. The time above this concentration is shown for each prolonged infusion.

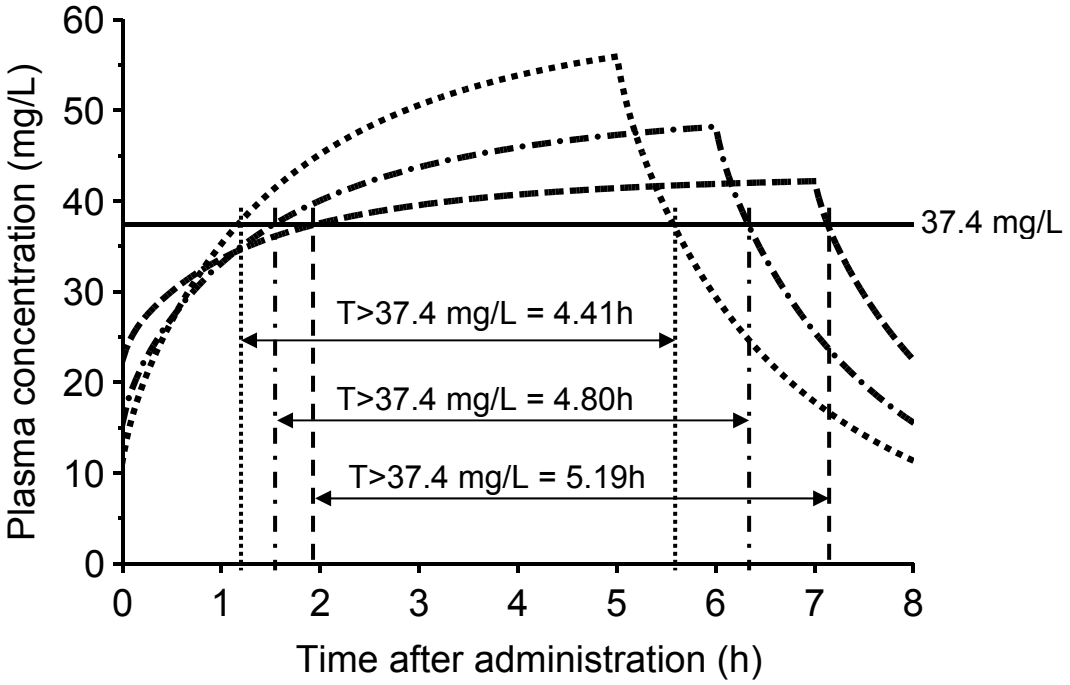


**Figure 3.6-4** Typical plasma concentration time profiles of ceftazidime in healthy volunteers with 70kg total body weight at steady-state. The dose was 2g ceftazidime q8h as 5h infusion, 6h infusion, 7h infusion, or continuous infusion.

The PKPD target for ceftazidime for near-maximal bacterial killing is about 65% $fT_{>MIC}$. In order to achieve higher PTAs than a continuous infusion for this target, it would be appreciable to achieve a concentration of 37.4 mg/L quickly and to maintain this concentration for the duration of the PKPD target, i. e. for 5.2h in this example (65% of an 8h dosing interval). If one prolongs the duration of infusion from 5h to 7h, both the time to reach 37.4 mg/L and the time of declining below 37.4 mg/L are shifted towards later time points (see Figure 3.6-4). Therefore, optimized prolonged infusions achieved about the same PTA vs. MIC profiles and PKPD breakpoints as continuous infusions.

As an alternative to prolonged and continuous infusion regimens, we studied the combination of a small loading dose to be followed by a prolonged infusion for the duration of the PKPD target. Importantly, this small loading dose is given at the beginning of each 8h dosing interval. In theory, such a loading dose + prolonged infusion regimen would achieve the highest PKPD breakpoint with the shortest duration of infusion. To estimate the possible

clinical advantage of the loading dose plus prolonged infusion regimens, we calculated the PTA expectation values for various MIC distributions for ceftazidime from the 2002 MYSTIC program in North America (273) and from the 2000 MYSTIC program in Europe in CF-patients (158).

### 3.6.3 Results

#### 3.6.3.1 PKPD breakpoints in CF-patients and healthy volunteers

The PKPD breakpoints for various dosage regimens of our five studied intravenous beta-lactams are shown in Table 3.6-1. For dose selection as mg/kg WT, the ratio of breakpoints in CF-patients and healthy volunteers was 0.5 [0.33 - 1.0] for the 0.5h infusion regimens and 0.75 [0.5 - 1.0] for the continuous infusion regimens (median [range]). CF-patients had lower PKPD breakpoints than healthy volunteers for dose selection as mg/kg WT, because CF-patients had (slightly) higher total clearances compared to healthy volunteers after size adjustment with linear scaling by WT (see Table 3.5-3).

Allometric scaling by FFM achieved similar clearances and volumes of distribution in CF-patients and healthy volunteers as shown in Table 3.5-3. Therefore, ratios of PKPD breakpoints slightly closer to 1.0 were achieved for “constant AUC” dosing based on the allometric model with FFM. The median [range] ratio was 0.67 [0.50 - 1.0] for 0.5h infusion and 1.0 [0.67 - 1.0] for continuous infusion (see Table 3.6-1).

**Table 3.6-1** PKPD breakpoints in CF-patients and healthy volunteers for dosing as mg/kg WT and for "constant AUC" dosing based on an allometric model with FFM

| Daily Dose | Infusion Duration | Interval | CF-patients / healthy volunteers: Dosing as mg/kg WT ($WT_{STD}$ = 70kg) | CF-patients / healthy volunteers: "Constant AUC" dosing allometric model by FFM ($FFM_{STD}$: 53kg) [a] |
|---|---|---|---|---|
| **Carumonam** | | | Breakpoints (mg/L) for the target $fT_{>MIC} \geq 60\%$ | |
| 6g/70kg | 0.25h | q8h | 3 / 6 | 4 / 8 |
| | 4h | q8h | 8 / 16 | 16 / 24 |
| | 24h | q24h | 16 / 16 | 16 / 24 |
| **Cefotiam** | | | Breakpoints (mg/L) for the target $fT_{>MIC} \geq 65\%$ | |
| 6g/70kg | 0.5h | q8h | 0.047 / 0.047 | 0.0625 / 0.0625 |
| | 5h | q8h | 1.5 / 2 | 2 / 3 |
| | 24h | q24h | 3 / 3 | 3 / 4 |
| **Cefpirome** | | | Breakpoints (mg/L) for the target $fT_{>MIC} \geq 65\%$ | |
| 4g/70kg | 0.5h | q12h | 1.5 / 2 | 1.5 / 2 |
| | 0.5h | q8h | 3 / 4 | |
| | 5h | q12h | 4 / 6 | 6 / 6 |
| | 5h | q8h | 8 / 12 | |
| | 24h | q24h | 12 / 16 | 16 / 16 |
| **Ceftazidime** | | | Breakpoints (mg/L) for the target $fT_{>MIC} \geq 65\%$ | |
| 6g/70kg | 0.5h | q8h | 1 / 3 | 2 / 4 |
| | 0.5h | q6h | 2 / 4 | |
| | 5h | q8h | 8 / 16 | 12 / 16 |
| | 4h | q6h | 12 / 16 | |
| | 24h | q24h | 12 / 16 | 16 / 16 |
| **Piperacillin** | | | Breakpoints (mg/L) for the target $fT_{>MIC} \geq 50\%$ | |
| 12g/70kg | 0.5h | q6h | 3 / 6 | 4 / 6 |
| | 3h | q6h | 16 / 24 | 24 / 24 |
| | 24h | q24h | 16 / 24 | 24 / 24 |

[a]: Doses were selected to achieve a constant average AUC for all values of FFM based on an allometric size model.

PKPD breakpoints were recorded with a step size of 1.5.

***Optimization of PKPD profiles:*** If one likes to increase the $fT_{>MIC}$ at the same daily dose, there are two possibilities: 1) Choosing a shorter dosing interval and splitting the same daily dose e. g. into four instead of three doses. 2) Using a longer duration of infusion (e. g. continuous or prolonged infusion instead of short-term infusion). Both options increase the PKPD breakpoint. As shown in Table 3.6-1 for the 0.5h infusion regimens, PKPD breakpoints were about twice as high for dosing 1.33 g cefpirome q8h compared to dosing 2 g cefpirome q12h. PKPD breakpoints were also about twice as high for dosing 1.5 g ceftazidime q6h compared to dosing 2 g ceftazidime q8h.

Compared to this moderate increase in PKPD breakpoints by a factor of about two for shorter dosing intervals and short-term infusions, a longer duration of infusion achieved a much larger increase in PKPD breakpoints. Table 3.6-2 compares the PKPD breakpoints for standard short-term infusion and mg/kg WT to the breakpoints for continuous infusion and “constant AUC” dose selection based on an allometric model for CF-patients (panel A) and healthy volunteers (panel B). The optimized dosage regimens achieved an increase in PKPD breakpoints by a factor of 11 [5.3-64] for CF-patients and by a factor of 5.3 [4.0-85] for healthy volunteers (median [range]).

We found in additional simulations that the duration of infusion which achieves the highest PKPD breakpoint is slightly longer than the dosing interval multiplied by the PKPD target. Thus, for an 8h dosing interval and a target of 65%, the optimal duration of infusion is slightly longer than 5.2h. The exact solution for the optimal duration of infusion depends on the specific characteristics of each beta-lactam. Importantly, prolonged infusions with an optimized duration achieved similar PKPD breakpoints compared to continuous infusion, as shown in Table 3.6-1 for cefotiam, cefpirome, ceftazidime, and piperacillin.

**Table 3.6-2** Increase in PKPD breakpoints for continuous infusion and "constant AUC" dosing based on an allometric model with FFM compared to standard short-term infusion and mg/kg WT dosing

The PKPD target for near-maximal bactericidal effect was used for all breakpoints. Dosage regimens were the same as shown in Table 3.6-1.

**Panel A:** PKPD breakpoints for CF-patients

| | **Standard regimen** Short-term intermittent infusion and mg/kg WT dosing | **Optimized regimen** Continuous infusion and "constant AUC" dose selection by the allometric model | **Ratio** optimized / standard |
|---|---|---|---|
| Carumonam | 3 mg/L | 16 mg/L | 5.3 |
| Cefotiam | 0.047 mg/L | 3 mg/L | 64 |
| Cefpirome | 1.5 mg/L | 16 mg/L | 11 |
| Ceftazidime | 1 mg/L | 16 mg/L | 16 |
| Piperacillin | 3 mg/L | 24 mg/L | 8.0 |
| | | **Median** | **11** |
| | | Min | 5.3 |
| | | Max | 64 |

**Panel B:** PKPD breakpoints for healthy volunteers

| | **Standard regimen** Short-term intermittent infusion and mg/kg WT dosing | **Optimized regimen** Continuous infusion and "constant AUC" dose selection by the allometric model | **Ratio** optimized / standard |
|---|---|---|---|
| Carumonam | 6 mg/L | 24 mg/L | 4.0 |
| Cefotiam | 0.047 mg/L | 4 mg/L | 85 |
| Cefpirome | 2 mg/L | 16 mg/L | 8.0 |
| Ceftazidime | 3 mg/L | 16 mg/L | 5.3 |
| Piperacillin | 6 mg/L | 24 mg/L | 4.0 |
| | | **Median** | **5.3** |
| | | Min | 4.0 |
| | | Max | 85 |

### 3.6.3.2 Allometric dose selection to achieve the same $fT_{>MIC}$

***For intermittent short-term infusion:*** We calculated the doses required to achieve the same $fT_{>MIC}$ for short-term infusion based on our new equation and evaluated these doses by MCS. These doses are summarized in Table 3.6-3. The third column shows the standard dose for mg/kg FFM dose selection (linear model) and the other columns show the doses predicted from our new equation. Importantly, the doses to achieve a constant $fT_{>MIC}$ were much higher than the doses calculated as mg/kg FFM, especially for the WT=15kg and WT=30kg group.

**Table 3.6-3** Doses of short-term infusions for the MCS in CF-patients with WT 15kg, 30kg, 50kg, or 70kg

| | | | Carumonam | Ceftazidime | Cefpirome | Cefotiam | Piperacillin |
|---|---|---|---|---|---|---|---|
| | | Dosing interval | q8h | q8h | q12h | q8h | q6h |
| | | $fT_{>MIC}$ Target | 60% | 65% | 65% | 65% | 50% |
| | | $t_{1/2,STD}$ | 2.0h | 1.48h | 2.07h | 0.931h | 0.69h |
| WT (kg) | FFM (kg) | Standard dose as mg/kg FFM | Allometric dose to achieve a constant $fT_{>MIC}$ | | | | |
| | | | Carumonam | Ceftazidime | Cefpirome | Cefotiam | Piperacillin |
| 15 | 11.4 | 0.43g | 0.94g | 1.35g | 1.46g | 2.64g | 1.77g [a] |
| 30 | 22.7 | 0.86g | 1.27g | 1.52g | 1.59g | 2.14g | 1.75g [a] |
| 50 | 37.9 | 1.43g | 1.65g | 1.77g | 1.80g | 2.01g | 1.86g [a] |
| 70 | 53.0 | 2.00g | 2.00g | 2.00g | 2.00g | 2.00g | 2.00g [a] |

[a]: A standard dose of 2g instead of 3g (as shown in Figure 3.6-5) is reported in this table to keep the numbers comparable to the other four drugs.

Figure 3.6-5 shows that CF-patients with various FFM achieved considerably different PTAs for dose selection as mg/kg FFM (left side). Dose selection based on our new equation with allometric dose selection by FFM to achieve the same $fT_{>MIC}$ yielded very similar PTA vs. MIC profiles for short-term infusions of all five studied beta-lactams.

## Dose selection as mg/kg FFM

**Carumonam** (target: $fT_{>MIC} \geq 60\%$)
0.25h infusion of 2g/53kg FFM q8h

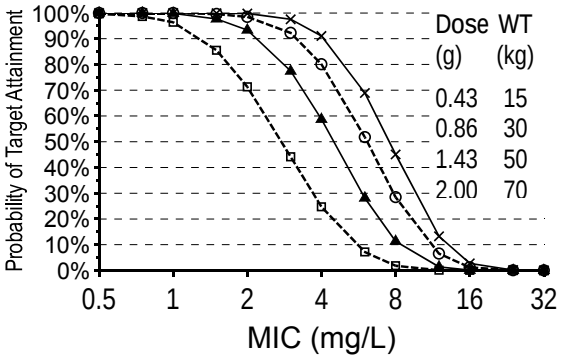


**Ceftazidime** (target: $fT_{>MIC} \geq 65\%$)
0.5h infusion of 2g/53kg FFM q8h

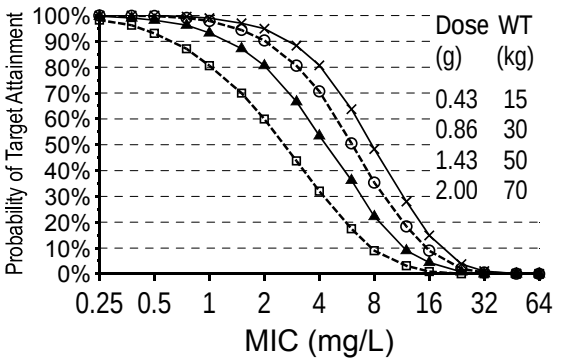


**Cefpirome** (target: $fT_{>MIC} \geq 65\%$)
0.5h infusion of 2g/53kg FFM q12h

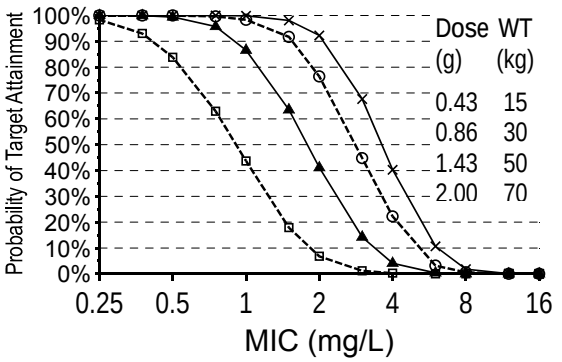


## Same $fT_{>MIC}$ dosing by an allometric model with FFM

**Carumonam** (target: $fT_{>MIC} \geq 60\%$)
0.25h infusion of 2g for 53kg FFM q8h

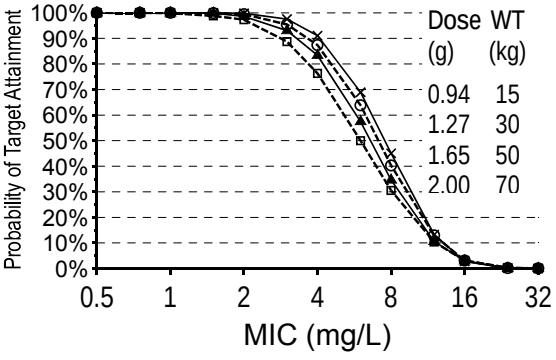


**Ceftazidime** (target: $fT_{>MIC} \geq 65\%$)
0.5h infusion of 2g for 53kg FFM q8h

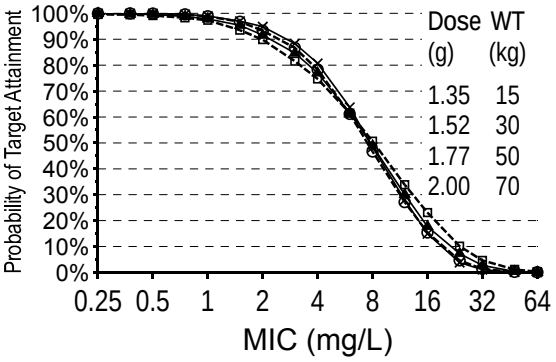


**Cefpirome** (target: $fT_{>MIC} \geq 65\%$)
0.5h infusion of 2g for 53 kg FFM q12h

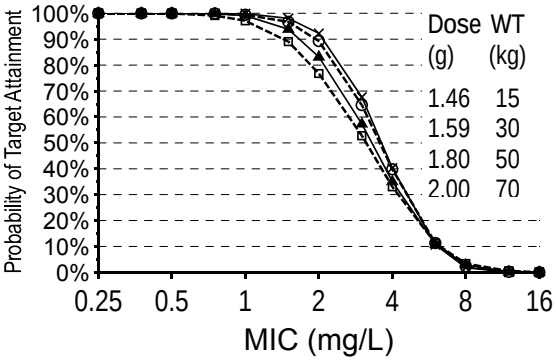


**Figure 3.6-5** Comparison of PTA vs. MIC profiles of short-term infusions for groups of CF-patients with various FFM (FFM was assumed to be 76% of WT for all groups of CF-patients)

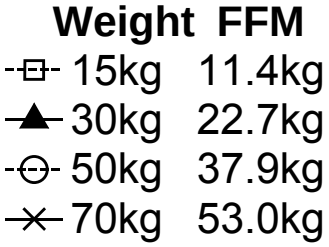

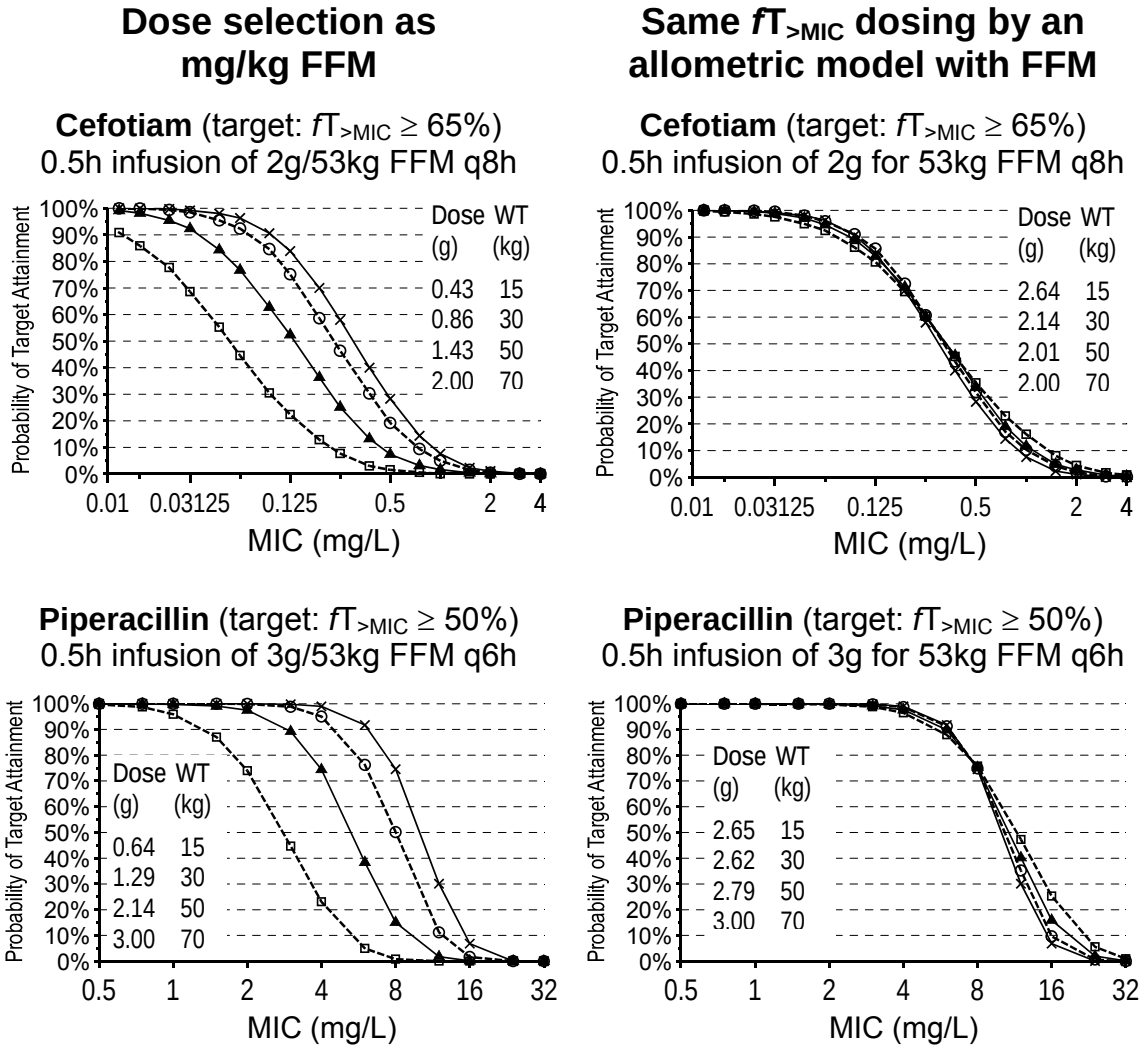


**Figure 3.6-5** Comparison of PTA vs. MIC profiles of short-term infusions for groups of CF-patients with various FFM (FFM was assumed to be 76% of WT for all groups of CF-patients) (continued)

Table 3.6-4 summarizes the PKPD breakpoints for CF-patients of various body size for the dosage regimens shown in Figure 3.6-5. The median [range] ratio of PKPD breakpoints relative to the WT=70kg group for dose selection as mg/kg FFM was 0.19 [0.12-0.25] for the WT=15kg group, 0.50 [0.33-0.50] for the WT=30kg group, and 0.75 [0.67-1.00] for the WT=50kg (see Table 3.6-4). On the contrary, PKPD breakpoints were virtually identical in all groups for allometric dosing to achieve the same $fT_{>MIC}$.

**Table 3.6-4** PKPD breakpoints for CF-patients with various WT (FFM) for short-term infusions and dose selection by mg/kg FFM

| | Standard dose for WT=70kg FFM=53kg | **PKPD breakpoint (mg/L)** *Total body weight* | | | | **Ratio relative to 70kg** *Total body weight* | | | |
|---|---|---|---|---|---|---|---|---|---|
| | | *15kg* | *30kg* | *50kg* | *70kg* | *15kg* | *30kg* | *50kg* | *70kg* |
| Carumonam | 2g q8h | 1 | 2 | 3 | 4 | 0.25 | 0.50 | 0.75 | 1.00 |
| Ceftazidime | 2g q8h | 0.5 | 1 | 2 | 2 | 0.25 | 0.50 | 1.00 | 1.00 |
| Cefpirome | 2g q12h | 0.375 | 0.75 | 1.5 | 2 | 0.19 | 0.38 | 0.75 | 1.00 |
| Cefotiam | 2g q8h | 0.012 | 0.031 | 0.063 | 0.094 | 0.12 | 0.33 | 0.67 | 1.00 |
| Piperacillin | 3g q6h | 1 | 3 | 4 | 6 | 0.17 | 0.50 | 0.67 | 1.00 |
| | | | | | **Median** | **0.19** | **0.50** | **0.75** | **1.00** |
| | | | | | Minimum | 0.12 | 0.33 | 0.67 | 1.00 |
| | | | | | Maximum | 0.25 | 0.50 | 1.00 | 1.00 |

***For continuous and prolonged infusion:*** The doses for linear dose selection as mg/kg FFM and allometric dose selection according to the "constant AUC" formula based on an allometric model with FFM are shown in Table 3.6-5.

**Table 3.6-5** Doses of continuous and prolonged infusion for the MCS in CF-patients with WT 15kg, 30kg, 50kg, or 70kg

| WT (kg) | FFM (kg) | Dose as mg/kg FFM | Allometric dose to achieve the same AUC for all FFMs | Ratio of "allometric dose" and "mg/kg FFM dose" |
|---|---|---|---|---|
| 15 | 11.4 | 1.29g / day | 1.89g / day | 1.47 |
| 30 | 22.7 | 2.57g / day | 3.18g / day | 1.24 |
| 50 | 37.9 | 4.29g / day | 4.66g / day | 1.09 |
| 70 | 53.0 | 6.00g / day | 6.00g / day | 1.00 |

The doses required to achieve the same average AUC for various FFMs are only slightly higher than the mg/kg FFM doses. Achieving the same AUC for a continuous infusion will result in achieving the same $fT_{>MIC}$.

The PTA vs. MIC profiles showed some differences for dose selection as mg/kg FFM. PKPD breakpoints of continuous infusions differed by a factor of about 1.33 to 2 between the WT=70kg group and the WT=15kg group for dose selection as mg/kg FFM (see left column of Figure 3.6-6 and Figure 3.6-7). Constant AUC dose selection by an allometric model with FFM achieved very similar PTA vs. MIC profiles for all studied FFMs (see right column of Figure 3.6-6 and Figure 3.6-7). This was expected for continuous infusion, because the underlying population PK models were based on an allometric size model with FFM.

Figure 3.6-6 (see right column) shows that “constant AUC” dose selection also achieved well comparable PTA vs. MIC profiles for optimized prolonged infusion for subject groups with different WT.

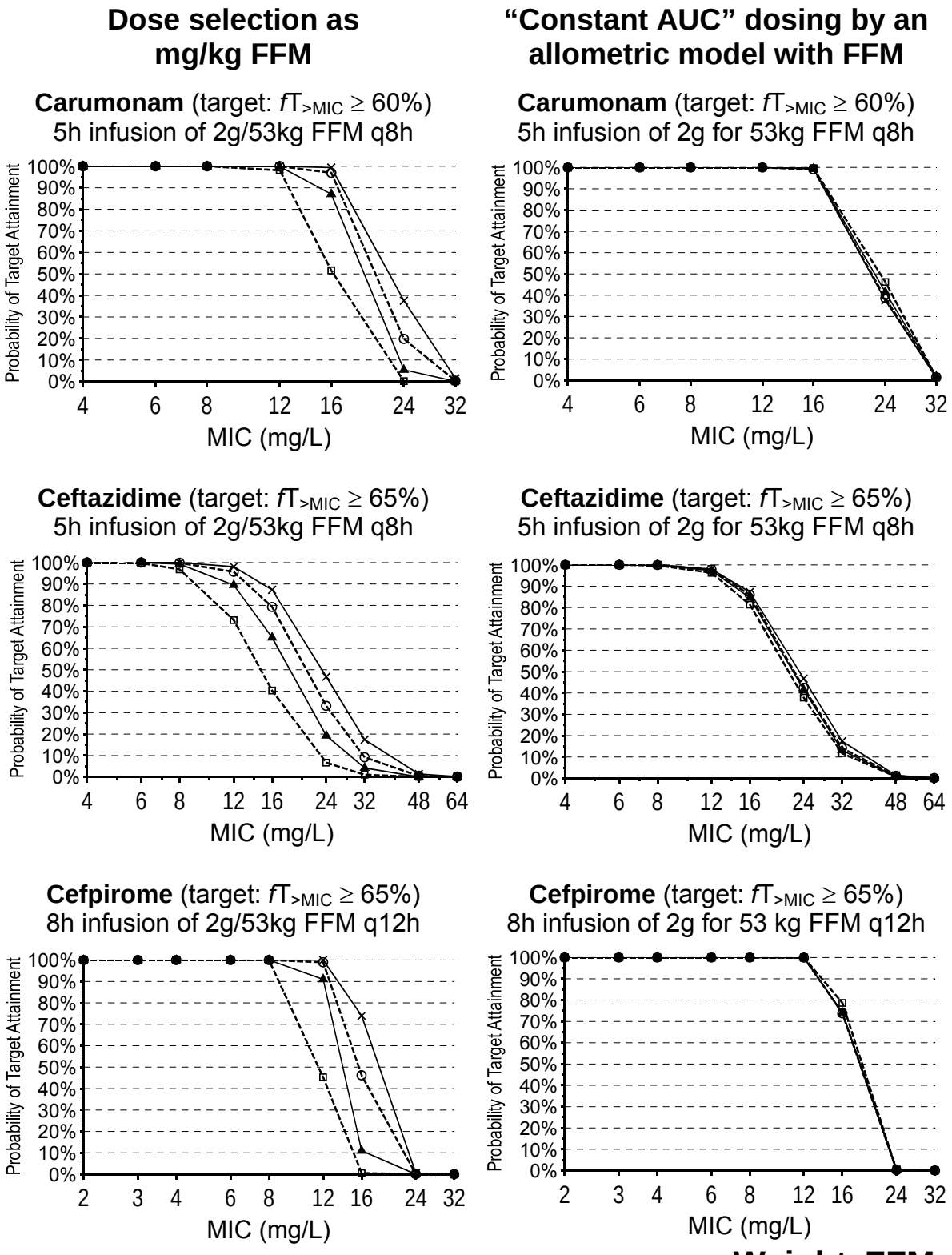


**Figure 3.6-6** Comparison of PTA vs. MIC profiles of prolonged infusions for groups of CF-patients with various FFM (FFM was assumed to be 76% of WT for all groups of CF-patients)

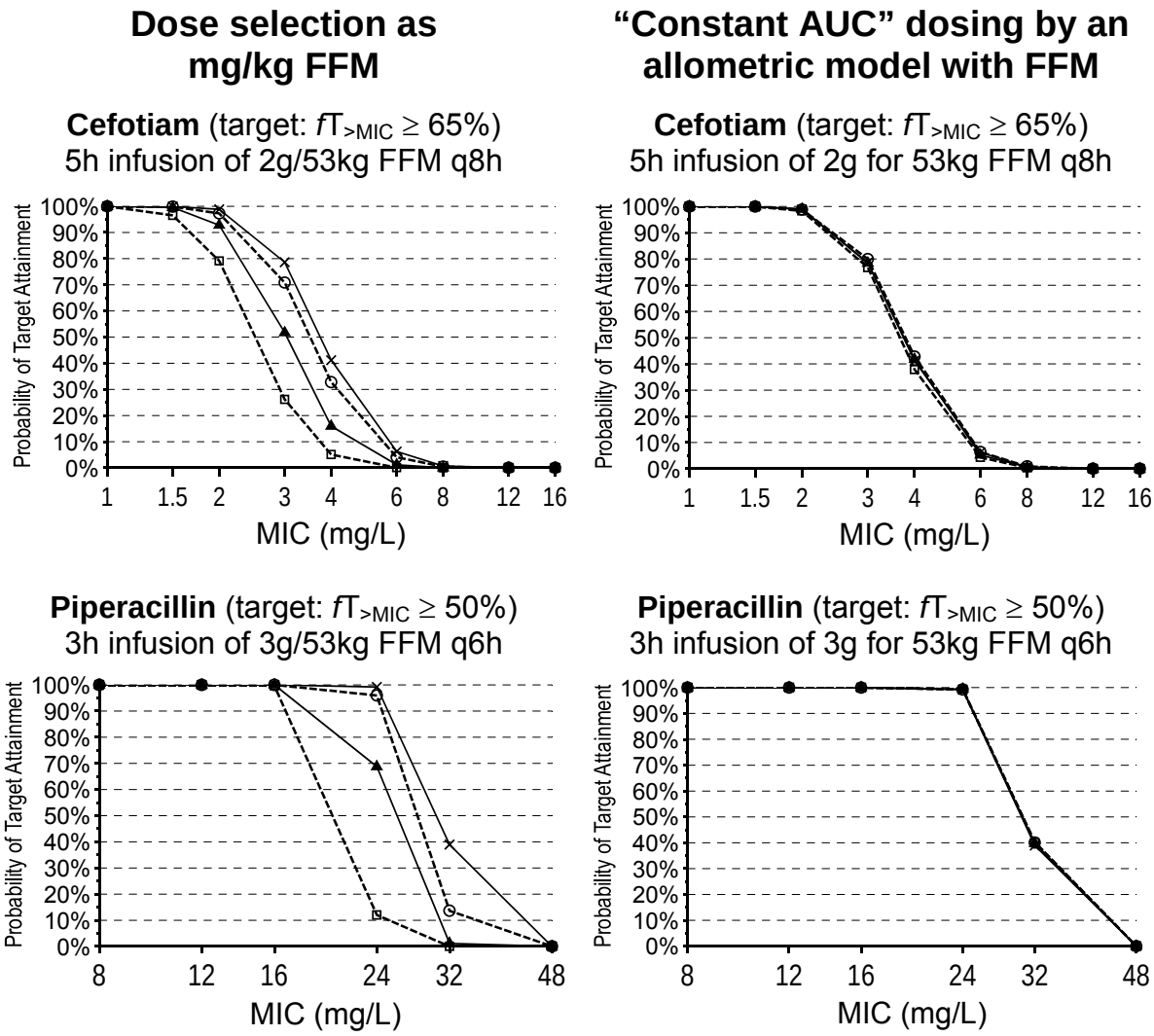


**Figure 3.6-6** Comparison of PTA vs. MIC profiles of prolonged infusions for groups of CF-patients with various FFM (FFM was assumed to be 76% of WT for all groups of CF-patients) (continued)

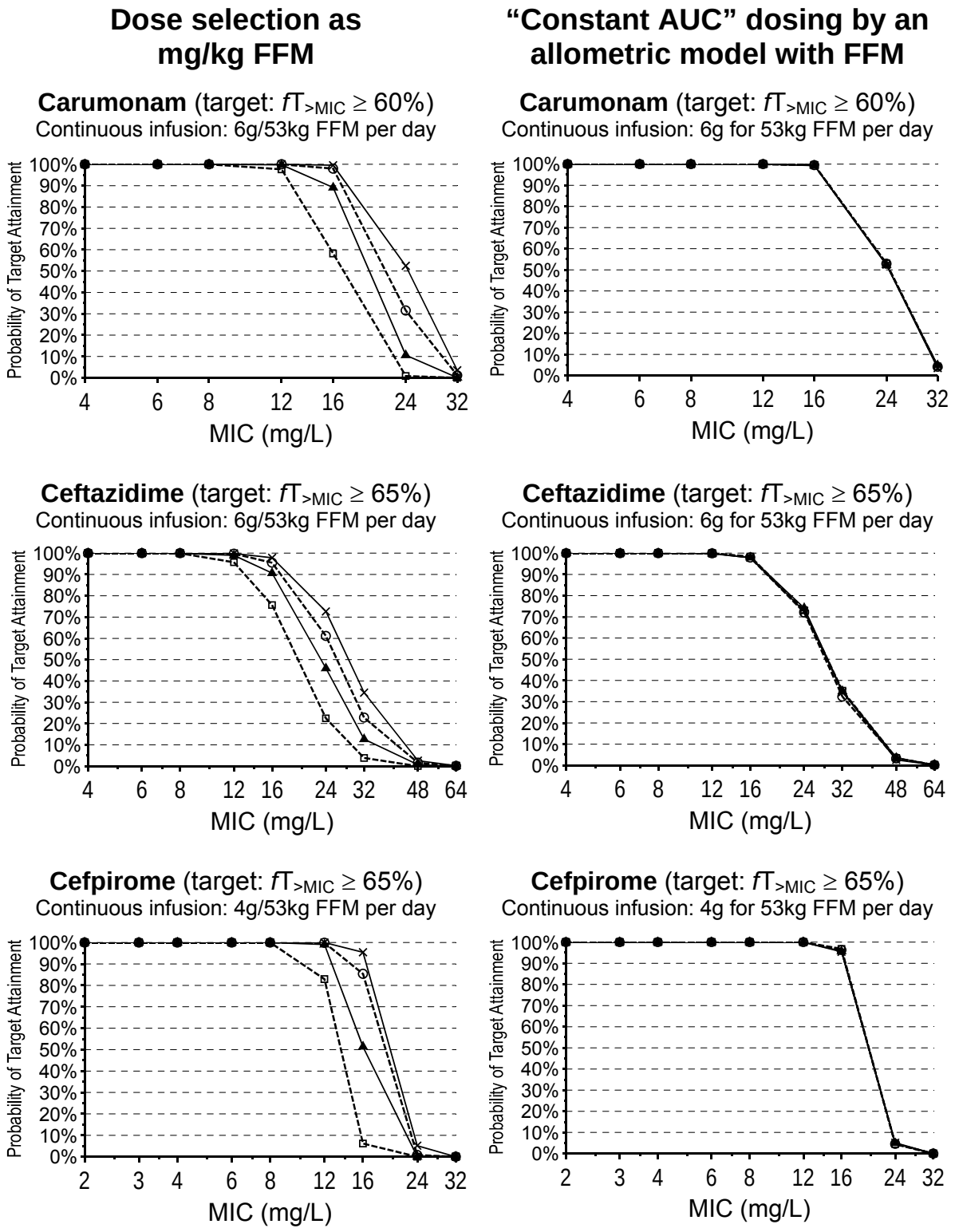


**Figure 3.6-7** Comparison of PTA vs. MIC profiles of continuous infusions for groups of CF-patients with various FFM (FFM was assumed to be 76% of WT for all groups of CF-patients)

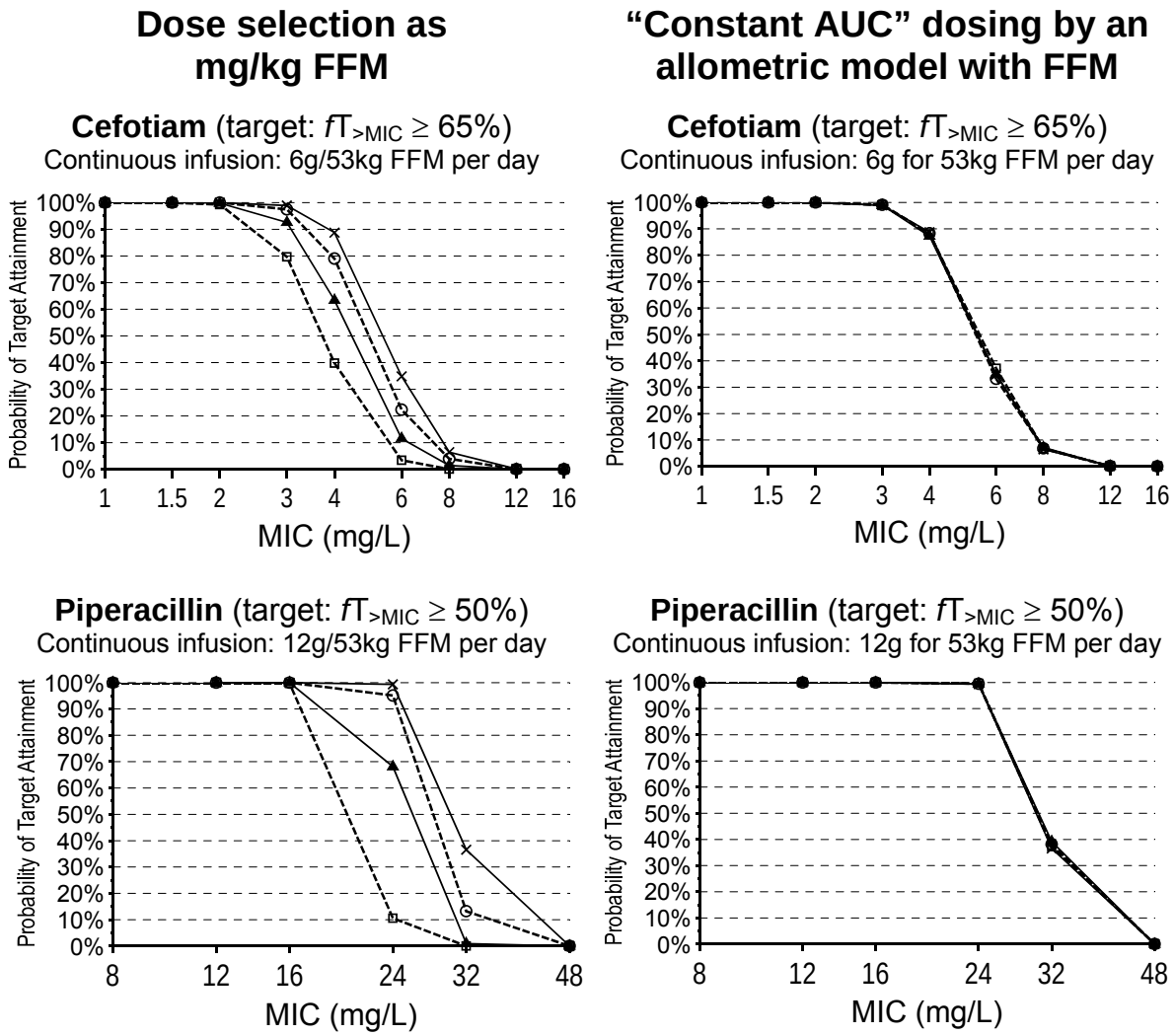


**Figure 3.6-7** Comparison of PTA vs. MIC profiles of continuous infusions for groups of CF-patients with various FFM (FFM was assumed to be 76% of WT for all groups of CF-patients) (continued)

### 3.6.3.3 Loading dose plus prolonged infusion dosage regimens

Figure 3.6-8 shows the range of predicted plasma concentrations for such a dosage regimen optimized to achieve the highest PTAs for the target $fT_{>MIC}$ ≥65% of dosing interval. We studied dosage regimens with a loading dose of 5%, 10%, 15%, etc. up to 50%. The best PTA vs. MIC profile was achieved with a loading dose of about 20% for ceftazidime.

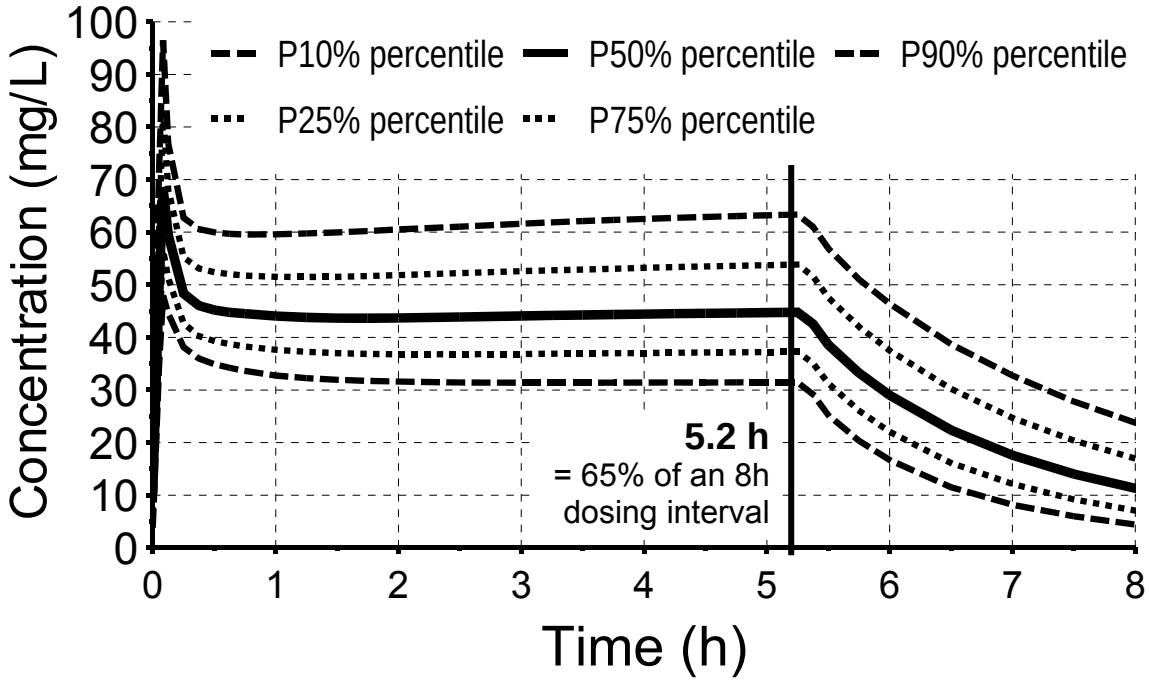


**Figure 3.6-8** Predicted plasma concentrations for a loading dose plus prolonged infusion regimen of ceftazidime at steady-state. 20% (0.4g) of the dose were given as 5min infusion which was followed by a 5.25h infusion of 80% (1.6g) of the dose.

The PTA vs. MIC profile of the optimized dosage regimen with a loading dose of 20% was better than the profiles of the three prolonged infusions and continuous infusions (see Figure 3.6-9). The advantages were most notable at an MIC of 32 mg/L in our example. We compared the PTA expectation values between standard short-term infusion, the prolonged infusion regimens, continuous infusion, and the optimized loading dose + prolonged infusion regimen (see Table 3.6-6). The loading dose plus prolonged infusion regimen achieved slightly higher PTA expectation values for ceftazidime compared to the other dosage regimens.

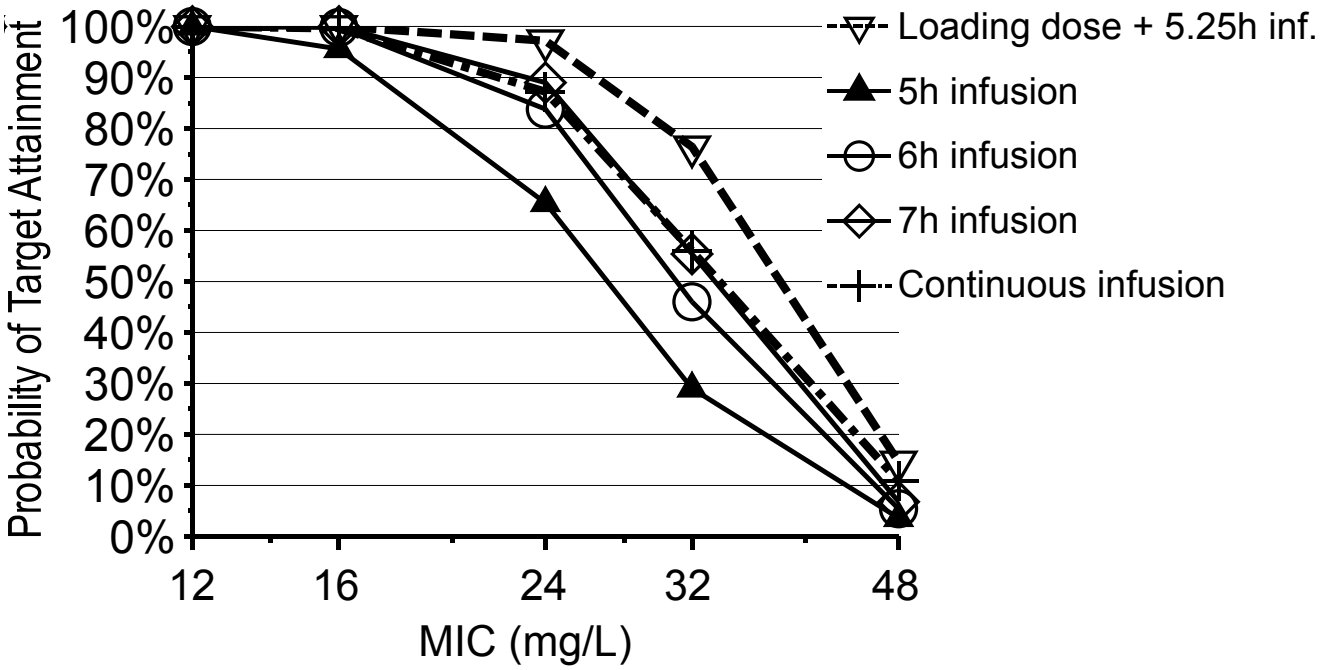


**Figure 3.6-9** Comparison of PTA vs. MIC profiles between continuous infusion, three prolonged infusion regimens, and the optimized loading dose plus prolonged infusion regimen

**Table 3.6-6** Comparison of PTA expectation values between standard-short term, prolonged, and continuous infusion as well as the optimized loading dose plus prolonged infusion regimen for ceftazidime

| **Dosage regimen** | **MYSTIC North America 2002** | | | | **MYSTIC Europe 2000** | |
|---|---|---|---|---|---|---|
| **2g q8h given as:** | *E. coli* | *K. pneumoniae* | *A. baumanii* | *P. aeruginosa* | *Staphylococcus* spp. | *P. aeruginosa* |
| 30min infusion | 95.5% | 90.3% | 55.3% | 80.2% | 28.9% | 63.6% |
| 5h infusion | 97.2% | 93.3% | 77.4% | 91.5% | 59.7% | 82.4% |
| 6h infusion | 97.7% | 94.6% | 82.4% | 92.9% | 64.3% | 84.7% |
| Continuous infusion | 98.1% | 95.4% | 85.4% | 93.7% | 66.6% | 85.8% |
| Loading dose plus prolonged infusion | 98.8% | 97.2% | 92.0% | 95.4% | 72.1% | 88.4% |

### 3.6.4 Discussion

The majority of MCS with beta-lactams in literature do not specifically account for the effect of covariates on PK parameters. Consequently, these MCS can not simulate the PTA vs. MIC profiles for subjects with specific covariates. Instead, these simulations assume that the PTA is calculated for subjects with the same covariates as the subjects studied in the original clinical trial.

However, it may be important to account for the effect of covariates on PK parameters and to simulate the PTA vs. MIC profiles for subjects with specific sets of covariates. We studied primarily adult CF-patients as shown in Table 3.5-1. One CF-patient had a WT of 14kg and ten CF-patients had a WT between 30 and 35kg. Our other 79 CF-patients had a WT between 35 and 81kg. Therefore, the predictions for CF-patients with a WT of 30kg in our MCS are reasonably supported by the CF-patients studied in our clinical trials. The PTA vs. MIC profiles for the group of CF-patients with a WT of 15kg is an extrapolation (except for the one CF-patient with a WT of 14kg). Although these MCS are supported by a standard allometric model, the results for the WT=15kg group should be interpreted with some caution.

We applied a standard allometric model which accounts for the effect of body size on clearance and assumes that body composition, renal, and hepatic function are comparable for CF-patients within the studied range in WT. Importantly, additional correction terms are required, when developmental changes in renal and hepatic function and developmental changes in body composition between newborns and adults occur (14, 26, 51, 62, 168, 324, 421, 534). As our beta-lactams are primarily eliminated renally, the maturation of renal clearance is most important for our MCS. Renal function has been shown to approach adult values after about one year of age (14, 121, 168, 388, 421). However, our MCS results should still be interpreted conservatively for young CF-patients, especially for CF-patients younger than about five years.

We could identify two reasons why CF-patients achieved systematically lower PTAs and PKPD breakpoints for short-term infusion and mg/kg WT

dose selection compared to healthy volunteers, when the demographic data (covariates) of the subjects in our clinical studies were used for MCS: 1) CF-patients had higher total clearances compared to healthy volunteers for linear scaling by WT (see Table 3.5-3). 2) Our CF-patients were smaller than our healthy volunteers and therefore our CF-patients were predicted to have a shorter elimination half-life by our allometric model. We used an allometric exponent of 0.75 for clearance and 1.0 for volume of distribution in our models. Sometimes the exponent of 0.67 for standard Euclidean geometry is discussed for clearance (see chapter 1.5). PKPD breakpoints for CF-patients with smaller body size would be much lower than shown in Table 3.6-4, if we used an exponent of 0.67 for our MCS.

Our equations for dose selection to achieve a constant $fT_{>MIC}$ for short-term infusion (see Figure 3.6-5) as well as for prolonged (see Figure 3.6-6) and continuous infusion (see Figure 3.6-7) achieved very similar PTA vs. MIC profiles in subjects of various body size. We could show that our formulas for dose selection achieved very similar PTA vs. MIC profiles for our five intravenous beta-lactams, although these equations were developed for a one-compartment model with intravenous bolus dose and do not consider random BSV.

Importantly, the doses required for a CF-patient with WT 15kg to achieve the same PKPD breakpoint as a CF-patient with WT 70kg for short-term infusion were substantially higher compared to the mg/kg WT doses (see Table 3.6-3). Even though this is a massive increase in doses of short-term infusions, such high doses have already been administered to CF-patients. Reed et al. (402) administered daily doses up to 900 mg/kg WT to CF-patients aged 12 years or less. Reed et al. (402) recommended doses not exceeding 600 mg/kg WT. Common piperacillin doses in adults without CF range from 9 g to 18 g daily. Assuming a WT of 70kg and mg/kg WT dose selection (linear model), this corresponds to 129 mg/kg and 257 mg/kg piperacillin daily.

As shown in Table 3.6-1 and Table 3.6-2, continuous infusion with allometric dose selection increased PKPD breakpoints in CF-patients by a factor of 11 [5.3 - 64] (median [range]) compared to short-term infusion with mg/kg WT dosing. This is a median increase in PKPD breakpoints by more

than three tube dilutions. An increase in mg/kg WT doses for short-term infusions by a factor of 11 [5.3 - 64] would be required to achieve the same PKPD breakpoint as for continuous infusion. Table 3.6-1 additionally shows that using a prolonged infusion time increased PKPD breakpoints more than administering the same daily dose with shorter dosing intervals as short-term infusions (i. e. same daily dose given q6h instead of q8h).

The PKPD profiles for continuous and prolonged infusions strongly suggest a clinical evaluation of these modes of administration. Besides a substantial increase in PKPD breakpoints, the differences in the required doses to achieve similar PTA vs. MIC profiles in subjects of various body size were much smaller for continuous and prolonged infusion (see Table 3.6-5) than for short-term infusion (see Table 3.6-3). Consequently, the differences in PTA vs. MIC profiles between dosing by an allometric size model and dosing based on mg/kg FFM were much smaller for continuous (see Figure 3.6-7) and prolonged infusion (see Figure 3.6-6) compared to short-term infusion (see Figure 3.6-5).

As a method to further increase the PKPD breakpoint at the same daily dose, we studied a loading dose plus prolonged infusion regimen. The loading dose is given at the beginning of each dosing interval to achieve effective concentrations as soon as possible (see Figure 3.6-4 and Figure 3.6-8). We found higher PTAs and higher PTA expectation values for the loading dose plus prolonged infusion regimen (see Figure 3.6-9 and Table 3.6-6) compared to continuous and optimized prolonged infusion.

The loading dose plus prolonged infusion regimen is the most flexible of the optimized regimens, as it has the shortest duration of infusion. The only additional workload is the switch in the infusion rate 5min after start of the infusion (at the transition between loading dose and prolonged infusion). We could show that any dosage regimen of a beta-lactam with an optimal PTA vs. MIC profile for a chosen $fT_{>MIC}$ target requires a duration of infusion which is at least as long as the $fT_{>MIC}$ multiplied by the dosing interval (i. e. about 5.2h duration of infusion for an 8h dosing interval and the target 65% $fT_{>MIC}$). Population PKPD models predict that the PKPD breakpoint for the chosen

target decreases notably, if the duration of infusion is less than this optimized value.

Therefore, if the PKPD target is known, it is possible to custom tailor an optimized dosage regimen which achieves both the best possible PTA vs. MIC profile and keeps the best possible flexibility for the patient (i. e. shortest duration of infusion for the selected PKPD target). Prolonged infusion and the new loading dose plus prolonged infusion regimen provide more flexibility for the patient and for administering other drugs or parenteral nutrition and might be superior to continuous infusion. Continuous infusion often requires an extra line which increases the risk for line infections.

However, such dosage regimens with an optimized PTA vs. MIC profile for beta-lactams are more inconvenient than standard short-term infusion, as the duration of infusion is much longer for the optimized dosage regimens. For an individual patient, these optimized dosage regimens probably have their greatest merit for treatment of severe infection or infections associated with a high mortality. Prevention of a chronic infection by *P. aeruginosa* in CF-patients probably warrants such an increased duration of infusion, as chronic infection by this pathogen is the most important factor for morbidity and mortality of CF-patients. On the population level, the use of dosage regimens with an optimized PTA vs. MIC profile might help to reduce the emergence of resistance. More data are required on this issue. If bacteria with a single step mutation were eradicated by an optimized dosage regimen before acquiring a second and third step of mutation, the use of optimized dosage regimens would have a great potential for limiting or slowing down the emergence of resistance. The final choice of the dosage regimen should account for the probability to cure each patient, the severity of disease, mortality associated with the disease, workload, costs, and convenience for applying the dosage regimen as well as for the potential for emergence of resistance.

In conclusion, CF-patients achieved lower PKPD breakpoints than healthy volunteers for short-term infusion of beta-lactams, when CF-patients and healthy volunteers had the same demographic data as in our clinical trials. The median [range] for the ratio of breakpoint in CF-patients divided by breakpoint in healthy volunteers was 0.50 [0.33 - 1.0] for short-term infusion

and mg/kg WT dose selection of our five intravenous beta-lactams. We identified two reasons for those systematically lower PKPD breakpoints in CF-patients: 1) CF-patients had higher clearances per kg WT and 2) The allometric model predicted CF-patients to have a shorter average elimination half-life compared to healthy volunteers, because our CF-patients were smaller. We developed and validated two formulas for dose selection to achieve similar PTA vs. MIC profiles for $fT_{>MIC}$ targets. A “constant AUC” dose selection based on an allometric size model achieved well comparable PTA vs. MIC profiles for continuous and optimized prolonged infusion for CF-patients of various body size. Our new equation for dose selection for short-term infusion also achieved very similar PTA vs. MIC profiles for CF-patients of various body size, but required substantially higher doses in smaller CF-patients due to their shorter half-life. Continuous infusion with allometric dose selection increased the PKPD breakpoints by a factor of 11 [5.3 - 64] (median [range]) compared to standard short-term infusion and mg/kg WT dose selection in CF-patients with the same demographic data as the CF-patients in our clinical studies. Prolonged infusion with an optimized duration achieved similar PKPD breakpoints compared to continuous infusion. The optimal duration of infusion for prolonged infusion was slightly longer than the PKPD target multiplied by the dosing interval (e.g. 65% $fT_{>MIC}$ times 8h = 5.2h). As an additional improvement, the proposed loading dose plus prolonged infusion regimen (loading dose being given at the beginning of each dosing interval) achieved slightly higher PTA expectation values than continuous infusion. Our MCS results suggest to evaluate the effectiveness and convenience of continuous and optimized prolonged infusion clinically. The disease severity and mortality, probability of cure for each individual patient, workload, cost, convenience for the patient, and potential for emergence of resistance have to be counterbalanced for the choice of the most appropriate dosage regimen.

# 4 Determination of PKPD breakpoints and optimization of dosage regimens for selected oral antibiotics

## 4.1 Background on specification of PKPD breakpoints

The PKPD breakpoint is a valuable measure to guide therapy. If the MIC of an infecting pathogen is known to be at or below the PKPD breakpoint, a high (e. g. >90%) probability for successful treatment is predicted. The method of determining a PKPD breakpoint is described in chapter 2.7.2.3. This method differs considerably from the method used to specify susceptibility breakpoints by national organizations in the US (CLSI), in Britain (BSAC), and in Germany (DIN). Some specific features of the methods used to determine breakpoints are shown in Table 4.1-1.

**Table 4.1-1** Comparison of the method used to specify the susceptibility breakpoint from the BSAC and the method used to specify the PKPD breakpoint

| | BSAC method (301) | Population PK & MCS |
|---|---|---|
| Accounts for the average plasma concentration time profile | Indirectly via the peak concentration and terminal half-life | Yes |
| Accounts for the patient specific variability and correlation of PK parameters | No | Yes |
| Specifically accounts for the dosage regimen in the patient population of interest | No | Yes |
| Accounts for nonlinear PK | No | Yes (if included in the population PK model) |
| Method predicts | Three categories: susceptible, intermediate, or resistant | Probability of target attainment at each MIC and for a whole MIC distribution |

The methodological comparison shown in Table 4.1-1 highlights some important advantages of the method for specifying the PKPD breakpoint as compared to the susceptibility breakpoints. There is a clear separation between PK and PD for determination of the PTA vs. MIC profile (see Figure 2.7-4 on page 65). The only input variable from the microbiological side is the PKPD target required to achieve e. g. near-maximal bacterial killing. The separation between PK and PD is not that strict for the BSAC method (301).

Due to those important advantages of specifying the PKPD breakpoint by population PK and MCS, Ambrose et al. (7) recently proposed re-evaluation of the cephem susceptibility breakpoints for Enterobacteriaceae. Therefore, we evaluated the PKPD breakpoint of several dosage regimens for cefuroxime axetil and performed a meta-analysis for oral ciprofloxacin and levofloxacin to determine their PKPD profile.

## 4.2 Pharmacokinetic-pharmacodynamic breakpoint and optimized dosage regimens of cefuroxime axetil

### 4.2.1 Chemical structure of cefuroxime and cefuroxime axetil

**Cefuroxime axetil**

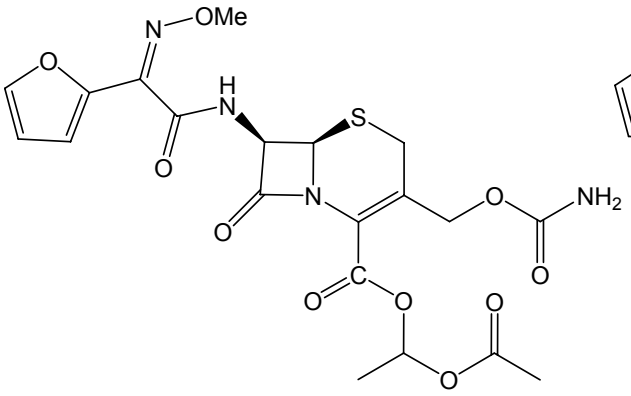

($C_{20}H_{22}N_4O_{10}S$, Mol. Wt.: 510.47)

**Cefuroxime**

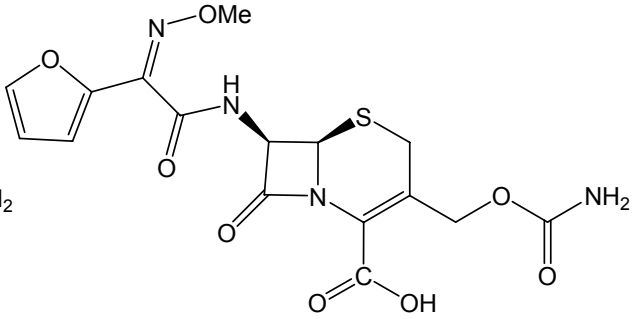

($C_{16}H_{16}N_4O_8S$, Mol. Wt.: 424.39)

**Chemical structure 4.2-1** Cefuroxime axetil and cefuroxime

### 4.2.2 Clinical use of cefuroxime axetil

Cefuroxime axetil is the acetoxyethyl-ester prodrug of cefuroxime. Cefuroxime axetil is reliably absorbed and can be taken with or without a meal, although its extent of absorption is enhanced under the influence of food (133). Cefuroxime has been successfully used in the treatment of upper and lower respiratory tract infections as well as genitourinary tract infections (442). Cefuroxime is active against *S. pyogenes*, *H. influenzae*, *M. catarrhalis*, *E. coli*, *K. pneumoniae*, *N. gonorrhoeae*, penicillin susceptible *S. pneumoniae*, and some isolates of penicillin intermediate *S. pneumoniae* (52, 53, 186, 187, 216, 285, 294, 313, 330, 381, 561). Cefuroxime is stable against the most common plasmid mediated beta-lactamases OXA-1, OXA-2, TEM-1, and TEM-2 of *E. coli* and SHV-1 of *K. pneumoniae* (442). There were no major

changes in the spectrum of susceptible pathogens for cefuroxime during the last decade, although some nosocomial isolates of Enterobacteriaceae became resistant due to production of TEM and SHV extended spectrum beta-lactamases (103, 438-441).

A susceptibility breakpoint of ≤1 mg/L has been determined for cefuroxime by the BSAC (56) and DIN (104). The susceptibility breakpoints from the CLSI (261, 352, 353) (formerly known as NCCLS) are ≤1 mg/L for *S. pneumoniae* and ≤4 mg/L for *H. influenzae*, Enterobacteriaceae, and Staphylococcus spp.

The encountered MICs of bacterial isolates are usually compared to those breakpoints to decide, whether a successful treatment outcome is to be expected. However, it has been repeatedly emphasized that both the PK and PD should be considered to determine the effectiveness of a drug (83, 107, 145, 218, 219, 476). The susceptibility breakpoint based on PKPD considerations has been determined by comparing the average plasma concentration time profiles of oral cefuroxime with the MICs of relevant pathogens by some authors (261, 313, 379). However, this approach ignores the true BSV in the plasma concentration time course. Ambrose et al. (7) incorporated the BSV into their MCS for intravenous cefuroxime based on literature data to determine the PKPD breakpoint, but did not estimate the full population PK model and did not study oral cefuroxime.

Population PK and MCS have not yet been used to determine the PKPD breakpoints for cefuroxime axetil and to predict the probability of successful treatment of infections caused by relevant pathogens. Therefore, our first objective was to determine the population PK of oral cefuroxime axetil in healthy volunteers. As our second objective, we derived the PTA vs. MIC profiles and the probability of successful treatment against various pathogens for a standard q12h dosage regimen of oral cefuroxime. We additionally studied for which pathogens dosing 250 mg cefuroxime axetil q8h instead of q12h may be advantageous.

### 4.2.3 Methods

The general clinical and sample handling procedures, the methods for PK analysis (including NCA and population PK), and the general methods for MCS are described in chapter 2.

***Subjects:*** Twenty-four (24) healthy, male, Caucasian volunteers participated in the study. Their demographic data were, average ± SD [range]: age 24.5 ± 3.3 yrs [18-31 yrs], weight 73.8 ± 9.2 kg [58.2-93.6 kg], and height 179 ± 8.0 cm [166-193 cm].

***Study design and drug administration:*** The study was a single dose, single-center study. All subjects received an oral cefuroxime axetil dose equivalent to 250 mg cefuroxime together with 240 mL low-carbonated, calcium-poor mineral water at room temperature. The study drug was administered directly after intake of a standardized breakfast with a significant amount of fat. This breakfast contained 4 slices of crisp bread (50 g), 20 g margarine, 2 slices (40 g) of cheese (30% fat content), 25 g marmalade, 100 mL fruit tea, and 100 mL milk (3.5% fat content).

***Blood sampling:*** Blood samples were drawn immediately before administration (0 min) as well as at 30, 60, and 90 min and at 2, 2.33, 2.67, 3, 3.33, 3.67, 4, 4.5, 5, 6, 8, 10, and 12 h after administration of study drug.

***Drug analysis:*** Samples were analyzed by means of an LC-MS/MS method, validated for 0.1 mL samples of human plasma. Plasma samples (0.1 mL) were diluted with buffer containing the internal standard and deproteinized by addition of 400 µL of acetonitrile. After thorough mixing, the samples were centrifuged for 5 min at 3,600 rpm at approximately +4 °C, and the acetonitrile was removed by extraction with 1 mL dichloromethane. The mixture was centrifuged again and 30 µL of the aqueous phase of each sample were then chromatographed on a reversed-phase column (Waters Symmetry® C8), eluted with an isocratic solvent system consisting of ammonium acetate buffer and acetonitrile (70/30, v/v) and monitored by LC-MS/MS with a MRM method as follows: Precursor → product ion for cefuroxime m/z 423 → m/z 207 and internal standard m/z 426 → m/z 156,

both analyses were in negative mode. Under these conditions cefuroxime and the internal standard were eluted after approximately 1.4 and 1.5 minutes, respectively. The Mac Quan software (version 1.5, PE Sciex, Thornhill, Ontario, Canada, 1991 - 1997) was used for evaluation of chromatograms.

The linearity of the cefuroxime calibration curve was shown from 0.00900 mg/L to 10.2 mg/L. The coefficient of correlation for all measured sequences of cefuroxime was at least 0.999. The lowest calibration standard of 0.00900 mg/L was set as the lower limit of quantification of the assay for cefuroxime in human plasma. For the spiked quality control standards of cefuroxime the inter-day precision ranged from 3.2 to 5.0% with an inter-day accuracy (relative error) between -4.3 to 2.1%. The intra-day precision and relative error of the cefuroxime assay ranged from 0.7 to 4.0% and between -0.1 and 3.4%.

***Population model:*** We tested one and two compartment disposition models with first-order, zero-order, or mixed-order (Michaelis-Menten) absorption with or without a lag-time.

***MCS:*** We compared dosage regimens of 250 mg oral cefuroxime q12h and 250 mg oral cefuroxime q8h both at steady-state and simulated 10,000 subjects for each dosage regimen in absence of residual error. We studied a range of MICs from 0.031 to 64 mg/L. As the protein binding for cefuroxime has been reported to range between 33 and 50% (136, 177, 442), we assumed an average protein binding of 42% for cefuroxime.

The PTA expectation value was calculated based on published MIC distributions. We used susceptibility data from the UK (330) collected in 2002 and 2003 on *H. influenzae* (n=581), *M. catarrhalis* (n=269), and *S. pneumoniae* (n=519), susceptibility data from Canada (561) collected in 2001 and 2002 on *H. influenzae* (n=1350), and susceptibility data from Germany (53) collected in 2002 on *H. influenzae* (n=300), *M. catarrhalis* (n=308), *S. pneumoniae* (n=331), and *S. pyogenes* (n=340). Additionally, we used susceptibility data from a global surveillance study (52) collected between 1997 and 2000 on penicillin susceptible *S. pneumoniae* (n=2102) and penicillin intermediate *S. pneumoniae* (n=1024), susceptibility data from a European surveillance study (187) collected between 1997 and 1999 on

*S. pneumoniae* (n=2018) and *S. pyogenes* (n=662), and susceptibility data from North America (186) collected between 1997 and 1999 on *S. pyogenes* (n=119).

### 4.2.4 Results

The results from NCA (see Table 4.2-1) and population PK analysis (see Table 4.2-2) were in good agreement. We found an average ± SD terminal half-life of 1.34 ± 0.13 h and peak concentrations of 2.64 ± 0.64 mg/L between 2 and 5 h post dose. The duration of total concentration above an MIC of 1 mg/L (equivalent to an non-protein bound concentration of about 0.58 mg/L) was 4.97 ± 0.79 h and the duration of total concentration above an MIC of 0.5 mg/L (equivalent to a non-protein bound concentration of about 0.29 mg/L) was 6.90 ± 0.77 h (see Table 4.2-1).

Cefuroxime axetil is rapidly metabolized to cefuroxime by nonspecific esterases in the intestinal mucosa and in blood. The VPCs showed that the oral absorption of cefuroxime axetil and subsequent metabolism to cefuroxime could not adequately be described by a first-order or a zero-order process either with or without a lag-time. The predictive performance of a mixed-order absorption model was better than that of the models with first-order or zero-order absorption.

Figure 4.2-1 shows the highly sufficient predictive performance of our final model for which the absorption from the gut into the central compartment was described as a Michaelis-Menten process. The population PK parameters of this model are shown in Table 4.2-2. The apparent maximum rate of absorption (Vmax/F) was 82.6 mg/h. During the first three hours, the rate of absorption was notably saturated, because the apparent amount in the gut compartment (Km/F) associated with 50% of Vmax/F was 20.0 mg and therefore 12.5 times lower than the dose of 250 mg.

**Table 4.2-1** PK parameters from NCA for 250 mg oral cefuroxime given as cefuroxime axetil

| Parameter | Unit | Average ± SD | Median [Min - Max] |
|---|---|---|---|
| Area under the curve from time zero to infinity | mg h $L^{-1}$ | 11.9 ± 2.49 | 11.6 [8.49 - 18.1] |
| Peak concentration | mg $L^{-1}$ | 2.64 ± 0.64 | 2.54 [1.65 - 3.90] |
| Time of peak concentration | mg $L^{-1}$ | 2.98 ± 0.73 | 2.83 [2.00 - 5.00] |
| Terminal half-life | h | 1.34 ± 0.13 | 1.35 [1.08 - 1.54] |
| Apparent total clearance | L $h^{-1}$ | 21.8 ± 4.29 | 21.5 [13.8 - 29.4] |
| Apparent volume of distribution during the terminal phase | L | 41.7 ± 7.64 | 44.4 [27.4 - 54.9] |
| Time of total concentration above 1 mg/L | h | 4.97 ± 0.79 | 4.90 [3.43 - 7.08] |
| Time of total concentration above 0.5 mg/L | h | 6.90 ± 0.77 | 6.75 [5.13 - 9.02] |

**Table 4.2-2** Population PK parameters for 250 mg oral cefuroxime given as cefuroxime axetil together with a fat-enhanced breakfast

| Parameter | Unit | Estimate | BSV (%)° |
|---|---|---|---|
| CL/F | L $h^{-1}$ | 21.9 | 19.1* |
| V/F | L | 40.3 | 17.6* |
| Tlag | min | 9.60 | 72.0 |
| Vmax/F | mg/h | 82.6 | 32.9** |
| Km/F | mg | 20.0 | 117** |
| $CV_C$ | % | 12.5 | |

°: Apparent coefficients of variation for the BSV.

*: Coefficient of correlation between the pair of random effects: r(CL,V) = 0.90.

**: Coefficient of correlation between the pair of random effects: r(Vmax,Km) = 0.59.

CL/F: apparent total clearance, V/F: apparent volume of distribution, F: extent of absorption, Tlag: lag-time of absorption, Vmax/F: apparent maximum rate of absorption from the gut into the central compartment, Km/F: apparent amount of drug in the gut compartment for which the rate of absorption is 50% of Vmax/F. $CV_C$: proportional residual error.

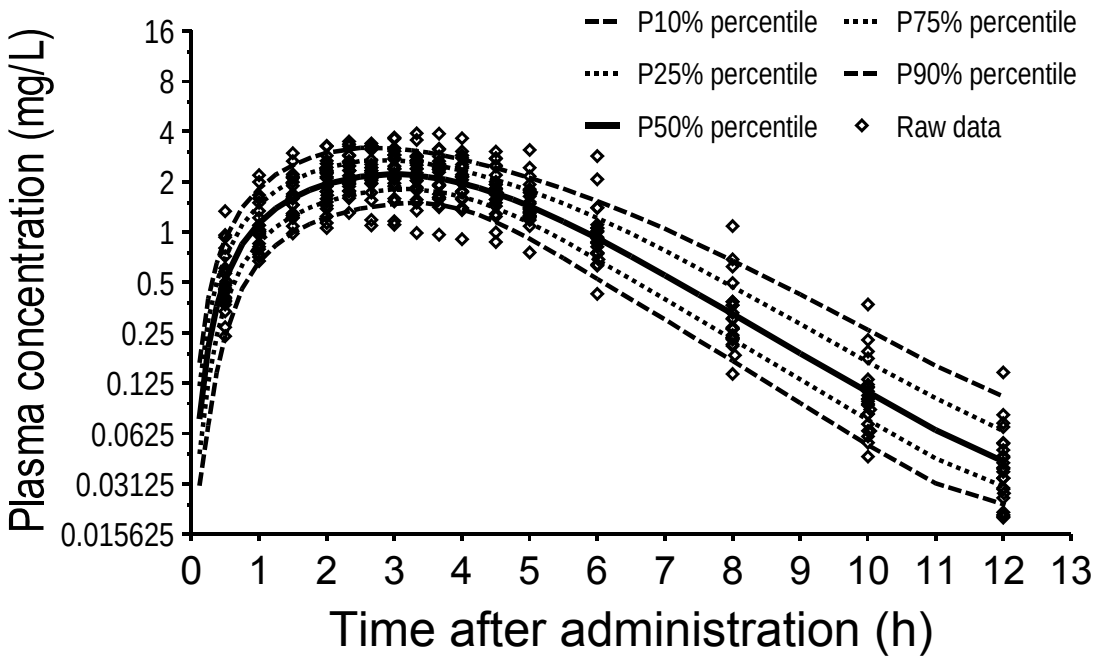


**Figure 4.2-1** VPC for a single oral cefuroxime axetil dose equivalent to 250 mg cefuroxime.

See chapter 2.6.3 for interpretation of VPCs.

After qualifying the predictive performance of our population PK model, we used this model to simulate plasma concentration time profiles for dosage regimens of 250 mg oral cefuroxime q12h or q8h. The derived PTA vs. MIC profiles for those regimens and for the PKPD targets $fT_{>MIC} \geq 40\%$ and $fT_{>MIC} \geq 65\%$ are shown in Figure 4.2-2. For the near-maximal kill target, the PKPD breakpoint increased by a factor of 4 from 0.094 mg/L for q12h dosing to 0.375 mg/L for q8h dosing. For the bacteriostasis target, the PKPD breakpoint increased by a factor of 2 from 0.375 mg/L for q12h dosing to 0.75 mg/L for q8h dosing.

We used the PTA vs. MIC profiles shown in Figure 4.2-2 to calculate the PTA expectation values against several pathogens which are commonly involved in infections treated with cefuroxime axetil. Table 4.2-3 shows that the PTA expectation values against *S. pyogenes* were >95% for both targets and both dosage regimens. High (>92%) PTA expectation values were also achieved against penicillin susceptible *S. pneumoniae* by both regimens and

for both targets, whereas the PTA expectation values were between 40 and 55% for the q8h regimen and between 18 and 48% for the q12h regimen against penicillin intermediate *S. pneumoniae*.

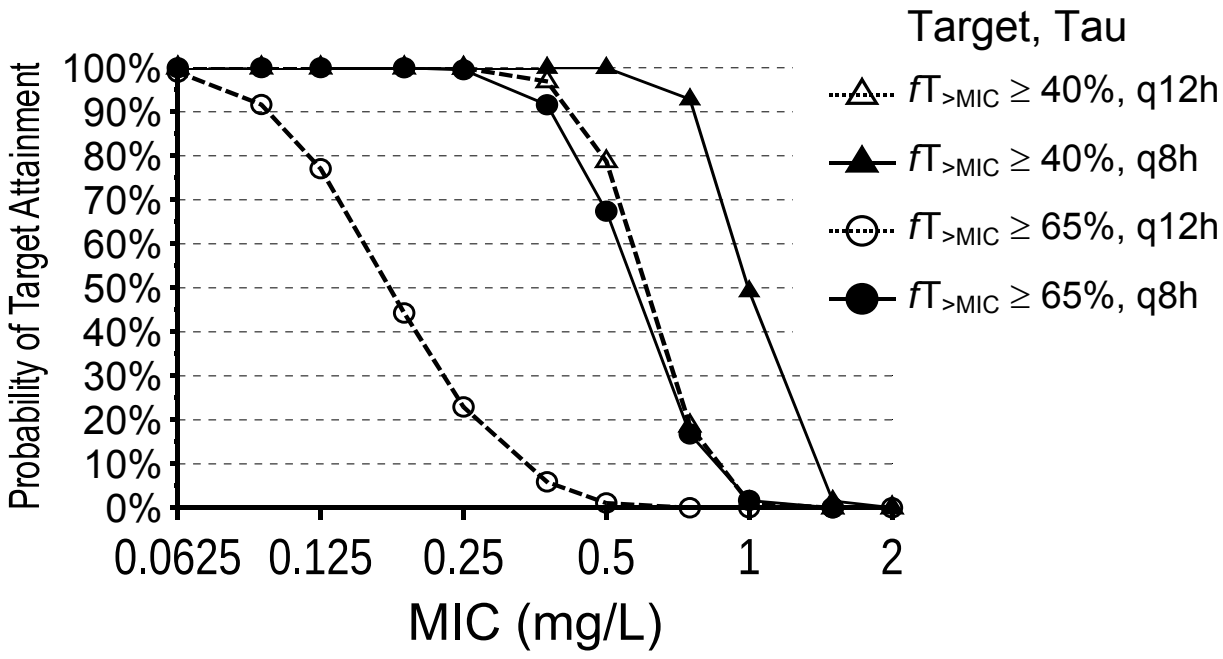


**Figure 4.2-2** Probability of target attainment vs. MIC profiles for 250 mg cefuroxime given as cefuroxime axetil either q12h (daily dose: 500 mg) or q8h (daily dose: 750 mg) for the PKPD targets $fT_{>MIC} \geq 40\%$ and $fT_{>MIC} \geq 65\%$

The q12h regimen achieved low (<47%) PTA expectation values against *H. influenzae* in the UK and in Canada. The q8h regimen achieved a PTA expectation value of 93.4% for the bacteriostasis target and of 72.3% for the near-maximal kill target for *H. influenzae* isolates from Germany. Cefuroxime had PTA expectation values ≤68% against *M. catarrhalis* (see Table 4.2-3), PTA expectation values ≤24% against methicillin-sensitive *S. aureus* (based on MIC data from Hoban et al. (186, 187), results not shown elsewhere), and PTA expectation values ≤2.6% against penicillin resistant *S. pneumoniae* (based on MIC data from Hoban et al. (186, 187) and Bouchillon et al. (52), results not shown elsewhere).

**Table 4.2-3** PTA expectation values for 250 mg cefuroxime given orally as cefuroxime axetil either q12h (daily dose: 500 mg) or q8h (daily dose: 750 mg) for the PKPD targets *f*T>MIC ≥ 40% and *f*T>MIC ≥ 65%

| **Pathogen** | **Region & year (no. of isolates)** | **PTA expectation value** | | | |
|---|---|---|---|---|---|
| | *PKPD Target* | $fT_{>MIC}$ ≥40% | | $fT_{>MIC}$ ≥65% | |
| | *Dosing* | *q12h* | *q8h* | *q12h* | *q8h* |
| *S. pyogenes* | Germany 2002 (n=340) (53) | 99.6% | 99.9% | 98.4% | 99.6% |
| | Europe 1997-1999 (n=662) (187) | 99.1% | 99.3% | 95.9% | 99.0% |
| | US & Canada 1997-1999 (n=119) (186) | 99.2% | 99.2% | 98.0% | 99.2% |
| *S. pneumoniae* | Germany 2002 (n=331) (53) | 97.5% | 98.0% | 92.8% | 97.3% |
| | UK 2002-2003 (n=519) (330) | 94.6% | 95.1% | 90.8% | 94.4% |
| | Europe 1997-1999 (n=2018) (187) | 72.0% | 74.5% | 63.2% | 71.5% |
| PSSP | Global 1997-2000 (n=2102) (52) | 98.5% | 99.1% | 92.4% | 98.3% |
| | Europe 1997-1999 (n=1274) (187) | 98.6% | 99.2% | 93.1% | 98.4% |
| PISP | Global 1997-2000 (n=1024) (52) | 47.7% | 55.1% | 20.7% | 46.0% |
| | Europe 1997-1999 (n=458) (187) | 41.7% | 50.2% | 18.3% | 39.9% |
| *H. influenzae* | UK 2002-2003 (n=581) (330) | 46.8% | 71.4% | 2.0% | 41.0% |
| | Canada 2001-2002 (n=1350) (561) | 21.2% | 50.0% | 4.2% | 19.3% |
| | Germany 2002 (n=300) (53) | 78.3% | 93.4% | 12.7% | 72.3% |
| *M. catarrhalis* | UK 2002-2003 (n=269) (330) | 39.2% | 68.1% | 2.4% | 35.0% |
| | Germany 2002 (n=308) (53) | 13.2% | 41.0% | 0.9% | 11.9% |

PSSP: Penicillin susceptible *S. pneumoniae*, PISP: Penicillin intermediate *S. pneumoniae*.

### 4.2.5 Discussion

Cefuroxime axetil has been used widely for more than a decade in the treatment of community-acquired upper and lower respiratory tract infections (including community-acquired pneumonia) (442). The causative pathogens of infections treated with cefuroxime axetil are often *S. pneumoniae*, *H. influenzae*, *M. catarrhalis*, and *S. pyogenes*. The reported $MIC_{90}$'s of cefuroxime against *H. influenzae* and *M. catarrhalis* are often 2 or 4 mg/L (381, 442). Whereas most isolates would be deemed susceptible by the CLSI breakpoint of ≤4 mg/L for those pathogens, a significant number of isolates would be deemed resistant according to the BSAC and DIN breakpoint of ≤1 mg/L for susceptibility. To decide which breakpoint might be more appropriate, we derived the PKPD breakpoint via population PK and MCS and predicted the probability of successful treatment with cefuroxime axetil.

One prerequisite for a MCS with cefuroxime axetil is to adequately describe the absorption and de-esterification of cefuroxime axetil to cefuroxime. PK studies in rats showed that these processes may be described by a mixed-order absorption process from the gut into the central compartment (424-426). Our population PK modeling also supported a mixed-order absorption model. We found an apparent Michaelis-Menten constant of 20.0 mg (117% coefficient of variation), an apparent maximum rate of absorption of 82.6 mg/h (32.9%), and a lag-time of 9.60 min (72%, see also Table 4.2-2). Figure 4.2-1 reveals the highly sufficient predictive performance of our final population PK model. The variability in the plasma concentration raw data was slightly wider between 3 and 5 h post dose than the variability predicted by our population PK model which might be due to variability in the gastric emptying. As this has little influence on the simulated $fT_{>MIC}$ values, it did not affect the PD profile of cefuroxime (see Figure 4.2-2) in our MCS.

Further support for the use of a saturable absorption model comes from dose linearity studies of cefuroxime axetil. Although the area under the plasma concentration time curve is dose linear between 125 and 1000 mg oral

cefuroxime after a meal, the peak concentrations at the 500 and 1000 mg dose level increase slightly less than dose proportional (8-fold increase in dose is associated with a 6.5-fold increase in average peak concentrations, (133)). This observation is not in agreement with a first-order absorption which would predict a proportional increase in peak concentrations. Our PK parameters from NCA (see Table 4.2-1) and from population PK (see Table 4.2-2) were within the range of those reported by other authors (133, 221, 456). Finn et al. (133) find an average area under the curve (AUC) in healthy volunteers of 12.9 mg*h/L for the tablet formulation of 250 mg cefuroxime given after a meal which was comparable to our AUC of 11.9 $\pm$ 2.49 mg*h/L. James et al. (221) report similar AUCs.

The average elimination half-life of cefuroxime is about 1.0-1.4 h in healthy volunteers and the average time of peak concentration is about 2-3 h post dose (133, 136, 221). For a q12h dosage regimen, there are on average about 7 half-lives between the peak concentration and the next dose. This causes a substantial (about 50 fold on average, see Figure 4.2-1) decline in the plasma concentration. However, there is BSV in the elimination half-life which may lead to very low trough concentrations for some subjects. This may explain why some of the clinical trials had microbiological eradication rates of less than 80% (442). Consequently, we explored the superiority of q8h dosage regimens compared to q12h dosing.

We used population PK to estimate the variability in the absorption and disposition parameters of cefuroxime to derive the PKPD breakpoints for oral cefuroxime. The PTA vs. MIC profiles in Figure 4.2-2 indicate that a standard dose of 250 mg oral cefuroxime q12h had a PKPD breakpoint of 0.094 mg/L for the near-maximal killing target ($fT_{>MIC} \geq 65\%$) and a PKPD breakpoint of 0.375 mg/L for the bacteriostasis target ($fT_{>MIC} \geq 40\%$). Most commonly, a PKPD breakpoint of $\leq$1 mg/L for susceptibility has been reported by other authors (261, 313, 379). Mason et al. (313) report that the time above MIC is 40% up to an MIC of about 2 mg/L after a dose of 15 mg/kg cefuroxime q12h. After correcting for a protein binding of 42%, this value corresponds to a breakpoint of about 1.2 mg/L for the target $fT_{>MIC} \geq 40\%$. Other authors (261,

379) report a PKPD breakpoint of 1.0 mg/L for the target $fT_{>MIC} \geq$ 40-50% for "standard doses" of cefuroxime. Our PKPD breakpoint of 0.375 mg/L (target: $fT_{>MIC} \geq$ 40%) for 250 mg oral cefuroxime q12h is about 32% lower than the breakpoint determined by Mason et al. (313) which would be about 0.55 mg/L at a dose of 250 mg cefuroxime q12h. There is also clinical data in children with pneumococcal acute otitis media which suggest a breakpoint of about 0.5 mg/L for oral cefuroxime (90). Besides a lower daily dose, incorporation of BSV into our MCS caused our PKPD breakpoints to be lower than those reported by other authors (261, 379) who based their breakpoint on average PK parameters and did not include BSV. However, it is important to account for BSV, because a patient with a half-life of 1.0 h will have a much shorter $fT_{>MIC}$ for a q12h dosing interval than a patient with a half-life of 1.5 h.

We found higher PKPD breakpoints for 250 mg oral cefuroxime q8h of 0.375 mg/L for the target $fT_{>MIC} \geq$ 65% and of 0.75 mg/L for the target $fT_{>MIC} \geq$ 40% (see Figure 4.2-2). Although the PKPD breakpoints increased for q8h dosing compared to q12h dosing by a factor of 4 for the target $fT_{>MIC} \geq$ 65% and by a factor of 2 for the target $fT_{>MIC} \geq$ 40%, it is important to assess the clinical relevance of this improvement. The PTA expectation values in Table 4.2-3 show that there was only a small improvement from q12h to q8h dosing for *S. pyogenes* and penicillin-susceptible *S. pneumoniae*, because the PTA expectation values were above 95% for *S. pyogenes* and above 92% for penicillin-susceptible *S. pneumoniae* for both regimens.

There were some advantages for the q8h dosage regimen for the near-maximal kill target, e. g. for penicillin susceptible *S. pneumoniae* (PTA expectation value 92-93% for q12h dosing vs. >98% for q8h dosing). Penicillin intermediate *S. pneumoniae* and *M. catarrhalis* isolates had PTA expectations values of ≤48% for q12h dosing and of ≤68% for q8h dosing for the bacteriostasis target. We observed the most pronounced advantage of q8h dosing for *H. influenzae*. Dosing 250 mg cefuroxime q8h achieved PTA expectation values for the bacteriostasis target of 50% for MIC data from Canada, 71% for MIC data from the US and 93% for MIC data from Germany (see Table 4.2-3).

To validate the results of our population PK analysis and MCS, we compared our PTA expectation values to the microbiological and clinical outcomes in clinical studies. Shah et al. (444) studied hospitalized patients and outpatients in 14 countries in Europe, Africa, and South America with acute exacerbation of chronic bronchitis (AECB) and find a 60% bacteriological overall cure rate for 250 mg oral cefuroxime twice daily. Interestingly 56% (22 of 39) of the *H. influenzae* isolates were eradicated. The authors report a clinical cure rate of 66% / 61% (per-protocol / intention-to-treat) at their clinical endpoint (5-14 days post treatment) and of 53% / 39% at the follow-up 3 to 4 weeks post treatment. Although the authors did not report actual MICs in those patients, the failures for the treatment of *H. influenzae* show a sub-optimal effectiveness of oral cefuroxime against this pathogen.

Chodosh et al. (74) find a significantly lower microbiological eradication rate for 500 mg oral cefuroxime bid (82%) vs. 500 mg oral ciprofloxacin bid (96%) in an outpatient trial with AECB patients. Cefuroxime eradicated *S. pneumoniae* in 100% of the cases (13/13), but had only an eradication rate of 76% (19/25) for *M. catarrhalis* and of 86% (19/22) for *H. influenzae*. De Abate et al. (99) conducted an outpatient trial with AECB patients and find a clinical cure rate of 77% for 250 mg oral cefuroxime bid which was significantly lower than the clinical cure rate of 89% for 400 mg gatifloxacin once daily. The microbiological eradication rate was 77% for cefuroxime and 90% for gatifloxacin. Notably, also a trial in patients with community-acquired pneumonia (131) showed a significantly lower microbiological eradication rate of *H. influenzae* for combinations of intravenous ceftriaxone (1 to 2g once daily or bid) and/or oral cefuroxime axetil (500 mg bid) compared to intravenous and/or oral levofloxacin (500 mg once daily). The eradication rates were 79% vs. 100%, respectively.

Consequently, if an infection by *H. influenzae* or *M. catarrhalis* is suspected and the MIC has not yet been determined, q8h dosing of oral cefuroxime should be considered for empiric therapy. As soon as the MIC is available and is below the PKPD breakpoint for 250 mg oral cefuroxime q12h, the dosing interval may be prolonged from q8h to q12h. In additional

simulations (data not shown), 500 mg oral cefuroxime q12h achieved similar PTA expectation values compared to 250 mg oral cefuroxime q8h.

In conclusion, we established a population PK model for oral cefuroxime which included a Michaelis-Menten type absorption from the gut into the central compartment. Our population PK model had a highly sufficient predictive performance and yielded a PKPD breakpoint of 0.375 mg/L for 250 mg oral cefuroxime q12h and of 0.75 mg/L for 250 mg oral cefuroxime q8h for the bacteriostasis target $fT_{>MIC} \geq 40\%$. These breakpoints were slightly lower than the susceptibility breakpoint of ≤1 mg/L provided by the BSAC and DIN, whereas the CLSI breakpoint of ≤4 mg/L is higher for most pathogens. Oral cefuroxime had good PTA expectation values against *S. pyogenes* (≥98%) and penicillin-susceptible *S. pneumoniae* (≥92%), but lower PTA expectation values against *M. catarrhalis* (≤68%), penicillin-intermediate *S. pneumoniae* (≤55%), and *H. influenzae* (≤93%) which varied between countries. If an infection by *H. influenzae* is suspected in empiric therapy, dosing 250 mg oral cefuroxime q8h instead of q12h might be considered to improve the probability of successful treatment. Future clinical trials to assess the effectiveness of cefuroxime axetil dosed q8h are warranted.

## 4.3 Meta-analysis of the pharmacokinetic-pharmacodynamic profile of oral ciprofloxacin and levofloxacin

### 4.3.1 Chemical structure of ciprofloxacin and levofloxacin

**Ciprofloxacin**

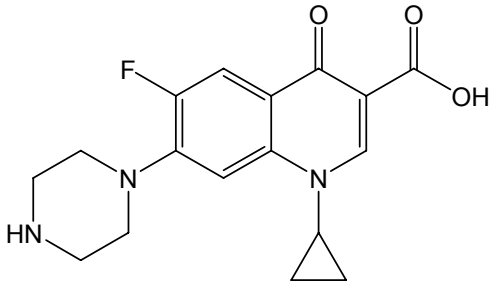


($C_{17}H_{18}FN_3O_3$, Mol. Wt.: 331.34)

**Levofloxacin**

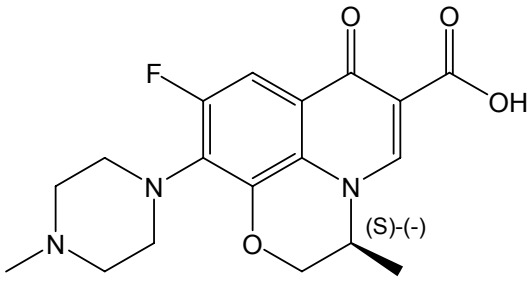


($C_{18}H_{20}FN_3O_4$, Mol. Wt.: 361.37)

**Chemical structure 4.3-1** Levofloxacin and ciprofloxacin

### 4.3.2 Advantages of a meta-analysis by population PK

The PKPD profile of several antibiotics is often compared by combining (literature) data on the PK from different studies. This approach may lack statistical consistency, since results from different subject groups, analytical laboratories, and investigators are pooled. Differences in demographic variables (e. g. body size) which may influence the PK parameters are not accounted for by such a comparison. Therefore, we performed a meta-analysis with data on oral levofloxacin and ciprofloxacin from a single laboratory to compare their PKPD profile via population PK and MCS.

Our first objective was to study the average PK parameters and their variability of extended release (XR) and immediate release (IR) oral ciprofloxacin and IR oral levofloxacin. Our second objective was to assess the PKPD breakpoint for both drugs and our third objective was to compare the PKPD profile of levofloxacin and ciprofloxacin against *S. pneumoniae*,

*P. aeruginosa*, *S. aureus*, *H. influenzae*, and *M. catarrhalis* for a range of *f*AUC/MIC targets.

### 4.3.3 Methods

The general clinical and sample handling procedures, the methods for PK analysis (including NCA and population PK), and the general methods for MCS are described in chapter 2.

***Study design:*** We used data from three single dose, two-way crossover studies in a total of n=38 healthy volunteers. Study 1 (n=12): 1000 mg XR ciprofloxacin vs. 500 mg IR levofloxacin; study 2 (n=14): 500 mg IR ciprofloxacin vs. 500 mg IR levofloxacin; study 3 (n=12): 500 mg IR ciprofloxacin vs. another comparator drug (data not shown here). Table 4.3-1 shows the demographic data. The average body weight differed by about 11% between study 1 and study 2.

***Drug administration and sample collection:*** Doses were administered as single oral doses in the fasting state together with 240 mL low carbonated mineral water. We took between eight and 14 blood samples from 0 to 32 h and seven or eight urine samples from 0 to 120 h from each patient in each study period. Blood samples were taken at pre-dose, 0.5, 1, 1.5, 2, 3, 4, 6, 8, 12, 16, 24, 28, and 32 h post dose in study 1. Blood sampling times in study 2 and 3 were: pre-dose, 1, 2, 3, 4, 6, 12, and 24 h post dose. It is important to note these differences in blood sampling times within the first two hours after dosing for interpretation of NCA results.

***Sample preparation:*** All sample handling was done under protection from daylight. Serum samples were thawed and vigorously mixed, then precipitated with acetonitrile/perchloric acid containing the internal standard. After centrifugation 10 µL of the supernatant were analyzed. Urine samples were thawed and vigorously mixed then diluted 1:100 with buffer containing the internal standard. 17 µL of the diluted sample were analyzed.

**Table 4.3-1** Demographic data (average ± SD and median [range])

| | Study 1 | Study 2 | Study 3 | All studies |
|---|---|---|---|---|
| Ciprofloxacin dose | 1000 mg XR | 500 mg IR | 500 mg IR | |
| Levofloxacin dose | 500 mg IR | 500 mg IR | | |
| Number of subjects (females / males) | 12 (6 / 6) | 14 (7 / 7) | 12 (6 / 6) | 38 (19 / 19) |
| Weight (kg) | 71.9 ± 13.9<br>68.5 [46-96] | 64.6 ± 9.5<br>65.2 [54-85] | 68.2 ± 8.5<br>66.0 [58-86] | 68.0 ± 10.9<br>65.8 [46-96] |
| Height (cm) | 170 ± 10.5<br>167 [157-190] | 172 ± 7.9<br>171 [160-184] | 172 ± 8.1<br>171 [159-187] | 171 ± 8.6<br>170 [157-190] |
| Age (yrs) | 32.9 ± 10.5<br>36.5 [19-45] | 23.0 ± 6.4<br>20.5 [18-40] | 27.7 ± 8.4<br>24.5 [19-42] | 27.6 ± 9.2<br>24.0 [18-45] |

***Assay conditions:*** Levofloxacin and ciprofloxacin were analyzed in one chromatographic run. Chromatographic separation was performed with a reversed phase column, isocratic solvent system [citric acid buffer containing ammonium perchlorate and acetonitrile containing ion-pair reagent (90/10, v/v)], and the effluent was monitored by fluorescence detection (excitation, 285 nm; emission, 480 nm). Turbochrom 3 software (version 3.2; 1991; PE Nelson, Cupertino, Calif.) was used for evaluation of chromatograms.

***Calibration row and spiked quality controls:*** The drug concentrations in serum and urine samples were measured by comparison with a serum and urine calibration row, respectively. Calibration standards were prepared by adding the defined amounts of standard solution of levofloxacin and ciprofloxacin to tested drug-free serum or urine.

Spiked quality controls (SQC) were prepared for determination of interassay variation by the addition of defined amounts of the stock solution or the spiked control of higher concentration to defined amounts of tested drug-free serum or urine. No interference was observed, for levofloxacin, ciprofloxacin or the internal standard in serum and urine. Weighted linear regression (1/peak height ratio) was performed for calibration.

The linearity of the calibration curve could be shown between concentrations of 0.00234 mg/L and 7.93 mg/L for levofloxacin and

0.00230 mg/L and 7.82 mg/L for ciprofloxacin in serum. The quantification levels were identical to the lowest calibration levels. The inter-assay precision of the SQCs in serum was 2.6% (6.41 mg/L), 2.6% (0.626 mg/L), 4.3% (0.0488 mg/L) and 7.2% (0.0122 mg/L) (range of accuracies of SQCs, 97.1% to 98.2%) for levofloxacin and 2.2% (6.40 mg/L), 2.4% (0.625 mg/L), 4.3% (0.0487 mg/L) and 7.7% (0.0122 mg/L) (range of accuracies of SQCs, 93.0% to 98.2%) for ciprofloxacin.

The linearity of the calibration curve could be shown between concentrations of 0.250 mg/L and 809 mg/L for levofloxacin and 0.248 mg/L and 800 mg/L for ciprofloxacin in urine. The quantification levels were identical to the lowest calibration levels. The inter-assay precision of the SQCs in urine was 2.1% (641 mg/L), 3.6% (62.0 mg/L), 2.3% (4.77 mg/L) and 3.3% (1.19 mg/L) (range of accuracies of SQCs, 98.3% to 100.8%) for levofloxacin and 2.4% (640 mg/L), 4.0% (61.9 mg/L), 3.4% (4.77 mg/L) and 6.3% (1.18 mg/L) (range of accuracies of SQCs, 99.9% to 101.8%) for ciprofloxacin.

***PK analysis:*** We considered one-, two-, and three compartment disposition models. The absorption was described as first-order or zero-order process both with or without an absorption lag-time. We incorporated body size by a standard allometric model based on WT with an allometric exponent of 0.75 for all clearance terms, and an exponent of 1.0 for all volume terms (see chapter 2.6.2.2 for details).

***MCS:*** We compared oral dosage regimens of 500 mg levofloxacin q24h, 500 mg ciprofloxacin (IR formulation) q12h, and 1000 mg ciprofloxacin (XR formulation) q24h in our MCS. We simulated the *f*AUC/MIC for at least 10,000 subjects per treatment. An average protein binding of 31% for levofloxacin (134) and of 30% for ciprofloxacin (190, 405, 560) was assumed.

We studied *f*AUC/MIC targets between 5 and 300. An AUC/MIC ratio of at least 125 for ciprofloxacin (which corresponds to a *f*AUC/MIC of 87.5 assuming a protein binding of 30%) is predictive for optimal clinical and microbiological outcomes in patients with serious infections by gram-negative microorganisms including *P. aeruginosa* (137). For gram-positive organisms, the required *f*AUC/MIC target for quinolones is lower than for gram-negative organisms. Several *in vitro* studies report a *f*AUC/MIC target between 30 and

55 for levofloxacin and ciprofloxacin against *S. pneumoniae* (277, 292, 293). Ambrose et al. (9) found a *f*AUC/MIC of 33.7 for levofloxacin against *S. pneumoniae* to be predictive of successful microbiological response in patients with community acquired respiratory tract infections. Preston et al. (107, 392) found a *f*AUC/MIC of 42 for levofloxacin against various organisms including *S. pneumoniae* and *S. aureus* to be predictive of successful microbiological response in patients with community acquired infections. We used MIC distributions from literature on penicillin susceptible *S. pneumoniae* isolates from 44 countries worldwide (52), *S. pneumoniae*, *H. influenzae*, and *M. catarrhalis* isolates from the UK (330), and *P. aeruginosa* and *S. aureus* isolates from Germany (205). These MIC distributions include MIC data of ciprofloxacin and levofloxacin for the same isolates.

### 4.3.4 Results

Figure 4.3-1 shows the average plasma concentration time profiles of ciprofloxacin (panel A) and levofloxacin (panel B). The average profiles for the 500 mg IR ciprofloxacin formulations in study 2 and 3 were virtually identical as were the average profiles for the 500 mg IR levofloxacin formulations in study 1 and 2. Table 4.3-2 lists the results from NCA for ciprofloxacin and Table 4.3-3 shows the NCA results for levofloxacin. It is important to keep in mind for interpretation of the NCA results that the majority of subjects had their peak concentration at the first sample (1 h post dose) for the ciprofloxacin and levofloxacin IR formulations in study 2 and 3. Consequently, the AUC from NCA is probably lower than the “true” AUC in study 2 and 3. This bias also affects the calculated total, renal, and nonrenal clearance.

The ciprofloxacin XR formulation showed a slower absorption / drug release than the IR formulations as indicated by the times to peak concentration (see Table 4.3-2). The terminal half-life of ciprofloxacin in plasma was estimated to be longer for the XR formulation than for the IR formulations, probably because of the different sampling schedule and higher ciprofloxacin dose of study 1 compared to studies 2 and 3.

**Panel A:** Ciprofloxacin

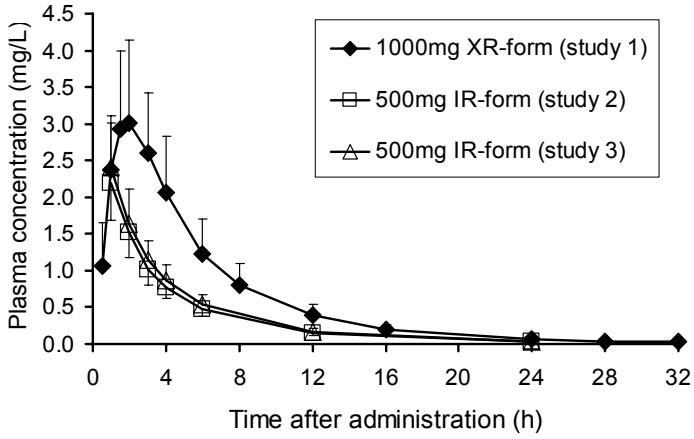


**Panel B:** Levofloxacin

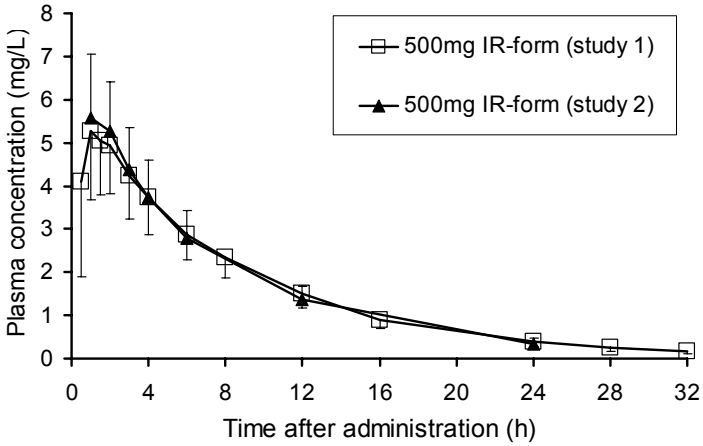


**Figure 4.3-1** Average ± SD concentrations of ciprofloxacin and levofloxacin

Population PK analysis was superior to NCA for the meta-analysis of the three studies, as population PK is not biased due to the different sampling schedules as described above. A three-compartment model with first-order absorption was most appropriate for ciprofloxacin and levofloxacin. Inclusion of a lag time for the oral absorption significantly improved the model fit and predictive performance. Inclusion of WT as covariate reduced the BSV in clearance, volume of distribution, and extent of absorption (due to the influence of body size both on clearance and volume of distribution) for ciprofloxacin and levofloxacin. Accounting for the differences in extent of absorption between different studies improved the objective function significantly and also improved the predictive performance. The highly sufficient predictive performance of our final models is shown in Figure 4.3-2.

**Table 4.3-2** PK parameters from NCA for ciprofloxacin

| | **Study 1** | **Study 2** | **Study 3** | **All studies** |
|---|---|---|---|---|
| Ciprofloxacin dose | 1000 mg XR | 500 mg IR | 500 mg IR | |
| Number of subjects | 12 | 14 | 12 | 38 |
| Time of peak concentration (h) | 1.96 ± 0.81<br>1.76 [1.00-4.00] | 1.00 ± 0.01<br>1.00 [0.97-1.03] | 1.09 ± 0.29<br>1.00 [1.00-2.00] | |
| Peak concentration (mg/L) | 3.28 ± 0.99<br>3.19 [1.45-4.92] | 2.18 ± 0.50<br>2.30 [1.40-2.95] | 2.46 ± 0.48<br>2.50 [1.61-3.18] | |
| Area under plasma concentration time curve (mg*h/L) | 19.4 ± 5.56<br>18.4 [7.82-28.3] | 9.04 ± 1.68<br>9.30 [6.64-11.9] | 9.98 ± 2.14<br>10.1 [6.19-14.4] | |
| Apparent total clearance (L/h) | 57.4 ± 24.6<br>54.2 [35.3-128] | 57.2 ± 10.9<br>53.8 [41.9-75.3] | 52.4 ± 12.1<br>49.4 [34.7-80.7] | 55.7 ± 16.4<br>52.9 [34.7-128] |
| Renal clearance (L/h) | 21.2 ± 3.44<br>21.3 [16.9-26.1] | 20.5 ± 2.05<br>19.9 [17.8-25.4] | 21.2 ± 8.73<br>19.4 [9.09-45.3] | 20.9 ± 5.27<br>19.8 [9.09-45.3] |
| Apparent nonrenal clearance (L/h) | 36.2 ± 24.8<br>30.3 [18.5-110] | 36.6 ± 11.4<br>33.7 [21.3-54.5] | 31.2 ± 6.98<br>32.2 [17.9-44.6] | 34.8 ± 15.8<br>31.7 [17.9-110] |
| Fraction excreted unchanged in urine (%) | 40.5 ± 9.9<br>43.1 [13.7-50.8] | 37.2 ± 8.1<br>38.6 [25.9-50.3] | 39.9 ± 9.3<br>42.7 [19.7-56.1] | 39.1 ± 9.0<br>40.8 [13.7-56.1] |
| Apparent volume of distribution during terminal phase (L) | 778 ± 1058<br>466 [246-4102] | 364 ± 111<br>330 [240-554] | 331 ± 83.3<br>309 [213-507] | 484 ± 617<br>352 [213-4102] |
| Terminal half-life in plasma (h) | 7.70 ± 4.76<br>6.20 [4.83-22.2] | 4.40 ± 0.91<br>4.61 [2.39-5.40] | 4.39 ± 0.56<br>4.20 [3.75-5.79] | 5.44 ± 3.09<br>4.83 [2.39-22.2] |
| Terminal half-life in urine (h) | 7.49 ± 4.57<br>5.88 [4.91-21.3] | 12.4 ± 5.89<br>11.0 [4.27-23.8] | 7.71 ± 3.09<br>6.79 [5.03-16.3] | 9.38 ± 5.18<br>7.41 [4.27-23.8] |

Table 4.3-4, Table 4.3-5, and Table 4.3-6 show the final estimates for the population PK models. As shown in Figure 4.3-2 (panel A), one subject most likely had a lower extent of absorption than all other subjects for the 1000 mg ciprofloxacin XR formulation. The terminal half-life of this subject was comparable to the half-life of the other subjects, therefore this subject probably had a lower extent of absorption and a clearance and volume of distribution within the range of the other subjects.

**Table 4.3-3** PK parameters from NCA for levofloxacin

| | **Study 1** | **Study 2** | **Studies 1 & 2** |
|---|---|---|---|
| Levofloxacin dose | 500 mg IR | 500 mg IR | |
| Number of subjects | 12 | 14 | 26 |
| Time of peak concentration (h) | 1.16 ± 0.50<br>1.00 [0.48-2.00] | 1.36 ± 0.50<br>1.00 [1.00-2.00] | 1.27 ± 0.50<br>1.00 [0.48-2.00] |
| Peak concentration (mg/L) | 6.17 ± 1.25<br>6.44 [3.29-7.54] | 6.07 ± 1.15<br>6.08 [3.93-7.74] | 6.12 ± 1.17<br>6.27 [3.29-7.74] |
| Area under the plasma concentration time curve (mg*h/L) | 49.2 ± 8.22<br>50.2 [35.5-63.5] | 46.9 ± 9.00<br>44.4 [34.7-68.9] | 48.0 ± 8.56<br>47.2 [34.7-68.9] |
| Apparent total clearance (L/h) | 10.4 ± 1.77<br>9.95 [7.87-14.1] | 11.0 ± 1.94<br>11.3 [7.26-14.4] | 10.7 ± 1.85<br>10.6 [7.26-14.4] |
| Renal clearance (L/h) | 8.40 ± 1.68<br>8.38 [5.82-12.4] | 8.91 ± 1.65<br>8.94 [6.27-11.9] | 8.68 ± 1.65<br>8.55 [5.82-12.4] |
| Apparent nonrenal clearance (L/h) | 2.02 ± 0.61<br>1.86 [1.30-3.13] | 2.08 ± 0.69<br>1.96 [0.989-3.20] | 2.05 ± 0.64<br>1.91 [0.989-3.20] |
| Fraction excreted unchanged in urine (%) | 80.4 ± 5.5<br>79.8 [74.0-88.2] | 81.2 ± 5.2<br>81.8 [69.6-86.7] | 80.8 ± 5.2<br>80.9 [69.6-88.2] |
| Apparent volume of distribution during terminal phase (L) | 93.8 ± 21.8<br>88.6 [67.3-126] | 92.4 ± 22.1<br>88.8 [62.6-129] | 93.0 ± 21.5<br>88.6 [62.6-129] |
| Terminal half-life in plasma (h) | 6.20 ± 0.71<br>5.98 [5.26-7.71] | 5.84 ± 0.99<br>5.64 [4.41-7.34] | 6.00 ± 0.88<br>5.95 [4.41-7.71] |
| Terminal half-life in urine (h) | 6.98 ± 0.80<br>7.02 [5.82-8.44] | 13.8 ± 2.86<br>13.6 [9.45-19.9] | 10.7 ± 4.09<br>9.79 [5.82-19.9] |

The coefficient of variation for the BSV in extent of absorption was 34% for the ciprofloxacin XR formulation and 18% for the ciprofloxacin IR formulation. Thus, the ciprofloxacin XR formulation had a 3.7-fold larger variance in extent of absorption compared to the IR formulation.

**A) Study 1: 1000 mg ciprofloxacin XR**

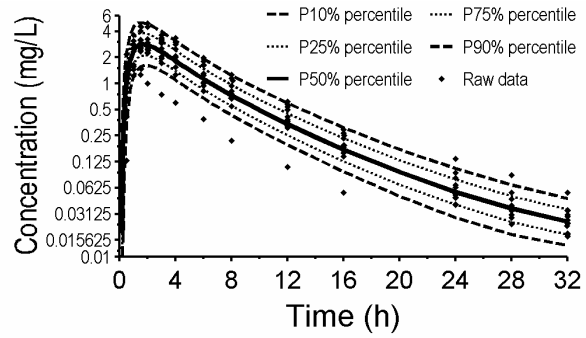


**B) Study 2: 500 mg ciprofloxacin IR**

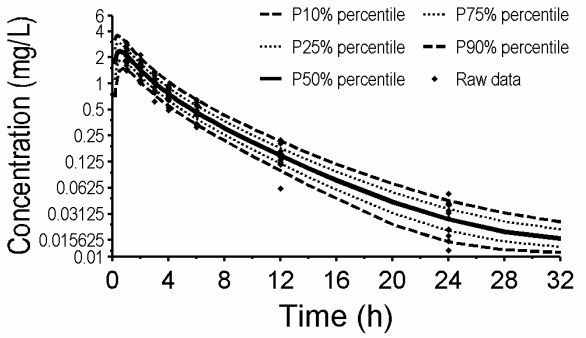


**C) Study 3: 500 mg ciprofloxacin IR**

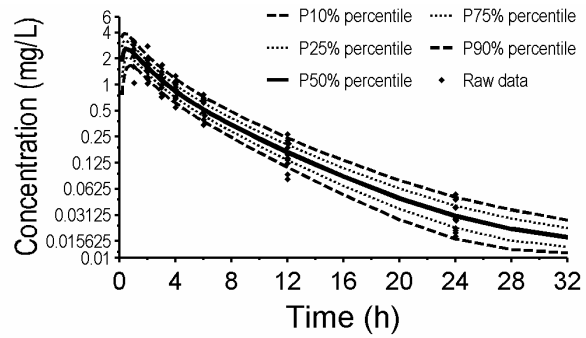


**D) Study 1: 500 mg levofloxacin IR**

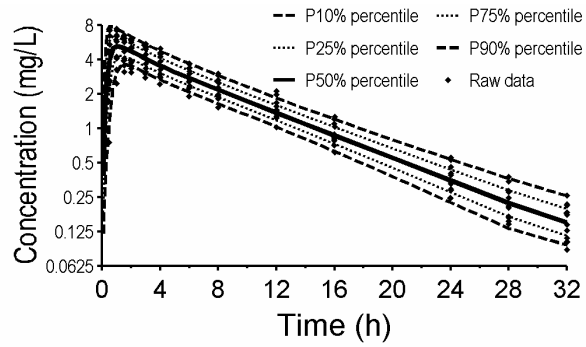


**E) Study 2: 500 mg levofloxacin IR**

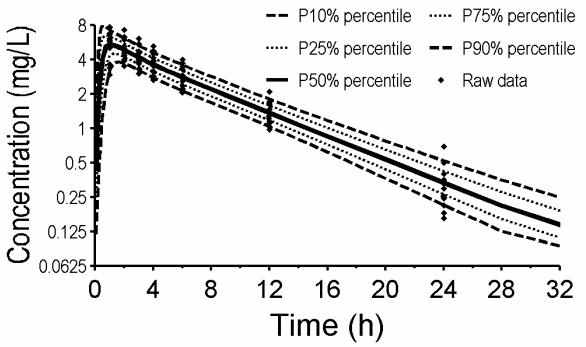


**Figure 4.3-2** VPCs based on at least 4,800 simulated subjects for the final models (see Table 4.3-4 and Table 4.3-5).

See chapter 2.6.3 for interpretation of VPCs.

**Table 4.3-4** Population PK parameters of ciprofloxacin after oral intake of a 1000 mg extended release (XR) formulation or 500 mg immediate release (IR) formulations.

Values are geometric means and apparent coefficients of variation for the BSV.

| **Parameter** | **Unit** | **1000 mg XR** | **500 mg IR** | |
|---|---|---|---|---|
| | | Study 1 | Study 2 | Study 3 |
| F (relative to XR) | | 1.00 (34%) | 1.01 (18%) | 1.18 (18%) |
| TLAG | min | 16.9 (37%) | (set to zero) | |
| TABS | min | 41.7 (42%) | 8.2 (90%) | |
| $CL_T/F$ § | L $h^{-1}$ | 54.9* (5.7%) | | |
| Vss/F §,° | L | 276* (15%) | | |
| V1/F § | L | 162* | | |
| V2/F § | L | 67.0* | | |
| V3/F § | L | 46.5* | | |
| $CLic_{shallow}/F$ § | L $h^{-1}$ | 32.6* | | |
| $CLic_{deep}/F$ § | L $h^{-1}$ | 4.58* | | |
| $CV_C$ | % | 11% | | |
| $SD_C$ | mg/L | 0.0072 | | |

*: Group estimate for a subject with WT = 70 kg.

§: Values are apparent clearances and apparent volumes of distribution with the extent of absorption of the XR formulation as reference.

°: Derived from PK parameter estimates. Vss was not an estimated model parameter.

F: extent of absorption (this factor also accounts for differences in the pharmaceutical content between the formulations used in each study), TLAG: lag time of absorption, TABS: half-life of absorption, $CL_T/F$: apparent total clearance, Vss/F: apparent volume of distribution at steady-state, V1/F: apparent volume of distribution for the central compartment, V2/F: apparent volume of distribution for the shallow peripheral compartment, V3/F: apparent volume of distribution for the deep peripheral compartment, $CLic_{shallow}/F$: apparent intercompartmental clearance between the central and the shallow peripheral compartment, $CLic_{deep}/F$: apparent intercompartmental clearance between the central and the deep peripheral compartment; $CV_C$ is the proportional and $SD_C$ is the additive residual error component for the plasma concentrations.

**Table 4.3-5** Population PK parameters of levofloxacin after oral intake of 500 mg immediate release (IR) formulations.

Values are population means and apparent coefficients of variation for the BSV

| Parameter | Unit | 500 mg IR | |
|---|---|---|---|
| | | Study 1 | Study 2 |
| F | | 1.00 (fixed) | 0.927 |
| TLAG | min | 17.8 (57%) | |
| TABS | min | 16.7 (73%) | |
| $CL_T/F$ § | L $h^{-1}$ | 10.5* (13%) | |
| Vss/F §,° | L | 80.5* | |
| V1/F § | L | 38.5* (33%) | |
| V2/F § | L | 19.2* (54%) | |
| V3/F § | L | 22.8* (35%) | |
| $CLic_{shallow}/F$ § | L $h^{-1}$ | 73.9* | |
| $CLic_{deep}/F$ § | L $h^{-1}$ | 16.1* | |
| $CV_C$ | % | 4.7% | |
| $SD_C$ | mg/L | 0.00035 | |

*: Group estimate for a subject with WT = 70 kg.

§: Values are apparent clearances and apparent volumes of distribution with the extent of absorption of the IR formulation of study 1 as reference.

°: Derived from PK parameter estimates. Vss was not an estimated model parameter.

See Table 4.3-4 for parameter explanations.

**Table 4.3-6** Variance-covariance matrix on log-scale (natural logarithm) for the BSV of levofloxacin (see Table 4.3-4 for parameter explanations)

| | **$CL_T$** | **V1** | **V2** | **V3** | **TABS** | **TLAG** |
|---|---|---|---|---|---|---|
| **$CL_T$** | 0.0175 | | | | | |
| **V1** | -0.00604 | 0.112 | | | | |
| **V2** | 0.0197 | -0.172 | 0.29 | | | |
| **V3** | 0.0217 | 0.0237 | -0.0177 | 0.126 | | |
| **TABS** | -0.00452 | 0.0182 | -0.0802 | 0.0547 | 0.535 | |
| **TLAG** | -0.00686 | 0.097 | -0.193 | -0.00637 | -0.0895 | 0.322 |

The higher BSV in extent of absorption for the ciprofloxacin XR formulation relative to the IR formulation had only a minor influence on the PTA vs. MIC profile for ciprofloxacin. Both the ciprofloxacin XR and IR formulation at a daily dose of 1000 mg achieved a PKPD breakpoint of about 0.25 mg/L for the target *f*AUC/MIC ≥ 33.7 (see Figure 4.3-3, panel A). The respective PKPD breakpoint for the target *f*AUC/MIC ≥ 87.5 was 0.0625 to 0.125 mg/L for ciprofloxacin (see Figure 4.3-3, panel B).

Levofloxacin achieved about two-fold higher PKPD breakpoints than ciprofloxacin. The PKPD breakpoint for levofloxacin at a daily dose of 500 mg was 0.5 mg/L for the *f*AUC/MIC ≥ 33.7 target and 0.25 mg/L for the *f*AUC/MIC ≥ 87.5 target (see Figure 4.3-3).

Combining the PTA vs. MIC profiles shown in Figure 4.3-3 with the MIC distributions for both drugs yields the PTA expectation values shown in Figure 4.3-4 for a range of PKPD targets. Both drugs achieved PTA expectation values above 95% for targets up to *f*AUC/MIC ≥ 90 against *H. influenzae* and *M. catarrhalis*. PTA expectation values were low for both drugs against *P. aeruginosa*. Levofloxacin achieved higher PTA expectation values against *S. pneumoniae* and *S. aureus* relative to ciprofloxacin.

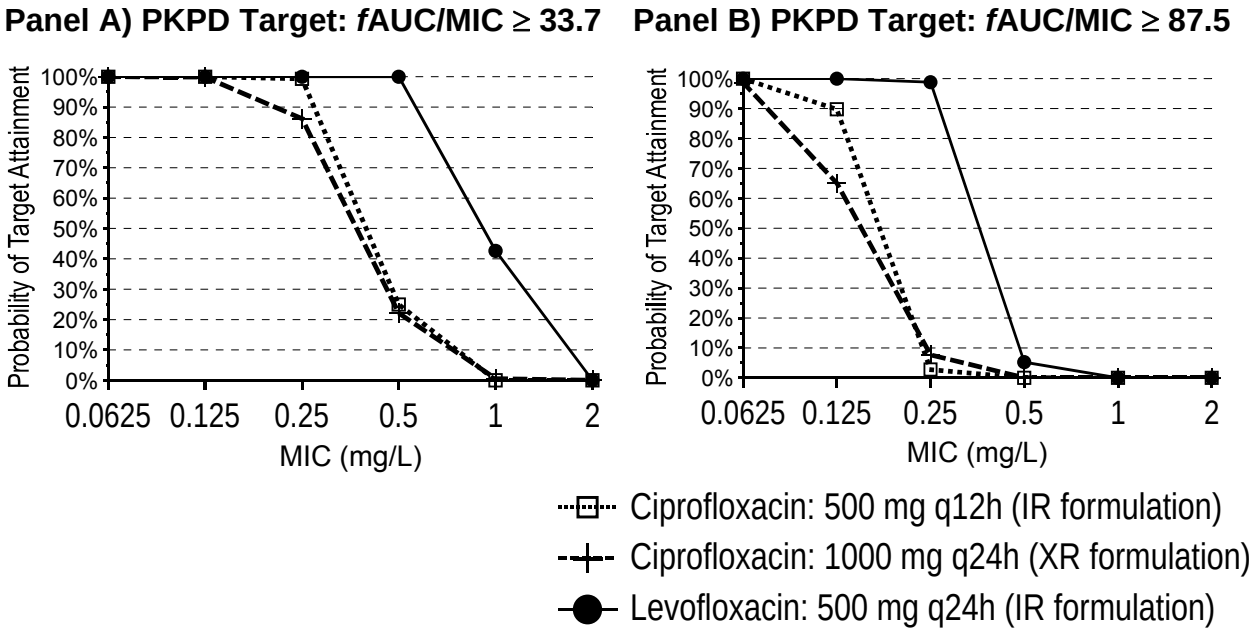


**Figure 4.3-3** Probability of target attainment for oral ciprofloxacin (daily dose: 1000 mg) and oral levofloxacin (daily dose: 500 mg)

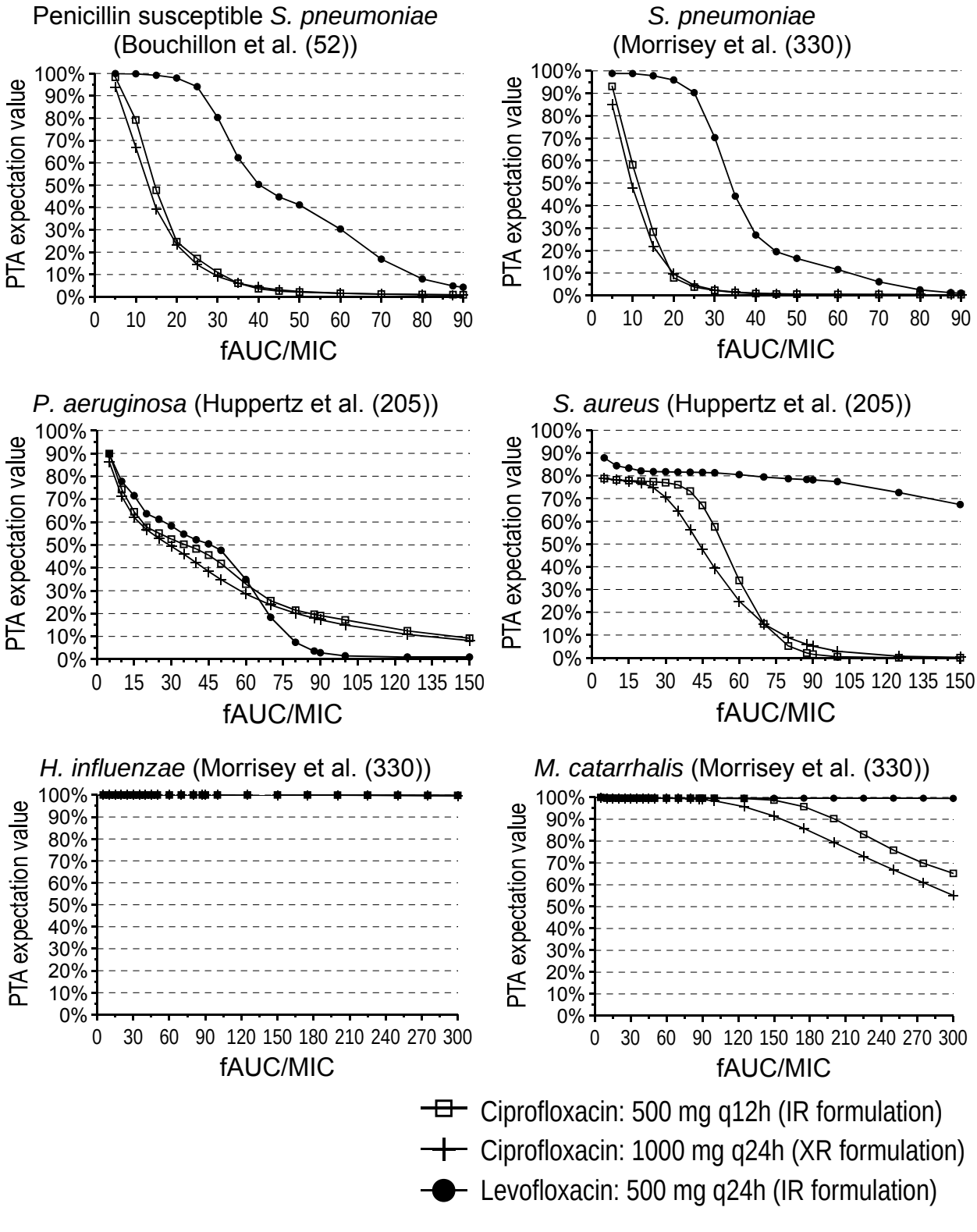


**Figure 4.3-4** PTA expectation values for oral ciprofloxacin (daily dose: 1000 mg) and oral levofloxacin (daily dose: 500 mg) for the MIC distribution of the respective study

### 4.3.5 Discussion

The growing emergence of resistance to antibiotics is a serious problem. Suboptimal antibiotic dosage regimens may kill the antibiotic-susceptible subpopulation of bacteria, while the antibiotic-resistant subpopulation amplifies and replaces the susceptible subpopulation during the course of therapy. Most of the PKPD targets for successful microbiological or clinical response have not been established to predict prevention of selection of resistant mutants.

The group of Drusano determined targets for quinolones for prevention of selection of resistant mutants. Jumbe et al. (239) used a non-neutropenic mouse thigh infection model with *P. aeruginosa*. They determined and prospectively validated an AUC/MIC target of 157 for levofloxacin to suppress amplification of the antibiotic-resistant subpopulation. Tam et al. (487) used an *in vitro* infection model to determine the AUC/MIC of garenoxacin which is required to suppress selection of amplification of the antibiotic-resistant subpopulation. They found that an AUC/MIC of 190 is predictive for this target. This *in vitro* infection model contains no granulocytes and therefore the AUC/MIC target is higher than in immuno-competent hosts like non-neutropenic mice. Importantly, the AUC/MIC target of 125 for ciprofloxacin which is predictive for optimal clinical and microbiological outcomes in patients with serious infections by gram-negative microorganisms including *P. aeruginosa* (137) is lower than the targets required for suppression of emergence of resistance.

*S. pneumoniae* develops resistance to quinolones typically in a stepwise manner (97, 110). A single mutation in the quinolone resistance-determining regions of gyrA or parC increases the MIC by about a factor of four. The strains achieve clinical resistance, if multiple mutations involving both genes occur, because the drug exposure in humans is insufficient to kill the strains with multiple mutations. It has been hypothesized (236) that the chance for emergence of resistance can be significantly reduced, if the dosage regimens achieve a drug exposure which can eradicate

subpopulations with a single mutation. Such an about fourfold higher drug exposure would represent the drug exposure to prevent emergence of resistance. The *f*AUC/MIC required for successful microbiological outcome for treatment of *S. pneumoniae* is about 33.7 for levofloxacin in patients with community acquired respiratory tract infections (9). Therefore, a resistance prevention exposure is likely to be a *f*AUC/MIC of roughly 135. The resistance prevention exposure probably varies for each combination of drug and pathogen and the exact resistance prevention exposure has not yet been determined for ciprofloxacin or levofloxacin against *S. pneumoniae*. However, these data suggest that it may be beneficial to achieve a higher *f*AUC/MIC than required for successful microbiological outcome.

Therefore, we examined a wide range of *f*AUC/MIC targets in our meta-analysis of ciprofloxacin and levofloxacin. A possible shortcoming of many PK studies in healthy volunteers is their small sample size. The BSV in total clearance might not be reliably estimated based on PK data from less than about 20 subjects. We therefore combined PK data from three cross-over studies with ciprofloxacin and levofloxacin to achieve a total sample size of 38 subjects for ciprofloxacin (data from three studies) and of 26 subjects for levofloxacin (data from two studies).

Our PK parameter estimates for levofloxacin and ciprofloxacin were well within the range of results reported by other authors (10, 134, 458, 461, 462, 464, 560) in healthy volunteers. We could show that population PK was superior to NCA, as population PK can account for differences in body size and differences in the pharmaceutical content of various formulations. Additionally, population PK is much more powerful than NCA, if datasets with considerably different sampling schedules are combined.

Our population PK models (see Table 4.3-4, Table 4.3-5, and Table 4.3-6) had a highly sufficient predictive performance (see Figure 4.3-2). We estimated the BSV for CL/F which includes both the BSV in clearance (CL) and the BSV in extent of absorption (F) for levofloxacin. CL/F had a low coefficient of variation of 13% in healthy volunteers for levofloxacin. We separated the variability in CL and F for ciprofloxacin, since the BSV in F was likely to be different for the ciprofloxacin XR and IR formulation. The BSV in F

had a coefficient of variation of 34% for the XR formulation and of 18% for the IR ciprofloxacin formulation (see Table 4.3-4). As the coefficient of variation was only 5.7% for CL of ciprofloxacin, CL/F had a coefficient of variation of about 35% for the XR formulation and of about 19% for the IR formulation which was higher than the BSV in CL/F of 13% for levofloxacin. Besides the administered dose, CL/F is the only PK parameter which determines the AUC. The lower BSV in CL/F for levofloxacin was the first reason why the PKPD breakpoint of levofloxacin was about twofold higher than for ciprofloxacin.

Although a usual daily dose of oral ciprofloxacin (1000 mg) is higher than the daily dose of oral levofloxacin (500 mg), ciprofloxacin had an about fivefold larger CL/F than levofloxacin (see Table 4.3-4 and Table 4.3-5). This is the second reason for the lower PKPD breakpoint of ciprofloxacin compared to levofloxacin Figure 4.3-3.

Interestingly, there was only a small difference in the PTA vs. MIC profile between the XR and IR ciprofloxacin formulation, although the BSV in CL/F was 3.4 fold larger for the XR formulation. We determined a PKPD breakpoint of about 0.25 mg/L for ciprofloxacin and of 0.5 mg/L for levofloxacin for the target *f*AUC/MIC $\geq$ 33.7 which represents a successful microbiological outcome against *S. pneumoniae* in community acquired respiratory tract infections (9). The PKPD breakpoint was lower for the PKPD target *f*AUC/MIC $\geq$ 87.5 (AUC/MIC $\geq$ 125) which represents optimal clinical and microbiological outcomes in patients with serious infections by gram-negative microorganisms including *P. aeruginosa* (137). Ciprofloxacin achieved a PKPD breakpoint of 0.0625 to 0.125 mg/L and levofloxacin of 0.25 mg/L for the target *f*AUC/MIC $\geq$ 87.5. Importantly, our PKPD breakpoints are lower than the susceptibility breakpoints set by national organizations.

The DIN (104) specified a breakpoint of $\leq$2 mg/L for susceptibility to levofloxacin and of $\leq$1 mg/L for ciprofloxacin. The susceptibility breakpoints of the CLSI (352) are $\leq$2 mg/L for levofloxacin and $\leq$1 mg/L for ciprofloxacin (for all pathogens reported in reference (352) except *N. gonorrhoeae*). Interestingly, the BSAC (56) specified in part lower breakpoints for ciprofloxacin: $\leq$0.12 mg/L for *S. pneumoniae*, $\leq$0.5 mg/L for

Enterobacteriaceae, *Acinetobacter*, *Pseudomonas*, *M. catarrhalis*, and *H. influenzae*, ≤1 mg/L for staphylococci. The BSAC breakpoints (56) for levofloxacin are: ≤2 mg/L for *S. pneumoniae* and ≤1 mg/L for Enterobacteriaceae, *Acinetobacter*, *Pseudomonas*, *M. catarrhalis*, and *H. influenzae*.

We determined the clinical relevance of our PKPD breakpoints by calculation of PTA expectation values for various MIC distributions from literature. These MIC distributions (52, 205, 330) contain MIC data for ciprofloxacin and levofloxacin for the same isolates. Both levofloxacin and ciprofloxacin achieved PTA expectation values of 100% for targets up to *f*AUC/MIC ≥ 300 (and above) against *H. influenzae* (see Figure 4.3-4). Levofloxacin achieved PTA expectation values of 100% for targets up to *f*AUC/MIC ≥ 300 (and above) for *M. catarrhalis*, whereas ciprofloxacin achieved lower PTA expectation values for targets higher than *f*AUC/MIC ≥ 100 against *M. catarrhalis*.

Both drugs achieved insufficient PTA expectation values against *P. aeruginosa* and should not be used as monotherapy against *P. aeruginosa* (see Figure 4.3-4). Ciprofloxacin achieved PTA expectation values below 10% against *S. pneumoniae* for the target *f*AUC/MIC ≥ 33.7. PTA expectation values for levofloxacin were only 50-55% for *S. pneumoniae* at the *f*AUC/MIC ≥ 33.7 target. Recently, Jumbe et al. (240) found in a mouse thigh infection model that pre-exposure to ciprofloxacin increases the mutational frequency of *S. pneumoniae* and increases the emergence of resistance to levofloxacin. Therefore, Jumbe et al. (240) proposed to minimize the use of ciprofloxacin in community acquired respiratory tract infections.

PTA expectation values for levofloxacin were higher against *S. aureus* relative to ciprofloxacin. PTA expectation values for ciprofloxacin were below 70% for targets higher than *f*AUC/MIC ≥ 30, whereas levofloxacin achieved PTA expectation values above 70% up to targets of *f*AUC/MIC ≥ 120. Therefore, levofloxacin might cause less emergence of resistance for *S. aureus* than ciprofloxacin.

In conclusion, we developed population PK models for oral ciprofloxacin and levofloxacin with a highly sufficient predictive performance. The PK of both drugs was adequately described by a three-compartment model with first order absorption including a lag time. For the PKPD target *f*AUC/MIC ≥ 33.7 representing successful microbiological outcome against *S. pneumoniae*, ciprofloxacin at a daily dose of 1000 mg achieved a PKPD breakpoint of 0.25 mg/L and levofloxacin at a daily dose of 500 mg achieved a PKPD breakpoint of 0.5 mg/L. For the PKPD target *f*AUC/MIC ≥ 87.5 representing successful outcome against serious infections by gram-negative pathogens including *P. aeruginosa*, ciprofloxacin achieved a PKPD breakpoint of 0.0625 to 0.125 mg/L and levofloxacin of 0.25 mg/L (same doses as above). Our PKPD breakpoints were considerably lower than most of the susceptibility breakpoints set by the DIN, CLSI, and BSAC for ciprofloxacin and levofloxacin. Both drugs achieved high PTA expectation values against *H. influenzae* and *M. catarrhalis*, whereas PTA expectation values did not support monotherapy against *P. aeruginosa* for both drugs. Ciprofloxacin also achieved insufficient PTA expectation values against *S. pneumoniae*. PTA expectation values for levofloxacin against *S. pneumoniae* were higher than for ciprofloxacin, but probably also did not support monotherapy against this pathogen in empiric treatment. Levofloxacin achieved superior PTA expectation values compared to ciprofloxacin against *S. aureus* and potentially causes less emergence of resistance of *S. aureus* than ciprofloxacin. Clinical studies are warranted to assess the clinical breakpoint of levofloxacin and ciprofloxacin. Further data are also needed on the potential for selection of resistant mutants due to exposure to levofloxacin or ciprofloxacin.

## 4.4 Conclusions on PKPD breakpoints and optimization of dosage regimens for antibiotics

The vast majority of susceptibility breakpoints set by national organizations like the DIN, BSAC, and CLSI for antibiotics have been determined without considering the BSV of PK parameters. Importantly, these susceptibility breakpoints are often not specific to a dosage regimen.

Our PKPD breakpoint for cefuroxime axetil for the bacteriostasis target was about ten times lower than the susceptibility breakpoint set by the CLSI for oral cefuroxime. Such pronounced differences suggest reconsideration of the CLSI breakpoint what has also been recently pointed out by Ambrose et al. (7) for intravenous cephalosporins. The PKPD breakpoint should be compared with the clinical success rates of infections caused by organisms with specific MICs. These success rates will ultimately guide the specification of the most reasonable clinical breakpoint for oral cefuroxime. We additionally studied optimized dosage regimens and their advantages for specific pathogens. Our models predicted advantages of dosing 250 mg oral cefuroxime q8h instead of q12h against some pathogens (e. g. *H. influenzae*).

Our MCS for oral ciprofloxacin and oral levofloxacin could separate pathogens with very high PTAs for both drugs (*H. influenzae* and *M. catarrhalis*), pathogens with insufficient PTAs for both drugs (*P. aeruginosa*), and pathogens with superior PTAs for levofloxacin compared to ciprofloxacin (*S. pneumoniae* and *S. aureus*) at standard doses.

Consequently, population PK in combination with MCS could provide valuable information for empiric therapy of oral cefuroxime, levofloxacin, and ciprofloxacin based on available data. Importantly, these methods account for the BSV and correlation of PK parameters and provide breakpoints which are specific to each dosage regimen. This technique has proven to be fast and cost-efficient and should be applied more frequently in the future.

# 5 Impact of between occasion variability on bioequivalence studies and individualized therapy

## 5.1 Background on different sources of variability and their therapeutic implications

The total variability in PK parameters (=population parameter variability, PPV) can be split into BSV and within subject variability (WSV). WSV can be further split into between occasion variability (BOV) and within occasion variability (WOV) (198) (see Figure 5.1-1). An occasion is usually defined as the shortest time period required to estimate a PK parameter (e. g. clearance) or to estimate a whole set of PK parameters (e. g. all structural parameters of a population PK model). For the work within this thesis, one study period was treated as one occasion.

Covariates such as total body weight or renal function can be used to predict the BSV which yields a predictable component of the BSV ($BSV_{Predictable}$) and a random component of BSV ($BSV_{Random}$). If the change of covariates like renal function is measured over time, such time dependent covariates can be used to split BOV into a predictable component ($BOV_{Predictable}$) and into a random component ($BOV_{Random}$). The predictable component of BSV and BOV is the fraction of variability that can be explained by use of a covariate model. The random component of BSV and BOV is the remaining unexplained variability due to some unobserved effects.

Holford (198) presented data on the PPV, BSV, and WSV of ten drugs. The coefficient of variation for those ten drugs ranged between 20 and 72% for PPV, between 11.8 and 57% for BSV, and between 15.6 and 53% for BOV. The average coefficients of variation for these ten example drugs are 51% for PPV, 41% for BSV, and 30% for WSV.

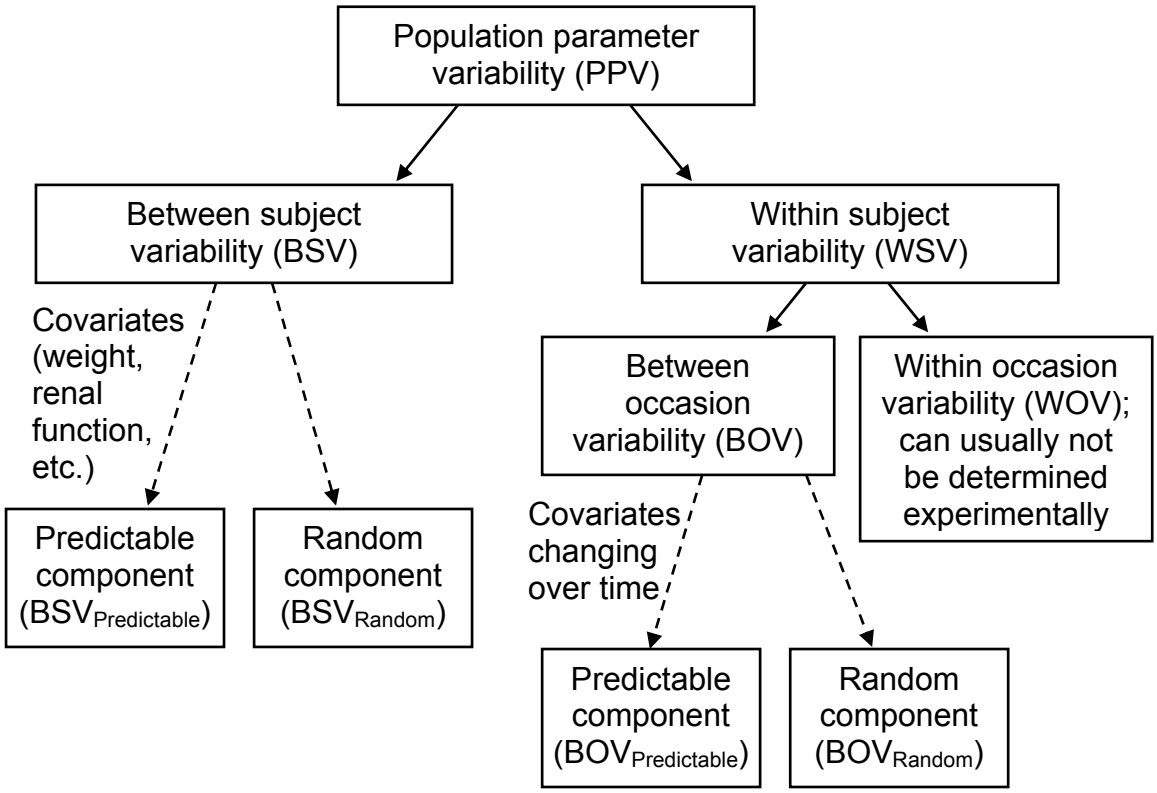


**Figure 5.1-1** Illustration of population parameter variability, BSV, and within subject variability

Definitions according to Holford (198):

PPV: Overall variability of a parameter (e. g. clearance).

BSV: Variability from subject to subject in the average value of a parameter for each individual.

BOV: Estimation of BOV requires that a subject is studied on more than one occasion (study period). The between occasion variability is the variability of an occasion specific parameter (e. g. clearance) around the average value in the respective individual.

WOV: Variability of a parameter (e. g. clearance) within an occasion e. g. due to variation in organ blood flow. For practical purposes, WOV e. g. of clearance is almost impossible to estimate.

If PPV, BSV, BOV, WSV, and WOV are expressed on variance scale, WSV is the sum of BOV and WOV and PPV is the sum of BSV and WSV.

If PPV, BSV, BOV, WSV, and WOV are expressed as coefficients of variation (=square root [SQRT] of the estimates on variance scale), the following equations apply:

$WSV = SQRT (BOV^2 + WOV^2)$

$PPV = SQRT (BSV^2 + WSV^2)$, e. g. a BSV of 40% and a WSV of 30% yield a PPV of 50%.

A high BOV is important for the applicability of therapeutic drug monitoring (TDM) and target concentration intervention (TCI). Both TDM and TCI assume that the plasma concentration time course is more closely linked to the drug effect than the size of the dose. In TDM, blood samples are drawn to quantify drug concentrations and to propose an “optimal” dosage regimen for an individual patient.

One of the key differences between TDM and TCI is that TDM assumes a therapeutic range of plasma concentrations, whereas TCI assumes one target concentration (195, 198). Within the therapeutic range, all concentrations are assumed to be equally “optimal”, whereas concentrations outside the therapeutic range are regarded as (highly) sub-optimal. The target concentration in TCI represents the optimal concentration balancing effectiveness and adverse effects (195, 198). Importantly, concentration and effect data from the individual patient can be used to select an individualized target concentration in TCI.

Besides the optimal target in TCI, one needs information about the disadvantage of not hitting this target precisely. Holford (195, 198) introduced the concept of safe and effective variability (SEV) which is used to rate deviations from the optimal target. The SEV is difficult to define and is unknown for most drugs. A practical approach would be the following (195, 198): The achieved concentration in the individual patient should fall within ±50% of the target concentration with a probability of 95% (for 95 of 100 subjects). If the distribution of predicted concentrations is approximately log-normal, then the coefficient of variation for the target concentration could be at most 25% for this drug (as the 95% confidence interval is about two times 25%). This coefficient of variation of 25% is the SEV in this example.

TCI uses covariates (e. g. weight or renal function) to reduce the random component of PPV ($PPV_{Random}$). However, TCI can not reduce WSV, since it is usually not possible to predict the random variability of an individual patient for a time period in the future. Therefore, the lowest achievable variability by use of TCI is the WSV.

If the WSV was greater than 25%, it would not be possible to achieve the criterion “95% probability to fall within ±50% of the target” for this drug

(see case D in Table 5.1-1). However, if the WSV was lower than 25%, TCI could be successfully applied to reduce the individual variability around the target concentration and to achieve the criterion (see case C in Table 5.1-1). Therefore, the relative size of SEV and WSV indicates, whether TCI can be successfully applied or not. Table 5.1-1 presents criteria for the applicability of various dosing strategies according to the SEV of the drug:

**Table 5.1-1** Criteria for the applicability of various dosing strategies

Table adapted from Holford (195, 198) (parameters explained in Figure 5.1-1).

| Case | Variability criterion | Dosing strategy | Comment |
|---|---|---|---|
| A | PPV < SEV | Give everyone the same dose | Very save and effective drug |
| B | PPV > SEV and $PPV_{Random}$ < SEV | Use patient covariates (e. g. weight) to adjust dose. (TCI not required) | Patient covariates can reduce $PPV_{Random}$ to fulfill the dosing criterion. |
| C | PPV > SEV, $PPV_{Random}$ > SEV, & WSV < SEV | Use TCI to adjust dose, as use of patient covariates alone is not sufficient due to $PPV_{Random}$ > SEV. | Blood concentrations from an individual patient are required to select doses. |
| D | WSV > SEV | TCI can not be used safely and effectively. | A high WSV precludes the safe and effective use of this drug. |

$PPV_{Random}$: Random component of population parameter variability.
On variance scale, $PPV_{Random} = BSV_{Random} + WSV$

We assessed the BOV of piperacillin and amoxicillin/clavulanic acid based on replicate administrations of the same formulation. BOV is always lower or equal to WSV. BOV and WSV are probably well comparable in healthy volunteers (assuming that WOV is small).

We additionally studied, if improvements in the pharmaceutical formulation of clavulanic acid may lead to a more reliable absorption of clavulanic acid (to achieve a lower BOV in extent of absorption of clavulanic acid).

## 5.2 Between occasion variability, saturable elimination, and optimized dosage regimens of piperacillin

The chemical structure of piperacillin is shown in chapter 3.3.1.1.

### 5.2.1 Clinical use of piperacillin / tazobactam

Piperacillin-tazobactam shows good bactericidal activity against *P. aeruginosa* and gram-positive microorganisms (499). Therefore, piperacillin-tazobactam is an attractive choice in the empiric treatment situation and is frequently used in the empirical treatment of hospital-acquired infections (297). Piperacillin is usually administered in combination with the beta-lactamase inhibitor tazobactam to prevent enzymatic degradation of piperacillin. There are still contradictory reports on the PK of piperacillin despite its use for more than two decades. Two recent papers (297, 520) studied the population PK of piperacillin and found evidence for a possibly saturable clearance of piperacillin. Vinks et al. (520) hypothesized a possible influence of genotype on clearance of piperacillin in CF-patients.

Bergan (38) reviewed the PK of acylureidopenicillins and concluded that drug exposure (as measured by AUC) increases more than proportionally with rising piperacillin doses, although the extent of saturability in piperacillin's elimination is rather small. This rather small extent is likely the reason why some authors propose a saturable clearance for piperacillin (16, 32, 39, 329, 493), whereas others find first-order (non-saturable) elimination (128, 129, 230, 363, 401, 483, 536, 548, 555). The protein binding of piperacillin is between 20 and 30% (13, 459). Tjandramaga et al. (493) report that about 70% of the renal excretion of piperacillin is by tubular secretion and 30% by passive glomerular filtration. Tubular secretion is the most obvious mechanism to explain mixed-order (capacity limited) renal elimination.

The microbiological and clinical success of beta-lactams can be best predicted by the $fT_{>MIC}$. Therefore, several authors proposed that continuous infusion (85, 108, 300, 340) and prolonged infusion (108) would be superior to

intermittent administration for this drug group. A loading dose at the initiation of therapy is often recommended to reach bactericidal concentrations as soon as possible. Several groups compared the clinical, microbiological, and economical outcome, bactericidal activity, and time above MIC between short-term and continuous infusion or studied treatment with continuous infusion, e. g. for meropenem (225, 271, 272, 336, 491), ceftazidime (36, 89, 284, 291, 335, 356) and piperacillin/tazobactam (162, 414). These trials concluded that clinical outcomes with continuous infusion were at least as safe and effective as intermittent treatment with short term infusions, and other measures (e. g. pharmacoeconomics) were superior for continuous infusion. However, the intermittent mode of administration is still the clinical standard, possibly due to the equipment and workload that is required for a continuous infusion.

We administered replicate doses of the same intravenous piperacillin formulation which allowed us to study the BOV of piperacillin. As our first objective, a population PK model was developed to fit the plasma and urine data simultaneously and to account for first-order and mixed-order (saturable) elimination of piperacillin. Our second objective was to determine the BOV of PK parameters. As our third objective, we compared the PTA between various dosage regimens by MCS to propose optimal piperacillin dosage regimens.

### 5.2.2 Methods

The general clinical and sample handling procedures, the methods for PK analysis (including NCA and population PK), and the general methods for MCS are described in chapter 2.

***Subjects:*** Four healthy Caucasian volunteers participated in the study. Table 5.2-1 shows the demographic statistics and a data summary.

***Study Design and Drug Administration:*** The study was conducted as a single-center, open, five-period replicate dose study. Each of the four subjects received the same formulation containing 4g piperacillin as 5min infusion as a single intravenous dose in each of the five study periods (occasions). Doses were given on days 1, 3, 10, 24, and 52. Piperacillin (4g) was dissolved in 50 mL sterile water for injection.

**Table 5.2-1** Data summary and demographic data

| | Min | Median | Max |
|---|---|---|---|
| Number of piperacillin plasma samples per subject (per subject and occasion) | 73 (13) | 76 (15) | 78 (16) |
| Number of piperacillin urine samples per subject (per subject and occasion) | 40 (7) | 41 (8) | 42 (10) |
| Age (y) | 22 | 23 | 24 |
| Weight (kg) | 67 | 77.5 | 85 |
| Height (cm) | 164 | 176 | 178 |
| Number of females / males | | 2 / 2 | |

***Sampling Schedule:*** Blood samples were drawn immediately before start of infusion, at the end of infusion as well as at 5, 10, 15, 20, 30, 45 min, and 1, 1.5, 2, 2.5, 3, 3.5, 4, 5, 6, 8, 10, 12, and 24 h after the end of each infusion. Urine was collected before drug administration, between the start of infusion and 1 h after the end of infusion, as well as at 1-2, 2-3, 3-4, 4-6, 6-8, 8-10, 10-12, and 12-24 h after the end of each infusion.

***Determination of Plasma and Urine Concentrations:*** Drug analysis of piperacillin in plasma is described in chapter 3.3.1.3 (see page 97 ff). For determination of piperacillin in urine 20 µL of the sample were diluted with 180 µL water. After mixing 40 µL were injected onto the HPLC-system. The linearity of the piperacillin calibration curves in urine was shown between 1.00 - 1000 mg/L, respectively. The inter-day precision and the analytical recovery of the spiked quality control standards of piperacillin in human urine ranged from 3.0 to 5.5% and was 92.0 to 97.9%, respectively.

**Population PK**

***Disposition and Drug elimination:*** The plasma and urinary excretion data allowed renal and nonrenal elimination mechanisms to be distinguished. We tested one, two, and three compartment disposition models and studied the following pathways for piperacillin elimination: 1) first-order nonrenal

($CL_{NR}$) and first-order renal clearance ($CL_R$), 2) first-order nonrenal clearance and mixed-order (Vmax and Km) renal elimination, and 3) first-order nonrenal clearance and parallel first-order + mixed-order renal elimination.

The formula for the population clearance ($CL_{POP}$) of the full model (model 3) as a function of the piperacillin concentration (C) in the central compartment contains the following components:

$$CL_{POP}(C) = CL_{NR} + CL_R + \frac{Vmax}{C + Km} \qquad \text{Formula 5.2-1}$$

This is a standard equation which is often applied for drugs with a non-saturable (glomerular filtration) and saturable component (tubular secretion) of renal elimination. This equation has also been applied for piperacillin by Lodise et al. (297) and Vinks et al. (520).

***Size:*** We applied the allometric size model with total body weight (WT) as size descriptor. The allometric exponent was 0.75 for clearance and 1.0 for volume of distribution as described in chapter 2.6.2.2.

***Individual PK model:*** In our population PK analysis, we did not separate the PPV its two components BSV and WSV, since we had only data on four subjects. Each of the five study periods was one occasion. We treated the dataset as if there were 20 separate individuals and estimated the PPV for this dataset. ANOVA statistics on log-scale were used to estimate the BOV of the individual PK parameters from population PK and from NCA.

PPV was estimated as variances but we report the square root of the estimates and refer to these values as PPV and BOV, respectively. We have expressed PPV and BOV in the text as a percentage, because these quantities are apparent coefficients of variation of a log-normal distribution. In our population PK model, $\eta_{PPV}$ is assumed to be a normally distributed random variable with mean zero and standard deviation PPV. We used an exponential parameter variability model for all PK parameters. The parameter variability model for Vmax, Km, CL, and Vss was specified as follows (see below for parameter explanations):

$$Vmax_{ij} = Vmax \cdot \exp(\eta_{PPV,VMAXij}) \cdot F_{Size,CL,i} \qquad \text{Formula 5.2-2}$$

$$Km_{ij} = Km \cdot \exp(\eta_{PPV,KMij}) \quad \text{Formula 5.2-3}$$

$$CL(C)_{ij} = \left( [CL_{NR} + CL_R] \cdot F_{Size,CL,i} + \frac{Vmax_{ij}}{C + Km_{ij}} \right) \cdot \exp(\eta_{PPV,CLij}) \quad \text{Formula 5.2-4}$$

$$Vss = V1 + V2 + V3 \quad \text{Formula 5.2-5}$$

$$Vss_{ij} = Vss \cdot \exp(\eta_{PPV,VSSij}) * F_{Size,V,i} \quad \text{Formula 5.2-6}$$

$F_{Size,V,i}$ and $F_{Size,CL,i}$ are the fractional changes in volume of distribution and clearance for the $i^{th}$ subject (with $WT_i$) standardized to a weight $WT_{STD}$ of 70 kg (see chapter 2.6.2.2 for details). $\eta_{PPV,NNij}$ is the value of $\eta_{PPV}$ for PK parameter NN for the $i^{th}$ subject at the $j^{th}$ occasion. The indices NNij denote the individual value for parameter NN for the $i^{th}$ subject at the $j^{th}$ occasion. C is the individual plasma concentration at the respective time point. $CL_R$, $CL_{NR}$, Vmax, V1, V2, V3, and Vss are the population estimates for a 70 kg subject.

***Assessment of PKPD profile:*** We compared the PKPD profile of various dosage regimens. Our studied dosage regimens comprised standard short-term (30min) infusion, prolonged (5h) infusion, and continuous infusion at daily doses between 9 and 18g per 70kg WT. We derived the PTA within the MIC range from 1 to 96 mg/L and used a protein binding of 30% for piperacillin (13, 459). We used the PKPD targets $fT_{>MIC} \geq 50\%$ of the dosing interval representing near-maximal killing and $fT_{>MIC} \geq 30\%$ representing bacteriostasis for penicillins (84, 107). Additionally, the targets $fT_{>MIC} \geq 40\%$, $fT_{>MIC} \geq 60\%$, $fT_{>MIC} \geq 70\%$, and $fT_{>MIC} = 100\%$ were studied.

### 5.2.3 Results

***Drug Concentrations:*** Figure 5.2-1 shows the average (± SD) plasma concentration time curves and Table 5.2-2 shows the results from NCA. Our PK parameters were in concordance with the results from other authors (38, 297, 520).

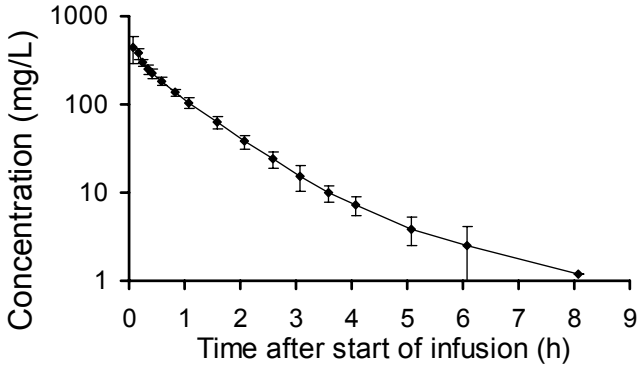


**Figure 5.2-1** Average (± SD) plasma concentrations after a 5min infusion of 4g piperacillin in healthy volunteers

**Table 5.2-2** PK parameters after a 5 min infusion of 4g piperacillin from NCA

| | **Average ± SD** | **Median [Min-Max]** |
|---|---|---|
| Peak concentration (mg/L) | 463 ± 127 | 465 [279 - 775] |
| Time to peak (min) | 6.8 ± 2.5 | 5 [5 - 11] |
| Total clearance (L/h) | 11.9 ± 1.34 | 11.9 [9.87 - 14.4] |
| Renal clearance (L/h) | 7.59 ± 0.86 | 7.81 [5.31 - 8.78] |
| Nonrenal clearance (L/h) | 4.33 ± 1.07 | 4.57 [2.21 - 6.30] |
| Volume of distribution at steady-state (L) | 12.7 ± 2.26 | 12.2 [9.47 - 16.9] |
| Fraction excreted unchanged in urine (%) | 63.9 ± 6.7 | 63.8 [52.8 - 79.8] |
| Terminal half-life (h) | 1.22 ± 0.461 | 1.04 [0.693 - 2.23] |
| Mean residence time (h) | 1.06 ± 0.15 | 1.01 [0.92 - 1.45] |

***Model Building:*** A three compartment disposition model was superior to a one and two compartment disposition model. The three compartment model with first-order nonrenal and first-order renal elimination (model 1) over-predicted the amounts excreted in urine by 16% at 1h and by 13% at 2h post end of infusion (comparison based on the simulated and observed medians). Model 2 (first-order nonrenal and mixed-order renal elimination) showed an under-prediction by 10% at 1h and an over-prediction by 14% at 2h post end of infusion for urinary excretion. The model with first-order nonrenal and

parallel first-order + mixed-order renal elimination (model 3) showed an under-prediction by 8% at 1h and an over-prediction by 6% at 2h post end of infusion for urinary excretion. Model 3 had an 11.9 points better objective function compared to model 2 and a 48.1 points better objective function compared to model 1. Model 3 had a highly sufficient predictive performance in plasma and urine (see Figure 5.2-2). Therefore, we selected model 3 as our final model.

All disposition parameters were scaled allometrically. Since the number of subjects in our study was small (4 subjects studied on 5 occasions), we did not seek to optimize the covariate model other than by including standard allometric models. PK parameter estimates of our final model are shown in Table 5.2-3. The estimates for the mixed-order renal elimination were 170 mg/h (50.4% coefficient of variation) for the maximum rate of elimination (Vmax) and 49.7 mg/L (150% CV) for the Michaelis-Menten constant (Km). Figure 5.2-3 shows clearance as a function of concentration. Total clearance is predicted to decrease from 13.5 L/h at a nominal concentration of 0 mg/L to 10.8 L/h at 200 mg/L for a typical 70 kg subject. The ANOVA with the individual PK parameter estimates revealed a low BOV for total clearance (8.5% CV) and volume of distribution at steady-state (16% CV), whereas Vmax (39%) and Km (117%) had a high BOV (see Table 5.2-4).

***PKPD profile:*** The PTA vs. MIC profiles are shown in Figure 5.2-4 for a range of PKPD targets. For the near-maximal kill target $fT_{>MIC} \geq 50\%$ continuous infusion of 9g/day and prolonged infusion of 3g q8h achieved robust (>90%) PTAs for MICs ≤16 mg/L. Those two regimens were superior to the 30min infusion regimens of 4g q8h and of 4g q6h.

Table 5.2-5 shows the PKPD breakpoints for all studied dosage regimens at various PKPD targets. A standard 30min infusion regimen of 4g q8h (daily dose: 12g) achieved a PKPD breakpoint of 4 mg/L for the near-maximal kill target. Giving 4g q6h (daily dose: 16g) increased the breakpoint to 12 mg/L and giving 3g q4h (daily dose: 18g) achieved a breakpoint of 24 mg/L. At a reduced daily dose of 9g, 5h infusion of 3g q8h achieved a breakpoint of 16-24 mg/L (PTA = 86% at an MIC of 24 mg/L). High dose 5h infusion of 6g q8h achieved a near-maximal kill breakpoint of 48 mg/L. The

PKPD breakpoints were more similar between our studied regimens for the bacteriostasis target $fT_{>MIC} \geq 30\%$. As expected, continuous infusion had its greatest benefit for the PKPD targets $fT_{>MIC} \geq 70\%$ and $fT_{>MIC} = 100\%$.

**Panel A: Plasma**

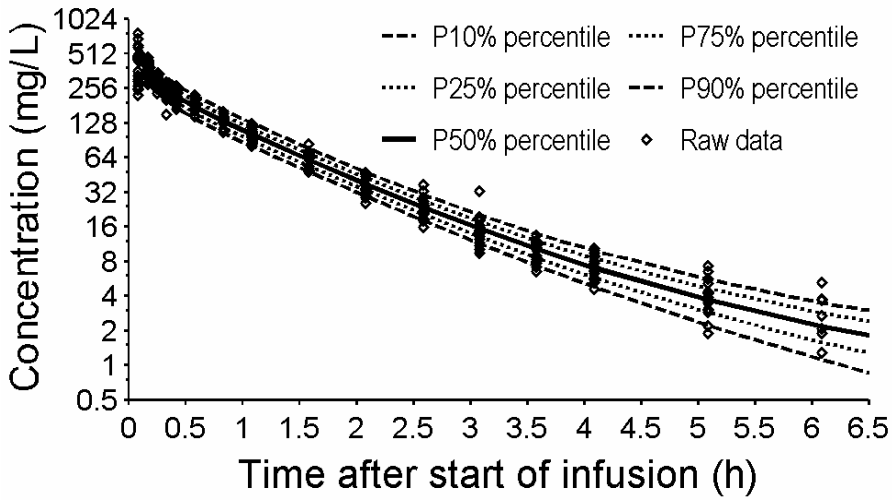


**Panel B: Urine**

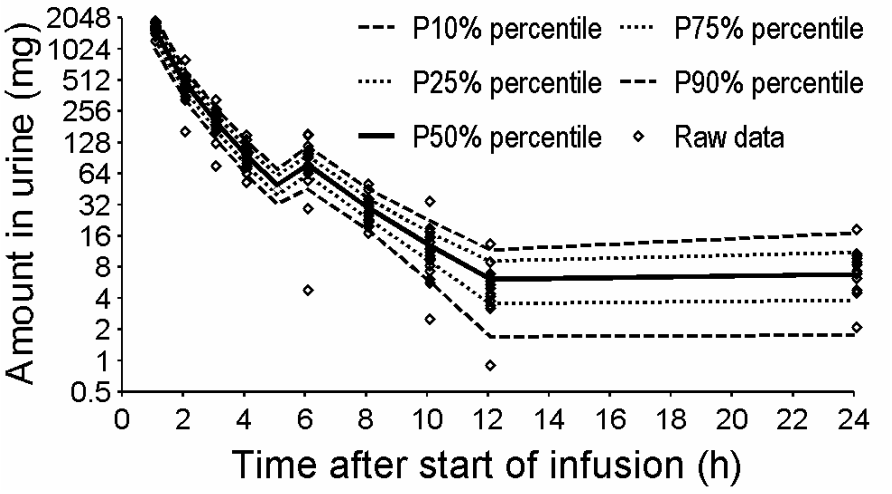


**Figure 5.2-2** VPCs for piperacillin

See chapter 2.6.3 for interpretation of VPCs.

**Table 5.2-3** Population parameter estimates of the three compartment model with first-order nonrenal elimination and parallel first-order and mixed-order renal elimination for piperacillin

| Parameter | Unit | Estimate | Parameter | Unit | Estimate |
|---|---|---|---|---|---|
| $CL_{NR}$ (for 70 kg) [a] | L $h^{-1}$ | 4.40 | PPVCLtot [c] | | 9.62% |
| $CL_R$ (for 70 kg) [a] | L $h^{-1}$ | 5.70 | | | |
| Vmax (for 70 kg) [a] | mg $h^{-1}$ | 170 | PPVVmax [d] | | 50.4% |
| Km | mg $L^{-1}$ | 49.7 | PPVKm [d] | | 150% |
| Vss (for 70 kg) [b,e] | L | 12.7 | PPVVss [c] | | 13.5% |
| V1 (for 70 kg) [b] | L | 7.00 | | | |
| V2 (for 70 kg) [b] | L | 2.95 | $CV_C$ | | 12.5% |
| V3 (for 70 kg) [b] | L | 2.71 | $SD_C$ | mg/L | 0.447 |
| $CLic_{shallow}$ (for 70 kg) [a] | L $h^{-1}$ | 12.7 | $CV_{AU}$ | | 24.6% |
| $CLic_{deep}$ (for 70 kg) [a] | L $h^{-1}$ | 1.28 | $SD_{AU}$ | mg | 3.89 |

[a]: The allometric model with a standard body weight of 70 kg and an exponent of 0.75 was used to scale the clearance terms and Vmax.

[b]: The allometric model with a standard body weight of 70 kg and an exponent of 1.0 was used to scale the volume of the central and both peripheral compartments.

[c]: Correlation between the pair of random effects: r(CLtot,Vss) = 0.84.

[d]: Correlation between the pair of random effects: r(Vmax,Km) = 0.99.

[e]: Derived from estimated PK parameters, not an estimated parameter.

$CL_{NR}$: nonrenal clearance describing the first-order nonrenal elimination, $CL_R$: renal clearance describing the first-order renal elimination, Vmax: maximum rate of elimination for the mixed-order renal elimination, Km: plasma concentration that results in a rate of 50% of Vmax. Vss: volume of distribution at steady-state, V1: volume of central compartment, V2: volume of shallow peripheral compartment, V3: volume of deep peripheral compartment. $CLic_{shallow}$: intercompartmental clearance between the central and shallow peripheral compartment. $CLic_{deep}$: intercompartmental clearance between the central and deep peripheral compartment. PPV: population parameter variability for total clearance (PPVCLtot), volume of distribution at steady-state (PPVVss), Vmax (PPVVmax), and Km (PPVKm). $CV_C$ is the proportional and $SD_C$ is the additive residual error component for the plasma concentrations. $CV_{AU}$ is the proportional and $SD_{AU}$ is the additive residual error component for the amounts excreted in urine.

**Table 5.2-4** ANOVA results for the between occasion variability of PK parameters

| Parameters from NCA | CV (%)[a] | Parameters from population PK analysis | CV (%)[a] |
|---|---|---|---|
| Total clearance | 8.5 | Maximum rate of mixed-order elimination (Vmax) | 39 |
| Renal clearance | 8.0 | Michaelis-Menten constant (Km) | 117 |
| Nonrenal clearance | 19 | | |
| Volume of distribution at steady-state | 16 | | |
| Mean residence time | 14 | | |
| Terminal half-life | 35 | | |

[a]: Apparent coefficient of variation for the variability of the individual PK parameter estimates between the five study periods (occasions) within subjects.

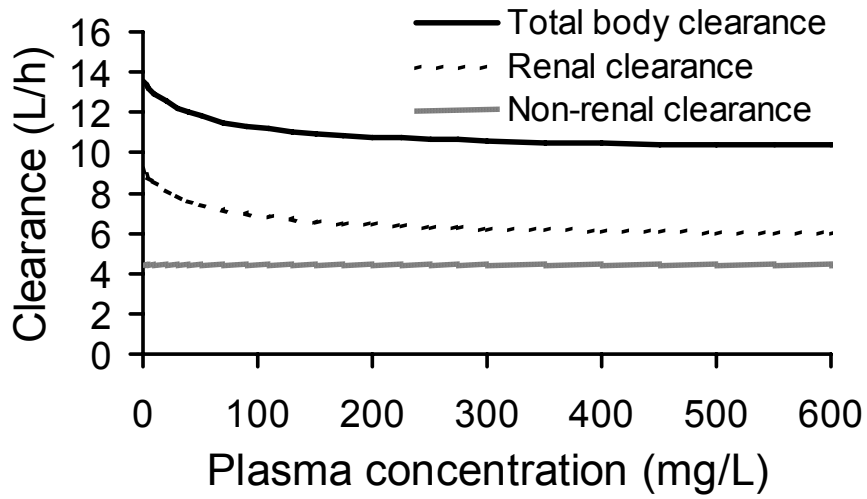


**Figure 5.2-3** Renal, nonrenal, and total clearance of piperacillin as a function of plasma concentration for a typical 70 kg subject

Nonrenal clearance is constant, whereas renal clearance has a mixed-order [saturable] and a first-order component and is therefore dependent on the plasma concentration.

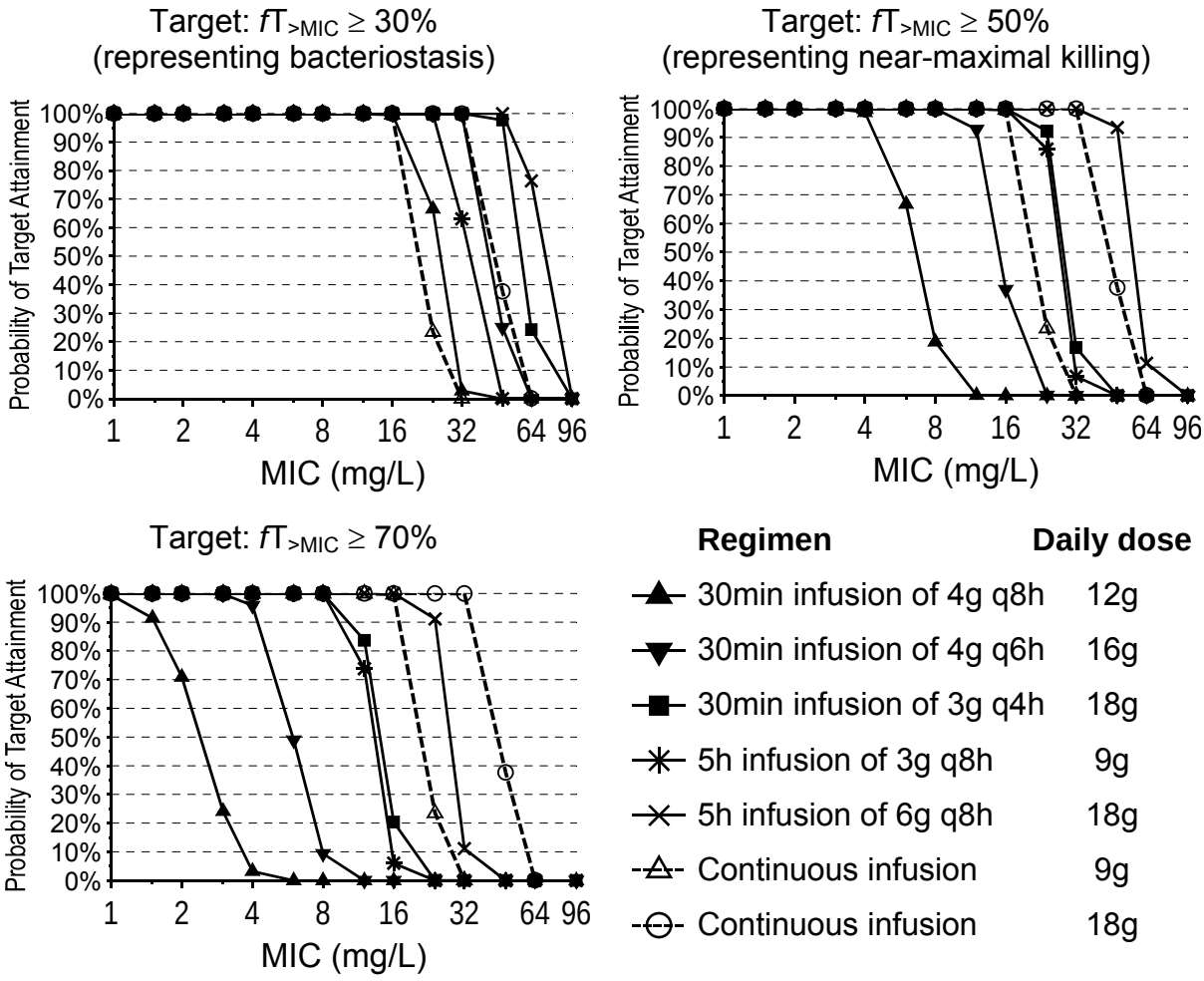


**Figure 5.2-4** Probabilities of target attainment vs. MIC profiles in healthy volunteers for various piperacillin dosage regimens at steady-state

### 5.2.4 Discussion

Piperacillin is frequently used in the empirical treatment of hospital-acquired infections. Recently, Lodise et al. (297) and Vinks et al. (520) used population PK and found evidence for a saturable elimination of piperacillin. Both groups find a high variability for Vmax and Km of the saturable elimination process. Vinks et al. (520) studied patients with cystic fibrosis and point out that some of the high BSV of Vmax and Km might be caused by variability in the genotype.

**Table 5.2-5** PKPD breakpoints for piperacillin in healthy volunteers

| | Daily Dose | Target: $fT_{>MIC}$ at least | | | | | |
|---|---|---|---|---|---|---|---|
| | | **30%** | 40% | **50%** | 60% | 70% | 100% |
| | | *PKPD breakpoint (mg/L)* | | | | | |
| 30 min infusion of 4g q8h | 12g | **16** | 8 | **4** | 2 | 1.5 | 0.375 |
| 30 min infusion of 4g q6h | 16g | **32** | 16 | **12** | 6 | 4 | 1 |
| 30 min infusion of 3g q4h | 18g | **48** | 32 | **24** | 16 | 8 | 3 |
| 5h infusion of 3g q8h | 9g | **24** | 24 | **16**[a] | 16 | 8 | 1 |
| 5h infusion of 6g q8h | 18g | **48** | 48 | **48** | 32 | 24 | 3 |
| Continuous infusion | 9g | **16** | 16 | **16** | 16 | 16 | **16** |
| Continuous infusion | 18g | **32** | 32 | **32** | 32 | 32 | **32** |

[a]: PTA was 86% at an MIC of 24 mg/L.

Saturable elimination should be incorporated in a population PK model, especially if dosage regimens with new doses or modes of administration are to be simulated. Before a population PK model is used in a MCS, VPCs are very important to assure, if the concentration time profiles simulated from a population PK model adequately mirror the central tendency and the variability of the observed concentrations. Lodise et al. (297) compared the predictive performance of their population PK models at 3h post dose, since they studied a 6h dosing interval and used the PKPD target $fT_{>MIC} \geq 50\%$.

We used population PK to study the renal and nonrenal elimination of piperacillin. Five replicate administrations of piperacillin over a period of 52 days were studied in four healthy volunteers to assess the BOV of PK parameters. We found that the elimination was best described by a first-order nonrenal and a parallel first-order + mixed-order renal elimination. Our final model had highly sufficient predictive performance in plasma and urine (see Figure 5.2-2). VPCs based on plasma and urine data revealed that simultaneous fitting of plasma concentrations and amounts excreted in urine was helpful to distinguish between elimination models.

Our population estimate for the Michaelis-Menten constant of the mixed-order renal elimination (Km) of 49.7 mg/L (apparent coefficient of variation of 150%) was comparable to the estimate from Vinks et al. (520), who find an average (± SD) Km of 83.8 ± 94.3 mg/L and a median Km of 44.9 ± 62.1 mg/L in CF-patients. Lodise et al. (297) report a higher Km of 245 ± 126 mg/L (average ± SD) for their dataset of 128 hospitalized patients. The maximum rate of the mixed-order renal elimination (Vmax) of 292 ± 501 mg/h (average ± SD) with a median of 142 mg/h from Lodise et al. is comparable to our estimate for Vmax of 170 mg/h (50.4% CV). Those differences might arise, since Vinks et al. and Lodise et al. both studied the combination of piperacillin and tazobactam, whereas we studied piperacillin alone. Although the PK of piperacillin is not much affected by the presence of tazobactam at dose ratios of 4:1 or 8:1 (459), this could contribute to the observed differences in Vmax and Km. Another possible reason is that we used plasma and urine data, whereas Lodise et al. and Vinks et. al did not use urine data for estimation of their population PK models. Our total clearance and volume of distribution at steady-state were comparable to the estimates from Lodise et al. (297) in healthy volunteers and Vinks et al. (520) in CF-patients.

We estimated a renal clearance of 5.70 L/h for the first-order component which corresponds to an unbound renal clearance of about 7.1-8.1 L/h (based on a protein binding of 20-30% for piperacillin (13, 459)). This estimate compares well to the expected glomerular filtration rate in healthy volunteers. Our estimate of 4.40 L/h for nonrenal clearance agrees well with the estimate of nonrenal clearance from NCA.

Tjandramaga et al. (493) and Bergan et al. (39) find a larger fraction of piperacillin excreted unchanged in urine at higher doses and Sörgel et al. (459, 460) report a higher fraction of unchanged piperacillin excreted in urine at steady-state than after single dose. Tjandramaga et al. (493) observe a decreased renal and a decreased nonrenal clearance with rising doses. However, Bergan et al. (38, 39) report a decreased nonrenal clearance and no changes in renal clearance with rising doses. Those observations suggest the existence of a saturable nonrenal elimination of piperacillin. We tried to

describe the nonrenal elimination as a mixed-order process. However, our data at a single dose level did not support a significant contribution of saturable nonrenal elimination.

As we had only data on four subjects at five occasions, we did not estimate the BOV in our population PK analysis. Instead, we used the individual PK parameter estimates to determine their BOV by ANOVA statistics. Lodise et al. (297) and Vinks et al. (520) both found a high variability for Vmax and Km of the saturable elimination process. As we had data on replicate administrations, we could estimate the BOV of those parameters. If demographic characteristics like body size, body composition, age, or genotype explained a major fraction of the variability in Vmax and Km, one would expect the BOV of Vmax and Km to be rather low. However, we found high BOVs with an apparent coefficient of variation of 117% for Km, 39% for Vmax, and 77% for the ratio of Vmax/Km.

In contrast, we found a much lower BOV for total clearance (8.5%), renal clearance (8.0%), nonrenal clearance (19%), and volume of distribution at steady-state (16%). These estimates are well comparable to the BOV of about 6% for total clearance after intravenous dosing of furosemide from Grahnen et al. (161) who performed a 6-period crossover study with four oral and two intravenous doses. The low BOV of total clearance and volume of distribution of piperacillin supports the use of TCI (195, 198) for piperacillin. Although beta-lactams have a wide therapeutic window, distinct serum-sicknesslike adverse reactions which seemed to be dose dependent (402) have been reported for piperacillin, e. g. during high dose empiric treatment of *P. aeruginosa* infections in CF-patients. Reed et al. (402) studied juvenile CF-patients and recommend doses of 600 mg/kg/day. If those high doses are of concern, TCI might help to optimize effectiveness and reduce toxicity.

As another possible option to reduce daily doses of piperacillin, we used MCS based on our final population PK model to simulate various dosage regimens and compared standard short-term (30min) infusions, prolonged (5h) infusions, and continuous infusion (see Table 5.2-5). The PTA was compared between those dosage regimens for the PKPD target $fT_{>MIC} \geq 30\%$ representing bacteriostasis and $fT_{>MIC} \geq 50\%$ representing near-maximal

killing of penicillins (84, 85, 107, 257). The selection of a pre-specified target deserves attention. There is variability in the required target among combinations of antibiotic x pathogen. Additionally, higher targets may be required to successfully treat infections by slow-growing bacteria in infection sites that require bactericidal activity such as endocarditis and osteomyelitis (84). Sometimes, higher targets of $fT_{>MIC} \geq 70\%$ or $fT_{>MIC} = 100\%$ are also discussed (337). To illustrate the influence of different PKPD targets on PTAs, we studied a range of targets between $fT_{>MIC} \geq 30\%$ and $fT_{>MIC} = 100\%$ (see Table 5.2-5 and Figure 5.2-4).

For the near-maximal kill target $fT_{>MIC} \geq 50\%$, 30min infusion of 4g q8h (daily dose: 12g) achieved a PKPD breakpoint of 4 mg/L. Administering 30min infusions of 4g q6h (daily dose: 16g) increased the PKPD breakpoint to 12 mg/L and giving 30min infusions of 3g q4h (daily dose: 18g) improved the PKPD breakpoint to 24 mg/L. We studied 5h infusions as an alternative dosage regimen which was specifically optimized for the PKPD target $fT_{>MIC} \geq 50\%$ for piperacillin. A 5h infusion of 3g q8h achieved a PKPD breakpoint of 16-24 mg/L (PTA = 86% at an MIC of 24 mg/L). Therefore, 5h prolonged infusion allows one to reduce the daily dose by a factor of 2 compared to 30min infusion of 3g q4h while achieving almost the same PTAs and PKPD breakpoints (see Figure 5.2-4 and Table 5.2-5). High dose 5h infusion of 6g q8h achieved a PKPD breakpoint of 48 mg/L. Consequently, 5h infusion of 6g q8h will have its greatest benefit compared to a standard 30min infusion of 4g q6h, if the MIC of the infecting pathogen falls between 12 and 48 mg/L.

Our PKPD breakpoints are comparable to the breakpoints reported by Lodise et al. (297) in hospitalized patients who found PTAs >95% for MICs ≤16 mg/L for a 30min piperacillin infusion of 3g q4h (in presence of tazobactam). For this dosage regimen Lodise et al. (297) find PTAs >95% for MICs ≤8 mg/L and a PTA of 72% at an MIC of 16 mg/L in healthy volunteers. Our PKPD breakpoint of 24 mg/L for this regimen in healthy volunteers was higher, because we estimated an about 16% lower total body clearance and a slightly smaller variability compared to the healthy volunteer data from Lodise et al. Another possible reason for this slight difference is that we used a model

with saturable clearance whereas Lodise et al. used a model with first-order elimination for MCS. However, these differences are small and, as has been shown by Lodise et al. (297) for piperacillin, a MCS based on healthy volunteer data is a conservative prediction for hospitalized patients.

A 5h prolonged infusion q8h is an inconvenient dosage regimen for the patient and seems justifiable for severe infections or for infections with high mortality. The potential for emergence of resistance should be considered, as prolonged infusion might decrease or slow down the emergence of resistance by preventing single step mutations. The most appropriate dosage regimen should also consider the convenience for the patient, workload, and costs (see end of chapter 3.6.4). These issues should be further studied clinically.

In conclusion we developed a population PK model with highly sufficient predictive performance for plasma and urine profiles. The renal elimination was saturable and best described by a parallel first-order and mixed-order process. The mixed-order renal elimination had a Vmax of 170 mg/h and a Km of 49.7 mg/L. The parameters of the mixed-order renal elimination had a high BOV of 39% for Vmax and of 117% for Km. However, those high BOVs had only a small influence on the BOV for total clearance of 8.5% (determined via NCA). Such a low BOV supports the use of TCI and TDM (195, 198). Standard 30min infusion of 4g q6h (daily dose: 16g) achieved robust (>90%) PTAs for MICs $\leq$12 mg/L for the near-maximal kill target $fT_{>MIC} \geq 50\%$. As alternative mode of administration at a lower daily dose of 9g, prolonged 5h infusion of 3g q8h achieved robust PTAs for MICs of 16-24 mg/L (PTA = 86% at an MIC of 24 mg/L). Therefore, 5h infusion of 3g q8h bears the advantage of a significant dose reduction (by a factor of about 2) compared to standard short-term infusions while achieving a similar PKPD profile. High dose 5h infusion of 6g q8h yielded robust PTAs for MICs $\leq$48 mg/L. High dose 5h infusion of 6g q8h is expected to be superior to 30min infusions of 4g q6h, if the MICs fall between 12 and 48 mg/L. Future clinical trials are warranted to show, if prolonged infusion is clinically superior to short-term infusion for piperacillin.

## 5.3 Impact of between occasion variability on the success of bioequivalence studies for oral amoxicillin / clavulanic acid

### 5.3.1 Chemical structure of amoxicillin and clavulanic acid

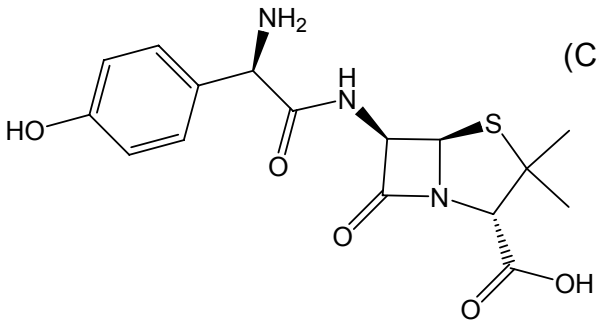


($C_{16}H_{19}N_3O_5S$, Mol. Wt.: 365.4)

**Chemical structure 5.3-1** Amoxicillin

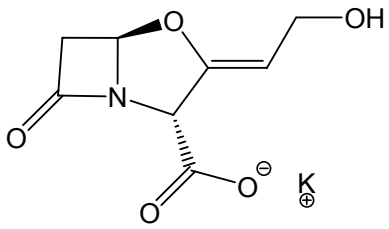


($C_8H_8KNO_5$, Mol. Wt.: 237.25)

**Chemical structure 5.3-2** Clavulanic acid

### 5.3.2 Background on the impact of a high between occasion variability on bioequivalence studies with beta-lactams

Bioequivalence studies comprise a critical part of generic drug development (556), especially for drugs with a high WSV like clavulanic acid. Both time and costs spent on bioequivalence studies are significant. WSV can be split into WOV and BOV. WOV can only be observed experimentally in exceptional cases (see chapter 5.1). In our crossover study with replicate doses of the same formulation, each study period comprised one occasion. A

high BOV of Cmax or AUC often requires more than 50 subjects for an adequately powered bioequivalence study with clavulanic acid.

It would be valuable for the pharmaceutical developer to know, whether it is BOV for the disposition of the drug or alternatively it is the release/absorption process that causes the high BOV in Cmax and AUC in a bioequivalence study. Such a high BOV can only be reduced by improvements in the pharmaceutical formulation, if it is due to modifiable variability in the drug release/absorption process. Only a few controlled clinical trials have been published on the BOV of drugs (123, 161, 208, 245, 446, 511-513). Idkaidek et al. (208) studied the BOV of Cmax and AUC for amoxicillin / clavulanic acid after replicate doses via NCA, but did not investigate the sources of the high BOV in Cmax and AUC for clavulanic acid.

The present procedure for assessment of bioequivalence most commonly uses plasma concentrations as a surrogate marker for clinical response. Although regulatory authorities require bioequivalence of beta-lactams to be shown based on Cmax and AUC, these parameters are probably not the most appropriate for beta-lactams. Convincing evidence from animal experiments (84, 107) shows that the time of non-protein bound concentration above the MIC best predicts microbiological and clinical response to beta-lactams (assuming a sufficient duration of antibiotic therapy).

We studied a replicate administration of the same oral amoxicillin / clavulanic acid formulation. Our objectives were: 1) To model the individual plasma concentration time curves for amoxicillin and clavulanic acid by use of population PK and to estimate the BOV in extent of absorption (BOVF), total clearance (BOVCL), and volume of distribution of the central compartment (BOVV1) as well as the BOV in all other absorption parameters. 2) To determine the effect of BOV on the chance to show bioequivalence in a two-way crossover study by simulations. 3) To study, if bioequivalence based on Cmax and AUC assures similarity in the PKPD profile for oral amoxicillin.

### 5.3.3 Methods

The general clinical and sample handling procedures, the methods for PK analysis (including NCA and population PK), and the general methods for MCS are described in chapter 2.

***Subjects:*** Twenty-four (24) healthy male Caucasian volunteers participated in the study. Table 5.3-1 shows the data summary including demographics.

***Study Design and Drug Administration:*** The study was conducted as a single-center, open, two-period, replicate dose study with a wash-out period of four days. Subjects received the same formulation containing 574 mg amoxicillin trihydrate equivalent to 500 mg amoxicillin and 148.9 mg potassium salt of clavulanic acid equivalent to 125 mg clavulanic acid as oral suspension (10 mL of Augmentan® forte dry-suspension, GlaxoSmithKline) as a single dose at each of the two occasions (study periods). The subjects received each dose of the study medication together with 240 mL of low carbonated, calcium-poor mineral water (room temperature). All doses were given in the fasting state.

***Blood Sampling:*** In total 18 blood samples were drawn at the following time points: pre-dose, and at 0.25, 0.5, 0.75, 1, 1.25, 1.5, 1.75, 2, 2.25, 2.5, 3, 4, 5, 6, 8, 10, and 12 hours after administration of the study drug.

**Table 5.3-1** Data summary and demographic data

| | **Average ± SD** | **Min** | **Median** | **Max** |
|---|---|---|---|---|
| Number of amoxicillin concentrations per subject (per subject and occasion) | | 34 (17) | 34 (17) | 34 (17) |
| Number of clavulanic acid concentrations per subject (per subject and occasion) | | 24 (11) | 28 (14) | 30 (15) |
| Renal function [a] | 98.8 ± 12.9 | 68.7 | 99.5 | 130 |
| Age (y) | 29 ± 6.8 | 19 | 26 | 44 |
| Weight at screening (kg) | 78.0 ± 6.7 | 62 | 77.5 | 91 |
| Weight at follow-up (kg) | 77.7 ± 6.8 | 61.5 | 77.5 | 90.5 |
| Height (cm) | 178 ± 5.4 | 171 | 176 | 192 |

[a]: Estimated renal function for a nominal 70 kg subject. We used the average of the estimated renal function at screening and at follow-up.

***Drug Analysis in Human Plasma:*** Samples were analyzed by means of an LC-MS/MS method, validated for 0.1 mL samples of human plasma. Plasma samples (0.1 mL) were mixed with buffer containing the internal standard and deproteinized by addition of acetonitrile. After thorough mixing, the samples were centrifuged. Each sample was chromatographed on a reversed-phase column, eluted with an isocratic solvent system consisting of buffer and acetonitrile and monitored by LC-MS/MS with a MRM method as follows. The MacQuan software (version 1.6, PE Sciex, Thornhill, Ontario, Canada, 1991 - 1998) was used for evaluation of chromatograms.

***Analysis of Amoxicillin:*** Precursor → product ion for amoxicillin m/z 366 → m/z 208 and internal standard m/z 350 → m/z 160. Under these conditions amoxicillin and the internal standard were eluted after approximately 0.7 and 0.8 minutes, respectively. The linearity of the amoxicillin calibration curve was shown from 0.0200 mg/L to 10.0 mg/L. The coefficient of correlation for all measured sequences of amoxicillin was at least 0.9995. The lowest calibration standard of 0.0200 mg/L was set as the lower limit of quantification of the assay for amoxicillin in human plasma. For the spiked quality control standards of amoxicillin the inter-day precision ranged from 3.6 to 9.2% with an inter-day accuracy (relative error) between -4.3 and 6.7%. The intra-day precision and relative error of the amoxicillin assay ranged from 2.1 to 9.1% and between -6.1 and 5.0%.

***Analysis of Clavulanic Acid:*** Precursor → product ion for clavulanic acid m/z 198 → m/z 108 and internal standard m/z 232 → m/z 140. Under these conditions clavulanic acid and the internal standard were eluted after approximately 2 minutes. The linearity of the clavulanic acid calibration curve was shown from 0.0500 mg/L to 8.00 mg/L. The coefficient of correlation for all measured sequences of clavulanic acid was at least 0.9997. The lowest calibration standard of 0.0500 mg/L was set as the lower limit of quantification of the assay for clavulanic acid in human plasma. For the spiked quality control standards of clavulanic acid the inter-day precision ranged from 2.7 to 5.4% with an inter-day accuracy (relative error) between -1.3 and 6.2%. The

intra-day precision and relative error of the clavulanic acid assay ranged from 0.7 to 2.6% and between -0.5 and 6.8%.

**Population PK**

***Structural model:*** A series of structurally different absorption models in combination with one or two compartment disposition models were tested. All absorption models were studied with or without a lag-time. The following absorption models were studied: 1) First-order absorption, 2) zero-order absorption, 3) Michaelis-Menten absorption, and 4) absorption models with two catenary absorption compartments. Figure 5.3-1 shows models 4a and 4b. Model 4b is a variant of one of the PK models proposed by Piotrovskij et al. (385) for amoxicillin.

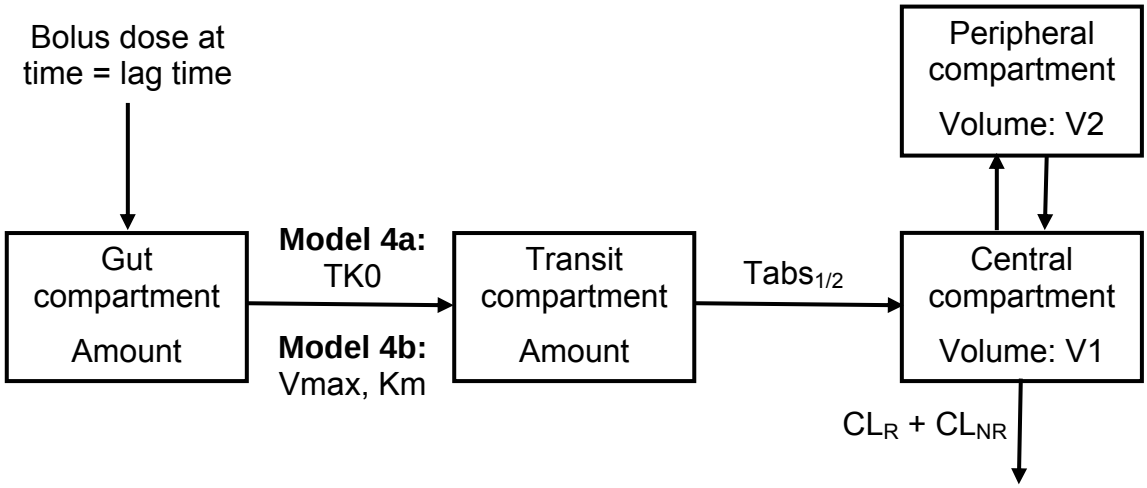


**Figure 5.3-1** Structural models with two catenary absorption compartments (clavulanic acid: model 4a, amoxicillin: model 4b)

The PK model shows two catenary absorption compartments (the gut and the transit compartment). When time equals lag-time, a bolus dose is given into the gut compartment. Models 4a and 4b differ in the link between the gut and transit compartment. A zero-order input (duration of zero-order input: TK0) links the gut with the transit compartment for model 4a, whereas a Michaelis-Menten process links those compartments for model 4b. Vmax is the maximum rate of drug transport from the gut to the transit compartment and Km is the amount of drug in the gut compartment that results in 50% of Vmax.

The transit compartment is linked by a first-order process (half-life: $Tabs_{1/2}$) with the central compartment. The drug is eliminated from the central compartment (volume: V1) by the sum of renal ($CL_R$) and nonrenal clearance ($CL_{NR}$). The peripheral compartment (volume: V2) is linked with the central compartment by the intercompartmental clearance (CLic). The peripheral compartment was not included for clavulanic acid, since the data supported only a one-compartment disposition model for clavulanic acid.

***Size:*** We applied the allometric size model with WT as size descriptor. The allometric exponent was 0.75 for clearance and 1.0 for volume of distribution as described in chapter 2.6.2.2.

***Clearance:*** We estimated glomerular filtration rate by the Cockcroft Gault formula (78) and used renal function (RF) as a covariate on renal clearance (see chapter 3.3.3.3, pages 131ff, for details). We used a standard glomerular filtration rate of 100 mL/min/70kg. We assumed a nonrenal ($CL_{NR}$) and a renal ($CL_R$) component of clearance. The renal clearance was assumed to be linearly related to renal function of the $i^{th}$ subject ($RF_i$). The group estimate of total clearance [$CL_{tot,i}(RF_i,WT_i)$] for subjects with a specific total body weight ($WT_i$) and renal function ($RF_i$) is:

$$CL_{tot}(RF_i, WT_i) = (CL_{NR} + RF_i \cdot CL_R) \cdot F_{Size,CL,i} \qquad \text{Formula 5.3-1}$$

$F_{Size,CL,i}$ is the fractional change in clearance for the $i^{th}$ subject (with $WT_i$) standardized to a weight $WT_{STD}$ of 70 kg (see chapter 2.6.2.2 for details).

***Individual PK model:*** We separated the PPV into its two components BSV and BOV. $\eta_{BSV}$ and $\eta_{BOV}$ are assumed to be normally distributed random variables with mean zero and standard deviation BSV and BOV, respectively. BSV and BOV were estimated as variances but we report the square root of the estimates. We have expressed these values in the text as a percentage because this quantity is an apparent coefficient of variation of a log-normal distribution.

The individual PK parameters were calculated as follows:

$$\eta_{PPVCLij} = \eta_{BSVCLi} + \eta_{BOVCLij} \qquad \text{Formula 5.3-2}$$

$$CL_{tot,ij}(RF_i, WT_i) = CL_{tot}(RF_i, WT_i) \cdot \exp(\eta_{PPVCLij}) \qquad \text{Formula 5.3-3}$$

$\eta_{BSVCLi}$ and $\eta_{BOVCLij}$ are $\eta_{BSV}$ and $\eta_{BOV}$ of CL for the $i^{th}$ subject at the $j^{th}$ occasion, respectively. $CL_{ij}(RF_i,WT_i)$ is the individual total clearance for the $i^{th}$ subject (with $RF_i$ and $WT_i$) at the $j^{th}$ occasion.

***Effect of BOV on the Chance of Showing Bioequivalence:*** We used the final model for amoxicillin and clavulanic acid to simulate the individual

plasma concentration time curves of 200 average bioequivalence studies (2x2 crossovers) with 24 subjects for each combination of BOVs.

The test and reference formulation were assumed to have the same average PK parameters and the same variability except for the modifications in the BOV terms as shown in the respective tables. We derived Cmax, $AUC_{0\text{-}last}$, and $AUC_{0\text{-}inf}$ from the simulated plasma concentration time curves via NCA. The width of the parametric 90% confidence intervals for the ratio of geometric means between the test and reference formulation for Cmax and AUC and the percentage of successful bioequivalence studies were recorded.

As the BOVF was much larger than BOVCL and BOVV1 for clavulanic acid, we studied the effect of different sizes of BOVF on the chance of showing bioequivalence for clavulanic acid. We studied the influence of BOVCL and BOVV1 on the chance of concluding bioequivalence for amoxicillin. In those simulations, the test and reference formulation had the same average rate and extent of absorption.

***Assessment of PD Profile:*** The $fT_{>MIC}$ can be used to predict the clinical and microbiological outcome for beta-lactams (84, 107). We simulated plasma concentration profiles of amoxicillin and derived the $fT_{>MIC}$ by linear interpolation between nominal sampling times for MICs between 0.25 and 4 mg/L. We used a plasma protein binding of 18% for amoxicillin (179). A $fT_{>MIC}$ of at least 50% of the dosing interval has been shown to be the PKPD target for near-maximal bacterial killing of penicillins (84, 107). We used this target for our analyses. The PTA was approximated by the frequency of achieving the target in 2,400 simulated plasma concentration time profiles for the chosen treatment schedule and parameter variability assumptions. The PKPD breakpoint was defined as the highest MIC with a PTA of at least 90%.

***Comparison of Bioequivalence and Similarity in PD Profiles:*** We compared bioequivalence and similarity in PD profiles of various amoxicillin formulations. The test formulation had a modified rate and extent of absorption compared to the reference formulation, but the variability terms were assumed to be the same for the test and reference formulation. For each test formulation, 100 bioequivalence studies (2x2 crossovers with 24 subjects) were simulated and evaluated. We studied non-bioequivalent formulations

with “similar” PD profiles which had a relative rate / extent of absorption of 80% / 80%, 100% / 100% (=reference formulation), 150% / 125%, and 200% / 175%, respectively. Additionally, we compared possibly bioequivalent formulations with “dissimilar” PD profiles. Those formulations had a relative rate / extent of absorption of 70% / 115%, 80% / 110%, 100% / 100% (=reference formulation), 125% / 90%, and 150% / 90%, respectively.

### 5.3.4 Results

***Drug Concentrations:*** Figure 5.3-2 shows the average (± SD) plasma concentration time curves for amoxicillin and clavulanic acid. NCA showed a maximum plasma concentration for amoxicillin of 7.79 ± 0.36 mg/L (average ± standard error) in period 1 and 8.00 ± 0.43 mg/L in period 2. The time to maximum plasma concentration was 1.43 ± 0.057 h in period 1 and 1.30 ± 0.067 h in period 2 for amoxicillin. For clavulanic acid the maximum plasma concentration was 2.49 ± 0.22 mg/L in period 1 and 2.64 ± 0.15 mg/L in period 2. The corresponding time points of maximum plasma concentration were 1.09 ± 0.047 h in period 1 and 1.13 ± 0.052 h in period 2.

***Model Building:*** For amoxicillin we found that a two compartment disposition model described the data better than a one compartment disposition model. For clavulanic acid the data did not support a two compartment disposition model hence we chose a one compartment disposition model. This was assessed by VPCs, the objective function, and standard residual plots.

The models with two catenary absorption compartments (models 4a and 4b, see Figure 5.3-1) were flexible enough to fit the shapes of the individual plasma concentration time curves. These models revealed a highly sufficient predictive performance in the VPCs (see Figure 5.3-3). Absorption models 1, 2, and 3 were either not flexible enough to fit the shape of the individual plasma concentration time profiles or showed considerable bias, too large variability, or both in the VPCs.

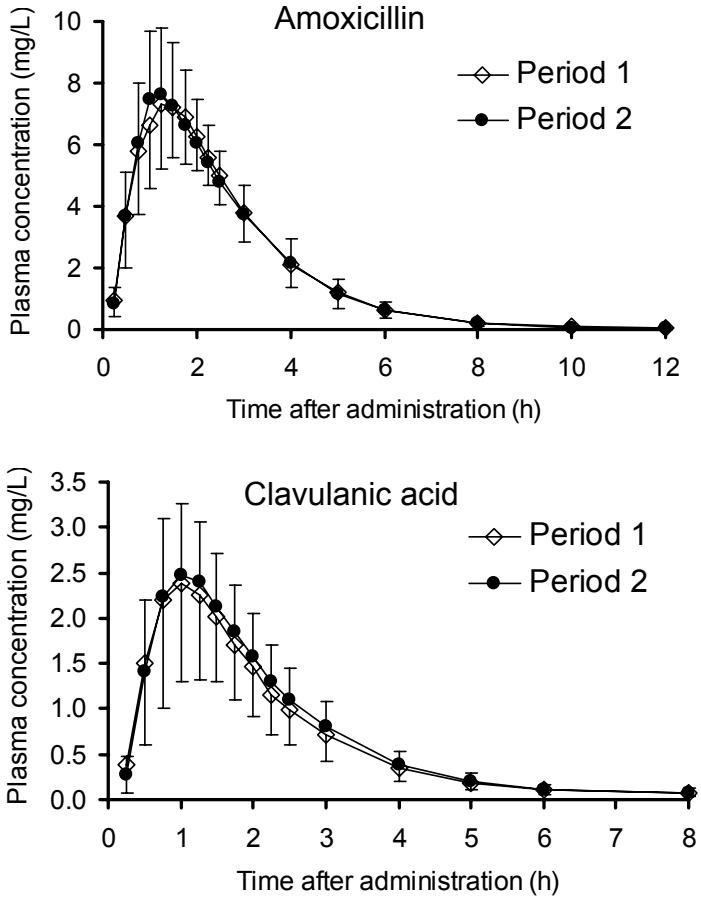


**Figure 5.3-2** Average ± SD plasma concentrations of amoxicillin and clavulanic acid in study periods 1 and 2 after a single oral administration of 500/125 mg amoxicillin / clavulanic acid

For amoxicillin, absorption models 4a and 4b had a similar predictive performance, but absorption model 4b had a 139 points better objective function relative to model 4a. We chose absorption model 4b with a two compartment disposition model as our final model for amoxicillin. For clavulanic acid model 4b had a 7.6 points better objective function relative to model 4a, but the predictive performance for model 4a was slightly better than for the more complex model 4b. We chose absorption model 4a with a one compartment disposition model as our final model for clavulanic acid.

All disposition parameters were scaled allometrically and we used a mixed additive and proportional error model for all PK models. Since we had only 24 subjects in our study, we did not seek to optimize the covariate model

other than by including standard allometric models and the model for renal function. Table 5.3-2 lists the estimates of the final population PK model for amoxicillin and clavulanic acid. Our PK parameters were in agreement with the results from other studies on amoxicillin and clavulanic acid in healthy volunteers (179, 208, 358, 385).

***Panel A:*** *Amoxicillin (model 4b)*

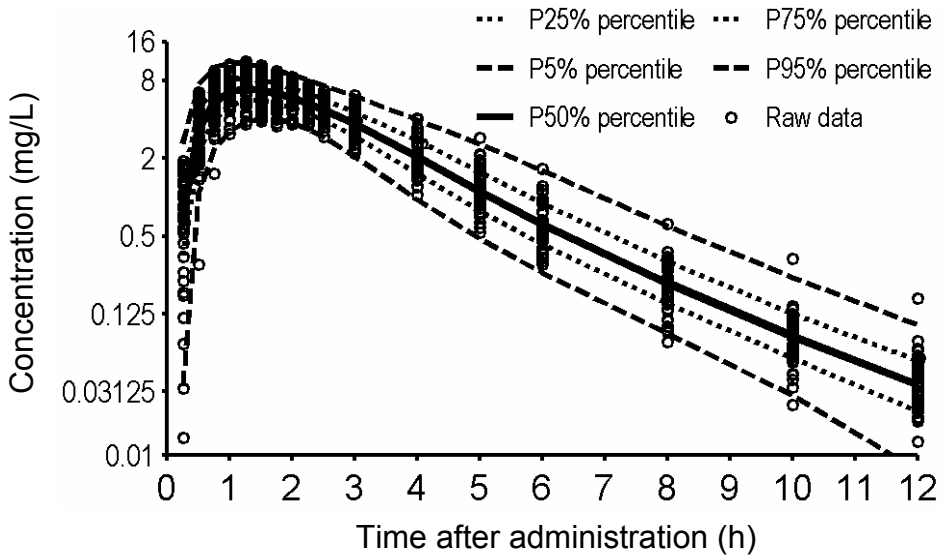


***Panel B:*** *Clavulanic acid (model 4a)*

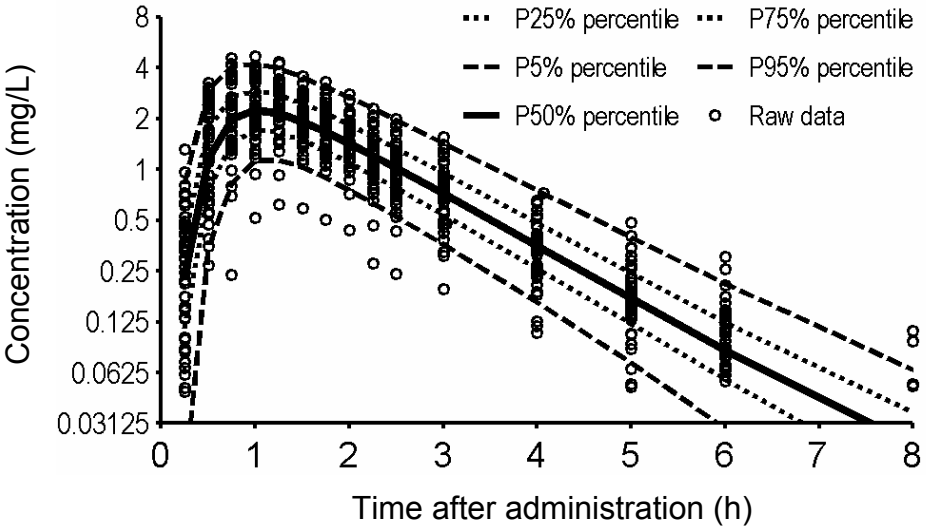


**Figure 5.3-3** VPCs for the final models shown in Table 5.3-2 based on 19,200 simulated profiles each

See chapter 2.6.3 for interpretation of VPCs.

**Table 5.3-2** Population parameter estimates for amoxicillin and clavulanic acid (see Figure 5.3-1 for explanation of PK parameters)

| Parameter | Unit | Amoxicillin (model 4b) | | | Clavulanic acid (model 4a) | | |
|---|---|---|---|---|---|---|---|
| | | Population estimate | BSV | BOV | Population estimate | BSV | BOV |
| F | | 1 (fixed) | 10.4% | 8.5% | 1 (fixed) | 23.7% | 25.2% |
| $CL_T$ (for 70 kg)[a] | L $h^{-1}$ | 21.6 | 11.9% | 9.6% | 22.5 | 8.39% | 1.4% |
| $CL_R$ (for 70 kg)[a] | L $h^{-1}$ | 15.0 | | | 10.2 | | |
| $CL_{NR}$ (for 70 kg)[a] | L $h^{-1}$ | 6.63 | | | 12.3 | | |
| Vss (for 70 kg)[b,e] | L | 15.8 | | | 30.2 | | |
| V1 (for 70 kg)[b] | L | 6.77 | 14.0% | 42.5% | 30.2 | 4.5% | 1.9% |
| V2 (for 70 kg)[b] | L | 9.04 | | | - | | |
| CLic (for 70 kg)[a] | L $h^{-1}$ | 5.45 | | | - | | |
| Tlag | min | 6.30 | 33.2% | 42.0% | 5.54 | 45.7%[d] | 46.4% |
| Vmax | mg/h | 784 | 75.3%[c] | 10.8% | - | | |
| Km | mg | 696 | 86.0%[c] | 7.5% | - | | |
| TK0 | min | - | | | 30.2 | 18.3%[d] | 26.3% |
| $Tabs_{1/2}$ | min | 14.5 | 0.90% | 48.0% | 11.3 | 43.2%[d] | 35.8% |
| $CV_{CONC}$ | | 8.15% | | | 7.33% | | |
| $SD_{CONC}$ | mg/L | 0.0112 | | | 0.0110 | | |

[a]: The allometric model with a standard body weight of 70 kg and an exponent of 0.75 was used to scale all clearance terms.

[b]: The allometric model with a standard body weight of 70 kg and an exponent of 1.0 was used to scale all volume terms.

[c]: r = correlation of random effects for pairs of parameters. $r_{BSV}$(Vmax,Km) = 0.978 for amoxicillin.

[d]: $r_{BSV}$(TK0,Tlag) = 0.687 and $r_{BSV}$(Tlag,Tabs) = -0.723 for clavulanic acid.

[e]: Derived from estimated PK parameters, not an estimated parameter.

-: Not included in the model.

BSV: Apparent coefficient of variation for between subject variability.

BOV: Apparent coefficient of variation for between occasion variability.

***Effect of BOV on the Chance of Showing Bioequivalence:*** Table 5.3-3 shows the chance of showing bioequivalence for clavulanic acid test formulations with various BOVF. The reference formulation had a BOVF of 25.2% which we estimated from the data of this study. As expected, a high BOVF resulted in wider 90% confidence intervals for the ratio of geometric means between the test and reference formulation for Cmax and AUC. Although the average rate and extent of absorption were identical for the test and the reference formulation, only 96% of the simulated bioequivalence studies (with n=24 subjects) concluded bioequivalence for "the ideal" test formulation with a BOVF of zero. For a test formulation with BOVF of 12.6%, 86.5% of the simulated studies showed bioequivalence. Therefore, BOVF had a pronounced effect on the chance of showing bioequivalence.

Table 5.3-4 shows the results of simulated bioequivalence studies for amoxicillin test and reference formulations with various combinations of BOVCL and BOVV1. Although the average rate and extent of absorption were identical for both formulations, a high BOVCL increased the width of the 90% confidence intervals and consequently reduced the chance of showing bioequivalence. However, a high BOVV1 had a surprisingly small influence on the width of the 90% confidence intervals for Cmax and, as expected, no effect on the width for AUC. As the BOVCL rises from zero to 80% for amoxicillin (with BOVV1 fixed at 42.5%), the percent of successful bioequivalence studies drops from 88% at BOVCL of 20% to 16.5% at BOVCL of 40% (see Table 5.3-4). The width of the 90% confidence intervals for AUC was more influenced by higher BOVCL values than the width for Cmax.

**Table 5.3-3** Influence of between occasion variability for extent of absorption (BOVF) on the results of bioequivalence studies (two-way crossovers with n=24 subjects) for clavulanic acid

| Test & reference formulation were identical except for | | Percentage of studies that passed the bioequivalence criterion of 80-125% for | | | |
|---|---|---|---|---|---|
| BOVF of the test formulation | BOVF of the reference formulation | Cmax | $AUC_{0\text{-last}}$ | $AUC_{0\text{-inf}}$ | All three statistics |
| 25.2% | 25.2% | 73% | 77.5% | 79% | 69% |
| 12.6% | 25.2% | 89% | 92% | 92.5% | 86.5% |
| 5% | 25.2% | 93% | 99% | 99.5% | 93% |
| 0% | 25.2% | 96% | 99.5% | 99.5% | 96% |
| 12.6% | 12.6% | 100% | 100% | 100% | 100% |
| 5% | 12.6% | 100% | 100% | 100% | 100% |
| 0% | 12.6% | 100% | 100% | 100% | 100% |
| 5% | 5% | 100% | 100% | 100% | 100% |
| 0% | 0% | 100% | 100% | 100% | 100% |

| Test & reference formulation were identical except for | | Median [Min-Max] width of the 90% confidence interval for the ratio of geometric means between the test and reference formulation | | |
|---|---|---|---|---|
| BOVF of the test formulation | BOVF of the reference formulation | Cmax (%) | $AUC_{0\text{-last}}$ (%) | $AUC_{0\text{-inf}}$ (%) |
| 25.2% | 25.2% | 26.7 [18.4 - 41.3] | 24.9 [15.6 - 37.5] | 24.7 [15.4 - 38.0] |
| 12.6% | 25.2% | 21.8 [11.7 - 35.0] | 20.0 [12.5 - 30.7] | 20.0 [12.6 - 30.7] |
| 5% | 25.2% | 20.4 [10.9 - 31.6] | 18.2 [10.1 - 27.2] | 18.0 [9.9 - 27.1] |
| 0% | 25.2% | 20.0 [13.5 - 29.3] | 17.5 [10.6 - 25.9] | 17.4 [10.8 - 26.6] |
| 12.6% | 12.6% | 15.8 [10.7 - 23.6] | 12.5 [8.1 - 18.2] | 12.5 [7.8 - 18.5] |
| 5% | 12.6% | 13.6 [6.1 - 19.2] | 10.0 [6.0 - 14.4] | 9.9 [5.9 - 14.4] |
| 0% | 12.6% | 12.8 [7.7 - 19.2] | 9.1 [5.7 - 12.6] | 9.0 [5.8 - 12.7] |
| 5% | 5% | 10.9 [6.4 - 16.5] | 5.6 [3.5 - 7.8] | 5.6 [3.5 - 7.9] |
| 0% | 0% | 9.4 [5.5 - 17.8] | 2.7 [1.7 - 4.1] | 2.7 [1.6 - 3.7] |

Both formulations are identical in rate and extent of absorption as well as in all other model parameters except BOVF as defined by the population PK model. BOVCL was 1.4% and BOVV1 was 1.9% for all simulations shown in this table. For all other model parameters, the final estimates of model 4a for clavulanic acid were used (see Table 5.3-2).

**Table 5.3-4** Influence of between occasion variability for clearance (BOVCL) and volume of central compartment (BOVV1) on the results of average bioequivalence studies (two-way crossovers with n=24 subjects) for amoxicillin

Note: Both amoxicillin formulations are identical in rate and extent of absorption as well as all other model parameters as defined by the population PK model.

| BOVCL for both formulations | BOVV1 for both formulations | Percentage of studies that passed the bioequivalence criterion of 80-125% for Cmax | $AUC_{0\text{-last}}$ | $AUC_{0\text{-inf}}$ | All three statistics |
|---|---|---|---|---|---|
| 0% | 0% | 100% | 100% | 100% | 100% |
| 9.6% | 42.5% | 98% | 100% | 100% | 98% |
| 0% | 42.5% | 100% | 100% | 100% | 100% |
| 10% | 42.5% | 98% | 100% | 100% | 98% |
| 15% | 42.5% | 97% | 100% | 100% | 97% |
| 20% | 42.5% | 94.5% | 91.5% | 91% | 88% |
| 30% | 42.5% | 76.5% | 65% | 64% | 59.5% |
| 40% | 42.5% | 50.5% | 21% | 19.5% | 16.5% |
| 80% | 42.5% | 0% | 0% | 0% | 0% |
| 9.6% | 0% | 100% | 100% | 100% | 100% |
| 9.6% | 20% | 99% | 100% | 100% | 99% |
| 9.6% | 40% | 98.5% | 100% | 100% | 98.5% |
| 9.6% | 80% | 94.5% | 100% | 100% | 94.5% |
| 9.6% | 120% | 68% | 100% | 100% | 68% |
| 9.6% | 160% | 25% | 93.5% | 100% | 25% |

BOVF was 8.5% for all simulations shown in this table. For all other model parameters, the final estimates of model 4b for amoxicillin were used (see Table 5.3-2).

*Table continues on next page.*

**Table 5.3-4** Influence of between occasion variability for clearance (BOVCL) and volume of central compartment (BOVV1) on the results of average bioequivalence studies (two-way crossovers with n=24 subjects) for amoxicillin

Note: Both amoxicillin formulations are identical in rate and extent of absorption as well as all other model parameters as defined by the population PK model.

| | | Median [Min-Max] width of the 90% confidence interval for the ratio of geometric means between the test and reference formulation | | |
|---|---|---|---|---|
| BOVCL for both formulations | BOVV1 for both formulations | Cmax (%) | $AUC_{0\text{-last}}$ (%) | $AUC_{0\text{-inf}}$ (%) |
| 0% | 0% | 13.7 [6.7 - 22] | 8.5 [5.5 - 12.3] | 8.6 [5.5 - 13.1] |
| 9.6% | 42.5% | 16.5 [9.2 - 25.9] | 12.6 [7.8 - 18.2] | 12.6 [7.8 - 18.3] |
| 0% | 42.5% | 14.8 [9.7 - 21.3] | 8.8 [4.9 - 12.1] | 8.8 [4.9 - 12.1] |
| 10% | 42.5% | 16.5 [9.2 - 26.2] | 12.9 [8.1 - 18.6] | 12.9 [8.1 - 18.8] |
| 15% | 42.5% | 18.4 [10.5 - 30.3] | 16.6 [10.6 - 24.7] | 16.7 [10.8 - 24.9] |
| 20% | 42.5% | 20.7 [12.3 - 34.9] | 20.8 [13.1 - 32.1] | 21.0 [13.5 - 32.4] |
| 30% | 42.5% | 26.4 [16.3 - 45.4] | 29.5 [17.3 - 48.5] | 29.6 [17.4 - 49.1] |
| 40% | 42.5% | 32.4 [18.6 - 56.6] | 38.7 [20.7 - 67.1] | 39.1 [20.7 - 68.3] |
| 80% | 42.5% | 58.7 [28.6 - 125.9] | 76.1 [31.6 - 163.7] | 78.7 [31.7 - 155.7] |
| 9.6% | 0% | 15.9 [9.4 - 23] | 13.1 [6.7 - 17.4] | 13.2 [6.7 - 18.6] |
| 9.6% | 20% | 15.8 [8.3 - 24.6] | 12.6 [7.8 - 18.2] | 12.6 [7.8 - 18.3] |
| 9.6% | 40% | 16.3 [9.1 - 25.7] | 12.6 [7.8 - 18.2] | 12.7 [7.9 - 18.3] |
| 9.6% | 80% | 19.7 [11.5 - 32.6] | 12.5 [7.9 - 18.1] | 12.7 [7.9 - 18.8] |
| 9.6% | 120% | 27.2 [15.3 - 54.2] | 13.2 [7.9 - 24.5] | 13.0 [8.6 - 21.2] |
| 9.6% | 160% | 39.8 [20.0 - 93.5] | 16.6 [9.0 - 45.9] | 14.1 [8.0 - 22.9] |

BOVF was 8.5% for all simulations shown in this table. For all other model parameters, the final estimates of model 4b for amoxicillin were used (see Table 5.3-2).

***Comparison of Bioequivalence and Similarity in PD Profiles:*** Figure 5.3-4 shows the median plasma concentration time curves of four amoxicillin formulations which would most likely be non-bioequivalent. However, those four formulations had very similar PTA vs. MIC profiles. The

maximum difference between all four curves in the PTA vs. MIC plot was <18% (highest - lowest curve).

Figure 5.3-5 shows the PTA vs. MIC profiles of the reference formulation, two test formulations with a chance to be bioequivalent of about 84% and two test formulations with a chance to be bioequivalent of about 25%. The latter two test formulations with a chance of about 25% to be bioequivalent had a 1.5-fold higher and a 2-fold lower PKPD breakpoint compared to the reference formulation.

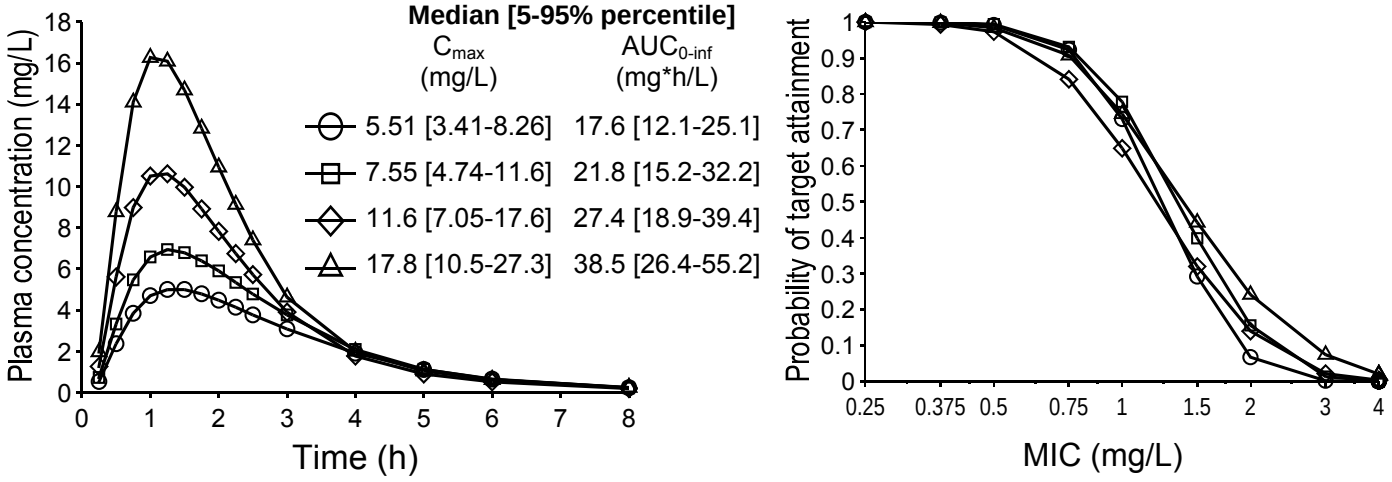


The average relative rate (Vmax) and extent (F) of absorption for the formulations shown in this plot were: 80% / 80% (circles), 100% / 100% (squares, reference formulation), 150% / 125% (diamonds), and 200% / 175% (triangles).

**Figure 5.3-4** Comparison of four non-bioequivalent formulations. Left panel: Median amoxicillin plasma concentrations of 2,400 simulated subjects for formulations with difference rates and extents of absorption. Right panel: Probabilities of target attainment for the same four formulations (target: $fT_{>MIC}$ at least 50% of the 8 h dosing interval)

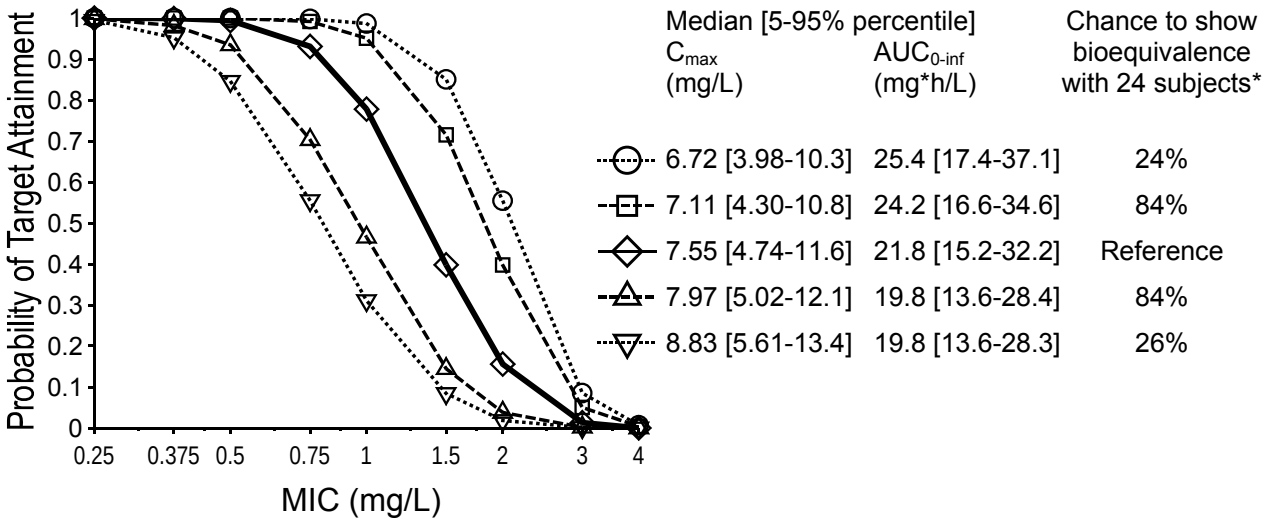


*: The chance of showing bioequivalence was calculated from 100 simulated two-way crossover studies with amoxicillin. Each 2x2 crossover study had a sample size of 24 subjects. The four test formulations were compared to the reference formulation.

The average relative rate (Vmax) and extent (F) of absorption for the formulations shown in this plot were: 70% / 115% (circles), 80% / 110% (squares), 100% / 100% (diamonds, reference formulation), 125% / 90% (up triangles) and 150% / 90% (down triangles).

**Figure 5.3-5** Comparison of five bioequivalent amoxicillin formulations. Each curve was derived from 2,400 simulated subjects for formulations with different rates and extents of absorption (target: $fT_{>MIC}$ at least 50% of an 8 h dosing interval)

### 5.3.5 Discussion

In this analysis three aspects of amoxicillin / clavulanic acid PK and PD were addressed. We estimated the BOV of amoxicillin and clavulanic acid and studied the influence of BOV in extent of absorption, clearance, and volume of central compartment on the chance of showing bioequivalence. As the clinical and microbiological outcome of beta-lactams is best described by $fT_{>MIC}$, we additionally studied, if bioequivalence assures similarity in the PD profile and vice versa.

We found that the high BOV of Cmax and AUC for clavulanic acid was predominantly determined by the 25.2% BOVF and not by a high BOVCL or BOVV1. Hence, improvements in the variability of the formulation may allow one to decrease the BOV of clavulanic acid, although the BOVF still includes both the BOV for the release from the formulation and for physiological changes. The pharmaceutical formulation is likely to be critical for the BOV of clavulanic acid absorption, since the BOVF for amoxicillin was only 8.5%. Variability in gastric transit time and gastric pH are likely to play a key role for degradation of clavulanic acid in the stomach. Our estimates for BOVF, BOVCL, and BOVV1 of amoxicillin and clavulanic acid were in agreement with the BOV for Cmax and AUC reported by Idkaidek et al. (208) from a bioequivalence study with replicate design.

Only a few reports on replicate administrations of the same formulation are available in literature that were studied in well-controlled trials in healthy volunteers (161, 208, 321, 504, 506, 512). Most of the available data on replicate doses of the same formulation come from datasets published by the FDA (55 datasets) (498) and from GlaxoSmithKline (22 datasets) (556). With the exception of the studies of Upton et al. (512, 513), Karlsson et al. (245), and Sheiner (446), none of these studies was analyzed by nonlinear mixed-effects modeling which has been shown to be a powerful approach to separate BOVF, BOVCL, and BOVV1 by Karlsson et al. (244, 245).

The importance of BOV on the chance of showing bioequivalence has been studied by el-Tahtawy et al. (123). They found that the width of the 90% confidence interval for the ratio of geometric means between the test and reference formulation decreases, if BOVCL and BOVV1 are absent. We were able to estimate the BOVF, BOVCL, and BOVV1, as well as the BOV for all absorption parameters of amoxicillin and clavulanic acid (see Table 5.3-2).

We studied the impact of BOVF, BOVCL, and BOVV1 on the results of bioequivalence studies with otherwise identical test and reference formulations. We used LC-MS/MS for bio-analysis and our data came exactly from the setting of a well-controlled, highly standardized bioequivalence study. Therefore, our study is well suitable to simulate bioequivalence studies which are commonly performed in generic drug development. In our simulations with

a range of BOVs for the test and reference formulation, a BOVF or BOVCL above about 15% increased the width of the 90% confidence intervals for the ratio of geometric means notably and therefore decreased the chance of showing bioequivalence (see Table 5.3-3 and Table 5.3-4). For a clavulanic acid reference formulation with BOVF 25.2%, the width of the 90% confidence interval for the ratio of geometric means decreased only by about 7% (median), even if the test formulation had zero BOVF (see Table 5.3-3). BOVCL directly influenced the width of the 90% confidence intervals (see Table 5.3-4). On the contrary, BOVV1 had no effect (as expected) on the width of the confidence intervals for AUC and surprisingly only a small effect on the width of the confidence intervals for Cmax.

Hence we could identify the sources of BOV which are critical for bioequivalence assessment. From a regulatory perspective, it may be important to know, whether a drug is highly variable (i. e. BOV > 30% for Cmax or AUC) due to a high BOVCL or BOVF. Improvements in the pharmaceutical formulation may reduce BOVF (e. g. by preventing degradation of the drug at low pH in stomach), whereas BOVCL is unlikely to be influenced by changes in the formulation. Therefore, widening of the bioequivalence limits from 80-125% to e. g. 75-133% seems justifiable only, if the high BOV of a drug is caused by a high BOVCL, but not by a high BOVF.

The structural model building was important for our analysis, as estimating the BOV terms for an oral formulation is a challenging task. To the best of our knowledge no population PK models for amoxicillin or clavulanic acid have been published. Allen et al. (5) used the STS approach and concluded that it is impossible to describe the absorption of clavulanic acid by standard absorption models. Piotrovskij et al. (385) also used the STS approach and came to the same conclusion for amoxicillin. They proposed a complex absorption model for amoxicillin. Our results were in agreement to the results from Allen et al. (5) and Piotrovskij et al. (385).

The absorption process involves disintegration, dissolution, and absorption from the GI tract into the portal vein. Finally, the absorbed drug must reach the venous blood at the site of sampling. Amoxicillin is an amphoteric compound with pKa values of 2.67 and 7.11. Tsuji et al. (507)

determined the solubility of amoxicillin at different pH values and found a U-shaped solubility curve with a minimum of 5.5 mg/mL at pH 5 and 37° C. They concluded that amoxicillin dissolves within 3-20 minutes at pH 3 under GI agitation conditions (and even faster at pH 1) and will most likely not precipitate at other pH conditions along the GI tract. Since we administered a dose of 500 mg amoxicillin as a suspension given with 240 mL water, amoxicillin solubility was probably not the rate limiting step of drug absorption in our study.

Several groups found evidence for a saturable (active) transport mechanism for the intestinal absorption of amoxicillin in animals (365, 496, 497) and in humans (76, 146, 371, 406, 453, 454, 541, 542). Additionally the lipophilicity of amoxicillin changes according to the local pH in the GI tract. The highest lipophilicity should be reached at the isoelectric point of amoxicillin at about pH 5, although most of the molecules will be present in their zwitterionic form at this pH. It was therefore not surprising that rather complex absorption models were required for amoxicillin. Clavulanic acid has a pKa of 2.7, is freely soluble in water and has an optimum stability in aqueous solution at pH 6.0 to 6.3 (492). More complex absorption models were also required for clavulanic acid. These models yielded excellent fits to the raw data and had a highly sufficient predictive performance (see Figure 5.3-3).

Our estimates for renal and non-renal clearance (see Table 5.3-2) resulted in an estimated fraction excreted unchanged in urine of 69% for amoxicillin and of 45% for clavulanic acid. These estimates were in agreement with the literature data. Urinary excretion of unchanged amoxicillin is reported as 86 ± 8% (average ± SD) of the drug and 43 ± 14% of clavulanic acid are excreted unchanged in the urine (179). It was encouraging that our model could estimate renal and non-renal clearance based on serum creatinine concentrations and plasma drug concentrations in absence of urinary excretion data.

After building the population PK models and studying the influence of BOV on the chance of showing bioequivalence, we studied whether bioequivalence in Cmax and AUC assures similarity in the PD profiles for

amoxicillin. We could show that bioequivalent formulations may have PKPD breakpoints which are 2-fold lower or 1.5-fold higher than the PKPD breakpoint of the reference formulation (see Figure 5.3-5). Although the clinical relevance of this observation needs to be determined, similarity in the PD profiles should be considered in parallel to standard bioequivalence testing based on Cmax and AUC.

In conclusion we developed population PK models for oral amoxicillin and clavulanic acid with a highly sufficient predictive performance. We could show that the high BOV often seen in bioequivalence studies with clavulanic acid was most likely due to the BOVF of 25.2% and not due to BOVCL or BOVV1. In simulations with various BOVs, a BOVF or BOVCL >15% decreased the chance of demonstrating bioequivalence notably. We found that amoxicillin test formulations with a 25% chance to be bioequivalent in a 2x2 crossover with 24 subjects may have a 2-fold lower or 1.5-fold higher PKPD breakpoint relative to the reference formulation. Therefore, bioequivalence did not guarantee similar PD profiles between the test and the reference formulation for beta-lactams. Similarity in the probability to achieve a PKPD target should be considered in parallel to bioequivalence for beta-lactams.

# 6 Monte Carlo simulations with beta-lactams

## 6.1 Background on Monte Carlo simulations

### 6.1.1 Purpose of a Monte Carlo simulation with antibiotics

Probably the most valuable information a pharmacometrician can provide for a physician in anti-infective chemotherapy is the expected probability of successful treatment. Large randomized controlled trials are required to assess the effectiveness (and safety) of a given drug and dosage regimen. However, the effectiveness of innovative dosage regimens has often not yet been evaluated. In absence of effectiveness data from a large clinical trial, MCS offer a tool to overcome this shortage of data. MCS combines the available information on the PK and PD with a PKPD target e. g. for near-maximal bactericidal activity. This target serves as surrogate marker, e. g. for successful microbiological outcome, in a MCS. By simulating several thousand virtual patients, the probability to achieve this target can be predicted for a given dose and mode of administration. The PTA is then combined with the expected susceptibility profile (MIC distribution) to predict the expected probability for successful microbiological outcome. If the microbiological outcome is the major determinant of clinical outcome, the PTA can be used to predict the probability of successful treatment. By use of PK data for a specific patient group and the MIC distribution of the local hospital, the probability of successful treatment can be predicted for the patients at each local hospital.

### 6.1.2 Monte Carlo simulation techniques applied in literature

Although MCS has become a standard technique since its first application to the field of anti-infective PKPD in 1998 (113), different methods are used and there is no generally applied method to assure the quality of a MCS. Methods like the VPC (VPC, see chapter 2.6.3) are not applied by the

majority of investigators performing MCS with antibiotics. This may be especially critical for a MCS with beta-lactams, because the PKPD target for beta-lactams is based on the time above MIC (T>MIC) which is much more difficult to accurately simulate than the AUC. Several factors determine the T>MIC. These comprise clearance, volume of distribution, intercompartmental distribution, rate of absorption, and duration of infusion, besides other factors. A possibly major shortcoming of virtually all MCS based on literature data is that the authors do not account for the correlation between clearance and volume of distribution (see chapter 2.6.2.3 and Figure 2.6-7 on page 50f).

The elimination half-life is very important in MCS with beta-lactams, especially for short-term infusions. Figure 6.1-1 shows the distribution of elimination half-lives for a simulation with or without correlation between clearance and volume of distribution. Clearance and volume of distribution both had a coefficient of variation of 30% in each simulation. The covariance was zero for the left box-whisker, whereas the simulation with covariance assumed a coefficient of correlation of 0.9 between clearance and volume of distribution (right box-whisker).

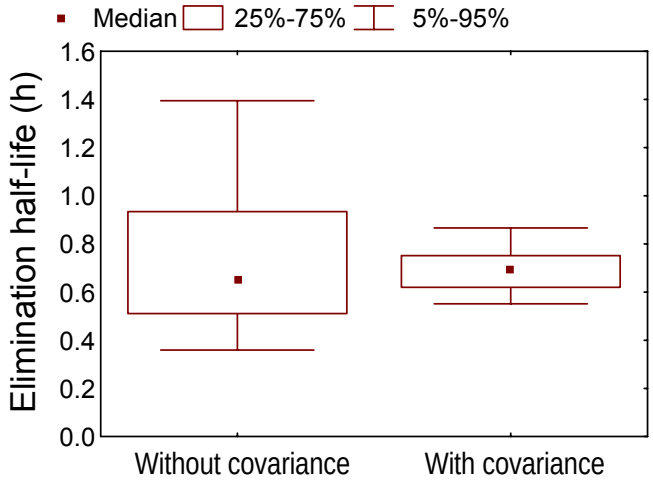


**Figure 6.1-1** Distribution of elimination half-lives for a simulation with or without covariance (coefficient of correlation: r = 0.9) between clearance and volume of distribution

The 5% percentiles differ by a factor of about 1.5 in those two simulations and this difference may affect the PTA vs. MIC profiles substantially. A correlation between clearance and volume of distribution can

be caused by several factors like: 1) Clearance and volume of distribution are both affected by body size. 2) BSV in protein binding can cause a correlation between clearance and volume of distribution. 3) BSV in extent of absorption affects both clearance and volume of distribution. Therefore, it is important to account for the correlation between PK parameters.

However, the coefficient of correlation (or the covariance) between clearance and volume of distribution is rarely reported in papers which used NCA for PK analysis. As many MCS with beta-lactams took clearance and volume of distribution data from literature and did not account for the correlation between clearance and volume of distribution, these results should be interpreted cautiously. This possible methodological shortcoming of several MCS in literature will not be discussed further here, since VPCs can be used to circumvent this possible problem, if individual concentration time raw data are available. Advantages of using VPCs will be described in detail below.

### 6.1.3 Uncertainty of Monte Carlo simulations

MCS is a powerful method to account for the BSV in PK parameters and for the variability in antimicrobial susceptibility (MIC distribution). However, there is uncertainty in the PK parameters (including the BSV terms), in the MIC distribution, in the PKPD target, and in the MCS methodology itself. Uncertainty in the PK parameters might become critically important, if the population PK model has been estimated from a small number of subjects or from sparse PK datasets (e. g. in pediatric or ICU patients). The influence of these sources of uncertainty on the results of a MCS for antibiotics has not yet been systematically studied.

## 6.2 Bias and uncertainty of Monte Carlo simulations with beta-lactams

### 6.2.1 Objectives

Our first objective was to compare various methods of qualifying a population PK model for subsequent use in a MCS. We were especially interested in the sensitivity of the MCS results to model misspecification. Our second objective was to derive meaningful confidence intervals for the results of a MCS based on the uncertainty in the PK parameters, in the MIC distribution, and in the PKPD target as well as uncertainty secondary to the MCS methodology. We present both results from simulation studies and real data examples.

### 6.2.2 Methods

The general clinical and sample handling procedures, the methods for PK analysis (including NCA and population PK), and the general methods for MCS are described in chapter 2.

We had two objectives which required both simulation and estimation procedures. We present the general methods of simulation, estimation, and derivation of PKPD results first. These methods and dosage regimens were used in the MCS, if not indicated otherwise. Then we describe the analysis plans for our two objectives.

***Population PK:*** Population PK was used to model the plasma concentration time profiles. We modeled the drug input for the oral absorption as a first order or zero order process from the gut into the central compartment and used a time-delimited zero order input into the central compartment for intravenous infusion. We estimated the BSV for all clearance and volume of distribution terms by assuming a log-normal distribution.

***MCS:*** The most predictive PKPD target for the microbiological outcome of beta-lactams is T>MIC (84, 107). We used the PKPD target T>MIC $\geq$ 40%

for bacteriostasis and T>MIC ≥ 70% for near-maximal bactericidal activity of cephalosporins in our simulations. We did not include protein binding in our simulations, because protein binding is of minor importance for low extraction ratio drugs (35) and a concentration independent protein binding does not influence the conclusions of our MCS. We simulated the plasma concentration time curves at steady-state after a 30 min intravenous infusion of 4,000 mg q8h for a test drug with beta-lactam like PK in absence of residual error for 2,000 to 10,000 subjects.

**Analysis plan for objective 1: Model selection for MCS**

***Model selection criteria:*** We compared the ability of NONMEM's objective function (-2 · log-likelihood + constant), residuals plots, and VPCs to select the most appropriate model for use in a MCS. We present two real data examples. Example one compares observed vs. predicted plots and residuals plots with the VPC and example two compares NONMEM's objective function with the VPC.

The first real data example is a population PK model for amoxicillin after intake of a 500 mg oral suspension. The structural model for this example was a two compartment disposition model. The oral absorption of amoxicillin did not follow a first order or zero order process. We described the absorption as a time delimited zero order input (including a lag-time) which was followed by a first order input process (without constraint at the transition between zero and first order input, see Holford et al. (196) for details). The second real data example compares a first order and a zero order absorption with a three compartment disposition model for levofloxacin. (Note: These models for levofloxacin did not include the final model for levofloxacin shown in Table 4.3-5 and Table 4.3-6.) We compared the objective function difference and the VPC to select the most appropriate population PK model.

***Bias in MCS results due to model misspecification:*** We intended to quantify the influence of model misspecification on the results of a MCS based on a simulation example. We simulated an example drug with a typical terminal half-life of 1.8 h which followed a two compartment model with first order PK. We will refer to this model as our "true model". We simulated

plasma concentrations after a single 30 min infusion of 4,000 mg from the true model for 48 subjects at the following time points: 7.5, 15, 22.5, 30, 45, 60, 75, and 90 min post start of infusion as well as 1.75, 2, 2.25, 2.5, 3, 3.5, 4, 4.5, 5, 6, 7, and 8 h post start of infusion. We estimated a one and a two compartment population PK model from those simulated concentrations and additionally derived clearance and volume of distribution via NCA. We calculated the geometric means and the coefficients of variation for clearance and volume of distribution during the terminal phase from NCA parameters by descriptive statistics.

We ran a MCS at steady-state for the true two compartment model, for the re-estimated two compartment model (=correct structural model), for the estimated one compartment model (=simplified structural model), and for a one compartment model based on the clearance and volume of distribution from NCA. We compared the PTA vs. MIC profiles between those four models. Additionally, we calculated the PTA expectation values for the targets T>MIC ≥40% and T>MIC ≥ 70% based on 32 published MIC distributions against *P. aeruginosa*, *S. aureus*, *E. coli, A. baumanii*, and *K. pneumoniae* (6, 158, 254, 273, 437, 467, 510) to compare PTA expectation values between those models for actual MIC data.

**Analysis plan for objective 2: Confidence intervals for MCS results**

***Uncertainty due to MCS methodology: How many subjects to simulate?*** We ran 5,000 replicates of a MCS with either 100, 500, 1000, 2000, or 10000 subjects for the true two compartment model. We calculated the PTA vs. MIC profile and the PTA expectation value for each of those replicates based on the 32 published MIC distributions shown above. We derived non-parametric 90% confidence intervals (5% to 95% percentile) of the PTA vs. MIC profiles and of the PTA expectation values. This simulation allowed us to estimate the uncertainty in the PTAs and PTA expectation values depending on the number of simulated subjects.

***Uncertainty in population PK parameters:*** We studied the influence of uncertainty in the estimated PK parameters on the results of a MCS for various numbers of subjects in the PK raw dataset. In the first step, we

simulated a raw dataset of 48 subjects based on the true two compartment model with 20 blood collections (observations) per subject at the time points shown above. We performed a non-parametric bootstrap (122, 376) by randomly drawing new PK datasets of various sample sizes from those 48 simulated subjects. Each subject could be drawn multiple times. We randomly generated 1,000 new raw datasets with 12, 24, or 48 subjects each.

In the second step, we estimated the PK parameters of a two compartment model for each of those 3 x 1,000 new datasets. This resulted in 1,000 sets of population PK parameter estimates for each sample size. The distribution of the population PK parameters from those 1,000 bootstrap runs per sample size represents the uncertainty in PK parameter estimates. In the third step, we ran a MCS with 2,500 subjects for each of those 3 x 1,000 parameter sets and derived the PTA vs. MIC profiles and the PTA expectation values for the 32 published MIC distributions shown above.

Additionally, we used the same three-step procedure to study 3,000 randomly generated new PK raw datasets with 12, 24, or 48 subjects for sparse plasma concentration data. The sparse datasets comprised an average ± SD of 4.4 ± 1.5 (median: 4, range: 2-8) randomly selected blood samples (observations) per subject instead of 20 observations per subject for the datasets with dense samples. These sparse data provided a more realistic estimate for the uncertainty in PK parameters for studies in patients from whom only a limited number of blood samples can be taken.

***Uncertainty in MIC distribution:*** MIC distributions used in a MCS may comprise less than 100 MIC samples. This is often the case, if the probability of successful treatment of a specific treatment group in a local hospital is of concern. We intended to estimate the influence of uncertainty arising from MIC distributions with various sample sizes on the results of a MCS. We used MIC distributions for *E. coli* (n=433) and *P. aeruginosa* (n=427) from the MYSTIC 2002 North America program (273) and for methicillin-susceptible *S. aureus* (MSSA, n=363) in the Americas (510) to randomly generate new MIC distributions by non-parametric bootstrapping. We randomly generated 5,000 new MIC distributions for each of the following sample sizes: 10, 20, 50, 100, 300, and 1,000 isolates per MIC distribution and pathogen. We

calculated the confidence interval for the PTA expectation value based on the true two compartment model in absence of uncertainty in PK parameters.

***Combined uncertainty in PK and in MIC distribution:*** We studied the uncertainty in the results of a MCS with uncertainty being present both in PK parameters and in MIC distribution. The MIC distribution consisted of 50 MIC samples. The MIC samples were randomly drawn from the MIC distribution for *E. coli* (n=433, (273)), *P. aeruginosa* (n=427, (273)), or MSSA (n=363, (510)) described above.

***Uncertainty in PKPD target:*** We studied various degrees of uncertainty in the PKPD target T>MIC. We ran 5,000 MCS with 10,000 subjects each based on the true two compartment model. We sampled population PKPD targets (same target for each subject in the population) from a normal distribution with mean ± SD of 65 ± 2.5%, 65 ± 5%, or 65 ± 10%. Additionally, we studied the influence of random BSV in the individual PKPD targets by using a normal distribution for the BSV which was centered around each randomly sampled population PKPD target. We derived the PTA expectation value for *E. coli* (n=433) and *P. aeruginosa* (n=427) (273).

### 6.2.3 Results

***Model selection for MCS:*** We compared NONMEM's objective function, residual plots and the VPC as criteria to select the most appropriate model for a MCS. Figure 6.2-1 shows a real data example for oral amoxicillin. The predicted vs. observed plot showed a convincing fit both on linear (panel A) and on log-log scale (panel B). The weighted residual vs. time plot (panel C) indicated no bias, whereas the VPC (panel D) showed a systematic overprediction and underprediction at different parts of the profile which would not have been discovered by the other diagnostic plots.

A) Observed vs. predicted plot – linear scale

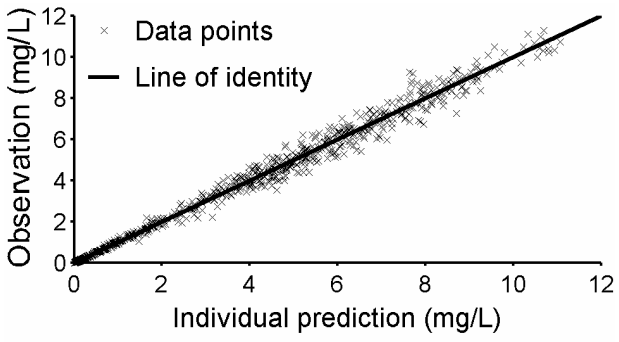


C) Weighted residual vs. time

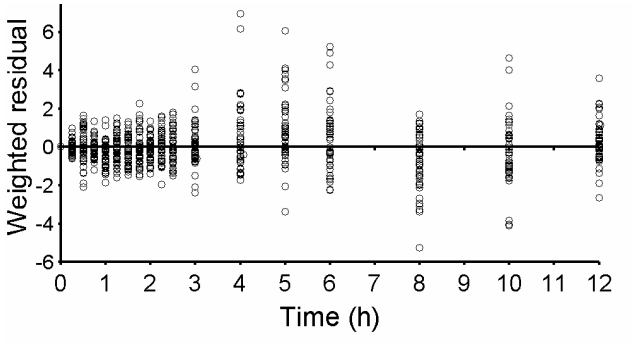


B) Observed vs. predicted plot – log-log scale

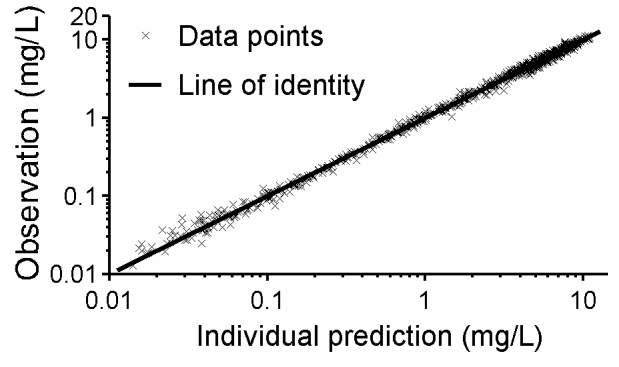


D) Visual predictive check – linear scale

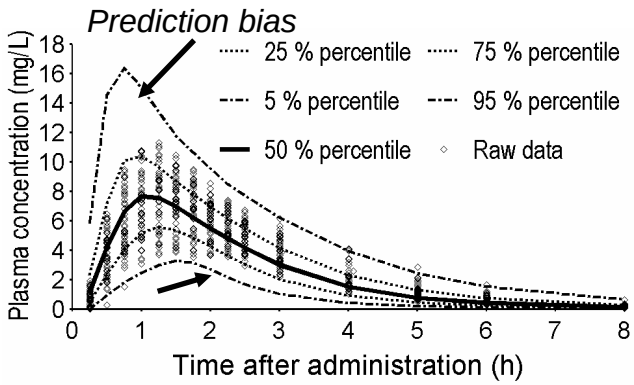


**Figure 6.2-1** Comparison of standard diagnostic plots and a VPC for a population PK model after 500 mg oral amoxicillin

**A) First order absorption** (NOTE: this is not the model shown in Table 4.3-5)

65 points better objective function, but worse predictive performance

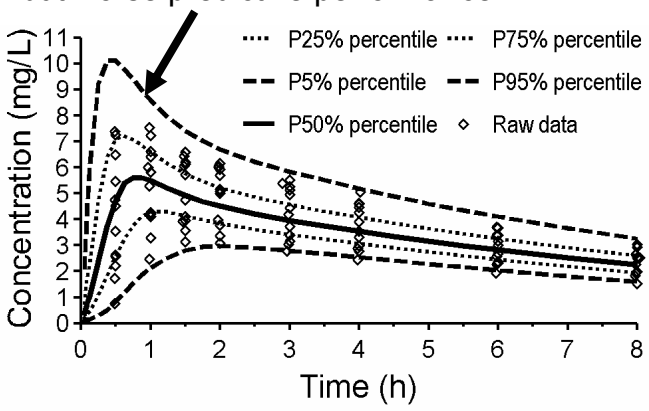


**B) Zero order absorption**

More reasonable predictive performance for peak concentrations

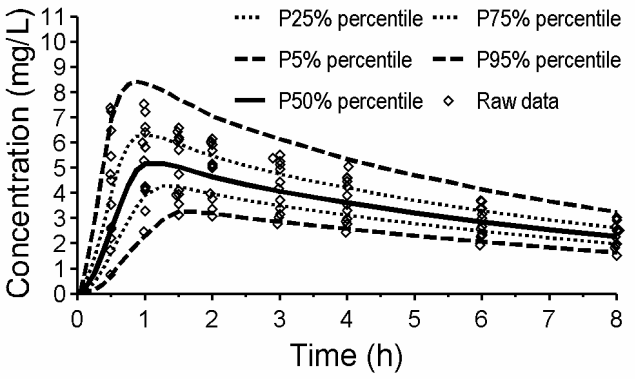


**Figure 6.2-2** VPC and objective functions of two population PK models for 500 mg oral levofloxacin (both models have three disposition compartments)

Furthermore, we compared NONMEM's objective function (-2 · log-likelihood + constant) to the VPC for a real data example after 500 mg oral levofloxacin (see Figure 6.2-2). The two structural models differed only in the absorption process. Both models included a lag time. The model with first order absorption had a 65 points better objective function than the model with zero order input. This was a pronounced difference in the objective function. The VPC revealed a much better predictive performance around the peak concentrations for the model with the worse objective function. Therefore, the VPC was superior to the objective function for selecting the most appropriate model for a MCS. This would especially be important, if the peak concentrations were used as PKPD target for a MCS with quinolones.

***Bias in MCS results due to model misspecification:*** We simulated the plasma concentration time curves for 48 subjects from the true two compartment model with frequent blood samples and re-estimated the PK parameters from those simulated concentrations for a one and a two compartment model. The estimated two compartment model closely matched the parameter estimates of the true two compartment model. The one compartment model overestimated clearance by 10% and underestimated volume of distribution at steady-state by 28%. The geometric mean volume of distribution during the terminal phase from NCA was 67% larger than the volume of distribution at steady-state of the true two compartment model. The individual volumes of distribution during the terminal phase were larger than the true volume of distribution at steady-state for 46 of 48 subjects.

We compared these population PK models in a MCS and simulated all dosage regimens at steady-state. The PTA vs. MIC profiles in Figure 6.2-3 were almost indistinguishable for the true and the re-estimated two compartment model. The estimated one compartment model under-predicted the PTA, whereas the MCS with the NCA estimates for clearance and volume of distribution over-predicted the PTAs both for a 30 min infusion (=true dosage regimen) and for a simplified bolus dose regimen.

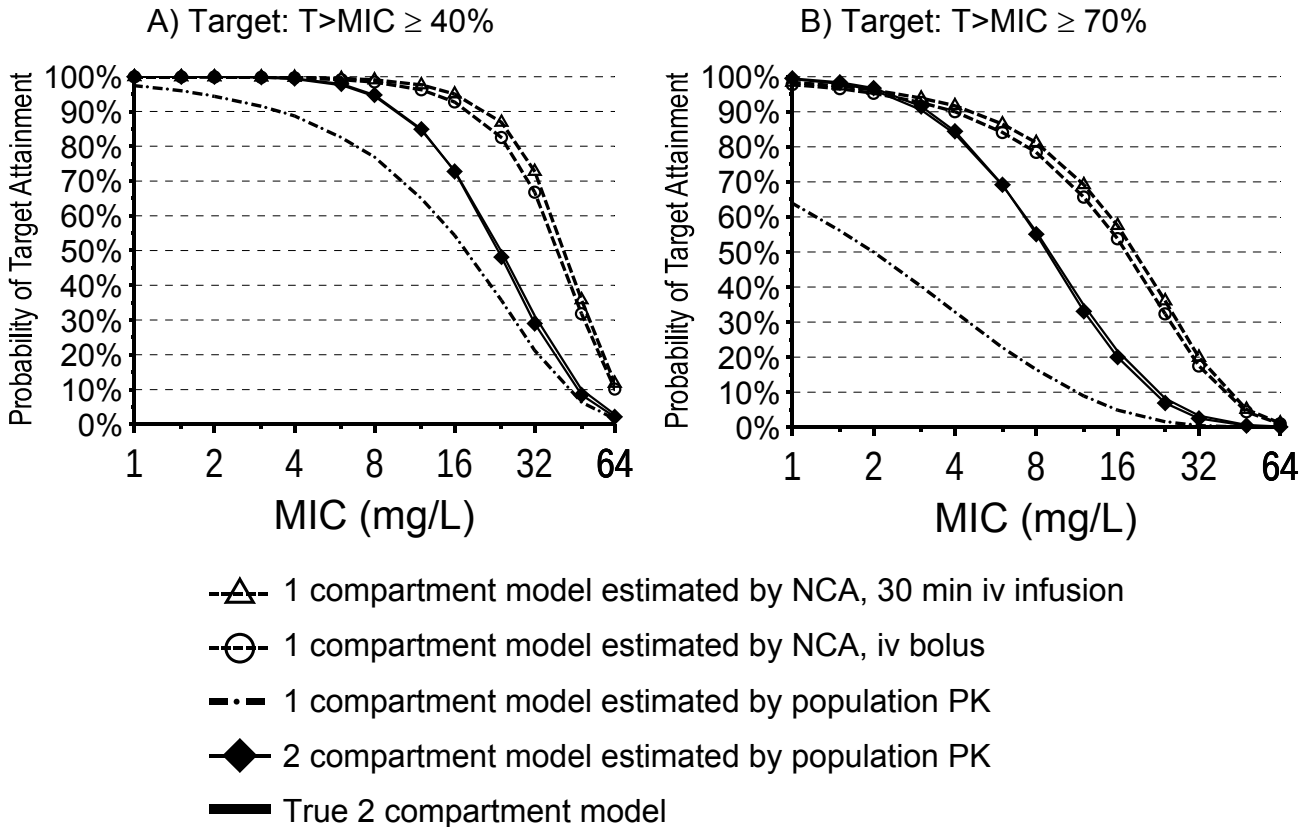


**Figure 6.2-3** Effect of model misspecification on PTA vs. MIC profiles at steady-state for various population PK models. Dosage regimen: 30 min infusion of 4,000 mg q8h at steady-state

Table 6.2-1 shows the influence of those biased PTAs on the PTA expectation values based on 32 MIC distributions. We separated the prediction errors based on the PTA expectation value for the true model. The estimated one compartment model showed a 6.9 to 25.8% median underprediction (maximum: 40.0% underprediction) and the MCS with the NCA parameters showed a 1.5 to 9.5% median overprediction (maximum: 24.9% overprediction). It should be noted that the overprediction for the population PK model based on the NCA parameters was up to 6.2% (98.2% for the one compartment model from NCA vs. 92.0% for the true two compartment model) in the 90-100% group (see Table 6.2-1).

**Table 6.2-1** Bias in PTA expectation values of the estimated population PK models compared to the true two compartment model for 32 MIC distributions in combination with the targets T>MIC ≥ 70% and T>MIC ≥ 40% (n=64 combinations in total, all dosage regimens simulated at steady-state)

| **PTA expectation value for the true model** (number of values within this range) | **Median (minimum to maximum)** | | | |
|---|---|---|---|---|
| | Re-estimated 2 compartment model | Estimated 1 compartment model | Non-compartmental analysis° | |
| | | | 30 min infusion | Bolus dose* |
| 90-100% (n=12) | 0.0% (-0.2 to 0.3%) | -6.9% (-38.5 to -1.2%) | 1.8% (0.6 to 6.2%) | 1.5% (0.5 to 5.4%) |
| 80-90% (n=12) | 0.0% (-0.1 to 0.3%) | -9.4% (-40.0 to -4.7%) | 4.9% (3.1 to 7.6%) | 4.0% (2.3 to 6.7%) |
| 65-80% (n=15) | -0.1% (-0.6 to 0.2%) | -22.1% (-38.3 to -5.9%) | 7.8% (4.1 to 15.5%) | 6.4% (3.5 to 13.3%) |
| 50-65% (n=14) | -0.2% (-0.6 to 0.2%) | -25.8% (-38.6 to -5.0%) | 8.6% (4.5 to 22.9%) | 7.5% (3.4 to 20.2%) |
| < 50% (n=11) | -0.2% (-1.0 to -0.1%) | -17.5% (-26.1 to -4.4%) | 9.5% (4.8 to 24.9%) | 8.2% (4.1 to 22.2%) |

°: Based on volume of distribution during the terminal phase.

*: The dosage regimen was simplified to a bolus dose instead of a 30 min infusion, because this simplification is sometimes used in a MCS with beta-lactams in literature.

***How many subjects to simulate:*** We ran 5,000 replicates of a MCS with various numbers of simulated subjects. Table 6.2-2 shows the PTAs and their non-parametric 90% confidence intervals at representative MICs. The 90% confidence intervals for the PTA had a width of about 3-6% for 1,000 simulated subjects, of about 2-4% for 2,000 simulated subjects, and of 1.6% or less for 10,000 simulated subjects. Importantly, these confidence intervals only include the uncertainty in the MCS methodology and include no uncertainty in PK parameters and no uncertainty in MIC distribution.

**Table 6.2-2** PTA and its 90% confidence intervals (5% - 95% percentile) depending on the number of subjects simulated (without uncertainty in PK parameters, without uncertainty in MIC distribution, and without uncertainty in PKPD target)

| Number of subjects simulated | Target: T>MIC ≥ 40% | | Target: T>MIC ≥ 70% | |
|---|---|---|---|---|
| | MIC 8 mg/L | MIC 16 mg/L | MIC 4 mg/L | MIC 8 mg/L |
| 100 | 94% (90 - 98%) | 72% (65 - 80%) | 83% (76 - 89%) | 54% (46 - 63%) |
| 500 | 94.0% (92.4 - 95.8%) | 72.4% (69.0 - 75.8%) | 83.2% (80.4 - 86.0%) | 54.8% (51.0 - 58.6%) |
| 1,000 | 94.1% (92.8 - 95.3%) | 72.4% (70.0 - 74.7%) | 83.1% (81.3 - 85.1%) | 54.6% (51.9 - 57.4%) |
| 2,000 | 94.1% (93.2 - 94.9%) | 72.4% (70.7 - 74.0%) | 83.2% (81.8 - 84.6%) | 54.7% (52.7 - 56.6%) |
| 10,000 | 94.1% (93.7 - 94.4%) | 72.4% (71.6 - 73.1%) | 83.1% (82.5 - 83.7%) | 54.7% (53.9 - 55.5%) |

Figure 6.2-4 shows the width of the 90% confidence intervals for the PTA expectation value plotted vs. the median PTA expectation value as a function of the number of simulated subjects. The width of these confidence intervals was smaller for higher PTA expectation values and was less than 2% for 2,000 simulated subjects and less than 1% for 10,000 simulated subjects in 62 of 64 studied cases.

***Uncertainty in population PK parameters:*** We estimated the uncertainty in PK parameters by non-parametric bootstrap techniques for dense and sparse plasma concentration time data with datasets of 12, 24, or 48 subjects. The resulting uncertainty in the PTA vs. MIC profiles is shown in Figure 6.2-5. The PTAs were slightly lower for the sparse data, because clearance was estimated to be about 4% higher, volume of the peripheral compartment was estimated to be about 6% smaller, and the BSV in clearance was estimated to be about 24% larger for the sparse data.

As expected, the 90% confidence intervals were wider for the datasets with sparse samples relative to the datasets with dense samples. However, the number of subjects influenced the width of the confidence intervals much more than the dense vs. sparse sampling.

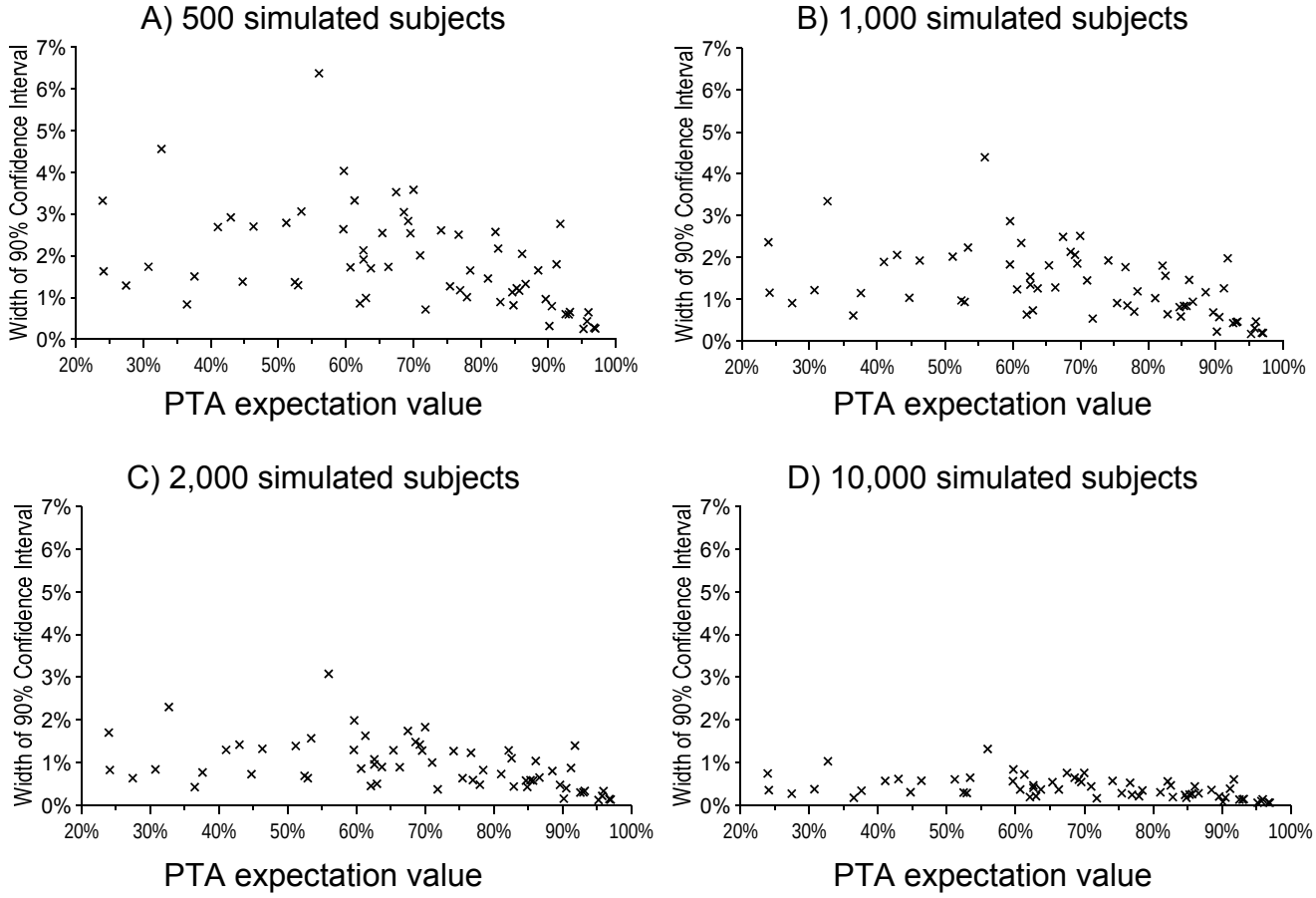


**Figure 6.2-4** Influence of the number of subjects simulated on the width of the 90% confidence intervals (5% - 95% percentiles) for the PTA expectation values (without uncertainty in PK parameters and without uncertainty in MIC distribution)

Each of the 64 data points represents the width for one of the 32 MIC distributions combined with one of the two targets T>MIC ≥ 40% or T>MIC ≥ 70%.

Even for dense PK data on 48 subjects, the width of the 90% confidence interval for the PTA was up to 21% (see Figure 6.2-5). The respective width of the 90% confidence intervals was up to 29% for dense PK data on 24 subjects and up to 44% for the dense PK data on 12 subjects. As shown in Figure 6.2-6, the width of the 90% confidence intervals for the PTA expectation values was up to 17% (20%) for dense (sparse) PK data on 48 subjects, up to 24% (28%) for dense (sparse) PK data on 24 subjects, and up to 35% (43%) for dense (sparse) PK data on 12 subjects.

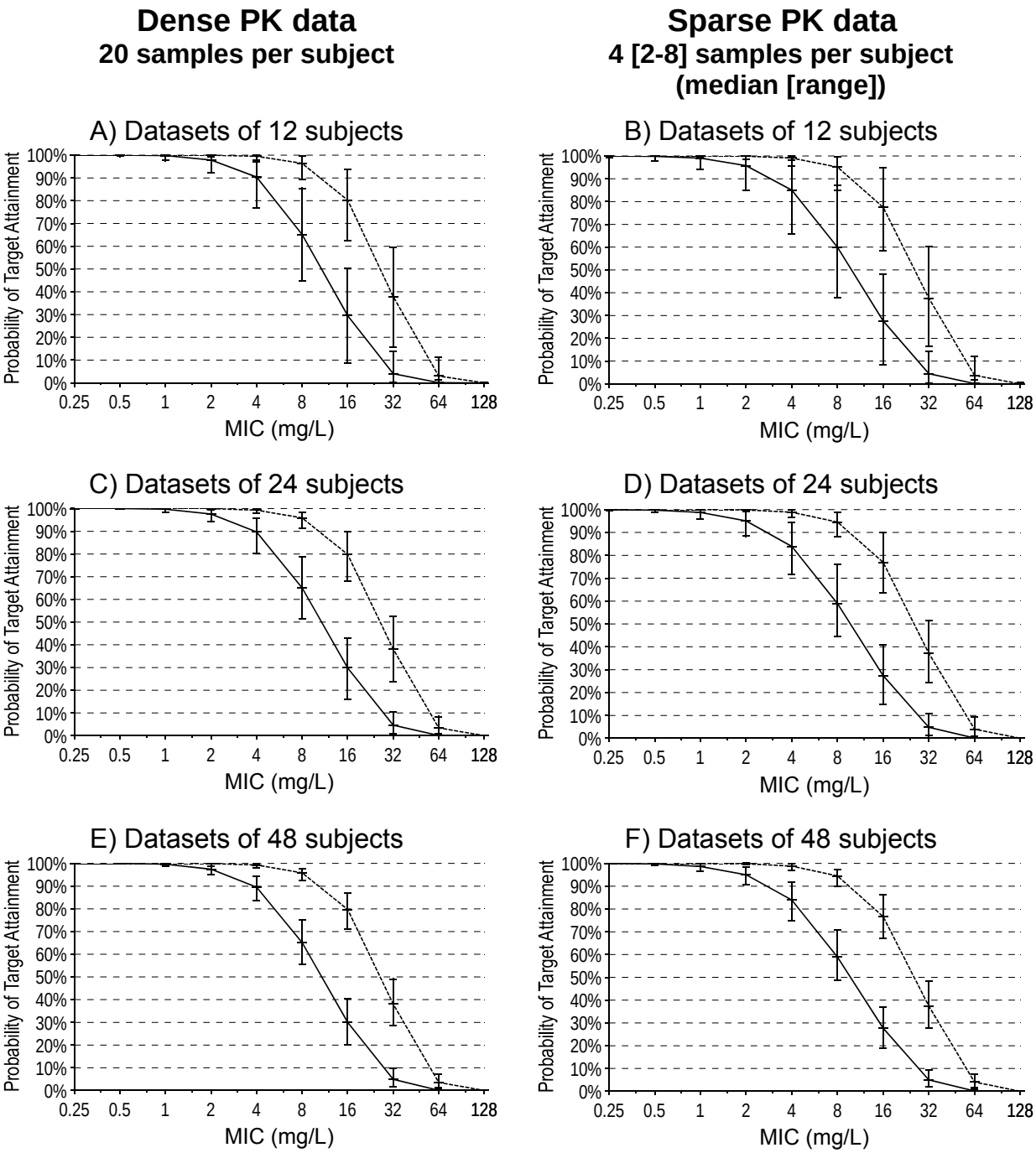


**Figure 6.2-5** Influence of uncertainty in PK parameters on the PTA vs. MIC profiles and their non-parametric 90% confidence intervals (5% - 95% percentiles) without uncertainty in PKPD target

The solid lines show the PTAs for the PKPD target T>MIC ≥ 70% and the dashed lines for T>MIC ≥ 40%. The markers are the median of 1,000 bootstrap estimates and the error bars are the non-parametric 90% confidence intervals (5% and 95% percentiles).

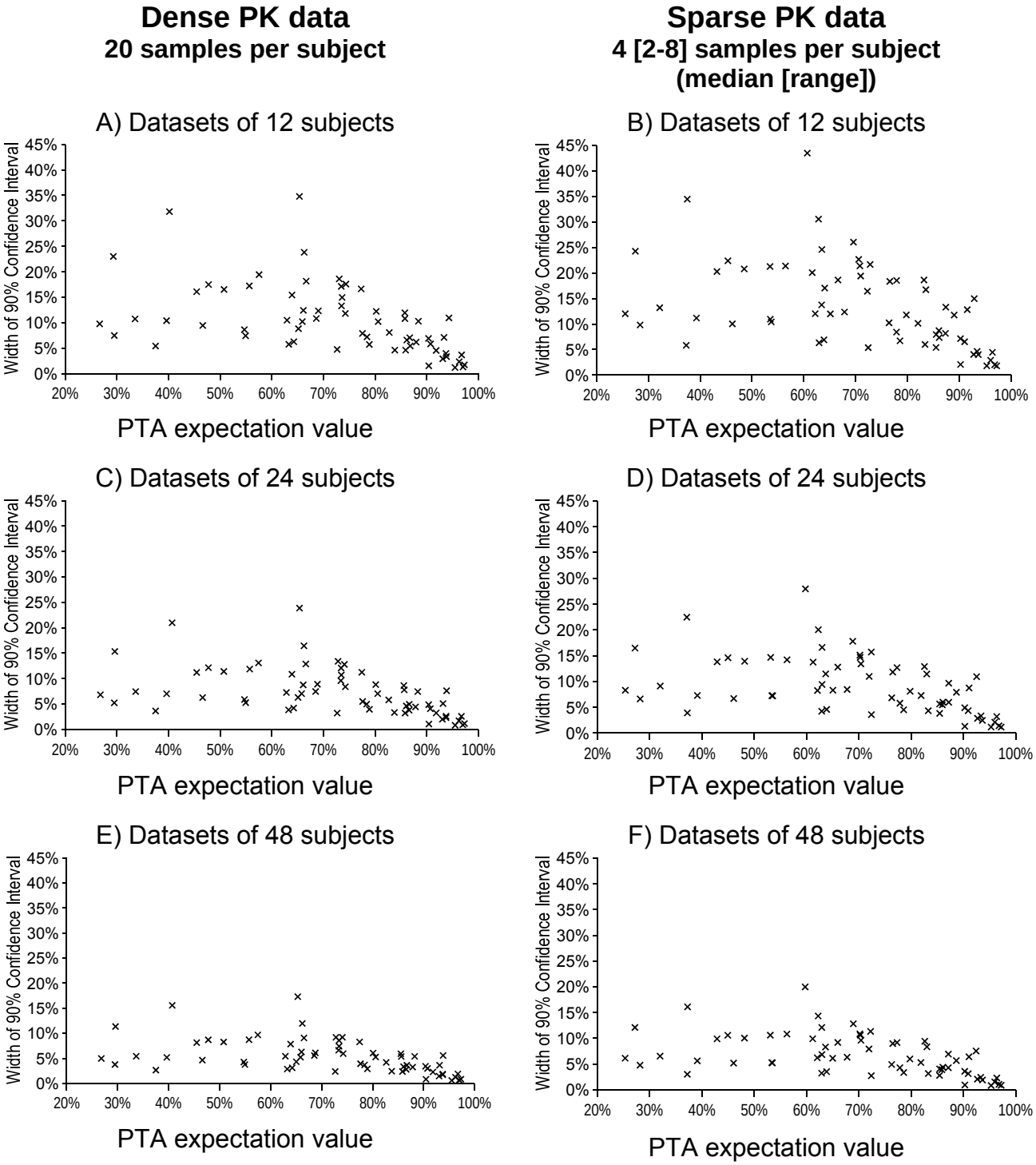


**Figure 6.2-6** Influence of uncertainty in PK parameters on the width of the 90% confidence intervals (5% - 95% percentiles) for the PTA expectation value without uncertainty in MIC distribution and without uncertainty in PKPD target

Each of the 64 data points represents the width for one of the 32 MIC distributions combined with one of the two targets T>MIC ≥ 40% or T>MIC ≥ 70%.

***Uncertainty in the MIC distribution:*** We studied the influence of uncertainty in the MIC distribution on the PTA expectation value for MIC distributions with 10 to 1,000 MIC samples. The results are shown in Table 6.2-3 (see *"Uncertainty in PD"*). The width of the 90% confidence intervals for the PTA expectation value was up to 37%, if only 10 MIC samples were available. The width was up to 26% for MIC distributions consisting of 20 MIC samples and up to 16% for MIC distributions consisting of 50 MIC samples. For MIC distributions based on 300 MIC samples, the 90% confidence intervals had a width of up to 7% and collecting 1,000 MIC samples resulted in a width of up to 4% for our examples. These results assume that there is no uncertainty in PK parameters and depend on the underlying MIC distribution. The confidence intervals for other MIC distributions can be wider or narrower.

***Combined uncertainty in the PK and in the PD:*** Table 6.2-3 shows the confidence intervals for the PTA expectation values, if there is only uncertainty in PK parameters (see *"Uncertainty in PK"*) and if there is uncertainty in PK parameters and in MIC distribution (see *"Uncertainty in PK & PD"*). The latter case is most relevant for PTA expectation values in actual practices, but still assumes that the PKPD target is known exactly. Uncertainty in the PK and PD contributed about equally to the combined uncertainty for the *E. coli* and the *P. aeruginosa* example, whereas uncertainty in PK was the predominant source of uncertainty for MSSA. The width of the 90% confidence intervals was 12-29% for sparse PK data on 24 subjects and MIC distributions with 50 samples, if both uncertainty in PK and PD were considered. The respective width for dense PK data on 24 subjects was 10-25% in our three examples.

***Uncertainty and variability in the PKPD target:*** We randomly sampled 5,000 population PKPD targets based on various standard deviations (see first three data rows of Table 6.2-4) to study the influence of uncertainty in the PKPD target on the results of a MCS. The population PKPD target was the same for all 10,000 subjects within one replicate of the MCS. The median PTAs and PTA expectation values were almost unaffected by the presence of uncertainty in the population PKPD target.

**Table 6.2-3** Median PTA expectation values and their 90% confidence intervals (5% - 95% percentile) for the target T>MIC ≥ 70% as a function of uncertainty in MIC distribution, uncertainty in PK parameters, or uncertainty in both (without uncertainty in PKPD target)

| Number of MIC isolates | Number of Subjects | *E. coli* | *P. aeruginosa* | MSSA |
|---|---|---|---|---|
| *Uncertainty in PD* | | | | |
| 10 | Infinite* | 92.8% (78.5-98.0%) | 61.8% (42.6-79.2%) | 57.1% (46.2-65.8%) |
| 20 | Infinite* | 91.8% (83.2-97.0%) | 61.7% (48.5-74.4%) | 56.2% (49.4-62.9%) |
| 50 | Infinite* | 91.5% (86.4-95.3%) | 61.7% (53.3-69.7%) | 56.3% (51.9-60.3%) |
| 100 | Infinite* | 91.3% (87.8-94.2%) | 61.6% (55.7-67.3%) | 56.2% (53.1-59.1%) |
| 300 | Infinite* | 91.2% (89.3-93.0%) | 61.5% (58.1-64.9%) | 56.1% (54.4-57.8%) |
| 1,000 | Infinite* | 91.2% (90.2-92.1%) | 61.5% (59.6-63.3%) | 56.1% (55.2-57.1%) |
| *Uncertainty in PK* | | | | |
| Infinite° | 12# | 91.6% (83.1-95.9%) | 63.5% (50.3-74.9%) | 60.7% (40.1-83.6%) |
| Infinite° | 24# | 91.1% (86.0-94.7%) | 63.0% (54.5-71.1%) | 59.8% (46.7-74.7%) |
| Infinite° | 48# | 91.1% (87.5-93.9%) | 62.9% (56.7-68.8%) | 59.8% (50.2-70.2%) |
| *Uncertainty in PK & PD* | | | | |
| 50 | 12# | 91.3% (81.9-97.4%) | 63.6% (48.2-77.5%) | 60.8% (39.6-83.4%) |
| 50 | 24# | 91.0% (84.1-96.4%) | 63.0% (51.4-74.1%) | 59.9% (46.3-74.9%) |
| 50 | 48# | 91.0% (85.0-95.7%) | 62.9% (52.9-72.6%) | 59.9% (49.5-70.8%) |

*: It was assumed that the PK parameters were known without uncertainty which would require an infinite number of subjects in the PK dataset.

°: It was assumed that the MIC distribution was known without uncertainty which would require an infinite number of MIC samples which characterize the observed MIC distribution.

#: Based on sparse PK raw datasets with an average ± SD of 4.4 ± 1.5 (median: 4, range: 2-8) blood samples per subject.

However, the confidence intervals were wider, if there was more uncertainty in the population PKPD target. For a population PKPD target of 65 ± 5%, the 90% confidence interval had a width of up to 25% for the PTAs and of up to 12% for the PTA expectation value in our examples. The presence of random BSV in the PKPD targets among the 10,000 subjects had almost no influence on the median PTAs and PTA expectation values and on their 90% confidence intervals (see last three data rows of Table 6.2-4).

**Table 6.2-4** Influence of uncertainty in the PKPD target T>MIC on PTAs and on PTA expectation values (without uncertainty in PK parameters and without uncertainty in MIC distribution).

The values are medians (5% - 95% percentiles) from 5,000 replicates of a MCS with 10,000 subjects each.

| **Target: T>MIC** | | **Probability of target attainment** | | | **PTA expectation value** | |
|---|---|---|---|---|---|---|
| Population Mean ± SD | Between subject variability | MIC 2 mg/L | MIC 4 mg/L | MIC 8 mg/L | *E. coli* (n=433) | *P. aeruginosa* (n=427) |
| 65 ± 2.5%* | 0% | 97.1% (95.3-98.1%) | 87.7% (83.8-90.7%) | 62.2% (55.9-68.7%) | 92.5% (90.9-93.6%) | 64.9% (61.7-67.8%) |
| 65 ± 5%* | 0% | 97.1% (93.7-98.8%) | 87.7% (80.1-93.1%) | 62.0% (49.9-74.6%) | 92.5% (89.6-94.4%) | 64.9% (58.7-70.5%) |
| 65 ± 10%* | 0% | 97.1% (88.5-99.7%) | 87.5% (69.7-97.2%) | 61.8% (37.9-85.4%) | 92.5% (85.0-95.8%) | 64.8% (51.6-76.0%) |
| 65 ± 2.5%* | 2.5%# | 96.9% (95.3-98.0%) | 87.5% (83.7-90.6%) | 62.2% (55.9-68.7%) | 92.4% (91.0-93.5%) | 64.8% (61.7-67.8%) |
| 65 ± 5%* | 5%# | 96.7% (93.3-98.6%) | 87.1% (79.4-93.0%) | 62.1% (49.8-74.5%) | 92.2% (89.3-94.4%) | 64.7% (58.5-70.6%) |
| 65 ± 10%* | 10%# | 95.9% (87.1-99.2%) | 85.9% (69.1-95.9%) | 61.8% (39.3-83.7%) | 91.7% (84.0-95.5%) | 64.3% (51.5-75.6%) |

*: We used T>MIC data from 10,000 simulated subjects. We sampled 5,000 population T>MIC targets based on a normal distribution. Within each of those 5,000 runs, the population target was the same for all 10,000 subjects.

#: We used the same procedure to sample random population targets as described above and added random BSV via a normal distribution for the individual targets around the sampled population target. For example, if a population target of 68% was sampled the distribution of individual targets was 68% ± 2.5%, 68% ± 5%, or 68% ± 10%.

### 6.2.4 Discussion

It is generally agreed upon that the PK and PD characteristics should be considered simultaneously for optimal dose selection in anti-infective chemotherapy. There is true BSV in the PK parameters and often much larger variability in the bacterial susceptibility. Population PK is a powerful method to

directly estimate the BSV. MCS combines the variability in the PK with the variability in the PD to predict the probability of successful treatment for a given drug and dosage regimen. Therefore, MCS offers the possibility to save a large amount of time and resources both in clinical trial development and in selection of optimal dosage regimens for empiric therapy.

Since the first application of a MCS in rational dose selection for phase II/III clinical trials (113), several MCS methods of various complexity have been applied to predict PTAs and PTA expectation values for antibiotic treatment (6, 8, 112-114, 116, 169, 239, 273, 274, 297, 326, 327, 339, 355, 558). Ideally the PK model used for MCS should be estimated via population PK. However, if such a model is not available, simplified one compartment models based on literature data are sometimes used to simulate the plasma concentration time curves. Although MCS has become increasingly popular, there is no standard method of how to assure the appropriateness of a population PK model and we are not aware of any systematic study about the influence of uncertainty in PK or PD on the results of a MCS for anti-infectives.

Therefore, our first objective was to compare various standard diagnostics with a new method to visually assess the predictive performance of a population PK model. Additionally, we studied the influence of model misspecification on the results of a MCS. Commonly applied statistics for model selection comprise both visual and statistical methods. A variety of diagnostic plots are often applied for visual inspection of the model fit, either based on population or on individual predictions. The log-likelihood is commonly used as statistical criterion to select the best model. The VPC addresses the simulation properties of a population PK model directly and it is this predictive performance which is most important for a MCS. The VPC compares the central tendency and variability of simulated plasma concentrations with the observed plasma concentrations. Lodise et al. (297) used a VPC to assess the predictive performance of various population PK models at the most relevant time point for their PKPD target 50% *f*T>MIC for piperacillin.

We could show in two real data examples that the VPC was superior to standard diagnostic plots (see Figure 6.2-1) and NONMEM's objective

function (see Figure 6.2-2) to assess the predictive performance of a population PK model. The VPC revealed the degree of model misprediction and at which part of the curve the prediction bias occurred. It allows one to decide, whether the prediction bias is likely to affect the results of a MCS. Standard diagnostic plots were more difficult to interpret and may even be misleading as shown in our two examples.

We further studied the influence of model misspecification on the results of a MCS. We simulated plasma concentrations from a two compartment population PK model and estimated the PK parameters with a one and a two compartment model from the simulated concentrations. Additionally, we determined clearance and volume of distribution via NCA and descriptive statistics. A MCS for each of those models showed that the results of the estimated two compartment model closely resembled the results for the true two compartment model (see Figure 6.2-3). The estimated one compartment model under-predicted the PTAs and both one compartment models based on the NCA parameters (30 min iv infusion and simplified bolus input) over-predicted the PTAs.

We put these mispredictions into clinical perspective by calculating the PTA expectation values. The estimated one compartment model under-predicted the PTA expectation values by up to 40% and the one compartment model from NCA over-predicted the PTA expectations values by up to 25% (see Table 6.2-1). Therefore, the use of a simplified PK model can result in considerable bias in the results of a MCS and we observed both over- and underpredictions. We therefore propose to use VPCs to assure the predictive performance of a population PK model as a routine check to qualify a population PK model for use in a MCS. If only published NCA parameters are available, the ability of the derived population PK model to recapitulate the NCA results (e. g. peak concentrations, their timing, and terminal half-life) should be assessed via predictive checks based on the derived population PK model (93, 553).

Our second objective was to determine the influence of uncertainty in the MCS methodology, PK parameters, MIC distribution, and PKPD target on the results of a MCS. Accounting for these sources of uncertainty allows one

to derive meaningful confidence intervals for the results of a MCS. These confidence intervals characterize the uncertainty in PTAs and in PTA expectation values secondary to a limited amount of available raw data and do not represent the BSV.

We studied the number of simulated subjects in a MCS as the first source of uncertainty. Table 6.2-2 shows that the 90% confidence intervals for the PTA had a width of about 4% for 2,000 simulated subjects and a width of about 2% for 10,000 simulated subjects. The confidence intervals for the PTA expectation values were narrower for PTA expectation values close to 100% (see Figure 6.2-4). The width of the 90% confidence intervals in the PTA expectation value was up to about 2% for 2,000 simulated subjects and up to about 1% for 10,000 simulated subjects. The width of these confidence intervals approaches zero for an infinite number of simulated subjects, because they only account for the uncertainty in the MCS methodology.

However, these confidence intervals do not account for the limited amount of available raw data used to derive the population PK model. There is uncertainty in population PK parameters which can be estimated by non-parametric bootstrap techniques (49, 126, 127, 154, 375, 376, 551). We derived the uncertainty in PK parameters for 6,000 randomly selected PK datasets of either 12, 24, or 48 subjects and dense or sparse sampling and ran a MCS for each of those estimated sets of population PK parameters. This method yields 6,000 PTA vs. MIC profiles and PTA expectation values. Figure 6.2-5 shows the non-parametric 90% confidence intervals for the PTA vs. MIC profiles and Figure 6.2-6 shows the width of the 90% confidence intervals for the PTA expectation values. As those probabilities are constraint between 0 and 100%, their confidence intervals were asymmetric.

As expected, the confidence intervals were slightly wider for the sparse than for the dense PK datasets, when compared at the same number of subjects. For the dense PK dataset, the width of the 90% confidence intervals for the PTA was up to 44% for 12 subjects, up to 29% for 24 subjects, and up to 21% for 48 subjects. For the sparse PK dataset, this width was up to 49% for 12 subjects, up to 32% for 24 subjects, and up to 22% for 48 subjects. The confidence intervals for 48 subjects with sparse data were much narrower

than the confidence intervals for 12 subjects with dense data, although these two datasets comprised about the same number of plasma samples. Therefore, it was preferable in our example to collect sparse data from a larger number of subjects and model them with population PK as compared to collecting dense data from a small number of subjects.

We observed a similar trend for the confidence intervals of the PTA expectation values. As the width of these confidence intervals depends on the MIC distribution, we studied in total 32 MIC distributions in combination with two PKPD targets (yielding 64 combinations). For the dense data, the width of the 90% confidence intervals for the PTA expectation value was up to 35% for 12 subjects, up to 24% for 24 subjects, and up to 17% for 48 subjects due to uncertainty in PK parameters. For the sparse data, these widths were up to 43% for 12 subjects, up to 28% for 24 subjects, and up to 20% for 48 subjects. Therefore, uncertainty in PK parameters may affect the results of a MCS to a considerable degree, especially for small PK datasets.

If the population PK parameters and the PKPD target were known exactly, uncertainty in MIC distribution caused a width of the 90% confidence intervals for PTA expectation values of about 12% for MIC distributions with 100 samples and of about 16% for MIC distributions with 50 samples (see Table 6.2-3). We studied three examples with uncertainty both in PK and in MIC distribution. Those sources of uncertainty contributed about equally to the combined uncertainty for *E. coli* and *P. aeruginosa* (see Table 6.2-3), whereas uncertainty in PK was the predominant source of uncertainty for the MSSA example. The width of the 90% confidence intervals was 12-29% for a sparse PK dataset with 24 subjects and MIC distributions with 50 samples, if both uncertainty in PK and PD was considered. The respective width for dense PK datasets was 10-25% in our three examples. These confidence intervals had a width of 15-44% for sparse PK data on 12 subjects and a width of 11-36% for dense PK data on 12 subjects (see Table 6.2-3).

Additionally, we considered uncertainty in the population PKPD target and BSV in the individual targets (see Table 6.2-4). The median PTAs and PTA expectation values were virtually unaffected by uncertainty in the population PKPD target. However, the width of the confidence intervals

increased, if the uncertainty in the population PKPD target was larger. The presence of random BSV in the PKPD target had only a small influence on PTAs, on PTA expectation values, and on their confidence intervals. Accounting for uncertainty in the population target is computationally straightforward, because the MCS can be repeated at each target of interest (e. g. for T>MIC targets of 60%, 65% and 70%).

Uncertainty in PK parameters, MIC distribution, and PKPD target represent the major determinants for the confidence intervals of the MCS results from a computational perspective. However, there are other experimental factors of uncertainty. A systematic error in the analytical assay (either proportional or additive) may result in biased estimates for clearance and volume of distribution. Such a bias can only be accounted for, if data from several investigators are combined in a meta-analysis. There is often not enough or even no data on the PK of a specific drug in the desired patient population. Although it may be possible to predict an age related change in renal function and body composition, critically ill patients often have a substantially larger BSV relative to healthy volunteers which cannot be predicted from healthy volunteer data. More research is required on the unbound drug concentrations and their variability in target tissues, and the PKPD targets for these target tissues need to be determined. Additionally, the meaning of the MIC might be compromised e. g. due to chemical instability *in vitro* which might be relevant for beta-lactams (303, 304). If these experimental conditions are critical, results of a MCS need to be interpreted with caution.

In conclusion, we could show that the VPC is an easy to interpret and powerful method to assure the predictive performance of a population PK model prior to its use in a MCS. The VPC was superior to standard diagnostic plots and NONMEM's objective function for selecting the most appropriate population PK model in a MCS. Use of a one instead of a two compartment model or deriving the PK parameters via NCA may result in biased results of a MCS. The bias in PTA expectation values ranged from -40% to +25% for our examples. We propose to assure the predictive performance of all PK models by a VPC prior to their use in a MCS. The 90% confidence intervals for the

PTA expectation value had a width of 12-29% (10-25%) for sparse (dense) PK data on 24 subjects and MIC distributions with 50 samples, if both uncertainty in PK and in MIC distribution were considered. These confidence intervals had a width of 15-44% (11-36%) for sparse (dense) PK data on 12 subjects. Uncertainty in the population PKPD target had only a small effect on the median PTAs and PTA expectation values, but had a pronounced effect on their confidence intervals. Simulating 2,000 (10,000) subjects in a MCS resulted in an about 5-times (10-times) smaller width of the 90% confidence intervals for the PTA expectation values than caused by the uncertainty in the PK for a dense PK dataset with 48 subjects. Consequently simulating 2,000 subjects was sufficient and simulating 10,000 subjects was highly sufficient to get an adequate estimate for the PTA expectation value. Meaningful confidence intervals for the results of a MCS should account for the uncertainty in PK parameters and in MIC distribution. Uncertainty in the population PKPD target can be accounted for by repeating those simulations at various PKPD targets. A statistical comparison of PTAs or PTA expectation values between two beta-lactams needs to account for the uncertainty in PK parameters and in MIC distribution. Further studies are required to determine the PKPD targets in specific patient populations.

# 7 Strengths, weaknesses, and alternative approaches

This chapter starts with a discussion of the strengths, weaknesses, and alternative approaches for each of the main chapters in this thesis. Chapter 7.5 presents a general discussion on the results and perspectives of this thesis.

## 7.1 Pharmacokinetic comparison between cystic fibrosis patients and healthy volunteers

### 7.1.1 Alternative approaches

We applied population PKPD modeling and MCS as a state-of-the-art technique to analyze our data in CF-patients and healthy volunteers. Additionally, NCA was used as a standard technique to apply the same method which has been used for most studies in literature.

We applied parametric population PK modeling. As an alternative approach, we could have applied non-parametric population PK analysis. Both the parametric and non-parametric approach have advantages and disadvantages. The possibly most important advantage of non-parametric population PK modeling is that this approach does not make any assumptions on the distribution of the parameter variability. Overall, we do not expect that the choice of parametric or non-parametric population PK modeling affects the conclusions of our analysis in CF-patients to a significant degree.

### 7.1.2 Strengths and weaknesses

As described above, we applied state-of-the-art computational methods to study the PK and PKPD profiles of our ten antibiotics in CF-patients. We performed a meta-analysis of ten studies from an in-house database to increase the power of our comparison, as our individual studies had a small sample size (eight to twelve CF-patients). Such a meta-analysis has rarely been performed in PK. We applied population PK and estimated the

uncertainty of our PK parameters via non-parametric bootstrap techniques which are both powerful techniques. It is important to account for the uncertainty of the individual studies, as the sample size and amount of information differ between studies. Although non-parametric bootstrapping requires a large amount of computation time, it improves the validity of the conclusions and is therefore justified. Such a meta-analysis is also rare, because the individual plasma and urine concentration raw data are required for analysis, but are often not available.

We used a mixed-effects meta-analysis and estimated the between drug variability for our PK comparison of CF-patients and healthy volunteers. This is superior to using a fixed-effects meta-analysis which assumes that the difference between CF-patients and healthy volunteers is the same for each drug. One limitation of our PK studies in CF-patients is that the sample sizes of the individual studies are small. Therefore, we could not estimate the effect of severity of the disease on the PK, as this would have required a sample size of 50 or more CF-patients for each drug. Most PK studies in CF-patients in literature studied less than 20 CF-patients.

It is an important advantage that all our studies in CF-patients had a healthy volunteer control group. After combining the PK data on our CF-patients, our dataset with 90 CF-patients and 111 healthy volunteers is probably one of the largest datasets currently available for CF-patients worldwide. Importantly, these data were collected in highly standardized clinical studies with very similar clinical protocols and clinical study performance. The samples were analyzed by HPLC in a single laboratory, the Institute for Biomedical and Pharmaceutical Research (Nürnberg-Heroldsberg, Germany). Many of the studies performed in the 1970s and 1980s used bio-assays for drug analysis (389) which are usually less specific and less precise compared to HPLC. Additionally, the PK data analysis was performed with virtually identical data analysis protocols by one pharmacometrician. Overall, these are strong arguments that heterogeneity among the studies combined in our meta-analysis was of no concern. There was also no publication bias in our meta-analysis, as we used the data of all available studies.

We used both linear and allometric size models for our comparison of CF-patients and healthy volunteers and studied various body size descriptors. Some of those descriptors accounted for body composition ($FFM_C$, $FFM_J$, $PNWT_C$, and $PNWT_J$) whereas other descriptors did not (WT and BSA). Overall, we found well comparable clearances and volumes of distribution for CF-patients and healthy volunteers, whereas some of the older studies found much larger differences between those two subject groups. Our CF-patients had a comparable age as our healthy volunteers (see Table 3.5-1), whereas many of the PK studies in literature compared CF-patients to (much) older healthy volunteer control groups (389, 408, 502).

Standard allometric models are intended to explain the differences in PK parameters between adult CF-patients and adult healthy volunteers. However, if one compares growing CF-patients with an age of e. g. ten years to adult healthy volunteers, it is possible that the younger CF-patients have a higher clearance, because their body is still growing (and probably has a higher energy need), whereas the body of adult healthy volunteers is not. Importantly, our CF-patients were on average only slightly younger than our healthy volunteers (see Table 3.5-1, page 256).

Another reason why data in CF-patients from the 1960s to 1980s might not be well comparable to CF-patients in 2000 is the median survival age. CF-patients had a median survival age of 14 years in 1969 and of 31.3 years in 1996 in the US (12). Therefore, an average 15 year old CF-patient in the 1960s might not be well comparable to a 15 year old CF-patient in 2000. It is difficult to study this effect retrospectively, however, this possible effect should be kept in mind for interpretation of data from older studies in CF-patients.

There are some important limitations for interpretation of our MCS in CF-patients. The two most important limitations are: 1) The PKPD targets for beta-lactams which we used in this thesis have not been derived in CF-patients. These targets were determined in mouse infection models (84, 107). 2) MCS which are based on a small number of e. g. eight CF-patients should be interpreted conservatively, since a small number of CF-patients might not be representative for the whole population of CF-patients.

There was no alternative to using the PKPD target from the mouse infection model (84, 107), since we are not aware of any PKPD targets which have been determined for CF-patients. Even though our sample size for the individual studies in CF-patients was low, it is still probably better to use MCS and interpret the results conservatively compared to doing nothing. Other limitations of MCS are discussed in chapter 7.2 and chapter 7.4.

## 7.2 Determination and use of PKPD breakpoints for oral antibiotics

### 7.2.1 Alternative approaches

Population PK in combination with MCS is a powerful technique to analyze the PK and PKPD profiles of oral antibiotics. As described above, non-parametric population PK would be an alternative to the parametric population PK approach which was applied in our analysis. However, this choice would probably not affect the results of our antibiotics in healthy volunteers significantly. We could show that population PK was most likely superior to NCA for our meta-analysis with ciprofloxacin and levofloxacin, as the sampling schedules differed notably between the three studies combined.

### 7.2.2 Strengths and weaknesses

We derived the PKPD breakpoints based on PK data from healthy volunteers with normal renal function. Based on our data alone, it is not possible to decide, whether our breakpoints also apply to patients. The BSV in sick patients is most often larger than the BSV in healthy volunteers and especially older patients may have an impaired renal function. Volume of distribution, especially for lipophilic drugs, tends to be larger in older patients due to a different body composition. As a consequence of a possibly reduced clearance and larger volumes of distribution in patients, half-lives tend to be (slightly) longer and more variable in patients. Therefore, our PKPD breakpoints derived from healthy volunteer data are probably lower than (or

comparable to) the breakpoints for patients. These alterations in patients may increase the PKPD breakpoints maybe by a factor of roughly 2 to 4. However, even those possibly higher PKPD breakpoints in patients are still (substantially) lower than some of the susceptibility breakpoints from national organizations for cefuroxime axetil, ciprofloxacin and levofloxacin.

One strength of our analysis is that we used population PK and accounted for the saturable rate of absorption of cefuroxime axetil. This is especially important, as the $fT_{>MIC}$ determines the microbiological and clinical success of cefuroxime. Our meta-analysis by population PK for ciprofloxacin and levofloxacin accounted for multiple covariates like differences in body size and differences in the pharmaceutical content of different ciprofloxacin and levofloxacin formulations. This is a considerable advantage of our population PK analysis compared to a meta-analysis based on NCA data.

## 7.3 Impact of between occasion variability on drug development and individualized therapy

### 7.3.1 Alternative approaches

Karlsson et al. (244, 245) showed that population PK (nonlinear mixed-effects modeling) is the most powerful technique to study the BOV of clearance, volume of distribution, extent of absorption, and other PK parameters. This method can simultaneously account for the presence of multiple covariates (like body size, renal function, etc.) in the subject population. If (multiple) covariates influence the PK parameters, population PK is especially superior to NCA and to the STS approach.

We used ANOVA statistics to separate BSV and BOV for piperacillin based on the individual PK parameter estimates, because it was not possible to separate these two random effects by population PK due to the low sample size of our piperacillin study.

### 7.3.2 Strengths and weaknesses

The sample size in our piperacillin study of four healthy volunteers was low. The variability of PK parameters in the whole population of healthy volunteers can not reliably be estimated based on data from four subjects. Therefore, our PKPD breakpoints for this piperacillin study need to be interpreted cautiously. Jonnson et al. (238) showed that population PK is the most powerful method to detect nonlinear PK. Although we had only data on four subjects for piperacillin, we could identify the parallel first-order and mixed-order renal elimination based on plasma and urine data at a single dose level. We obtained reasonable estimates for the glomerular filtration rate and tubular secretion of piperacillin. It was encouraging that our estimates were very similar to the population PK results of a larger crossover study with two dose levels of piperacillin (results not shown in this thesis).

Our study on oral amoxicillin / clavulanic acid was well suitable to draw conclusions for generic drug development, since this study was performed under the highly standardized procedures commonly applied for bioequivalence studies. Drug analysis was performed by LC-MS/MS which is especially important for clavulanic acid. We could show that population PK was superior to NCA for analysis of these data. Limitations apply to our conclusions on the breakpoint of oral amoxicillin, as this breakpoint was determined for healthy volunteers who might have a (slightly) different breakpoint compared to patients (see chapter 7.2.2).

## 7.4 How much can we “trust” Monte Carlo simulations?

MCS is a technique that has become increasingly popular in anti-infective chemotherapy since its first application in this field in 1998. However, the assumptions and uncertainty of the MCS methods are not always considered. This may lead to biased and less reliable conclusions.

We applied a state-of-the-art technique to assess the uncertainty of MCS via population PK and non-parametric bootstrap techniques. To the best of my knowledge, this combination of methods has been applied for the first

time for MCS of antibiotics. This method is especially appealing, as the uncertainty in PK parameters is directly estimated and non-parametric bootstrapping does not make any assumptions on the uncertainty distribution.

There are several important issues to be considered for interpretation of MCS results. We compared several methods for selecting the most appropriate population PK model and assessed the uncertainty in MCS results from a data analytical perspective. However, a MCS relies on several assumptions which need to be discussed carefully for interpretation of MCS.

*Possibly critical assumptions of a MCS:*

1. Has the population PK model been derived in the desired patient population?
2. Are the studied subjects representative for the desired patient population?
3. Is the sample size large enough to estimate the population PK model reliably?
4. Has the clinical part of the study been performed reliably to prevent a systematic bias in the plasma concentration time raw data?
5. Does the analytical assay yield unbiased plasma concentrations?
6. Has the PKPD target been derived for the specific infection in the patient population of interest?
7. Is the method for determination of MICs reliable?
8. Is the assumed PKPD relationship adequate for the concentrations of the antibiotic and pathogen at the site of action?
9. Is the drug related response the most important determinant of successful therapy?

In many situations, those assumptions cannot easily be assured based on the available data from the PK study. Violating one or more of the above mentioned assumptions may shift PKPD breakpoints towards higher or lower values. However, a large amount of *in vitro* data and experiments in animals (84, 107) show that there is a predictive relationship between the concentration time course and the microbiological success. Given the possibly critical assumptions above, the results of a MCS should be interpreted

conservatively. Violating the assumptions may cause a misprediction of a MCS. However, such a misprediction should always be used to further improve and refine the MCS technique and to reconsider the assumptions, as mispredictions (outliers) might even be more informative than accurate predictions from a methodological point of view.

## 7.5 General discussion of the results and perspectives of this thesis

### 7.5.1 Discussion of the work presented in this thesis

The results presented in this thesis were based on a large and homogeneous in-house database of the Institute for Biomedical and Pharmaceutical Research (IBMP). The clinical studies were performed with a high degree of standardization and the clinical study protocols were well comparable. The sample analyses were performed in a single bio-analytical laboratory which is an extremely valuable advantage for the validity of the conclusions in this thesis.

Based on those datasets of ten studies in CF-patients and healthy volunteers and six additional studies in healthy volunteers, we performed PKPD data analyses and simulations which all followed very similar PK analysis protocols and which were done by one pharmacometrician. We used parametric population PK analysis in NONMEM® as primary analysis method for all studies. NONMEM® is a stable, fast, and efficient population PK program which can be automated by some additional programming. Alternatively, we could have used non-parametric population PK which offers both advantages and disadvantages to parametric population PK analysis in NONMEM® (see chapter 2.8).

We analyzed some of the datasets in parallel with non-parametric population PK and observed similar results for our parametric population PK analysis (data not shown). Non-parametric population PK is probably considerably better than parametric population PK, if the distribution of PK

parameters in the parameter variability model does not follow e. g. a normal distribution on log-scale. This would be the case for multi-modal distributions. However, volume of distribution and glomerular filtration are unlikely to follow a multi-modal distribution after accounting for body size and body composition. The renal route of elimination is the primary route for almost all of our studied antibiotics. Polymorphisms of the drug transporters might occur for the active tubular secretion of our beta-lactams and quinolones. However, such a polymorphism of renal clearance has not yet been described for beta-lactams or quinolones *in vivo*. As most of our studies had a sample size of 30 subjects or less, it is unlikely that we could have observed such a polymorphism for renal clearance. Therefore, parametric and non-parametric population PK would probably yield comparable results for our studies. Additionally, there are considerable theoretical arguments that the choice of parametric or non-parametric population PK did not affect our conclusions to a significant degree.

Our data analyses served both explorative and confirmative purposes. Most of our analyses were explorative analyses. These comprised the PK comparison between CF-patients and healthy volunteers, derivation of PKPD breakpoints, optimization of dosage regimens, studying the elimination pathways of piperacillin, studying the importance of BOV, and comparing bioequivalence with similarity in PTA vs. MIC profiles for amoxicillin. Population PK is a powerful technique for those analyses, as various sources of variability and the effect of covariates can be accounted for simultaneously. We could also show in a confirmative analysis that allometric size models based on FFM or PNWT were more appropriate for dose selection of CF-patients compared to linear size models based on WT. This confirmative analysis would not have been possible without the large database of PK data in CF-patients and healthy volunteers from the IBMP.

Additionally, we developed a new method to determine the uncertainty of MCS for beta-lactams. This method allows one to compare the probability of successful treatment between two (or more) beta-lactams statistically which has not been possible previously. Our method combines non-parametric bootstrapping and MCS of beta-lactams. Non-parametric bootstrapping has

been used in fields other than anti-infective PKPD, but has not yet been applied to MCS of beta-lactams. Our simulation study provided a rough estimate of the expected uncertainty and their sources for the results of a MCS with beta-lactams. Besides assessing the uncertainty of MCS with beta-lactams, this simulation study compared various methods of MCS. Importantly, our results suggested that more than half of the published MCS with beta-lactams are possibly flawed due to the use of PK parameters from NCA. This study underlines the need for a standardized methodology of how to apply MCS with beta-lactams. Irrespective of the applied method, we found that VPCs should always be performed to qualify a population PK model for MCS. Severely biased MCS results can occur which might otherwise not be discovered.

A set of programs was developed within this thesis which can perform VPCs for all population PK models of interest efficiently. We applied VPCs for all models in this thesis and used it as our primary method to qualify models for use in MCS. Based on our final population PK models, we explored various optimized dosage regimens for eight beta-lactams. All these MCS were based on a full population PK model qualified via VPCs. Although this method has been published and applied since 1998, only very few authors used full population PK models for MCS of beta-lactams. We are not aware of any published MCS study which compared optimized antibiotic dosage regimens as systematically as in this thesis. Besides continuous and prolonged infusion, we assessed the advantages of a loading dose plus prolonged infusion regimen which has not yet been studied previously (see chapter 3.6.3.3). Many of our PKPD breakpoints were (substantially) lower than the breakpoints used by national organizations like the DIN, BSAC, and CLSI. These lower PKPD breakpoints suggest reconsidering the use of these antibiotics. The programs for automated MCS of antibiotics developed within this thesis were an essential tool to generate those MCS at the required rate.

We are not aware of any MCS in beta-lactams which incorporated allometric theory. Allometric size models were shown to be superior to linear size models in our meta-analysis of the CF-studies. Based on standard allometric equations, we developed and validated two equations to select

beta-lactam doses in patients of various body size. These equations should predict the beta-lactam doses which are required to achieve similar PTA vs. MIC profiles in patients of various body size (excluding small children for whom additional correction terms are required).

The first equation is the exact theoretical solution for a continuous infusion. We could show that this equation is also a good approximation for optimized prolonged infusion, as it achieved very similar PTA vs. MIC profiles in patients of various body size for our five beta-lactams. The second equation was a new equation developed by the author of this thesis and provides an approximate solution for short-term infusion of beta-lactams. This formula worked well for our five intravenous beta-lactams. However, this formula shows that very high beta-lactam doses are required in patients with a WT of 15 or 30kg compared to patients with a WT of 70kg for short-term infusion. This was a very important observation for optimal dose selection in children and adults of small body size (excluding children in the first years of life).

Overall, our MCS results strongly suggest evaluation of optimized dosage regimens for beta-lactams clinically. The possible advantages (higher probability of successful treatment, possibly less emergence of resistance, and possibly lower costs) of these optimized dosage regimens have to be counterbalanced with the disadvantages of a higher workload and less convenience for the patient. The severity and mortality associated with the disease and the availability of only a few new antibiotics will need to be considered. Those decisions should balance the arguments from an interdisciplinary group of physicians, nurses, microbiologists, pharmacologists, pharmacometricians, and others.

### 7.5.2 Future perspectives

The present methodology for predicting the probability of successful antibiotic treatment accounts for the BSV of PK parameters. The vast majority of MCS used PKPD statistics like the *f*AUC/MIC, *f*Cmax/MIC, or *f*T>MIC to predict the probability of successful treatment. More clinical studies are

required to assess the critical target of those PKPD statistics for special patient groups like for CF-patients.

Importantly, these PKPD statistics do not account for the full time course of drug concentration during the whole duration of therapy. More models on the time course of drug related response over the whole duration of therapy are required. These models should address the probability of selection of resistant mutants for an individual patient. Optimal trial design techniques should be applied more frequently to prove that the optimized dosage regimens proposed in this thesis and by others result in superior probabilities of cure and maybe less emergence of resistance compared to standard short-term infusions. Those MCS and clinical studies should propose dosing guidelines which have been proven to optimize effectiveness and minimize emergence of resistance. These dosage regimens should give specific guidance for the optimal duration of antibiotics therapy for each patient group, as duration of therapy is possibly an important factor for emergence of resistance.

These efforts are driven by the fact that only a few new antibiotics have been developed during the last decade. Therefore, the effectiveness of the antibiotics which have been proven to be safe and effective should be preserved as long as possible. By the same token, regulatory authorities worldwide should continue their efforts to support derivation of optimal dosage regimens for new anti-infectives. These techniques should consider MCS as presented in this thesis. Rational dose selection in patients with specific covariates should consider covariate specific MCS (e. g. for pediatrics, lean, or overweight patients or patients with specific renal function) as performed in this thesis. Additionally, PKPD targets should be derived for special patient groups during phase II and phase III clinical trials in drug development. Population PKPD and clinical trial design should be used more frequently to gain more information during drug development.

As the next step, it would be very appealing to combine population PKPD models, which predict the probability of successful treatment and selection of resistant mutants, with epidemiological models. This combination

of models might predict the spread of resistant bacteria over a hospital ward, the whole hospital, a whole country, or even worldwide.

As a more short-term goal, visualization of modeling results via MCS should be used to stimulate discussions among colleagues. These techniques can predict trial results extremely fast compared to running the clinical trial. An online interface should be built in the future which performs a standard population PK analysis and MCS and which does not require the user to be an expert in population PKPD. This thesis presented the first steps of such an analysis by developing an automated MCS system for antibiotics.

After convincing physicians and other people involved that there are considerable advantages of applying population PKPD and MCS techniques for rational dose selection, the results of MCS can be implemented in hand-held computer devices which can propose optimal dosage regimens for a physician on-the-fly. A meta-analysis working group for population PKPD models of antibiotics should propose the best available population PK model for each drug and each patient group. Then, only the hospital specific susceptibility data have to be incorporated in such a hand-held device. Such software packages still have to be developed and a meta-analysis PKPD working group would probably require scientists to share their concentration time raw data. However, the merits of saving the effectiveness of currently available antibiotics warrants these efforts. Ideally, such meta-analyses and the original raw data should be published by the originator of a new antibiotic. After marketing, regulatory authorities or international organizations should take care of the population PKPD models which are intended to be incorporated in hand-held devices. If new data on the PKPD principles of antibiotic treatment become available, these data should be critically evaluated by the regulatory authorities or international organizations and incorporated in the population PKPD models to achieve the maximal benefit for the patients.

# 8 Summary

***Background:*** Population pharmacokinetic-pharmacodynamic (PKPD) modeling and simulations were applied to identify optimal dosage regimens for antibiotics. As the emergence of bacterial resistance is increasing and as only a few new antibiotics became available during the last decade, optimal use of established agents and preserving their effectiveness seems vital.

***Objectives:*** 1) To find the descriptor of body size and body composition which allows to achieve target concentrations and target effects in patients with cystic fibrosis (CF) most precisely. 2) To identify the mode of administration with the highest probability of successful treatment for intravenous beta-lactams. 3) To develop formulas for optimal dose selection which achieve similar probabilities of successful treatment in patients of various body size for beta-lactams. 4) To determine the highest minimal inhibitory concentration (MIC) with a robust (≥90%) probability of successful treatment (this MIC is called PKPD breakpoint). 5) To assess the effect of variability in PK parameters between study periods (between occasion variability: BOV) on the applicability of target concentration intervention and on generic drug development. 6) To compare various criteria to select a population PK model for Monte Carlo simulations (MCS). 7) To assess the bias and uncertainty of MCS of beta-lactams in order to statistically compare the probability of successful treatment between various beta-lactams.

***General methods:*** Drug analysis in plasma and urine was performed by HPLC or LC-MS/MS in a single laboratory, at the IBMP. Drug analysis was not done by the author of this thesis. We used non-compartmental analysis and parametric population PK analysis for all studies. We used non-parametric bootstrapping to assess the uncertainty of PK parameters for our meta-analysis of the PK in CF-patients and healthy volunteers. Plasma concentration time profiles for several thousand virtual subjects were simulated by MCS which account for average PK parameters, their between subject variability (BSV), and patient specific demographic data. Convincing literature data show that the duration of non-protein bound concentration above MIC ($fT_{>MIC}$) best predicts the microbiological and clinical success of

beta-lactams and the area under the non-protein bound concentration curve divided by the MIC (*f*AUC/MIC) best predicts success for quinolones. We used PKPD targets from literature that were based on the $fT_{>MIC}$ or *f*AUC/MIC, respectively. Achieving a PKPD target was used as a surrogate measure for successful treatment. In our MCS, we calculated the $fT_{>MIC}$ or *f*AUC/MIC for all simulated concentration profiles and compared it to the value of the PKPD target. The fraction of subjects who achieved the target at the respective MIC approximates the probability of target attainment (PTA). The PTA can be interpreted as probability of successful treatment under certain assumptions.

**Studies in CF-patients**

***Methods:*** We had data from ten studies (seven beta-lactams and three quinolones) in CF-patients which all included a healthy volunteer control group. Clinical procedures were very similar for all ten studies. Both subject groups had study conditions as similar as possible. We had data on 90 CF-patients (average ± SD, age: 21±3.6 yrs) and on 111 healthy volunteers (age: 25±3.5 yrs). We compared the average clearance and volume of distribution between CF-patients and healthy volunteers for various body size descriptors including total body weight (WT), fat-free mass (FFM), and predicted normal weight (PNWT). We considered linear and allometric scaling of PK parameters by body size and used a meta-analysis based on population PK parameters for the comparison of CF-patients and healthy volunteers. Target concentrations can be achieved more precisely, if a size descriptor reduces the random, unexplained BSV. Therefore, we studied the reduction of unexplained BSV for each size descriptor relative to linear scaling by WT, since doses for CF-patients are commonly selected as mg/kg WT.

***Results:*** Without accounting for body size, average total clearance was 15% lower (p=0.005) and volume of distribution at steady-state was 17% lower (p=0.001) in CF-patients compared to healthy volunteers. For linear scaling by WT, average total clearance in CF-patients divided by total clearance in healthy volunteers was 1.15 (p=0.013). This ratio was 1.06 (p=0.191) for volume of distribution. A ratio of 1.0 indicates that CF-patients and healthy volunteers of the same body size have identical average

clearances or volumes of distribution. For allometric scaling by FFM or PNWT, the ratio of total clearance and volume of distribution between CF-patients and healthy volunteers was within 0.80 and 1.25 for almost all drugs and the average ratio was close to 1. Allometric scaling by FFM or PNWT reduced the unexplained BSV in renal clearance by 24 to 27% (median of 10 drugs) relative to linear scaling by WT. The unexplained BSV was reduced for seven or eight of the ten drugs by more than 15% and the remaining two or three drugs had essentially unchanged (±15%) unexplained BSVs in renal clearance.

***Conclusions:*** The PK in CF-patients was comparable to the PK in healthy volunteers after accounting for body size and body composition by allometric scaling with FFM or PNWT. Target concentrations and target effects in CF-patients can be achieved most precisely by dose selection based on an allometric size model with FFM or PNWT. Future studies are warranted to study the clinical superiority of allometric dosing by FFM or PNWT compared to dose selection as mg/kg WT in CF-patients.

**Optimized dosage regimens for beta-lactams**

***Methods:*** We studied the optimal duration of infusion to reach the highest PTA and compared PKPD breakpoints between optimized prolonged infusion, continuous infusion, and standard short-term infusion at the same daily dose via MCS for the five intravenous beta-lactams studied in our CF-trials. We used our final population PK models that were based on allometric size models with FFM to derive PKPD breakpoints for CF-patients of various FFM. We developed formulas for optimal dose selection in patients of various body size. These formulas were based on standard allometric theory and were evaluated for our five intravenous beta-lactams from the CF-studies.

***Results:*** The optimal duration of infusion was slightly longer than the PKPD target multiplied by the dosing interval. For an 8h dosing interval and the PKPD target $fT_{>MIC}$ at least 50% of the dosing interval, a 5h infusion q8h yielded similar PTAs compared to continuous infusion at the same daily dose. When doses were selected as mg/kg FFM (linear model), continuous and optimized prolonged infusion increased the PKPD breakpoints in CF-patients

by a factor of 8.0 [5.3-64] (median [range]) compared to short-term infusions for our five intravenous beta-lactams.

For continuous infusions and dose selection as mg/kg FFM, our MCS identified about 1.5 times lower PKPD breakpoints in CF-patients with a FFM of 11.4kg compared to CF-patients with a FFM of 53kg. Rearrangement of the standard allometric scaling equation clearance ~ (body size)$^{0.75}$ yields the following equation which should achieve a constant average area under the concentration time curve (AUC) for patients of various FFM:

$$\text{Dose}(\text{FFM}_i) = \text{Dose}_{STD} \cdot \left( \frac{\text{FFM}_i}{\text{FFM}_{STD}} \right)^{0.75} \quad \text{(formula is known in literature)}$$

Body size is described as fat-free mass (FFM), $\text{Dose}_{STD}$ is the standard dose for a patient of standard FFM ($\text{FFM}_{STD}$). $\text{FFM}_i$ is FFM of the $i^{th}$ patient. This formula is the exact theoretical solution to achieve similar $f\text{T}_{>MIC}$ values in patients of various FFM for continuous infusion. We were the first who showed that dose selection by this formula achieved similar $f\text{T}_{>MIC}$ values and PTAs in patients of various FFM for optimized prolonged infusion of beta-lactams. For 0.5h infusions and dose selection as mg/kg FFM, our MCS identified about 5.3 [4-8] times (median [range]) lower PKPD breakpoints in CF-patients with a FFM of 11.4kg compared to CF-patients with a FFM of 53kg. We developed a new formula to achieve similar $f\text{T}_{>MIC}$ values and PTAs in patients of various FFM for short-term infusion of beta-lactams:

$$\text{Dose}(\text{FFM}_i) = \text{Dose}_{STD} \frac{\text{FFM}_i}{\text{FFM}_{STD}} \exp\left\{ \frac{\%\text{target} \cdot \text{Tau} \cdot \ln(2)}{\text{half-life}_{STD}} \cdot \left[ \left( \frac{\text{FFM}_{STD}}{\text{FFM}_i} \right)^{0.25} - 1 \right] \right\}$$

Tau is the dosing interval, %target is the PKPD target, and $\text{half-life}_{STD}$ is the typical half-life of a patient with $\text{FFM}_{STD}$ (other parameters same as above). Dose selection by this formula achieved similar PTAs for our five intravenous beta-lactams. However, the required doses in small patients were very high.

***Conclusions:*** The optimal duration for prolonged infusion of beta-lactams was slightly longer than the PKPD target multiplied by the dosing interval. We developed and successfully validated a new equation for allometric dose selection of beta-lactams for short-term infusion and we

evaluated a formula for allometric dose selection for prolonged infusion. As both we and others found considerable evidence that allometric size models are superior to linear size models, beta-lactam doses for continuous and optimized prolonged infusion should be selected by the “constant AUC” formula shown above. Very high doses were required for short-term infusion of beta-lactams to achieve similar PTAs in small patients. Therefore, optimized prolonged infusion of beta-lactams with “constant AUC” dose selection appears as the optimal choice from a PKPD point of view and its superiority to short-term infusion and mg/kg dose selection should be evaluated clinically. The increased workload and inconvenience of prolonged infusion should be counterbalanced with higher probabilities of cure, severity of disease, and a possibly lower chance for selection of resistant mutants.

**PKPD breakpoints**

***Methods:*** We used the population PK models from our studies in CF-patients to derive PKPD breakpoints. We estimated a population PK model from a study in 24 healthy volunteers who were dosed with 250mg oral cefuroxime. Additionally, we estimated population PK models for data from three studies with 38 (in total) healthy volunteers who received 500 or 1000mg oral ciprofloxacin and 500mg levofloxacin. We assessed PKPD breakpoints of standard and optimized dosage regimens of all antibiotics via MCS.

***Results:*** Optimized dosage regimens of cefpirome, cefotiam, and carumonam achieved PKPD breakpoints that supported their use in CF-patients against *S. aureus* and *H. influenzae* depending on the local susceptibility pattern. PKPD breakpoints of oral cefaclor and oral cefadroxil in CF-patients were lower and the MIC of the infecting pathogen should be measured before start of therapy by these agents. Monotherapy with oral ciprofloxacin against *P. aeruginosa* in CF-patients achieved insufficiently low PKPD breakpoints. Continuous infusion of piperacillin or ceftazidime achieved promising PKPD breakpoints in CF-patients which might be sufficient to treat infections caused by *P. aeruginosa* depending on its local susceptibility. Our PKPD breakpoint for oral cefuroxime was substantially lower than the MIC breakpoints for susceptibility specified by national organizations. We also found considerably lower PKPD breakpoints for oral ciprofloxacin and oral

levofloxacin compared to the breakpoints from national organizations. Levofloxacin and ciprofloxacin achieved insufficient PTAs against *P. aeruginosa*, whereas levofloxacin achieved higher PTAs against *S. pneumoniae* and *S. aureus* compared to ciprofloxacin at standard doses.

***Conclusions:*** Our MCS predicted promising probabilities of successful treatment for optimized dosage regimens of our intravenous beta-lactams in CF-patients. Ciprofloxacin monotherapy should not be used for empiric treatment of *P. aeruginosa* in CF-patients. Our PKPD breakpoints for oral cefuroxime, ciprofloxacin, and levofloxacin suggest critical reconsideration of susceptibility breakpoints specified by national organizations.

**Studies on the between occasion variability (BOV)**

***Methods:*** We studied the PK in four healthy volunteers who received the same formulation of 4g piperacillin as single dose in five subsequent study periods. In another study, 24 healthy volunteers received 500/125mg oral amoxicillin / clavulanic acid on two subsequent study periods. We estimated the population PK and BOV of piperacillin, amoxicillin, and clavulanic acid. Additionally, we simulated 2x2 crossover bioequivalence studies with 24 subjects to assess the chance of showing bioequivalence and the PKPD breakpoints for amoxicillin test formulations with various rates and extents of absorption compared to the reference formulation.

***Results:*** Piperacillin had a low BOV in total clearance of 8.5% (coefficient of variation). Clavulanic acid had a high BOV of 25% for extent of absorption. Simulations with a range of BOVs showed that a BOV in extent of absorption or clearance above about 15% decreased the chance of showing bioequivalence notably. Amoxicillin test formulations with a 25% chance to be bioequivalent could have a 2-fold lower or 1.5-fold higher PKPD breakpoint relative to the reference formulation.

***Conclusions:*** The low BOV for piperacillin would support its use for target concentration intervention and therapeutic drug monitoring. The high BOV in peak concentrations and AUCs often observed in bioequivalence studies with clavulanic acid was most likely caused by its instability to gastric acid. Bioequivalence did not guarantee similar PKPD breakpoints for

amoxicillin test and reference formulations. Similarity in PKPD breakpoints should be considered in parallel to bioequivalence for beta-lactams.

**Bias and uncertainty for Monte Carlo simulations of beta-lactams**

***Methods:*** We compared various model selection criteria of models to be used for MCS based on two real data examples. We studied the bias of MCS results, if PK parameters and their variability are derived via non-compartmental analysis. This method has been applied by more than half of the MCS published on beta-lactams. The uncertainty in MCS results was determined by non-parametric bootstrap techniques and subsequent MCS.

***Results:*** Visual predictive checks were easy to interpret and more powerful than other criteria of model selection for a MCS. Use of PK parameters from non-compartmental analysis may result in considerable bias in the MCS results. Uncertainty in population PK parameters (very important), uncertainty in MIC distribution (important, especially for MIC distributions with less than about 300 isolates), and uncertainty in PKPD target were the major sources of uncertainty in results of a MCS from a data analytical perspective.

***Conclusions:*** Visual predictive checks should always be performed to qualify a population PK model for MCS. MCS should be based on estimated population PK models, as the use of PK parameters from non-compartmental analysis can considerably bias the results of a MCS for beta-lactams. We performed the first analysis of the uncertainty of MCS with beta-lactams. Uncertainty in PK parameters and in the MIC distribution were identified as most important sources of uncertainty for a MCS with beta-lactams (besides uncertainty in the PKPD target). Uncertainty in PK parameters and in MIC distribution must be considered for a statistical comparison of the MCS results between various beta-lactams.

Overall, various aspects of population PKPD modeling and applications of MCS were shown in this thesis. An interactive interplay of modeling, simulations, and visualization of results may be very valuable to select doses in individual patients, for drug development, and to stimulate discussions among colleagues. These methods have been shown to be fast and cost-efficient and will hopefully become more widely used in the future.

# 9 Zusammenfassung

***Hintergrund:*** In dieser Arbeit wurden populations-pharmakokinetische (PK) und -pharmakodynamische (PD) Modelle und Simulationen verwendet, um optimale Dosierungsregime von Antibiotika abzuleiten. Da die Resistenzentwicklung von Bakterien immer mehr voranschreitet und in den letzten zehn Jahren nur wenige neue Antibiotika auf den Markt kamen, erscheint eine optimale Therapie mit bewährten Antibiotika sowie die Erhaltung der Wirksamkeit dieser Substanzen sehr wichtig.

***Zielsetzungen:*** 1) Den Deskriptor für Körpergröße und Körperzusammensetzung zu finden, mit dem Ziel-Konzentrationen und Ziel-Effekte in Mukoviszidose-Patienten (engl.: „cystic fibrosis“, CF-Patienten) am genauesten erzielt werden können. 2) Suche nach Dosierungsregimen mit der höchsten Wahrscheinlichkeit für erfolgreiche Therapie mit intravenösen Beta-Laktamen. 3) Entwicklung und Validierung von Formeln, mit denen die Beta-Laktam-Dosen für Patienten unterschiedlicher Körpergröße berechnet werden können, so dass Patienten verschiedener Körpergröße ähnliche Erfolgswahrscheinlichkeiten erzielen. 4) Bestimmung der höchsten minimalen Hemmkonzentration (MHK) mit einer Erfolgswahrscheinlichkeit von mindestens 90% für alle untersuchten Antibiotika. (Diese MHK wird als PKPD Grenzwert bezeichnet). 5) Untersuchung des Einflusses von Variabilität der PK Parameter zwischen den Studienperioden (engl.: „between occasion variability“, BOV) auf die Anwendbarkeit von individualisierter Therapie und auf die generische Arzneimittelentwicklung. 6) Vergleich verschiedener Auswahlkriterien für Populations-PK-Modelle, die in Monte-Carlo-Simulationen (MCS) verwendet werden sollen. 7) Bestimmung von systematischen Abweichungen und der Unsicherheit von MCS für Beta-Laktame. Nur wenn die Unsicherheit in MCS berücksichtigt wird, können die Erfolgswahrscheinlichkeiten mehrerer Antibiotika statistisch verglichen werden.

***Allgemeine Methoden:*** Die Analytik in Plasma und Urin wurde mittels HPLC oder LC-MS/MS in einem einzigen Labor durchgeführt, im Labor des IBMP. An der Analytik war der Autor dieser Arbeit nicht beteiligt. Wir verwendeten nicht-kompartimentelle Analyse und parametrische Populations-

PK-Analyse in allen Studien. Wir verwendeten nicht-parametrische Bootstrap-Techniken um die Unsicherheit in den PK-Parametern für unsere Meta-Analyse der PK in CF-Patienten und gesunden Probanden zu bestimmen. Die Plasma-Konzentrations-Zeit-Profile für mehrere tausend Probanden wurden mittels MCS simuliert. MCS berücksichtigt die mittleren PK-Parameter, deren Variabilität zwischen Probanden (engl.: „between subject variability“, BSV), und die patientenspezifischen demographischen Daten. Überzeugende Ergebnisse aus der Literatur zeigen, dass die Dauer der nicht-proteingebundenen Konzentration oberhalb der MHK ($fT_{>MHK}$) am besten den mikrobiologischen und klinischen Erfolg von Beta-Laktamen vorhersagt und dass die Fläche unter der nicht-proteingebundenen Konzentration dividiert durch die MHK (*f*AUC/MHK) am besten den Erfolg für Chinolone anzeigt. Wir verwendeten PKPD Zielwerte aus der Literatur die auf der $fT_{>MHK}$ oder der *f*AUC/MHK basieren. Das Erreichen eines PKPD Zielwertes wurde als Surrogat für erfolgreiche Behandlung angesehen. In unseren MCS berechneten wir die $fT_{>MHK}$- oder *f*AUC/MHK-Werte für jedes simulierte Konzentrations-Zeit-Profil und verglichen diesen Wert mit dem PKPD Zielwert. Der Anteil an Probanden, welcher den Zielwert bei der jeweiligen MHK erreicht, ist näherungsweise die Erfolgswahrscheinlichkeit für den Zielwert (engl.: „probability of target attainment“, PTA). Die PTA kann unter bestimmten Annahmen als Wahrscheinlichkeit für erfolgreiche Therapie interpretiert werden.

**Studien in CF-Patienten**

***Methoden:*** Wir verwendeten Daten von zehn Studien (sieben Beta-Laktame und drei Chinolone) in CF-Patienten, die alle über eine Kontrollgruppe mit gesunden Probanden verfügten. Die klinische Durchführung dieser Studien war sehr gut vergleichbar. CF-Patienten und gesunde Probanden hatten so ähnliche Studienbedingungen wie möglich. Unser Datensatz beinhaltete 90 CF-Patienten (Mittelwert ± SD, Alter: 21±3.6 Jahre) und 111 gesunde Probanden (Alter: 25±3.5 Jahre). Wir verglichen die mittlere Clearance und das mittlere Verteilungsvolumen zwischen CF-Patienten und gesunden Probanden nach Normierung auf

verschiedene Deskriptoren für Körpergröße. Diese beinhalteten Gesamtkörpergewicht (WT), fettfreie Körpermasse (FFM) und das vorhergesagte Normalgewicht (engl.: „predicted normal weight“, PNWT). Wir verwendeten lineare und allometrische Skalierung der PK Parameter mit der Körpergröße und verglichen die Populations-PK-Parameter zwischen CF-Patienten und gesunden Probanden in einer Meta-Analyse. Zielkonzentrationen können präziser erreicht werden, wenn ein Deskriptor für die Körpergröße die zufällige, unerklärte BSV verringert. Daher untersuchten wir die Verringerung der unerklärten BSV für einige Körpergrößen-Deskriptoren. Lineares Skalieren mit WT nahmen wir als Vergleichswert für die BSV, da die Dosen für CF-Patienten meist als mg/kg WT berechnet werden.

***Ergebnisse:*** Ohne Beachtung der Körpergröße war die mittlere Gesamtkörperclearance um 15% niedriger (p=0.005) in CF-Patienten und das Verteilungsvolumen im Steady-State um 17% niedriger (p=0.001) in CF-Patienten verglichen mit gesunden Probanden. Bei linearer Skalierung mit WT, war die mittlere Gesamtkörperclearance in CF-Patienten dividiert durch die Gesamtkörperclearance in Gesunden 1.15 (p=0.013). Dieser Quotient betrug 1.06 (p=0.191) für das Verteilungsvolumen. Bei einem Quotienten von 1.0 hätten CF-Patienten und gesunde Probanden der gleichen Körpergröße identische mittlere Clearances bzw. Verteilungsvolumina. Für allometrisches Skalieren mit FFM oder PNWT lagen fast alle Quotienten für Gesamtkörperclearance und Verteilungsvolumen zwischen CF-Patienten und Gesunden zwischen 0.80 und 1.25 und die mittleren Quotienten waren nahe 1.0. Allometrisches Skalieren mit FFM oder PNWT reduzierte die unerklärte BSV in der renalen Clearance um 24 bis 27% (Median der 10 Substanzen) verglichen mit linearem Skalieren mit WT. Sieben oder acht der zehn Substanzen hatten eine Verringerung der unerklärten BSV in der renalen Clearance um mehr als 15% und die übrigen zwei bzw. drei Substanzen erreichten eine ähnliche (±15%) unerklärte BSV für renale Clearance.

***Schlussfolgerungen:*** Die PK in CF-Patienten war vergleichbar mit der PK in Gesunden, wenn man Körpergröße und Körperzusammensetzung durch allometrisches Skalieren mit FFM oder PNWT berücksichtigte. Zielkonzentrationen und Zieleffekte in CF-Patienten konnten durch

allometrisches Skalieren mit FFM oder PNWT am genausten erreicht werden. Zukünftige Studien in CF-Patienten zur klinischen Überlegenheit von allometrischer Dosiswahl mit FFM oder PNWT verglichen mit Dosiswahl als mg/kg WT sollten durchgeführt werden.

**Optimierte Dosierungsregime für Beta-Laktame**

***Methoden:*** Wir untersuchten die optimale Dauer einer Infusion, um die höchste PTA zu erzielen. Wir verglichen die PKPD Grenzwerte zwischen optimierter verlängerter Infusion, kontinuierlicher Infusion und Standard-Kurzzeitinfusion alle bei der gleichen Tagesdosis mittels MCS für die fünf intravenös gegebenen Beta-Laktame aus unseren CF-Studien. Wir verwendeten die Populations-PK-Modelle aus diesen Studien um die PKPD Grenzwerte für CF-Patienten unterschiedlicher Körpergröße vorherzusagen. Diese Populations-PK-Modelle basierten auf allometrischer Skalierung mit FFM. Wir entwickelten Formeln für die optimale Dosiswahl in Patienten mit unterschiedlicher FFM. Diese Formeln basierten auf allometrischer Theorie und wir testeten sie für die fünf intravenös gegebenen Beta-Laktame aus den CF-Studien.

***Ergebnisse:*** Die optimale Dauer der Infusion war etwas länger als der PKPD Zielwert multipliziert mit dem Dosierungsintervall. Für ein 8h-Intervall und den PKPD Zielwert $fT_{>MHK}$ mindestens 50% des Dosierungsintervalls, erreichte eine 5h Infusion q8h ähnliche PTAs wie kontinuierliche Infusion bei gleicher Tagesdosis. Wenn die Dosis als mg/kg FFM gewählt wurde (lineares Modell), so erhöhte eine kontinuierliche Infusion und optimierte verlängerte Infusion den PKPD-Grenzwerte in CF-Patienten auf das 8.0 [5.3-64] Fache (Median [Bereich]) verglichen mit Kurzzeitinfusion für unsere fünf intravenös gegebenen Beta-Laktame.

Für kontinuierliche Infusion und Dosiswahl als mg/kg FFM zeigte unsere MCS etwa 1.5-fach tiefere PKPD-Grenzwerte in CF-Patienten mit einem FFM von 11.4kg verglichen mit CF-Patienten mit einem FFM von 53kg. Aus der allometrischen Gleichung Clearance ~ Körpergröße$^{0.75}$ kann man die folgende Formel ableiten. Diese Formel soll die Dosis vorhersagen, welche die gleiche mittlere Fläche unter der Konzentrations-Zeit-Kurve (AUC) in Patienten mit unterschiedlicher FFM erzielt:

$$\text{Dosis}(\text{FFM}_i) = \text{Dosis}_{STD} \cdot \left( \frac{\text{FFM}_i}{\text{FFM}_{STD}} \right)^{0.75}$$ (Formel ist bekannt in der Literatur)

Körpergröße wird durch die fettfreie Körpermasse (FFM) beschrieben, $\text{Dosis}_{STD}$ ist die Standard-Dosis für Patienten mit Standard-FFM ($\text{FFM}_{STD}$). $\text{FFM}_i$ ist FFM für den i-ten Patienten. Diese Formel ist die exakte theoretische Lösung für kontinuierliche Infusion um gleiche $fT_{>MHK}$-Werte in Patienten mit unterschiedlicher FFM zu erzielen. Wir konnten als erste zeigen, dass Dosiswahl mit dieser Formel auch ähnliche $fT_{>MHK}$-Werte und PTAs für optimierte verlängerte Infusion in Patienten mit unterschiedlichem FFM erzielt.

Für 0.5h Infusionen und Dosiswahl als mg/kg FFM zeigte unsere MCS 5.3 [4-8] fach (Median [Bereich]) tiefere PKPD-Grenzwerte in CF-Patienten mit einem FFM von 11.4kg verglichen mit CF-Patienten mit einem FFM von 53kg. Wir entwickelten eine neue Formel, um ähnliche $fT_{>MHK}$-Werte und PTAs für Kurzzeitinfusion von Beta-Laktamen in Patienten mit unterschiedlicher FFM zu erzielen:

$$\text{Dosis}(\text{FFM}_i) = \text{Dosis}_{STD} \frac{\text{FFM}_i}{\text{FFM}_{STD}} \exp\left\{ \frac{\%\text{Zielwert} \cdot \text{Tau} \cdot \ln(2)}{\text{Halbwertszeit}_{STD}} \cdot \left[ \left( \frac{\text{FFM}_{STD}}{\text{FFM}_i} \right)^{0.25} - 1 \right] \right\}$$

Tau ist das Dosierungsintervall, %Zielwert ist der PKPD Zielwert und $\text{Halbwertszeit}_{STD}$ ist die typische terminale Halbwertszeit eines Patienten mit $\text{FFM}_{STD}$ (alle anderen Abkürzungen wie oben). Dosiswahl mit dieser Formel erzielte ähnliche PTAs für unsere fünf intravenös gegebenen Beta-Laktame. Jedoch waren die dazu benötigten Dosen in kleinen Patienten sehr groß.

***Schlussfolgerungen:*** Die optimale Dauer für verlängerte Infusion von Beta-Laktamen war etwas länger als der PKPD-Zielwert multipliziert mit dem Dosierungsintervall. Wir entwickelten und validierten erfolgreich eine neue Formel, um Beta-Laktam Dosen für Kurzzeitinfusionen nach einem allometrischen Körpergrößenmodell zu wählen. Wir testeten ferner erfolgreich eine Formel zur allometrischen Dosiswahl für optimierte verlängerte Infusion für Patienten unterschiedlicher Körpergröße. Sowohl wir als auch andere fanden erhebliche Beweise dafür, dass allometrische Körpergrößenmodelle linearen Körpergrößenmodellen überlegen sind. Daher sollten Beta-Laktam-

Dosen für kontinuierliche und optimierte verlängerte Infusion mit der oben beschriebenen Formel für eine konstante AUC gewählt werden. Für Kurzzeitinfusionen wurden sehr hohe Dosen benötigt, um ähnliche PTAs in kleineren Patienten zu erzielen. Daher erscheint eine verlängerte Infusion mit optimierter Dauer mit Dosiswahl anhand einer konstanten AUC als die optimale Wahl für Beta-Laktame aus Sicht der PKPD. Die Überlegenheit dieses Dosierungsregimes gegenüber Kurzzeitinfusion und mg/kg Dosiswahl sollte klinisch geprüft werden. Der zusätzliche Arbeitsaufwand und die Unannehmlichkeiten für den Patienten durch verlängerte Infusion sollten gegen die höhere Wahrscheinlichkeit für Heilung, den Schweregrad der Erkrankung und eine möglicherweise niedrigere Chance auf Selektion resistenter Mutanten abgewogen werden.

**PKPD-Grenzwerte**

***Methoden:*** Wir verwendeten die Populations-PK-Modelle aus unseren CF-Studien um die PKPD Grenzwerte abzuleiten. Wir schätzten ein Populations-PK-Modell mit Daten aus einer Studie mit 24 gesunden Probanden (Dosis: 250mg orales Cefuroxim) ab. Außerdem schätzten wir Populations-PK-Modelle für Daten aus drei Studien mit insgesamt 38 gesunden Probanden ab (Dosis: 500 oder 1000mg orales Ciprofloxacin und 500mg Levofloxacin). Wir bestimmten die PKPD-Grenzwerte von Standard- und optimierten Dosierungsregimen für alle Antibiotika mit MCS.

***Ergebnisse:*** Optimierte Dosierungsregime mit Cefpirom, Cefotiam und Carumonam erzielten PKPD-Grenzwerte, welche den Einsatz dieser Substanzen gegen *S. aureus* und *H. influenzae* in CF-Patienten als vielversprechend erscheinen lassen. Das ist jedoch von der lokal vorliegenden MHK-Verteilung abhängig. Orales Cefaclor und Cefadroxil erreichten niedrigere PKPD-Grenzwerte in CF-Patienten und die MHK der Infektionskeime sollte bestimmt werden, bevor diese Substanzen eingesetzt werden. Monotherapie mit oralem Ciprofloxacin gegen *P. aeruginosa* erreichte nur unzureichende PKPD-Grenzwerte in CF-Patienten. Kontinuierliche Infusion mit Piperacillin oder Ceftazidim erzielte PKPD-Grenzwerte in CF-Patienten, die als vielversprechend für den Einsatz gegen *P. aeruginosa* angesehen werden können. Dabei sollte die lokale Resistenzlage von

*P. aeruginosa* berücksichtigt werden. Unsere PKPD-Grenzwerte für orales Cefuroxim waren wesentlich niedriger als die MHK-Grenzwerte für Empfindlichkeit, die von nationalen Organisationen festgelegt wurden. Wir fanden auch wesentlich tiefere PKPD-Grenzwerte für orales Ciprofloxacin und orales Levofloxacin verglichen mit den Grenzwerten von nationalen Organisationen. Levofloxacin und Ciprofloxacin erreichten unzureichende PTAs gegen *P. aeruginosa*. Levofloxacin erzielte höhere PTAs gegen *S. pneumoniae* und *S. aureus* als Ciprofloxacin bei Standard-Dosen.

***Schlussfolgerungen:*** Unsere MCS sagte vielversprechende Wahrscheinlichkeiten für erfolgreiche Therapie für optimierte Dosierungsregime unserer intravenös gegebenen Beta-Laktame in CF-Patienten vorher. Monotherapie mit oralem Ciprofloxacin sollte nicht für die empirische Therapie gegen *P. aeruginosa* in CF-Patienten verwendet werden. Unsere PKPD-Grenzwerte für orales Cefuroxim, Ciprofloxacin und Levofloxacin legen nahe, dass die MHK-Grenzwerte einiger nationaler Organisationen kritisch überdacht werden sollten.

**Studien zur Variabilität der PK zwischen Studienperioden (BOV)**

***Methoden:*** Wir untersuchten die PK in vier gesunden Probanden, die die gleiche Formulierung von 4g Piperacillin an fünf aufeinanderfolgenden Studienperioden als Einmaldosen erhielten. In einer anderen Studie untersuchten wir 24 gesunde Probanden, die 500/125mg orales Amoxicillin / Clavulansäure an zwei aufeinanderfolgenden Studienperioden erhielten. Wir bestimmten die Populations-PK-Parameter und die BOV von Piperacillin, Amoxicillin und Clavulansäure. Zusätzlich simulierten wir 2x2 Crossover-Bioäquivalenz-Studien mit 24 Probanden, um die Chance auf Bioäquivalenz und die PKPD-Grenzwerte für Amoxicillin-Test-Formulierungen mit verschiedener Geschwindigkeit und Ausmaß der Resorption relativ zur Vergleichsformulierung zu untersuchen.

***Ergebnisse:*** Die BOV für die Gesamtkörperclearance von Piperacillin war mit einem Variationskoeffizienten (CV) von 8.5% gering. Clavulansäure hatte eine hohe BOV für das Ausmaß der Resorption (25% CV). Simulationen mit verschiedenen BOVs zeigten, dass eine BOV von mehr als ca. 15% für Ausmaß der Resorption oder Clearance die Chance Bioäquivalenz zu zeigen

merklich verringerte. Amoxicillin Test-Formulierungen mit einer ca. 25%igen Chance auf Bioäquivalenz konnten um einen Faktor von 2 niedrigere oder um einen Faktor von 1.5 höhere PKPD-Grenzwerte haben, relativ zur Vergleichs-formulierung.

***Schlussfolgerungen:*** Die kleine BOV für Piperacillin würde den erfolgreichen Einsatz von „target concentration intervention“ und von therapeutischem „drug monitoring“ erlauben. Die hohe BOV in den Maximal-Konzentrationen und in den AUCs, welche oft in Bioäquivalenz-Studien mit Clavulansäure gefunden wird, wurde wahrscheinlich durch die Säureinstabilität von Clavulansäure im Magen verursacht. Bioäquivalenz garantierte nicht ähnliche PKPD-Grenzwerte für die Test- und Referenz-Formulierung für Amoxicillin. Daher sollte die Ähnlichkeit der PKPD-Grenzwerte parallel zur Bioäquivalenz für Beta-Laktame untersucht werden.

**Systematische Fehler und Unsicherheit von Monte-Carlo-Simulationen (MCS) für Beta-Laktame**

***Methoden:*** Wir verglichen verschiedene Kriterien zur Modell-Auswahl für MCS auf Basis von zwei Datensätzen aus realen Studien. Wir untersuchten den systematischen Fehler von MCS-Ergebnissen, wenn PK-Parameter und ihre Variabilität mittels nicht-kompartimenteller Analyse bestimmt werden. Diese Methode wurde von mehr als der Hälfte der MCS für Beta-Laktame in der Literatur angewandt. Die Unsicherheit in den MCS-Ergebnissen wurde durch nicht-parametrische Bootstrap-Techniken und anschließende MCS bestimmt.

***Ergebnisse:*** Ein visueller Vergleich der vorhergesagten und gemessenen Konzentrationen war eine leicht zu interpretierende Methode und war besser geeignet als andere Kriterien, um ein Modell für eine MCS zu qualifizieren. Die Verwendung von PK-Parametern aus der nicht-kompartimentellen Analyse konnte zu merklich verfälschten MCS-Ergebnissen führen. Unsicherheit in den Populations-PK Parametern (am wichtigsten), Unsicherheit in der MHK-Verteilung (v. a. wichtig, wenn die MHK-Verteilung weniger als 300 Proben beinhaltet) und Unsicherheit im PKPD Zielwert waren die Hauptquellen für Unsicherheit in den MCS-Ergebnissen aus datenanalytischer Sicht.

***Schlussfolgerungen:*** Visuelle Kontrollen – wie oben beschrieben – sollten immer durchgeführt werden, um ein Populations-PK-Modell für eine MCS zu qualifizieren. MCS für Beta-Laktame sollten auf einem abgeschätzten Populations-PK-Modell basieren, da die Verwendung von PK-Parametern aus der nicht-kompartimentellen Analyse die MCS-Ergebnisse erheblich verfälschen kann. Wir führten die erste systematische Analyse der Unsicherheit einer MCS mit Beta-Laktamen durch. Unsicherheit in den PK-Parametern und in der MHK-Verteilung waren die wichtigsten Quellen von Unsicherheit für MCS mit Beta-Laktamen (neben der Unsicherheit im PKPD Zielwert). Unsicherheit in den PK-Parametern und in der MHK-Verteilung müssen berücksichtigt werden, wenn man die MCS-Ergebnisse verschiedener Beta-Laktame statistisch vergleichen möchte.

In dieser Doktorarbeit wurden verschiedene Aspekte von Populations-PKPD-Modellierung und -Anwendungen von Monte-Carlo-Simulationen gezeigt. Ein interaktives Zusammenspiel von Modellierung, Simulationen und Visualisierung von Ergebnissen kann sehr hilfreich sein, um individuelle Dosen optimal zu wählen, die klinische Entwicklung zu optimieren und die Diskussion von Ergebnissen zu fördern. Diese Methoden sind nachweislich schnell und kosteneffizient und sie werden hoffentlich in der Zukunft auf breiterer Basis Anwendung finden.

## 10 List of abbreviations

| | |
|---|---|
| AECB | acute exacerbation of chronic bronchitis |
| ANOVA | analysis of variance |
| ANCOVA | analysis of covariance |
| AUC | area under the curve |
| $AUC_{0\text{-last}}$ | AUC from time of administration up to the last quantifiable concentration |
| $AUC_{0\text{-}\infty}$ | AUC from time of administration up to time infinity |
| AUMC | area under the first moment concentration time curve |
| BDV | between drug variability |
| bid | twice daily |
| BOV | between occasion variability |
| BSA | body surface area |
| BSAC | British Society for Antimicrobial Chemotherapy |
| BSV | between subject variability |
| Caco-2 | a cell monolayer absorption model based on colon cancer cells |
| CF | cystic fibrosis |
| CL | clearance |
| $C_{last}$ | last quantifiable concentration |
| $CL_{ic}$ | intercompartmental clearance |
| $CL_R$ | renal clearance |
| $CL_{NR}$ | nonrenal clearance |
| CLSI | Clinical and Laboratory Standards Institute (formerly known as NCCLS) |
| $CL_T$ or $CL_{TOT}$ | total body clearance |
| Cmax | maximum observed plasma concentration |
| CV | coefficient of variation |
| DIN | Deutsches Institut für Normung |
| *E. coli* | *Escherichia coli* |
| F | Extent of absorption |
| *f*AUC/MIC | ratio of the free (non-protein bound) area under the concentration time curve over 24h to the MIC |

| | |
|---|---|
| $FCYF_{CLR}$ | Average renal clearance in CF-patients divided by average renal clearance in healthy volunteers after adjustment for body size |
| $FCYF_{CLNR}$ | Average nonrenal clearance in CF-patients divided by average nonrenal clearance in healthy volunteers after adjustment for body size |
| $FCYF_{CLT}$ | Average total clearance in CF-patients divided by average total clearance in healthy volunteers after adjustment for body size |
| $FCYF_{V}$ | Average volume of distribution at steady-state in CF-patients divided by average volume of distribution at steady-state in healthy volunteers after adjustment for body size |
| FDA | US Food and Drug Administration |
| $FFM_C$ | fat-free mass estimated by the formula of Cheymol & James |
| $FFM_J$ | fat-free mass estimated by the formula of Janmahasatian et al. |
| $fT_{>MIC}$ | time that the free (non-protein bound) plasma concentration remains above the MIC of a pathogen |
| GI | gastrointestinal |
| HPLC | high performance liquid chromatography |
| HT | height |
| IBMP | Institute for Biomedical and Pharmaceutical research |
| ICAAC | Interscience Conference on Antimicrobial Agents and Chemotherapy |
| ICU | intensive care unit |
| IR | Immediate release |
| iv | intravenous |
| Km | Michalis-Menten constant; concentration or amount resulting in 50% of the maximum rate of drug transport (Vmax) for a mixed-order process |
| *K. pneumoniae* | *Klebsiella pneumoniae* |
| $\lambda_z$ | terminal slope of the time vs. logarithmic concentration curve |
| LBM | lean body mass |
| LC-MS/MS | liquid chromatography with tandem mass spectrometry |
| ln | natural logarithm |
| log | logarithm (natural logarithm, if not otherwise specified) |
| MBRT | mean body residence time |
| MCS | Monte Carlo simulations or Monte Carlo simulation |
| MHK | Minimale Hemmkonzentration |
| MIC | minimum inhibitory concentration |
| MIT | mean input time |

| | |
|---|---|
| Mol. Wt. | molecular weight |
| MRM | multiple reaction monitoring |
| MRSA | methicillin-resistant *Staphylococcus aureus* |
| MRT | mean residence time |
| MS/MS | tandem mass spectrometry |
| MSSA | methicillin-susceptible *Staphylococcus aureus* |
| MYSTIC | a global antimicrobial surveillance program |
| m/z | mass to charge ratio |
| NCA | non-compartmental analysis |
| NCCLS | National Committee for Clinical Laboratory Standards (now known as CLSI) |
| NONMEM® | nonlinear mixed effects modeling and the name of a very frequently applied population PK program |
| *P. aeruginosa* | *Pseudomonas aeruginosa* |
| PD | pharmacodynamics or pharmacodynamic |
| PEPT1 | peptide transporter expressed in the intestine |
| PK | pharmacokinetics or pharmacokinetic |
| PKPD | pharmacokinetics-pharmacodynamics |
| $PNWT_C$ | predicted normal weight estimated by the formula of Cheymol & James |
| $PNWT_J$ | predicted normal weight estimated by the formula of Janmahasatian et al. |
| po | per oral |
| PPV | population parameter variability |
| PTA | probability of target attainment |
| q | quaque, every |
| q8h | every 8 hours |
| qd | once daily |
| qid | four times daily |
| *S. aureus* | *Staphylococcus aureus* |
| *S. epidermidis* | *Staphylococcus epidermidis* |
| *S. pneumoniae* | *Streptococcus pneumoniae* |
| SD | standard deviation |
| SEV | Save and effective variability |
| SENTRY | a global antimicrobial surveillance program |
| SQC | spiked quality control |
| SRM | selected reaction monitoring |
| STS | standard-two-stage |

| | |
|---|---|
| $t_{1/2}$ | half-life (terminal half-life, if not otherwise specified) |
| TABS | half-life of absorption |
| TCI | target concentration intervention |
| TDM | therapeutic drug monitoring |
| tid | three times daily |
| TK0 | duration of zero-order input (duration of infusion) |
| TLAG | absorption lag-time |
| tmax | time to peak concentration |
| US | United States |
| UV | ultraviolet |
| V | volume of distribution |
| V1 | volume of distribution of the central compartment |
| V2 | volume of distribution of the (shallow) peripheral compartment |
| V3 | volume of distribution of the deep peripheral compartment |
| Vmax | Maximum rate of drug transport of a mixed-order process |
| VPC | visual predictive check |
| Vss | volume of distribution at steady-state |
| Vz | volume of distribution during the terminal phase |
| WOV | within occasion variability |
| WSV | within subject variability |
| WT | total body weight |
| XR | extended release |

# 11 References


1. **Abelson Storby, K., A. Osterlund, and G. Kahlmeter.** 2004. Antimicrobial resistance in Escherichia coli in urine samples from children and adults: a 12 year analysis. Acta Paediatr **93:**487-91.
2. **Abramowsky, C. R., and G. L. Swinehart.** 1982. The nephropathy of cystic fibrosis: a human model of chronic nephrotoxicity. Hum Pathol **13:**934-9.
3. **Adam, D., and P. Gierschik.** 1980. Vergleichende Untersuchungen zur Pharmakokinetik von Cefadroxil und Amoxicillin nach oraler Nüchterngabe. Infection **8:**S561-S572.
4. **Ahmed, A., S. Hafiz, M. Rafiq, N. Tariq, E. M. Abdulla, S. Hussain, R. Azim, S. J. Siddiqui, A. Awan, K. Z. Khan, and A. Fareed.** 2002. Determination of antimicrobial activity of Cefaclor on common respiratory tract pathogens in Pakistan. J Pak Med Assoc **52:**7-11.
5. **Allen, G. D., P. E. Coates, and B. E. Davies.** 1988. On the absorption of clavulanic acid. Biopharm Drug Dispos **9:**127-36.
6. **Ambrose, P. G., S. M. Bhavnani, and R. N. Jones.** 2003. Pharmacokinetics-pharmacodynamics of cefepime and piperacillin-tazobactam against Escherichia coli and Klebsiella pneumoniae strains producing extended-spectrum beta-lactamases: report from the ARREST program. Antimicrob Agents Chemother **47:**1643-6.
7. **Ambrose, P. G., S. M. Bhavnani, R. N. Jones, W. A. Craig, and M. N. Dudley.** 2004. Presented at the 44th Interscience Conference on Antimicrobial Agents and Chemotherapy, Washington, DC, October 30 to November 2, 2004.
8. **Ambrose, P. G., and D. M. Grasela.** 2000. The use of Monte Carlo simulation to examine pharmacodynamic variance of drugs: fluoroquinolone pharmacodynamics against Streptococcus pneumoniae. Diagn Microbiol Infect Dis **38:**151-7.
9. **Ambrose, P. G., D. M. Grasela, T. H. Grasela, J. Passarell, H. B. Mayer, and P. F. Pierce.** 2001. Pharmacodynamics of fluoroquinolones against Streptococcus pneumoniae in patients with community-acquired respiratory tract infections. Antimicrob Agents Chemother **45:**2793-7.
10. **Aminimanizani, A., P. Beringer, and R. Jelliffe.** 2001. Comparative pharmacokinetics and pharmacodynamics of the newer fluoroquinolone antibacterials. Clin Pharmacokinet **40:**169-87.
11. **Andes, D., and W. A. Craig.** 2002. Pharmacodynamics of the new fluoroquinolone gatifloxacin in murine thigh and lung infection models. Antimicrob Agents Chemother **46:**1665-70.
12. **Anonymous.** 1998. Cystic fibrosis foundation patient registry 1997 annual data report. Cystic Fibrosis Foundation, Bethesda, MD, USA.
13. **Anonymous.** Revised 5 April 1999. Piperacillin sodium and tazobactam sodium (Zosyn) product information. Lederle Laboratories, Pearl River, N.Y.
14. **Aperia, A., and P. Herin.** 1976. Effect of arterial blood pressure reduction on renal hemodynamics in the developing lamb. Acta Physiol Scand **98:**387-94.
15. **Armstrong, G. C., R. Wise, R. M. Brown, and J. Hancox.** 1981. Comparison of ceftazidime and cefamandole pharmacokinetics and blister fluid concentrations. Antimicrob Agents Chemother **20:**356-8.
16. **Aronoff, G. R., R. S. Sloan, M. E. Brier, and F. C. Luft.** 1983. The effect of piperacillin dose on elimination kinetics in renal impairment. Eur J Clin Pharmacol **24:**543-7.
17. **Aronoff, S. C., and J. D. Klinger.** 1985. Comparison of cefpiramide (HR-810) and four anti-pseudomonal beta-lactam agents against pseudomonas isolates from children with cystic fibrosis. J Antimicrob Chemother **15:**545-9.
18. **Aronson, J. K.** 2005. Metameta-analysis. Br J Clin Pharmacol **60:**117-9.
19. **Arvidsson, A., G. Alvan, and B. Strandvik.** 1983. Difference in renal handling of cefsulodin between patients with cystic fibrosis and normal subjects. Acta Paediatr Scand **72:**293-4.

20. **Asahi, Y., S. Miyazaki, and K. Yamaguchi.** 1995. In vitro and in vivo antibacterial activities of BO-2727, a new carbapenem. Antimicrob Agents Chemother **39:**1030-7.
21. **Ashdown, L. R.** 1988. In vitro activities of the newer beta-lactam and quinolone antimicrobial agents against Pseudomonas pseudomallei. Antimicrob Agents Chemother **32:**1435-6.
22. **Augsberger, A.** 1962. Old and new rules for dosage determination in paediatrics. Triangle **5:**200-7.
23. **Augsberger, A.** 1951. Quantitative notes on the therapeutic use of cardiac glycosides. I. Variability of need and tolerance. Med Welt **20:**1471-5.
24. **Badian, M., V. Malerczyk, J. D. Collins, G. T. Dixon, M. Verho, and H. G. Eckert.** 1988. Safety, tolerance and pharmacokinetics of 2.0 g cefpirome (HR 810) after single and multiple dosing. Chemotherapy **34:**367-73.
25. **Bakker, W., A. A. Vinks, J. W. Mouton, P. de Jonge, J. G. Verzijl, and H. G. Heijerman.** 1993. [Continuous intravenous home treatment of airway infections using ceftazidime administration via portable pump in patients with cystic fibrosis; a multicenter study]. Ned Tijdschr Geneeskd **137:**2486-91.
26. **Balis, F. M., P. A. Pizzo, J. Eddy, C. Wilfert, R. McKinney, G. Scott, R. F. Murphy, P. F. Jarosinski, J. Falloon, and D. G. Poplack.** 1989. Pharmacokinetics of zidovudine administered intravenously and orally in children with human immunodeficiency virus infection. J Pediatr **114:**880-4.
27. **Bandak, S. I., M. R. Turnak, B. S. Allen, L. D. Bolzon, D. A. Preston, S. K. Bouchillon, and D. J. Hoban.** 2001. Antibiotic susceptibilities among recent clinical isolates of Haemophilus influenzae and Moraxella catarrhalis from fifteen countries. Eur J Clin Microbiol Infect Dis **20:**55-60.
28. **Barbato, F., M. I. La Rotonda, and P. Morrica.** 1991. pH-Dependence of hydrophobic parameters in a set of cephaloporin antibiotics. Pharmacochemical Library **16:**99-102.
29. **Barbhaiya, R. H.** 1996. A pharmacokinetic comparison of cefadroxil and cephalexin after administration of 250, 500 and 1000 mg solution doses. Biopharm Drug Dispos **17:**319-30.
30. **Barbhaiya, R. H., U. A. Shukla, C. R. Gleason, W. C. Shyu, R. B. Wilber, R. R. Martin, and K. A. Pittman.** 1990. Phase I study of multiple-dose cefprozil and comparison with cefaclor. Antimicrob Agents Chemother **34:**1198-203.
31. **Barraclough, M., and C. J. Taylor.** 1996. Twenty-four hour ambulatory gastric and duodenal pH profiles in cystic fibrosis: effect of duodenal hyperacidity on pancreatic enzyme function and fat absorption. J Pediatr Gastroenterol Nutr **23:**45-50.
32. **Batra, V. K., J. A. Morrison, K. C. Lasseter, and V. A. Joy.** 1979. Piperacillin kinetics. Clin Pharmacol Ther **26:**41-53.
33. **Beal, S. L., A. J. Boeckmann, L. B. Sheiner, and NONMEM Project Group.** 1999. NONMEM Users Guides, Version 5 ed. University of California at San Francisco, San Francisco.
34. **Benedict, F. G.** 1938. Vital Energetics: A Study in Comparative Basal Metabolism. Carnegie Institution of Washington, Washington, DC.
35. **Benet, L. Z., and B. A. Hoener.** 2002. Changes in plasma protein binding have little clinical relevance. Clin Pharmacol Ther **71:**115-21.
36. **Benko, A. S., D. M. Cappelletty, J. A. Kruse, and M. J. Rybak.** 1996. Continuous infusion versus intermittent administration of ceftazidime in critically ill patients with suspected gram-negative infections. Antimicrob Agents Chemother **40:**691-5.
37. **Berg, U., E. Kusoffsky, and B. Strandvik.** 1982. Renal function in cystic fibrosis with special reference to the renal sodium handling. Acta Paediatr Scand **71:**833-8.
38. **Bergan, T.** 1981. Overview of acylureidopenicillin pharmacokinetics. Scand J Infect Dis Suppl **29:**33-48.
39. **Bergan, T., and J. D. Williams.** 1982. Dose dependence of piperacillin pharmacokinetics. Chemotherapy **28:**153-9.
40. **Bergeret, M., N. Boutros, and J. Raymond.** 2004. In vitro combined bactericidal activity of cefpirome and glycopeptides against glycopeptides and oxacillin-resistant staphylococci. Int J Antimicrob Agents **23:**247-53.

41. **Bergeret, M., and J. Raymond.** 1999. In-vitro bactericidal activity of cefpirome and cefamandole in combination with glycopeptides against methicillin-resistant Staphylococcus aureus. J Antimicrob Chemother **43:**291-4.
42. **Bergeron, M. G., and M. Bernier.** 1994. Bactericidal activity of cefpirome (HR 810) against 513 gram-negative bacteria isolated from blood of septicemic patients. Infection **22:**299-305.
43. **Berube, D., F. Vallee, A. C. Panneton, M. G. Bergeron, and M. LeBel.** 1988. Pharmacokinetics of carumonam after single and multiple 1- and 2-g dosage regimens. Antimicrob Agents Chemother **32:**354-7.
44. **Bhakta, D. R., I. Leader, R. Jacobson, B. Robinson-Dunn, R. E. Honicky, and A. Kumar.** 1992. Antibacterial properties of investigational, new, and commonly used antibiotics against isolates of Pseudomonas cepacia in Michigan. Chemotherapy **38:**319-23.
45. **Bilello, J. A., P. A. Bilello, K. Stellrecht, J. Leonard, D. W. Norbeck, D. J. Kempf, T. Robins, and G. L. Drusano.** 1996. Human serum alpha 1 acid glycoprotein reduces uptake, intracellular concentration, and antiviral activity of A-80987, an inhibitor of the human immunodeficiency virus type 1 protease. Antimicrob Agents Chemother **40:**1491-7.
46. **Blaser, J., B. B. Stone, M. C. Groner, and S. H. Zinner.** 1987. Comparative study with enoxacin and netilmicin in a pharmacodynamic model to determine importance of ratio of antibiotic peak concentration to MIC for bactericidal activity and emergence of resistance. Antimicrob Agents Chemother **31:**1054-60.
47. **Blumer, J. L., R. C. Stern, J. D. Klinger, T. S. Yamashita, C. M. Meyers, A. Blum, and M. D. Reed.** 1985. Ceftazidime therapy in patients with cystic fibrosis and multiply-drug-resistant pseudomonas. Am J Med **79:**37-46.
48. **Bonacorsi, S., F. Fitoussi, S. Lhopital, and E. Bingen.** 1999. Comparative in vitro activities of meropenem, imipenem, temocillin, piperacillin, and ceftazidime in combination with tobramycin, rifampin, or ciprofloxacin against Burkholderia cepacia isolates from patients with cystic fibrosis. Antimicrob Agents Chemother **43:**213-7.
49. **Bonate, P. L.** 1998. Coverage and precision of confidence intervals for area under the curve using parametric and non-parametric methods in a toxicokinetic experimental design. Pharm Res **15:**405-10.
50. **Bosso, J. A., P. G. Black, and J. M. Matsen.** 1987. Ciprofloxacin versus tobramycin plus azlocillin in pulmonary exacerbations in adult patients with cystic fibrosis. Am J Med **82:**180-4.
51. **Boucher, F. D., J. F. Modlin, S. Weller, A. Ruff, M. Mirochnick, S. Pelton, C. Wilfert, R. McKinney, Jr., M. J. Crain, M. M. Elkins, and et al.** 1993. Phase I evaluation of zidovudine administered to infants exposed at birth to the human immunodeficiency virus. J Pediatr **122:**137-44.
52. **Bouchillon, S. K., D. J. Hoban, J. L. Johnson, B. M. Johnson, D. L. Butler, K. A. Saunders, L. A. Miller, and J. A. Poupard.** 2004. In vitro activity of gemifloxacin and contemporary oral antimicrobial agents against 27247 Gram-positive and Gram-negative aerobic isolates: a global surveillance study. Int J Antimicrob Agents **23:**181-96.
53. **Brauers, J., S. Bagel, and M. Kresken.** 2005. Aktuelle Resistanzsituation bei bakteriellen Erregern von ambulant erworbenen Atemwegsinfektionen. Chemotherapie Journal **14:**45-53.
54. **Bretschneider, B., M. Brandsch, and R. Neubert.** 1999. Intestinal transport of beta-lactam antibiotics: analysis of the affinity at the H+/peptide symporter (PEPT1), the uptake into Caco-2 cell monolayers and the transepithelial flux. Pharm Res **16:**55-61.
55. **Brisson, A. M., A. Bryskier, L. Millerioux, and J. B. Fourtillan.** 1984. Pharmacokinetics of cefotiam administered intravenously and intramuscularly to healthy adults. Antimicrob Agents Chemother **26:**513-8.
56. **British Society for Antimicrobial Chemotherapy.** 2005. BSAC Disc Diffusion Method for Antimicrobial Susceptibility Testing. Version 4 January 2005.
57. **Brody, S.** 1945. Bioenergetics and Growth. Reinhold Publishing Corporation, New York.
58. **Brogard, J. M., F. Jehl, B. Willemin, A. M. Lamalle, J. F. Blickle, and H. Monteil.** 1989. Clinical pharmacokinetics of cefotiam. Clin Pharmacokinet **17:**163-74.

59. **Brumfitt, W., and J. M. Hamilton-Miller.** 1999. Cefaclor into the millennium. J Chemother **11:**163-78.
60. **Buck, R. E., and K. E. Price.** 1977. Cefadroxil, a new broad-spectrum cephalosporin. Antimicrob Agents Chemother **11:**324-30.
61. **Burgess, D. S.** 1999. Pharmacodynamic principles of antimicrobial therapy in the prevention of resistance. Chest **115:**19S-23S.
62. **Burns, L. E., J. E. Hodgman, and A. B. Cass.** 1959. Fatal circulatory collapse in premature infants receiving chloramphenicol. N Engl J Med **261:**1318-21.
63. **Bustad, A., D. Terziivanov, R. Leary, R. Port, A. Schumitzky, and R. Jelliffe.** 2006. Parametric and nonparametric population methods: their comparative performance in analysing a clinical dataset and two Monte Carlo simulation studies. Clin Pharmacokinet **45:**365-83.
64. **Buts, J. P., C. L. Morin, C. C. Roy, A. Weber, and A. Bonin.** 1978. One-hour blood xylose test: a reliable index of small bowel function. J Pediatr **92:**729-33.
65. **Canton, R., N. Cobos, J. de Gracia, F. Baquero, J. Honorato, S. Gartner, A. Alvarez, A. Salcedo, A. Oliver, and E. Garcia-Quetglas.** 2005. Antimicrobial therapy for pulmonary pathogenic colonisation and infection by Pseudomonas aeruginosa in cystic fibrosis patients. Clin Microbiol Infect **11:**690-703.
66. **Caplan, A., and S. Gross.** 1968. Hematologic and serologic studies in cystic fibrosis. J Pediatr **73:**540-7.
67. **Casey, J. R., and M. E. Pichichero.** 2004. Meta-analysis of cephalosporin versus penicillin treatment of group A streptococcal tonsillopharyngitis in children. Pediatrics **113:**866-82.
68. **Castello, M., and C. Mari.** 1995. Pseudomonas aeruginosa colonization in Turin CF center. Microbiological and therapeutic observations. Minerva Pediatr **47:**175-85.
69. **Cavallo, J. D., R. Fabre, F. Leblanc, M. H. Nicolas-Chanoine, and A. Thabaut.** 2000. Antibiotic susceptibility and mechanisms of beta-lactam resistance in 1310 strains of pseudomonas aeruginosa: a French multicentre study (1996). J Antimicrob Chemother **46:**133-6.
70. **Cavallo, J. D., F. Leblanc, and R. Fabre.** 2000. Surveillance of Pseudomonas aeruginosa sensitivity to antibiotics in France and distribution of beta-lactam resistance mechanisms: 1998 GERPB study. Pathol Biol (Paris) **48:**472-7.
71. **Cavell, B.** 1981. Gastric emptying in infants with cystic fibrosis. Acta Paediatr Scand **70:**635-8.
72. **Cheymol, G.** 2000. Effects of obesity on pharmacokinetics implications for drug therapy. Clin Pharmacokinet **39:**215-31.
73. **Chiba, K., M. Tsuchiya, J. Kato, K. Ochi, Z. Kawa, and T. Ishizaki.** 1989. Cefotiam disposition in markedly obese athlete patients, Japanese sumo wrestlers. Antimicrob Agents Chemother **33:**1188-92.
74. **Chodosh, S., J. McCarty, S. Farkas, M. Drehobl, R. Tosiello, M. Shan, L. Aneiro, and S. Kowalsky.** 1998. Randomized, double-blind study of ciprofloxacin and cefuroxime axetil for treatment of acute bacterial exacerbations of chronic bronchitis. The Bronchitis Study Group. Clin Infect Dis **27:**722-9.
75. **Christensson, B. A., I. Nilsson-Ehle, B. Ljungberg, A. Lindblad, A. S. Malmborg, L. Hjelte, and B. Strandvik.** 1992. Increased oral bioavailability of ciprofloxacin in cystic fibrosis patients. Antimicrob Agents Chemother **36:**2512-7.
76. **Chulavatnatol, S., and B. G. Charles.** 1994. Determination of dose-dependent absorption of amoxycillin from urinary excretion data in healthy subjects. Br J Clin Pharmacol **38:**274-7.
77. **Church, D. A., J. F. Kanga, R. J. Kuhn, T. T. Rubio, W. A. Spohn, J. C. Stevens, B. G. Painter, B. E. Thurberg, D. C. Haverstock, R. Y. Perroncel, and R. M. Echols.** 1997. Sequential ciprofloxacin therapy in pediatric cystic fibrosis: comparative study vs. ceftazidime/tobramycin in the treatment of acute pulmonary exacerbations. The Cystic Fibrosis Study Group. Pediatr Infect Dis J **16:**97-105; discussion 123-6.
78. **Cockcroft, D. W., and M. H. Gault.** 1976. Prediction of creatinine clearance from serum creatinine. Nephron **16:**31-41.

79. **Cole, P.** 1997. Pharmacologic and clinical comparison of cefaclor in immediate-release capsule and extended-release tablet forms. Clin Ther **19:**617-25; discussion 603.
80. **Conway, S. P., K. G. Brownlee, M. Denton, and D. G. Peckham.** 2003. Antibiotic treatment of multidrug-resistant organisms in cystic fibrosis. Am J Respir Med **2:**321-32.
81. **Cox, K. L., J. N. Isenberg, and M. E. Ament.** 1982. Gastric acid hypersecretion in cystic fibrosis. J Pediatr Gastroenterol Nutr **1:**559-65.
82. **Craig, M., H. Haddad, and H. Shwachman.** 1957. The pathological changes in the liver in cystic fibrosis of the pancreas. Am J Dis Child **93:**357-369.
83. **Craig, W. A.** 1998. Choosing an antibiotic on the basis of pharmacodynamics. Ear Nose Throat J **77:**7-11; discussion 11-2.
84. **Craig, W. A.** 1998. Pharmacokinetic/pharmacodynamic parameters: rationale for antibacterial dosing of mice and men. Clin Infect Dis **26:**1-12.
85. **Craig, W. A., and S. C. Ebert.** 1992. Continuous infusion of beta-lactam antibiotics. Antimicrob Agents Chemother **36:**2577-83.
86. **Currie, B. J.** 2003. Melioidosis: an important cause of pneumonia in residents of and travellers returned from endemic regions. Eur Respir J **22:**542-50.
87. **Cutler, R. E., A. D. Blair, and M. R. Kelly.** 1979. Cefadroxil kinetics in patients with renal insufficiency. Clin Pharmacol Ther **25:**514-21.
88. **Cystic Fibrosis Foundation Patient Registry.** 2002. 2001 Annual Data Report to the Center Directors. Cystic Fibrosis Foundation, Bethesda, MD, USA.
89. **Daenen, S., Z. Erjavec, D. R. Uges, H. G. De Vries-Hospers, P. De Jonge, and M. R. Halie.** 1995. Continuous infusion of ceftazidime in febrile neutropenic patients with acute myeloid leukemia. Eur J Clin Microbiol Infect Dis **14:**188-92.
90. **Dagan, R., O. Abramson, E. Leibovitz, D. Greenberg, R. Lang, S. Goshen, P. Yagupsky, A. Leiberman, and D. M. Fliss.** 1997. Bacteriologic response to oral cephalosporins: are established susceptibility breakpoints appropriate in the case of acute otitis media? J Infect Dis **176:**1253-9.
91. **Dagan, R., E. Leibovitz, D. M. Fliss, A. Leiberman, M. R. Jacobs, W. Craig, and P. Yagupsky.** 2000. Bacteriologic efficacies of oral azithromycin and oral cefaclor in treatment of acute otitis media in infants and young children. Antimicrob Agents Chemother **44:**43-50.
92. **Dance, D. A.** 2002. Melioidosis. Curr Opin Infect Dis **15:**127-32.
93. **Dansirikul, C., M. Choi, and S. B. Duffull.** 2005. Estimation of pharmacokinetic parameters from non-compartmental variables using Microsoft Excel. Comput Biol Med **35:**389-403.
94. **Dantzig, A. H., L. B. Tabas, and L. Bergin.** 1992. Cefaclor uptake by the proton-dependent dipeptide transport carrier of human intestinal Caco-2 cells and comparison to cephalexin uptake. Biochim Biophys Acta **1112:**167-73.
95. **Daschner, F. D., K. A. Hemmer, P. Offermann, and J. Slanicka.** 1982. Pharmacokinetics of cefotiam in normal humans. Antimicrob Agents Chemother **22:**958-60.
96. **David, T. J., and J. Devlin.** 1989. Continuous infusion of ceftazidime in cystic fibrosis. Lancet **1:**1454-5.
97. **Davies, T. A., G. A. Pankuch, B. E. Dewasse, M. R. Jacobs, and P. C. Appelbaum.** 1999. In vitro development of resistance to five quinolones and amoxicillin-clavulanate in Streptococcus pneumoniae. Antimicrob Agents Chemother **43:**1177-82.
98. **Davis, R. L., J. R. Koup, J. Williams-Warren, A. Weber, L. Heggen, D. Stempel, and A. L. Smith.** 1987. Pharmacokinetics of ciprofloxacin in cystic fibrosis. Antimicrob Agents Chemother **31:**915-9.
99. **De Abate, C. A., R. A. McIvor, P. McElvaine, and e. al.** 1999. Smokers treated with gatifloxacin had a high clinical cure rate: gatifloxacin vs cefuroxime axetil in patients with acute exacerbations of chronic bronchitis. J Respir Dis **20 Suppl.:**S23-9.
100. **de Groot, R., B. D. Hack, A. Weber, D. Chaffin, B. Ramsey, and A. L. Smith.** 1990. Pharmacokinetics of ticarcillin in patients with cystic fibrosis: a controlled prospective study. Clin Pharmacol Ther **47:**73-8.

101. **de Groot, R., and A. L. Smith.** 1987. Antibiotic pharmacokinetics in cystic fibrosis. Differences and clinical significance. Clin Pharmacokinet **13:**228-53.
102. **Deeter, R. G., D. L. Kalman, M. P. Rogan, and S. C. Chow.** 1992. Therapy for pharyngitis and tonsillitis caused by group A beta-hemolytic streptococci: a meta-analysis comparing the efficacy and safety of cefadroxil monohydrate versus oral penicillin V. Clin Ther **14:**740-54.
103. **Dellamonica, P.** 1994. Cefuroxime axetil. Int J Antimicrob Agents **4:**23-36.
104. **Deutsches Institut für Normung e. V.** 2004. Medizinische Mikrobiologie - Empfindlichkeitsprüfung von mikrobiellen Krankheitserregern gegen Chemotherapeutika - Teil 4: Bewertungsstufen für die minimale Hemmkonzentration - MHK-Grenzwerte von antibakteriellen Wirkstoffen. DIN 58940-4. Beuth Verlag, Berlin.
105. **Doring, G., S. P. Conway, H. G. Heijerman, M. E. Hodson, N. Hoiby, A. Smyth, and D. J. Touw.** 2000. Antibiotic therapy against Pseudomonas aeruginosa in cystic fibrosis: a European consensus. Eur Respir J **16:**749-67.
106. **Dost, F. H.** 1953. Der Blutspiegel: Kinetik der Konzentrationsabläufe in der Kreislaufflüssigkeit. Georg Thieme, Leipzig, Germany.
107. **Drusano, G. L.** 2004. Antimicrobial pharmacodynamics: critical interactions of 'bug and drug'. Nat Rev Microbiol **2:**289-300.
108. **Drusano, G. L.** 2003. Prevention of resistance: a goal for dose selection for antimicrobial agents. Clin Infect Dis **36:**S42-50.
109. **Drusano, G. L., and W. A. Craig.** 1997. Relevance of pharmacokinetics and pharmacodynamics in the selection of antibiotics for respiratory tract infections. J Chemother **9 Suppl 3:**38-44.
110. **Drusano, G. L., D. E. Johnson, M. Rosen, and H. C. Standiford.** 1993. Pharmacodynamics of a fluoroquinolone antimicrobial agent in a neutropenic rat model of Pseudomonas sepsis. Antimicrob Agents Chemother **37:**483-90.
111. **Drusano, G. L., S. L. Preston, C. Fowler, M. Corrado, B. Weisinger, and J. Kahn.** 2004. Relationship between fluoroquinolone area under the curve: minimum inhibitory concentration ratio and the probability of eradication of the infecting pathogen, in patients with nosocomial pneumonia. J Infect Dis **189:**1590-7.
112. **Drusano, G. L., S. L. Preston, M. H. Gotfried, L. H. Danziger, and K. A. Rodvold.** 2002. Levofloxacin penetration into epithelial lining fluid as determined by population pharmacokinetic modeling and monte carlo simulation. Antimicrob Agents Chemother **46:**586-9.
113. **Drusano, G. L., S. L. Preston, C. Hardalo, R. Hare, C. Banfield, D. Andes, O. Vesga, and W. A. Craig.** 2001. Use of preclinical data for selection of a phase II/III dose for evernimicin and identification of a preclinical MIC breakpoint. Antimicrob Agents Chemother **45:**13-22.
114. **Drusano, G. L., S. L. Preston, M. Van Guilder, D. North, M. Gombert, M. Oefelein, L. Boccumini, B. Weisinger, M. Corrado, and J. Kahn.** 2000. A population pharmacokinetic analysis of the penetration of the prostate by levofloxacin. Antimicrob Agents Chemother **44:**2046-51.
115. **Drusano, G. L., H. C. Standiford, B. Fitzpatrick, J. Leslie, P. Tangtatsawasdi, P. Ryan, B. Tatem, M. R. Moody, and S. C. Schimpff.** 1984. Comparison of the pharmacokinetics of ceftazidime and moxalactam and their microbiological correlates in volunteers. Antimicrob Agents Chemother **26:**388-93.
116. **Dudley, M. N., and P. G. Ambrose.** 2000. Pharmacodynamics in the study of drug resistance and establishing in vitro susceptibility breakpoints: ready for prime time. Curr Opin Microbiol **3:**515-21.
117. **Duffull, S. B., M. J. Dooley, B. Green, S. G. Poole, and C. M. Kirkpatrick.** 2004. A standard weight descriptor for dose adjustment in the obese patient. Clin Pharmacokinet **43:**1167-78.
118. **Duffull, S. B., F. Mentre, and L. Aarons.** 2001. Optimal design of a population pharmacodynamic experiment for ivabradine. Pharm Res **18:**83-9.
119. **Duffull, S. B., S. Retout, and F. Mentre.** 2002. The use of simulated annealing for finding optimal population designs. Comput Methods Programs Biomed **69:**25-35.
120. **Eagle, H., R. Fleischman, and M. Levy.** 1953. "Continuous" vs. "discontinuous" therapy with penicillin; the effect of the interval between injections on therapeutic efficacy. N Engl J Med **248:**481-8.

121. **Edwards, D. J., and K. Stoeckel.** 1992. The pharmacokinetics of new oral cephalosporins in children. Chemotherapy **38 Suppl 2:**2-9.
122. **Efron, B., and R. J. Tibshirani.** 1986. Bootstrap methods for standard errors, confidence intervals and other measures of statistical accuracy. Stat Sci **1:**54-77.
123. **el-Tahtawy, A. A., A. J. Jackson, and T. M. Ludden.** 1994. Comparison of single and multiple dose pharmacokinetics using clinical bioequivalence data and Monte Carlo simulations. Pharm Res **11:**1330-6.
124. **Elkhaili, H., J. D. Peter, D. Pompei, D. Levless-Than-Or-Eq Slanteque, L. Linger, Y. Salmon, J. Salmon, and H. Monteil.** 1998. Pharmacokinetics in vivo and pharmacodynamics ex vivo/in vitro of meropenem and cefpirome in the Yucatan micropig model: continuous infusion versus intermittent injection. Clin Microbiol Infect **4:**18-26.
125. **Elphick, H. E., and A. Tan.** 2005. Single versus combination intravenous antibiotic therapy for people with cystic fibrosis. Cochrane Database Syst Rev**:**CD002007.
126. **Ette, E. I.** 1997. Stability and performance of a population pharmacokinetic model. J Clin Pharmacol **37:**486-95.
127. **Ette, E. I., and L. C. Onyiah.** 2002. Estimating inestimable standard errors in population pharmacokinetic studies: the bootstrap with Winsorization. Eur J Drug Metab Pharmacokinet **27:**213-24.
128. **Evans, M. A., P. Wilson, T. Leung, and J. D. Williams.** 1978. Pharmacokinetics of piperacillin following intravenous administration. J Antimicrob Chemother **4:**255-61.
129. **Evans, M. A. L., T. Leung, P. Wilson, and J. D. Williams.** 1979. Pharmacokinetics of intravenously administered antibiotics: a study of piperacillin, a new semi-synthetic penicillin. Drugs Exp. Clin. Res. **5:**111-116.
130. **Figueredo, V. M., and H. C. Neu.** 1988. Synergy of ciprofloxacin with fosfomycin in vitro against Pseudomonas isolates from patients with cystic fibrosis. J Antimicrob Chemother **22:**41-50.
131. **File, T. M., Jr., J. Segreti, L. Dunbar, R. Player, R. Kohler, R. R. Williams, C. Kojak, and A. Rubin.** 1997. A multicenter, randomized study comparing the efficacy and safety of intravenous and/or oral levofloxacin versus ceftriaxone and/or cefuroxime axetil in treatment of adults with community-acquired pneumonia. Antimicrob Agents Chemother **41:**1965-72.
132. **Finkelstein, E., and K. Hall.** 1979. Aminoglycoside clearance in patients with cystic fibrosis. J Pediatr **94:**163-4.
133. **Finn, A., A. Straughn, M. Meyer, and J. Chubb.** 1987. Effect of dose and food on the bioavailability of cefuroxime axetil. Biopharm Drug Dispos **8:**519-26.
134. **Fish, D. N., and A. T. Chow.** 1997. The clinical pharmacokinetics of levofloxacin. Clin Pharmacokinet **32:**101-19.
135. **Fondacaro, J. D., J. E. Heubi, and F. W. Kellogg.** 1982. Intestinal bile acid malabsorption in cystic fibrosis: a primary mucosal cell defect. Pediatr Res **16:**494-8.
136. **Foord, R. D.** 1976. Cefuroxime: human pharmacokinetics. Antimicrob Agents Chemother **9:**741-7.
137. **Forrest, A., D. E. Nix, C. H. Ballow, T. F. Goss, M. C. Birmingham, and J. J. Schentag.** 1993. Pharmacodynamics of intravenous ciprofloxacin in seriously ill patients. Antimicrob Agents Chemother **37:**1073-81.
138. **Frase, L. L., A. D. Strickland, G. W. Kachel, and G. J. Krejs.** 1985. Enhanced glucose absorption in the jejunum of patients with cystic fibrosis. Gastroenterology **88:**478-84.
139. **Frederiksen, B., C. Koch, and N. Hoiby.** 1997. Antibiotic treatment of initial colonization with Pseudomonas aeruginosa postpones chronic infection and prevents deterioration of pulmonary function in cystic fibrosis. Pediatr Pulmonol **23:**330-5.
140. **Frederiksen, B., C. Koch, and N. Hoiby.** 1999. Changing epidemiology of Pseudomonas aeruginosa infection in Danish cystic fibrosis patients (1974-1995). Pediatr Pulmonol **28:**159-66.
141. **Frederiksen, B., S. Lanng, C. Koch, and N. Hoiby.** 1996. Improved survival in the Danish center-treated cystic fibrosis patients: results of aggressive treatment. Pediatr Pulmonol **21:**153-8.
142. **Frydman, A. M., Y. Le Roux, M. A. Lefebvre, F. Djebbar, J. B. Fourtillan, and J. Gaillot.** 1986. Pharmacokinetics of pefloxacin after repeated intravenous and oral

administration (400 mg bid) in young healthy volunteers. J Antimicrob Chemother **17 Suppl B:**65-79.
143. **Fung-Tomc, J. C., E. Huczko, T. Stickle, B. Minassian, B. Kolek, K. Denbleyker, D. Bonner, and R. Kessler.** 1995. Antibacterial activities of cefprozil compared with those of 13 oral cephems and 3 macrolides. Antimicrob Agents Chemother **39:**533-8.
144. **Gaillard, J. L., P. Cahen, C. Delacourt, C. Silly, M. Le Bourgeois, C. Coustere, J. de Blic, G. Lenoir, and P. Scheinmann.** 1995. Correlation between activity of beta-lactam agents in vitro and bacteriological outcome in acute pulmonary exacerbations of cystic fibrosis. Eur J Clin Microbiol Infect Dis **14:**291-6.
145. **Garraffo, R., H. B. Drugeon, and D. Chiche.** 1997. Pharmacokinetics and pharmacodynamics of two oral forms of cefuroxime axetil. Fundam Clin Pharmacol **11:**90-5.
146. **Garrigues, T. M., U. Martin, J. E. Peris-Ribera, and L. F. Prescott.** 1991. Dose-dependent absorption and elimination of cefadroxil in man. Eur J Clin Pharmacol **41:**179-83.
147. **Georgopoulos, A., A. Buxbaum, U. Straschil, and W. Graninger.** 1998. Austrian national survey of prevalence of antimicrobial resistance among clinical isolates of Streptococcus pneumoniae 1994-96. Scand J Infect Dis **30:**345-9.
148. **Gerber, M. A.** 1986. A comparison of cefadroxil and penicillin V in the treatment of streptococcal pharyngitis in children. Drugs **32 Suppl 3:**29-32.
149. **Giamarellos-Bourboulis, E. J., P. Grecka, A. Tsitsika, C. Tympanidou, and H. Giamarellou.** 2000. In-vitro activity of FK 037 (Cefoselis), a novel 4(th) generation cephalosporin, compared to cefepime and cefpirome on nosocomial staphylococci and gram-negative isolates. Diagn Microbiol Infect Dis **36:**185-91.
150. **Giamarellou, H.** 1996. Clinical experience with the fourth generation cephalosporins. J Chemother **8 Suppl 2:**91-104.
151. **Gibson, R. L., J. L. Burns, and B. W. Ramsey.** 2003. Pathophysiology and management of pulmonary infections in cystic fibrosis. Am J Respir Crit Care Med **168:**918-51.
152. **Girard, P., and F. Mentré.** 2005. A comparison of estimation methods in nonlinear mixed effects models using a blind analysis. Abstr 834. PAGE. Abstracts of the Annual Meeting of the Population Approach Group in Europe **14**.
153. **Gobburu, J. V., and N. H. Holford.** 2001. Vz, the terminal phase volume: time for its terminal phase? J Biopharm Stat **11:**373-5.
154. **Gobburu, J. V., and J. Lawrence.** 2002. Application of resampling techniques to estimate exact significance levels for covariate selection during nonlinear mixed effects model building: some inferences. Pharm Res **19:**92-8.
155. **Goldfarb, J., R. C. Stern, M. D. Reed, T. S. Yamashita, C. M. Myers, and J. L. Blumer.** 1987. Ciprofloxacin monotherapy for acute pulmonary exacerbations of cystic fibrosis. Am J Med **82:**174-9.
156. **Gooch, W. M., 3rd, L. Kaminester, G. W. Cole, R. Binder, M. R. Morman, J. M. Swinehart, M. Wisniewski, H. M. Yilmaz, and J. J. Collins.** 1991. Clinical comparison of cefuroxime axetil, cephalexin and cefadroxil in the treatment of patients with primary infections of the skin or skin structures. Dermatologica **183:**36-43.
157. **Goodchild, M. C., G. M. Murphy, A. M. Howell, S. A. Nutter, and C. M. Anderson.** 1975. Aspects of bile acid metabolism in cystic fibrosis. Arch Dis Child **50:**769-78.
158. **Goossens, H.** 2000. MYSTIC (Meropenem Yearly Susceptibility Test Information Collection) results from Europe: comparison of antibiotic susceptibilities between countries and centre types. MYSTIC Study Group (European centres only). J Antimicrob Chemother **46 Suppl T2:**39-52.
159. **Gosden, C. M., and J. R. Gosden.** 1984. Fetal abnormalities in cystic fibrosis suggest a deficiency in proteolysis of cholecystokinin. Lancet **2:**541-6.
160. **Graham, G., I. Gueorguieva, and K. Dickens.** 2005. A program for the optimum design of pharmacokinetic, pharmacodynamic, drug metabolism and drug-drug interaction models. Comput Methods Programs Biomed **78:**237-49.
161. **Grahnen, A., M. Hammarlund, and T. Lundqvist.** 1984. Implications of intraindividual variability in bioavailability studies of furosemide. Eur J Clin Pharmacol **27:**595-602.

162. **Grant, E. M., J. L. Kuti, D. P. Nicolau, C. Nightingale, and R. Quintiliani.** 2002. Clinical efficacy and pharmacoeconomics of a continuous-infusion piperacillin-tazobactam program in a large community teaching hospital. Pharmacotherapy **22:**471-83.
163. **Green, B., and S. B. Duffull.** 2003. Prospective evaluation of a D-optimal designed population pharmacokinetic study. J Pharmacokinet Pharmacodyn **30:**145-61.
164. **Green, B., and S. B. Duffull.** 2004. What is the best size descriptor to use for pharmacokinetic studies in the obese? Br J Clin Pharmacol **58:**119-33.
165. **Griese, M., I. Muller, and D. Reinhardt.** 2002. Eradication of initial Pseudomonas aeruginosa colonization in patients with cystic fibrosis. Eur J Med Res **7:**79-80.
166. **Guard, R. W., F. A. Khafagi, M. C. Brigden, and L. R. Ashdown.** 1984. Melioidosis in Far North Queensland. A clinical and epidemiological review of twenty cases. Am J Trop Med Hyg **33:**467-73.
167. **Guggenbichler, J. P., and G. Kienel.** 1979. Bioavailability of oral antibiotics in cystic fibrosis. Monogr Paediatr **10:**34-40.
168. **Guignard, J. P., A. Torrado, S. M. Mazouni, and E. Gautier.** 1976. Renal function in respiratory distress syndrome. J Pediatr **88:**845-50.
169. **Gumbo, T., A. Louie, M. R. Deziel, L. M. Parsons, M. Salfinger, and G. L. Drusano.** 2004. Selection of a moxifloxacin dose that suppresses drug resistance in Mycobacterium tuberculosis, by use of an in vitro pharmacodynamic infection model and mathematical modeling. J Infect Dis **190:**1642-51.
170. **Hadorn, B., G. Zoppi, D. H. Shmerling, A. Prader, I. McIntyre, and C. M. Anderson.** 1968. Quantitative assessment of exocrine pancreatic function in infants and children. J Pediatr **73:**39-50.
171. **Hallynck, T. H., H. H. Soep, J. A. Thomis, J. Boelaert, R. Daneels, and L. Dettli.** 1981. Should clearance be normalised to body surface or to lean body mass? Br J Clin Pharmacol **11:**523-6.
172. **Hampel, B., H. Lode, J. Wagner, and P. Koeppe.** 1982. Pharmacokinetics of cefadroxil and cefaclor during an eight-day dosage period. Antimicrob Agents Chemother **22:**1061-3.
173. **Hanaki, H., H. Akagi, Y. Masaru, T. Otani, A. Hyodo, and K. Hiramatsu.** 1995. TOC-39, a novel parenteral broad-spectrum cephalosporin with excellent activity against methicillin-resistant Staphylococcus aureus. Antimicrob Agents Chemother **39:**1120-6.
174. **Hansch, C., A. Leo, and D. Hoekman.** 1995. Exploring QSAR: hydrophobic, electronic abd steric constants. American Chemical Society, Washington.
175. **Hanzlik, P. J.** 1912. The absorption of sodium iodide. J. Pharmacol. Exptl. Therap. **3:**387-421.
176. **Hanzlik, P. J., G. L. Laqueur, and H. B. Moy.** 1950. Phenobarbital administered continuously with and without deficient diets. Stanford Med Bull **8:**133-43.
177. **Hara, T., H. Saeki, A. Yamamoto, K. Ohta, T. Suzuki, M. Ara, M. Sugawara, Y. Sano, H. Sakuma, and K. Satoh.** 1988. Concentrations of cefuroxime in the skin. Jpn J Antibiot **41:**10-7.
178. **Harding, S. M., A. J. Monro, J. E. Thornton, A. J. Munro, and M. I. J. Hogg.** 1981. The comparative pharmacokinetics of ceftazidime and cefotaxime in healthy volunteers. J Antimicrob Chemother **8 (Suppl. B):**262-272.
179. **Hardman, J. G., L. E. Limbird, P. B. Molinoff, R. W. Ruddon, and A. Goodman Gilman.** 1996. Goodman & Gilman's: The pharmacological basis of therapeutics, 9th ed. McGraw-Hill, New York.
180. **Hasegawa, K., K. Yamamoto, N. Chiba, R. Kobayashi, K. Nagai, M. R. Jacobs, P. C. Appelbaum, K. Sunakawa, and K. Ubukata.** 2003. Diversity of ampicillin-resistance genes in Haemophilus influenzae in Japan and the United States. Microb Drug Resist **9:**39-46.
181. **Hausman, M. S.** 1980. Treatment of urinary infections with cefadroxil: controlled comparison of high-compliance oral dosage regimens. Urology **15:**40-3.
182. **Hedman, A., Y. Adan-Abdi, G. Alvan, B. Strandvik, and A. Arvidsson.** 1988. Influence of the glomerular filtration rate on renal clearance of ceftazidime in cystic fibrosis. Clin Pharmacokinet **15:**57-65.

183. **Hedman, A., G. Alvan, B. Strandvik, and A. Arvidsson.** 1990. Increased renal clearance of cefsulodin due to higher glomerular filtration rate in cystic fibrosis. Clin Pharmacokinet **18:**168-75.
184. **Hemmingsen, A. M.** 1950. Rep. Stenographic Mem. Hosp. (Copenhagen) **4:**1-58.
185. **Henwood, C. J., D. M. Livermore, D. James, and M. Warner.** 2001. Antimicrobial susceptibility of Pseudomonas aeruginosa: results of a UK survey and evaluation of the British Society for Antimicrobial Chemotherapy disc susceptibility test. J Antimicrob Chemother **47:**789-99.
186. **Hoban, D. J., S. K. Bouchillon, J. L. Johnson, G. G. Zhanel, D. L. Butler, K. A. Saunders, L. A. Miller, and J. A. Poupard.** 2003. Comparative in vitro potency of amoxycillin-clavulanic acid and four oral agents against recent North American clinical isolates from a global surveillance study. Int J Antimicrob Agents **21:**425-33.
187. **Hoban, D. J., S. K. Bouchillon, J. L. Johnson, G. G. Zhanel, D. L. Butler, K. A. Saunders, L. A. Miller, and J. A. Poupard.** 2003. Comparative in vitro surveillance of amoxicillin-clavulanic acid and four oral comparators against 21232 clinical isolates from europe. Eur J Clin Microbiol Infect Dis **22:**261-7.
188. **Hodson, M. E., C. M. Roberts, R. J. Butland, M. J. Smith, and J. C. Batten.** 1987. Oral ciprofloxacin compared with conventional intravenous treatment for Pseudomonas aeruginosa infection in adults with cystic fibrosis. Lancet **1:**235-7.
189. **Hoeger, P. H.** 2004. Antimicrobial susceptibility of skin-colonizing S. aureus strains in children with atopic dermatitis. Pediatr Allergy Immunol **15:**474-7.
190. **Hoffken, G., H. Lode, C. Prinzing, K. Borner, and P. Koeppe.** 1985. Pharmacokinetics of ciprofloxacin after oral and parenteral administration. Antimicrob Agents Chemother **27:**375-9.
191. **Hoiby, N.** 1993. Antibiotic therapy for chronic infection of pseudomonas in the lung. Annu Rev Med **44:**1-10.
192. **Hoiby, N., B. Frederiksen, and T. Pressler.** 2005. Eradication of early Pseudomonas aeruginosa infection. J Cyst Fibros **4 Suppl 2:**49-54.
193. **Holford, N. H.** 1996. A size standard for pharmacokinetics. Clin Pharmacokinet **30:**329-32.
194. **Holford, N. H.** 2001. Target concentration intervention: beyond Y2K. Br J Clin Pharmacol **52 Suppl 1:**55S-59S.
195. **Holford, N. H.** 1999. Target concentration intervention: beyond Y2K. Br J Clin Pharmacol **48:**9-13.
196. **Holford, N. H., R. J. Ambros, and K. Stoeckel.** 1992. Models for describing absorption rate and estimating extent of bioavailability: application to cefetamet pivoxil. J Pharmacokinet Biopharm **20:**421-42.
197. **Holford, N. H., and L. B. Sheiner.** 1982. Kinetics of pharmacologic response. Pharmacol Ther **16:**143-66.
198. **Holford, N. H. G.** 2003, posting date. Individualization: Why, How, When? The Role of Between and Within Subject Variability in Using Drug Concentration Measurements to Individualize Dose. [Online.]
199. **Holland, D. J., A. Wesley, D. Drinkovic, and B. J. Currie.** 2002. Cystic Fibrosis and Burkholderia pseudomallei Infection: An Emerging Problem? Clin Infect Dis **35:**e138-40.
200. **Hoogkamp-Korstanje, J. A., and J. van der Laag.** 1983. Piperacillin and tobramycin in the treatment of Pseudomonas lung infections in cystic fibrosis. J Antimicrob Chemother **12:**175-83.
201. **Howe, C., A. Sampath, and M. Spotnitz.** 1971. The pseudomallei group: a review. J Infect Dis **124:**598-606.
202. **Hu, T. M., and W. L. Hayton.** 2001. Allometric scaling of xenobiotic clearance: uncertainty versus universality. AAPS PharmSci **3:**E29.
203. **Huls, C. E., R. A. Prince, D. K. Seilheimer, and J. A. Bosso.** 1993. Pharmacokinetics of cefepime in cystic fibrosis patients. Antimicrob Agents Chemother **37:**1414-6.
204. **Humbert, G., A. Leroy, J. P. Fillastre, and M. Godin.** 1979. Pharmacokinetics of cefadroxil in normal subjects and in patients with renal insufficiency. Chemotherapy **25:**189-95.

205. **Huppertz, K., and B. Wiedemann.** 2000. GENARS-Project established. Chemotherapie Journal **9:**200-121.
206. **Husson, M. O., A. Fruchart, and D. Izard.** 1998. Comparative study of the bactericidal activity of cefepime and cefpirome in association with glycopeptides against Staphylococci sensitive and resistant to methicillin. Pathol Biol (Paris) **46:**279-83.
207. **Hutabarat, R. M., J. D. Unadkat, C. Sahajwalla, S. McNamara, B. Ramsey, and A. L. Smith.** 1991. Disposition of drugs in cystic fibrosis. I. Sulfamethoxazole and trimethoprim. Clin Pharmacol Ther **49:**402-9.
208. **Idkaidek, N. M., A. Al-Ghazawi, and N. M. Najib.** 2004. Bioequivalence evaluation of two brands of amoxicillin/clavulanic acid 250/125 mg combination tablets in healthy human volunteers: use of replicate design approach. Biopharm Drug Dispos **25:**367-72.
209. **Igari, J., T. Oguri, N. Hiramatsu, K. Akiyama, and T. Koyama.** 2003. Post-marketing surveillance of antibacterial activities of cefozopran against various clinical isolates--II. Gram-negative bacteria. Jpn J Antibiot **56:**458-96.
210. **Ikemoto, H., K. Watanabe, T. Mori, J. Igari, T. Oguri, H. Kawaguchi, Y. Shimizu, H. Matsumiya, A. Saito, T. Terai, H. Inoue, T. Nakadate, C. Ito, T. Yosida, Y. Tanno, I. Ohno, K. Nishioka, M. Arakawa, K. Igarashi, K. Wada, M. Okada, K. Ozaki, N. Aoki, N. Kitamura, M. Touyama, and et al.** 1997. Susceptibilities of bacteria isolated from patients with respiratory infectious diseases to antibiotics (1995). Jpn J Antibiot **50:**421-59.
211. **Ikemoto, H., K. Watanabe, T. Mori, J. Igari, T. Oguri, K. Kobayashi, K. Satou, H. Matsumiya, A. Saito, T. Terai, Y. Tanno, K. Nishioka, M. Arakawa, K. Wada, M. Okada, K. Ozaki, N. Aoki, N. Kitamura, O. Sekine, Y. Suzuki, M. Matsuda, H. Tanimoto, K. Nakata, Y. Nakamori, N. Kusano, and et al.** 1996. Susceptibilities of bacteria isolated from patients with respiratory infectious diseases to antibiotics (1994). Jpn J Antibiot **49:**419-55.
212. **Ikemoto, H., K. Watanabe, T. Mori, J. Igari, T. Oguri, K. Kobayashi, K. Satou, H. Matsumiya, A. Saito, T. Terai, Y. Tanno, K. Nishioka, M. Arakawa, K. Wada, M. Okada, K. Ozaki, N. Aoki, N. Kitamura, O. Sekine, Y. Suzuki, H. Tanimoto, K. Nakata, Y. Nakamori, T. Nakatani, N. Kusano, and et al.** 1996. Susceptibilities of bacteria isolated from patients with respiratory infectious diseases to antibiotics (1992). Jpn J Antibiot **49:**34-70.
213. **Ikemoto, H., K. Watanabe, T. Mori, J. Igari, T. Oguri, Y. Shimizu, T. Terai, H. Inoue, T. Nakadate, C. Ito, T. Yoshida, I. Ohno, Y. Tanno, M. Arakawa, K. Igarashi, M. Okada, K. Ozaki, N. Aoki, N. Kitamura, O. Sekine, Y. Suzuki, K. Nakata, T. Nakatani, H. Inagawa, and N. Kusano.** 1998. Susceptibilities of bacteria isolated from patients with lower respiratory infectious diseases to antibiotics (1996). Jpn J Antibiot **51:**437-74.
214. **Ishii, Y., J. Alba, S. Kimura, K. Shiroto, and K. Yamaguchi.** 2005. Evaluation of antimicrobial activity of beta-lactam antibiotics using Etest against clinical isolates from 60 medical centres in Japan. Int J Antimicrob Agents **25:**296-301.
215. **Isles, A., M. Spino, E. Tabachnik, H. Levison, J. Thiessen, and S. MacLeod.** 1983. Theophylline disposition in cystic fibrosis. Am Rev Respir Dis **127:**417-21.
216. **Ison, C. A., J. W. Mouton, K. Jones, K. A. Fenton, and D. M. Livermore.** 2004. Which cephalosporin for gonorrhoea? Sex Transm Infect **80:**386-8.
217. **Jackson, M. A., H. Kusmiesz, S. Shelton, C. Prestidge, R. I. Kramer, and J. D. Nelson.** 1986. Comparison of piperacillin vs. ticarcillin plus tobramycin in the treatment of acute pulmonary exacerbations of cystic fibrosis. Pediatr Infect Dis **5:**440-3.
218. **Jacobs, M. R.** 2003. How can we predict bacterial eradication? Int J Infect Dis **7 Suppl 1:**S13-20.
219. **Jacobs, M. R., S. Bajaksouzian, A. Zilles, G. Lin, G. A. Pankuch, and P. C. Appelbaum.** 1999. Susceptibilities of Streptococcus pneumoniae and Haemophilus influenzae to 10 oral antimicrobial agents based on pharmacodynamic parameters: 1997 U.S. Surveillance study. Antimicrob Agents Chemother **43:**1901-8.

220. **Jaehde, U., F. Sorgel, U. Stephan, and W. Schunack.** 1994. Effect of an antacid containing magnesium and aluminum on absorption, metabolism, and mechanism of renal elimination of pefloxacin in humans. Antimicrob Agents Chemother **38:**1129-33.
221. **James, N. C., K. H. Donn, J. J. Collins, I. M. Davis, T. L. Lloyd, R. W. Hart, and J. R. Powell.** 1991. Pharmacokinetics of cefuroxime axetil and cefaclor: relationship of concentrations in serum to MICs for common respiratory pathogens. Antimicrob Agents Chemother **35:**1860-3.
222. **James, W.** 1976. Research on Obesity. Her Majesty's Stationery Office, London.
223. **Janmahasatian, S.** 2005. Quantification of Lean Body Weight (thesis). The University of Queensland, Brisbane.
224. **Janmahasatian, S., S. B. Duffull, S. Ash, L. C. Ward, N. M. Byrne, and B. Green.** 2005. Quantification of lean bodyweight. Clin Pharmacokinet **44:**1051-65.
225. **Jaruratanasirikul, S., and S. Sriwiriyajan.** 2003. Comparison of the pharmacodynamics of meropenem in healthy volunteers following administration by intermittent infusion or bolus injection. J Antimicrob Chemother **52:**518-21.
226. **Jennings, M. B., J. M. McCarty, N. M. Scheffler, A. D. Puopolo, and C. D. Rothermel.** 2003. Comparison of azithromycin and cefadroxil for the treatment of uncomplicated skin and skin structure infections. Cutis **72:**240-4.
227. **Jensen, T., S. S. Pedersen, C. H. Nielsen, N. Hoiby, and C. Koch.** 1987. The efficacy and safety of ciprofloxacin and ofloxacin in chronic Pseudomonas aeruginosa infection in cystic fibrosis. J Antimicrob Chemother **20:**585-94.
228. **Johansen, H. K., and N. Hoiby.** 1992. Seasonal onset of initial colonisation and chronic infection with Pseudomonas aeruginosa in patients with cystic fibrosis in Denmark. Thorax **47:**109-11.
229. **Johansen, H. K., L. Norregaard, P. C. Gotzsche, T. Pressler, C. Koch, and N. Hoiby.** 2004. Antibody response to Pseudomonas aeruginosa in cystic fibrosis patients: a marker of therapeutic success?--A 30-year cohort study of survival in Danish CF patients after onset of chronic P. aeruginosa lung infection. Pediatr Pulmonol **37:**427-32.
230. **Johnson, C. A., C. E. Halstenson, J. S. Kelloway, B. E. Shapiro, S. W. Zimmerman, A. Tonelli, R. Faulkner, A. Dutta, J. Haynes, D. S. Greene, and et al.** 1992. Single-dose pharmacokinetics of piperacillin and tazobactam in patients with renal disease. Clin Pharmacol Ther **51:**32-41.
231. **Johnson, D. M., D. J. Biedenbach, M. L. Beach, M. A. Pfaller, and R. N. Jones.** 2000. Antimicrobial activity and in vitro susceptibility test development for cefditoren against Haemophilus influenzae, Moraxella catarrhalis, and Streptococcus species. Diagn Microbiol Infect Dis **37:**99-105.
232. **Jones, M. E., R. S. Blosser-Middleton, I. A. Critchley, J. A. Karlowsky, C. Thornsberry, and D. F. Sahm.** 2003. In vitro susceptibility of Streptococcus pneumoniae, Haemophilus influenzae and Moraxella catarrhalis: a European multicenter study during 2000-2001. Clin Microbiol Infect **9:**590-9.
233. **Jones, R. N.** 1999. Summation: beta-lactam resistance surveillance in the Asia-Western Pacific region. Diagn Microbiol Infect Dis **35:**333-8.
234. **Jones, R. N., M. R. Jacobs, J. A. Washington, and M. A. Pfaller.** 1997. A 1994-95 survey of Haemophilus influenzae susceptibility to ten orally administered agents. A 187 clinical laboratory center sample in the United States. Diagn Microbiol Infect Dis **27:**75-83.
235. **Jones, R. N., M. A. Pfaller, S. D. Allen, E. H. Gerlach, P. C. Fuchs, and K. E. Aldridge.** 1991. Antimicrobial activity of cefpirome. An update compared to five third-generation cephalosporins against nearly 6000 recent clinical isolates from five medical centers. Diagn Microbiol Infect Dis **14:**361-4.
236. **Jones, R. N., C. M. Rubino, S. M. Bhavnani, and P. G. Ambrose.** 2003. Worldwide antimicrobial susceptibility patterns and pharmacodynamic comparisons of gatifloxacin and levofloxacin against Streptococcus pneumoniae: report from the Antimicrobial Resistance Rate Epidemiology Study Team. Antimicrob Agents Chemother **47:**292-6.
237. **Jones, R. N., and W. R. Wilson.** 1998. Epidemiology, laboratory detection, and therapy of penicillin-resistant streptococcal infections. Diagn Microbiol Infect Dis **31:**453-9.

238. **Jonsson, E. N., J. R. Wade, and M. O. Karlsson.** 2000. Nonlinearity detection: advantages of nonlinear mixed-effects modeling. AAPS PharmSci **2:**E32.
239. **Jumbe, N., A. Louie, R. Leary, W. Liu, M. R. Deziel, V. H. Tam, R. Bachhawat, C. Freeman, J. B. Kahn, K. Bush, M. N. Dudley, M. H. Miller, and G. L. Drusano.** 2003. Application of a mathematical model to prevent in vivo amplification of antibiotic-resistant bacterial populations during therapy. J Clin Invest **112:**275-85.
240. **Jumbe, N. L., A. Louie, M. H. Miller, W. Liu, M. R. Deziel, V. H. Tam, R. Bachhawat, and G. L. Drusano.** 2006. Quinolone efflux pumps play a central role in emergence of fluoroquinolone resistance in Streptococcus pneumoniae. Antimicrob Agents Chemother **50:**310-7.
241. **Jusko, W. J., L. L. Mosovich, L. M. Gerbracht, M. E. Mattar, and S. J. Yaffe.** 1975. Enhanced renal excretion of dicloxacillin in patients with cystic fibrosis. Pediatrics **56:**1038-44.
242. **Kahlmeter, G.** 2003. An international survey of the antimicrobial susceptibility of pathogens from uncomplicated urinary tract infections: the ECO.SENS Project. J Antimicrob Chemother **51:**69-76.
243. **Kaplan, S. L., B. Afghani, P. Lopez, E. Wu, D. Fleishaker, B. Edge-Padbury, S. Naberhuis-Stehouwer, and J. B. Bruss.** 2003. Linezolid for the treatment of methicillin-resistant Staphylococcus aureus infections in children. Pediatr Infect Dis J **22:**S178-85.
244. **Karlsson, M. O., and L. B. Sheiner.** 1994. Estimating bioavailability when clearance varies with time. Clin Pharmacol Ther **55:**623-37.
245. **Karlsson, M. O., and L. B. Sheiner.** 1993. The importance of modeling interoccasion variability in population pharmacokinetic analyses. J Pharmacokinet Biopharm **21:**735-50.
246. **Kataoka, D., and Y. Tanaka.** 2004. The combination of aztreonam and cefozopran against Stenotrophomonas maltophilia. J Infect Chemother **10:**62-4.
247. **Kattwinkel, J., L. M. Taussig, B. E. Statland, and J. I. Verter.** 1973. The effects of age on alkaline phosphatase and other serologic liver function tests in normal subjects and patients with cystic fibrosis. J Pediatr **82:**234-42.
248. **Kavi, J., J. M. Andrews, J. P. Ashby, G. Hillman, and R. Wise.** 1988. Pharmacokinetics and tissue penetration of cefpirome, a new cephalosporin. J Antimicrob Chemother **22:**911-6.
249. **Kearns, G. L.** 1993. Hepatic drug metabolism in cystic fibrosis: recent developments and future directions. Ann Pharmacother **27:**74-9.
250. **Kearns, G. L., W. R. Crom, K. H. Karlson, Jr., G. B. Mallory, Jr., and W. E. Evans.** 1996. Hepatic drug clearance in patients with mild cystic fibrosis. Clin Pharmacol Ther **59:**529-40.
251. **Kearns, G. L., B. C. Hilman, and J. T. Wilson.** 1982. Dosing implications of altered gentamicin disposition in patients with cystic fibrosis. J Pediatr **100:**312-8.
252. **Kemmerich, B., H. Warns, H. Lode, K. Borner, P. Koeppe, and H. Knothe.** 1983. Multiple-dose pharmacokinetics of ceftazidime and its influence on fecal flora. Antimicrob Agents Chemother **24:**333-8.
253. **Kercsmar, C. M., R. C. Stern, M. D. Reed, C. M. Myers, D. Murdell, and J. L. Blumer.** 1983. Ceftazidime in cystic fibrosis: pharmacokinetics and therapeutic response. J Antimicrob Chemother **12 Suppl A:**289-95.
254. **Kiffer, C. R., C. Mendes, J. L. Kuti, and D. P. Nicolau.** 2004. Pharmacodynamic comparisons of antimicrobials against nosocomial isolates of escherichia coli, klebsiella pneumoniae, acinetobacter baumannii and pseudomonas aeruginosa from the MYSTIC surveillance program: the OPTAMA Program, South America 2002. Diagn Microbiol Infect Dis **49:**109-16.
255. **Kim, M. K., C. Nightingale, and D. Nicolau.** 2003. Influence of sex on the pharmacokinetic interaction of fleroxacin and ciprofloxacin with caffeine. Clin Pharmacokinet **42:**985-96.
256. **Kimura, T., T. Yamamoto, M. Mizuno, Y. Suga, S. Kitade, and H. Sezaki.** 1983. Characterization of aminocephalosporin transport across rat small intestine. J Pharmacobiodyn **6:**246-53.
257. **Kirby, W. M.** 1945. Bacteriostatic and lytic actions of penicillin on sensitive and resistant staphylococci. J Clin Invest **24:**165-169.

258. **Kleiber, M.** 1932. Body size and metabolism. Hilgardia **6:**315-353.
259. **Kleiber, M.** 1961. The Fire of Life. John Wiley and Sons, Inc., New York, London.
260. **Koeppe, P., D. Hoffler, and K. Strobel.** 1987. Pharmacokinetics and dose recommendations of carumonam in renal failure. Arzneimittelforschung **37:**65-9.
261. **Koeth, L. M., D. Felmingham, M. R. Jacobs, and F. Rossi.** 2004. Antimicrobial resistance of Streptococcus pneumoniae and Haemophilus influenzae in Sao Paulo, Brazil from 1996 to 2000. Int J Antimicrob Agents **23:**356-61.
262. **Kruger-Thiemer, E.** 1957. Possibilities of biochemical reactions of isoniazid. Beitr Klin Tuberk Spezif Tuberkuloseforsch **117:**179-86.
263. **Kruger-Thiemer, E., and P. Bunger.** 1965. The role of the therapeutic regimen in dosage design. I. Chemotherapy **10:**61-73.
264. **Kruger-Thiemer, E., and P. Bunger.** 1965. The role of the therapeutic regimen in dosage design. II. Chemotherapy **10:**129-44.
265. **Kumamoto, Y., T. Hirose, A. Yokoo, Y. Hikichi, S. Shigeta, Y. Shiraiwa, H. Kameoka, H. Yoshida, H. Tazaki, H. Iri, H. Uchida, Y. Kobayashi, S. Matsuda, M. Fujime, K. Fujita, R. Kitagawa, J. Igari, T. Oguri, N. Kosakai, K. Yamaguchi, F. Kashitani, S. Yonezu, Y. Yamanaka, M. Takaha, F. Iori, and et al.** 1996. Comparative studies on activities of antimicrobial agents against causative organisms isolated from patients with urinary tract infections (1994). I. Susceptibility distribution. Jpn J Antibiot **49:**465-93.
266. **Kumamoto, Y., T. Tsukamoto, T. Hirose, A. Yokoo, M. Fujime, K. Fujita, S. Shigeta, J. Watanabe, J. Igari, M. Ogiwara, K. Ishibashi, T. Oguri, H. Yoshida, Y. Imafuku, K. Yamaguchi, T. Matsumoto, F. Kashitani, M. Murai, H. Ooe, M. Nishikawa, K. Watanabe, Y. Kobayashi, H. Uchida, T. Oka, C. Mochida, and et al.** 1999. Comparative studies on activities of antimicrobial agents against causative organisms isolated from patients with urinary tract infections (1997). I. Susceptibility distribution. Jpn J Antibiot **52:**93-129.
267. **Kumamoto, Y., T. Tsukamoto, M. Matsukawa, Y. Kunishima, T. Hirose, O. Yamaguti, K. Ishibashi, S. Shigeta, T. Suzutani, H. Yoshida, Y. Imafuku, M. Murai, K. Watanabe, Y. Kobayashi, H. Uchida, S. Matsuda, S. Sato, M. Fujime, K. Fujita, J. Igari, T. Oguri, K. Yamaguchi, N. Furuya, T. Deguchi, S. Ishihara, H. Ooe, M. Nishikawa, T. Oka, M. Kitamura, Y. Fukuhara, S. Kamidono, S. Arakawa, H. Kumon, K. Monden, T. Matsumoto, K. Takahashi, S. Naito, T. Egashira, S. Kohno, Y. Miyazaki, Y. Hirakata, and S. Aoki.** 2004. Comparative studies on activities of antimicrobial agents against causative organisms isolated from patients with urinary tract infections (2002). I. Susceptibility distribution. Jpn J Antibiot **57:**246-74.
268. **Kumamoto, Y., T. Tsukamoto, K. Watanabe, Y. Kobayashi, T. Hirose, M. Matsukawa, H. Uchida, S. Takahashi, Y. Kunishima, S. Matsuda, S. Sato, M. Ogihara, K. Ishibashi, S. Shigeta, M. Fujime, K. Fujita, H. Yoshida, Y. Imafuku, J. Igari, M. Murai, T. Oguri, K. Yamaguchi, T. Matsumoto, F. Kashitani, T. Furuhama, H. Kumon, K. Monden, H. Ooe, M. Nishikawa, S. Kohno, Y. Miyazaki, K. Izumikawa, T. Yamaguchi, C. Mochida, T. Oka, M. Kitamura, Y. Takano, and Y. Matsuoka.** 2001. Comparative studies on activities of antimicrobial agents against causative organisms isolated from patients with urinary tract infections (1999). I. Susceptibility distribution. Jpn J Antibiot **54:**185-216.
269. **Kumamoto, Y., T. Tsukamoto, K. Watanabe, Y. Kobayashi, M. Matsukawa, H. Uchida, Y. Kunishima, T. Hirose, S. Matsuda, S. Sato, S. Shigeta, M. Fujime, K. Fujita, O. Yamaguti, M. Ogihara, K. Ishibashi, J. Igari, K. Takahashi, T. Oguri, H. Yoshida, Y. Imafuku, K. Yamaguchi, N. Furuya, F. Kashitani, M. Murai, H. Ooe, M. Nishikawa, H. Kumon, K. Monden, T. Oka, M. Kitamura, S. Kohno, K. Tomono, Y. Miyazaki, Y. Matsuoka, Y. Fukuhara, Y. Hirakata, and S. Aoki.** 2003. Comparative studies on activities of antimicrobial agents against causative organisms isolated from patients with urinary tract infections (2001). I. Susceptibility distribution. Jpn J Antibiot **56:**396-423.
270. **Kurz, C. C., W. Marget, K. Harms, and R. M. Bertele.** 1986. A cross-over study on the effectiveness of ofloxacin and ciprofloxacin administered orally. Infection **14 Suppl 1:**S82-6.

271. **Kuti, J. L., P. K. Dandekar, C. H. Nightingale, and D. P. Nicolau.** 2003. Use of Monte Carlo simulation to design an optimized pharmacodynamic dosing strategy for meropenem. J Clin Pharmacol **43:**1116-23.
272. **Kuti, J. L., C. H. Nightingale, R. F. Knauft, and D. P. Nicolau.** 2004. Pharmacokinetic properties and stability of continuous-infusion meropenem in adults with cystic fibrosis. Clin Ther **26:**493-501.
273. **Kuti, J. L., C. H. Nightingale, and D. P. Nicolau.** 2004. Optimizing pharmacodynamic target attainment using the MYSTIC antibiogram: data collected in North America in 2002. Antimicrob Agents Chemother **48:**2464-70.
274. **Kuti, J. L., C. H. Nightingale, R. Quintiliani, and D. P. Nicolau.** 2002. Pharmacodynamic profiling of continuously infused piperacillin/tazobactam against Pseudomonas aeruginosa using Monte Carlo analysis. Diagn Microbiol Infect Dis **44:**51-7.
275. **Kuzemko, J., and C. Crawford.** 1989. Continuous infusion of ceftazidime in cystic fibrosis. Lancet **2:**385.
276. **La Rosa, F., S. Ripa, M. Prenna, A. Ghezzi, and M. Pfeffer.** 1982. Pharmacokinetics of cefadroxil after oral administration in humans. Antimicrob Agents Chemother **21:**320-2.
277. **Lacy, M. K., W. Lu, X. Xu, P. R. Tessier, D. P. Nicolau, R. Quintiliani, and C. H. Nightingale.** 1999. Pharmacodynamic comparisons of levofloxacin, ciprofloxacin, and ampicillin against Streptococcus pneumoniae in an in vitro model of infection. Antimicrob Agents Chemother **43:**672-7.
278. **Larsen, G. L., R. J. Barron, R. A. Landay, E. K. Cotton, M. A. Gonzalez, and J. G. Brooks.** 1980. Intravenous aminophylline in patients with cystic fibrosis. Pharmacokinetics and effect on pulmonary function. Am J Dis Child **134:**1143-8.
279. **LeBel, M.** 1991. Fluoroquinolones in the treatment of cystic fibrosis: a critical appraisal. Eur J Clin Microbiol Infect Dis **10:**316-24.
280. **LeBel, M., M. G. Bergeron, F. Vallee, C. Fiset, G. Chasse, P. Bigonesse, and G. Rivard.** 1986. Pharmacokinetics and pharmacodynamics of ciprofloxacin in cystic fibrosis patients. Antimicrob Agents Chemother **30:**260-6.
281. **Leclercq-Foucart, J., P. Forget, F. Sodoyez-Goffaux, and A. Zappitelli.** 1986. Intestinal permeability to [51Cr]EDTA in children with cystic fibrosis. J Pediatr Gastroenterol Nutr **5:**384-7.
282. **Leeder, J. S., M. Spino, A. F. Isles, A. M. Tesoro, R. Gold, and S. M. MacLeod.** 1984. Ceftazidime disposition in acute and stable cystic fibrosis. Clin Pharmacol Ther **36:**355-62.
283. **Lees, C. M., and R. L. Smyth.** 2000. The current management of cystic fibrosis. Int J Clin Pract **54:**171-9.
284. **Lemmen, S. W., I. Engels, and F. D. Daschner.** 1997. Serum bactericidal activity of ceftazidime administered as continuous infusion of 3 g over 24 h versus intermittent bolus infusion of 2 g against Pseudomonas aeruginosa in healthy volunteers. J Antimicrob Chemother **39:**841-2.
285. **Lesmana, M., C. I. Lebron, D. Taslim, P. Tjaniadi, D. Subekti, M. O. Wasfy, J. R. Campbell, and B. A. Oyofo.** 2001. In vitro antibiotic susceptibility of Neisseria gonorrhoeae in Jakarta, Indonesia. Antimicrob Agents Chemother **45:**359-62.
286. **Levy, J., A. L. Smith, J. R. Koup, J. Williams-Warren, and B. Ramsey.** 1984. Disposition of tobramycin in patients with cystic fibrosis: a prospective controlled study. J Pediatr **105:**117-24.
287. **Lewis, M. T., K. Yamaguchi, D. J. Biedenbach, and R. N. Jones.** 1999. In vitro evaluation of cefepime and other broad-spectrum beta-lactams in 22 medical centers in Japan: a phase II trial comparing two annual organism samples. The Japan Antimicrobial Resistance Study Group. Diagn Microbiol Infect Dis **35:**307-15.
288. **Liassine, N., J. Bille, C. Breer, R. Frei, J. Wust, and R. Auckenthaler.** 1997. In vitro activity of cefpirome against microorganisms isolated in haematology, oncology and intensive care units in Switzerland. Scand J Infect Dis **29:**615-21.
289. **Lietman, P. S.** 1988. Pharmacokinetics of antimicrobial drugs in cystic fibrosis. Beta-lactam antibiotics. Chest **94:**115S-120S.

290. **Linder, C. W., K. Nelson, S. Paryani, J. R. Stallworth, and J. L. Blumer.** 1993. Comparative evaluation of cefadroxil and cephalexin in children and adolescents with pyodermas. Cefadroxil Once Daily Pyoderma Study Group. Clin Ther **15:**46-56.
291. **Lipman, J., C. D. Gomersall, T. Gin, G. M. Joynt, and R. J. Young.** 1999. Continuous infusion ceftazidime in intensive care: a randomized controlled trial. J Antimicrob Chemother **43:**309-11.
292. **Lister, P. D., and C. C. Sanders.** 1999. Pharmacodynamics of levofloxacin and ciprofloxacin against Streptococcus pneumoniae. J Antimicrob Chemother **43:**79-86.
293. **Lister, P. D., and C. C. Sanders.** 1999. Pharmacodynamics of trovafloxacin, ofloxacin, and ciprofloxacin against Streptococcus pneumoniae in an in vitro pharmacokinetic model. Antimicrob Agents Chemother **43:**1118-23.
294. **Llanes, R., J. Sosa, D. Guzman, A. Llop, E. A. Valdes, I. Martinez, S. Palma, and M. I. Lantero.** 2003. Antimicrobial susceptibility of Neisseria gonorrhoeae in Cuba (1995-1999): implications for treatment of gonorrhea. Sex Transm Dis **30:**10-4.
295. **Lode, H., R. Stahlmann, G. Dzwillo, and P. Koeppe.** 1980. Comparative pharmacokinetics of oral cephalosporins: cephalexin, cefaclor and cefadroxil. Arzneimittelforschung **30:**505-9.
296. **Lode, H., R. Stahlmann, and P. Koeppe.** 1979. Comparative pharmacokinetics of cephalexin, cefaclor, cefadroxil, and CGP 9000. Antimicrob Agents Chemother **16:**1-6.
297. **Lodise, T. P., Jr., B. Lomaestro, K. A. Rodvold, L. H. Danziger, and G. L. Drusano.** 2004. Pharmacodynamic profiling of piperacillin in the presence of tazobactam in patients through the use of population pharmacokinetic models and Monte Carlo simulation. Antimicrob Agents Chemother **48:**4718-24.
298. **Maass, L., V. Malerczyk, and M. Verho.** 1987. Pharmacokinetics of cefpirome (HR 810), a new cephalosporin derivative administered intramuscularly and intravenously to healthy volunteers. Infection **15:**207-10.
299. **Maass, L., V. Malerczyk, M. Verho, P. Hajdu, K. Seeger, and N. Klesel.** 1987. Dose linearity testing of intravenous cefpirome (HR 810), a novel cephalosporin derivate. Infection **15:**202-6.
300. **MacGowan, A. P., and K. E. Bowker.** 1998. Continuous infusion of beta-lactam antibiotics. Clin Pharmacokinet **35:**391-402.
301. **MacGowan, A. P., and R. Wise.** 2001. Establishing MIC breakpoints and the interpretation of in vitro susceptibility tests. J Antimicrob Chemother **48 Suppl 1:**17-28.
302. **Mack, G., P. J. Cooper, and N. Buchanan.** 1991. Effects of enzyme supplementation on oral absorption of ciprofloxacin in patients with cystic fibrosis. Antimicrob Agents Chemother **35:**1484-5.
303. **MacKenzie, F. M., K. E. Milne, and I. M. Gould.** 2004. Reassessment of cefaclor breakpoints for Haemophilus influenzae. J Chemother **16:**329-33.
304. **MacKenzie, F. M., K. E. Milne, and I. M. Gould.** 2004. Reassessment of the cefaclor breakpoint for Streptococcus pneumoniae. Int J Antimicrob Agents **23:**337-42.
305. **Mager, H., and G. Goller.** 1995. Analysis of pseudo-profiles in organ pharmacokinetics and toxicokinetics. Stat Med **14:**1009-24.
306. **Mager, H., and G. Goller.** 1998. Resampling methods in sparse sampling situations in preclinical pharmacokinetic studies. J Pharm Sci **87:**372-8.
307. **Malerczyk, V., L. Maass, M. Verho, P. Hajdu, N. Klesel, and R. Rangoonwala.** 1987. Single and multiple dose pharmacokinetics of intravenous cefpirome (HR 810), a novel cephalosporin derivative. Infection **15:**211-4.
308. **Manno, G., M. Cruciani, L. Romano, S. Scapolan, M. Mentasti, R. Lorini, and L. Minicucci.** 2005. Antimicrobial use and Pseudomonas aeruginosa susceptibility profile in a cystic fibrosis centre. Int J Antimicrob Agents **25:**193-7.
309. **Manoharan, M., U. Jaehde, H. U. Koch, U. Malter, K. G. Naber, and F. Sorgel.** 1988. High-performance liquid chromatographic assays for gyrase inhibitors in plasma, urine, several body fluids, and tissues. Rev Infect Dis **10:**S98-S100.
310. **Marchetti, F., L. Giglio, M. Candusso, D. Faraguna, and B. M. Assael.** 2004. Early antibiotic treatment of pseudomonas aeruginosa colonisation in cystic fibrosis: a critical review of the literature. Eur J Clin Pharmacol **60:**67-74.

311. **Marino, E. L., A. Dominguez-Gil, and C. Muriel.** 1982. Influence of dosage form and administration route on the pharmacokinetic parameters of cefadroxil. Int J Clin Pharmacol Ther Toxicol **20:**73-7.
312. **Martini, N., M. Agostini, G. Barlocco, L. Bozzini, L. Castellani, A. Messori, G. Scroccaro, and G. Mastella.** 1984. Serum and sputum concentrations of azlocillin, cefoperazone and ceftazidime in patients with cystic fibrosis. J Clin Hosp Pharm **9:**303-9.
313. **Mason, E. O., Jr., L. B. Lamberth, N. L. Kershaw, B. L. Prosser, A. Zoe, and P. G. Ambrose.** 2000. Streptococcus pneumoniae in the USA: in vitro susceptibility and pharmacodynamic analysis. J Antimicrob Chemother **45:**623-31.
314. **Mathai, D., P. R. Rhomberg, D. J. Biedenbach, and R. N. Jones.** 2002. Evaluation of the in vitro activity of six broad-spectrum beta-lactam antimicrobial agents tested against recent clinical isolates from India: a survey of ten medical center laboratories. Diagn Microbiol Infect Dis **44:**367-77.
315. **McCarty, J. M., S. J. Tilden, P. Black, J. C. Craft, J. Blumer, W. Waring, and N. A. Halsey.** 1988. Comparison of piperacillin alone versus piperacillin plus tobramycin for treatment of respiratory infections in children with cystic fibrosis. Pediatr Pulmonol **4:**201-4.
316. **McNulty, C. A., G. M. Garden, J. Ashby, and R. Wise.** 1985. Pharmacokinetics and tissue penetration of carumonam, a new synthetic monobactam. Antimicrob Agents Chemother **28:**425-7.
317. **Mendes, C., and P. J. Turner.** 2001. Unit differences in pathogen occurrence arising from the MYSTIC program European database (1997-2000). Diagn Microbiol Infect Dis **41:**191-6.
318. **Mercado, F. F., P. J. Santella, and C. A. Fernandez.** 1978. Clinical experience with cefadroxil in upper and lower respiratory tract infections. J Int Med Res **6:**271-9.
319. **Merrikin, D. J., J. Briant, and G. N. Rolinson.** 1983. Effect of protein binding on antibiotic activity in vivo. J Antimicrob Chemother **11:**233-8.
320. **Meulemans, A., P. Vicart, J. Mohler, and M. Vulpillat.** 1988. Determination of antibiotic lipophilicity with a micromethod: application to brain permeability in man and rats. Chemotherapy **34:**90-5.
321. **Meyer, M. C., A. B. Straughn, E. J. Jarvi, K. S. Patrick, F. R. Pelsor, R. L. Williams, R. Patnaik, M. L. Chen, and V. P. Shah.** 2000. Bioequivalence of methylphenidate immediate-release tablets using a replicated study design to characterize intrasubject variability. Pharm Res **17:**381-4.
322. **Michalsen, H., and T. Bergan.** 1981. Pharmacokinetics of netilmicin in children with and without cystic fibrosis. Antimicrob Agents Chemother **19:**1029-31.
323. **Miller, M. E., and D. M. Kornhauser.** 1994. Bromide pharmacokinetics in cystic fibrosis. Arch Pediatr Adolesc Med **148:**266-71.
324. **Miller, R. P., R. J. Roberts, and L. J. Fischer.** 1976. Acetaminophen elimination kinetics in neonates, children, and adults. Clin Pharmacol Ther **19:**284-94.
325. **Mimeault, J., F. Vallee, R. Seelmann, F. Sorgel, M. Ruel, and M. LeBel.** 1990. Altered disposition of fleroxacin in patients with cystic fibrosis. Clin Pharmacol Ther **47:**618-28.
326. **Moczygemba, L. R., C. R. Frei, and D. S. Burgess.** 2004. Pharmacodynamic modeling of carbapenems and fluoroquinolones against bacteria that produce extended-spectrum beta-lactamases. Clin Ther **26:**1800-7.
327. **Montgomery, M. J., P. M. Beringer, A. Aminimanizani, S. G. Louie, B. J. Shapiro, R. Jelliffe, and M. A. Gill.** 2001. Population pharmacokinetics and use of Monte Carlo simulation to evaluate currently recommended dosing regimens of ciprofloxacin in adult patients with cystic fibrosis. Antimicrob Agents Chemother **45:**3468-73.
328. **Morgan, D. J., and K. M. Bray.** 1994. Lean body mass as a predictor of drug dosage. Implications for drug therapy. Clin Pharmacokinet **26:**292-307.
329. **Morrison, J. A., and V. K. Batra.** 1979. Pharmacokinetics of piperacillin sodium in man. Drugs Exp. Clin. Res. **5:**105-110.
330. **Morrissey, I., M. Robbins, L. Viljoen, and D. F. Brown.** 2005. Antimicrobial susceptibility of community-acquired respiratory tract pathogens in the UK during 2002/3 determined locally and centrally by BSAC methods. J Antimicrob Chemother **55:**200-8.

331. **Morse, D. R., M. L. Furst, R. D. Lefkowitz, D. D'Angelo, and J. V. Esposito.** 1990. A comparison of erythromycin and cefadroxil in the prevention of flare-ups from asymptomatic teeth with pulpal necrosis and associated periapical pathosis. Oral Surg Oral Med Oral Pathol **69:**619-30.
332. **Mosteller, R. D.** 1987. Simplified calculation of body-surface area. N Engl J Med **317:**1098.
333. **Mouton, J., A. Horrevorts, S. Overbeek, and e. al.** 1993. Pharmacokinetics of ceftazidime during continuous and intermittent infusion in adult cystic fibrosis patients. In: Mouton JW, editor. Pharmacokinetic and pharmacodynamic studies of betalactam antibiotics in volunteers and patients with cystic fibrosis [thesis]. University of Rotterdam, Rotterdam.
334. **Mouton, J. W., M. N. Dudley, O. Cars, H. Derendorf, and G. L. Drusano.** 2005. Standardization of pharmacokinetic/pharmacodynamic (PK/PD) terminology for anti-infective drugs: an update. J Antimicrob Chemother **55:**601-7.
335. **Mouton, J. W., A. M. Horrevorts, P. G. Mulder, E. P. Prens, and M. F. Michel.** 1990. Pharmacokinetics of ceftazidime in serum and suction blister fluid during continuous and intermittent infusions in healthy volunteers. Antimicrob Agents Chemother **34:**2307-11.
336. **Mouton, J. W., and M. F. Michel.** 1991. Pharmacokinetics of meropenem in serum and suction blister fluid during continuous and intermittent infusion. J Antimicrob Chemother **28:**911-8.
337. **Mouton, J. W., and N. Punt.** 2001. Use of the t > MIC to choose between different dosing regimens of beta-lactam antibiotics. J Antimicrob Chemother **47:**500-1.
338. **Mouton, J. W., N. Punt, and A. A. Vinks.** 2005. A retrospective analysis using Monte Carlo simulation to evaluate recommended ceftazidime dosing regimens in healthy volunteers, patients with cystic fibrosis, and patients in the intensive care unit. Clin Ther **27:**762-72.
339. **Mouton, J. W., A. Schmitt-Hoffmann, S. Shapiro, N. Nashed, and N. C. Punt.** 2004. Use of Monte Carlo simulations to select therapeutic doses and provisional breakpoints of BAL9141. Antimicrob Agents Chemother **48:**1713-8.
340. **Mouton, J. W., and A. A. Vinks.** 1996. Is continuous infusion of beta-lactam antibiotics worthwhile?--efficacy and pharmacokinetic considerations. J Antimicrob Chemother **38:**5-15.
341. **Mouton, J. W., and A. A. Vinks.** 2005. Pharmacokinetic/pharmacodynamic modelling of antibacterials in vitro and in vivo using bacterial growth and kill kinetics: the minimum inhibitory concentration versus stationary concentration. Clin Pharmacokinet **44:**201-10.
342. **Mrestani, Y., M. Janich, H. H. Ruttinger, and R. H. Neubert.** 2000. Characterization of partition and thermodynamic properties of cephalosporins using micellar electrokinetic chromatography in glycodeoxycholic acid solution. J Chromatogr A **873:**237-46.
343. **Muller, M., B. Rohde, A. Kovar, A. Georgopoulos, H. G. Eichler, and H. Derendorf.** 1997. Relationship between serum and free interstitial concentrations of cefodizime and cefpirome in muscle and subcutaneous adipose tissue of healthy volunteers measured by microdialysis. J Clin Pharmacol **37:**1108-13.
344. **Mulrow, C. D.** 1994. Rationale for systematic reviews. BMJ **309:**597-9.
345. **Murakawa, T., H. Sakamoto, S. Fukada, S. Nakamoto, T. Hirose, N. Itoh, and M. Nishida.** 1980. Pharmacokinetics of ceftizoxime in animals after parenteral dosing. Antimicrob Agents Chemother **17:**157-64.
346. **Muranushi, N., K. Horie, K. Masuda, and K. Hirano.** 1994. Characteristics of ceftibuten uptake into Caco-2 cells. Pharm Res **11:**1761-5.
347. **Muranushi, N., T. Yoshikawa, M. Yoshida, T. Oguma, K. Hirano, and H. Yamada.** 1989. Transport characteristics of ceftibuten, a new oral cephem, in rat intestinal brush-border membrane vesicles: relationship to oligopeptide and amino beta-lactam transport. Pharm Res **6:**308-12.
348. **Nakashima, E., A. Tsuji, S. Kagatani, and T. Yamana.** 1984. Intestinal absorption mechanism of amino-beta-lactam antibiotics. III. Kinetics of carrier-mediated transport across the rat small intestine in situ. J Pharmacobiodyn **7:**452-64.

349. **Nakayama, I., Y. Akieda, E. Yamaji, Y. Nitta, M. Ohishi, K. Katagiri, N. Imamura, and K. Takase.** 1992. Single- and multiple-dose pharmacokinetics of intravenous cefpirome (HR810) to healthy volunteers. J Clin Pharmacol **32:**256-66.
350. **National Committee for Clinical Laboratory Standards.** 2000. Methods for dilution antimicrobial susceptibility tests for bacteria that grow aerobically, 5th edition ed. Approved standard. National Committee for Clinical Laboratory Standards, Wayne, PA.
351. **National Committee for Clinical Laboratory Standards.** 2001. Performance standards for antimicrobial susceptibility testing eleventh informational supplement, M100-S11. NCCLS, Wayne, PA.
352. **National Committee for Clinical Laboratory Standards.** 2002. Performance standards for antimicrobial susceptibility testing: supplemental tables. M100-S12, vol. 22. National Committee for Clinical Laboratory Standards, Wayne, PA.
353. **National Committee for Clinical Laboratory Standards.** 2004. Performance Standards for Antimicrobial Susceptibility Testing; Forteenth Informational Supplement. NCCLS document M100-S14, Wayne, PA.
354. **Nestorov, I., G. Graham, S. Duffull, L. Aarons, E. Fuseau, and P. Coates.** 2001. Modeling and stimulation for clinical trial design involving a categorical response: a phase II case study with naratriptan. Pharm Res **18:**1210-9.
355. **Nicolau, D. P., and P. G. Ambrose.** 2001. Pharmacodynamic profiling of levofloxacin and gatifloxacin using Monte Carlo simulation for community-acquired isolates of Streptococcus pneumoniae. Am J Med **111 Suppl 9A:**13S-18S; discussion 36S-38S.
356. **Nicolau, D. P., C. H. Nightingale, M. A. Banevicius, Q. Fu, and R. Quintiliani.** 1996. Serum bactericidal activity of ceftazidime: continuous infusion versus intermittent injections. Antimicrob Agents Chemother **40:**61-4.
357. **Niklas, K. J.** 1994. Plant Allometry: The Scaling of Form and Process. University of Chicago Press, Chicago.
358. **Nilsson-Ehle, I., H. Fellner, S. A. Hedstrom, P. Nilsson-Ehle, and J. Sjovall.** 1985. Pharmacokinetics of clavulanic acid, given in combination with amoxycillin, in volunteers. J Antimicrob Chemother **16:**491-8.
359. **Norrby, S. R.** 1983. Ceftazidime in clinical practice - a summary. J Antimicrob Chemother **12 Suppl A:**405-8.
360. **O'Carroll, M. R., T. J. Kidd, C. Coulter, H. V. Smith, B. R. Rose, C. Harbour, and S. C. Bell.** 2003. Burkholderia pseudomallei: another emerging pathogen in cystic fibrosis. Thorax **58:**1087-91.
361. **O'Sullivan, T. A., J. P. Wang, J. D. Unadkat, S. M. al-Habet, W. F. Trager, A. L. Smith, S. McNamara, and M. L. Aitken.** 1993. Disposition of drugs in cystic fibrosis. V. In vivo CYP2C9 activity as probed by (S)-warfarin is not enhanced in cystic fibrosis. Clin Pharmacol Ther **54:**323-8.
362. **Obana, Y., T. Murakami, H. Kuzui, and T. Nishino.** 1990. Bacterial combination effect between carumonam and eight other antibiotics. Jpn J Antibiot **43:**2094-101.
363. **Occhipinti, D. J., S. L. Pendland, L. L. Schoonover, E. B. Rypins, L. H. Danziger, and K. A. Rodvold.** 1997. Pharmacokinetics and pharmacodynamics of two multiple-dose piperacillin-tazobactam regimens. Antimicrob Agents Chemother **41:**2511-7.
364. **Oguma, T., H. Yamada, M. Sawaki, and N. Narita.** 1991. Pharmacokinetic analysis of the effects of different foods on absorption of cefaclor. Antimicrob Agents Chemother **35:**1729-35.
365. **Oh, D. M., P. J. Sinko, and G. L. Amidon.** 1992. Characterization of the oral absorption of several aminopenicillins: determination of intrinsic membrane absorption parameters in the rat intestine in situ. Int J Pharm **85:**181-7.
366. **Okuda, J., M. Otsuki, T. Oh, and T. Nishino.** 2000. In vitro activity of DU-6681a, an active form of the new oral carbapenem compound DZ-2640, in comparison with that of R-95867, faropenem and oral cephalosporins. J Antimicrob Chemother **46:**101-8.
367. **Paalzow, L. K.** 1995. Torsten Teorell, the father of pharmacokinetics. Ups J Med Sci **100:**41-6.
368. **Paap, C. M., and M. C. Nahata.** 1990. Clinical pharmacokinetics of antibacterial drugs in neonates. Clin Pharmacokinet **19:**280-318.
369. **Padoan, R., A. Brienza, R. M. Crossignani, G. Lodi, A. Giunta, B. M. Assael, F. Granata, E. Passarella, P. A. Vallaperta, and L. Xerri.** 1983. Ceftazidime in

treatment of acute pulmonary exacerbations in patients with cystic fibrosis. J Pediatr **103:**320-4.

370. **Padoan, R., W. Cambisano, D. Costantini, R. M. Crossignani, M. L. Danza, G. Trezzi, and A. Giunta.** 1987. Ceftazidime monotherapy vs. combined therapy in Pseudomonas pulmonary infections in cystic fibrosis. Pediatr Infect Dis J **6:**648-53.
371. **Paintaud, G., G. Alvan, M. L. Dahl, A. Grahnen, J. Sjovall, and J. O. Svensson.** 1992. Nonlinearity of amoxicillin absorption kinetics in human. Eur J Clin Pharmacol **43:**283-8.
372. **Panneton, A. C., M. G. Bergeron, and M. LeBel.** 1988. Pharmacokinetics and tissue penetration of fleroxacin after single and multiple 400- and 800-mg-dosage regimens. Antimicrob Agents Chemother **32:**1515-20.
373. **Paradis, D., F. Vallee, S. Allard, C. Bisson, N. Daviau, C. Drapeau, F. Auger, and M. LeBel.** 1992. Comparative study of pharmacokinetics and serum bactericidal activities of cefpirome, ceftazidime, ceftriaxone, imipenem, and ciprofloxacin. Antimicrob Agents Chemother **36:**2085-92.
374. **Park, R. W., and R. J. Grand.** 1981. Gastrointestinal manifestations of cystic fibrosis: a review. Gastroenterology **81:**1143-61.
375. **Parke, J., and B. G. Charles.** 2000. Factors affecting oral cyclosporin disposition after heart transplantation: bootstrap validation of a population pharmacokinetic model. Eur J Clin Pharmacol **56:**481-7.
376. **Parke, J., N. H. Holford, and B. G. Charles.** 1999. A procedure for generating bootstrap samples for the validation of nonlinear mixed-effects population models. Comput Methods Programs Biomed **59:**19-29.
377. **Paulfeuerborn, W., H. J. Muller, K. Borner, P. Koeppe, and H. Lode.** 1993. Comparative pharmacokinetics and serum bactericidal activities of SCE-2787 and ceftazidime. Antimicrob Agents Chemother **37:**1835-41.
378. **Payen, S., R. Serreau, A. Munck, Y. Aujard, Y. Aigrain, F. Bressolle, and E. Jacqz-Aigrain.** 2003. Population pharmacokinetics of ciprofloxacin in pediatric and adolescent patients with acute infections. Antimicrob Agents Chemother **47:**3170-8.
379. **Peric, M., F. A. Browne, M. R. Jacobs, and P. C. Appelbaum.** 2003. Activity of nine oral agents against gram-positive and gram-negative bacteria encountered in community-acquired infections: use of pharmacokinetic/pharmacodynamic breakpoints in the comparative assessment of beta-lactam and macrolide antimicrobial agents. Clin Ther **25:**169-77.
380. **Permin, H., C. Koch, N. Hoiby, H. O. Christensen, A. F. Moller, and S. Moller.** 1983. Ceftazidime treatment of chronic Pseudomonas aeruginosa respiratory tract infection in cystic fibrosis. J Antimicrob Chemother **12 Suppl A:**313-23.
381. **Perry, C. M., and R. N. Brogden.** 1996. Cefuroxime axetil. A review of its antibacterial activity, pharmacokinetic properties and therapeutic efficacy. Drugs **52:**125-58.
382. **Petitjean, O., B. Pangon, N. Brion, M. Tod, C. Chaplain, V. Le Gros, K. Louchahi, and P. Allouch.** 1993. Pharmacokinetics and bactericidal activities of one 800-milligram dose versus two 400-milligram doses of intravenously administered pefloxacin in healthy volunteers. Antimicrob Agents Chemother **37:**737-40.
383. **Pfaller, M. A., R. N. Jones, and D. J. Biedenbach.** 2001. Antimicrobial resistance trends in medical centers using carbapenems: report of 1999 and 2000 results from the MYSTIC program (USA). Diagn Microbiol Infect Dis **41:**177-82.
384. **Pierard, D., K. Emmerechts, and S. Lauwers.** 1998. Comparative in-vitro activity of cefpirome against isolates from intensive care and haematology/oncology units. Belgian Multicentre Study Group. J Antimicrob Chemother **41:**443-50.
385. **Piotrovskij, V. K., G. Paintaud, G. Alvan, and T. Trnovec.** 1994. Modeling of the saturable time-constrained amoxicillin absorption in humans. Pharm Res **11:**1346-51.
386. **Pitt, T. L., M. Sparrow, M. Warner, and M. Stefanidou.** 2003. Survey of resistance of Pseudomonas aeruginosa from UK patients with cystic fibrosis to six commonly prescribed antimicrobial agents. Thorax **58:**794-6.
387. **Postnikov, S. S., S. Semykin, S. V. Polikarpova, and V. P. Nazhimov.** 2002. Pefloxacin in the treatment of patients with mucoviscidosis. Antibiot Khimioter **47:**13-5.

388. **Prandota, J.** 1985. Clinical pharmacokinetics of changes in drug elimination in children. Dev Pharmacol Ther **8:**311-28.
389. **Prandota, J.** 1988. Clinical pharmacology of antibiotics and other drugs in cystic fibrosis. Drugs **35:**542-78.
390. **Prandota, J.** 1987. Drug disposition in cystic fibrosis: progress in understanding pathophysiology and pharmacokinetics. Pediatr Infect Dis J **6:**1111-26.
391. **Preston, D. A., and M. R. Turnak.** 2000. Assumed versus approved breakpoints. Antimicrob Agents Chemother **44:**3243-5.
392. **Preston, S. L., G. L. Drusano, A. L. Berman, C. L. Fowler, A. T. Chow, B. Dornseif, V. Reichl, J. Natarajan, and M. Corrado.** 1998. Pharmacodynamics of levofloxacin: a new paradigm for early clinical trials. Jama **279:**125-9.
393. **Prince, A. S., and H. C. Neu.** 1980. Use of piperacillin, a semisynthetic penicillin, in the therapy of acute exacerbations of pulmonary disease in patients with cystic fibrosis. J Pediatr **97:**148-51.
394. **Querol-Ferrer, V., R. Zini, and J. P. Tillement.** 1991. The blood binding of cefotiam and cyclohexanol, metabolites of the prodrug cefotiam hexetil, in-vitro. J Pharm Pharmacol **43:**863-6.
395. **Quintiliani, R.** 1986. Efficacy of a twice-daily regimen of cefadroxil in the treatment of respiratory tract infections. Drugs **32 Suppl 3:**43-9.
396. **Raeissi, S. D., J. Li, and I. J. Hidalgo.** 1999. The role of an alpha-amino group on H+ -dependent transepithelial transport of cephalosporins in Caco-2 cells. J Pharm Pharmacol **51:**35-40.
397. **Rains, C. P., H. M. Bryson, and D. H. Peters.** 1995. Ceftazidime. An update of its antibacterial activity, pharmacokinetic properties and therapeutic efficacy. Drugs **49:**577-617.
398. **Rajagopalan, P., and M. R. Gastonguay.** 2003. Population pharmacokinetics of ciprofloxacin in pediatric patients. J Clin Pharmacol **43:**698-710.
399. **Rappaz, I., L. A. Decosterd, J. Bille, M. Pilet, N. Belaz, and M. Roulet.** 2000. Continuous infusion of ceftazidime with a portable pump is as effective as thrice-a-day bolus in cystic fibrosis children. Eur J Pediatr **159:**919-25.
400. **Reed, M.** 1997. The pathophysiology and treatment of cystic fibrosis. J Pediatr Pharm Pract **2:**285-308.
401. **Reed, M. D., J. Goldfarb, T. S. Yamashita, E. Lemon, and J. L. Blumer.** 1994. Single-dose pharmacokinetics of piperacillin and tazobactam in infants and children. Antimicrob Agents Chemother **38:**2817-26.
402. **Reed, M. D., R. C. Stern, C. M. Myers, J. D. Klinger, T. S. Yamashita, and J. L. Blumer.** 1987. Therapeutic evaluation of piperacillin for acute pulmonary exacerbations in cystic fibrosis. Pediatr Pulmonol **3:**101-9.
403. **Reed, M. D., R. C. Stern, C. M. Myers, T. S. Yamashita, and J. L. Blumer.** 1988. Lack of unique ciprofloxacin pharmacokinetic characteristics in patients with cystic fibrosis. J Clin Pharmacol **28:**691-9.
404. **Reed, M. D., R. C. Stern, C. A. O'Brien, D. A. Crenshaw, and J. L. Blumer.** 1987. Randomized double-blind evaluation of ceftazidime dose ranging in hospitalized patients with cystic fibrosis. Antimicrob Agents Chemother **31:**698-702.
405. **Reeves, D. S., M. J. Bywater, H. A. Holt, and L. O. White.** 1984. In-vitro studies with ciprofloxacin, a new 4-quinolone compound. J Antimicrob Chemother **13:**333-46.
406. **Reigner, B. G., W. Couet, J. P. Guedes, J. B. Fourtillan, and T. N. Tozer.** 1990. Saturable rate of cefatrizine absorption after oral administration to humans. J Pharmacokinet Biopharm **18:**17-34.
407. **Retout, S., F. Mentre, and R. Bruno.** 2002. Fisher information matrix for non-linear mixed-effects models: evaluation and application for optimal design of enoxaparin population pharmacokinetics. Stat Med **21:**2623-39.
408. **Rey, E., J. M. Treluyer, and G. Pons.** 1998. Drug disposition in cystic fibrosis. Clin Pharmacokinet **35:**313-29.
409. **Rey, L. C., and C. K. Farhat.** 1997. Prevalence of Haemophilus influenzae resistant to ampicillin, cefaclor, cefotaxime, chloramphenicol and cotrimoxazol isolated from laboratories in the city of Sao Paulo, Brazil. J Pediatr (Rio J) **73:**26-31.
410. **Reynolds, R., J. Shackcloth, D. Felmingham, and A. MacGowan.** 2003. Antimicrobial susceptibility of lower respiratory tract pathogens in Great Britain and

Ireland 1999-2001 related to demographic and geographical factors: the BSAC Respiratory Resistance Surveillance Programme. J Antimicrob Chemother **52:**931-43.
411. **Ribbing, J., and E. N. Jonsson.** 2004. Power, selection bias and predictive performance of the Population Pharmacokinetic Covariate Model. J Pharmacokinet Pharmacodyn **31:**109-34.
412. **Richard, D. A., S. Nousia-Arvanitakis, V. Sollich, B. J. Hampel, B. Sommerauer, and U. B. Schaad.** 1997. Oral ciprofloxacin vs. intravenous ceftazidime plus tobramycin in pediatric cystic fibrosis patients: comparison of antipseudomonas efficacy and assessment of safety with ultrasonography and magnetic resonance imaging. Cystic Fibrosis Study Group. Pediatr Infect Dis J **16:**572-8.
413. **Richards, D. M., and R. N. Brogden.** 1985. Ceftazidime. A review of its antibacterial activity, pharmacokinetic properties and therapeutic use. Drugs **29:**105-61.
414. **Richerson, M. A., P. G. Ambrose, K. Q. Bui, and et al.** 1999. Pharmacokinetic and economic evaluation of piperacillin/tazobactam administered either as continuous or intermittent infusion with once-daily gentamicin. Infectious Disease in Clinical Practice **8:**195-200.
415. **Robinson, C. A., R. J. Kuhn, J. Craigmyle, M. I. Anstead, and J. E. Kanga.** 2001. Susceptibility of pseudomonas aeruginosa to cefepime versus ceftazidime in patients with cystic fibrosis. Pharmacotherapy **21:**1320-4.
416. **Rode, J. W., and D. D. Webling.** 1981. Melioidosis in the Northern Territory of Australia. Med J Aust **1:**181-4.
417. **Rosenthal, A., L. N. Button, and K. T. Khaw.** 1977. Blood volume changes in patients with cystic fibrosis. Pediatrics **59:**588-94.
418. **Rosselli, P.** 1986. Frequency of isolation and drug resistance of bacterial strains isolated from respiratory material in patients with cystic fibrosis. Quad Sclavo Diagn **22:**273-82.
419. **Rossi, F., D. Andreazzi, M. Maffucci, and A. A. Pereira.** 2001. Susceptibility of S. pneumoniae to various antibiotics aong strains isolated from patients and healthy carriers in different regions of Brazil(1999-2000). Braz J Infect Dis **5:**305-12.
420. **Rouan, M. C., J. B. Lecaillon, J. Guibert, J. Modai, and J. P. Schoeller.** 1985. Pharmacokinetics of cefotiam in humans. Antimicrob Agents Chemother **27:**177-80.
421. **Routledge, P. A.** 1994. Pharmacokinetics in children. J Antimicrob Chemother **34 Suppl A:**19-24.
422. **Rubio, T. T.** 1987. Ciprofloxacin: comparative data in cystic fibrosis. Am J Med **82:**185-8.
423. **Rubner, M.** 1883. Über den Einfluss der Körpergrösse auf Stoff- und Kraftwechsel. Z. Biol. **19:**536-562.
424. **Ruiz-Balaguer, N., A. Nacher, V. G. Casabo, and M. Merino.** 1997. Nonlinear intestinal absorption kinetics of cefuroxime axetil in rats. Antimicrob Agents Chemother **41:**445-8.
425. **Ruiz-Balaguer, N., A. Nacher, V. G. Casabo, and M. Merino Sanjuan.** 2002. Intestinal transport of cefuroxime axetil in rats: absorption and hydrolysis processes. Int J Pharm **234:**101-11.
426. **Ruiz-Carretero, P., M. Merino-Sanjuan, A. Nacher, and V. G. Casabo.** 2004. Pharmacokinetic models for the saturable absorption of cefuroxime axetil and saturable elimination of cefuroxime. Eur J Pharm Sci **21:**217-23.
427. **Rye, P. J., G. Roberts, R. E. Staugas, and A. J. Martin.** 1994. Coagulopathy with piperacillin administration in cystic fibrosis: two case reports. J Paediatr Child Health **30:**278-9.
428. **Sader, H. S., and R. N. Jones.** 1994. In vitro antimicrobial activity of cefpirome against ceftazidime-resistant isolates from two multicenter studies. Eur J Clin Microbiol Infect Dis **13:**675-9.
429. **Saiman, L., F. Mehar, W. W. Niu, H. C. Neu, K. J. Shaw, G. Miller, and A. Prince.** 1996. Antibiotic susceptibility of multiply resistant Pseudomonas aeruginosa isolated from patients with cystic fibrosis, including candidates for transplantation. Clin Infect Dis **23:**532-7.
430. **Saitoh, H., C. Gerard, and B. J. Aungst.** 1996. The secretory intestinal transport of some beta-lactam antibiotics and anionic compounds: a mechanism contributing to poor oral absorption. J Pharmacol Exp Ther **278:**205-11.

431. **San Gabriel, P., J. Zhou, S. Tabibi, Y. Chen, M. Trauzzi, and L. Saiman.** 2004. Antimicrobial susceptibility and synergy studies of Stenotrophomonas maltophilia isolates from patients with cystic fibrosis. Antimicrob Agents Chemother **48:**168-71.
432. **Sanchez-Pico, A., J. E. Peris-Ribera, C. Toledano, F. Torres-Molina, V. G. Casabo, A. Martin-Villodre, and J. M. Pla-Delfina.** 1989. Non-linear intestinal absorption kinetics of cefadroxil in the rat. J Pharm Pharmacol **41:**179-85.
433. **Sandberg, T., C. Henning, S. Iwarson, and O. Paulsen.** 1985. Cefadroxil once daily for three or seven days versus amoxycillin for seven days in uncomplicated urinary tract infections in women. Scand J Infect Dis **17:**83-7.
434. **Santella, P. J., B. Tanrisever, and E. Berman.** 1978. An overview of results of world-wide clinical trials with cefadroxil. J Int Med Res **6:**441-51.
435. **Sauermann, R., G. Delle-Karth, C. Marsik, I. Steiner, M. Zeitlinger, B. X. Mayer-Helm, A. Georgopoulos, M. Muller, and C. Joukhadar.** 2005. Pharmacokinetics and pharmacodynamics of cefpirome in subcutaneous adipose tissue of septic patients. Antimicrob Agents Chemother **49:**650-5.
436. **Schaefer, H. G., H. Stass, J. Wedgwood, B. Hampel, C. Fischer, J. Kuhlmann, and U. B. Schaad.** 1996. Pharmacokinetics of ciprofloxacin in pediatric cystic fibrosis patients. Antimicrob Agents Chemother **40:**29-34.
437. **Schulin, T.** 2002. In vitro activity of the aerosolized agents colistin and tobramycin and five intravenous agents against Pseudomonas aeruginosa isolated from cystic fibrosis patients in southwestern Germany. J Antimicrob Chemother **49:**403-6.
438. **Schumacher, H., B. Bengtsson, H. Bjerregaard-Andersen, and T. G. Jensen.** 1998. Detection of extended-spectrum beta-lactamases. The reliability of methods for susceptibility testing as used in Denmark. Apmis **106:**979-86.
439. **Schumacher, H., J. Scheibel, and J. K. Moller.** 2000. Cross-resistance patterns among clinical isolates of Klebsiella pneumoniae with decreased susceptibility to cefuroxime. J Antimicrob Chemother **46:**215-21.
440. **Schumacher, H., U. Skibsted, D. S. Hansen, and J. Scheibel.** 1997. Cefuroxime resistance in Klebsiella pneumoniae. Susceptibility to cefotaxime and ceftazidime despite production of ESBLs. Apmis **105:**708-16.
441. **Schumacher, H., U. Skibsted, R. Skov, and J. Scheibel.** 1996. Cefuroxime resistance in Escherichia coli. Resistance mechanisms and prevalence. Apmis **104:**531-8.
442. **Scott, L. J., D. Ormrod, and K. L. Goa.** 2001. Cefuroxime axetil: an updated review of its use in the management of bacterial infections. Drugs **61:**1455-500.
443. **Scully, B. E., M. Nakatomi, C. Ores, S. Davidson, and H. C. Neu.** 1987. Ciprofloxacin therapy in cystic fibrosis. Am J Med **82:**196-201.
444. **Shah, P. M., F. P. Maesen, A. Dolmann, N. Vetter, E. Fiss, and R. Wesch.** 1999. Levofloxacin versus cefuroxime axetil in the treatment of acute exacerbation of chronic bronchitis: results of a randomized, double-blind study. J Antimicrob Chemother **43:**529-39.
445. **Shalit, I., H. R. Stutman, M. I. Marks, S. A. Chartrand, and B. C. Hilman.** 1987. Randomized study of two dosage regimens of ciprofloxacin for treating chronic bronchopulmonary infection in patients with cystic fibrosis. Am J Med **82:**189-95.
446. **Sheiner, L. B.** 1992. Bioequivalence revisited. Stat Med **11:**1777-88.
447. **Sheiner, L. B.** 1984. The population approach to pharmacokinetic data analysis: rationale and standard data analysis methods. Drug Metab Rev **15:**153-71.
448. **Sheldon, C. D., B. K. Assoufi, and M. E. Hodson.** 1993. Regular three monthly oral ciprofloxacin in adult cystic fibrosis patients infected with Pseudomonas aeruginosa. Respir Med **87:**587-93.
449. **Shibl, A. M., and S. S. Hussein.** 1992. Surveillance of Streptococcus pneumoniae serotypes in Riyadh and their susceptibility to penicillin and other commonly prescribed antibiotics. J Antimicrob Chemother **29:**149-57.
450. **Shinagawa, N., J. Yura, T. Manabe, K. Mashita, S. Ishikawa, A. Mizuno, K. Hirata, R. Denno, M. Mukaiya, K. Ishibiki, Y. Ushijima, N. Aikawa, K. Takuma, S. Iwai, M. Kunimatsu, H. Kinoshita, K. Morimoto, M. Fujimoto, H. Tanimura, H. Ohnishi, K. Noguchi, S. Mizobata, Y. Umemoto, K. Orita, S. Oda, and et al.** 1996. Isolation rate of E. coli from surgical infections and their susceptibilities. Jpn J Antibiot **49:**456-64.

451. **Shinagawa, N., J. Yura, T. Manabe, K. Mashita, S. Ishikawa, A. Mizuno, K. Hirata, R. Denno, M. Mukaiya, K. Ishibiki, Y. Ushijima, N. Aikawa, K. Takuma, S. Iwai, M. Kunimatsu, K. Ohtsuka, H. Kinoshita, K. Morimoto, M. Fujimoto, H. Tanimura, H. Ohnishi, Y. Umemoto, S. Sakaguchi, H. Dounishi, S. Oda, and et al.** 1996. Isolation rate of Pseudomonas aeruginosa from surgical infections and their susceptibilities. Jpn J Antibiot **49:**544-54.
452. **Simon, C.** 1980. Pharmacokinetics of cefadroxil, a new oral cephalosporin. Arzneimittelforschung **30:**502-4.
453. **Sjovall, J., G. Alvan, J. E. Akerlund, J. O. Svensson, G. Paintaud, C. E. Nord, and B. Angelin.** 1992. Dose-dependent absorption of amoxicillin in patients with an ileostomy. Eur J Clin Pharmacol **43:**277-81.
454. **Sjovall, J., G. Alvan, and D. Westerlund.** 1985. Dose-dependent absorption of amoxycillin and bacampicillin. Clin Pharmacol Ther **38:**241-50.
455. **Sollich, V., E. Kloditz, R. Schuster, W. Handrick, S. Bromme, W. Rumler, R. Patsch, H. Kharari, and F. B. Spencker.** 1993. Oral ciprofloxacin therapy in juvenile patients with cystic fibrosis--results of a prospective pilot study. Kinderarztl Prax **61:**211-4.
456. **Sommers, D. K., M. Van Wyk, P. E. Williams, and S. M. Harding.** 1984. Pharmacokinetics and tolerance of cefuroxime axetil in volunteers during repeated dosing. Antimicrob Agents Chemother **25:**344-7.
457. **Sookpranee, T., M. Sookpranee, M. A. Mellencamp, and L. C. Preheim.** 1991. Pseudomonas pseudomallei, a common pathogen in Thailand that is resistant to the bactericidal effects of many antibiotics. Antimicrob Agents Chemother **35:**484-9.
458. **Sorgel, F., J. Bulitta, and M. Kinzig-Schippers.** 2001. How well do gyrase inhibitors work? The pharmacokinetics of quinolones. Pharm Unserer Zeit **30:**418-27.
459. **Sorgel, F., and M. Kinzig.** 1993. The chemistry, pharmacokinetics and tissue distribution of piperacillin/tazobactam. J Antimicrob Chemother **31 Suppl A:**39-60.
460. **Sorgel, F., and M. Kinzig.** 1994. Pharmacokinetic characteristics of piperacillin/tazobactam. Intensive Care Med **20 Suppl 3:**S14-20.
461. **Sorgel, F., and M. Kinzig.** 1993. Pharmacokinetics of gyrase inhibitors, Part 1: Basic chemistry and gastrointestinal disposition. Am J Med **94:**44S-55S.
462. **Sorgel, F., and M. Kinzig.** 1993. Pharmacokinetics of gyrase inhibitors, Part 2: Renal and hepatic elimination pathways and drug interactions. Am J Med **94:**56S-69S.
463. **Sorgel, F., R. Metz, K. Naber, R. Seelmann, and P. Muth.** 1988. Pharmacokinetics and body fluid penetration of fleroxacin in healthy volunteers. J Antimicrob Chemother **22 Suppl D:**155-67.
464. **Sorgel, F., K. G. Naber, U. Jaehde, A. Reiter, R. Seelmann, and G. Sigl.** 1989. Gastrointestinal secretion of ciprofloxacin. Evaluation of the charcoal model for investigations in healthy volunteers. Am J Med **87:**62S-65S.
465. **Sourgens, H., H. Derendorf, and H. Schifferer.** 1997. Pharmacokinetic profile of cefaclor. Int J Clin Pharmacol Ther **35:**374-80.
466. **Soussy, C. J., M. Chanal, E. Derlot, F. Goldstein, and J. Duval.** 1994. In vitro antibacterial activity of cefpirome: a new cephalosporin; results of a multicenter study. Pathol Biol (Paris) **42:**754-60.
467. **Spencker, F. B., L. Staber, T. Lietz, R. Schille, and A. C. Rodloff.** 2003. Development of resistance in Pseudomonas aeruginosa obtained from patients with cystic fibrosis at different times. Clin Microbiol Infect **9:**370-9.
468. **Spino, M.** 1991. Pharmacokinetics of drugs in cystic fibrosis. Clin Rev Allergy **9:**169-210.
469. **Spino, M., R. P. Chai, A. F. Isles, J. W. Balfe, R. G. Brown, J. J. Thiessen, and S. M. MacLeod.** 1985. Assessment of glomerular filtration rate and effective renal plasma flow in cystic fibrosis. J Pediatr **107:**64-70.
470. **Spino, M., R. P. Chai, A. F. Isles, J. J. Thiessen, A. Tesoro, R. Gold, and S. M. MacLeod.** 1984. Cloxacillin absorption and disposition in cystic fibrosis. J Pediatr **105:**829-35.
471. **Spyker, D. A., L. L. Gober, W. M. Scheld, M. A. Sande, and W. K. Bolton.** 1982. Pharmacokinetics of cefaclor in renal failure: effects of multiple doses and hemodialysis. Antimicrob Agents Chemother **21:**278-81.

472. **Spyker, D. A., B. L. Thomas, M. A. Sande, and W. K. Bolton.** 1978. Pharmacokinetics of cefaclor and cephalexin: dosage nomograms for impaired renal function. Antimicrob Agents Chemother **14:**172-7.
473. **Stead, R. J., H. G. Kennedy, M. E. Hodson, and J. C. Batten.** 1985. Adverse reactions to piperacillin in adults with cystic fibrosis. Thorax **40:**184-6.
474. **Steckelberg, J. M., M. S. Rouse, B. M. Tallan, D. R. Osmon, N. K. Henry, and W. R. Wilson.** 1993. Relative efficacies of broad-spectrum cephalosporins for treatment of methicillin-susceptible Staphylococcus aureus experimental infective endocarditis. Antimicrob Agents Chemother **37:**554-8.
475. **Stern, R. C.** 1996. Denmark to the rescue. Pediatr Pulmonol **21:**151-2.
476. **Stoeckel, K., W. L. Hayton, and D. J. Edwards.** 1995. Clinical pharmacokinetics of oral cephalosporins. Antibiot Chemother **47:**34-71.
477. **Strandvik, B., A. S. Malmborg, H. Alfredson, and A. Ericsson.** 1983. Clinical results and pharmacokinetics of ceftazidime treatment in patients with cystic fibrosis. J Antimicrob Chemother **12 Suppl A:**283-7.
478. **Stratchounski, L. S., O. I. Kretchikova, G. K. Reshedko, O. U. Stetsiouk, M. M. Kandalov, O. A. Egorova, L. M. Boyko, E. L. Ryabkova, G. D. Tarasova, and B. M. Blokhin.** 2001. Antimicrobial susceptibility of nasopharyngeal isolates of Haemophilus influenzae from healthy children in day-care centres: results of multicentre study in Russia. Int J Antimicrob Agents **18:**347-51.
479. **Strenkoski, L. C., and D. E. Nix.** 1993. Cefpirome clinical pharmacokinetics. Clin Pharmacokinet **25:**263-73.
480. **Strober, W., G. Peter, and R. H. Schwartz.** 1969. Albumin metabolism in cystic fibrosis. Pediatrics **43:**416-26.
481. **Stuck, A. E., F. J. Frey, P. Heizmann, R. Brandt, and E. Weidekamm.** 1989. Pharmacokinetics and metabolism of intravenous and oral fleroxacin in subjects with normal and impaired renal function and in patients on continuous ambulatory peritoneal dialysis. Antimicrob Agents Chemother **33:**373-81.
482. **Stutman, H. R., I. Shalit, M. I. Marks, R. Greenwood, S. A. Chartrand, and B. C. Hilman.** 1987. Pharmacokinetics of two dosage regimens of ciprofloxacin during a two-week therapeutic trial in patients with cystic fibrosis. Am J Med **82:**142-5.
483. **Sullivan, M. C., C. H. Nightingale, R. Quintiliani, and K. Sweeney.** 1993. Comparison of the pharmacokinetic and pharmacodynamic activity of piperacillin and mezlocillin. Pharmacotherapy **13:**607-12.
484. **Susanto, M., and L. Z. Benet.** 2002. Can the enhanced renal clearance of antibiotics in cystic fibrosis patients be explained by P-glycoprotein transport? Pharm Res **19:**457-62.
485. **Szyndler, J. E., S. J. Towns, P. P. van Asperen, and K. O. McKay.** 2005. Psychological and family functioning and quality of life in adolescents with cystic fibrosis. J Cyst Fibros **4**:135-44.
486. **Taccetti, G., S. Campana, and L. Marianelli.** 1999. Multiresistant non-fermentative gram-negative bacteria in cystic fibrosis patients: the results of an Italian multicenter study. Italian Group for Cystic Fibrosis microbiology. Eur J Epidemiol **15:**85-8.
487. **Tam, V. H., A. Louie, M. R. Deziel, W. Liu, R. Leary, and G. L. Drusano.** 2005. Bacterial-population responses to drug-selective pressure: examination of garenoxacin's effect on Pseudomonas aeruginosa. J Infect Dis **192:**420-8.
488. **Tam, V. H., S. L. Preston, and G. L. Drusano.** 2003. Optimal sampling schedule design for populations of patients. Antimicrob Agents Chemother **47:**2888-91.
489. **Teorell, T.** 1937. Kinetics of distribution of substances administered to the body. I: The extravascular modes of administration. Arch Intern Pharmacodyn **57:**205-225.
490. **Teorell, T.** 1937. Kinetics of distribution of substances administered to the body. II: The intravascular mode of administration. Arch Intern Pharmacodyn **57:**226-240.
491. **Thalhammer, F., F. Traunmuller, I. El Menyawi, M. Frass, U. M. Hollenstein, G. J. Locker, B. Stoiser, T. Staudinger, R. Thalhammer-Scherrer, and H. Burgmann.** 1999. Continuous infusion versus intermittent administration of meropenem in critically ill patients. J Antimicrob Chemother **43:**523-7.
492. **The United States pharmacopeia.** 2002. The national formulary. USP, NF 21st ed. The United States Pharmacopeial Convention, Inc., Rockville, MD.

493. **Tjandramaga, T. B., A. Mullie, R. Verbesselt, P. J. De Schepper, and L. Verbist.** 1978. Piperacillin: human pharmacokinetics after intravenous and intramuscular administration. Antimicrob Agents Chemother **14:**829-37.
494. **Tjandramaga, T. B., A. Van Hecken, A. Mullie, R. Verbesselt, P. J. De Schepper, and L. Verbist.** 1982. Comparative pharmacokinetics of ceftazidime and moxalactam. Antimicrob Agents Chemother **22:**237-41.
495. **Tod, M., F. Mentre, Y. Merle, and A. Mallet.** 1998. Robust optimal design for the estimation of hyperparameters in population pharmacokinetics. J Pharmacokinet Biopharm **26:**689-716.
496. **Torres-Molina, F., J. E. Peris-Ribera, M. C. Garcia-Carbonell, J. C. Aristorena, L. Granero, and J. M. Pla-Delfina.** 1992. Nonlinearities in amoxycillin pharmacokinetics. I. Disposition studies in the rat. Biopharm Drug Dispos **13:**23-38.
497. **Torres-Molina, F., J. E. Peris-Ribera, M. C. Garcia-Carbonell, J. C. Aristorena, and J. M. Pla-Delfina.** 1992. Nonlinearities in amoxycillin pharmacokinetics. II. Absorption studies in the rat. Biopharm Drug Dispos **13:**39-53.
498. **Tothfalusi, L., and L. Endrenyi.** 2001. Evaluation of some properties of individual bioequivalence (IBE) from replicate-design studies. Int J Clin Pharmacol Ther **39:**162-6.
499. **Touw, D. J.** 1998. Clinical pharmacokinetics of antimicrobial drugs in cystic fibrosis. Pharm World Sci **20:**149-60.
500. **Touw, D. J., A. A. Vinks, H. G. Heijerman, and W. Bakker.** 1996. Prospective evaluation of a dose prediction algorithm for intravenous tobramycin in adolescent and adult patients with cystic fibrosis. Ther Drug Monit **18:**118-23.
501. **Touw, D. J., A. A. Vinks, H. G. Heijerman, J. Hermans, and W. Bakker.** 1994. Suggestions for the optimization of the initial tobramycin dose in adolescent and adult patients with cystic fibrosis. Ther Drug Monit **16:**125-31.
502. **Touw, D. J., A. A. Vinks, J. W. Mouton, and A. M. Horrevorts.** 1998. Pharmacokinetic optimisation of antibacterial treatment in patients with cystic fibrosis. Current practice and suggestions for future directions. Clin Pharmacokinet **35:**437-59.
503. **Toyosawa, T., S. Miyazaki, A. Tsuji, K. Yamaguchi, and S. Goto.** 1993. In vitro and in vivo antibacterial activities of E1077, a novel parenteral cephalosporin. Antimicrob Agents Chemother **37:**60-6.
504. **Trantow, T., R. Herzog, H. Fuder, J. Ise, and P. W. Lucker.** 1995. A pilot study on the determination of the relative bioavailability of levo-thyroxine. Methods Find Exp Clin Pharmacol **17:**333-43.
505. **Trenholme, G. M., J. C. Pottage, Jr., and P. H. Karakusis.** 1985. Use of ceftazidime in the treatment of nosocomial lower respiratory infections. Am J Med **79:**32-6.
506. **Tsang, Y. C., R. Pop, P. Gordon, J. Hems, and M. Spino.** 1996. High variability in drug pharmacokinetics complicates determination of bioequivalence: experience with verapamil. Pharm Res **13:**846-50.
507. **Tsuji, A., E. Nakashima, S. Hamano, and T. Yamana.** 1978. Physicochemical properties of amphoteric beta-lactam antibiotics I: Stability, solubility, and dissolution behavior of amino penicillins as a function of pH. J Pharm Sci **67:**1059-66.
508. **Tsuji, A., E. Nakashima, I. Kagami, and T. Yamana.** 1981. Intestinal absorption mechanism of amphoteric beta-lactam antibiotics I: Comparative absorption and evidence for saturable transport of amino-beta-lactam antibiotics by in situ rat small intestine. J Pharm Sci **70:**768-72.
509. **Turner, A., S. J. Pedler, F. Carswell, G. R. Spencer, and D. C. Speller.** 1984. Serum and sputum concentrations of ceftazidime in patients with cystic fibrosis. J Antimicrob Chemother **14:**521-7.
510. **Turner, P. J.** 2000. MYSTIC (Meropenem Yearly Susceptibility Test Information Collection): a global overview. J Antimicrob Chemother **46 Suppl T2:**9-23.
511. **Upton, R. A., S. Riegelman, and L. B. Sheiner.** 1980. Bioavailability assessment as influenced by variation in drug disposition, p. 77-85. *In* K. S. Albert (ed.), Drug Absorption and Disposition: Statistical Considerations. American Pharmaceutical Association Academy of Pharmaceutical Sciences, Washington, D.C.
512. **Upton, R. A., J. F. Thiercelin, T. W. Guentert, S. M. Wallace, J. R. Powell, L. Sansom, and S. Riegelman.** 1982. Intraindividual variability in theophylline

pharmacokinetics: statistical verification in 39 of 60 healthy young adults. J Pharmacokinet Biopharm **10:**123-34.
513. **Upton, R. A., J. F. Thiercelin, J. K. Moore, and S. Riegelman.** 1982. A method for estimating within-individual variability in clearance and in volume of distribution from standard bioavailability studies. J Pharmacokinet Biopharm **10:**135-46.
514. **Vaisman, N., P. B. Pencharz, M. Corey, G. J. Canny, and E. Hahn.** 1987. Energy expenditure of patients with cystic fibrosis. J Pediatr **111:**496-500.
515. **Vawter, G. F., and H. Shwachman.** 1979. Cystic fibrosis in adults: an autopsy study. Pathol Annu **14 Pt 2:**357-82.
516. **Verhaegen, J., and L. Verbist.** 1998. In-vitro activity of 21 beta-lactam antibiotics against penicillin-susceptible and penicillin-resistant Streptococcus pneumoniae. J Antimicrob Chemother **41:**381-5.
517. **Viaene, E., H. Chanteux, H. Servais, M. P. Mingeot-Leclercq, and P. M. Tulkens.** 2002. Comparative stability studies of antipseudomonal beta-lactams for potential administration through portable elastomeric pumps (home therapy for cystic fibrosis patients) and motor-operated syringes (intensive care units). Antimicrob Agents Chemother **46:**2327-32.
518. **Vinks, A. A.** 2002. The application of population pharmacokinetic modeling to individualized antibiotic therapy. Int J Antimicrob Agents **19:**313-22.
519. **Vinks, A. A., R. W. Brimicombe, H. G. Heijerman, and W. Bakker.** 1997. Continuous infusion of ceftazidime in cystic fibrosis patients during home treatment: clinical outcome, microbiology and pharmacokinetics. J Antimicrob Chemother **40:**125-33.
520. **Vinks, A. A., J. G. Den Hollander, S. E. Overbeek, R. W. Jelliffe, and J. W. Mouton.** 2003. Population pharmacokinetic analysis of nonlinear behavior of piperacillin during intermittent or continuous infusion in patients with cystic fibrosis. Antimicrob Agents Chemother **47:**541-7.
521. **Vinks, A. A., D. J. Touw, H. G. Heijerman, M. Danhof, G. P. de Leede, and W. Bakker.** 1994. Pharmacokinetics of ceftazidime in adult cystic fibrosis patients during continuous infusion and ambulatory treatment at home. Ther Drug Monit **16:**341-8.
522. **Visalli, M. A., M. R. Jacobs, and P. C. Appelbaum.** 1998. Activities of three quinolones, alone and in combination with extended-spectrum cephalosporins or gentamicin, against Stenotrophomonas maltophilia. Antimicrob Agents Chemother **42:**2002-5.
523. **Visalli, M. A., M. R. Jacobs, and P. C. Appelbaum.** 1998. Determination of activities of levofloxacin, alone and combined with gentamicin, ceftazidime, cefpirome, and meropenem, against 124 strains of Pseudomonas aeruginosa by checkerboard and time-kill methodology. Antimicrob Agents Chemother **42:**953-5.
524. **Vogelman, B., S. Gudmundsson, J. Leggett, J. Turnidge, S. Ebert, and W. A. Craig.** 1988. Correlation of antimicrobial pharmacokinetic parameters with therapeutic efficacy in an animal model. J Infect Dis **158:**831-47.
525. **Walstad, R. A., K. B. Hellum, S. Blika, L. G. Dale, T. Fredriksen, K. I. Myhre, and G. R. Spencer.** 1983. Pharmacokinetics and tissue penetration of ceftazidime: studies on lymph, aqueous humour, skin blister, cerebrospinal and pleural fluid. J Antimicrob Chemother **12 Suppl A:**275-82.
526. **Wang, J. P., J. D. Unadkat, S. M. al-Habet, T. A. O'Sullivan, J. Williams-Warren, A. L. Smith, and B. Ramsey.** 1993. Disposition of drugs in cystic fibrosis. IV. Mechanisms for enhanced renal clearance of ticarcillin. Clin Pharmacol Ther **54:**293-302.
527. **Watanabe, N., K. Katsu, M. Moriyama, and K. Kitoh.** 1988. In vitro evaluation of E1040, a new cephalosporin with potent antipseudomonal activity. Antimicrob Agents Chemother **32:**693-701.
528. **Waterhouse, T. H., S. Redmann, S. B. Duffull, and J. A. Eccleston.** 2005. Optimal Design for Model Discrimination and Parameter Estimation for Itraconazole Population Pharmacokinetics in Cystic Fibrosis Patients. J Pharmacokinet Pharmacodyn **32:**521-45.
529. **Watkins, J. B., A. M. Tercyak, P. Szczepanik, and P. D. Klein.** 1977. Bile salt kinetics in cystic fibrosis: influence of pancreatic enzyme replacement. Gastroenterology **73:**1023-8.

530. **Weber, A. M., C. C. Roy, L. Chartrand, G. Lepage, O. L. Dufour, C. L. Morin, and R. Lasalle.** 1976. Relationship between bile acid malabsorption and pancreatic insufficiency in cystic fibrosis. Gut **17:**295-9.
531. **Weber, A. M., C. C. Roy, C. L. Morin, and R. Lasalle.** 1973. Malabsorption of bile acids in children with cystic fibrosis. N Engl J Med **289:**1001-5.
532. **Weidekamm, E., R. Portmann, K. Suter, C. Partos, D. Dell, and P. W. Lucker.** 1987. Single- and multiple-dose pharmacokinetics of fleroxacin, a trifluorinated quinolone, in humans. Antimicrob Agents Chemother **31:**1909-14.
533. **Weidekamm, E., K. Stockel, and D. Dell.** 1987. A new trifluorinated quinolone: Ro 23-6240 (AM 833). Drugs Exp Clin Res **13:**85-90.
534. **Weiss, C. F., A. J. Glazko, and J. K. Weston.** 1960. Chloramphenicol in the newborn infant. A physiologic explanation of its toxicity when given in excessive doses. N Engl J Med **262:**787-94.
535. **Weizman, Z., P. R. Durie, H. R. Kopelman, S. M. Vesely, and G. G. Forstner.** 1986. Bile acid secretion in cystic fibrosis: evidence for a defect unrelated to fat malabsorption. Gut **27:**1043-8.
536. **Welling, P. G., W. A. Craig, R. W. Bundtzen, F. W. Kwok, A. U. Gerber, and P. O. Madsen.** 1983. Pharmacokinetics of piperacillin in subjects with various degrees of renal function. Antimicrob Agents Chemother **23:**881-7.
537. **West, G. B., and J. H. Brown.** 2005. The origin of allometric scaling laws in biology from genomes to ecosystems: towards a quantitative unifying theory of biological structure and organization. J Exp Biol **208:**1575-92.
538. **West, G. B., J. H. Brown, and B. J. Enquist.** 1999. The fourth dimension of life: fractal geometry and allometric scaling of organisms. Science **284:**1677-9.
539. **West, G. B., J. H. Brown, and B. J. Enquist.** 1997. A general model for the origin of allometric scaling laws in biology. Science **276:**122-6.
540. **West, G. B., W. H. Woodruff, and J. H. Brown.** 2002. Allometric scaling of metabolic rate from molecules and mitochondria to cells and mammals. Proc Natl Acad Sci U S A **99 Suppl 1:**2473-8.
541. **Westphal, J. F., A. Deslandes, J. M. Brogard, and C. Carbon.** 1991. Reappraisal of amoxycillin absorption kinetics. J Antimicrob Chemother **27:**647-54.
542. **Westphal, J. F., J. H. Trouvin, A. Deslandes, and C. Carbon.** 1990. Nifedipine enhances amoxicillin absorption kinetics and bioavailability in humans. J Pharmacol Exp Ther **255:**312-7.
543. **White, C. R., and R. S. Seymour.** 2005. Allometric scaling of mammalian metabolism. J Exp Biol **208:**1611-9.
544. **Wible, K., M. Tregnaghi, J. Bruss, D. Fleishaker, S. Naberhuis-Stehouwer, and M. Hilty.** 2003. Linezolid versus cefadroxil in the treatment of skin and skin structure infections in children. Pediatr Infect Dis J **22:**315-23.
545. **Wise, R., J. M. Andrews, and K. A. Bedford.** 1981. Cefoperazone and cefotiam--two new cephalosporins: an in-vitro comparison. J Antimicrob Chemother **7:**343-52.
546. **Wise, R., J. M. Andrews, and N. Brenwald.** 1996. In vitro activity of the tricyclic beta-lactam GV104326. Antimicrob Agents Chemother **40:**1248-53.
547. **Wise, R., D. Griggs, and J. M. Andrews.** 1988. Pharmacokinetics of the quinolones in volunteers: a proposed dosing schedule. Rev Infect Dis **10 Suppl 1:**S83-9.
548. **Wise, R., M. Logan, M. Cooper, and J. M. Andrews.** 1991. Pharmacokinetics and tissue penetration of tazobactam administered alone and with piperacillin. Antimicrob Agents Chemother **35:**1081-4.
549. **Wood, R. E., T. F. Boat, and C. F. Doershuk.** 1976. Cystic fibrosis. Am Rev Respir Dis **113:**833-78.
550. **Yaffe, S. J., L. M. Gerbracht, L. L. Mosovich, M. E. Mattar, M. Danish, and W. J. Jusko.** 1977. Pharmacokinetics of methicillin in patients with cystic fibrosis. J Infect Dis **135:**828-31.
551. **Yafune, A., and M. Ishiguro.** 1999. Bootstrap approach for constructing confidence intervals for population pharmacokinetic parameters. I: A use of bootstrap standard error. Stat Med **18:**581-99.
552. **Yamamoto, T., P. Naigowit, S. Dejsirilert, D. Chiewsilp, E. Kondo, T. Yokota, and K. Kanai.** 1990. In vitro susceptibilities of Pseudomonas pseudomallei to 27 antimicrobial agents. Antimicrob Agents Chemother **34:**2027-9.

553. **Yano, Y., S. L. Beal, and L. B. Sheiner.** 2001. Evaluating pharmacokinetic/pharmacodynamic models using the posterior predictive check. J Pharmacokinet Pharmacodyn **28:**171-92.
554. **Yoshikawa, T., N. Muranushi, M. Yoshida, T. Oguma, K. Hirano, and H. Yamada.** 1989. Transport characteristics of ceftibuten (7432-S), a new oral cephem, in rat intestinal brush-border membrane vesicles: proton-coupled and stereoselective transport of ceftibuten. Pharm Res **6:**302-7.
555. **Zaghloul, I., N. Kuck, and A. Yacobi.** 1997. The effect of tazobactam on the pharmacokinetics and the antibacterial activity of piperacillin in dogs. Int. J. Pharm. **153:**115-121.
556. **Zariffa, N. M., S. D. Patterson, D. Boyle, and M. Hyneck.** 2000. Case studies, practical issues and observations on population and individual bioequivalence. Stat Med **19:**2811-20.
557. **Zeitlinger, M. A., C. Marsik, A. Georgopoulos, M. Muller, G. Heinz, and C. Joukhadar.** 2003. Target site bacterial killing of cefpirome and fosfomycin in critically ill patients. Int J Antimicrob Agents **21:**562-7.
558. **Zelenitsky, S., R. Ariano, G. Harding, and A. Forrest.** 2005. Evaluating ciprofloxacin dosing for Pseudomonas aeruginosa infection by using clinical outcome-based Monte Carlo simulations. Antimicrob Agents Chemother **49:**4009-14.
559. **ZeLuff, B., M. Catchpole, P. Lowe, H. Koornhof, and L. Gentry.** 1986. Cefadroxil compared with cefaclor in the treatment of streptococcal pneumonia in adults. Drugs **32 Suppl 3:**39-42.
560. **Zhanel, G. G., K. Ennis, L. Vercaigne, A. Walkty, A. S. Gin, J. Embil, H. Smith, and D. J. Hoban.** 2002. A critical review of the fluoroquinolones: focus on respiratory infections. Drugs **62:**13-59.
561. **Zhanel, G. G., L. Palatnick, K. A. Nichol, D. E. Low, and D. J. Hoban.** 2003. Antimicrobial resistance in Haemophilus influenzae and Moraxella catarrhalis respiratory tract isolates: results of the Canadian Respiratory Organism Susceptibility Study, 1997 to 2002. Antimicrob Agents Chemother **47:**1875-81.
562. **Zlotos, G., A. Bucker, M. Kinzig-Schippers, F. Sorgel, and U. Holzgrabe.** 1998. Plasma protein binding of gyrase inhibitors. J Pharm Sci **87:**215-20.

**Curriculum Vitae**

| | |
|---|---|
| Name | Jürgen Bernd Bulitta |
| Date of birth | August 09, 1979 |
| Place of birth | Neustadt a.d. Aisch, Germany |
| Nationality | German |
| Marital status: | Unmarried |

**Studies:**

| | |
|---|---|
| Since November 2003 | Ph.D. student at the Institute for Biomedical and Pharmaceutical Research (IBMP) in Nürnberg-Heroldsberg, Germany, supervisor: Professor Dr Fritz Sörgel,<br><br>and the Department of Pharmaceutical Chemistry, University of Würzburg, Germany, supervisor: Professor Dr Ulrike Holzgrabe |
| July 2005 to January 2006 | Internship in population pharmacokinetic data analysis and simulations at the Ordway Research Institute, Albany, NY, USA, supervisor: Professor Dr George Drusano |
| January 2005 to May 2005 | Internship in modeling, simulations and meta-analyses of pharmacokinetic and pharmacodynamic data at the University of Queensland, Brisbane, Australia, supervisor: Professor Dr Stephen Duffull |
| October 2004 to January 2005 | Internship in population pharmacokinetics and pharmacodynamics with NONMEM and automatic data processing at the University of Auckland, Auckland, New Zealand, supervisor: Professor Dr Nick Holford |
| October 1999 to October 2003 | Chemistry studies (“Diplom Chemie”) at the Friedrich-Alexander-University, Erlangen-Nürnberg, Germany |
| August 1998 to August 1999 | Civilian service at the Martha-Maria elderly home, Nürnberg, Germany |
| July 1998 to October 2003 | Scientific co-worker at the Institute for Biomedical and Pharmaceutical Research (IBMP) in Nürnberg-Heroldsberg, Germany, supervisor: Professor Dr Fritz Sörgel |
| 1990 - 1998 | Lyceum Scheinfeld (“Gymnasium Scheinfeld”), Scheinfeld, Bavaria, Germany |
| 1986 - 1990 | Primary School Scheinfeld, Scheinfeld, Bavaria, Germany |